UCSF
UC San Francisco Electronic Theses and Dissertations

Title
Mechanisms Regulating the Expression and Function of MXR

Permalink
https://escholarship.org/uc/item/8dr5j9nq

Author
Eclov, Rachel

Publication Date
2013

Peer reviewed|Thesis/dissertation

eScholarship.org Powered by the California Digital Library
University of California

Mechanisms Regulating the Expression and Function of MXR

by

Rachel J. Eclov

DISSERTATION

Submitted in partial satisfaction of the requirements for the degree of

DOCTOR OF PHILOSOPHY

in

Pharmaceutical Sciences and Pharmacogenomics

in the

GRADUATE DIVISION

© 2013 Rachel Jean Eclov

This thesis is dedicated to my husband Neville,

with whom I share the times of struggle and success.

Acknowledgements

This thesis is the compilation of many hours spent in the lab researching or on the computer searching the literature and writing. However much effort I put in, it would never have been completed without physical, mental and emotional contributions from many people. Although below I acknowledge many of those who have helped me, there are also many unnamed individuals who shared with me their insight, protocols, cells, reagents and techniques. To both those named and unnamed, you have my thanks and gratitude for easing my passage and bringing me through this journey.

The foremost person that has my utmost gratitude is my advisor, *Dr. Deanna Kroetz*. It has been an honor to have a mentor with compassion, who is both a great scientist and scholar, and capable of recalling every piece of knowledge or literature she's ever read. Even though the last few months have been frantic and stressful, she has my heartfelt thanks for her continued diligence in combing through my thesis time and time again. Deanna has also contributed to my development as a scientist and I appreciate how she has always challenged me to think critically about the literature and experimental setups so I learned how to address research questions from different angles and with the correct forethought. I am also appreciative of Deanna's open mind to different research avenues, such as epigenetics, and allowing me to try out new techniques in the lab. Finally, because I have always had a knack for pronouncing words incorrectly, I especially appreciate Deanna's willingness to reiterate to me the correct pronunciation, especially with words like canalicular.

I would also like to thank the members of my thesis and oral committees, who gave me valuable advice and suggestions on the direction of my thesis. *Dr. Nadav Ahituv*,

who before he was the chair of my orals committee, opened my eyes to the world of epigenetics and transporter gene regulation. I am also grateful for his willingness to collaborate with me on the *in vivo* portions of my research. *Dr. John Witte*, for your ever upbeat attitude, enthusiasm for my results and realistic research suggestions. Members of my orals committee: *Dr. Kathy Giacomini*, who was gracious enough to find time in her busy schedule to enlighten me on different aspects of transporters and write me numerous letters of recommendations through the years, and *Dr. Pui-Yan Kwok* who knows everything on genetic analysis.

The other Pharmaceutical Science and Pharmacogenomic (PSPG) faculty members including my academic advisor *Dr. Steve Hamilton*, who took the time to make sure I was academically and emotionally on track. The PSPG administrator *Debbie Acoba* for her diligence and willingness to complete paperwork, and making sure that the years of my graduate studies were full of department funded outings. Additionally, I would like to thank the multitude of staff at the University of California San Francisco, especially those at the Cell Culture Facility and Cell Imaging Facility, who made my life run smoother. Also, a very special and heartfelt thanks to our purchasing analyst *Hubert Sylvester*, without whose patience and prompt actions I would never have received any of my reagents.

From the beginning of my time in the Kroetz lab, I had guidance and endless day-to-day help from three wonderful individuals, for whom I have a great deal of appreciation and gratitude. *Dr. Yingmei Lui*, whose knowledge on immunocytochemistry was a great asset in a coworker. To *Dr. Hisa Fukushima*, who never said no; her infectious smile and generosity were the reasons I was never afraid of joining the Kroetz

lab. Last, but never least, *Dr. Svetlana Markova*, who assisted me on many projects, taught me a multitude of skills and always had the time and ability to answer to any question. Sveta also became a close friend of mine and I'll be forever grateful for being able to share my years in the Kroetz lab with her.

The atmosphere in which I spent my graduate career was both educational and entertaining, and there are numerous people who have my thanks for making it that way. First, thank you to all the current and past members of the Kroetz lab, particularly *Dr. Mike Baldwin*, *Dr. Leslie Chinn*, *Mike Martin* and *Janine Micheli* for their technical help, valuable suggestions and willingness to eat anything I baked without regard to fat or calories. Second, a special thank you to *Aparna Chhibber,* who promptly fielded my computer programming questions and assisted with many SNP correlations. Also, thank you to the endless flow of Swedish pharmacy students and international postdoctoral fellows in the Kroetz lab, who in addition to showing me novel techniques, all stole into my heart and I cannot wait to travel the world and visit them. I would also like to thank all the past and present members of Giacomini lab, who I have always thought of as our sister lab, for being great friends and scientists, and their always willingness to share reagents, equipment and space. Specifically, I would like to thank *Dr. Sook Wah Yee*; if I am ever half as good a scientist as her, I will be satisfied.

There are many people who collaborated with me, and without their assistance I would not have the wonderful collection of data described in the following pages. Thank you to (a very soon to be doctor) *Mee Jean Kim* and *Dr. Robin Smith* for your time and effort collecting the *in vivo* enhancer data for me. Thank you to *Shripa Patel* from the PAN facility at Stanford University for never giving up on my DNA methylation

sequencing project. Also, my many mentees, especially *Xiaomin Liang*. I am grateful that they allowed me to practice my teaching and assisted me during their brief time in the Kroetz lab.

My time at UCSF was a section of my life that, while it was happening, I thought could never possibly end, and now that it has, I look back and realize the years flew by in the blink of an eye. This is due to those in San Francisco that shared life outside of lab with me. Among these individuals are my fellow PSPG students; your intelligence and work ethic always gave me a benchmark to strive toward. Also, the many people who allowed me to relax by playing soccer with them, especially the members of Wakiza, Das Foot and iSoccer; I will miss each and every one of them. A special thanks to *Dr. Marcia Campbell Scott*, for listening and understanding about my endless lab stories, and her husband "*Uncle Andrew*" for giving my husband an outlet for all things soccer so I didn't have to be it (and also for your casserole).

My graduate work was built upon other years of my life that was sculpted by many special people. I would like to thank my parents *Barb and Chris LaFond*, who did an excellent job teaching me that only hard work and perseverance will allow me to succeed. I also appreciate their assumptions that I would complete anything I set out to do, which gave me the confidence to actually do it. To my beautiful "sister" *Jessica Paulson*, I appreciate being able to share the good and bad aspects of writing a thesis with her and the never ending Disney related materials with which she has supplied me. Her encouragement and support means the world to me. To my siblings *Lynda, Lisa* and *Chris*, for their provision of reading materials and attempts to understand my research. To

my family-in-law, *Theresa* and *Jon Eclov*, who understand the effort it takes to get an advanced degree and always provide a stimulating conversation.

Finally I thank my intelligent husband, *Neville Eclov*; there are not words that will adequately express my gratitude for his support and love. In addition to spending many weekends in lab with me in order to keep me sane, he has always believed in my capacities as a scientist. Also, I must express my appreciation to him as a sounding board for my scientific thoughts and for his time spent diligently editing my thesis; without his efforts my thesis would never have been completed. Finally, I need to thank him for not giving up on me, or letting me give up, even though I have sat in my pajamas over the past several months and taken every frustration out on him.

I would also like to acknowledge my financial support. These studies were funded by the NIH grant GM61390, American Foundation for Pharmaceutical Education Predoctoral fellowship, NIGMS Predoctoral Training Grant 2 T32 GM07175 and are part of the Pharmacogenetics of Membrane Transporters project in the Pharmacogenetics Research Network.

Rachel Eclov

Abstract

ABCG2 encodes for a multidrug efflux transporter called the mitoxantrone resistance protein (MXR, BCRP) that mediates the efflux of substrates out of the cell and is important in detoxification. The present study was focused on the expression and function of MXR amino acid variants, activity of the *ABCG2* promoter and promoter variants, characterization of *ABCG2* locus *cis*-regulatory elements and variant enhancers, and examination of DNA methylation around *ABCG2*. MXR expression, localization and activity were characterized using whole cells and inside-out vesicles. The Q141K variant had reduced expression. MXR I206L had increased efflux of pheophorbide A and both V12M and D620N had increased ATPase activity. The activity of *ABCG2* regulatory elements was tested in *in vitro* and *in vivo* luciferase assays. Two promoter SNPs (rs76656413 and rs59370292) had decreased *in vivo* liver enhancer activity. Six regions with *in vivo* liver enhancer activity and several enhancer SNPs (rs9999111, rs12508471, rs72873421, rs149713212 and rs2725263) with altered activity *in vivo* were identified. Association of these SNPs with ABCG2, PPM1K or PDK2 expression in different tissues was detected. *In vitro* assays were used to identify nuclear receptor response elements. The *ABCG2* promoter responded to multiple nuclear receptor ligands, and the promoter SNP rs66664036 had a significantly increased response to 17β-estradiol. Nine rifampin, six 17β-estradiol and three dexamethasone responsive regions were identified. Enhancer SNP rs12508471 had decreased response to 17β-estradiol and increased response to dexamethasone, while rs573519157 had an increased and rs190754327 had a decreased response to 17β-estradiol. Finally, methylation of CpG islands in the *ABCG2* locus was correlated with the expression of ABCG2 in human liver and kidney tissues. There was

no correlation of whole CpG island methylation with ABCG2 expression. However, a CpG site within CpG4 correlated with ABCG2 expression in the kidney, and part or all of select CpG islands had significantly lower methylation in liver than in kidney. The genetic and epigenetic regulation of the *ABCG2* gene locus described in this dissertation may contribute to clinical variation in ABCG2 expression.

TABLE OF CONTENTS

LIST OF TABLES

LIST OF FIGURES

LIST OF EQUATIONS

Chapter 1 : Function and Regulation of the Mitoxantrone Resistance Protein

1.1 Overview

The mitoxantrone resistance protein (MXR; BCRP; ABCG2), referred to here as MXR, is an efflux transporter expressed apically in several tissues with a broad range of both exogenous and endogenous substrates. The transport activity, tissue distribution and specific cellular localization of MXR suggest that it plays a pivotal role in endogenous substrate disposition as well as the protection and detoxification of the body from xenobiotics. Overexpression of MXR is associated with drug resistance to a variety of anticancer drugs, and its expression has been linked with decreased disease-free survival in several different cancers. An individual's susceptibility to certain drug-induced side effects has also been linked to MXR expression or nonsynonymous single nucleotide polymorphisms (SNPs) in the MXR gene *ABCG2*. Initial reports on common *ABCG2* SNPs suggest that amino acid altering SNPs have significant effects on substrate selectivity, transport function, expression and localization. However, these SNP-associated changes in MXR function do not account for all of the variation in MXR expression or the pharmacokinetic and pharmacodynamic properties of MXR substrates. The details of ABCG2 regulation are not well known, but the evidence is accumulating for regulation by methylation, transcription factors and nuclear receptors. Here, we discuss the current literature on the different mechanisms which alter MXR expression and function.

1.2 Introduction

Both drug metabolizing enzymes and transporters contribute to drug distribution, elimination, response and toxicity. The ATP-binding cassette (ABC) transporters comprise a superfamily of membrane transporter proteins that utilize the energy from ATP hydrolysis to translocate substrates, against their concentration gradient, across both extra- and intracellular membranes[1]. These membrane bound proteins are responsible for the biological distribution of both endogenous and exogenous compounds. The ABC transporters represent one of the largest families of transporters, with seven highly diverse families (ABCA to ABCG)[1]. The importance of these membrane transporters in drug disposition is evident from the recently published guidelines on drug transporters[2].

The efficacy of cancer therapy is often limited by the development of drug resistance by cancer cells. One method of resistance is attributed to efflux membrane transporters, which become upregulated and efflux chemotherapeutics from the cancer cell, thus conferring cancer cell resistance by reducing the internal concentration of the drug. One of the main efflux transporters indicated in multidrug resistance during chemotherapy is the mitoxantrone resistance protein (MXR)[3]. MXR is a high capacity transporter that recognizes a wide variety of substrates, including chemotherapeutics ranging from anthracenes to kinase inhibitors[4]. Since the expression of MXR can lead to drug resistance, MXR is a prognostic factor in both hematopoietic and solid cancers, as well as an indicator for possible drug toxicity[3].

There are multiple nonsynonymous variants of MXR, many of which are rare; MXR is a highly polymorphic transporter with over 80 single nucleotide polymorphisms (SNPs) in its gene, *ABCG2*[5–11]. The transport functions of the common nonsynonymous

variants and many unnatural variants of MXR have been investigated[12]. Due to difficulties in monitoring the transport efficacy of an efflux transporter, these reports are often limited to one variant against several substrates or one substrate for several variants. However, since MXR has multiple binding regions for substrate interactions, several nonsynonymous variants have been shown to possess altered substrate specificity and activity[13]. This indicates that each variant should be screened against whole panels of MXR substrates to determine if there are any differences in its transport capabilities. There are many assays being utilized for the characterization of MXR variants, and these tools must continue to be optimized and utilized so that future generations of therapeutics may be screened[14].

Although nonsynonymous variants of MXR have been shown to alter MXR function, and possibly substrate specificity, their frequency does not account for all the reported variability in MXR expression, as individuals with reference MXR still have variability in expression[15]. Therefore, in order to effectively evade multidrug resistance, we must understand the mechanisms that regulate the expression of the gene that codes for MXR, *ABCG2*. Recent research has highlighted the role of the *ABCG2* promoter and its hypomethylation in the regulation of MXR expression[16]. However, there is growing evidence for additional regulation of *ABCG2*, including that of alternate promoters, enhancers and nuclear receptor (NR) response elements[16].

By understanding both drug-drug interactions and underlying DNA differences that alter the expression or function of a drug response protein, we could predict drug toxicity and efficacy, bringing us closer to personalized medicine[17,18]. Here, we describe the current literature regarding MXR and *ABCG2* regulation, including the MXR protein

itself, MXR substrates and inhibitors, the nonsynonymous variants of MXR, and regulation of *ABCG2* via DNA methylation and its promoter, enhancers and NRs.

1.3 The Mitoxantrone Resistance Protein

The mitoxantrone resistance protein (MXR) is a 75 kDa membrane transporter first isolated from a mitoxantrone resistant human colon carcinoma cell line[19,20]. It was independently isolated from a doxorubicin resistant human breast cancer cell line (MCF-7 AdVp) and named the breast cancer resistance protein (BCRP)[21]. Shortly thereafter, the protein was isolated from placental tissue and named the ABC transporter of the placenta (ABCP)[22]. MXR transport is unidirectional, and since it localizes to the plasma membrane, it transports substrates from the cytoplasm out of the cell. Since its discovery, MXR has been shown to transport numerous endogenous and exogenous substrates, thus becoming a major player in clinical studies of the pharmacokinetics of its substrates.

1.3.1 *Tissue Distribution*

MXR is expressed in many tissues and protects the body from natural dietary toxins and carcinogens. Expression of MXR has been reported in the intestinal and colon epithelium[21,23–25], where it effluxes substrates out of the epithelium cell and back into the lumen, limiting the absorption of MXR substrates. It is also highly expressed in the bile canalicular membrane of hepatocytes[21,23–25], where it transports substrates and many of their conjugates into the bile, increasing their elimination from the body. MXR is expressed at lower levels in the renal cortex tubules[21,24,25], where it mediates the excretion of substrates into the urine. MXR is expressed in the ducts and lobules of the breast[23],

where it effluxes nutrients, toxins, carcinogens or drugs from the circulation into milk. It is expressed in the placental syncytiotrophoblasts[21–28], where it works to protect the fetus from endogenous hormones and toxins by moving substrates in the fetal circulation to the maternal circulation[26]. MXR is also present in the endothelium of veins and capillaries, most importantly at the blood-brain barrier where it keeps its substrates from penetrating into the brain[23,25,29]. Finally, MXR is expressed in the side population of hematopoietic stem cells; it has been proposed that its role there is the protection of the progenitor cells[30–32].

1.3.2 *Localization*

MXR is a plasma membrane protein and is generally not expressed on other intracellular membranes[33]. This allows MXR to efflux its substrates out of the cell. There have been reports of MXR having altered cellular localization in times of nutrient deprivation, such as low folate, when it then relocates to vesicle membranes under the assumption it helps to sequester nutrients in these vesicles[34]. MXR has apical localization in the epithelium of the small intestine and colon and the liver bile canaliculi, indicating a role of MXR in systemic exposure through the regulation of digestive uptake, thus secreting substances into the bile for their elimination and preventing substrates from entering circulation from the gut[23]. MXR is also localized to the apical side of most breast ducts and lobules, where it moves substrates into the milk[23]. Finally, MXR has mainly apical localization in placental syncytiotrophoblasts[23], with one report of some cytoplasmic staining in these cells[24], where it moves substrates into the maternal circulation.

1.3.3 *Structure*

MXR and related ABCG subfamily members are half-transporters consisting of one nucleotide binding domain (NBD) and a membrane spanning domain (MSD) that consists of six transmembrane (TM) α-helices[35,36]. Compared to other ABC transporters, the orientation of the MXR NBD and MSD is reversed. The NBD is at the amino-terminal end of the protein, including an intracellular stretch that has the ATP binding site (Walker A and B motifs) and the C signature motif of ABC transporter, before the MSD and finally the acid terminal end of the protein (see Figure 1.1)[37]. The NBD stretches from residues 1-396, and the MSD from residues 397-655[37]. There is a N-glycosylation site at Asp590 in the extracellular loop connecting TM5 with TM6[38], and the Cys603 amino acid, also in this loop, is responsible for disulfide bond formation between MXR oligomers[39]. The Arg363 and T402-G410 residues are relevant for correct biogenesis, folding and membrane insertion of the MXR protein[40,41]. Additionally, the R482 amino acid is critical in substrate interaction[42].

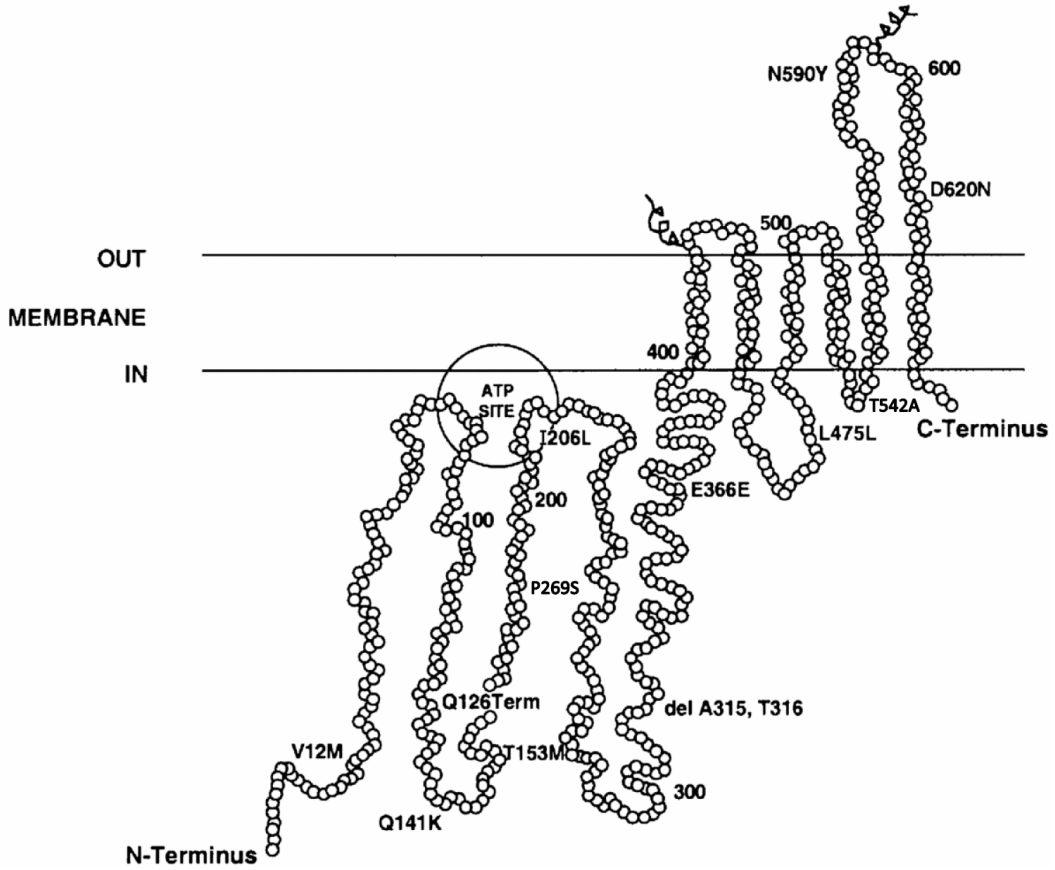

Figure 1.1 Structure of the MXR transporter. A schematic representation of MXR membrane organization with nonsynonymous variant locations indicated. Figure was obtained from Polgar and Bates[43] with additional variants added.

1.3.4 *Oligomerization*

The MXR protein is unique among the multidrug resistant transporters because it is a half transporter and needs to form oligomers in order to create a functional unit. The MXR protein migrates on a gel as a monomer at ~70-75 kDa under reducing conditions and as a dimer at 140-180 kDa (depending on glycosylation and other modifications) under non-reducing conditions[44,45]. However, in human cells the minimal stable functional unit of MXR is a homotetramer, and it has potential to have higher forms of oligomerization, including as a homo-dodecamer[44]. Cys603 is responsible for disulfide

bond formation between MXR oligomers[39]. However, the formation of intra-molecular disulfide bonds between MXR proteins is not necessary for activity and transport function[3]. The formation of higher order oligomers of MXR would provide multiple binding sites and flexibility in the protein's recognition of substrates. Multiple homology modeling and structural analysis help to elucidate the structure of MXR *in vivo*[37]; however, additional structural data are needed to confirm the current two dimensional structure predictions and make a three dimensional map of the functional transporter.

1.4 Therapeutic Substrates of MXR

The MXR protein is extremely flexible in its substrate recognition. Ongoing functional characterization of the transporter adds to the list of MXR substrates, which includes a broad spectrum of synthetic and endogenous compounds[3,37]. The substrate specificity of MXR overlaps with that of other multidrug transporters, and it has been suggested that the dual role of these transporters assists in synergistic protection of the body and its organs[1,46]. MXR was first discovered in cellular resistance to chemotherapeutic agents; since then many classes of chemotherapeutics have been tested in cytotoxicity assays and identified as MXR substrates. Additionally, a number of other non-chemotherapeutic compounds such as statins, antiretrovirals and antibiotics have been shown to be transported by MXR (see Table 1.1).

1.4.1 *Anthracenes and Topoisomerase Inhibitors*

The ability of many anticancer agents to elicit their cytotoxic effects depends on intracellular access of the drug. The overexpression of efflux transporters, such as MXR,

leads to reduced intracellular accumulation of anticancer agents and drug resistance. Mitoxantrone is an anthracenedione anticancer agent[47] used in combination therapies to treat prostate and breast cancers and multiple sclerosis[48–50]. Resistance to mitoxantrone is a hallmark of MXR overexpressing cell lines[19,20,33,51–57]. Mitoxantrone stimulates MXR ATPase activity[58], but direct kinetics for this compound have not been reported. The anthracene derivative bisantrene also shows reduced accumulation in MXR expressing cell lines[20]. Additionally, cells resistant to mitoxantrone exhibit cross-resistance to other topoisomerase inhibitors including etoposide[51,57,59], GV196771[60], indolocarbazole[61], becatecarin[62], NB-506 and J-107088[63].

1.4.2 *Antimetabolites*

Many antimetabolites, which are chemotherapeutic agents that interfere with rapidly dividing cells, are also MXR substrates. The most well-characterized antimetabolite substrate of MXR is methotrexate (MTX). Methorexate is an antifolate that competitively inhibits the dihydrofolate reductase enzyme, making it an effective agent to treat many types of cancers and rheumatoid arthritis[64]. The ability for MXR to transport MTX was first identified in cell lines that overexpressed MXR and had resistance to MTX[57,65]. MTX is a high capacity, low affinity substrate of MXR with reported K_m values of 0.68 – 1.3 mM[55,64,66]. MXR also transports MTX diglutamates and triglutamates, but it cannot transport MTX with more than three glutamates[55,64,66]. Another metabolite of MTX, 7-hydroxy-methotrexate is also transported by MXR[55].

Although MXR can transport MTX and folic acid[55], it cannot transport the reduced folate leucovorin[66]. Interestingly, most lipophilic antifolates are much better

substrates of the mutant G482 MXR[67], but MTX transport is specific to reference R482 MXR[68]. Other antifolates such as GW1843, tomudex, pyrimethamine and trimethrexate are also substrates of MXR[67,69]. Other antimetabolites can be transported by MXR, including pyrimidine analogs like 5-fluorouracil[57] and multiple purine analogs such as clofarabine, fludarabine, 6-mercaptopurine and 6-mercaptopurine riboside[70]. Additionally, nucleotide and nucleoside analogs are MXR substrates, specifically CdAMP and cladribine[70]. Considering the wide breadth of antimetabolites that are MXR substrates, emerging antimetabolite therapies should be screened through MXR substrate assays.

1.4.3 *Anthracyclines*

The MCF-7 AdVp cell line overexpresses MXR and accumulates the anthracycline daunorubicin (daunomycin) to a lesser extent than the parental cell line[20]. Additionally, both daunorubicin and doxorubicin were shown to stimulate MXR ATPase activity[58]. However, these cells harbor a R482G/T variant MXR protein, and reference MXR is not capable of transporting daunorubicin[71,72]. The MCF-7 AdVp cells are also cross-resistant to doxorubicin[51], epirubicin[56,71] and pirarubicin[57]. The transport of many anthracyclines is attributed to the R482G/T mutation in MXR, including idarubicin[71]. The R482G/T MXR variant is not found in humans, but these data provide information regarding the determinants of MXR substrate specificity.

1.4.4 *Camptothecin Analogues*

Camptothecin is an anticancer agent that works through inhibition of DNA topoisomerase I and its derivative irinotecan, a cytotoxic camptothecin whose active metabolite is SN-38, a commonly used anti-cancer agent for treatment of colorectal, lung and gastric tumors[73]. Although camptothecin itself is not transported by MXR[74], many of its derivatives, including irinotecan (CPT-11)[75–77], the irinotecan active metabolite SN-38 (7-ethyl-10-hydroxycamptothecin)[54,56,74–78], SN-38 glucuronide[76,78], topotecan[20,33,52–54,56,74,75,79], 9-aminocamptothecin[52,56,74,75,80], homocamptothecin[77] and diflomotecan[77,81], are MXR substrates. Thus, overexpression of MXR causes cancer cell line resistance to SN-38 and irinotecan[82,83]. The structural comparison of camptothecin analogues transported by MXR has given insight into key features of MXR substrates. Since irinotecan analogues with a hydroxyl group at position 10 or 11 of their A ring are good substrates for MXR, hydrogen bond formation is considered to be involved in substrate recognition and/or transport[84]. Additionally, negative potential at position 10 or 11 of the A ring[85] and a polar group at position 9 or 10[80] are both important for substrate recognition by MXR. Continued elucidation of the structural features of MXR substrates will inform the development of anticancer agents with lower potential for drug resistance.

Although camptothecin derivatives are effective anticancer agents, they are often accompanied by side effects; these side effects have been linked to several efflux drug transporters including MXR[73]. In MXR knockout mice, topotecan plasma levels are increased and milk accumulation is decreased relative to reference[86]. Elacridar (GF120918), a non-selective inhibitor of ABC transporters, increases plasma topotecan levels and increases fetal topotecan exposure, demonstrating the potential for clinically

significant drug-drug interactions involving MXR[79]. In human studies, decreased function *ABCG2* alleles have been associated with irinotecan induced neutropenia[87,88], oral bioavailability of topotecan[89] and diflomotecan[81], and extensive plasma accumulation of SN-38 and its glucuronide[90]. The development of campthothecin derivatives that are not MXR substrates would be expected to improve the benefit-risk ratio for these agents.

1.4.5 *Kinase Inhibitors*

Many new anticancer agents have been developed to target specific mitogenic pathways within cancer cells. Many of these mitogenic pathways are regulated by kinases, and inhibition of these kinases is an effective anticancer therapy. Tyrosine kinase inhibitors (TKIs) were first developed for treatment of hematopoietic malignancies, and efflux of these compounds can lead to drug resistance[91]. MXR expression is high in many hematopoietic cancers[92,93], making TKIs that are not substrates of MXR a useful strategy for future development.

The first TKI, imatinib mesylate, is transported in MXR overexpressing cell lines[94,95], and individuals develop "pharmacokinetic resistance" to imatinib through the overexpression of MXR[96]. Many other TKIs, including lapatinib, dasatinib, gefitinib, vandetanib and erlotinib are also substrates of MXR[97–102]. Most TKIs were initially thought to be inhibitors of MXR, but it is now clear that agents such as nilotinib, dasatinib and CI1033 are high-affinity substrates of MXR that at high concentrations inhibit the transporter[103,104]. Most TKIs, like erlotinib, stimulate the ATPase activity of MXR, supporting the claim that they are MXR substrates[105]. *Abcg2*-/- mice have

increased bioavailability of erlotinib[99] and increased sorafenib penetration into the brain[106], illustrating the importance of MXR in TKI pharmacokinetics. MXR also plays a role in the transport of the cylin-dependent kinase/Aurora kinase inhibitor JNJ-7706621[107]. MXR should therefore be evaluated in the development of all kinase inhibitors.

1.4.6 *Statins*

Statins target HMG-CoA reductase and are used in the treatment of coronary heart disease[108]. Statins are widely used and generally well-tolerated; however, serious complications such as myopathy may occur[108]. The ABCG family is associated with the transport of cholesterol steroids[36], and MXR transports a number of statins, including rosuvastatin[109] and pitavastatin[110] (see Table 1.1). Patients with reduced function variants of MXR had higher exposure to rosuvastatin[111], fluvastatin, pravastatin and simvastatin[112], higher liver levels and a greater therapeutic response[108]. Noncoding SNPs in the *ABCG2* locus are associated with greater response to rosuvastatin[113]. Although individuals with these variants might exhibit improved drug response, they also have the potential for drug toxicities. The use of statins as a gout treatment has also been proposed because they are able to alter ABCG2 expression[114]. Thus, identification of statins that are substrates of MXR, of MXR variants with lower transport of these compounds and of the pathways involved in the statin regulation of MXR is important for assessing the benefit-risk ratio in patients.

1.4.7 *Antiretrovirals*

The development of antiretroviral therapy (ART) has led to significant declines in human immunodeficiency virus (HIV) associated morbidity and mortality[115]. Although combination therapy is now a hallmark of ART, there are numerous drug resistance and metabolic complications that are associated with HIV treatment[115]. Overexpression of MXR *in vitro* leads to increased resistance to the nucleoside reverse transcriptase inhibitor (NRTI) zidovudine (AZT) as a result of decreased cellular accumulation of AZT and its metabolites[116,117]. Similarly, lamivudine has reduced activity in MXR overexpressing cells[116]. Antiretroviral drugs are competitive inhibitors of MXR, and multiple antiretrovirals (in order of IC_{50} rank: lopinavir, nelfinavir, delavirdine, efavirenz, saquinavir, atazanavir, amprenavir and abacavir) increased pheophorbide A accumulation in a MXR expressing cell line[118]. Identification of ART agents that can inhibit MXR in combination treatment settings could provide avenues to circumvent resistance.

1.4.8 *Antibiotics*

The ability of MXR to transport antibiotics, especially into milk, is of particular interest not only in humans, but in cows as well. MXR can transport a number of antibiotics including ciprofloxacin, ofloxacin, norfloxacin, erythromycin, tetracycline, rifampicin and enrofloxacin[119–121]. MXR alters the pharmacokinetics, hepatobiliary excretion and milk secretion of nitrofurantoin[122]. It also mediates the biliary excretion of ciprofloxacin, grepafloxacin, ofloxacin and ulifloxacin, and the tubular secretion of ciprofloxacin and grepafloxacin[123]. Identification of antibiotic substrates of MXR is necessary to limit infant exposure and reduce antibiotic accumulation in cow's milk.

1.4.9 *Other Therapeutic Drugs*

Sulfasalazine, a prodrug for 5-aminosalicylic acid, is an anti-inflammatory medication used for rheumatoid arthritis and inflammatory bowel disease[124,125]. Sulfasalazine is a high affinity (K_m = 0.7 μM) substrate of MXR[126,127] and is used clinically as a marker of MXR activity[128–130]. MXR transports other immunomodulators including the anti-inflammatory diclofenac[131], the antirheumatic drug leflunomide and its metabolite A771726 (teriflunomide)[132].

MXR also transports numerous other therapeutic compounds that treat everything from parasites to sclerosis (see Table 1.1). MXR transports drugs that work in the gastric tract such as the proton pump inhibitor pantroprazole, which can also inhibit MXR[133], and the antiulcerative agent cimetidine[134]. Since MXR is expressed in the apical side of the intestinal epithelium, its efflux of these compounds back into the lumen might aid in their therapeutic action or work to reduce plasma levels of the drug. For example, *Abcg2*-/- mice have increased plasma concentrations and decreased milk accumulation of cimetidine[86]. MXR also transports several antidiabetic agents such as glyburide[135,136], and is responsible for the biliary excretion of troglitazone sulfate, the major metabolite of the antidiabetic agent troglitazone[137]. MXR also mediates the transfer of glyburide across the human placenta from fetus to maternal circulation[138]. Finally, the expression of MXR at the blood brain barrier can impact any of its antipsychotic substrates that need to enter the CNS, such as the depression medicine befloxatone[139]. Prazosin, a drug used to treat anxiety, post-traumatic stress disorder and panic disorder, has reduced accumulation in cells overexpressing MXR[20]. Expression of MXR may influence the pharmacological or toxicological actions of its many substrates.

Table 1.1. Therapeutic Substrates of MXR

Statins	***Quinoline Alkaloids***	***Antimetabolites***
nitrofurantoin[140]	irinotecan[75–77,82,83]	methotrexate[55,57,64–66]
pitavastatin[110,141]	SN-38[54,56,74–78,82,83]	MTX diglutamate[55,64,66]
pravastatin[112,142]	SN-38-glucuronide[76,78]	MTX triglutamate[64,66]
lamivudine[143]	topotecan[20,33,52–54,56,74,75,79,86]	7-hydroxy-MTX[55]
fluvastatin[112]	9-aminocamptothecin[52,56,74,75,80]	GW1843[69]
simvastatin[112]	homocaptothecin[77]	trimethrexate[67]
rosuvastatin[109,111]	diflomotecan[77,81]	tomudex[69]
	NX211[75]	pyrimethamine[67]
Kinase Inhibitors	DX-8951f [52,144]	5-fluorouracil[57]
gefitinib[97,98,101]	gimatecan[145]	CdAMP[70]
erlotinib[97,99,105]	belotecan[146]	cladribine[70]
imatinib[94–96]		clofarabine[70]
lapatinib[100]	***Others***	fludarabine[70]
nilotinib[103]	prazosin[20]	6-mercaptopurine (6MP)[70]
dasatinib[102,103]	Iodoarylazidoprazosin[147]	6MP riboside[70]
vandetanib[101]	mycophenolic acid glucuronide[148]	
sorafenib[106]	azidopine[147]	***Immunomodulators***
tandutinib[149]	nitrendipine[147]	diclofenac[131]
CP-724,714[150]	nicardipine[147]	leflunomide[132]
symadex[151]	nifedipine[147]	teriflunomide[132]
*CI1033[104]	cimetidine[86,134]	albendazol sulfozide[152]
JNJ-7706621[107]	*pantroprazole[133]	sulfasalazine[126–130]
	glyburide[135,136,138]	
Antibiotics	troglitazone sulfate[137]	***Topoisomerase Inhibitors***
ciprofloxacin[119,123]	TH-337[153]	mitoxantrone[19,20,33,51–58]
ofloxacin[119,123]	*dipyridamole[154]	bisantrene[20]
norfloxacin[119]	ME3327[155]	aza-antrapyrazole[53,156]
erythromycin[120]	PM-5[155]	etoposide[51,57,59]
tetracycline[120]	*oxfendazole[152]	teniposide[59]
rifampicin[120]	moxidectin[157]	indolocarbazole[61]
enrofloxacin[121]	zoledronic acid[158]	NB-506[63]
nitrofurantoin[122]	riluzole[159]	J-107088[63]
grepafloxacin[123]	olmesartan medoxomil[160]	GV196771[60]
ulifloxacin[123]	befloxatone[139]	*becatecarin[62]
	4-methylumbelliferone (4Mu) sulfate[161]	
Anthracyclines[#]	4Mu glucuronide[161]	***Antiretrovirals***
doxorubicin[51,58]	E3040 sulfate[161]	zidovudine (ZVD)[116,117]
epirubicin[56,71]	2,4-dinitrophenyl-S-glutathione[161]	ZDV metabolites[116,117]
pirarubicin[57]	albendazol sulfoxide[152]	lamivudine[116,143]
	ortataxel[162]	ganciclovir[163]
	bicalutamide[164]	
	*NSC73306[165]	

*Also inhibits MXR at higher concentrations
[#]Substrates of the R482G/T variant MXR

1.5 Natural Substrates of MXR

The tissue distribution and localization of the MXR transporter supports an important role in detoxification and protection. This role was illuminated in MXR knockout mice, which develop phototoxicity due to accumulation of the porphyrin class of dietary toxins[166]. Since then it has been shown that MXR is responsible for the protection of the body from other dietary toxins such as carcinogens[167]. Additionally, MXR is responsible for the distribution of many natural compounds, including flavonoids, folic acid, steroids, and bile acids (see Table 1.2). Identification of the natural substrates of MXR adds to the knowledge of its function in the body and could help in identifying structurally similar therapeutic substrates of MXR.

1.5.1 *Porphyrins*

Porphyrins are naturally occurring aromatic compounds that bind and form complexes with metals. The most common porphyrin is heme, which gives blood cells their red color and their ability to transport iron. The buildup of porphyrins, either in cells or *in vivo*, leads to phototoxicity. *Abcg2*-/- mice experience phototoxicity due to the accumulation of porphyrins[166], which led to their establishment as MXR substrates[10,168]. Pheophorbide A, a natural dietary toxin, accumulates in MXR knockout mice to cause phototoxicity[166] and is a specific MXR substrate and good *in vitro* probe for MXR function[169]. Levels of protoporphyrin IX (a derivative of heme) are also increased in the erthyrocytes of *Abcg2*-/- mice[166], and protoporphyrin IX was later determined to be a substrate of MXR[170]. MXR mediates the transport of other porphyrins, including

hematoporphyrin[10,171] and 3-(1'-hexyloxyethyl)-3-devinyl pyropeophorbide-A (HPPH)[172], and is important for the biliary excretion of porphyrins[173].

Transport of porphyrins by MXR is consistent with phototoxicity caused by some MXR inhibitors and substrates[174]. The MXR specific inhibitor fumetrimorgin C (FTC) blocks phytoporphyrin (phylloerythrin) transported in MXR expressing cell lines[173]. Additionally, the reduced accumulation of pyropheophorbide A methyl ester, chlorine e6 and protoporphyrin IX (generated by treating with 5-aminolevulinic acid) in a MXR overexpressing cell line was reversible by FTC treatment[175]. The continued characterization of porphyrin substrates of MXR could give new insight into the mechanisms that lead to clinical phototoxicity and its prevention.

1.5.2 *Carcinogens*

One of the most common food carcinogens is 2-amino-1-methyl-6-phenylimidazo[4,5-b]pyridine (PhIP). MXR transports PhIP[134], along with other carcinogens including Benzo[a]pyrene-3-sulfate and Benzo[a]pyrene-3-glucuronide[176]. The ability of MXR to protect against carcinogen exposure is evident from reports that *Abcg2-/-* mice have higher plasma levels of PhIP due to impaired hepatobiliary and intestinal excretion of PhIP[167] and have decreased PhIP transport into milk[86]. MXR reduces systemic exposure to the heterocyclic amines 2-amino-3-methylimidazo[4,5-f]quinoline (IQ) and 3-amino-1,4-dimethyl-5H-pyrido[4,3-b]indole (Trp-P-1) and the potent human hepatocarcinogen aflatoxin B1[177]. The ability of MXR to reduce systemic exposure to carcinogens is associated with cancer susceptibility. For example, prostate cancer patients with reduced function alleles of MXR had a significantly shorter survival

time[178]. Reduced function MXR variants were also associated with increased risk of diffuse large B-cell lymphoma[179]. Mechanisms that reduce MXR expression could result in cancer prevention.

1.5.3 *Flavonoids*

Fruits, vegetables and beverages are all important sources of flavonoids[180–182]. Flavonoids are polyphenolic compounds that are characterized as flavonols, flavones, flavanones, flavanols, isoflavones, chalcones, or anthocyanidins. These compounds are all widely distributed throughout the plant kingdom; the two most common flavonols (which are the most common flavonoids) are quercetin and kaempferol[181,183]. Quercetin and kaempferol are major constituents of Ginkgo biloba extract, and both are MXR substrates[184]. Lumen absorption of quercetin and the quercetin glucuronides is limited by MXR efflux[185]. Additionally, plasma concentrations of quercetin and isorhamnetin (methylated metabolite of quercetin) increase in MXR knockout mice[185].

Many flavonoids have biological activity, such as riboflavin (vitamin B_2) which is secreted into milk by MXR[186]. MXR transports many of the flavonoids (see Table 1.2), including hesperetin and its metabolites and flavopiridol[187–189]. Flavopiridol is a cyclin-dependent kinase inhibitor being developed as an acute myeloid leukemia (AML) treatment. MXR overexpressing cells are resistant to flavopiridol[189] and ABCG2 mRNA levels correlate with flavopiridol cytotoxicity in AML blast cell samples[93]. The importance of MXR in flavopiridol activity requires careful study.

Some flavonoids have weak estrogenic activities and are called phytoestrogens. Some phytoestrogens, including genistein, naringenin, acacetin and kaempferol,

potentiate the cytotoxicity of SN-38 and mitoxantrone and increase cellular accumulation of topotecan[190]. Studies in *Abcg2 -/-* mice have shown increases in AUC of genistein[191,192], plasma levels of diadzein[192] and the accumulation of inulin in the brain and testis[192]. Thus, MXR is important in limiting the oral availability and distribution of phytoestrogens into the brain, testis, epididymis and fetus[192]. Alterations in MXR expression or function could impact the bioavailability and tissue exposure to phytoestrogens.

1.5.4 *Hormones*

In addition to many phytoestrogens, MXR transports many other hormones including estrone 3-sulfate (E1S), dehydroepiandrosterone sulfate (DHEAS) and the estrogen metabolites 17β-estradiol sulfate and 17β-estradiol-17β-D-glucuronide ($E_2$17βG)[161,193]. Data on whether MXR can transport estrogen are conflicting, as there are reports of MXR transport of 17β-estradiol[120] and non-transport of free estrogen and 17β-estradiol[193]. MXR transport of estrogen conjugates is well supported; the K_m for E1S ranges from 3.6-16.6 μM[161,194] and the K_m for $E_2$17βG is 44.2 μM[66]. MXR is implicated in the bioavailability of estrogens and is responsible for the biliary excretion of the 3-*O*-sulfate conjugate of 17α-ethinylestradiol, a component of oral contraceptives[195]. The expression of MXR could affect many hormonal processes, especially in tissues where both hormones and MXR are prevalent, such as the placenta, breast and testes.

1.5.5 *Dyes and Fluorescent Compounds*

There are many different dyes and fluorescent compounds utilized in the laboratory setting, including Hoechst 33342 dye and D-luciferin (substrate of the firefly luciferase), that are substrates of MXR[196,197]. Many of the dyes that are transported by MXR are used in flow cytometry assays. For example, the expression of MXR in hematopoietic pluripotent progenitor cells is a major contributor to the efflux of Hoechst 33342[198,199]. Two other cell imaging agents, rhodamine 123 and Bodipy-prazosin, are actively transported from cells by MXR[58,71], have reduced accumulation in MXR overexpressing cell lines[20] and their efflux is inhibitable by the MXR specific inhibitor FTC[200]. These dyes have also been utilized *in vivo*; for example, MXR transports Bodipy-prazosin away from the mouse fetus[136]. The newly developed fluorescent bile salt analogues cholyl-L-lysyl-fluorescein and cholylglycylamido fluorescein are being developed as *in vivo* tools to monitor liver transporter function[201,202].

1.5.6 *Other Natural Substrates*

MXR is located on the apical membrane of the bile canalicular membrane and transports bile acids such as cholate and deoxycholate[120,202]. Additionally, MXR is expressed in the kidney and mediates urate secretion at the brush border membrane of renal proximal tubule cells[203]. MXR also transports uric acid, and *ABCG2* polymorphisms and gene expression levels have been repeatedly associated with gout[204–206]. Determining mechanisms that regulate the expression and function of MXR could lead to new pathways to identify individuals at risk for gout.

There are many other dietary nutrients that are transported by MXR, including folic acid and vitamin K[55,66,207]. Resveratrol, the natural phenol found in the skin of red grapes and other fruits and that is associated with increased life span, is transported by MXR[55]. Glutathione (GSH), the major endogenous thiol antioxidant with a critical role in the preservation of cellular redox balance as well as the detoxification of exogenous and endogenous compounds, is also transported by MXR[208]. Finally, MXR transports phenethyl isothiocyanates; isothiocyanates are non-nutrient constituents abundant in cruciferous vegetables that inhibit carcinogenesis[209].

MXR is also important for the transport of cellular components. The potent sphingolipid mediator sphingosine 1-phosphate (S1P) is transported by MXR[210]. Additionally, the phospholipid phosphatidylserine, usually kept on the inner-leaflet of the cell membrane, is also transported by MXR[211]. The most interesting cellular compound that MXR transports is amyloid β[212], a component of amyloid plaques indicated in the causation of Alzheimer's disease[212]. Therefore, the expression and function of MXR at the blood-brain barrier could be playing a role in the accumulation of amyloid β, and therapies designed to increase MXR expression or function could be beneficial in Alzheimer patients.

Table 1.2. Natural Substrates of MXR

Porphyrins	***Carcinogens***
pheophorbide A[166,168,169]	PhIP[86,134,167]
protoporphyrin IX[166,168,170,175]	benzo[a]pyrene-3-sulfate[176]
phytoporphyrin[173]	benzo[a]pyrene-3-glucuronide[176]
pyropheophorbide A methyl ester[175]	IQ[177]
chlorine e6[175]	Trp-P-1[177]
hematoporphyrin[10,171]	aflatoxin B_1[177]
HPPH[172]	
zinc mesoporphyrin[168]	***Flavonoids***
heme[168]	genistein[190–192]
hemin[168]	naringenin[190]
zinc protoporphyrin IX[168]	acacetin[190]
copper protoporphyrin IX[168]	kaempferol[184,190]
	flavopiridol[189]
Steroids/Hormones	riboflavin[186]
estrone 3-sulfate[161,193,194]	quercetin[185]
DHEAS[161]	quercetin glucuronides[185]
E(2)17β glucuronide[66,161]	isorhamnetin[185]
17β-estradiol sulfate[193]	hesperetin[188]
oestradiol[120]	hesperetin 7-O-glucuronide[187]
3-*O*-sulfate 17α-ethinylestradiol[195]	inulin[192]
	daidzein[192]
Bile Acids	
glycoCA[202]	***Dyes***
tauroCA[202]	rhodamine 123[20,58]
taurolithocholic acid-3-sulfate[202]	bodipy-prazosin[58,71,136,200]
cholic acid/cholate[120,202]	hoechst 33342[58,71,198,199]
deoxycholate[120]	eFluxxID® Green[213]
	eFluxxID® Gold[213]
Dietary Compounds	D-luciferin[196,197]
uric acid/urate[203,204]	cholyl-L-lysyl-fluorescein[201]
folic acid[55]	cholylglycylamido fluorescein[202]
vitamin K[207]	bodipy-dihydropyridine[147]
plumbagin[207]	
resveratrol[55]	***Others***
phenethyl isothiocyanates[209]	sphingosine 1-phosphate[210]
glutathione[208]	phospholipid phosphatidylserine[211]
	amyloid β[212]

1.6 MXR Inhibitors

There are currently many natural products and synthetic inhibitors of MXR (see Table 1.3), and many libraries of compounds are being screened for their ability to inhibit

MXR function[196,214]. Identification of dietary compounds and therapeutics that inhibit MXR could aid in the understanding of drug-drug interactions and the prevention of drug toxicity. MXR inhibitors are identified through assays utilizing a well characterized substrate of MXR and screening for whether target compounds can alter transport. This has led to the discovery of multiple competitive and noncompetitive inhibitors (see Table 1.3). Competitive inhibitors act as substrates with high affinity for a MXR substrate binding sites, preventing binding and active transport of other substrates. Non-competitive inhibitors can act in various ways, for example by blocking the ATPase activity that is necessary for transport of xenobiotics across the plasma membrane. Typical examples of noncompetitive inhibitors of MXR are cyclosporine A and sodium orthovanadate[58,215].

1.6.1 *Prototypical MXR Inhibitors*

One of the most common specific and potent inhibitors of MXR, fumitremorgin C (FTC), is an indolyl diketopiperazine isolated from *Aspergillus fumigatus* and is not transported by MXR[53,200,216,217]. FTC inhibits the ATPase activity of MXR[218] and reverses mitoxantrone, doxorubicin and topotecan resistance[53,216]. Depending on the MXR substrate, FTC has IC_{50} values in the range of 0.5-10 μM[53,58,216,219]. Although FTC is a potent MXR inhibitor, it is not being developed for clinical use because it causes severe *in vivo* neurotoxicity, including tremors and convulsions. There are many FTC analogs that have also been targeted as specific MXR inhibitors, although many also have severe cytotoxicity[220]. The most promising FTC analogs for use in the clinic are Ko134 and Ko143, which are both potent and specific MXR inhibitors without cytotoxicity[98,221].

Two more common inhibitors of MXR are the benzimidazoles pantoprazole and omeprazole, which inhibit MTX transport with IC_{50} values around 13 μM and 36 μM, respectively[133]. Pantoprazole, a proton pump inhibitor, is a common treatment for acid reflux, acts through competitive inhibition and is also transported by MXR[133]. Co-treatment with pantoprazole reduces imatinib clearance and increases imatinib penetration into mouse brain[94]. Development of an effective and safe MXR inhibitor would be beneficial particularly for the treatment of brain tumors.

MXR also has overlap in its inhibitor profile with P-glycoprotein (P-gp), another common ABC transporter. The P-gp inhibitor tariquidar inhibits MXR-mediated pheophorbide A transport[169]. Another P-gp inhibitor elacridar (GF120918) reverses MXR-dependent cellular resistance to topotecan and other camptothecin derivatives[75,222], to etoposide[59] and to mitoxatrone and MTX[65,221,222]. Elacridar also works *in vivo* and during co-treatment increases topotecan plasma and fetal concentrations in mice[79], reduces imatinib clearance and increases imatinib penetration into mouse brain[94]. Possibly due to its dual inhibition of both MXR and P-gp, elacridar increases the oral bioavailability of topotecan by 50% in patients[223]. Since elacridar can be used *in vivo* to inhibit ABC transporters, it is a promising clinical combination therapeutic for reversal of drug resistance or improvement of chemotherapeutic bioavailability.

1.6.2 *Hormones*

Many sulfate and glucoronide conjugates of estrogen derivates and other hormones are transported by MXR, but their parent compounds are not[193]. However, free estrogens like estrone and 17β-estradiol increase the cellular accumulation of topotecan,

mitoxantrone and SN-38 in MXR overexpressing cell lines[134,224]. Estrogen antagonists and agonist screens found that diethylstilbestrol, estrone, tamoxifen, toremifene, TAG-11 and TAG-139 all reverse MXR-mediated SN-38 and topotecan resistance[225]. Therefore, estrogen levels in tissues could play a role in target site concentrations of MXR substrates.

Glucocorticoids regulate growth, metabolic, developmental and immune functions, and glucocorticoid derivatives are widely prescribed to treat immune disorders[226]. The natural glucocorticoid corticosterone and the glucocorticoid drugs beclomethasone, 6α-methylprednisolone, dexamethasone and triamcinolone inhibit, but are not transported by, MXR[134]. The impact of glucocorticoid treatment on MXR substrates *in vivo* requires further study.

1.6.3 *Tyrosine Kinase Inhibitors*

Tyrosine kinase inhibitors (TKIs) are anticancer agents given as single or combination therapies for many cancers and are particularly important in the treatment of hematopoietic malignancies[101]. Initially, both imatinib and gefitinib were reported to reverse MXR-mediated topotecan and SN-38 resistance, without being transported by MXR[227–229]. They have both since been shown to be transported by MXR, functioning as competitive inhibitors of the transporter[97,230,231]. Erlotinib reverses MXR-mediated drug resistance[105], but it also stimulates MXR ATPase activity and is a substrate[97]. Recent data suggests that nilotinib, imatinib, dasatinib, lapatinib and sunitinib all function as MXR substrates at low concentrations[231–234] but inhibit MXR at higher concentrations[103].

1.6.4 *Natural Inhibitors*

The interaction of naturally occurring compounds with drugs is of clinical significance and may explain individual variability in drug pharmacokinetics. Extracts of isoflavonoids from food sources inhibit MXR-mediated transport[235]. Flavones are the most potent MXR inhibitors[236], but multiple flavonoids, including phytoestrogens, also inhibit transporter function[190,235,237–241]. The glucoside derivatives of flavonoids have significantly reduced MXR inhibitory capabilities[235,237]. Some of the most potent flavonoid inhibitors of MXR include coumestrol[235], chrysin[237], biochanin A[237], quercetin[241], retusin and ayanin[240]. Although administration of chrysin did not affect topotecan pharmacokinetics in rats or mice[242], *in vivo* experiments should focus on flavonoids given in combination as found in food, since MXR inhibition may be additive[243].

Many chalcones, which are phenols and structurally related to flavonoids (they are flavonoid precursors), and indolylphenylpropenones are MXR inhibitors[244]. Curcumin is a phenol linked with beneficial effects in many diseases, particularly at low doses where it reduces amyloid β accumulation in Alzheimer models[245]. The major forms of curcuminoids in turmeric powder, curcumin, demethoxycurcumin and bisdemethoxycurcumin, are all noncompetative inhibitors of MXR[246]. Additionally, tetrahydrocurcumin, a major curcumin metabolite, also inhibits MXR[247]. Further studies investigating the complex interaction of amyloid β, curcumin and MXR would be beneficial to the study of Alzheimers.

Table 1.3. MXR Inhibitors

Kinase Inhibitors
*imatinib[94,227,229–232]
*gefitinib[97,98,196,228,229]
EKI-785[229]
sunitinib[234,248]
*nilotinib[103,231,232]
*dasatinib[103,231]
*erlotinib[97,105]
*lapatinib[100,233]
*CI1033[104]
bisindolylmaleimides IV[251]
indolocarbazole[251]
bisindolylmaleimides V[251]
arcyriaflavin A[251]
K252c[251]
UCN-01[169]
purvalanol A[171]
WHI-P180[171]
LY294002[254]

Estrogens
estrone[224,225]
17β-estradiol[134,224]
diethylstilbestrol[225]
tamoxifen[225]
toremifene[225]
TAG-11[225]
TAG-139[225]

Glucocorticoids
corticosterone[134]
beclomethasone[134]
6α-methylprednisolone[134]
dexamethasone[134]
triamcinolone[134]

Analog Screens
dihydropyridines[253]
pyridines (I_m)[253]
chromanones[262]
taxanes[263]

Natural Compounds
coumestrol[235]
genistein[121,190,191,235,237,243]
daidzein[235,237,238]
biochanin A[235,237,239,243]
glycitein[235]
prunetin[235]
chrysin[237,242,243]
7,8-benzoflavone[242]
apigenin[237,243]
fisetin[237]
hesperetin[237,238,243]
kaempferol[190,237,243]
naringenin[190,237,243]
phloretin[237]
quercetin[237,238,241]
silybin[237]
silymarin[237,238,243]
resveratrol[238]
kaempferide[239]
5,7-dimethoxyflavone[239]
8-methylflavone[239]
acacetin[190]
chalcones[244]
indolylphenylpropenones[244]
curcumin[246]
demethoxycurcumin[246]
bisdemethoxycurcumin[246]
tetrahydrocurcumin[247]
caffeine[260]
naringenin-7-glucoside[190]
6-prenylchrysin[236]
tectochrysin[236]

Antipsychotics
clozapine[249]
paliperidone[249]
chlorpromazine[249]
quetiapine[249]
olanzapine[249]
haloperidol[249]
reserpine[32]
risperidone[249]

Others
cyclosporine A[58,215]
orthovanadate[58]
fumitremorginC[53,58,200,216–219]
Ko134[98,221]
Ko143[98,221,249]
digoxin[134]
elacridar[59,65,75,221,222]
novobiocin[54,250]
glafenine[196]
tracazolate[196]
calcimycin[196]
doxazosin mesylate[196]
tariquidar[169]
tryprostatin A[211]
biricodar[252]
*Dipyridamole[154]
nicardipine[154,253]
nitrendipine[154,253]
nimodipine[154]
niguldipine[253]
PZ-39[255,256]
ortataxel[257]
tRA96023[257]
XR9577[258]
WK-X-34[258,259]
WK-X-50[258]
WK-X-84[258]
albendazole sulfoxide[121]

Antiretrovirals
lopinavir[118]
nelfinavir[118,261]
delavirdine[118]
efavirenz[118]
saquinavir[118,261]
atazanavir[118]
amprenavir[118]
abacavir[118]
ritonavir[261]

*indicates also substrate of MXR

1.7 Physiological Function of MXR

Separate from its role in cancer resistance and pharmacokinetics, MXR has an important function in the body. The tissue distribution and substrate and inhibitor profiles of MXR indicate its importance for the distribution of nutrients, especially into the milk, and the defense of tissues from carcinogens and phototoxic compounds. Although therapeutic MXR inhibitors are being developed or are already in clinical use, the disruption of the physiological function of MXR must be considered in developing such strategies.

1.7.1 *Distribution of Dietary Compounds*

MXR regulates the absorption of dietary compounds, and its cellular localization is altered in times of nutrient deprivation. During times of low folate, MXR localizes to the membrane of intracellular vesicles where it assists in sequestering nutrients[34]. Additionally, MXR is expressed in the ducts and tubules of the breast, where it contributes to the secretion of nutrients, particularly riboflavin (vitamin B_2), into milk[186].

The expression of MXR in the lumen serves to reduce overall systemic exposure to various compounds. The distribution of phytoestrogens are altered in *Abcg2 -/-* mice, which have increased AUC of genistein[191,192], plasma levels of diadzein[192], brain and testis accumulation of inulin[192], and plasma concentrations of quercetin and isorhamnetin (methylated metabolite of quercetin)[185]. Although phytoestrogens are not strictly nutrients, they are considered beneficial due to their estrogenic and anti-estrogenic effects[264].

1.7.2 *Tissue Defense*

MXR plays an important role in protecting the brain, fetus, prostate and eye[46]. In *Abcg2 -/-* mice, there is increased exposure to the dietary carcinogen PhIP[167] and hepatocarcinogen aflatoxin B_1[177]. Additionally, MXR reduces the systemic exposure to the heterocyclic amines IQ and Trp-P-1[177]. MXR also plays a role in the placental barrier and the protection of the fetus from glyburide, Bodipy-prazosin and bile acids[136,202]. The inhibition of MXR in mice via elacridar treatment increased fetal topotecan exposure[79]. Reduced MXR function limits the accumulation of PhIP, topotecan and cimetidine into mouse milk[86] and simultaneously increases systemic and fetal exposure to harmful compounds. As a result of both the natural protective role of MXR against carcinogens[265] and its ability to efflux chemotherapeutics out of cancer cells[266], MXR expression is associated with decreased progression-free and disease-free survival in a variety of cancers[267–275].

1.7.3 *Phototoxicity*

MXR knockout mice develop phototoxic skin lesions due to the accumulation of chlorophyll-derivative porphyrins from natural dietary sources that are MXR substrates[166], particularly pheophorbide A[10,168,169]. Phototoxicity has been reported in healthy individuals with chlorophyll rich diets[276], and it is also a well known side effect of several therapeutic agents that are MXR substrates[277–280] and inhibitors[281]. Low functioning nonsynonymous alleles of MXR have reduced porphyrin transport[282], and this could contribute to human phototoxicity in individuals treated with a number of MXR substrates such as statins[277] and imatinib[278]. MXR transports many photosensitizers

with structures similar to that of pheophorbide A and increases photodynamic resistance to pheophorbide A, pyropheophorbide A methyl ester, chlorine e6 and 5-aminolevulinic acid in photodynamic therapy (PDT)[175]. PDT is an anticancer treatment in which a tumor-selective photosensitizer is administered and light is activated to cause cell death through the generation of reactive oxygen species[175]. MXR needs to be studied as a possible mechanism for the development of cellular resistance to this therapy.

The accumulation of porphyrins is also relevant to cytotoxicity that occurs during hypoxia. Normally, MXR protects tissues during hypoxia by effluxing heme and porphyrin compounds out of the cell[283]. This is most relevant to stem cells as it reduces erythropoietic protophyria by effluxing protoporphyrin IX[170]. Additionally, the major endogenous thiol antioxidant glutathione (GSH), which has an extensive role in the preservation of cellular redox balance, is transported by MXR[208]. Therefore, the expression and function of MXR in individual cells can be relevant for their survival upon exposure to hypoxia.

1.8 MXR Variants

Nonsynonymous variants of *ABCG2* and other ABC membrane transporters have been implicated in the *in vivo* drug disposition, therapeutic efficacy and adverse drug reactions of their substrates[35,284–286]. There are several common and many rare nonsynonymous variants of *ABCG2* (see Figure 1.1 and Table 1.4)[5–11]. The minor allele frequencies (MAFs) of *ABCG2* variants are population-specific[5–11]. The effects of transporter variants on different substrates are not always the same; in fact, 14% of variants in membrane transporters exhibited substrate specific defects in transport[287]. The

transport function of the common nonsynonymous variants and many unnatural variants of *ABCG2* have been investigated[12]. The functional studies and phenotype association of *ABCG2* nonsynonymous variants[8,285,288] indicate that some variants of MXR have substrate-dependent alterations in transport abilities.

1.8.1 *V12M*

The V12M variant is located in the NH_2-terminal intracellular region of the MXR transporter (see Figure 1.1). The V12M polymorphism is most common in Asian and Caucasian populations with MAFs ranging from 2-45%[5–11]. Although there have been a few reports of altered V12M localization[289] and lower V12M protein expression in cells[10] and Hispanic livers[15], the majority of reports indicate no effect of this variant on mRNA or protein[6,9,282,290–292]. There is evidence for substrate-dependent effects of the V12M variant as it causes lower porphyrin[10] and higher methotrexate[293] transport. The V12M variant also has protective effects (higher IC_{50}) against pheophorbide A[6] and SN-38[282]. However, the V12M variant was similar to reference MXR in its mitoxantrone stimulated ATPase activity[294], as well as sensitivity to mitoxantrone[282,292]. Patients homozygous for the V12M variant had worse survival in diffuse large B-cell lymphoma[179] and response to imatinib mesylate treatment[295].

1.8.2 *Q141K*

The Q141K variant lies between the Walker A motif and the ABC signature region (see Figure 1.1). The Q141K variant is very common, with MAFs in Asian and Caucasian populations ranging from 6-36%[5–11]. Reports on alteration in MXR function

are contradictory. Some reports show that Q141K exhibits lower SN-38[294], porphyrin[10], urate[203] and glyburide[135] transport, and lower IC_{50}s for imatinib[296], topotecan[89], Symadex (C-1311)[151], SN-38 and mitoxantrone[9,282,292]. Other reports show that Q141K has similar mitoxantrone stimulated ATPase activity[294], pheophorbide A IC_{50}[6] and MTX ATP-dependent transport[293] compared to reference. The Q141K transporter has lower protein expression, but mRNA levels are unaffected[6,9,10,27,290–292,297,298]. However, intestinal mRNA and protein levels are not affected by the Q141K[130,268]. Alterations in Q141K protein levels have been linked to an increase in proteasomal degradation[299,300]. Thus, studies that normalized for MXR expression (as opposed to total protein) saw no changes in Q141K function[291], indicating that the Q141K protein functions properly, but has reduced expression due to higher protein degradation.

MXR Q141K is associated with altered pharmacokinetics and multiple adverse events. The Q141K variant transporter alters the pharmacokinetic parameters of SN-38 and its glucuronide[88,90], gefitinib[97], sulfasalazine[130,301], topotecan[89], diflomotecan[81], mycophenolic acid glucuronide[148], fluvastatin, pravastatin and simvastatin[112], and rosuvastatin[111] but has no effect on the pharmacokinetic properties of imatinib[296], nitrofurantoin[140], irinotecan[90], pitavastatin[141], pravastatin[142] or lamivudine[143]. MXR Q141K is also associated with chemotherapy-induced diarrhea[302,303], acute lymphoblastic leukemia complications[304] and neutropenia in cancer patients treated with irinotecan[87,88]. Due to the reduction in urate transport by the Q141K variant, it is estimated that this SNP is responsible for 10% of gout cases in Caucasians[203]. Finally, lower expression of Q141K could have ramification in the protection of the body from carcinogens. This is consistent with reports of MXR Q141K association with increased risk and worse

survival in patients with diffuse large B-cell lymphoma[179]. The Q141K variant transporter is also associated with poorer survival in patients who were younger at diagnosis or had bulky tumors[179]. The MXR V12M/Q141K haplotype was associated with the worst overall survival in diffuse large B-cell lymphoma[179]. Collectively, these data suggest that both V12M and Q141K MXR transporters can have significant effects on pharmacokinetics and pharmacodynamics.

1.8.3 *R482 Mutations*

The MXR R482T variant was identified from a doxorubicin resistant cell line, but has not been found in human samples. This mutation is located in the intracellular domain near the third transmembrane helix, a region important in other ABC transporters for the recognition of substrates, and drastically changes the substrate antagonist-specific profile of MXR[71]. Both the MXR R482T and R482G mutants cannot transport MTX[65], but are 100 to 1000-fold more resistant to the antifolates GW1843 and Tomudex[69] and lipophilic antifolates[67]. Additionally, the 482G and 482T variants, but not reference MXR, transport rhodamine 123, daunorubicin and LysoTracker Green[71]. Due to the position of R482 near transmembrane 3 and its ability to alter the MXR substrate profile, it has been proposed that this residue is important for the interaction of MXR with charged substrates (like MTX and rhodamine 123) but not with neutral unconjugated sterols, bile acids or antibiotics[120]. Continued research on these mutations could inform our understanding of acquired drug resistance.

Table 1.4 Nonsynonymous Variants of MXR

SNP ID	Position[1]	Δnt[2]	ΔAA[3]	MAF[4] (%)	Sources
rs2231137	34	G>A	Val12Met	0.0-45	5,8,10,11,27,143,268,289,292, 305–310
-	38	C>T	Ser13Leu	0.3	307
-	151	G>T	Gly51Cys	0.1	11
-	-	-	Lys86Met	-	218
rs2231139	376	C>T	Gln126Stop	0.0-3	8,10,11,143,307,308,311
rs2231142	421	C>A	Gln141Lys	0.0-41	5,8,10,11,27,90,143,268,289,292, 305–311
-	458	C>T	Thr153Met	3.3	10,11
-	479	G>A	Arg160Gln	0.3-0.5	8,10,307
rs1061017	496	C>G	Gln166Gly	0.3	11
rs12721643	626	A>C	Ile206Leu	0.6-20	8,10,11,268,305
rs1061018	623	T>C	Phe208Ser	0.3	10,11
rs3116448	742	T>C	Ser248Pro	0.5	10,11
rs34678167	805	C>T	Pro269Ser	0.2-0.8	143,305,309
-	1060	G>A	Gly354Arg	0.3	307
-	1291	T>C	Phe431Leu	0.3-0.8	8,10,11,307,311
-	1322	G>A	Ser441Asn	0.5	8,10,311
-	-	-	Arg482Ala	-	218
rs192169063	1465	T>C	Phe489Leu	0.5-0.8	8,10,307,311
-	1515	C>-	Phe506Stop	0.3	307
rs35965584	1624	A>G	Thr542Ala	1.9	305,312
-	1711	T>A	Phe571Leu	0.5	10
-	1723	C>T	Arg575Stop	0.3	8,10,307
rs34264773	1768	A>T	Asn590Tyr	0.0-1.1	8,10,11
rs34783571	1858	G>A	Asp620Asn	0.5-1.1	8,10,11,305,306,313
-	34/421	G>A/C>A	Val12Met/ Gln141Lys	0.6-1.5	305,309,311

[1]Position in cDNA

[2]Change in nucleotide, variants without indicated change are not natural

[3]Change in amino acid

[4]Minor allele frequency in percent from all reported populations, individual population MAFs are reported elsewhere[5–11]

1.9 ABCG2 mRNA

The expression of ABCG2 mRNA is an important determinant of MXR expression and function and is altered by many types of stimuli, ranging from hypoxia to xenobiotic exposure[314–320]. This regulatory control of MXR expression gives cells the ability to adapt to excessive or reduced levels of endogenous substrates which are essential for their survival. Characterizing the variability in ABCG2 throughout the body is important in understanding how expression impacts both systemic and target site drug exposure.

1.9.1 *mRNA variability*

Reports on the expression of ABCG2 in different normal tissues show wide variability in ABCG2 expression levels. As much as a 500-fold change in mRNA expression has been noted across human liver samples, without detectable copy number variations[15]. In human intestine, ABCG2 levels vary 1.8- to 78-fold[130,268]. In a cohort of human liver and kidney samples collected as part of the Pharmacogenetics of Membrane Transporters project, large variation in ABCG2 mRNA was detected (see Figure 1.2). Additionally, overexpression of ABCG2 is seen in cancers[92,268–275], with reports of ABCG2 mRNA levels varying 1000-fold in the blast cells of leukemic patients[92] and 200-fold in AML blast cell samples[93]. Higher expression of ABCG2 mRNA has been linked to decreased disease-free survival of patients with several types of cancers[268–275]. This variability of ABCG2 expression is not accounted for by the Q141K variant with reduced protein stability or other non-synonymous variants of *ABCG2*[15], and additional mechanisms must contribute to variation in expression[321].

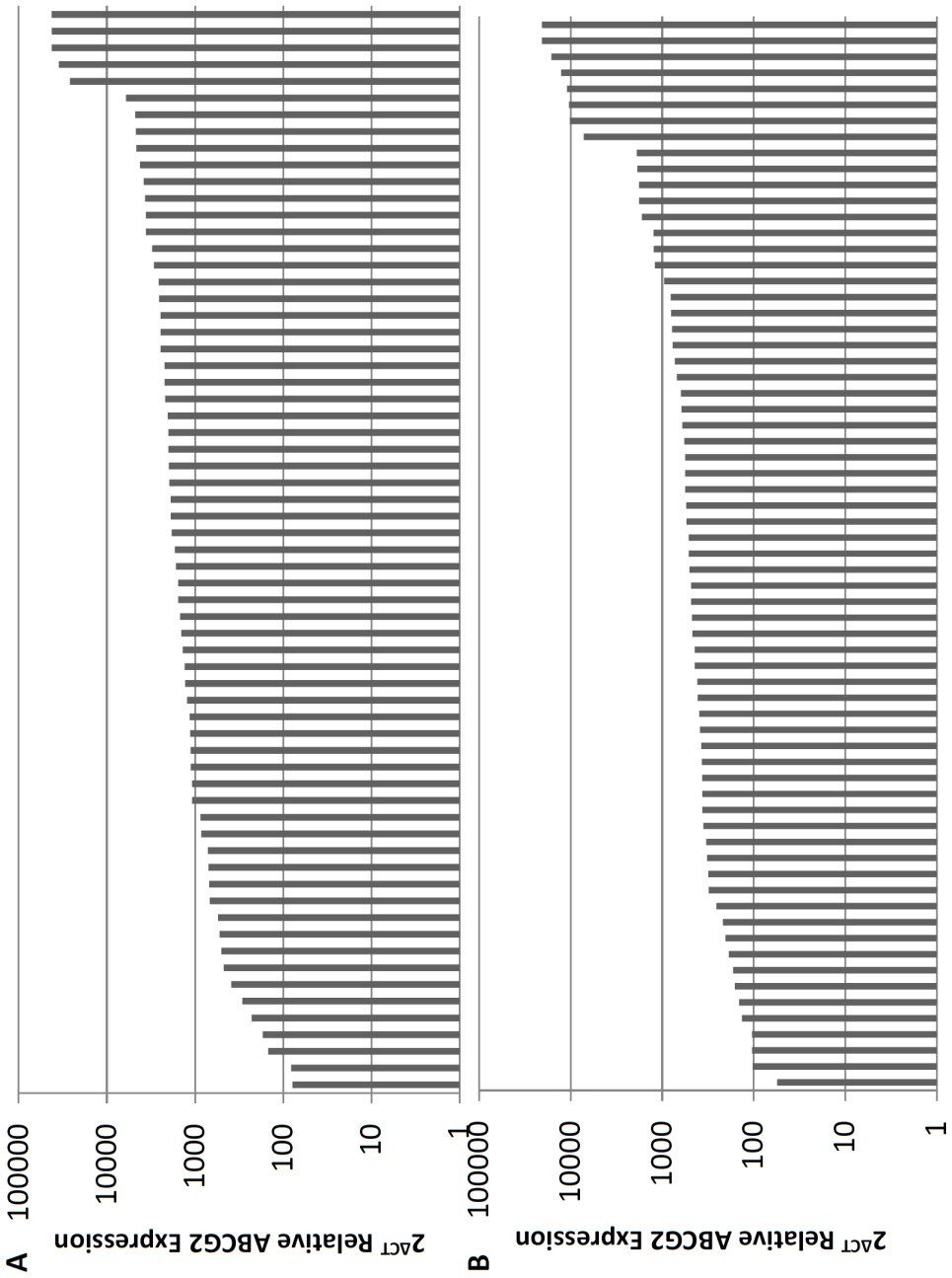

Figure 1.2 Expression profile of ABCG2 mRNA in human tissues. ABCG2 mRNA expression in 60 human (A) kidney and (B) liver tissues, determined by qRT-PCR and displayed as $2^{\Delta Ct}$ relative expression. The mRNA expression of ABCG2 was normalized to the geometric mean of GAPDH, β-2 microglobin, and β-actin, then quantile normalized as described in *Chapter 5 Materials and Methods*. Each sample is represented by a column along the x-axis.

1.9.2 *Splice variants*

In addition to variation in expression, there are eleven ABCG2 mRNA splice variants reported in the National Center for Biotechnology Information (NCBI) website (http://www.ncbi.nlm.nih.gov/IEB/Research/Acembly/av.cgi?db=human&l=ABCG2). Of these, the major splice variants are prominent in different tissues. Several tissue-specific isoforms of *ABCG2* occur due to the creation of splice variants of the 5'-UTR from use of alternate promoters[322–324]. The most common of the exon 1 splice variants is called E1a[15,325], and it is generated by the use of any one of three adjacent promoters and is commonly detected in drug-resistant cell lines[323]. E1b is associated with lower ABCG2 mRNA in livers[15], and its murine equivalent is expressed in the intestine[324]. E1c, which has an intron 1 that is approximately 90 kb longer than the other exon 1 splice variants, is detected in human leukemia[322] and during murine erythroid differentiation[326].

1.10 *ABCG2* and its regulation

MXR is transcribed by *ABCG2* located on the anti-strand of chromosome 4q22 between *PKD2* and *PPM1K*[21]. *ABCG2* spans over 66 kb and includes 15 introns and 16 exons[22]. The translational start site is located in exon 2, the Walker A domain in exon 3 and the Walker B and ABC signature domains in exon 6[22] (see Figure 1.3). *ABCG2* is highly conserved; it is known as the white protein in *Drosophila* and has been found in all sequenced vertebrates[16]. Due to the wide variability in ABCG2 expression, mechanisms that are important in the regulation of ABCG2 are of increasing importance.

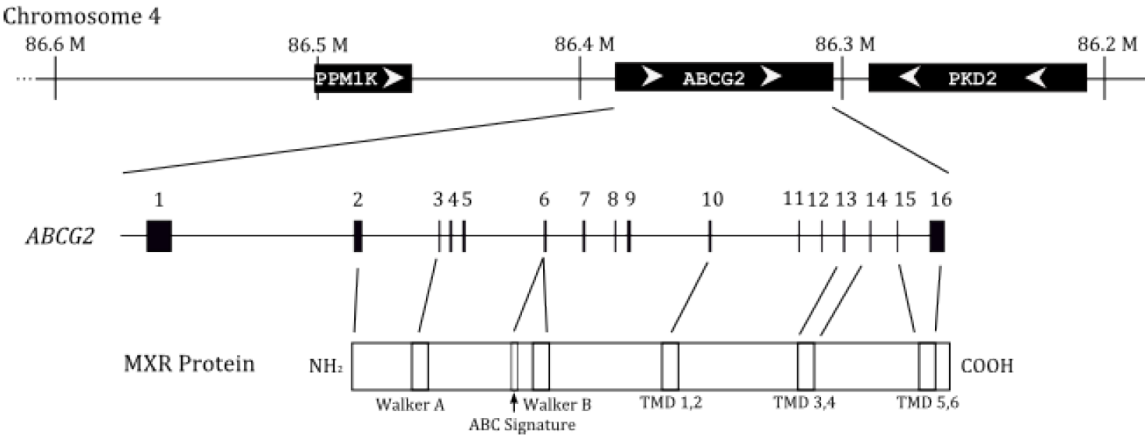

Figure 1.3. Orientation of the *ABCG2* locus and MXR protein. Diagram depicts the orientation and location of the *ABCG2* gene on chromosome 4, followed by an enlarged version of the *ABCG2* gene with the introns (horizontal line) and exons (vertical lines) noted. Finally, the organization of the MXR protein is depicted; boxes are the location of important physical features, and lines connect these features with the exons that code for them. Abbreviations are as follows: M, Morgans; TMD, transmembrane domain; ABC, ATP-binding cassette. Figure adapted from Bailey- Dell[325] with all components to scale.

1.10.1 *Promoter*

The basal *ABCG2* promoter is a TATA-less sequence that instead includes a CCAAT box and numerous Sp1, AP-1 and AP-2 sites 312 bp upstream of the transcriptional start site[325]. An alternate promoter for *ABCG2* is used to generate one of the 5' UTR mRNA variants[322]. The basal -628/+362 *ABCG2* promoter segment had suppressed activity in MCF-7 cells, whereas the -312/+362 promoter segment was highly active[325].

The proximal promoter of *ABCG2* also has a functional aryl hydrocarbon receptor (AhR) response element between -194 to -190[327,328] that overlaps with its functional

progesterone receptor (PR)[317] and estrogen receptor (ER)[329] response elements. There is an NF-κB response element at -23, which works in concert with estrogen to increase ABCG2 expression[315]. Additionally, there is a hypoxia inducible factor (HIF)-1α response element between -116 and -112[330] and an antioxidant response element at -431 to -420[331]. Recently, an interferon-γ activated sequence at -448/-422 was shown to increase the *ABCG2* promoter activity upon stimulation of the JAK2/STAT5 pathway by prolactin[332]. This overlaps with the antioxidant response element stimulated by Nrf2 in stem cells[331]. The cMyc-Max protein also binds to the unmethylated proximal promoter of *ABCG2* to activate *ABCG2* transcription in human leukemic hematopoietic progenitor cells[333,334].

Although the *ABCG2* proximal promoter has many transcription factor (TF) response elements, SNPs within the *ABCG2* promoter have not yet been associated with its mRNA levels. There has been a report of an adjacent promoter haplotype -15622C/T and 1143C/T conferring lower MXR expression, and thus it was associated with higher erlotinib PK parameters[335]. Further studies of this polymorphism and other promoter polymorphisms are required to understand their contribution to the variation in ABCG2 mRNA.

1.10.2 *Methylation*

DNA methylation occurs by the addition of a methyl group to the 5' position of cytosine (C) when it is directly linked with a guanine (G). DNA methylation occurs in the human genome at these "CpG" sites (the 'p' refers to the phosphate group linking the two nucleotides)[336]. CpG sites cluster in specific regions of the genome at a frequency higher

than what would randomly be expected throughout the genome, and these regions are termed CpG islands (CGIs)[337,338]. Promoters are often associated with a high frequency of CpG sites[339,340], and when these multiple CpG sites over a gene's promoter are methylated, it causes gene suppression[337]. Additionally, methylation of CpG sites has been shown to affect the binding of TFs, especially over gene promoters[341,342].

The *ABCG2* basal promoter is on the edge of a large CGI that covers most of the *ABCG2* proximal promoter and the core of which is just upstream of the transcriptional start site[325]. Normally, minimal to absent methylation of the *ABCG2* promoter CGI has been reported in human liver tissues[343] and in renal cell lines[344]. Treatment with the demethylating agent 5-aza-2'-deoxycytidine or other xenobiotics in cell lines induces ABCG2 expression, whereas the hypermethylated *ABCG2* promoter is associated with gene silencing[344–348]. The degree of *ABCG2* promoter methylation correlates to ABCG2 mRNA levels in cancer cell lines[344–347] and hypomethylation of the *ABCG2* promoter contributes to drug-resistance in cell lines and patients[344–349]. Additionally, demethylation of the *ABCG2* promoter has also been correlated with metastasis and stage of cancer, but not with the development of cancer itself[350]. Methylation of the *ABCG2* promoter may determine the allele-specific expression profile in certain tissues, specifically in placenta[27]. Further research on the impact of *ABCG2* promoter methylation in normal and malignant tissues is warranted.

1.11 Nuclear Receptors

Recent research has highlighted that SNPs in non-coding genomic regions can affect gene transcription and expression levels of metabolizing enzymes and membrane

transporters, and thus drug disposition[321,351]. Additional variation in enzyme and transporter expression can be mediated by ligand-activated TFs from the nuclear receptor (NR) family; these TFs stimulate drug detoxification pathways to temporarily alter gene expression in response to changes in the cell environment[352,353].

NRs are ligand-dependent TFs, and theirligands include a variety of fatty acids, vitamins and steroids[354] that bind to consensus sequences in the genome and promote the transcription or transrepression of target genes[355]. NRs exist as homo- and heterodimers with each partner recognizing specific DNA sequences, called response elements[356]. These response elements exist as direct, indirect or inverted half-sites separated by variable length nucleotide spacers[357].

NRs have been classified depending upon their binding partner and the type of response element to which they bind[356]. Class I NRs include the steroid hormones and bind to inverted repeats[358], and Class II NRs are heterodimeric partners of RXR and bind to direct repeats[359]. The other two classes of NRs are orphan receptors binding to direct repeats and NRs acting as monomers to bind to a single half-site[356,357]. NRs can also be categorized based upon their mechanism of action, which includes their ligand binding while the NR is located in the cytosol (Type I) or nucleus (Type II)[360]. The large number of heterodimer combinations between different NRs and their diversity of isoform expression depending on cell type and development could generate significant diversity in gene regulation[361].

The expression of ABCG2 is altered by many types of stimuli, including hypoxia[314], inflammation[315], xenobiotics[316], hormones[317,318] and nutrients[319,320]. There is much evidence supporting the regulation of *ABCG2* by NR pathways, including those for

the ER, PR, AhR, HIF, pregnane X receptor (PXR), constitutive androstane receptor (CAR), glucocorticoid receptor (GR), retinoid-related orphan receptor (ROR), peroxisome proliferator-activated receptor (PPAR) and NF-E2 related factor-2 (Nrf2)[314–320,328–331,362]. The understanding of the pathways and xenobiotics that regulate ABCG2 expression could have application clinically. For example, it has been proposed to utilize statins as a treatment of gout because statins are able to alter ABCG2 expression[114]. Since ~13% of current drugs target NRs[363], it is imperative we understand the NR transcriptional regulation of drug enzymes and transporters, especially *ABCG2*.

1.11.1 *Estrogen Receptor*

The ER is a class I and type I NR and is usually activated by 17β-estradiol (E_2), but can be activated or suppressed by several other types of estrogens[357]. The ER has two forms, ERα and ERβ, that have specific tissue expression and regulate overlapping but different cellular pathways[357]. The ER is important in many cellular processes, including growth, differentiation, inflammation and function of the sexual organs[364]. The ER also plays a major role in many cancers, including breast, ovarian, colorectal, prostate, and endometrial[364]. The ER binds to estrogen responsive elements (ERE) almost exclusively in *cis*-regulatory regions; it has only been found to bind to 4% of the proximal promoters for estrogen responsive genes[365]. Additionally, ER works in concert with many other TFs and co-factors to activate its target genes. The presence of the general TFs AP-1, Sp1 and CREB1, substantially increase the modulation of activity with estrogen treatment[364,366–369]. Additionally, GATA3 is integral to the ERα receptor pathway in several tissues, including kidney and breast[370]. Other transcriptional co-factors, like p300, AP-2γ and

FoxA1, directly interact with ER and work as long-range tethering sites for the ERα-mediated transcription[368,371]. ER dimerizes with many other NRs, including the hepatic nuclear factor (HNF)-4, thyroid receptor (TR), retinoic acid receptor (RAR), retinoid X receptor (RXR), and the vitamin D receptor (VDR)[361]. The type of response that ERs elicit upon ligand binding depends on the expression of the two ER forms, which ER ligand has bound, other cofactors that are present and chromosome conformation[364].

Stimulation of ER both induces[318,372,373] and downregulates[224,374,375] ABCG2 expression. The ability of ER to either increase or decrease ABCG2 expression depends on both the tissue and presence of other NR[224,318,372–375]. Additionally, ER often shares response elements with the progesterone receptor (PR), such as the ER/PR element found in the *ABCG2* proximal promoter[317]. The ER and PR have a normal role in the upregulation of ABCG2 during pregnancy to augment protection of the fetus[26,79,329]. Understanding the ER regulation pathway for *ABCG2* is vital because of the role both of these proteins play in the placenta and mammary tissues[26,28].

1.11.2 *Glucocorticoid Receptor*

The GR is another type I, class I NR that is expressed in almost every tissue and is activated by glucocorticoids[376]. After being released from its repressors by one of its ligands, GR works to trans-repress target genes by binding to other TFs in the nucleus such as AP-1 or NF-κB and inhibiting them from activating transcription of the target gene[377]. Glucocorticoids have a broad endogenous role in the body, including regulation of growth, metabolic, immune and stress related pathways, and are critical for the function of the central nervous, digestive, hematopoietic, renal, and reproductive

systems[226,376,378,379]. Due to the powerful anti-inflammatory and immunosuppressive action of glucocorticoids, they are widely utilized for treatment of acute and chronic inflammatory diseases, autoimmune diseases, organ transplant rejection, and malignancies of the lymphoid system[378,380].

The majority of glucocorticoid response elements (GREs) are >10 kb from the transcriptional start site of glucocorticoid responsive genes, with only 9% of GREs in the proximal promoter[381]. The ~1000 bp surrounding a GRE is evolutionarily conserved and the level of conservation for a predicted GRE is correlated to the extent of GR occupancy at that element[382]. Many other TFs are associated with GREs, including AP-1, ETS, C/EBP or HNF4[381]. AP-2 also interacts with GR[383], and is implicated along with PPAR and the liver X receptor (LXR) in cell response to inflammation[379,384].

The GR ligand dexamethasone increases the expression of both PXR and RXR[385], which in turn increases the expression of genes by increasing activity of NR/RXR dimers[386,387]. Due to dexamethasone's ability to induce PXR expression, dexamethasone is capable of acting via direct GR-dependent mechanisms at either low concentrations or short exposure and via a PXR-dependent mechanism at high concentration or long exposure[386,388,389]. Dexamethasone decreases ABCG2 expression both *in vivo*[390] and i*n vitro*[391]. Both GR and PXR regulatory elements of *ABCG2* must be identified and characterized in order to understand the pathways that dexamethasone utilizes to regulate *ABCG2*.

1.11.3 *Retinoid X Receptor*

The RXR proteins RXRα/β are essential dimerization partners of many steroid hormone receptors and other NRs, including PXR, LXR, CAR, PPAR and the farnesoid X receptor (FXR). However, a biological role and ligand for RXR has not been identified[359]. RXRα interacts with HNF4α, and both RXRα and HNF4α interact with ERα[361]. In addition to the importance of RXRα and ERα in the placenta, HNF4α and RXRα are important liver specific nuclear factors[359,392]. Thus, the pathways of RXR/NR regulation and their target tissues overlap with that of the MXR protein and give support for the possible regulation of *ABCG2* by RXR/NR dimers.

The function of RXR/NR dimers can be repressed by the interaction of the octamer 1 (Oct-1, POU2F1) TF[393]. In addition to RXR, Oct-1 interacts with GR, AR and PR[393–395]. Additionally, RXR dimerized with PPAR, CAR or LXR binds to GR or ER response elements, inhibiting the ER or GR response[396–399]. The restrictive expression patterns for RXRα/β and the activation or repression of gene expression being dependent on interaction with other co-factors could explain how this NR affects expression of genes in selected tissues[359].

1.11.4 *Pregnane X Receptor*

PXR is a NR critical in the regulation of hepatic genes and drug metabolizing enzymes and transporters[400]. PXR is a Type I, Class II NR that is activated by a variety of ligands including steroids, bile acids and antibiotics[401]. The most common PXR ligand is rifampin[402]. Upon binding of its ligand, PXR dissociates from its regulatory proteins in the cytoplasm, translocates to the nucleus and alters gene expression through

heterodimerizing with RXR. PXR is predominantly expressed in liver, small intestine and colon, as well as other tissues, cancer cell lines and tumor samples[401].

The expression of PXR mRNA is correlated with the expression of ABCG2 mRNA[403,404], and rifampin induces ABCG2 expression[316,405]. PXR is also activated by other ligands, including statins and the bile acid lithocholic acid[406]. Since *ABCG2* is integral in statin response[108] and the development of gout[204], PXR is a candidate for linking ABCG2 expression with disease or drug response. The ability of rifampin to induce ABCG2 expression and the correlation of PXR with ABCG2 indicate that PXR can regulate *ABCG2*[316,403–405]. Additionally, the identification of PXR response elements and a better understanding of the PXR induction pathway for *ABCG2* could identify new therapeutic targets.

1.11.5 *Farnesoid and Liver X Receptors*

LXR and FXR both dimerize with RXR and are Type II and Class II NRs highly expressed in the intestine and liver[407]. These NRs bind DNA in a complex with corepressors and become active once the ligand displaces the corepressors and recruits coactivators[407]. FXR is a known regulator of bile acid[408], lipid homeostasis[409] and drug metabolizing and transport genes[352], especially those involved in statin response[410–412]. Lower expressing variants of FXR in combination with reduced function of ABCG2 have recently been linked to statin response[413]. LXR binds to cholesterol metabolites, regulates cholesterol turnover and hepatic glucose metabolism and represses a set of inflammatory genes in immune cells[399]. Additionally, LXR is implicated along with PPAR in cell response to inflammation[379,384]. Unlike the other ABCG genes[407], there has been no FXR

or LXR response elements identified for *ABCG2*. The identification of these elements would aid in the understanding of the effects of FXR and LXR dynamics on *ABCG2* regulation during homeostasis and drug targeting of bile acid, cholesterol and lipid pathways.

1.11.6 *Aryl Hydrocarbon Receptor*

The aryl hydrocarbon receptor (AhR) is a Class I, Type II NR that translocates to the nucleus upon ligand binding and dimerizes with the aryl hydrocarbon receptor nuclear translocator (ARNT)[414] or ER[415]. Additionally, AhR dimerizes with several other NR[414] and has recently been shown to recognize nontraditional AhRE motifs[416,417]. Many carcinogens are known ligands of AhR and through AhR induce multiple metabolizing enzymes and drug transporters[418]. Exposure to carcinogens causes DNA damage that leads to DNA mutations[419], and exposure to exogenous carcinogens are a factor in the development, severity and aggressiveness of cancer. ABCG2 expression is increased with carcinogen exposure[176,420,421]. The expression of ABCG2 and activity of its promoter are both altered by exposure to AhR ligands[327,328,422]. This induction of ABCG2 expression through the AhR pathway would allow the body to protect itself, and its vital organs, from exposure to these carcinogens.

1.11.7 *COUP-TFII*

Chicken ovalbumin upstream promoter-transcription factor II (COUP-TFII), is a member of the steroid NR family and is important in glucose, cholesterol and xenobiotic metabolism pathways[423]. COUP-TFII binds to the same direct repeat segments as VDR,

TR, RAR, RXR, PPAR and HNF4[423]. Therefore, COUP-TFII exerts negative regulatory function on these NRs by competing for their common response element, forming inactive heterodimers or tethering the corepressor silencing mediator for retinoid and thyroid hormone receptor (SMRT), and tightening the chromatin structure[423–425]. In contrast, the binding of GR stimulates COUP-TFII induced transactivation by attracting cofactors, while COUP-TFII binding will repress the GR-governed transcriptional activity[424]. The restrictive expression patterns for COUP-TF[426] and its dynamic interactions with many other NRs could explain how it affects expression of genes in selected tissues.

1.12 Summary

The MXR protein is expressed apically in numerous tissues, especially those relevant for drug absorption and excretion, and has a number of natural and synthetic substrates and inhibitors. The MXR transporter has several amino acid variants implicated in altered drug response and cancer risk. Finally, the wide variability in mRNA expression of ABCG2 can be attributed to the activity of the basal *ABCG2* promoter, DNA methylation and regulation by NRs. Much has been done to understand the role MXR plays in protection from toxins, drug pharmacokinetics, pharmacodynamics, and toxicity, cancer risk and severity, and distribution of nutrients and natural compounds. However, little is known about the function and substrate profiles of amino acid variants of MXR and the mechanisms that regulate *ABCG2.* These mechanisms need to be fully elucidated to aid in the translation of MXR pharmacogenomics into clinical application.

1.13 Focus of Thesis

1.13.1 *Rationale*

There is interindividual variability in the therapeutic response, pharmacokinetic and pharmacodynamic profiles of MXR substrates, as well as in the expression of MXR among healthy individuals and in cancerous tissues. It was been demonstrated that ABCG2 responds to different stimuli and is thus altered through exposure to different compounds. Additionally, *ABCG2* is polymorphic and many of its nonsynonymous variants have not been characterized; of those that have, there are conflicting reports on substrate-dependent effects, activity and localization. Therefore, in addition to continued characterization of *ABCG2* nonsynonymous variants, the mechanisms and *cis*-regulatory elements involved in regulation of *ABCG2* and the corresponding effects of SNPs within these elements must be examined.

1.13.2 *Hypotheses*

First, I hypothesize that some MXR variants exhibit altered substrate profiles, expression and localization compared to the reference transporter. Second, I hypothesize that SNPs within the *ABCG2* proximal promoter and *cis*-regulatory elements of the *ABCG2* locus affect the ability of these elements to regulate transcription. Third, I hypothesize that the activity of some *cis*-regulatory elements in the *ABCG2* locus can be attributed to regulation by nuclear receptors. Finally, I hypothesize that DNA methylation patterns in the *ABCG2* locus are tissue-specific and regulate the transcription of *ABCG2*.

1.13.3 *Specific aims*

1. Characterize nonsynonymous variants of *ABCG2*. Cell based assays were used to examine *in vitro* expression and localization, and flow cytometry and inside-out membrane vesicles were used to examine ATPase, indirect and direct transport activity of MXR variant transporters (Chapter 2).
2. Examine the effects of SNPs on *ABCG2* promoter activity through *in silico* transcription factor binding predictions, *in vitro* luciferase assays and an *in vivo* hydrodynamic tail vein assay (Chapter 3).
3. Identify *cis*-regulatory elements in the *ABCG2* gene locus through *in silico* predictions, *in vitro* luciferase assays and an *in vivo* hydrodynamic tail vein assay (Chapter 4). Similar methods were used to examine the effects of SNPs within these elements on their activity, and enhancer variants were associated with gene expression (Chapter 5).
4. Examine the response to nuclear receptor ligands of *in silico* predicted *cis*-regulatory elements in the *ABCG2* locus, the *ABCG2* promoter and their SNPs through *in vitro* luciferase assays (Chapter 6).
5. Examine epigenetic DNA modifications in the *ABCG2* locus in human liver and kidney tissues and their association with ABCG2 expression (Chapter 7).

Collectively, these studies will enhance our understanding of how genetic and epigenetic changes influence MXR function and expression. The results from this research will drive future clinical investigations examining how interindividual variation in MXR expression and function contributes to differences in drug response.

1.14 References

(1) Schinkel, A. H.; Jonker, J. W. Mammalian drug efflux transporters of the ATP binding cassette (ABC) family: an overview. *Advanced drug delivery reviews* **2003**, *55*, 3–29.

(2) Giacomini, K. M.; Huang, S.-M.; Tweedie, D. J.; Benet, L. Z.; Brouwer, K. L. R.; Chu, X.; Dahlin, A.; Evers, R.; Fischer, V.; Hillgren, K. M.; Hoffmaster, K. a; Ishikawa, T.; Keppler, D.; Kim, R. B.; Lee, C. a; Niemi, M.; Polli, J. W.; Sugiyama, Y.; Swaan, P. W.; Ware, J. a; Wright, S. H.; Yee, S. W.; Zamek-Gliszczynski, M. J.; Zhang, L. Membrane transporters in drug development. *Nature reviews. Drug discovery* **2010**, *9*, 215–36.

(3) Mo, W.; Zhang, J.-T. Human ABCG2: structure, function, and its role in multidrug resistance. *International journal of biochemistry and molecular biology* **2012**, *3*, 1–27.

(4) Mao, Q.; Unadkat, J. D. Role of the breast cancer resistance protein (ABCG2) in drug transport. *The AAPS journal* **2005**, *7*, E118–33.

(5) Kim, K.; Joo, H.-J.; Park, J.-Y. ABCG2 polymorphisms, 34G>A and 421C>A in a Korean population: analysis and a comprehensive comparison with other populations. *Journal of clinical pharmacy and therapeutics* **2010**, *35*, 705–12.

(6) Tamura, A.; Onishi, Y.; An, R.; Koshiba, S.; Wakabayashi, K.; Hoshijima, K.; Priebe, W.; Yoshida, T.; Kometani, S.; Matsubara, T.; Mikuriya, K.; Ishikawa, T. In vitro evaluation of photosensitivity risk related to genetic polymorphisms of human ABC transporter ABCG2 and inhibition by drugs. *Drug metabolism and pharmacokinetics* **2007**, *22*, 428–40.

(7) Wakabayashi, K.; Tamura, A.; Saito, H.; Onishi, Y.; Ishikawa, T. Human ABC transporter ABCG2 in xenobiotic protection and redox biology. *Drug metabolism reviews* **2006**, *38*, 371–91.

(8) Ishikawa, T.; Tamura, A.; Saito, H.; Wakabayashi, K.; Nakagawa, H. Pharmacogenomics of the human ABC transporter ABCG2: from functional evaluation to drug molecular design. *Die Naturwissenschaften* **2005**, *92*, 451–63.

(9) Yanase, K.; Tsukahara, S.; Mitsuhashi, J.; Sugimoto, Y. Functional SNPs of the breast cancer resistance protein-therapeutic effects and inhibitor development. *Cancer letters* **2006**, *234*, 73–80.

(10) Tamura, A.; Watanabe, M.; Saito, H.; Nakagawa, H.; Kamachi, T.; Okura, I.; Ishikawa, T. Functional validation of the genetic polymorphisms of human ATP-binding cassette (ABC) transporter ABCG2: identification of alleles that are defective in porphyrin transport. *Molecular pharmacology* **2006**, *70*, 287–96.

(11) Yoshioka, S.; Katayama, K.; Okawa, C.; Takahashi, S.; Tsukahara, S.; Mitsuhashi, J.; Sugimoto, Y. The identification of two germ-line mutations in the human breast cancer resistance protein gene that result in the expression of a low/non-functional protein. *Pharmaceutical research* **2007**, *24*, 1108–17.

(12) Gradhand, U.; Kim, R. B. Pharmacogenomics of MRP transporters (ABCC1-5) and BCRP (ABCG2). *Drug metabolism reviews* **2008**, *40*, 317–54.

(13) Giri, N.; Agarwal, S.; Shaik, N.; Pan, G.; Chen, Y.; Elmquist, W. F. Substrate-Dependent Breast Cancer Resistance Protein (Bcrp1 / Abcg2) -Mediated Interactions : Consideration of Multiple Binding Sites in in Vitro Assay Design. *Pharmacology* **2009**, *37*, 560–570.

(14) Hegedus, C.; Szakács, G.; Homolya, L.; Orbán, T. I.; Telbisz, A.; Jani, M.; Sarkadi, B. Ins and outs of the ABCG2 multidrug transporter: an update on in vitro functional assays. *Advanced drug delivery reviews* **2009**, *61*, 47–56.

(15) Poonkuzhali, B.; Lamba, J.; Strom, S.; Sparreboom, A.; Thummel, K.; Watkins, P.; Schuetz, E. Association of breast cancer resistance protein/ABCG2 phenotypes and novel promoter and intron 1 single nucleotide polymorphisms. *Drug metabolism and disposition: the biological fate of chemicals* **2008**, *36*, 780–95.

(16) Robey, R. W.; To, K. K. K.; Polgar, O.; Dohse, M.; Fetsch, P.; Dean, M.; Bates, S. E. ABCG2: a perspective. *Advanced drug delivery reviews* **2009**, *61*, 3–13.

(17) Evans, W. E.; Relling, M. V Moving towards individualized medicine with pharmacogenomics. *Nature* **2004**, *429*, 464–8.

(18) Daly, A. K. Pharmacogenetics and human genetic polymorphisms. *The Biochemical journal* **2010**, *429*, 435–49.

(19) Miyake, K.; Mickley, L.; Litman, T.; Zhan, Z.; Robey, R.; Cristensen, B.; Brangi, M.; Greenberger, L.; Dean, M.; Fojo, T.; Bates, S. E. Molecular cloning of cDNAs which are highly overexpressed in mitoxantrone-resistant cells: demonstration of homology to ABC transport genes. *Cancer research* **1999**, *59*, 8–13.

(20) Litman, T.; Brangi, M.; Hudson, E.; Fetsch, P.; Abati, A.; Ross, D. D.; Miyake, K.; Resau, J. H.; Bates, S. E. The multidrug-resistant phenotype associated with overexpression of the new ABC half-transporter, MXR (ABCG2). *Journal of cell science* **2000**, *113 (Pt 1*, 2011–21.

(21) Doyle, L. a; Yang, W.; Abruzzo, L. V; Krogmann, T.; Gao, Y.; Rishi, a K.; Ross, D. D. A multidrug resistance transporter from human MCF-7 breast cancer cells. *Proceedings of the National Academy of Sciences of the United States of America* **1998**, *95*, 15665–70.

(22) Allikmets, R.; Schriml, L. M.; Hutchinson, A.; Romano-Spica, V.; Dean, M. A human placenta-specific ATP-binding cassette gene (ABCP) on chromosome 4q22 that is involved in multidrug resistance. *Cancer research* **1998**, *58*, 5337–9.

(23) Maliepaard, M.; Scheffer, G. L.; Faneyte, I. F.; Gastelen, A. Van; Pijnenborg, A. C. L. M. Subcellular Localization and Distribution of the Breast Cancer Resistance Protein Transporter in Normal Human Tissues Subcellular Localization and Distribution of the Breast Cancer Resistance Protein Transporter in Normal Human Tissues 1. **2001**, 3458–3464.

(24) Fetsch, P. a; Abati, A.; Litman, T.; Morisaki, K.; Honjo, Y.; Mittal, K.; Bates, S. E. Localization of the ABCG2 mitoxantrone resistance-associated protein in normal tissues. *Cancer letters* **2006**, *235*, 84–92.

(25) Doyle, L. A.; Ross, D. D. Multidrug resistance mediated by the breast cancer resistance protein BCRP (ABCG2). *Oncogene* **2003**, *22*, 7340–58.

(26) Mao, Q. BCRP/ABCG2 in the placenta: expression, function and regulation. *Pharmaceutical research* **2008**, *25*, 1244–55.

(27) Kobayashi, D.; Ieiri, I.; Hirota, T.; Takane, H. Functional assessment of ABCG2 (BCRP) gene polymorphisms to protein expression in human placenta. *Drug metabolism and* **2005**, *33*, 94–101.

(28) Yeboah, D.; Sun, M.; Kingdom, J.; Baczyk, D.; Lye, S. J.; Matthews, S. G.; Gibb, W. Expression of breast cancer resistance protein (BCRP / ABCG2) in human placenta throughout gestation and at term before and after labor. **2006**, *1258*, 1251–1258.

(29) Cooray, H. C.; Blackmore, C. G.; Maskell, L.; Barrand, M. a Localisation of breast cancer resistance protein in microvessel endothelium of human brain. *Neuroreport* **2002**, *13*, 2059–63.

(30) Abbott, B. L. ABCG2 (BCRP): a cytoprotectant in normal and malignant stem cells. *Clinical advances in hematology & oncology : H&O* **2006**, *4*, 63–72.

(31) Hirschmann-Jax, C.; Foster, a E.; Wulf, G. G.; Nuchtern, J. G.; Jax, T. W.; Gobel, U.; Goodell, M. a; Brenner, M. K. A distinct “side population” of cells with high drug efflux capacity in human tumor cells. *Proceedings of the National Academy of Sciences of the United States of America* **2004**, *101*, 14228–33.

(32) Zhou, S.; Schuetz, J. D.; Bunting, K. D.; Colapietro, a M.; Sampath, J.; Morris, J. J.; Lagutina, I.; Grosveld, G. C.; Osawa, M.; Nakauchi, H.; Sorrentino, B. P. The ABC transporter Bcrp1/ABCG2 is expressed in a wide variety of stem cells and is a molecular determinant of the side-population phenotype. *Nature medicine* **2001**, *7*, 1028–34.

(33) Rocchi, E.; Khodjakov, a; Volk, E. L.; Yang, C. H.; Litman, T.; Bates, S. E.; Schneider, E. The product of the ABC half-transporter gene ABCG2 (BCRP/MXR/ABCP) is expressed in the plasma membrane. *Biochemical and biophysical research communications* **2000**, *271*, 42–6.

(34) Lemos, C.; Kathmann, I.; Giovannetti, E.; Beliën, J. a M.; Scheffer, G. L.; Calhau, C.; Jansen, G.; Peters, G. J. Cellular folate status modulates the expression of BCRP and MRP multidrug transporters in cancer cell lines from different origins. *Molecular cancer therapeutics* **2009**, *8*, 655–64.

(35) Choudhuri, S.; Klaassen, C. D. Structure, function, expression, genomic organization, and single nucleotide polymorphisms of human ABCB1 (MDR1), ABCC (MRP), and ABCG2 (BCRP) efflux transporters. *International journal of toxicology* **2006**, *25*, 231–59.

(36) Kusuhara, H.; Sugiyama, Y. ATP-binding cassette, subfamily G (ABCG family). *Pflügers Archiv : European journal of physiology* **2007**, *453*, 735–44.

(37) Ni, Z.; Bikadi, Z.; Rosenberg, M. F.; Mao, Q. Structure and function of the human breast cancer resistance protein (BCRP/ABCG2). *Current drug metabolism* **2010**, *11*, 603.

(38) Mohrmann, K.; Van Eijndhoven, M. a J.; Schinkel, A. H.; Schellens, J. H. M. Absence of N-linked glycosylation does not affect plasma membrane localization of breast cancer resistance protein (BCRP/ABCG2). *Cancer chemotherapy and pharmacology* **2005**, *56*, 344–50.

(39) Shigeta, J.; Katayama, K.; Mitsuhashi, J.; Noguchi, K.; Sugimoto, Y. BCRP/ABCG2 confers anticancer drug resistance without covalent dimerization. *Cancer science* **2010**, *101*, 1813–21.

(40) Polgar, O.; Ierano, C.; Tamaki, A.; Stanley, B.; Ward, Y.; Xia, D.; Tarasova, N.; Robey, R. W.; Bates, S. E. Mutational analysis of threonine 402 adjacent to the GXXXG dimerization motif in transmembrane segment 1 of ABCG2. *Biochemistry* **2010**, *49*, 2235–45.

(41) Polgar, O.; Ediriwickrema, L. S.; Robey, R. W.; Sharma, A.; Hegde, R. S.; Li, Y.; Xia, D.; Ward, Y.; Dean, M.; Ozvegy-Laczka, C.; Sarkadi, B.; Bates, S. E. Arginine 383 is a crucial residue in ABCG2 biogenesis. *Biochimica et biophysica acta* **2009**, *1788*, 1434–43.

(42) Ozvegy-Laczka, C.; Köblös, G.; Sarkadi, B.; Váradi, A. Single amino acid (482) variants of the ABCG2 multidrug transporter: major differences in transport capacity and substrate recognition. *Biochimica et biophysica acta* **2005**, *1668*, 53–63.

(43) Polgar, O.; Bates, S. E. ABC transporters in the balance: is there a role in multidrug resistance? *Biochemical Society transactions* **2005**, *33*, 241–5.

(44) Xu, J.; Liu, Y.; Yang, Y.; Bates, S.; Zhang, J. Characterization of oligomeric human half-ABC transporter ATP-binding cassette G2. *The Journal of biological chemistry* **2004**, *279*, 19781–9.

(45) Bhatia, A.; Schäfer, H.-J.; Hrycyna, C. a Oligomerization of the human ABC transporter ABCG2: evaluation of the native protein and chimeric dimers. *Biochemistry* **2005**, *44*, 10893–904.

(46) Leslie, E. M.; Deeley, R. G.; Cole, S. P. C. Multidrug resistance proteins: role of P-glycoprotein, MRP1, MRP2, and BCRP (ABCG2) in tissue defense. *Toxicology and applied pharmacology* **2005**, *204*, 216–37.

(47) Posner, L. E.; Dukart, G.; Goldberg, J.; Bernstein, T.; Cartwright, K. Mitoxantrone: an overview of safety and toxicity. *Investigational new drugs* **1985**, *3*, 123–32.

(48) Scott, L. J.; Figgitt, D. P. Mitoxantrone: a review of its use in multiple sclerosis. *CNS drugs* **2004**, *18*, 379–96.

(49) Carles, J.; Castellano, D.; Climent, M. Á.; Maroto, P.; Medina, R.; Alcaraz, A. Castration-resistant metastatic prostate cancer: current status and treatment possibilities. *Clinical & translational oncology : official publication of the Federation of Spanish Oncology Societies and of the National Cancer Institute of Mexico* **2012**, *14*, 169–76.

(50) Atiba, J. O.; Green, S. J.; Hynes, H. E.; Osborne, C. K.; Miller, T. P.; Davidner, M. Phase II evaluation of mitoxantrone plus cis-platinum in patients with advanced breast cancer. A Southwest Oncology Group study. *Investigational new drugs* **1994**, *12*, 129–32.

(51) Nakagawa, M.; Schneider, E.; Dixon, K. H.; Horton, J.; Kelley, K.; Morrow, C.; Cowan, K. H. Reduced intracellular drug accumulation in the absence of P-glycoprotein (mdr1) overexpression in mitoxantrone-resistant human MCF-7 breast cancer cells. *Cancer research* **1992**, *52*, 6175–81.

(52) Ishii, M.; Iwahana, M.; Mitsui, I.; Minami, M.; Imagawa, S. Growth inhibitory effect of a new camptothecin analog , DX-8951f , on various drug-resistant sublines including BCRP-mediated camptothecin derivative- resistant variants derived from the human lung cancer cell line PC-6. **2000**, 353–362.

(53) Rabindran, S. K.; Ross, D. D.; Doyle, L. A.; Yang, W.; Greenberger, L. M. Fumitremorgin C reverses multidrug resistance in cells transfected with the breast cancer resistance protein. *Cancer research* **2000**, *60*, 47–50.

(54) Shiozawa, K.; Oka, M.; Soda, H.; Yoshikawa, M.; Ikegami, Y.; Tsurutani, J.; Nakatomi, K.; Nakamura, Y.; Doi, S.; Kitazaki, T.; Mizuta, Y.; Murase, K.; Yoshida, H.; Ross, D. D.; Kohno, S. Reversal of breast cancer resistance protein (BCRP/ABCG2)-mediated drug resistance by novobiocin, a coumermycin antibiotic. *International journal of cancer. Journal international du cancer* **2004**, *108*, 146–51.

(55) Breedveld, P.; Pluim, D.; Cipriani, G.; Dahlhaus, F.; Van Eijndhoven, M. A. J.; De Wolf, C. J. F.; Kuil, A.; Beijnen, J. H.; Scheffer, G. L.; Jansen, G.; Borst, P.; Schellens, J. H. M. The effect of low pH on breast cancer resistance protein (ABCG2)-mediated transport of methotrexate, 7-hydroxymethotrexate, methotrexate diglutamate, folic acid, mitoxantrone, topotecan, and resveratrol in in vitro drug transport models. *Molecular pharmacology* **2007**, *71*, 240–9.

(56) Brangi, M.; Litman, T.; Ciotti, M.; Nishiyama, K.; Kohlhagen, G.; Takimoto, C.; Robey, R.; Pommier, Y.; Fojo, T.; Bates, S. E. Camptothecin resistance: role of the ATP-binding cassette (ABC), mitoxantrone-resistance half-transporter (MXR), and potential for glucuronidation in MXR-expressing cells. *Cancer research* **1999**, *59*, 5938–46.

(57) Yuan, J.; Lv, H.; Peng, B.; Wang, C.; Yu, Y.; He, Z. Role of BCRP as a biomarker for predicting resistance to 5-fluorouracil in breast cancer. *Cancer chemotherapy and pharmacology* **2009**, *63*, 1103–10.

(58) Ozvegy, C.; Litman, T.; Szakács, G.; Nagy, Z.; Bates, S.; Váradi, a; Sarkadi, B. Functional characterization of the human multidrug transporter, ABCG2, expressed in insect cells. *Biochemical and biophysical research communications* **2001**, *285*, 111–7.

(59) Allen, J. D.; Van Dort, S. C.; Buitelaar, M.; Van Tellingen, O.; Schinkel, A. H. Mouse breast cancer resistance protein (Bcrp1/Abcg2) mediates etoposide resistance and transport, but etoposide oral availability is limited primarily by P-glycoprotein. *Cancer research* **2003**, *63*, 1339–44.

(60) Polli, J. W.; Baughman, T. M.; Humphreys, J. E.; Jordan, K. H.; Mote, A. L.; Webster, L. O.; Barnaby, R. J.; Vitulli, G.; Bertolotti, L.; Read, K. D.; Serabjit-Singh, C. J. The systemic exposure of an N-methyl-D-aspartate receptor antagonist is limited in mice by the P-glycoprotein and breast cancer resistance protein efflux transporters. *Drug metabolism and disposition: the biological fate of chemicals* **2004**, *32*, 722–6.

(61) Nakagawa, R.; Hara, Y.; Arakawa, H.; Nishimura, S.; Komatani, H. ABCG2 confers resistance to indolocarbazole compounds by ATP-dependent transport. *Biochemical and biophysical research communications* **2002**, *299*, 669–75.

(62) Robey, R. W.; Obrzut, T.; Shukla, S.; Polgar, O.; Macalou, S.; Bahr, J. C.; Di Pietro, A.; Ambudkar, S. V; Bates, S. E. Becatecarin (rebeccamycin analog, NSC 655649) is a transport substrate and induces expression of the ATP-binding cassette transporter, ABCG2, in lung carcinoma cells. *Cancer chemotherapy and pharmacology* **2009**, *64*, 575–83.

(63) Komatani, H.; Kotani, H.; Hara, Y.; Nakagawa, R.; Matsumoto, M.; Arakawa, H.; Nishimura, S. Identification of breast cancer resistant protein/mitoxantrone resistance/placenta-specific, ATP-binding cassette transporter as a transporter of NB-506 and J-107088, topoisomerase I inhibitors with an indolocarbazole structure. *Cancer research* **2001**, *61*, 2827–32.

(64) Volk, E. L.; Schneider, E. Wild-type breast cancer resistance protein (BCRP/ABCG2) is a methotrexate polyglutamate transporter. *Cancer research* **2003**, *63*, 5538–43.

(65) Volk, E. L.; Farley, K. M.; Wu, Y.; Li, F.; Robey, R. W.; Schneider, E. Overexpression of wild-type breast cancer resistance protein mediates methotrexate resistance. *Cancer research* **2002**, *62*, 5035–40.

(66) Chen, Z.; Robey, R. W.; Belinsky, M. G.; Shchaveleva, I.; Ren, X.; Sugimoto, Y.; Ross, D. D.; Bates, S. E.; Kruh, G. D. Transport of methotrexate, methotrexate polyglutamates, and 17beta-estradiol 17-(beta-D-glucuronide) by ABCG2: effects of acquired mutations at R482 on methotrexate transport. *Cancer research* **2003**, *63*, 4048–54.

(67) Bram, E.; Ifergan, I.; Shafran, A.; Berman, B.; Jansen, G.; Assaraf, Y. G. Mutant Gly482 and Thr482 ABCG2 mediate high-level resistance to lipophilic antifolates. *Cancer chemotherapy and pharmacology* **2006**, *58*, 826–34.

(68) Mitomo, H.; Kato, R.; Ito, A.; Kasamatsu, S.; Ikegami, Y.; Kii, I.; Kudo, A.; Kobatake, E.; Sumino, Y.; Ishikawa, T. A functional study on polymorphism of the ATP-binding cassette transporter ABCG2: critical role of arginine-482 in methotrexate transport. *The Biochemical journal* **2003**, *373*, 767–74.

(69) Shafran, A.; Ifergan, I.; Bram, E.; Jansen, G.; Kathmann, I.; Peters, G. J.; Robey, R. W.; Bates, S. E.; Assaraf, Y. G. ABCG2 harboring the Gly482 mutation confers high-level resistance to various hydrophilic antifolates. *Cancer research* **2005**, *65*, 8414–22.

(70) De Wolf, C.; Jansen, R.; Yamaguchi, H.; De Haas, M.; Van de Wetering, K.; Wijnholds, J.; Beijnen, J.; Borst, P. Contribution of the drug transporter ABCG2 (breast cancer resistance protein) to resistance against anticancer nucleosides. *Molecular cancer therapeutics* **2008**, *7*, 3092–102.

(71) Robey, R. W.; Honjo, Y.; Morisaki, K.; Nadjem, T. a; Runge, S.; Risbood, M.; Poruchynsky, M. S.; Bates, S. E. Mutations at amino-acid 482 in the ABCG2 gene affect substrate and antagonist specificity. *British journal of cancer* **2003**, *89*, 1971–8.

(72) Honjo, Y.; Hrycyna, C. A.; Yan, Q. W.; Medina-Pérez, W. Y.; Robey, R. W.; Van de Laar, A.; Litman, T.; Dean, M.; Bates, S. E. Acquired mutations in the MXR/BCRP/ABCP gene alter substrate specificity in MXR/BCRP/ABCP-overexpressing cells. *Cancer research* **2001**, *61*, 6635–9.

(73) De Jong, F. a; De Jonge, M. J. a; Verweij, J.; Mathijssen, R. H. J. Role of pharmacogenetics in irinotecan therapy. *Cancer letters* **2006**, *234*, 90–106.

(74) Maliepaard, M.; Van Gastelen, M. A.; De Jong, L. A.; Pluim, D.; Van Waardenburg, R. C.; Ruevekamp-Helmers, M. C.; Floot, B. G.; Schellens, J. H. Overexpression of the BCRP/MXR/ABCP gene in a topotecan-selected ovarian tumor cell line. *Cancer research* **1999**, *59*, 4559–63.

(75) Maliepaard, M.; Van Gastelen, M. A.; Tohgo, A.; Hausheer, F. H.; Van Waardenburg, R. C.; De Jong, L. A.; Pluim, D.; Beijnen, J. H.; Schellens, J. H. Circumvention of breast cancer resistance protein (BCRP)-mediated resistance to camptothecins in vitro using non-substrate drugs or the BCRP inhibitor GF120918. *Clinical cancer research : an official journal of the American Association for Cancer Research* **2001**, *7*, 935–41.

(76) Nakatomi, K.; Yoshikawa, M.; Oka, M.; Ikegami, Y.; Hayasaka, S.; Sano, K.; Shiozawa, K.; Kawabata, S.; Soda, H.; Ishikawa, T.; Tanabe, S.; Kohno, S. Transport of 7-ethyl-10-hydroxycamptothecin (SN-38) by breast cancer resistance protein ABCG2 in human lung cancer cells. *Biochemical and biophysical research communications* **2001**, *288*, 827–32.

(77) Bates, S. E.; Medina-Pérez, W. Y.; Kohlhagen, G.; Antony, S.; Nadjem, T.; Robey, R. W.; Pommier, Y. ABCG2 mediates differential resistance to SN-38 (7-ethyl-10-hydroxycamptothecin) and homocamptothecins. *The Journal of pharmacology and experimental therapeutics* **2004**, *310*, 836–42.

(78) Kawabata, S.; Oka, M.; Shiozawa, K.; Tsukamoto, K.; Nakatomi, K.; Soda, H.; Fukuda, M.; Ikegami, Y.; Sugahara, K.; Yamada, Y.; Kamihira, S.; Doyle, L. a; Ross, D. D.; Kohno, S. Breast cancer resistance protein directly confers SN-38 resistance of lung cancer cells. *Biochemical and biophysical research communications* **2001**, *280*, 1216–23.

(79) Jonker, J. W.; Smit, J. W.; Brinkhuis, R. F.; Maliepaard, M.; Beijnen, J. H.; Schellens, J. H.; Schinkel, A. H. Role of breast cancer resistance protein in the bioavailability and fetal penetration of topotecan. *Journal of the National Cancer Institute* **2000**, *92*, 1651–6.

(80) Rajendra, R.; Gounder, M. K.; Saleem, A.; Schellens, J. H. M.; Ross, D. D.; Bates, S. E.; Sinko, P.; Rubin, E. H. Differential Effects of the Breast Cancer Resistance Protein on the Cellular Accumulation and Cytotoxicity of 9-Aminocamptothecin and 9-Nitrocamptothecin Differential Effects of the Breast Cancer Resistance Protein on the Cellular Accumulation and Cytotox. *Cancer* **2003**, 3228–3233.

(81) Sparreboom, A.; Gelderblom, H.; Marsh, S.; Ahluwalia, R.; Obach, R.; Principe, P.; Twelves, C.; Verweij, J.; McLeod, H. L. Diflomotecan pharmacokinetics in relation to ABCG2 421C>A genotype. *Clinical pharmacology and therapeutics* **2004**, *76*, 38–44.

(82) Bessho, Y.; Oguri, T.; Achiwa, H.; Muramatsu, H.; Maeda, H.; Niimi, T.; Sato, S.; Ueda, R. Role of ABCG2 as a biomarker for predicting resistance to CPT-11/SN-38 in lung cancer. *Cancer science* **2006**, *97*, 192–8.

(83) Takahata, T.; Ookawa, K.; Suto, K.; Tanaka, M.; Yano, H.; Nakashima, O.; Kojiro, M.; Tamura, Y.; Tateishi, T.; Sakata, Y.; Fukuda, S. Chemosensitivity determinants of irinotecan hydrochloride in hepatocellular carcinoma cell lines. *Basic & clinical pharmacology & toxicology* **2008**, *102*, 399–407.

(84) Ishikawa, T.; Ikegami, Y.; Sano, K.; Nakagawa, H.; Sawada, S. Transport mechanism-based drug molecular design: novel camptothecin analogues to circumvent ABCG2-associated drug resistance of human tumor cells. *Current pharmaceutical design* **2006**, *12*, 313–25.

(85) Nakagawa, H.; Saito, H.; Ikegami, Y.; Aida-Hyugaji, S.; Sawada, S.; Ishikawa, T. Molecular modeling of new camptothecin analogues to circumvent ABCG2-mediated drug resistance in cancer. *Cancer letters* **2006**, *234*, 81–9.

(86) Jonker, J. W.; Merino, G.; Musters, S.; Van Herwaarden, A. E.; Bolscher, E.; Wagenaar, E.; Mesman, E.; Dale, T. C.; Schinkel, A. H. The breast cancer resistance protein BCRP (ABCG2) concentrates drugs and carcinogenic xenotoxins into milk. *Nature medicine* **2005**, *11*, 127–9.

(87) Sai, K.; Saito, Y.; Maekawa, K.; Kim, S.-R.; Kaniwa, N.; Nishimaki-Mogami, T.; Sawada, J.; Shirao, K.; Hamaguchi, T.; Yamamoto, N.; Kunitoh, H.; Ohe, Y.; Yamada, Y.; Tamura, T.; Yoshida, T.; Matsumura, Y.; Ohtsu, A.; Saijo, N.; Minami, H. Additive effects of drug transporter genetic polymorphisms on irinotecan pharmacokinetics/pharmacodynamics in Japanese cancer patients. *Cancer chemotherapy and pharmacology* **2010**, *66*, 95–105.

(88) Jada, S. R.; Lim, R.; Wong, C. I.; Shu, X.; Lee, S. C.; Zhou, Q.; Goh, B. C.; Chowbay, B. Role of UGT1A1*6, UGT1A1*28 and ABCG2 c.421C>A polymorphisms in irinotecan-induced neutropenia in Asian cancer patients. *Cancer science* **2007**, *98*, 1461–7.

(89) Sparreboom, A.; Loos, W. J.; Burger, H.; Sissung, T. M.; Verweij, J.; Figg, W. D.; Nooter, K.; Gelderblom, H. Effect of ABCG2 genotype on the oral bioavailability of topotecan. *Cancer biology & therapy* **2005**, *4*, 650–8.

(90) De Jong, F. a; Marsh, S.; Mathijssen, R. H. J.; King, C.; Verweij, J.; Sparreboom, A.; McLeod, H. L. ABCG2 pharmacogenetics: ethnic differences in allele frequency and assessment of influence on irinotecan disposition. *Clinical cancer research : an official journal of the American Association for Cancer Research* **2004**, *10*, 5889–94.

(91) Lemos, C.; Jansen, G.; Peters, G. J. Drug transporters: recent advances concerning BCRP and tyrosine kinase inhibitors. *British journal of cancer* **2008**, *98*, 857–62.

(92) Ross, D. D.; Karp, J. E.; Chen, T. T.; Doyle, L. A. Expression of breast cancer resistance protein in blast cells from patients with acute leukemia. *Blood* **2000**, *96*, 365–8.

(93) Nakanishi, T.; Karp, J. E.; Tan, M.; Doyle, L. A.; Peters, T.; Yang, W.; Wei, D.; Ross, D. D. Quantitative analysis of breast cancer resistance protein and cellular resistance to flavopiridol in acute leukemia patients. *Clinical cancer research : an official journal of the American Association for Cancer Research* **2003**, *9*, 3320–8.

(94) Breedveld, P.; Pluim, D.; Cipriani, G.; Wielinga, P.; Van Tellingen, O.; Schinkel, A. H.; Schellens, J. H. M. The effect of Bcrp1 (Abcg2) on the in vivo pharmacokinetics and brain penetration of imatinib mesylate (Gleevec): implications for the use of breast cancer resistance protein and P-glycoprotein inhibitors to enable the brain penetration of imatinib in pat. *Cancer research* **2005**, *65*, 2577–82.

(95) Burger, H.; Van Tol, H.; Boersma, A. W. M.; Brok, M.; Wiemer, E. a C.; Stoter, G.; Nooter, K. Imatinib mesylate (STI571) is a substrate for the breast cancer resistance protein (BCRP)/ABCG2 drug pump. *Blood* **2004**, *104*, 2940–2.

(96) Burger, H.; Nooter, K. Pharmacokinetic resistance to imatinib mesylate: role of the ABC drug pumps ABCG2 (BCRP) and ABCB1 (MDR1) in the oral bioavailability of imatinib. *Cell cycle (Georgetown, Tex.)* **2004**, *3*, 1502–5.

(97) Li, J.; Cusatis, G.; Brahmer, J.; Sparreboom, A.; Robey, R. W.; Bates, S. E.; Hidalgo, M.; Baker, S. D. Association of variant ABCG2 and the pharmacokinetics of epidermal growth factor receptor tyrosine kinase inhibitors in cancer patients. *Cancer biology & therapy* **2007**, *6*, 432–8.

(98) Elkind, N. B.; Szentpétery, Z.; Apáti, A.; Ozvegy-Laczka, C.; Várady, G.; Ujhelly, O.; Szabó, K.; Homolya, L.; Váradi, A.; Buday, L.; Kéri, G.; Német, K.; Sarkadi, B. Multidrug transporter ABCG2 prevents tumor cell death induced by the

epidermal growth factor receptor inhibitor Iressa (ZD1839, Gefitinib). *Cancer research* **2005**, *65*, 1770–7.

(99) Marchetti, S.; De Vries, N. a; Buckle, T.; Bolijn, M. J.; Van Eijndhoven, M. a J.; Beijnen, J. H.; Mazzanti, R.; Van Tellingen, O.; Schellens, J. H. M. Effect of the ATP-binding cassette drug transporters ABCB1, ABCG2, and ABCC2 on erlotinib hydrochloride (Tarceva) disposition in in vitro and in vivo pharmacokinetic studies employing Bcrp1-/-/Mdr1a/1b-/- (triple-knockout) and wild-type mice. *Molecular cancer therapeutics* **2008**, *7*, 2280–7.

(100) Polli, J. W.; Humphreys, J. E.; Harmon, K. A.; Castellino, S.; O'Mara, M. J.; Olson, K. L.; John-Williams, L. S.; Koch, K. M.; Serabjit-Singh, C. J. The role of efflux and uptake transporters in [N-{3-chloro-4-[(3-fluorobenzyl)oxy]phenyl}-6-[5-({[2-(methylsulfonyl)ethyl]amino}methyl)-2-furyl]-4-quinazolinamine (GW572016, lapatinib) disposition and drug interactions. *Drug metabolism and disposition: the biological fate of chemicals* **2008**, *36*, 695–701.

(101) Azzariti, A.; Porcelli, L.; Simone, G. M.; Quatrale, A. E.; Colabufo, N. a; Berardi, F.; Perrone, R.; Zucchetti, M.; D'Incalci, M.; Xu, J. M.; Paradiso, A. Tyrosine kinase inhibitors and multidrug resistance proteins: interactions and biological consequences. *Cancer chemotherapy and pharmacology* **2010**, *65*, 335–46.

(102) Hiwase, D. K.; Saunders, V.; Hewett, D.; Frede, A.; Zrim, S.; Dang, P.; Eadie, L.; To, L. B.; Melo, J.; Kumar, S.; Hughes, T. P.; White, D. L. Dasatinib cellular uptake and efflux in chronic myeloid leukemia cells: therapeutic implications. *Clinical cancer research : an official journal of the American Association for Cancer Research* **2008**, *14*, 3881–8.

(103) Hegedus, C.; Ozvegy-Laczka, C.; Apáti, a; Magócsi, M.; Német, K.; Orfi, L.; Kéri, G.; Katona, M.; Takáts, Z.; Váradi, a; Szakács, G.; Sarkadi, B. Interaction of nilotinib, dasatinib and bosutinib with ABCB1 and ABCG2: implications for altered anti-cancer effects and pharmacological properties. *British journal of pharmacology* **2009**, *158*, 1153–64.

(104) Erlichman, C.; Boerner, S. A.; Hallgren, C. G.; Spieker, R.; Wang, X. Y.; James, C. D.; Scheffer, G. L.; Maliepaard, M.; Ross, D. D.; Bible, K. C.; Kaufmann, S. H. The HER tyrosine kinase inhibitor CI1033 enhances cytotoxicity of 7-ethyl-10-hydroxycamptothecin and topotecan by inhibiting breast cancer resistance protein-mediated drug efflux. *Cancer research* **2001**, *61*, 739–48.

(105) Shi, Z.; Peng, X.-X.; Kim, I.-W.; Shukla, S.; Si, Q.-S.; Robey, R. W.; Bates, S. E.; Shen, T.; Ashby, C. R.; Fu, L.-W.; Ambudkar, S. V; Chen, Z.-S. Erlotinib (Tarceva, OSI-774) antagonizes ATP-binding cassette subfamily B member 1 and ATP-binding cassette subfamily G member 2-mediated drug resistance. *Cancer research* **2007**, *67*, 11012–20.

(106) Agarwal, S.; Sane, R.; Ohlfest, J. R.; Elmquist, W. F. The role of the breast cancer resistance protein (ABCG2) in the distribution of sorafenib to the brain. *The Journal of pharmacology and experimental therapeutics* **2011**, *336*, 223–33.

(107) Seamon, J. a; Rugg, C. a; Emanuel, S.; Calcagno, A. M.; Ambudkar, S. V; Middleton, S. a; Butler, J.; Borowski, V.; Greenberger, L. M. Role of the ABCG2 drug transporter in the resistance and oral bioavailability of a potent cyclin-dependent kinase/Aurora kinase inhibitor. *Molecular cancer therapeutics* **2006**, *5*, 2459–67.

(108) Generaux, G. T.; Bonomo, F. M.; Johnson, M.; Doan, K. M. M. Impact of SLCO1B1 (OATP1B1) and ABCG2 (BCRP) genetic polymorphisms and inhibition on LDL-C lowering and myopathy of statins. *Xenobiotica; the fate of foreign compounds in biological systems* **2011**, *41*, 639–51.

(109) Huang, L.; Wang, Y.; Grimm, S. ATP-dependent transport of rosuvastatin in membrane vesicles expressing breast cancer resistance protein. *Drug metabolism and disposition: the biological fate of chemicals* **2006**, *34*, 738–42.

(110) Hirano, M.; Maeda, K.; Matsushima, S.; Nozaki, Y.; Kusuhara, H.; Sugiyama, Y. Involvement of BCRP (ABCG2) in the biliary excretion of pitavastatin. *Molecular pharmacology* **2005**, *68*, 800–7.

(111) Zhang, W.; Yu, B.-N.; He, Y.-J.; Fan, L.; Li, Q.; Liu, Z.-Q.; Wang, A.; Liu, Y.-L.; Tan, Z.-R.; Fen-Jiang; Huang, Y.-F.; Zhou, H.-H. Role of BCRP 421C>A polymorphism on rosuvastatin pharmacokinetics in healthy Chinese males. *Clinica chimica acta; international journal of clinical chemistry* **2006**, *373*, 99–103.

(112) Keskitalo, J. E. J.; Pasanen, M. K. M.; Neuvonen, P. J.; Niemi, M. Different effects of the ABCG2 c. 421C> A SNP on the pharmacokinetics of fluvastatin, pravastatin and simvastatin. *Pharmacogenomics* **2009**, *10*, 1617–1624.

(113) Chasman, D. I.; Giulianini, F.; MacFadyen, J.; Barratt, B. J.; Nyberg, F.; Ridker, P. M. Genetic determinants of statin-induced low-density lipoprotein cholesterol reduction: the Justification for the Use of Statins in Prevention: an Intervention Trial Evaluating Rosuvastatin (JUPITER) trial. *Circulation. Cardiovascular genetics* **2012**, *5*, 257–64.

(114) Rodrigues, A. C.; Curi, R.; Genvigir, F. D. V.; Hirata, M. H.; Hirata, R. D. C. The expression of efflux and uptake transporters are regulated by statins in Caco-2 and HepG2 cells. *Acta pharmacologica Sinica* **2009**, *30*, 956–64.

(115) Temesgen, Z.; Warnke, D.; Kasten, M. J. Current status of antiretroviral therapy. *Expert opinion on pharmacotherapy* **2006**, *7*, 1541–54.

(116) Wang, X.; Furukawa, T.; Nitanda, T.; Okamoto, M.; Sugimoto, Y.; Akiyama, S.-I.; Baba, M. Breast cancer resistance protein (BCRP/ABCG2) induces cellular resistance to HIV-1 nucleoside reverse transcriptase inhibitors. *Molecular pharmacology* **2003**, *63*, 65–72.

(117) Wang, X.; Nitanda, T.; Shi, M.; Okamoto, M.; Furukawa, T.; Sugimoto, Y.; Akiyama, S.; Baba, M. Induction of cellular resistance to nucleoside reverse transcriptase inhibitors by the wild-type breast cancer resistance protein. *Biochemical pharmacology* **2004**, *68*, 1363–70.

(118) Weiss, J.; Rose, J.; Storch, C. H.; Ketabi-Kiyanvash, N.; Sauer, A.; Haefeli, W. E.; Efferth, T. Modulation of human BCRP (ABCG2) activity by anti-HIV drugs. *The Journal of antimicrobial chemotherapy* **2007**, *59*, 238–45.

(119) Merino, G.; Álvarez, A. I.; Pulido, M. M. M. M. M.; Molina, A. J. A. J.; Schinkel, A. H. A. H. A. H.; Prieto, J. G. J. G.; Alvarez, A. I. Breast cancer resistance protein (BCRP/ABCG2) transports fluoroquinolone antibiotics and affects their oral availability, pharmacokinetics, and milk secretion. *Drug metabolism and disposition* **2006**, *34*, 690–695.

(120) Janvilisri, T.; Shahi, S.; Venter, H.; Balakrishnan, L.; Van Veen, H. W. Arginine-482 is not essential for transport of antibiotics, primary bile acids and unconjugated sterols by the human breast cancer resistance protein (ABCG2). *The Biochemical journal* **2005**, *385*, 419–26.

(121) Pulido, M. M.; Molina, A. J.; Merino, G.; Mendoza, G.; Prieto, J. G.; Alvarez, A. I. Interaction of enrofloxacin with breast cancer resistance protein (BCRP/ABCG2): influence of flavonoids and role in milk secretion in sheep. *Journal of veterinary pharmacology and therapeutics* **2006**, *29*, 279–87.

(122) Merino, G.; Jonker, J. W.; Wagenaar, E.; Van Herwaarden, A. E.; Schinkel, A. H. The breast cancer resistance protein (BCRP/ABCG2) affects pharmacokinetics, hepatobiliary excretion, and milk secretion of the antibiotic nitrofurantoin. *Molecular pharmacology* **2005**, *67*, 1758–64.

(123) Ando, T.; Kusuhara, H.; Merino, G.; Alvarez, A. I.; Schinkel, A. H.; Sugiyama, Y. Involvement of breast cancer resistance protein (ABCG2) in the biliary excretion mechanism of fluoroquinolones. *Drug metabolism and disposition: the biological fate of chemicals* **2007**, *35*, 1873–9.

(124) Cantini, F.; Niccoli, L.; Nannini, C.; Kaloudi, O.; Bertoni, M.; Cassarà, E. Psoriatic arthritis: a systematic review. *International journal of rheumatic diseases* **2010**, *13*, 300–17.

(125) Ford, A. C.; Achkar, J.-P.; Khan, K. J.; Kane, S. V; Talley, N. J.; Marshall, J. K.; Moayyedi, P. Efficacy of 5-aminosalicylates in ulcerative colitis: systematic

review and meta-analysis. *The American journal of gastroenterology* **2011**, *106*, 601–16.

(126) Jani, M.; Szabó, P.; Kis, E.; Molnár, E.; Glavinas, H.; Krajcsi, P.; Ani, M. J.; Zabó, P. S.; Is, E. K.; Olnár, É. M.; Lavinas, H. G.; Rajcsi, P. K. Kinetic characterization of sulfasalazine transport by human ATP-binding cassette G2. *Biological & pharmaceutical bulletin* **2009**, *32*, 497–9.

(127) Van der Heijden, J.; De Jong, M. C.; Dijkmans, B. A. C.; Lems, W. F.; Oerlemans, R.; Kathmann, I.; Scheffer, G. L.; Scheper, R. J.; Assaraf, Y. G.; Jansen, G. Acquired resistance of human T cells to sulfasalazine: stability of the resistant phenotype and sensitivity to non-related DMARDs. *Annals of the rheumatic diseases* **2004**, *63*, 131–7.

(128) Adkison, K. K.; Vaidya, S. S.; Lee, D. Y.; Koo, S. H.; Li, L.; Mehta, A. A.; Gross, A. S.; Polli, J. W.; Humphreys, J. E.; Lou, Y.; Lee, E. J. D. Oral sulfasalazine as a clinical BCRP probe substrate: pharmacokinetic effects of genetic variation (C421A) and pantoprazole coadministration. *Journal of pharmaceutical sciences* **2010**, *99*, 1046–62.

(129) Kusuhara, H.; Furuie, H.; Inano, A.; Sunagawa, A.; Yamada, S.; Wu, C.; Fukizawa, S.; Morimoto, N.; Ieiri, I.; Morishita, M.; Sumita, K.; Mayahara, H.; Fujita, T.; Maeda, K.; Sugiyama, Y. Pharmacokinetic interaction study of sulphasalazine in healthy subjects and the impact of curcumin as an in vivo inhibitor of BCRP. *British journal of pharmacology* **2012**, *166*, 1793–1803.

(130) Urquhart, B. L.; Ware, J. a; Tirona, R. G.; Ho, R. H.; Leake, B. F.; Schwarz, U. I.; Zaher, H.; Palandra, J.; Gregor, J. C.; Dresser, G. K.; Kim, R. B. Breast cancer resistance protein (ABCG2) and drug disposition: intestinal expression, polymorphisms and sulfasalazine as an in vivo probe. *Pharmacogenetics and genomics* **2008**, *18*, 439–48.

(131) Lagas, J. S.; Van der Kruijssen, C. M. M.; Van de Wetering, K.; Beijnen, J. H.; Schinkel, A. H. Transport of diclofenac by breast cancer resistance protein (ABCG2) and stimulation of multidrug resistance protein 2 (ABCC2)-mediated drug transport by diclofenac and benzbromarone. *Drug metabolism and disposition: the biological fate of chemicals* **2009**, *37*, 129–36.

(132) Kis, E.; Nagy, T.; Jani, M.; Molnár, E.; Jánossy, J.; Ujhellyi, O.; Német, K.; Herédi-Szabó, K.; Krajcsi, P. Leflunomide and its metabolite A771726 are high affinity substrates of BCRP: implications for drug resistance. *Annals of the rheumatic diseases* **2009**, *68*, 1201–7.

(133) Breedveld, P.; Zelcer, N.; Pluim, D.; Sönmezer, O.; Tibben, M. M.; Beijnen, J. H.; Schinkel, A. H.; Van Tellingen, O.; Borst, P.; Schellens, J. H. M. Mechanism of the pharmacokinetic interaction between methotrexate and benzimidazoles:

potential role for breast cancer resistance protein in clinical drug-drug interactions. *Cancer research* **2004**, *64*, 5804–11.

(134) Pavek, P.; Merino, G.; Wagenaar, E.; Bolscher, E.; Novotna, M.; Jonker, J. W.; Schinkel, A. H. Human breast cancer resistance protein: interactions with steroid drugs, hormones, the dietary carcinogen 2-amino-1-methyl-6-phenylimidazo(4,5-b)pyridine, and transport of cimetidine. *The Journal of pharmacology and experimental therapeutics* **2005**, *312*, 144–52.

(135) Pollex, E. K.; Anger, G.; Hutson, J.; Koren, G.; Piquette-Miller, M. Breast cancer resistance protein (BCRP)-mediated glyburide transport: effect of the C421A/Q141K BCRP single-nucleotide polymorphism. *Drug metabolism and disposition: the biological fate of chemicals* **2010**, *38*, 740–4.

(136) Cygalova, L. H.; Hofman, J.; Ceckova, M.; Staud, F. Transplacental pharmacokinetics of glyburide, rhodamine 123, and BODIPY FL prazosin: effect of drug efflux transporters and lipid solubility. *The Journal of pharmacology and experimental therapeutics* **2009**, *331*, 1118–25.

(137) Enokizono, J.; Kusuhara, H.; Sugiyama, Y. Involvement of breast cancer resistance protein (BCRP/ABCG2) in the biliary excretion and intestinal efflux of troglitazone sulfate, the major metabolite of troglitazone with a cholestatic effect. *Drug metabolism and disposition: the biological fate of chemicals* **2007**, *35*, 209–14.

(138) Gedeon, C.; Anger, G.; Piquette-Miller, M.; Koren, G. Breast cancer resistance protein: mediating the trans-placental transfer of glyburide across the human placenta. *Placenta* **2008**, *29*, 39–43.

(139) Tournier, N.; Valette, H.; Peyronneau, M.-A.; Saba, W.; Goutal, S.; Kuhnast, B.; Dollé, F.; Scherrmann, J.-M.; Cisternino, S.; Bottlaender, M. Transport of selected PET radiotracers by human P-glycoprotein (ABCB1) and breast cancer resistance protein (ABCG2): an in vitro screening. *Journal of nuclear medicine : official publication, Society of Nuclear Medicine* **2011**, *52*, 415–23.

(140) Adkison, K. K.; Vaidya, S. S.; Lee, D. Y.; Koo, S. H.; Li, L.; Mehta, A. a; Gross, A. S.; Polli, J. W.; Lou, Y.; Lee, E. J. D. The ABCG2 C421A polymorphism does not affect oral nitrofurantoin pharmacokinetics in healthy Chinese male subjects. *British journal of clinical pharmacology* **2008**, *66*, 233–9.

(141) Ieiri, I.; Suwannakul, S.; Maeda, K.; Uchimaru, H.; Hashimoto, K.; Kimura, M.; Fujino, H.; Hirano, M.; Kusuhara, H.; Irie, S.; Higuchi, S.; Sugiyama, Y. SLCO1B1 (OATP1B1, an Uptake Transporter) and ABCG2 (BCRP, an Efflux Transporter) Variant Alleles and Pharmacokinetics of Pitavastatin in Healthy Volunteers. *Clinical Pharmacology & Therapeutics* **2007**, *82*, 541–547.

(142) Ho, R. H.; Choi, L.; Lee, W.; Mayo, G.; Schwarz, U. I.; Tirona, R. G.; Bailey, D. G.; Michael Stein, C.; Kim, R. B. Effect of drug transporter genotypes on pravastatin disposition in European- and African-American participants. *Pharmacogenetics and genomics* **2007**, *17*, 647–56.

(143) Kim, H.-S.; Sunwoo, Y. E.; Ryu, J. Y.; Kang, H.-J.; Jung, H.-E.; Song, I.-S.; Kim, E.-Y.; Shim, J.-C.; Shon, J.-H.; Shin, J.-G. The effect of ABCG2 V12M, Q141K and Q126X, known functional variants in vitro, on the disposition of lamivudine. *British journal of clinical pharmacology* **2007**, *64*, 645–54.

(144) Van Hattum, a H.; Hoogsteen, I. J.; Schlüper, H. M. M.; Maliepaard, M.; Scheffer, G. L.; Scheper, R. J.; Kohlhagen, G.; Pommier, Y.; Pinedo, H. M.; Boven, E. Induction of breast cancer resistance protein by the camptothecin derivative DX-8951f is associated with minor reduction of antitumour activity. *British journal of cancer* **2002**, *87*, 665–72.

(145) Marchetti, S.; Oostendorp, R. L.; Pluim, D.; Van Eijndhoven, M.; Van Tellingen, O.; Schinkel, A. H.; Versace, R.; Beijnen, J. H.; Mazzanti, R.; Schellens, J. H. In vitro transport of gimatecan (7-t-butoxyiminomethylcamptothecin) by breast cancer resistance protein, P-glycoprotein, and multidrug resistance protein 2. *Molecular cancer therapeutics* **2007**, *6*, 3307–13.

(146) Li, H.; Jin, H.-E.; Kim, W.; Han, Y.-H.; Kim, D.-D.; Chung, S.-J.; Shim, C.-K. Involvement of P-glycoprotein, multidrug resistance protein 2 and breast cancer resistance protein in the transport of belotecan and topotecan in Caco-2 and MDCKII cells. *Pharmaceutical research* **2008**, *25*, 2601–12.

(147) Shukla, S.; Robey, R. W.; Bates, S. E.; Ambudkar, S. V The calcium channel blockers, 1,4-dihydropyridines, are substrates of the multidrug resistance-linked ABC drug transporter, ABCG2. *Biochemistry* **2006**, *45*, 8940–51.

(148) Miura, M.; Kagaya, H.; Satoh, S.; Inoue, K.; Saito, M.; Habuchi, T.; Suzuki, T. Influence of drug transporters and UGT polymorphisms on pharmacokinetics of phenolic glucuronide metabolite of mycophenolic acid in Japanese renal transplant recipients. *Therapeutic drug monitoring* **2008**, *30*, 559–64.

(149) Yang, J. J.; Milton, M. N.; Yu, S.; Liao, M.; Liu, N.; Wu, J.-T.; Gan, L.; Balani, S. K.; Lee, F. W.; Prakash, S.; Xia, C. Q. P-glycoprotein and breast cancer resistance protein affect disposition of tandutinib, a tyrosine kinase inhibitor. *Drug metabolism letters* **2010**, *4*, 201–12.

(150) Feng, B.; Xu, J. J.; Bi, Y.-A.; Mireles, R.; Davidson, R.; Duignan, D. B.; Campbell, S.; Kostrubsky, V. E.; Dunn, M. C.; Smith, A. R.; Wang, H. F. Role of hepatic transporters in the disposition and hepatotoxicity of a HER2 tyrosine kinase inhibitor CP-724,714. *Toxicological sciences : an official journal of the Society of Toxicology* **2009**, *108*, 492–500.

(151) Bram, E. E.; Adar, Y.; Mesika, N.; Sabisz, M.; Skladanowski, A.; Assaraf, Y. G. Structural Determinants of Imidazoacridinones Facilitating Antitumor Activity Are Crucial for Substrate Recognition by ABCG2. **2009**, *75*, 1149–1159.

(152) Merino, G.; Jonker, J. W.; Wagenaar, E.; Pulido, M. M.; Molina, A. J.; Alvarez, A. I.; Schinkel, A. H. Transport of anthelmintic benzimidazole drugs by breast cancer resistance protein (BCRP/ABCG2). *Drug metabolism and disposition: the biological fate of chemicals* **2005**, *33*, 614–8.

(153) Meng, F.; Cai, X.; Duan, J.; Matteucci, M. G.; Hart, C. P. A novel class of tubulin inhibitors that exhibit potent antiproliferation and in vitro vessel-disrupting activity. *Cancer chemotherapy and pharmacology* **2008**, *61*, 953–63.

(154) Zhang, Y.; Gupta, A.; Wang, H.; Zhou, L.; Vethanayagam, R. R.; Unadkat, J. D.; Mao, Q. BCRP transports dipyridamole and is inhibited by calcium channel blockers. *Pharmaceutical research* **2005**, *22*, 2023–34.

(155) Kondo, C.; Onuki, R.; Kusuhara, H.; Suzuki, H.; Suzuki, M.; Okudaira, N.; Kojima, M.; Ishiwata, K.; Jonker, J. W.; Sugiyama, Y. Lack of improvement of oral absorption of ME3277 by prodrug formation is ascribed to the intestinal efflux mediated by breast cancer resistant protein (BCRP/ABCG2). *Pharmaceutical research* **2005**, *22*, 613–8.

(156) Hazlehurst, L. A.; Foley, N. E.; Gleason-guzman, M. C.; Line, M. C.; Hacker, M. P.; Cress, A. E.; Greenberger, L. W.; Jong, M. C. De; Dalton, W. S. Multiple Mechanisms Confer Drug Resistance to Mitoxantrone in the Human 8226 Myeloma Cell Line Multiple Mechanisms Confer Drug Resistance to Mitoxantrone in the Human 8226. **1999**, 1021–1028.

(157) Perez, M.; Blazquez, A. G.; Real, R.; Mendoza, G.; Prieto, J. G.; Merino, G.; Alvarez, A. I. In vitro and in vivo interaction of moxidectin with BCRP/ABCG2. *Chemico-biological interactions* **2009**, *180*, 106–12.

(158) Kars, M. D.; Işeri, O. D.; Ural, A. U.; Gündüz, U. In vitro evaluation of zoledronic acid resistance developed in MCF-7 cells. *Anticancer research* **2007**, *27*, 4031–7.

(159) Milane, A.; Vautier, S.; Chacun, H.; Meininger, V.; Bensimon, G.; Farinotti, R.; Fernandez, C. Interactions between riluzole and ABCG2/BCRP transporter. *Neuroscience letters* **2009**, *452*, 12–6.

(160) Yamada, A.; Maeda, K.; Kamiyama, E.; Sugiyama, D.; Kondo, T.; Shiroyanagi, Y.; Nakazawa, H.; Okano, T.; Adachi, M.; Schuetz, J. D.; Adachi, Y.; Hu, Z.; Kusuhara, H.; Sugiyama, Y. Multiple human isoforms of drug transporters contribute to the hepatic and renal transport of olmesartan, a selective antagonist of the angiotensin II AT1-receptor. *Drug metabolism and disposition: the biological fate of chemicals* **2007**, *35*, 2166–76.

(161) Suzuki, M.; Suzuki, H.; Sugimoto, Y.; Sugiyama, Y. ABCG2 transports sulfated conjugates of steroids and xenobiotics. *The Journal of biological chemistry* **2003**, *278*, 22644–9.

(162) Brooks, T. A.; Minderman, H.; O'Loughlin, K. L.; Pera, P.; Ojima, I.; Baer, M. R.; Bernacki, R. J.; Brooks, T. Taxane-based reversal agents modulate drug resistance mediated by P-glycoprotein, multidrug resistance protein, and breast cancer resistance protein. *Molecular cancer therapeutics* **2003**, *2*, 1195–205.

(163) Hu, W.; Liu, W. Side populations of glioblastoma cells are less sensitive to HSV-TK/GCV suicide gene therapy system than the non-side population. *In vitro cellular & developmental biology. Animal* **2010**, *46*, 497–501.

(164) Colabufo, N. A.; Pagliarulo, V.; Berardi, F.; Contino, M.; Inglese, C.; Niso, M.; Ancona, P.; Albo, G.; Pagliarulo, A.; Perrone, R. Bicalutamide failure in prostate cancer treatment: involvement of Multi Drug Resistance proteins. *European journal of pharmacology* **2008**, *601*, 38–42.

(165) Wu, C.-P.; Shukla, S.; Calcagno, A. M.; Hall, M. D.; Gottesman, M. M.; Ambudkar, S. V Evidence for dual mode of action of a thiosemicarbazone, NSC73306: a potent substrate of the multidrug resistance linked ABCG2 transporter. *Molecular cancer therapeutics* **2007**, *6*, 3287–96.

(166) Jonker, J. W.; Buitelaar, M.; Wagenaar, E.; Van Der Valk, M. a; Scheffer, G. L.; Scheper, R. J.; Plosch, T.; Kuipers, F.; Elferink, R. P. J. O.; Rosing, H.; Beijnen, J. H.; Schinkel, A. H. The breast cancer resistance protein protects against a major chlorophyll-derived dietary phototoxin and protoporphyria. *Proceedings of the National Academy of Sciences of the United States of America* **2002**, *99*, 15649–54.

(167) Van Herwaarden, A. E.; Jonker, J. W.; Wagenaar, E.; Brinkhuis, R. F.; Schellens, J. H. M.; Beijnen, J. H.; Schinkel, A. H. The breast cancer resistance protein (Bcrp1/Abcg2) restricts exposure to the dietary carcinogen 2-amino-1-methyl-6-phenylimidazo[4,5-b]pyridine. *Cancer research* **2003**, *63*, 6447–52.

(168) Desuzinges-Mandon, E.; Arnaud, O.; Martinez, L.; Huché, F.; Di Pietro, A.; Falson, P. ABCG2 transports and transfers heme to albumin through its large extracellular loop. *The Journal of biological chemistry* **2010**, *285*, 33123–33.

(169) Robey, R. W.; Steadman, K.; Polgar, O.; Morisaki, K.; Blayney, M.; Mistry, P.; Bates, S. E. Pheophorbide a is a specific probe for ABCG2 function and inhibition. *Cancer research* **2004**, *64*, 1242–6.

(170) Zhou, S.; Zong, Y.; Ney, P. a; Nair, G.; Stewart, C. F.; Sorrentino, B. P. Increased expression of the Abcg2 transporter during erythroid maturation plays a role in decreasing cellular protoporphyrin IX levels. *Blood* **2005**, *105*, 2571–6.

(171) An, R.; Hagiya, Y.; Tamura, A.; Li, S.; Saito, H.; Tokushima, D.; Ishikawa, T. Cellular phototoxicity evoked through the inhibition of human ABC transporter ABCG2 by cyclin-dependent kinase inhibitors in vitro. *Pharmaceutical research* **2009**, *26*, 449–58.

(172) Zheng, X.; Morgan, J.; Pandey, S. K.; Chen, Y.; Tracy, E.; Baumann, H.; Missert, J. R.; Batt, C.; Jackson, J.; Bellnier, D. a; Henderson, B. W.; Pandey, R. K. Conjugation of 2-(1'-hexyloxyethyl)-2-devinylpyropheophorbide-a (HPPH) to carbohydrates changes its subcellular distribution and enhances photodynamic activity in vivo. *Journal of medicinal chemistry* **2009**, *52*, 4306–18.

(173) Robey, R. W.; Fetsch, P. a; Polgar, O.; Dean, M.; Bates, S. E. The livestock photosensitizer, phytoporphyrin (phylloerythrin), is a substrate of the ATP-binding cassette transporter ABCG2. *Research in veterinary science* **2006**, *81*, 345–9.

(174) Lankerani, L.; Baron, E. D. Photosensitivity to exogenous agents. *Journal of cutaneous medicine and surgery* **2005**, *8*, 424–31.

(175) Robey, R. W.; Steadman, K.; Polgar, O.; Bates, S. E. ABCG2-mediated transport of photosensitizers: potential impact on photodynamic therapy. *Cancer biology & therapy* **2005**, *4*, 187–94.

(176) Ebert, B.; Seidel, A.; Lampen, A. Identification of BCRP as transporter of benzo[a]pyrene conjugates metabolically formed in Caco-2 cells and its induction by Ah-receptor agonists. *Carcinogenesis* **2005**, *26*, 1754–63.

(177) Van Herwaarden, A. E.; Wagenaar, E.; Karnekamp, B.; Merino, G.; Jonker, J. W.; Schinkel, A. H. Breast cancer resistance protein (Bcrp1/Abcg2) reduces systemic exposure of the dietary carcinogens aflatoxin B1, IQ and Trp-P-1 but also mediates their secretion into breast milk. *Carcinogenesis* **2006**, *27*, 123–30.

(178) Gardner, E. R.; Ahlers, C. M.; Shukla, S.; Sissung, T. M.; Ockers, S. B.; Price, D. K.; Hamada, A.; Robey, R. W.; Steinberg, S. M.; Ambudkar, S. V; Dahut, W. L.; Figg, W. D. Association of the ABCG2 C421A polymorphism with prostate cancer risk and survival. *BJU international* **2008**, *102*, 1694–9.

(179) Hu, L.-L.; Wang, X.-X.; Chen, X.; Chang, J.; Li, C.; Zhang, Y.; Yang, J.; Jiang, W.; Zhuang, S.-M. BCRP gene polymorphisms are associated with susceptibility and survival of diffuse large B-cell lymphoma. *Carcinogenesis* **2007**, *28*, 1740–4.

(180) Scalbert, A.; Williamson, G. Dietary intake and bioavailability of polyphenols. *The Journal of nutrition* **2000**, *130*, 2073S–85S.

(181) Manach, C.; Scalbert, A.; Morand, C.; Rémésy, C.; Jiménez, L. Polyphenols: food sources and bioavailability. *The American journal of clinical nutrition* **2004**, *79*, 727–47.

(182) Somerset, S. M.; Johannot, L. Dietary flavonoid sources in Australian adults. *Nutrition and cancer* **2008**, *60*, 442–9.

(183) De Vries, J. H.; Janssen, P. L.; Hollman, P. C.; Van Staveren, W. A.; Katan, M. B. Consumption of quercetin and kaempferol in free-living subjects eating a variety of diets. *Cancer letters* **1997**, *114*, 141–4.

(184) An, G.; Gallegos, J.; Morris, M. E. The Bioflavonoid Kaempferol Is an Abcg2 Substrate and Inhibits Abcg2-Mediated Quercetin Efflux ABSTRACT : **2011**, *39*, 426–432.

(185) Sesink, A. L. A.; Arts, I. C. W.; De Boer, V. C. J.; Breedveld, P.; Schellens, J. H. M.; Hollman, P. C. H.; Russel, F. G. M. Breast cancer resistance protein (Bcrp1/Abcg2) limits net intestinal uptake of quercetin in rats by facilitating apical efflux of glucuronides. *Molecular pharmacology* **2005**, *67*, 1999–2006.

(186) Van Herwaarden, A. E.; Wagenaar, E.; Merino, G.; Jonker, J. W.; Rosing, H.; Beijnen, J. H.; Schinkel, A. H. Multidrug transporter ABCG2/breast cancer resistance protein secretes riboflavin (vitamin B2) into milk. *Molecular and cellular biology* **2007**, *27*, 1247–53.

(187) Brand, W.; Oosterhuis, B.; Krajcsi, P.; Barron, D.; Dionisi, F.; Van Bladeren, P. J.; Rietjens, I. M. C. M.; Williamson, G. Interaction of hesperetin glucuronide conjugates with human BCRP, MRP2 and MRP3 as detected in membrane vesicles of overexpressing baculovirus-infected Sf9 cells. *Biopharmaceutics & drug disposition* **2011**, *32*, 530–5.

(188) Brand, W.; Van der Wel, P. A. I.; Rein, M. J.; Barron, D.; Williamson, G.; Van Bladeren, P. J.; Rietjens, I. M. C. M. Metabolism and transport of the citrus flavonoid hesperetin in Caco-2 cell monolayers. *Drug metabolism and disposition: the biological fate of chemicals* **2008**, *36*, 1794–802.

(189) Robey, R. W.; Medina-Pérez, W. Y.; Nishiyama, K.; Lahusen, T.; Miyake, K.; Litman, T.; Senderowicz, A. M.; Ross, D. D.; Bates, S. E. Overexpression of the ATP-binding cassette half-transporter, ABCG2 (Mxr/BCrp/ABCP1), in flavopiridol-resistant human breast cancer cells. *Clinical cancer research : an official journal of the American Association for Cancer Research* **2001**, *7*, 145–52.

(190) Imai, Y.; Tsukahara, S.; Asada, S.; Sugimoto, Y. Phytoestrogens/flavonoids reverse breast cancer resistance protein/ABCG2-mediated multidrug resistance. *Cancer research* **2004**, *64*, 4346–52.

(191) Yang, Z.; Zhu, W.; Gao, S.; Yin, T.; Jiang, W.; Hu, M. Breast cancer resistance protein (ABCG2) determines distribution of genistein phase II metabolites: reevaluation of the roles of ABCG2 in the disposition of genistein. *Drug metabolism and disposition: the biological fate of chemicals* **2012**, *40*, 1883–93.

(192) Enokizono, J.; Kusuhara, H.; Sugiyama, Y. Effect of breast cancer resistance protein (Bcrp/Abcg2) on the disposition of phytoestrogens. *Molecular pharmacology* **2007**, *72*, 967–75.

(193) Imai, Y.; Asada, S.; Tsukahara, S.; Ishikawa, E.; Tsuruo, T.; Sugimoto, Y. Breast cancer resistance protein exports sulfated estrogens but not free estrogens. *Molecular pharmacology* **2003**, *64*, 610–8.

(194) Mao, Q.; Conseil, G.; Gupta, A.; Cole, S. P. C.; Unadkat, J. D. Functional expression of the human breast cancer resistance protein in Pichia pastoris. *Biochemical and biophysical research communications* **2004**, *320*, 730–7.

(195) Han, Y.; Busler, D.; Hong, Y.; Tian, Y.; Chen, C.; Rodrigues, A. D. Transporter studies with the 3-O-sulfate conjugate of 17alpha-ethinylestradiol: assessment of human liver drug transporters. *Drug metabolism and disposition: the biological fate of chemicals* **2010**, *38*, 1072–82.

(196) Zhang, Y.; Byun, Y.; Ren, Y. R.; Liu, J. O.; Laterra, J.; Pomper, M. G. Identification of inhibitors of ABCG2 by a bioluminescence imaging-based high-throughput assay. *Cancer research* **2009**, *69*, 5867–75.

(197) Zhang, Y.; Bressler, J. P.; Neal, J.; Lal, B.; Bhang, H.-E. C.; Laterra, J.; Pomper, M. G. ABCG2/BCRP expression modulates D-Luciferin based bioluminescence imaging. *Cancer research* **2007**, *67*, 9389–97.

(198) Scharenberg, C. W.; Harkey, M. A.; Torok-Storb, B. The ABCG2 transporter is an efficient Hoechst 33342 efflux pump and is preferentially expressed by immature human hematopoietic progenitors. *Blood* **2002**, *99*, 507–12.

(199) Kim, M.; Turnquist, H.; Jackson, J.; Sgagias, M.; Yan, Y.; Gong, M.; Dean, M.; Sharp, J. G.; Cowan, K. The multidrug resistance transporter ABCG2 (breast cancer resistance protein 1) effluxes Hoechst 33342 and is overexpressed in hematopoietic stem cells. *Clinical cancer research : an official journal of the American Association for Cancer Research* **2002**, *8*, 22–8.

(200) Robey, R. W.; Honjo, Y.; Van de Laar, A.; Miyake, K.; Regis, J. T.; Litman, T.; Bates, S. E. A functional assay for detection of the mitoxantrone resistance protein, MXR (ABCG2). *Biochimica et biophysica acta* **2001**, *1512*, 171–82.

(201) De Waart, D. R.; Häusler, S.; Vlaming, M. L. H.; Kunne, C.; Hänggi, E.; Gruss, H.; Oude Elferink, R. P. J.; Stieger, B. Hepatic transport mechanisms of cholyl-L-lysyl-fluorescein. *The Journal of pharmacology and experimental therapeutics* **2010**, *334*, 78–86.

(202) Blazquez, A. G.; Briz, O.; Romero, M. R.; Rosales, R.; Monte, M. J.; Vaquero, J.; Macias, R. I. R.; Cassio, D.; Marin, J. J. G. Characterization of the role of ABCG2

as a bile acid transporter in liver and placenta. *Molecular pharmacology* **2012**, *81*, 273–83.

(203) Woodward, O. M.; Köttgen, A.; Coresh, J.; Boerwinkle, E.; Guggino, W. B.; Köttgen, M. Identification of a urate transporter, ABCG2, with a common functional polymorphism causing gout. *Proceedings of the National Academy of Sciences of the United States of America* **2009**, *106*, 10338–42.

(204) Reginato, A. M.; Mount, D. B.; Yang, I.; Choi, H. K. The genetics of hyperuricaemia and gout. *Nature reviews. Rheumatology* **2012**, *8*, 610–21.

(205) Tan, Y.-C.; Blumenfeld, J.; Rennert, H. Autosomal dominant polycystic kidney disease: genetics, mutations and microRNAs. *Biochimica et biophysica acta* **2011**, *1812*, 1202–12.

(206) Peters, D. J.; Spruit, L.; Saris, J. J.; Ravine, D.; Sandkuijl, L. A.; Fossdal, R.; Boersma, J.; Van Eijk, R.; Nørby, S.; Constantinou-Deltas, C. D. Chromosome 4 localization of a second gene for autosomal dominant polycystic kidney disease. *Nature genetics* **1993**, *5*, 359–62.

(207) Shukla, S.; Wu, C.-P.; Nandigama, K.; Ambudkar, S. V The naphthoquinones, vitamin K3 and its structural analogue plumbagin, are substrates of the multidrug resistance linked ATP binding cassette drug transporter ABCG2. *Molecular cancer therapeutics* **2007**, *6*, 3279–86.

(208) Brechbuhl, H. M.; Min, E.; Kariya, C.; Frederick, B.; Raben, D.; Day, B. J. Select cyclopentenone prostaglandins trigger glutathione efflux and the role of ABCG2 transport. *Free radical biology & medicine* **2009**, *47*, 722–30.

(209) Ji, Y.; Morris, M. E. Membrane transport of dietary phenethyl isothiocyanate by ABCG2 (breast cancer resistance protein). *Molecular pharmaceutics* **2005**, *2*, 414–9.

(210) Takabe, K.; Kim, R. H.; Allegood, J. C.; Mitra, P.; Ramachandran, S.; Nagahashi, M.; Harikumar, K. B.; Hait, N. C.; Milstien, S.; Spiegel, S. Estradiol induces export of sphingosine 1-phosphate from breast cancer cells via ABCC1 and ABCG2. *The Journal of biological chemistry* **2010**, *285*, 10477–86.

(211) Woehlecke, H.; Pohl, A.; Alder-Baerens, N.; Lage, H.; Herrmann, A. Enhanced exposure of phosphatidylserine in human gastric carcinoma cells overexpressing the half-size ABC transporter BCRP (ABCG2). *The Biochemical journal* **2003**, *376*, 489–95.

(212) Tai, L. M.; Loughlin, a J.; Male, D. K.; Romero, I. a P-glycoprotein and breast cancer resistance protein restrict apical-to-basolateral permeability of human brain endothelium to amyloid-beta. *Journal of cerebral blood flow and metabolism :*

official journal of the International Society of Cerebral Blood Flow and Metabolism **2009**, *29*, 1079–83.

(213) Lebedeva, I. V; Pande, P.; Patton, W. F. Sensitive and specific fluorescent probes for functional analysis of the three major types of mammalian ABC transporters. *PloS one* **2011**, *6*, e22429.

(214) Henrich, C. J.; Robey, R. W.; Bokesch, H. R.; Bates, S. E.; Shukla, S.; Ambudkar, S. V; Dean, M.; McMahon, J. B. New inhibitors of ABCG2 identified by high-throughput screening. *Molecular cancer therapeutics* **2007**, *6*, 3271–8.

(215) Qadir, M.; O'Loughlin, K. L.; Fricke, S. M.; Williamson, N. a; Greco, W. R.; Minderman, H.; Baer, M. R. Cyclosporin A is a broad-spectrum multidrug resistance modulator. *Clinical cancer research : an official journal of the American Association for Cancer Research* **2005**, *11*, 2320–6.

(216) Rabindran, S. K.; He, H.; Singh, M.; Brown, E.; Collins, K. I.; Annable, T.; Greenberger, L. M. Reversal of a novel multidrug resistance mechanism in human colon carcinoma cells by fumitremorgin C. *Cancer research* **1998**, *58*, 5850–8.

(217) Minderman, H.; Suvannasankha, A.; O'Loughlin, K. L.; Scheffer, G. L.; Scheper, R. J.; Robey, R. W.; Baer, M. R. Flow cytometric analysis of breast cancer resistance protein expression and function. *Cytometry* **2002**, *48*, 59–65.

(218) Ozvegy, C.; Váradi, A.; Sarkadi, B. Characterization of drug transport, ATP hydrolysis, and nucleotide trapping by the human ABCG2 multidrug transporter. Modulation of substrate specificity by a point mutation. *The Journal of biological chemistry* **2002**, *277*, 47980–90.

(219) Noguchi, K.; Kawahara, H.; Kaji, A.; Katayama, K.; Mitsuhashi, J.; Sugimoto, Y. Substrate-dependent bidirectional modulation of P-glycoprotein-mediated drug resistance by erlotinib. *Cancer science* **2009**, *100*, 1701–7.

(220) Van Loevezijn, a; Allen, J. D.; Schinkel, a H.; Koomen, G. J. Inhibition of BCRP-mediated drug efflux by fumitremorgin-type indolyl diketopiperazines. *Bioorganic & medicinal chemistry letters* **2001**, *11*, 29–32.

(221) Allen, J. D.; Van Loevezijn, A.; Lakhai, J. M.; Van der Valk, M.; Van Tellingen, O.; Reid, G.; Schellens, J. H. M.; Koomen, G.-J.; Schinkel, A. H. Potent and specific inhibition of the breast cancer resistance protein multidrug transporter in vitro and in mouse intestine by a novel analogue of fumitremorgin C. *Molecular cancer therapeutics* **2002**, *1*, 417–25.

(222) De Bruin, M.; Miyake, K.; Litman, T.; Robey, R.; Bates, S. E. Reversal of resistance by GF120918 in cell lines expressing the ABC half-transporter, MXR. *Cancer letters* **1999**, *146*, 117–26.

(223) Kruijtzer, C. M. F. Increased Oral Bioavailability of Topotecan in Combination With the Breast Cancer Resistance Protein and P-Glycoprotein Inhibitor GF120918. *Journal of Clinical Oncology* **2002**, *20*, 2943–2950.

(224) Imai, Y.; Tsukahara, S.; Ishikawa, E.; Tsuruo, T.; Sugimoto, Y. Estrone and 17beta-estradiol reverse breast cancer resistance protein-mediated multidrug resistance. *Japanese journal of cancer research : Gann* **2002**, *93*, 231–5.

(225) Sugimoto, Y.; Tsukahara, S.; Imai, Y.; Ueda, K.; Tsuruo, T. Reversal of breast cancer resistance protein-mediated drug resistance by estrogen antagonists and agonists. *Molecular cancer therapeutics* **2003**, *2*, 105–12.

(226) Charmandari, E.; Kino, T.; Chrousos, G. P. Glucocorticoids and their actions: an introduction. *Annals of the New York Academy of Sciences* **2004**, *1024*, 1–8.

(227) Houghton, P. J.; Germain, G. S.; Harwood, F. C.; Schuetz, J. D.; Stewart, C. F.; Buchdunger, E.; Traxler, P. Imatinib mesylate is a potent inhibitor of the ABCG2 (BCRP) transporter and reverses resistance to topotecan and SN-38 in vitro. *Cancer research* **2004**, *64*, 2333–7.

(228) Nakamura, Y.; Oka, M.; Soda, H.; Shiozawa, K.; Yoshikawa, M.; Itoh, A.; Ikegami, Y.; Tsurutani, J.; Nakatomi, K.; Kitazaki, T.; Doi, S.; Yoshida, H.; Kohno, S. Gefitinib ("Iressa", ZD1839), an epidermal growth factor receptor tyrosine kinase inhibitor, reverses breast cancer resistance protein/ABCG2-mediated drug resistance. *Cancer research* **2005**, *65*, 1541–6.

(229) Ozvegy-Laczka, C.; Hegedus, T.; Várady, G.; Ujhelly, O.; Schuetz, J. D.; Váradi, A.; Kéri, G.; Orfi, L.; Német, K.; Sarkadi, B. High-affinity interaction of tyrosine kinase inhibitors with the ABCG2 multidrug transporter. *Molecular pharmacology* **2004**, *65*, 1485–95.

(230) Nakanishi, T.; Shiozawa, K.; Hassel, B. a; Ross, D. D. Complex interaction of BCRP/ABCG2 and imatinib in BCR-ABL-expressing cells: BCRP-mediated resistance to imatinib is attenuated by imatinib-induced reduction of BCRP expression. *Blood* **2006**, *108*, 678–84.

(231) Dohse, M.; Scharenberg, C.; Shukla, S.; Robey, R. W.; Volkmann, T.; Deeken, J. F.; Brendel, C.; Ambudkar, S. V; Neubauer, A.; Bates, S. E. Comparison of ATP-binding cassette transporter interactions with the tyrosine kinase inhibitors imatinib, nilotinib, and dasatinib. *Drug metabolism and disposition: the biological fate of chemicals* **2010**, *38*, 1371–80.

(232) Brendel, C.; Scharenberg, C.; Dohse, M.; Robey, R. W.; Bates, S. E.; Shukla, S.; Ambudkar, S. V; Wang, Y.; Wennemuth, G.; Burchert, a; Boudriot, U.; Neubauer, a Imatinib mesylate and nilotinib (AMN107) exhibit high-affinity interaction with

ABCG2 on primitive hematopoietic stem cells. *Leukemia : official journal of the Leukemia Society of America, Leukemia Research Fund, U.K* **2007**, *21*, 1267–75.

(233) Dai, C.; Tiwari, A. K.; Wu, C.-P.; Su, X.-D.; Wang, S.-R.; Liu, D.; Ashby, C. R.; Huang, Y.; Robey, R. W.; Liang, Y.; Chen, L.; Shi, C.-J.; Ambudkar, S. V; Chen, Z.-S.; Fu, L. Lapatinib (Tykerb, GW572016) reverses multidrug resistance in cancer cells by inhibiting the activity of ATP-binding cassette subfamily B member 1 and G member 2. *Cancer research* **2008**, *68*, 7905–14.

(234) Dai, C.; Liang, Y.; Wang, Y.; Tiwari, A. K.; Yan, Y.; Wang, F.; Chen, Z.; Tong, X.; Fu, L. Sensitization of ABCG2-overexpressing cells to conventional chemotherapeutic agent by sunitinib was associated with inhibiting the function of ABCG2. *Cancer letters* **2009**, *279*, 74–83.

(235) Tamaki, H.; Satoh, H.; Hori, S.; Ohtani, H.; Sawada, Y. Inhibitory effects of herbal extracts on breast cancer resistance protein (BCRP) and structure-inhibitory potency relationship of isoflavonoids. *Drug metabolism and pharmacokinetics* **2010**, *25*, 170–9.

(236) Ahmed-Belkacem, A.; Pozza, A.; Muñoz-Martínez, F.; Bates, S. E.; Castanys, S.; Gamarro, F.; Di Pietro, A.; Pérez-Victoria, J. M. Flavonoid structure-activity studies identify 6-prenylchrysin and tectochrysin as potent and specific inhibitors of breast cancer resistance protein ABCG2. *Cancer research* **2005**, *65*, 4852–60.

(237) Zhang, S.; Yang, X.; Morris, M. E. Flavonoids are inhibitors of breast cancer resistance protein (ABCG2)-mediated transport. *Molecular pharmacology* **2004**, *65*, 1208–16.

(238) Cooray, H. C.; Janvilisri, T.; Van Veen, H. W.; Hladky, S. B.; Barrand, M. a Interaction of the breast cancer resistance protein with plant polyphenols. *Biochemical and biophysical research communications* **2004**, *317*, 269–75.

(239) An, G.; Morris, M. E. Effects of single and multiple flavonoids on BCRP-mediated accumulation, cytotoxicity and transport of mitoxantrone in vitro. *Pharmaceutical research* **2010**, *27*, 1296–308.

(240) Pick, A.; Müller, H.; Mayer, R.; Haenisch, B.; Pajeva, I. K.; Weigt, M.; Bönisch, H.; Müller, C. E.; Wiese, M. Structure-activity relationships of flavonoids as inhibitors of breast cancer resistance protein (BCRP). *Bioorganic & medicinal chemistry* **2011**, *19*, 2090–102.

(241) Yoshikawa, M.; Ikegami, Y.; Sano, K.; Yoshida, H.; Mitomo, H.; Sawada, S.; Ishikawa, T. Transport of SN-38 by the wild type of human ABC transporter ABCG2 and its inhibition by quercetin, a natural flavonoid. *Journal of experimental therapeutics & oncology* **2004**, *4*, 25–35.

(242) Zhang, S.; Wang, X.; Sagawa, K.; Morris, M. E. Flavonoids chrysin and benzoflavone, potent breast cancer resistance protein inhibitors, have no significant effect on topotecan pharmacokinetics in rats or mdr1a/1b (-/-) mice. *Drug metabolism and disposition: the biological fate of chemicals* **2005**, *33*, 341–8.

(243) Zhang, S.; Yang, X.; Morris, M. E. Combined effects of multiple flavonoids on breast cancer resistance protein (ABCG2)-mediated transport. *Pharmaceutical research* **2004**, *21*, 1263–73.

(244) Valdameri, G.; Gauthier, C.; Terreux, R.; Kachadourian, R.; Day, B. J.; Winnischofer, S. M. B.; Rocha, M. E. M.; Frachet, V.; Ronot, X.; Di Pietro, A.; Boumendjel, A. Investigation of chalcones as selective inhibitors of the breast cancer resistance protein: critical role of methoxylation in both inhibition potency and cytotoxicity. *Journal of medicinal chemistry* **2012**, *55*, 3193–200.

(245) Lim, G. P.; Chu, T.; Yang, F.; Beech, W.; Frautschy, S. a; Cole, G. M. The curry spice curcumin reduces oxidative damage and amyloid pathology in an Alzheimer transgenic mouse. *The Journal of neuroscience : the official journal of the Society for Neuroscience* **2001**, *21*, 8370–7.

(246) Chearwae, W.; Shukla, S.; Limtrakul, P.; Ambudkar, S. V Modulation of the function of the multidrug resistance-linked ATP-binding cassette transporter ABCG2 by the cancer chemopreventive agent curcumin. *Molecular cancer therapeutics* **2006**, *5*, 1995–2006.

(247) Limtrakul, P.; Chearwae, W.; Shukla, S.; Phisalphong, C.; Ambudkar, S. V Modulation of function of three ABC drug transporters, P-glycoprotein (ABCB1), mitoxantrone resistance protein (ABCG2) and multidrug resistance protein 1 (ABCC1) by tetrahydrocurcumin, a major metabolite of curcumin. *Molecular and cellular biochemistry* **2007**, *296*, 85–95.

(248) Kawahara, H.; Noguchi, K.; Katayama, K.; Mitsuhashi, J.; Sugimoto, Y. Pharmacological interaction with sunitinib is abolished by a germ-line mutation (1291T>C) of BCRP/ABCG2 gene. *Cancer science* **2010**, *101*, 1493–500.

(249) Wang, J.-S.; Zhu, H.-J.; Markowitz, J. S.; Donovan, J. L.; Yuan, H.-J.; Devane, C. L. Antipsychotic drugs inhibit the function of breast cancer resistance protein. *Basic & clinical pharmacology & toxicology* **2008**, *103*, 336–41.

(250) Yang, C.-H.; Chen, Y.-C.; Kuo, M.-L. Novobiocin sensitizes BCRP/MXR/ABCP overexpressing topotecan-resistant human breast carcinoma cells to topotecan and mitoxantrone. *Anticancer research 23*, 2519–23.

(251) Robey, R. W.; Shukla, S.; Steadman, K.; Obrzut, T.; Finley, E. M.; Ambudkar, S. V; Bates, S. E. Inhibition of ABCG2-mediated transport by protein kinase

inhibitors with a bisindolylmaleimide or indolocarbazole structure. *Molecular cancer therapeutics* **2007**, *6*, 1877–85.

(252) Minderman, H.; O'Loughlin, K. L.; Pendyala, L.; Baer, M. R. VX-710 (biricodar) increases drug retention and enhances chemosensitivity in resistant cells overexpressing P-glycoprotein, multidrug resistance protein, and breast cancer resistance protein. *Clinical cancer research : an official journal of the American Association for Cancer Research* **2004**, *10*, 1826–34.

(253) Zhou, X.; Yang, X.; Wang, Q.; Coburn, R. A.; Morris, M. E. Effects of dihydropyridines and pyridines on multidrug resistance mediated by breast cancer resistance protein: in vitro and in vivo studies. *Drug metabolism and disposition: the biological fate of chemicals* **2005**, *33*, 1220–8.

(254) Imai, Y.; Yoshimori, M.; Fukuda, K.; Yamagishi, H.; Ueda, Y. The PI3K/Akt inhibitor LY294002 reverses BCRP-mediated drug resistance without affecting BCRP translocation. *Oncology reports* **2012**, *27*, 1703–9.

(255) Peng, H.; Dong, Z.; Qi, J.; Yang, Y.; Liu, Y.; Li, Z.; Xu, J.; Zhang, J.-T. A novel two mode-acting inhibitor of ABCG2-mediated multidrug transport and resistance in cancer chemotherapy. *PloS one* **2009**, *4*, e5676.

(256) Peng, H.; Qi, J.; Dong, Z.; Zhang, J.-T. Dynamic vs static ABCG2 inhibitors to sensitize drug resistant cancer cells. *PloS one* **2010**, *5*, e15276.

(257) Minderman, H.; Brooks, T. a; O'Loughlin, K. L.; Ojima, I.; Bernacki, R. J.; Baer, M. R. Broad-spectrum modulation of ATP-binding cassette transport proteins by the taxane derivatives ortataxel (IDN-5109, BAY 59-8862) and tRA96023. *Cancer chemotherapy and pharmacology* **2004**, *53*, 363–9.

(258) Jekerle, V.; Klinkhammer, W.; Reilly, R. M.; Piquette-Miller, M.; Wiese, M. Novel tetrahydroisoquinolin-ethyl-phenylamine based multidrug resistance inhibitors with broad-spectrum modulating properties. *Cancer chemotherapy and pharmacology* **2007**, *59*, 61–9.

(259) Jekerle, V.; Klinkhammer, W.; Scollard, D. a; Breitbach, K.; Reilly, R. M.; Piquette-Miller, M.; Wiese, M. In vitro and in vivo evaluation of WK-X-34, a novel inhibitor of P-glycoprotein and BCRP, using radio imaging techniques. *International journal of cancer. Journal international du cancer* **2006**, *119*, 414–22.

(260) Ding, R.; Shi, J.; Pabon, K.; Scotto, K. W. Xanthines down-regulate the drug transporter ABCG2 and reverse multidrug resistance. *Molecular pharmacology* **2012**, *81*, 328–37.

(261) Gupta, A.; Zhang, Y.; Unadkat, J. D.; Mao, Q. HIV protease inhibitors are inhibitors but not substrates of the human breast cancer resistance protein (BCRP/ABCG2). *The Journal of pharmacology and experimental therapeutics* **2004**, *310*, 334–41.

(262) Boumendjel, A.; Nicolle, E.; Moraux, T.; Gerby, B.; Blanc, M.; Ronot, X.; Boutonnat, J. Piperazinobenzopyranones and phenalkylaminobenzopyranones: potent inhibitors of breast cancer resistance protein (ABCG2). *Journal of medicinal chemistry* **2005**, *48*, 7275–81.

(263) Brooks, T. A.; Minderman, H.; O'Loughlin, K. L.; Pera, P.; Ojima, I.; Baer, M. R.; Bernacki, R. J.; Brooks, T. Taxane-based reversal agents modulate drug resistance mediated by P-glycoprotein, multidrug resistance protein, and breast cancer resistance protein. *Molecular cancer therapeutics* **2003**, *2*, 1195–205.

(264) Zhao, E.; Mu, Q. Phytoestrogen biological actions on Mammalian reproductive system and cancer growth. *Scientia pharmaceutica* **2011**, *79*, 1–20.

(265) Jonker, J. W.; Merino, G.; Musters, S.; Van Herwaarden, A. E.; Bolscher, E.; Wagenaar, E.; Mesman, E.; Dale, T. C.; Schinkel, A. H. The breast cancer resistance protein BCRP (ABCG2) concentrates drugs and carcinogenic xenotoxins into milk. *Nature medicine* **2005**, *11*, 127–9.

(266) Noguchi, K.; Katayama, K.; Mitsuhashi, J.; Sugimoto, Y. Functions of the breast cancer resistance protein (BCRP/ABCG2) in chemotherapy. *Advanced drug delivery reviews* **2009**, *61*, 26–33.

(267) Kim, Y. H.; Ishii, G.; Goto, K.; Ota, S.; Kubota, K.; Murata, Y.; Mishima, M.; Saijo, N.; Nishiwaki, Y.; Ochiai, A. Expression of breast cancer resistance protein is associated with a poor clinical outcome in patients with small-cell lung cancer. *Lung cancer (Amsterdam, Netherlands)* **2009**, *65*, 105–11.

(268) Zamber, C. P.; Lamba, J. K.; Yasuda, K.; Farnum, J.; Thummel, K.; Schuetz, J. D.; Schuetz, E. G. Natural allelic variants of breast cancer resistance protein (BCRP) and their relationship to BCRP expression in human intestine. *Pharmacogenetics* **2003**, *13*, 19–28.

(269) Suvannasankha, a; Minderman, H.; O'Loughlin, K. L.; Nakanishi, T.; Greco, W. R.; Ross, D. D.; Baer, M. R. Breast cancer resistance protein (BCRP/MXR/ABCG2) in acute myeloid leukemia: discordance between expression and function. *Leukemia : official journal of the Leukemia Society of America, Leukemia Research Fund, U.K* **2004**, *18*, 1252–7.

(270) Suvannasankha, A.; Minderman, H.; O'Loughlin, K. L.; Nakanishi, T.; Ford, L. a; Greco, W. R.; Wetzler, M.; Ross, D. D.; Baer, M. R. Breast cancer resistance protein (BCRP/MXR/ABCG2) in adult acute lymphoblastic leukaemia: frequent

expression and possible correlation with shorter disease-free survival. *British journal of haematology* **2004**, *127*, 392–8.

(271) Benderra, Z.; Faussat, A.-M.; Sayada, L.; Perrot, J.-Y.; Chaoui, D.; Marie, J.-P.; Legrand, O. Breast cancer resistance protein and P-glycoprotein in 149 adult acute myeloid leukemias. *Clinical cancer research : an official journal of the American Association for Cancer Research* **2004**, *10*, 7896–902.

(272) Tsunoda, S.; Okumura, T.; Ito, T.; Kondo, K.; Ortiz, C.; Tanaka, E.; Watanabe, G.; Itami, A.; Sakai, Y.; Shimada, Y. ABCG2 expression is an independent unfavorable prognostic factor in esophageal squamous cell carcinoma. *Oncology* **2006**, *71*, 251–8.

(273) Usuda, J.; Tsunoda, Y.; Ichinose, S.; Ishizumi, T.; Ohtani, K.; Maehara, S.; Ono, S.; Tsutsui, H.; Ohira, T.; Okunaka, T.; Furukawa, K.; Sugimoto, Y.; Kato, H.; Ikeda, N. Breast cancer resistant protein (BCRP) is a molecular determinant of the outcome of photodynamic therapy (PDT) for centrally located early lung cancer. *Lung cancer (Amsterdam, Netherlands)* **2010**, *67*, 198–204.

(274) Uggla, B.; Ståhl, E.; Wågsäter, D.; Paul, C.; Karlsson, M. G.; Sirsjö, A.; Tidefelt, U. BCRP mRNA expression v. clinical outcome in 40 adult AML patients. *Leukemia research* **2005**, *29*, 141–6.

(275) Yoh, K. Breast Cancer Resistance Protein Impacts Clinical Outcome in Platinum-Based Chemotherapy for Advanced Non-Small Cell Lung Cancer. *Clinical Cancer Research* **2004**, *10*, 1691–1697.

(276) Jitsukawa, K.; Suizu, R.; Hidano, A. Chlorella photosensitization. New phytophotodermatosis. *International journal of dermatology* **1984**, *23*, 263–8.

(277) Wan, P.; Moat, S.; Anstey, A. Pellagra: a review with emphasis on photosensitivity. *The British journal of dermatology* **2011**, *164*, 1188–200.

(278) Ho, A. Y. L.; Deacon, A.; Osborne, G.; Mufti, G. J. Precipitation of porphyria cutanea tarda by imatinib mesylate? *British journal of haematology* **2003**, *121*, 375.

(279) Brazzelli, V.; Prestinari, F.; Barbagallo, T.; Rona, C.; Orlandi, E.; Passamonti, F.; Locatelli, F.; Zecca, M.; Villani, S.; Borroni, G. A long-term time course of colorimetric assessment of the effects of imatinib mesylate on skin pigmentation: a study of five patients. *Journal of the European Academy of Dermatology and Venereology : JEADV* **2007**, *21*, 384–7.

(280) Brazzelli, V.; Muzio, F.; Manna, G.; Moggio, E.; Vassallo, C.; Orlandi, E.; Fiandrino, G.; Lucioni, M.; Borroni, G. Photoinduced dermatitis and oral lichenoid

reaction in a chronic myeloid leukemia patient treated with imatinib mesylate. *Photodermatology, photoimmunology & photomedicine* **2012**, *28*, 2–5.

(281) Boumendjel, a; Macalou, S.; Valdameri, G.; Pozza, a; Gauthier, C.; Arnaud, O.; Nicolle, E.; Magnard, S.; Falson, P.; Terreux, R.; Carrupt, P.; Payen, L.; Di Pietro, a Targeting the multidrug ABCG2 transporter with flavonoidic inhibitors: in vitro optimization and in vivo validation. *Current medicinal chemistry* **2011**, *18*, 3387–401.

(282) Tamura, A.; Wakabayashi, K.; Onishi, Y.; Takeda, M.; Ikegami, Y.; Sawada, S.; Tsuji, M.; Matsuda, Y.; Ishikawa, T. Re-evaluation and functional classification of non-synonymous single nucleotide polymorphisms of the human ATP-binding cassette transporter ABCG2. *Cancer Science* **2007**, *98*, 231–239.

(283) Krishnamurthy, P.; Schuetz, J. D. The ABC transporter Abcg2/Bcrp: role in hypoxia mediated survival. *Biometals : an international journal on the role of metal ions in biology, biochemistry, and medicine* **2005**, *18*, 349–58.

(284) IEIRI, I. Functional Significance of Genetic Polymorphisms in P-glycoprotein (MDR1, ABCB1) and Breast Cancer Resistance Protein (BCRP, ABCG2). *Drug metabolism and pharmacokinetics* **2011**.

(285) Cascorbi, I. Role of pharmacogenetics of ATP-binding cassette transporters in the pharmacokinetics of drugs. *Pharmacology & therapeutics* **2006**, *112*, 457–73.

(286) Sarkadi, B.; Homolya, L.; Szakács, G.; Váradi, A. Human multidrug resistance ABCB and ABCG transporters: participation in a chemoimmunity defense system. *Physiological reviews* **2006**, *86*, 1179–236.

(287) Urban, T. J.; Sebro, R.; Hurowitz, E. H.; Leabman, M. K.; Badagnani, I.; Lagpacan, L. L.; Risch, N.; Giacomini, K. M. Functional genomics of membrane transporters in human populations. *Genome research* **2006**, *16*, 223–30.

(288) Meyer, H. E.; Kroemer, H. K. *Drug Transporters: In Vitro and In Vivo Evidence for the Importance of Breast Cancer Resistance Protein Transporters (BCRP/MXR/ABCP/ABCG2)*; Fromm, M. F.; Kim, R. B., Eds.; Springer Berlin Heidelberg: Berlin, Heidelberg, 2011; Vol. 201.

(289) Mizuarai, S.; Aozasa, N.; Kotani, H. Single nucleotide polymorphisms result in impaired membrane localization and reduced atpase activity in multidrug transporter ABCG2. *International journal of cancer. Journal international du cancer* **2004**, *109*, 238–46.

(290) Tamura, A.; Wakabayashi, K.; Onishi, Y.; Nakagawa, H.; Tsuji, M.; Matsuda, Y.; Ishikawa, T. Genetic polymorphisms of human ABC transporter ABCG2: development of the standard method for functional validation of SNPs by using the

Flp recombinase system. *Journal of experimental therapeutics & oncology* **2006**, *6*, 1–11.

(291) Kondo, C.; Suzuki, H.; Itoda, M.; Ozawa, S.; Sawada, J.; Kobayashi, D.; Ieiri, I.; Mine, K.; Ohtsubo, K.; Sugiyama, Y. Functional analysis of SNPs variants of BCRP/ABCG2. *Pharmaceutical research* **2004**, *21*, 1895–903.

(292) Ingelheim, B.; Imai, Y.; Nakane, M.; Kage, K.; Tsukahara, S.; Ishikawa, E.; Tsuruo, T.; Miki, Y.; Sugimoto, Y. C421A polymorphism in the human breast cancer resistance protein gene is associated with low expression of Q141K protein and low-level drug resistance. *Molecular cancer therapeutics* **2002**, *1*, 611–6.

(293) Ishikawa, T.; Sakurai, A.; Kanamori, Y.; Nagakura, M.; Hirano, H.; Takarada, Y.; Yamada, K.; Fukushima, K.; Kitajima, M. High-speed screening of human ATP-binding cassette transporter function and genetic polymorphisms: new strategies in pharmacogenomics. *Methods in enzymology* **2005**, *400*, 485–510.

(294) Morisaki, K.; Robey, R. W.; Ozvegy-Laczka, C.; Honjo, Y.; Polgar, O.; Steadman, K.; Sarkadi, B.; Bates, S. E. Single nucleotide polymorphisms modify the transporter activity of ABCG2. *Cancer chemotherapy and pharmacology* **2005**, *56*, 161–72.

(295) Kim, D. H. D.; Sriharsha, L.; Xu, W.; Kamel-Reid, S.; Liu, X.; Siminovitch, K.; Messner, H. a.; Lipton, J. H. Clinical relevance of a pharmacogenetic approach using multiple candidate genes to predict response and resistance to imatinib therapy in chronic myeloid leukemia. *Clinical cancer research : an official journal of the American Association for Cancer Research* **2009**, *15*, 4750–8.

(296) Gardner, E. R.; Burger, H.; Van Schaik, R. H.; Van Oosterom, A. T.; De Bruijn, E. a; Guetens, G.; Prenen, H.; De Jong, F. a; Baker, S. D.; Bates, S. E.; Figg, W. D.; Verweij, J.; Sparreboom, A.; Nooter, K. Association of enzyme and transporter genotypes with the pharmacokinetics of imatinib. *Clinical pharmacology and therapeutics* **2006**, *80*, 192–201.

(297) Sugimoto, Y.; Tsukahara, S.; Ishikawa, E.; Mitsuhashi, J. Breast cancer resistance protein: molecular target for anticancer drug resistance and pharmacokinetics/pharmacodynamics. *Cancer science* **2005**, *96*, 457–65.

(298) Kasza, I.; Várady, G.; Andrikovics, H.; Koszarska, M.; Tordai, A.; Scheffer, G. L.; Németh, A.; Szakács, G.; Sarkadi, B. Expression Levels of the ABCG2 Multidrug Transporter in Human Erythrocytes Correspond to Pharmacologically Relevant Genetic Variations. *PloS one* **2012**, *7*, e48423.

(299) Furukawa, T.; Wakabayashi, K.; Tamura, A.; Nakagawa, H.; Morishima, Y.; Osawa, Y.; Ishikawa, T. Major SNP (Q141K) variant of human ABC transporter

ABCG2 undergoes lysosomal and proteasomal degradations. *Pharmaceutical research* **2009**, *26*, 469–79.

(300) Wakabayashi-Nakao, K.; Tamura, A.; Furukawa, T.; Nakagawa, H.; Ishikawa, T. Quality control of human ABCG2 protein in the endoplasmic reticulum: ubiquitination and proteasomal degradation. *Advanced drug delivery reviews* **2009**, *61*, 66–72.

(301) Yamasaki, Y.; Ieiri, I.; Kusuhara, H.; Sasaki, T.; Kimura, M.; Tabuchi, H.; Ando, Y.; Irie, S.; Ware, J.; Nakai, Y.; Higuchi, S.; Sugiyama, Y. Pharmacogenetic characterization of sulfasalazine disposition based on NAT2 and ABCG2 (BCRP) gene polymorphisms in humans. *Clinical pharmacology and therapeutics* **2008**, *84*, 95–103.

(302) Kim, I.-S.; Kim, H.-G.; Kim, D. C.; Eom, H.-S.; Kong, S.-Y.; Shin, H.-J.; Hwang, S.-H.; Lee, E.-Y.; Lee, G.-W. ABCG2 Q141K polymorphism is associated with chemotherapy-induced diarrhea in patients with diffuse large B-cell lymphoma who received frontline rituximab plus cyclophosphamide/doxorubicin/vincristine/prednisone chemotherapy. *Cancer science* **2008**, *99*, 2496–501.

(303) Cusatis, G.; Gregorc, V.; Li, J.; Spreafico, A.; Ingersoll, R. G.; Verweij, J.; Ludovini, V.; Villa, E.; Hidalgo, M.; Sparreboom, A.; Baker, S. D. Pharmacogenetics of ABCG2 and adverse reactions to gefitinib. *Journal of the National Cancer Institute* **2006**, *98*, 1739–42.

(304) Erdilyi, D. J.; Kámory, E.; Csókay, B.; Andrikovics, H.; Tordai, a; Kiss, C.; Filni-Semsei, a; Janszky, I.; Zalka, a; Fekete, G.; Falus, a; Kovács, G. T.; Szalai, C. Synergistic interaction of ABCB1 and ABCG2 polymorphisms predicts the prevalence of toxic encephalopathy during anticancer chemotherapy. *The pharmacogenomics journal* **2008**, *8*, 321–7.

(305) Nguyen, T. D.; Gow, J. M.; Chinn, L. W.; Kelly, L.; Jeong, H.; Huang, C. C.; Stryke, D.; Kawamoto, M.; Johns, S. J.; Carlson, E.; Taylor, T.; Ferrin, T. E.; Sali, A.; Giacomini, K. M.; Kroetz, D. L. PharmGKB submission update: IV. PMT submissions of genetic variations in ATP-Binding cassette transporters to the PharmGKB network. *Pharmacological reviews* **2006**, *58*, 1–2.

(306) Honjo, Y.; Morisaki, K.; Huff, L.; Robey, R. W.; Hung, J.; Dean, M.; Bates, S. E. Single-nucleotide polymorphism (SNP) analysis in the ABC half-transporter ABCG2 (MXR/BCRP/ABCP1). *Cancer biology & ...* **2002**, *2*, 696–702.

(307) Aekawa, K. M.; Toda, M. I.; Ai, K. S.; Aito, Y. S.; Aniwa, N. K.; Hirao, K. S.; Amaguchi, T. H.; Unitoh, H. K.; Amamoto, N. Y.; Amura, T. T.; Inami, H. M.; Ubota, K. K.; Htsu, A. O.; Maekawa, K.; Itoda, M.; Sai, K.; Saito, Y. Genetic

variation and haplotype structure of the ABC transporter gene ABCG2 in a Japanese population. *Drug metabolism and* **2006**, *21*, 109–121.

(308) Imai, Y.; Nakane, M.; Kage, K.; Tsukahara, S.; Ishikawa, E.; Tsuruo, T.; Miki, Y.; Sugimoto, Y. C421A polymorphism in the human breast cancer resistance protein gene is associated with low expression of Q141K protein and low-level drug resistance. *Molecular cancer therapeutics* **2002**, *1*, 611–6.

(309) Lee, S. S.; Jeong, H.; Yi, J.; Jung, H.; Jang, J.; Kim, E.; Lee, S.; Shin, J.; Al, L. E. E. E. T. Identification and Functional Assessment of BCRP Polymorphisms in a Korean Population. *Pharmacology* **2007**, *35*, 623–632.

(310) Bäckström, G.; Taipalensuu, J.; Melhus, H.; Brändström, H.; Svensson, A.-C.; Artursson, P.; Kindmark, A. Genetic variation in the ATP-binding cassette transporter gene ABCG2 (BCRP) in a Swedish population. *European journal of pharmaceutical sciences : official journal of the European Federation for Pharmaceutical Sciences* **2003**, *18*, 359–64.

(311) ITODA, M.; SAITO, Y.; SHIRAO, K. Eight novel single nucleotide polymorphisms in ABCG2/BCRP in Japanese cancer patients administered irinotacan. *Drug metabolism and …* **2003**, *18*, 212–217.

(312) Ishikawa, T.; Nakagawa, H.; Hagiya, Y.; Nonoguchi, N.; Miyatake, S.-I.; Kuroiwa, T. Key Role of Human ABC Transporter ABCG2 in Photodynamic Therapy and Photodynamic Diagnosis. *Advances in pharmacological sciences* **2010**, *2010*, 587306.

(313) Bosch, T. M.; Kjellberg, L. M.; Bouwers, A.; Koeleman, B. P. C.; Schellens, J. H. M.; Beijnen, J. H.; Smits, P. H. M.; Meijerman, I. Detection of single nucleotide polymorphisms in the ABCG2 gene in a Dutch population. *American journal of pharmacogenomics : genomics-related research in drug development and clinical practice* **2005**, *5*, 123–31.

(314) Cheng, G. M. Y.; To, K. K. W. Adverse Cell Culture Conditions Mimicking the Tumor Microenvironment Upregulate ABCG2 to Mediate Multidrug Resistance and a More Malignant Phenotype. *ISRN oncology* **2012**, *2012*, 746025.

(315) Pradhan, M.; Bembinster, L. a; Baumgarten, S. C.; Frasor, J. Proinflammatory cytokines enhance estrogen-dependent expression of the multidrug transporter gene ABCG2 through estrogen receptor and NF{kappa}B cooperativity at adjacent response elements. *The Journal of biological chemistry* **2010**, *285*, 31100–6.

(316) Jigorel, E.; Vee, M. Le; Boursier-neyret, C.; Parmentier, Y.; Fardel, O. Differential Regulation of Sinusoidal and Canalicular Hepatic Drug Transporter Expression by Xenobiotics Activating Drug-Sensing Receptors in Primary Human Hepatocytes ABSTRACT : **2006**, *34*, 1756–1763.

(317) Wang, H.; Lee, E.; Zhou, L.; Leung, P. C. K.; Ross, D. D.; Unadkat, J. D.; Mao, Q. Progesterone receptor (PR) isoforms PRA and PRB differentially regulate expression of the breast cancer resistance protein in human placental choriocarcinoma BeWo cells. *Molecular pharmacology* **2008**, *73*, 845–54.

(318) Zhang, Y.; Zhou, G.; Wang, H.; Zhang, X.; Wei, F.; Cai, Y.; Yin, D. Transcriptional upregulation of breast cancer resistance protein by 17beta-estradiol in ERalpha-positive MCF-7 breast cancer cells. *Oncology* **2006**, *71*, 446–55.

(319) Lemos, C.; Kathmann, I.; Giovannetti, E.; Dekker, H.; Scheffer, G. L.; Calhau, C.; Jansen, G.; Peters, G. J. Folate deprivation induces BCRP (ABCG2) expression and mitoxantrone resistance in Caco-2 cells. *International journal of cancer. Journal international du cancer* **2008**, *123*, 1712–20.

(320) Lemos, C.; Kathmann, I.; Giovannetti, E.; Calhau, C.; Jansen, G.; Peters, G. J. Impact of cellular folate status and epidermal growth factor receptor expression on BCRP/ABCG2-mediated resistance to gefitinib and erlotinib. *British journal of cancer* **2009**, *100*, 1120–7.

(321) Smith, R. P.; Lam, E. T.; Markova, S.; Yee, S. W.; Ahituv, N. Pharmacogene regulatory elements: from discovery to applications. *Genome medicine* **2012**, *4*, 45.

(322) Campbell, P. K.; Zong, Y.; Yang, S.; Zhou, S.; Rubnitz, J. E.; Sorrentino, B. P. Identification of a novel, tissue-specific ABCG2 promoter expressed in pediatric acute megakaryoblastic leukemia. *Leukemia research* **2011**, *35*, 1321–9.

(323) Nakanishi, T.; Bailey-Dell, K. J.; Hassel, B. a; Shiozawa, K.; Sullivan, D. M.; Turner, J.; Ross, D. D. Novel 5' untranslated region variants of BCRP mRNA are differentially expressed in drug-selected cancer cells and in normal human tissues: implications for drug resistance, tissue-specific expression, and alternative promoter usage. *Cancer research* **2006**, *66*, 5007–11.

(324) Natarajan, K.; Xie, Y.; Nakanishi, T.; Beck, W. T.; Bauer, K. S.; Ross, D. D. Identification and characterization of the major alternative promoter regulating Bcrp1/Abcg2 expression in the mouse intestine. *Biochimica et biophysica acta* **2011**, *1809*, 295–305.

(325) Bailey-Dell, K. J.; Hassel, B.; Doyle, L. a; Ross, D. D. Promoter characterization and genomic organization of the human breast cancer resistance protein (ATP-binding cassette transporter G2) gene. *Biochimica et biophysica acta* **2001**, *1520*, 234–41.

(326) Zong, Y.; Zhou, S.; Fatima, S.; Sorrentino, B. P. Expression of mouse Abcg2 mRNA during hematopoiesis is regulated by alternative use of multiple leader exons and promoters. *The Journal of biological chemistry* **2006**, *281*, 29625–32.

(327) To, K. K. W.; Robey, R.; Zhan, Z.; Bangiolo, L.; Bates, S. E. Upregulation of ABCG2 by romidepsin via the aryl hydrocarbon receptor pathway. *Molecular cancer research : MCR* **2011**, *9*, 516–27.

(328) Tan, K. P.; Wang, B.; Yang, M.; Boutros, P. C.; Macaulay, J.; Xu, H.; Chuang, A. I.; Kosuge, K.; Yamamoto, M.; Takahashi, S.; Wu, A. M. L.; Ross, D. D.; Harper, P. A.; Ito, S. Aryl Hydrocarbon Receptor Is a Transcriptional Activator of the Human Breast Cancer Resistance Protein (BCRP / ABCG2) □. **2010**.

(329) Ee, P. L. R. Identification of a Novel Estrogen Response Element in the Breast Cancer Resistance Protein (ABCG2) Gene. *Cancer Research* **2004**, *64*, 1247–1251.

(330) Krishnamurthy, P.; Ross, D. D.; Nakanishi, T.; Bailey-Dell, K.; Zhou, S.; Mercer, K. E.; Sarkadi, B.; Sorrentino, B. P.; Schuetz, J. D. The stem cell marker Bcrp/ABCG2 enhances hypoxic cell survival through interactions with heme. *The Journal of biological chemistry* **2004**, *279*, 24218–25.

(331) Singh, A.; Wu, H.; Zhang, P.; Happel, C. Expression of ABCG2 (BCRP) is regulated by Nrf2 in cancer cells that confers side population and chemoresistance phenotype. *Molecular cancer ...* **2010**, *9*, 2365–2376.

(332) Wu, A. M. L.; Dalvi, P.; Lu, X.; Yang, M.; Riddick, D. S.; Matthews, J.; Clevenger, C. V; Ross, D. D.; Harper, P. a; Ito, S. *Induction of Multidrug Resistance Transporter ABCG2 by Prolactin in Human Breast Cancer Cells.*; 2012.

(333) Herkert, B.; Eilers, M. Transcriptional repression: the dark side of myc. *Genes & cancer* **2010**, *1*, 580–6.

(334) Porro, A.; Iraci, N.; Soverini, S.; Diolaiti, D.; Gherardi, S.; Terragna, C.; Durante, S.; Valli, E.; Kalebic, T.; Bernardoni, R.; Perrod, C.; Haber, M.; Norris, M. D.; Baccarani, M.; Martinelli, G.; Perini, G. c-MYC Oncoprotein Dictates Transcriptional Profiles of ATP-Binding Cassette Transporter Genes in Chronic Myelogenous Leukemia CD34+ Hematopoietic Progenitor Cells. *Molecular cancer research : MCR* **2011**, *9*, 1054–66.

(335) Rudin, C. M.; Liu, W.; Desai, A.; Karrison, T.; Jiang, X.; Janisch, L.; Das, S.; Ramirez, J.; Poonkuzhali, B.; Schuetz, E.; Fackenthal, D. L.; Chen, P.; Armstrong, D. K.; Brahmer, J. R.; Fleming, G. F.; Vokes, E. E.; Carducci, M. A.; Ratain, M. J. Pharmacogenomic and pharmacokinetic determinants of erlotinib toxicity. *Journal of clinical oncology : official journal of the American Society of Clinical Oncology* **2008**, *26*, 1119–27.

(336) Ehrlich, M.; Gama-Sosa, M. Amount and distribution of 5-methylcytosine in human DNA from different types of tissues or cells. *Nucleic acids ...* **1982**, *10*, 11–14.

(337) Takai, D.; Jones, P. a Comprehensive analysis of CpG islands in human chromosomes 21 and 22. *Proceedings of the National Academy of Sciences of the United States of America* **2002**, *99*, 3740–5.

(338) Bird, A. CpG-rich islands and the function of DNA methylation. *Nature* **1986**.

(339) Cooper, S. J.; Trinklein, N. D.; Anton, E. D.; Nguyen, L.; Myers, R. M. Comprehensive analysis of transcriptional promoter structure and function in 1% of the human genome. *Genome research* **2006**, *16*, 1–10.

(340) Larsen, F.; Gundersen, G.; Lopez, R.; Prydz, H. CpG islands as gene markers in the human genome. *Genomics* **1992**, *13*, 1095–107.

(341) Reik, W.; Murrell, A. Silence across the border. **2000**, *405*, 408–409.

(342) Wolffe, a P. Transcriptional control: imprinting insulation. *Current biology : CB* **2000**, *10*, R463–5.

(343) Ding, S.; Gong, B.-D.; Yu, J.; Gu, J.; Zhang, H.-Y.; Shang, Z.-B.; Fei, Q.; Wang, P.; Zhu, J.-D. Methylation profile of the promoter CpG islands of 14 "drug-resistance" genes in hepatocellular carcinoma. *World journal of gastroenterology : WJG* **2004**, *10*, 3433–40.

(344) To, K. K. W.; Zhan, Z.; Bates, S. E. Aberrant promoter methylation of the ABCG2 gene in renal carcinoma. *Molecular and cellular biology* **2006**, *26*, 8572–85.

(345) Nakano, H.; Nakamura, Y.; Soda, H.; Kamikatahira, M.; Uchida, K.; Takasu, M.; Kitazaki, T.; Yamaguchi, H.; Nakatomi, K.; Yanagihara, K.; Kohno, S.; Tsukamoto, K. Methylation status of breast cancer resistance protein detected by methylation-specific polymerase chain reaction analysis is correlated inversely with its expression in drug-resistant lung cancer cells. *Cancer* **2008**, *112*, 1122–30.

(346) Turner, J. G.; Gump, J. L.; Zhang, C.; Cook, J. M.; Marchion, D.; Hazlehurst, L.; Munster, P.; Schell, M. J.; Dalton, W. S.; Sullivan, D. M. ABCG2 expression, function, and promoter methylation in human multiple myeloma. *Blood* **2006**, *108*, 3881–9.

(347) Bram, E.; Stark, M.; Raz, S.; Assaraf, Y. Chemotherapeutic drug-induced ABCG2 promoter demethylation as a novel mechanism of acquired multidrug resistance. *Neoplasia (New York, NY)* **2009**, *11*, 1359–1370.

(348) Chen, M.; Xue, X.; Wang, F.; An, Y.; Tang, D.; Xu, Y.; Wang, H.; Yuan, Z.; Gao, W.; Wei, J.; Zhang, J.; Miao, Y. Expression and promoter methylation analysis of ATP-binding cassette genes in pancreatic cancer. *Oncology reports* **2012**, *27*, 265–9.

(349) Bram, E.; Stark, M.; Raz, S. Chemotherapeutic drug-induced ABCG2 promoter demethylation as a novel mechanism of acquired multidrug resistance. *Neoplasia (New York, NY)* **2009**, *11*, 1359–1370.

(350) Hiraki, M.; Kitajima, Y.; Sato, S.; Mitsuno, M.; Koga, Y.; Nakamura, J.; Hashiguchi, K.; Noshiro, H.; Miyazaki, K. Aberrant gene methylation in the lymph nodes provides a possible marker for diagnosing micrometastasis in gastric cancer. *Annals of surgical oncology* **2010**, *17*, 1177–86.

(351) Georgitsi, M.; Zukic, B.; Pavlovic, S.; Patrinos, G. P. Transcriptional regulation and pharmacogenomics. *Pharmacogenomics* **2011**, *12*, 655–73.

(352) Tirona, R. Molecular mechanisms of drug transporter regulation. *Drug Transporters* **2011**, *201*.

(353) Urquhart, B.; Tirona, R.; Kim, R. Nuclear receptors and the regulation of drug-metabolizing enzymes and drug transporters: implications for interindividual variability in response to drugs. *The Journal of Clinical …* **2007**.

(354) Germain, P.; Staels, B.; Dacquet, C.; Spedding, M.; Laudet, V. Overview of Nomenclature of Nuclear Receptors. **2006**, *58*, 685–704.

(355) Schupp, M.; Lazar, M. a Endogenous ligands for nuclear receptors: digging deeper. *The Journal of biological chemistry* **2010**, *285*, 40409–15.

(356) Mangelsdorf, D. J.; Thummel, C.; Beato, M.; Herrlich, P.; Schütz, G.; Umesono, K.; Blumberg, B.; Kastner, P.; Mark, M.; Chambon, P.; Evans, R. M. The nuclear receptor superfamily: the second decade. *Cell* **1995**, *83*, 835–9.

(357) Olefsky, J. M. Nuclear receptor minireview series. *The Journal of biological chemistry* **2001**, *276*, 36863–4.

(358) Klinge, C. M.; Bodenner, D. L.; Desai, D.; Niles, R. M.; Traish, a M. Binding of type II nuclear receptors and estrogen receptor to full and half-site estrogen response elements in vitro. *Nucleic acids research* **1997**, *25*, 1903–12.

(359) Germain, P.; Chambon, P.; Eichele, G.; Evans, R. M.; Lazar, M. A.; Leid, M.; De Lera, A. R.; Lotan, R.; Mangelsdorf, D. J.; Gronemeyer, H. International Union of Pharmacology. LXIII. Retinoid X receptors. *Pharmacological reviews* **2006**, *58*, 760–72.

(360) Novac, N.; Heinzel, T. Nuclear receptors: overview and classification. *Current drug targets. Inflammation and allergy* **2004**, *3*, 335–46.

(361) Lee, S. K.; Choi, H. S.; Song, M. R.; Lee, M. O.; Lee, J. W. Estrogen receptor, a common interaction partner for a subset of nuclear receptors. *Molecular endocrinology (Baltimore, Md.)* **1998**, *12*, 1184–92.

(362) Szatmari, I.; Vámosi, G.; Brazda, P.; Balint, B. L.; Benko, S.; Széles, L.; Jeney, V.; Ozvegy-Laczka, C.; Szántó, A.; Barta, E.; Balla, J.; Sarkadi, B.; Nagy, L. Peroxisome proliferator-activated receptor gamma-regulated ABCG2 expression confers cytoprotection to human dendritic cells. *The Journal of biological chemistry* **2006**, *281*, 23812–23.

(363) Overington, J. P.; Al-Lazikani, B.; Hopkins, A. L. How many drug targets are there? *Nature reviews. Drug discovery* **2006**, *5*, 993–6.

(364) Zhao, C.; Gao, H.; Liu, Y.; Papoutsi, Z.; Jaffrey, S.; Gustafsson, J.-A.; Dahlman-Wright, K. Genome-wide mapping of estrogen receptor-beta-binding regions reveals extensive cross-talk with transcription factor activator protein-1. *Cancer research* **2010**, *70*, 5174–83.

(365) Carroll, J. S.; Meyer, C. a; Song, J.; Li, W.; Geistlinger, T. R.; Eeckhoute, J.; Brodsky, A. S.; Keeton, E. K.; Fertuck, K. C.; Hall, G. F.; Wang, Q.; Bekiranov, S.; Sementchenko, V.; Fox, E. a; Silver, P. a; Gingeras, T. R.; Liu, X. S.; Brown, M. Genome-wide analysis of estrogen receptor binding sites. *Nature genetics* **2006**, *38*, 1289–97.

(366) Safe, S. Transcriptional activation of genes by 17 beta-estradiol through estrogen receptor-Sp1 interactions. *Vitamins and hormones* **2001**, *62*, 231–52.

(367) Schultz, J. R.; Petz, L. N.; Nardulli, A. M. Cell- and ligand-specific regulation of promoters containing activator protein-1 and Sp1 sites by estrogen receptors alpha and beta. *The Journal of biological chemistry* **2005**, *280*, 347–54.

(368) Dutertre, M.; Smith, C. L. Ligand-independent interactions of p160/steroid receptor coactivators and CREB-binding protein (CBP) with estrogen receptor-alpha: regulation by phosphorylation sites in the A/B region depends on other receptor domains. *Molecular endocrinology (Baltimore, Md.)* **2003**, *17*, 1296–314.

(369) Acevedo, M. L.; Kraus, W. L. Mediator and p300 / CBP-Steroid Receptor Coactivator Complexes Have Distinct Roles , but Function Synergistically , during Estrogen Receptor α -Dependent Transcription with Chromatin Templates Mediator and p300 / CBP-Steroid Receptor Coactivator Complexes. **2003**.

(370) Wilson, B. J. Does GATA3 act in tissue-specifi c pathways ? A meta-analysis-based approach. **2008**, 1–6.

(371) Tan, S. K.; Lin, Z. H.; Chang, C. W.; Varang, V.; Chng, K. R.; Pan, Y. F.; Yong, E. L.; Sung, W. K.; Sung, W. K.; Cheung, E. AP-2γ regulates oestrogen receptor-mediated long-range chromatin interaction and gene transcription. *The EMBO journal* **2011**, *30*, 2569–81.

(372) Ee, P. L. R.; He, X.; Ross, D. D.; Beck, W. T. Modulation of breast cancer resistance protein (BCRP / ABCG2) gene expression using RNA interference Modulation of breast cancer resistance protein (BCRP / ABCG2) gene expression using RNA interference. **2005**, 1577–1584.

(373) Yasuda, S.; Kobayashi, M.; Itagaki, S.; Hirano, T.; Iseki, K. Response of the ABCG2 promoter in T47D cells and BeWo cells to sex hormone treatment. *Molecular biology reports* **2009**, *36*, 1889–96.

(374) Wang, H.; Zhou, L.; Gupta, A.; Vethanayagam, R. R.; Zhang, Y.; Unadkat, J. D.; Mao, Q. Regulation of BCRP/ABCG2 expression by progesterone and 17beta-estradiol in human placental BeWo cells. *American journal of physiology. Endocrinology and metabolism* **2006**, *290*, E798–807.

(375) Imai, Y.; Ishikawa, E.; Asada, S.; Sugimoto, Y. Estrogen-mediated post transcriptional down-regulation of breast cancer resistance protein/ABCG2. *Cancer research* **2005**, *65*, 596–604.

(376) Lu, N. Z.; Wardell, S. E.; Burnstein, K. L.; Defranco, D.; Fuller, P. J.; Giguere, V.; Hochberg, R. B.; McKay, L.; Renoir, J.; Weigel, N. L.; Wilson, E. M.; McDonnell, D. P.; Cidlowski, J. A. International Union of Pharmacology. LXV. The pharmacology and classification of the nuclear receptor superfamily: glucocorticoid, mineralocorticoid, progesterone, and androgen receptors. *Pharmacological reviews* **2006**, *58*, 782–97.

(377) Ray, a; Prefontaine, K. E. Physical association and functional antagonism between the p65 subunit of transcription factor NF-kappa B and the glucocorticoid receptor. *Proceedings of the National Academy of Sciences of the United States of America* **1994**, *91*, 752–6.

(378) Oakley, R. H.; Cidlowski, J. a Cellular processing of the glucocorticoid receptor gene and protein: new mechanisms for generating tissue-specific actions of glucocorticoids. *The Journal of biological chemistry* **2011**, *286*, 3177–84.

(379) Glass, C. K.; Saijo, K. Nuclear receptor transrepression pathways that regulate inflammation in macrophages and T cells. *Nature reviews. Immunology* **2010**, *10*, 365–76.

(380) Rhen, T.; Cidlowski, J. a Antiinflammatory action of glucocorticoids--new mechanisms for old drugs. *The New England journal of medicine* **2005**, *353*, 1711–23.

(381) So, A. Y.-L.; Chaivorapol, C.; Bolton, E. C.; Li, H.; Yamamoto, K. R. Determinants of cell- and gene-specific transcriptional regulation by the glucocorticoid receptor. *PLoS genetics* **2007**, *3*, e94.

(382) So, A. Y.-L.; Cooper, S. B.; Feldman, B. J.; Manuchehri, M.; Yamamoto, K. R. Conservation analysis predicts in vivo occupancy of glucocorticoid receptor-binding sequences at glucocorticoid-induced genes. *Proceedings of the National Academy of Sciences of the United States of America* **2008**, *105*, 5745–9.

(383) Wong, D. L.; Siddall, B. J.; Ebert, S. N.; Bell, R. A.; Her, S. Phenylethanolamine N-methyltransferase gene expression: synergistic activation by Egr-1, AP-2 and the glucocorticoid receptor. *Brain research. Molecular brain research* **1998**, *61*, 154–61.

(384) Huang, W.; Glass, C. K. Nuclear receptors and inflammation control: molecular mechanisms and pathophysiological relevance. *Arteriosclerosis, thrombosis, and vascular biology* **2010**, *30*, 1542–9.

(385) Pascussi, J. M.; Drocourt, L.; Fabre, J. M.; Maurel, P.; Vilarem, M. J. Dexamethasone induces pregnane X receptor and retinoid X receptor-alpha expression in human hepatocytes: synergistic increase of CYP3A4 induction by pregnane X receptor activators. *Molecular pharmacology* **2000**, *58*, 361–72.

(386) Pascussi, J. M.; Drocourt, L.; Gerbal-Chaloin, S.; Fabre, J. M.; Maurel, P.; Vilarem, M. J. Dual effect of dexamethasone on CYP3A4 gene expression in human hepatocytes. Sequential role of glucocorticoid receptor and pregnane X receptor. *European journal of biochemistry / FEBS* **2001**, *268*, 6346–58.

(387) Yamaguchi, S.; Murata, Y.; Nagaya, T.; Hayashi, Y.; Ohmori, S.; Nimura, Y.; Seo, H. Glucocorticoids increase retinoid-X receptor alpha (RXRalpha) expression and enhance thyroid hormone action in primary cultured rat hepatocytes. *Journal of molecular endocrinology* **1999**, *22*, 81–90.

(388) Bhadhprasit, W.; Sakuma, T.; Hatakeyama, N.; Fuwa, M.; Kitajima, K.; Nemoto, N. Involvement of Glucocorticoid Receptor and Pregnane X Receptor in the Regulation of Mouse CYP3A44 Female-Predominant Expression by Glucocorticoid Hormone ABSTRACT : **2007**, *35*, 1880–1885.

(389) Honorat, M.; Mesnier, A.; Di Pietro, A.; Lin, V.; Cohen, P.; Dumontet, C.; Payen, L. Dexamethasone down-regulates ABCG2 expression levels in breast cancer cells. *Biochemical and biophysical research communications* **2008**, *375*, 308–14.

(390) Petropoulos, S.; Gibb, W.; Matthews, S. G. Glucocorticoid regulation of placental breast cancer resistance protein (Bcrp1) in the mouse. *Reproductive sciences (Thousand Oaks, Calif.)* **2011**, *18*, 631–9.

(391) Elahian, F.; Kalalinia, F.; Behravan, J. Dexamethasone downregulates BCRP mRNA and protein expression in breast cancer cell lines. *Oncology research* **2009**, *18*, 9–15.

(392) Schrem, H.; Klempnauer, J.; Borlak, J. Liver-enriched transcription factors in liver function and development. Part I: the hepatocyte nuclear factor network and liver-specific gene expression. *Pharmacological reviews* **2002**, *54*, 129–58.

(393) Kakizawa, T.; Miyamoto, T.; Ichikawa, K.; Kaneko, A.; Suzuki, S.; Hara, M.; Nagasawa, T.; Takeda, T.; Mori, J. i; Kumagai, M.; Hashizume, K. Functional interaction between Oct-1 and retinoid X receptor. *The Journal of biological chemistry* **1999**, *274*, 19103–8.

(394) Préfontaine, G. G.; Walther, R.; Giffin, W.; Lemieux, M. E.; Pope, L.; Haché, R. J. Selective binding of steroid hormone receptors to octamer transcription factors determines transcriptional synergism at the mouse mammary tumor virus promoter. *The Journal of biological chemistry* **1999**, *274*, 26713–9.

(395) Préfontaine, G. G.; Lemieux, M. E.; Giffin, W.; Schild-poulter, C.; Pope, L.; Lacasse, E.; Haché, R. J. G. Recruitment of Octamer Transcription Factors to DNA by Glucocorticoid Receptor Recruitment of Octamer Transcription Factors to DNA by Glucocorticoid Receptor. **1998**.

(396) Nuñez, S. B.; Medin, J. a; Braissant, O.; Kemp, L.; Wahli, W.; Ozato, K.; Segars, J. H. Retinoid X receptor and peroxisome proliferator-activated receptor activate an estrogen responsive gene independent of the estrogen receptor. *Molecular and cellular endocrinology* **1997**, *127*, 27–40.

(397) Keller, H.; Givel, F.; Perroud, M.; Wahli, W. Signaling cross-talk between peroxisome proliferator-activated receptor/retinoid X receptor and estrogen receptor through estrogen response elements. *Molecular endocrinology (Baltimore, Md.)* **1995**, *9*, 794–804.

(398) Min, G.; Kim, H.; Bae, Y.; Petz, L.; Kemper, J. K. Inhibitory cross-talk between estrogen receptor (ER) and constitutively activated androstane receptor (CAR). CAR inhibits ER-mediated signaling pathway by squelching p160 coactivators. *The Journal of biological chemistry* **2002**, *277*, 34626–33.

(399) Nader, N.; Ng, S. S. M.; Wang, Y.; Abel, B. S.; Chrousos, G. P.; Kino, T. Liver x receptors regulate the transcriptional activity of the glucocorticoid receptor: implications for the carbohydrate metabolism. *PloS one* **2012**, *7*, e26751.

(400) Konno, Y.; Negishi, M.; Kodama, S. The roles of nuclear receptors CAR and PXR in hepatic energy metabolism. *Drug metabolism and pharmacokinetics* **2008**, *23*, 8–13.

(401) Chen, Y.; Nie, D. Pregnane X receptor and its potential role in drug resistance in cancer treatment. *Recent patents on anti-cancer drug discovery* **2009**, *4*, 19–27.

(402) Lehmann, J. M.; McKee, D. D.; Watson, M. a; Willson, T. M.; Moore, J. T.; Kliewer, S. a The human orphan nuclear receptor PXR is activated by compounds that regulate CYP3A4 gene expression and cause drug interactions. *The Journal of clinical investigation* **1998**, *102*, 1016–23.

(403) Albermann, N.; Schmitz-Winnenthal, F. H.; Z'graggen, K.; Volk, C.; Hoffmann, M. M.; Haefeli, W. E.; Weiss, J. Expression of the drug transporters MDR1/ABCB1, MRP1/ABCC1, MRP2/ABCC2, BCRP/ABCG2, and PXR in peripheral blood mononuclear cells and their relationship with the expression in intestine and liver. *Biochemical pharmacology* **2005**, *70*, 949–58.

(404) Gahir, S. S.; Piquette-miller, M. Gestational and Pregnane X Receptor-Mediated Regulation of Placental ATP-Binding Cassette Drug Transporters in Mice □. **2011**, 465–471.

(405) Lemmen, J.; Tozakidis, I. E. P.; Galla, H.-J. Pregnane X receptor upregulates ABC-transporter Abcg2 and Abcb1 at the blood-brain barrier. *Brain research* **2012**, 1–13.

(406) Kliewer, S. a.; Goodwin, B.; Willson, T. M. The nuclear pregnane X receptor: a key regulator of xenobiotic metabolism. *Endocrine reviews* **2002**, *23*, 687–702.

(407) Kalaany, N. Y.; Mangelsdorf, D. J. LXRS and FXR: the yin and yang of cholesterol and fat metabolism. *Annual review of physiology* **2006**, *68*, 159–91.

(408) Makishima, M. Identification of a Nuclear Receptor for Bile Acids. *Science* **1999**, *284*, 1362–1365.

(409) Parks, D. J. Bile Acids: Natural Ligands for an Orphan Nuclear Receptor. *Science* **1999**, *284*, 1365–1368.

(410) Kast, H. R.; Goodwin, B.; Tarr, P. T.; Jones, S. A.; Anisfeld, A. M.; Stoltz, C. M.; Tontonoz, P.; Kliewer, S.; Willson, T. M.; Edwards, P. A. Regulation of multidrug resistance-associated protein 2 (ABCC2) by the nuclear receptors pregnane X receptor, farnesoid X-activated receptor, and constitutive androstane receptor. *The Journal of biological chemistry* **2002**, *277*, 2908–15.

(411) Meyer Zu Schwabedissen, H. E.; Böttcher, K.; Chaudhry, A.; Kroemer, H. K.; Schuetz, E. G.; Kim, R. B. Liver X receptor α and farnesoid X receptor are major transcriptional regulators of OATP1B1. *Hepatology (Baltimore, Md.)* **2010**, *52*, 1797–807.

(412) Ohtsuka, H.; Abe, T.; Onogawa, T.; Kondo, N.; Sato, T.; Oshio, H.; Mizutamari, H.; Mikkaichi, T.; Oikawa, M.; Rikiyama, T.; Katayose, Y.; Unno, M. Farnesoid X receptor, hepatocyte nuclear factors 1alpha and 3beta are essential for transcriptional activation of the liver-specific organic anion transporter-2 gene. *Journal of gastroenterology* **2006**, *41*, 369–77.

(413) Hu, M.; Lui, S. S. H.; Tam, L.-S.; Li, E. K.; Tomlinson, B. The farnesoid X receptor -1G>T polymorphism influences the lipid response to rosuvastatin. *Journal of lipid research* **2012**, *53*, 1384–9.

(414) Hankinson, O. Role of coactivators in transcriptional activation by the aryl hydrocarbon receptor. *Archives of biochemistry and biophysics* **2005**, *433*, 379–86.

(415) Ahmed, S.; Valen, E.; Sandelin, A.; Matthews, J. Dioxin increases the interaction between aryl hydrocarbon receptor and estrogen receptor alpha at human promoters. *Toxicological sciences : an official journal of the Society of Toxicology* **2009**, *111*, 254–66.

(416) Patel, R. D.; Murray, I. a; Flaveny, C. a; Kusnadi, A.; Perdew, G. H. Ah receptor represses acute-phase response gene expression without binding to its cognate response element. *Laboratory investigation; a journal of technical methods and pathology* **2009**, *89*, 695–707.

(417) Advance, T. High-resolution genome-wide mapping of AHR and ARNT binding sites by ChIP-Seq High-resolution genome-wide mapping of AHR and ARNT binding sites by ChIP-Seq Raymond Lo * and Jason Matthews * * Department of Pharmacology and Toxicology , University of Toron. **2012**.

(418) Nguyen, L. P.; Bradfield, C. a The search for endogenous activators of the aryl hydrocarbon receptor. *Chemical research in toxicology* **2008**, *21*, 102–16.

(419) Pfeifer, G. P.; Denissenko, M. F.; Olivier, M.; Tretyakova, N.; Hecht, S. S.; Hainaut, P. Tobacco smoke carcinogens, DNA damage and p53 mutations in smoking-associated cancers. *Oncogene* **2002**, *21*, 7435–51.

(420) Ebert, B.; Seidel, A.; Lampen, A. Phytochemicals induce breast cancer resistance protein in Caco-2 cells and enhance the transport of benzo[a]pyrene-3-sulfate. *Toxicological sciences : an official journal of the Society of Toxicology* **2007**, *96*, 227–36.

(421) Advance, T. The fungicide prochloraz and environmental pollutant dioxin induce the ABCG2 transporter in bovine mammary epithelial cells by the arylhydrocarbon receptor signalling pathway. **2012**.

(422) Tompkins, L. M.; Li, H.; Li, L.; Lynch, C.; Xie, Y.; Nakanishi, T.; Ross, D. D.; Wang, H. A novel xenobiotic responsive element regulated by aryl hydrocarbon

receptor is involved in the induction of BCRP/ABCG2 in LS174T cells. *Biochemical pharmacology* **2010**, *80*, 1754–61.

(423) Qiu, Y.; Krishnan, V.; Pereira, F. A.; Tsai, S. Y.; Tsai, M. J. Chicken ovalbumin upstream promoter-transcription factors and their regulation. *The Journal of steroid biochemistry and molecular biology* **1996**, *56*, 81–5.

(424) De Martino, M. U.; Alesci, S.; Chrousos, G. P.; Kino, T. Interaction of the glucocorticoid receptor and the chicken ovalbumin upstream promoter-transcription factor II (COUP-TFII): implications for the actions of glucocorticoids on glucose, lipoprotein, and xenobiotic metabolism. *Annals of the New York Academy of Sciences* **2004**, *1024*, 72–85.

(425) Shibata, H.; Nawaz, Z.; Tsai, S. Y.; O'Malley, B. W.; Tsai, M. J. Gene silencing by chicken ovalbumin upstream promoter-transcription factor I (COUP-TFI) is mediated by transcriptional corepressors, nuclear receptor-corepressor (N-CoR) and silencing mediator for retinoic acid receptor and thyroid hormone receptor (SMRT). *Molecular endocrinology (Baltimore, Md.)* **1997**, *11*, 714–24.

(426) Park, J.-I.; Tsai, S. Y.; Tsai, M.-J. Molecular mechanism of chicken ovalbumin upstream promoter-transcription factor (COUP-TF) actions. *The Keio journal of medicine* **2003**, *52*, 174–81.

Chapter 2 : Functional Characterization of MXR Variants

2.1. Abstract

The mitoxantrone resistance protein (MXR, BCRP, ABCG2) is an efflux membrane transporter with nonsynonymous variants that may alter the pharmacokinetic and pharmacodynamic properties of MXR substrates. In the present study, the expression and function of the MXR nonsynonymous variants V12M, Q141K, I206L, P269S, T542A, D620N and V12M/Q141K are characterized. Transient and stable expression of MXR variants in MCF-7 and HEK293 Flp-in cells, respectively, was used to investigate MXR function. Inhibitable efflux of MXR substrates was measured using flow cytometry and the localization and expression of the variant proteins was determined using Western blots and immunohistochemistry. Inside-out vesicles from the stable cell lines were used to test the ATPase and uptake activity of the MXR proteins. The V12M variant exhibits reduced protein expression but higher ATPase activity than the MXR reference protein. The Q141K variant also exhibited lower whole cell and membrane protein expression, consistent with published data. The first characterization of the T542A variant and V12M/Q141K transporters indicated no alteration in expression or function. The I206L had increased inhibitable efflux of the pheophorbide A compound and D620N had higher vanadate-sensitive ATPase activity. There was no alteration in localization of the MXR variants. In conclusion, MXR nonsynonymous variants have substrate-dependent alterations in function that may contribute to the interindividual variability in the pharmacokinetics and pharmacodynamics of MXR substrates.

2.2. Introduction

The mitoxantrone resistance protein (MXR, BCRP, ABCG2) is a member of the ATP-binding cassette (ABC) transporter family[1]. MXR and other ABCG subfamily members are half-transporters consisting of one nucleotide binding domain (NBD) and six transmembrane domains[2,3]. The functional MXR efflux transporter is found as both a homodimer and a tetramer [4,5]. MXR, located on the apical plasma membrane, transports a wide variety of compounds including nutrients, natural dietary toxins, cytotoxic agents and fluorescent drugs[6,78]. It is expressed in many tissues, including the intestine[9–12], liver[9–12], breast[10], placenta[9–16] and blood-brain barrier[10,12,17], thus playing an important role in the detoxification and protection of the body[8,18,19]. Not only has wide variability of ABCG2 expression been reported in normal tissues[20–22], but overexpression of ABCG2 is seen in some tumors[22–30] and has been associated with disease-free survival [22,24–30]. Overexpression of MXR also confers resistance to a variety of anticancer agents, including mitoxantrone, camptothecins (irinotecan, topotecan, SN-38) and anthracyclines[31–33].

Nonsynonymous variants of MXR and other ABC membrane transporters have been implicated in *in vivo* drug disposition, therapeutic efficacy and adverse drug reactions of their substrates[2,69–71]. The effects of transporter variants on different substrates are not always similar; in fact, 14% of variants in membrane transporters exhibited substrate specific defects in transport[72]. MXR has increased flexibility compared to other transporters and multiple substrate binding domains that have different inhibitor and substrate interactions[73]. MXR mutations occurring at the 482 amino acid are only found in drug-resistant cells lines. However the mutations exhibit extensive

substrate and antagonist specific activity[74]. The functional studies and phenotype association of other MXR nonsynonymous variants[7,70,75] indicate that some variants of MXR have substrate-dependent alterations in transport abilities. Thus, it is necessary to systematically characterize the substrate-dependent effects of *ABCG2* genetic variants.

MXR was initially identified in a cell line resistant to mitoxantrone[34,35], an anthracenedione derivative anticancer agent[36]. It is used in combination therapies to treat prostate and breast cancers and multiple sclerosis[37–39]. Mitoxantrone is often used in growth inhibition assays to measure the activity of the MXR protein[40], however its kinetic parameters for MXR (K_m and V_{max}) have never been reported. In fact, many MXR substrates are still lacking kinetic analysis. With the development of *ABCG2* Flp-in stable cell lines[41] and isolation techniques for inside-out vesicles[42], kinetic assays are now possible.

MXR knockout mice (*Abcg2*-/-) experience phototoxicity due to the accumulation of porphyrins[43], especially pheoporbide A, which are established MXR substrates[44,45]. Normally, MXR protects tissues during hypoxia by effluxing heme and porphyrin compounds out of the cell[46]. Phototoxicity is also a well known side effect of several anticancer kinase inhibitors[47–50], which are also MXR inhibitors[51], and it occurs in healthy individuals with chlorophyll rich diets[52]. Pheophorbide A is not a substrate of P-gp or MRP1 and has been targeted as a potential MXR specific probe[53]. However, nonsynonymous alleles of MXR have reduced porphyrin transport[54] which may contribute to cellular resistance to photodynamic therapy[55] and cause clinical phototoxicity.

Sulfasalazine is another specific substrate of MXR[56]. Sulfasalazine, of which 5-aminosalicylic acid is the active metabolite, is an anti-inflammatory medication used for rheumatoid arthritis and inflammatory bowel disease[57,58]. It has been used as a successful clinical marker of MXR activity and MXR inhibition[59,60]. It has also been used as a successful *in vivo* probe for MXR low-functioning alleles in healthy patients[21]. Understanding the contribution of MXR variants to sulfasalazine exposure and efficacy could lead to further use of this drug as an MXR probe substrate or help in facilitating optimal drug therapy for the widely occurring systemic inflammatory diseases.

Irinotecan, a cytotoxic camptothecin whose active metabolite is SN-38, is a commonly used anti-cancer agent for treatment of colorectal, lung and gastric tumors[61]. Both irinotecan and its active metabolite SN-38 are transported by MXR[62,63]. Overexpression of MXR can cause resistance to SN-38 and irinotecan *in vitro*[64,65]. The Q141K MXR variant has been associated with SN-38 pharmacokinetics[66], reduced *in vitro* transport[67] and severity of irinotecan-induced neutropenia[66]. There is also a report of one homozygous Q141K individual with extensive SN-38 accumulation[68]. Further clarification of the effect of Q141K on SN-38 transport and the investigation of other MXR variants could enhance our understanding of irinotecan pharmacogenomics.

Current research on MXR nonsynonymous variants focuses on variants with high, or frequent, minor allele frequencies (MAFs). However, decreased function variants of other membrane transporters have significantly lower allele frequencies and are more likely to alter evolutionarily conserved amino acid residues[72]. Aside from two variants, V12M and Q141K, most of the reported MXR variants have low MAFs. Therefore, it is important to determine if MXR variants, regardless of their MAFs, have altered function.

In this study, the effect of nonsynonymous variants identified in the SOPHIE cohort was investigated for their effect on the expression and function of MXR. The SOPHIE cohort is a group of ethnically diverse group of individuals who have donated DNA and are willing to be a part of future clinical pharmacogenomic studies[76]. Transiently and stably transfected cell lines were used to look at mRNA and protein expression, protein localization, and cellular efflux. Inside-out vesicles from the stably transfected cells were used to examine MXR vanadate-sensitive ATPase activity after stimulation with different MXR substrates. Preliminary studies were performed in inside-out vesicles to examine the kinetic parameters of mitoxantrone, SN38, pheophorbide A and sulfasalazine transport by MXR variants.

2.3. Materials and Methods

2.3.1. Chemicals and Materials

Mitoxantrone, sulfasalazine, doxorubicin hydrochloride, verapamil, pantoprazole sodium hydrate, protease inhibitor cocktail, CelLytic™ MT Lysis Buffer, Tween 20, sodium orthovanadate, fumitremorgin C (FTC), ouabain, sodium azide, estrone-3-sulfate, bis-tris propane (BTP), KCl, acridine orange, NADH, phosphol(enol)pyruvic acid (PEP), lactic dehydrogenase (LD) and pyruvate kinase (PK), creatine phosphate, creatine kinase, EGTA, $MgCl_2$, ATP magnesium salt, NaOH, sodium dodecyl sulfate (SDS), Triton X-100, Nunc LabTek II 2-well glass chamber slides and Potter-Elvenjem homogenizers were all purchased from Sigma Aldrich (St. Louis, MO). The 2X TaqMan Universal PCR Master Mix and Taqman probes ABCG2 hs01053796_m1, GAPDH Hs99999905_m1 and GusB Hs99999908_m1 were purchased from Applied Biosystems (Carlsbad, CA).

Vesicles made from mock transfected (BD CT) and MXR overexpressing (BD BCRP) Sf9 cells and 488-Alexa goat anti-mouse secondary antibody were purchased from BD Biosciences (San Jose, CA). Non-fat dried milk and 0.45 μm nitrocellulose membranes were both purchased from Bio-Rad (Hercules, CA). Pierce BCA assay kits and 1.1 mL polypropylene flow cytometer tubes were purchased from Thermo Scientific (Rockford IL). RNase Easy Mini Kits, QIAquick PCR Purification Kits and QIAprep Miniprep Kits were all purchased from Qiagen (Valencia, CA). The human embryonic kidney (HEK293) Flp-in cell line, high-glucose Dulbecco's modified Eagle's medium (DMEM), Opti-Minimal Essential Medium (Opti-MEM), dithiothreitol (DTT), BioRad Kaleidoscope Protein Ladder, NuPage 4X Sample buffer, β-mercapthanone, NuPage 20X running buffer, NuPage 20X transfer buffer, NOVEX-NuPAGE 4-12% Bis-Tris SDS-PAGE gels, GAPDH antibody (mouse anti-human), pOG44 vector, pcDNA5/FRT vector, DH5α competent cells, ProLong Gold Antifade plus DAPI mounting reagent, SuperScript® III First-Strand Synthesis System and Lipofectamine 2000 were all purchased from Invitrogen (Carlsbad, CA). The 100 mm LB Amp-100 agar plates, LB Broth supplemented with 100 μg/mL ampicilin and 10X MOPS buffer were purchased from Teknova (Hollister, CA). DMSO, 1X phosphate buffered saline (PBS), 0.05% trypsin, hygromycin, Tris-HCl, EDTA, HEPES and 100X penicillin and streptomycin were all purchased from the UCSF Cell Culture Facility (San Francisco, CA). Methanol and acetone were both purchased from Fisher Scientific (Pittsburgh, PA). High-Fidelity Phusion Buffer, Phusion High-Fidelity DNA Polymerase, bovine serum albumin (BSA), *Dpn*I, and *Dpn*I digestion buffer were all purchased from New England Biolabs (Ipswich, MA). All other materials including the human breast adenocarcinoma (MCF-7) cell line

(American Type Culture Collection, Manassas, VA), 10% fetal bovine serum (FBS, Axenia BioLogix, Dixon, CA), Improved Minimum Essential Medium (IMEM) without phenol red (Mediatech Inc, Manassas, VA), anti-human ABCG2 antibody 5D3 PE conjugated (eBioscience, San Diego, CA), mouse anti-human ABCG2 antibody BXP-21 (Santa Cruz, Paso Robles, CA), goat anti-mouse secondary antibody 800CW IRDye (LiCore, Lincoln NE), PD Multitrap G-25 Sephadex columns (GE Healthcare Biosciences, Pittsburgh, PA), 0.45 μM mixed cellulose ester (MCE) filter plates (Millipore, Billerica, MA), HYPERflasks (Corning, Corning, NY), PiColorLock ATPase Assay kits (Innova Biosciences, Cambridge, United Kingdom) and dNTPs (Denville, Metuchen, NJ) were all purchased from the indicated manufacturers. The human breast adenocarcinoma doxorubicin and verapamil resistant cell line (MCF-7 AdVp) was a generous gift from Susan Bates (National Cancer Institute, Bethesda, MD).

2.3.2. Genetic Analysis of ABCG2 Coding Region

SNPs in the *ABCG2* coding regions were retrieved for all available ethnic populations from publicly available databases, including 1000 Genomes (phase 1 release 02/14/2012)[77], dbSNP build 135, and HapMap release 28[78] and were combined with those from the SOPHIE cohort reported in the Pharmacogenetics of Membrane Transporter Database (http://pharmacogenetics.ucsf.edu/, UCSF, San Francisco, CA)[76]. Additional non-synonymous variants of MXR were extracted from previously published sequencing studies[79–82]. Details regarding the sequencing of SOPHIE samples for *ABCG2* coding SNPs have already been published[83]. Genotypes from 1000 Genomes (phase 1 release 05/21/2011) were used for calculating haplotypes. Haplotypes were determined

by downloading each region's genotype and information files from the 1000 Genomes browser for all available ethnic groups combined. Genotype and information files were then loaded into Haploview version 4.2[84] and linkage disequilibrium analysis was performed using all available SNPs. The potential effect of non-synonymous variants on MXR function were predicted using the Grantham scale[85], SIFT[86] and PolyPhen[87] prediction programs. Evolutionary conservation was determined by alignment of orthologous amino acid sequences from six species (chimp, dog, cow, mouse, rat and zebrafish) to that of the human sequence using the UCSC genome browser (http://genome.ucsc.edu/).

2.3.3. Cloning of MXR and Site Directed Mutagenesis for MXR Variant Plasmids

MXR was previously cloned in the Kroetz lab from human placental cDNA into the pcDNA5/FRT vector using the primers in Table 2.1. Variants where then introduced into the reference MXR pcDNA5/FRT plasmid. Site-directed mutagenesis (SDM) primers for each of the MXR nonsynonymous SNPs (Table 2.1) were designed using the PrimerX© program and synthesized by Integrated DNA Technologies (San Diego, CA). PCR reaction components for all primers are as follows: 1X High-Fidelity Phusion Buffer, 1 unit Phusion High-Fidelity DNA Polymerase, 200 nM dNTPs, 1 μM each primer and 100 ng reference MXR pcDNA5/FRT vector, all in a final volume of 50 μL. PCR reaction conditions for all primers are as follows: an initial cycle for 30 sec at 98°C, followed by 16 cycles of 10 sec at 98°C, melting temperature (varies per primer pair) for 30 sec and 3.5 min at 72°C, then a final extension for 10 min at 72°C. The SDM PCR reactions were then digested for at least 20 min at 37°C with 1 unit *Dpn*I. The reactions

were purified using the QIAquick PCR purification kit per the manufacturer's protocol, and 5 µL of the purified SDM reaction was transformed into 35 µL DH5α competent cells. After growing for 24 hr on 100 mm LB Amp-100 agar plates, single colonies were expanded overnight at 37°C with shaking in LB broth supplemented with 100 µg/mL ampicillin. DNA was isolated from the bacteria using the QIAprep Miniprep Kit per the manufacturer's protocol, and the plasmid was sequenced with the RVPrimer3 and other primers listed in Table 2.2 to confirm the presence of the SNP at the correct location. The DNA concentration was checked using a NanoDrop Spectrophotometer (Thermo Scientific) and stored at -20°C.

Table 2.1. Cloning and SDM Primers for MXR Variants

Variant	Primer Sequence[1]	Tm[2] (°C)
WT	CCTGAGCTCGTCCCCTGGATGTC	53
	GAGAACTGTAAGGGACAGGTATG	
V12M	GTCGAAGTTTTTATCCCAATGTCACAAGG	61
	CCTTGTGACATTGGGATAAAAACTTCGAC	
Q141K	CGGTGAGAGCAAAACTTAAAGTTCTCAGCAGC	64.7
	GCTGCTGAGAACTTTAAGTTTTGCTCTCACCG	
I206L	CACTGATCCTTCCCTCTTGTTCTTGGATGAG	64.4
	CTCATCCAAGAACAAGAGGGAAGGATCAGTG	
P269S	TCCTGAGCAGACCCGTGGAACATAA	64.6
	TTATGTTCCACGGGTCTGCTCAGGA	
T542A	GCAACACTTCTCATGGCCATCTGTTTTGTG	64.7
	CACAAAACAGATGGCCATGAGAAGTGTTGC	
D620N	AAAGCAGGGCATCAATCTCTCACCCTG	64.4
	CAGGGTGAGAGATTGATGCCCTGCTTT	

[1]Forward and reverse primers per SNP

[2]Melting temperature used for annealing step of PCR

Abbreviations: PCR, polymerase chain reaction; Tm, Temperature

Table 2.2. Sequencing Primers for MXR pcDNA5/FRT

Primer	Sequence
F3:294	GGAACGCACCGTGCACATGC
1003F	TAAAGTGGCAGACTCCAAGGTT
1749F	GATTCTACTGGAATCCAGAACAGAGC
2218R	TCGTGGAATGCTGAAGTACTGAAGCC
R2:2569	CAGTGTGATGGCAAGGGAACAG

Abbreviations: F, Forward; R, Reverse

2.3.4. Cell Culture

HEK293 Flp-in cells were grown in high-glucose DMEM supplemented with 10% FBS, 100 units/mL penicillin and 0.1 mg/mL streptomycin. The MCF-7 cell line was grown in IMEM without phenol red, supplemented with 10% FBS, 100 units/mL penicillin and 0.1mg/mL streptomycin. The MCF-7 ADVP cell line was grown in IMEM without phenol red, supplemented with 10% FBS, 100 units/mL penicillin, 0.1mg/mL streptomycin, 3 μg/ml doxorubicin and 5 μg/ml verapamil. All cell lines were grown in a 5% CO_2 incubator at 37°C. To maintain cells, they were split upon reaching confluency by treatment with 0.05% Trypsin-EDTA, washing with 1X PBS and suspension in fresh media at a 1:5 to 1:20 dilution.

2.3.5. Transient Transfection of MCF-7 Cells

For transient transfections, we utilized the parent cell line of the MCF-7 Ad/Vp cell line from which MXR was cloned, the MCF-7 cell line[9]. MCF-7 cells have low background expression of MXR (data not shown) and have been utilized through the literature in MXR transport assays[9,88]. MCF-7 cells were split with 0.05% Trypsin-EDTA, seeded at ~2 x 10^6 cells in a T-25 plate and transfected once they reached 95% confluency in fresh IMEM with 10% FBS, but without antibiotics and phenol red. Cells

were then transfected with Lipofectamine 2000 following guidelines suggested in the manufacturer's protocol. In short, 25 μL of Lipofectamine 2000 was diluted with 600 μL Opti-MEM and incubated for 5 min, then gently mixed with a 625 μL solution of 10 μg pcDNA5/FRT constructs diluted with Opti-MEM. The DNA-Lipofectamine mixture was allowed to incubate at room temperature for 30 min before being placed onto cells with 4 mL of antibiotic-free media. All cell lines were incubated with their transfection agents for 18-24 hr before use in the efflux assays.

2.3.6. Creation of Stable HEK293 Flp-in Cells

The stable HEK293 Flp-in cell lines were created by transfection of HEK293 Flp-in cells followed by selection with hygromycin. The HEK293 Flp-in cell line are commercially available cells that have an engineered single Flp-in site to ensure one cDNA clone of *ABCG2* is inserted at a controlled location; similar Flp-in cells have been used in other MXR experiments[41]. Also, the HEK293 Flp-in parent cell is the HEK293T cells, which have low to undetectable expression of MXR (data not shown). HEK293 Flp-in cells were split with 0.05% Trypsin-EDTA, seeded at ~5 x 10^5 cells per well of a 6-well plate and transfected once they reached 80% confluency in fresh DMEM with 10% FBS, but without antibiotics. Cells were then transfected with Lipofectamine 2000 following guidelines suggested in the manufacturer's protocol. In short, 10 μL of Lipofectamine 2000 was diluted to 250 μL with Opti-MEM and incubated for 5 min, then gently mixed with a 250 μL solution of 0.4 μg ABCG2-pcDNA5/FRT plasmid plus 3.6 μg pOG44 DNA diluted with Opti-MEM. The DNA-Lipofectamine mixture was allowed to incubate at room temperature for 30 min before being placed onto cells with 1.5 mL of

antibiotic-free media. All cell lines were incubated with their transfection agents for 6-8 hr, and then the transfection media was removed and fresh DMEM with 10% FBS and antibiotics added. After 24 hr, the media was again changed to DMEM media supplemented with 75 μg/mL hygromycin. Media was refreshed again after 48 hr with DMEM plus 75 μg/mL hygromycin and the cells were continually selected for 1 to 2 weeks in the hygromycin media, until colonies were visible. Per each variant, ~10 colonies were selected and expanded in DMEM plus 75 μg/mL hygromycin until confluent in a T-25 plate. Cells were then split with 0.05% trypsin and aliquots were taken for membrane expression analysis using flow cytometry, with additional aliquots for protein and mRNA extraction. Colonies of HEK293 Flp-in cells stably expressing variant MXR proteins with MXR expression levels similar to that of WT were selected for further studies. Colonies from cells transfected with empty pcDNA5/FRT vector that had the lowest level of MXR expression were also selected for further studies.

2.3.7. Protein and mRNA Extraction from Cells

To obtain whole cell lystates, transiently transfected MCF-7 cells and stably transfected HEK293 Flp-in cells were grown to confluency, then rinsed with 1X PBS and trypsinized with 0.05% trypsin until detached. Cells were then centrifuged at 500*g*, and the pellet was rinsed with 1X PBS. Up to 5 x 10^6 cells were resuspended in 500 μL of CelLytic MT lysis buffer plus 1:1000 protease inhibitor cocktail following the manufacturer's protocol. Cells were incubated at 4°C for 15 min and then centrifuged at 14,000*g* for 10 min at 4°C. Protein concentration of the supernant was determined using a

Pierce BCA assay kit following the manufacturer's protocol. Lysates were kept at -80°C until analyzed for protein expression.

To obtain mRNA from transiently and stably transfected cells, after trypsinizing and washing cells as above, mRNA was extracted from 5 x 10^6 cells using the RNase Easy Mini Kit following the manufacturer's protocol. The RNA concentration was determined using spectrophotometry and kept at -20°C until assayed for mRNA expression levels.

2.3.8. MXR Immunoblots

Whole cell lysates and membrane fractions (as vesicles) from transient or stably transfected cells (MCF-7 or HEK293 Flp-in, respectively) and whole cell lysates from drug-resistant MCF-7 ADVP cells were characterized by Western blotting. Either 10 μg whole cell lysate or 5 μg of membrane fractions mixed with 1X NuPage LDS sample buffer and 5% v/v β-mercapthanone were loaded per lane of a 4-12% Bis-Tris SDS-PAGE gel. Samples were separated alongside a BioRad kaleidoscope protein ladder at 120 V for 2 hr, or until the dye front reached the end of the gel, with 1X NuPAGE MOPS SDS running buffer in the XCell SureLock™ electrophoresis cell (Invitrogen). Samples were then transferred to a 0.45 μm nitrocellulose membrane using 1X NuPAGE transfer buffer in the Xcell II Blot Module (Invitrogen) at 32 V for 1.5 hr. Membranes were washed three times with 1X PBS for 5 min and then blocked for 1 hr at room temperature with 2% nonfat dried milk in 1X PBS. Membranes were incubated with BXP-21 mouse anti-human primary MXR antibody (1:500) in 2% nonfat dried milk plus 0.1% Tween (PBS-T) overnight at 4°C with rocking, then primary GAPDH goat anti-human antibody

at 1:20,000 was added for 1 hr. Membranes were washed three times with 1X PBS-T for 5 min and then incubated with IRDye 800CW goat anti-mouse secondary antibody at 1:10,000 for 1 hr at room temperature. Membranes were rinsed three times with 1X PBS-T for 5 min and a final time with 1X PBS before imaging both 800 and 700 nm channels on an Odyssey® Classic infrared scanner (LiCore). Densitometric analysis was performed using ImageJ[89]. Expression of MXR was normalized to that of GAPDH and variant MXR expression was compared to the reference MXR plasmid.

2.3.9. Flow Cytometry

Membrane expression of MXR was determined in either transiently transfected MCF-7 cells or stably transfected HEK293 Flp-in cells via flow cytometry. At least 48 hr prior to an experiment, media was changed to IMEM with 10% FBS and 1X Pen-Strep but without phenol red. When cells reached confluency, they were washed with 1X PBS and then treated with 0.05% trypsin until detached, centrifuged at 500*g* for 5 min and washed with 1X PBS. Cells were then resuspended at 1 x 10^5 cells per tube, centrifuged at 500*g* and the pellet washed with 200 µL of 1X PBS. Cells were resuspended in 500 µL of 1:250 5D3-PE conjugated primary MXR antibody and incubated for 1 hr at room temperature in the dark. Cells were centrifuged at 500*g* for 5 min and the pellet washed twice with 500 µL 1X PBS. The pellet was resuspended in 300 µL 10% FBS in 1X PBS (10% FBS-PBS) and internal fluorescence of the cell measured on a FACSCalibur flow cytometer (BD Biosciences, San Jose, CA) channel 2 (FL2-H) after gating for live cells based on forward (FSC) and side (SSC) scatter. For each sample, 5,000-10,000 events

were captured and recorded as histograms with counts on the y-axis and log fluorescence on the x-axis.

The capability of transiently transfected MCF-7 cells to efflux mitoxantrone, doxorubicin and pheophorbide A was measured by flow cytometry. Cells were grown to confluency in IMEM with 10% FBS and 1X PBS but without phenol red and then trypsinized with 0.05% trypsin until detached. Cells were centrifuged at 500*g* for 5 min, the pellet washed with 1X PBS and 5 x 10^5 cells transferred to a 1.1 mL polypropylene tube. Cells were centrifuged again at 500*g* for 5 min and the pellet resuspended in 250 μL of 100 μM pantoprazole in phenol-free IMEM media, or inhibitor-free phenol-free IMEM media for 30 min at 37°C. An aliquot (250 μL) of 2X drug solution in phenol-free IMEM, with or without 100 μM pantoprazole, was added to the cells and incubated for 30 min at 37°C. Final drug concentrations were 10 μM mitoxantrone, 10 μM doxorubicin and 1 μM pheophorbide A. Cells were centrifuged at 500*g* for 5 min at room temperature and resuspended in 500 μL phenol-free IMEM and incubated for 30 min at 37°C. Cells were then centrifuged at 500*g* for 5 min at 4°C and the pellet washed twice with 500 μL ice cold 1X PBS. Samples were resuspended in ice cold 10% FBS-PBS and kept on ice until analysis on a FACSCalibur flow cytometer channels 3 and 4 (FL3-H, FL4-H) after gating for live cells based on forward (FSC) and side (SSC) scatter. For each sample, 5,000-10,000 events were captured and recorded as histograms with counts on the y-axis and log fluorescence on the x-axis. Each experiment was replicated two to seven times.

2.3.10. Immunocytochemistry

Localization of MXR proteins in stably transfected HEK293 Flp-in cell lines was determined using fluorescent antibodies and a laser-scanning confocal microscope. Stably transfected cells were plated at 1 x 10^5 per well on 2-well glass chamber slides and grown until 80% confluent in IMEM with 10% FBS, 1X Pen-Strep and no phenol red. Media was then aspirated off the cells, the cells were washed twice with 2 mL 1X PBS per well, fixed with ice cold 300 µL 1:1 v/v methanol and acetone at -20°C for 10 min and gently washed twice with 1X PBS. Nonspecific binding sites were blocked with 300 µL 1X PBS plus 1.5 mg/mL BSA per well for 1 hr at room temperature. Cells were then incubated with BXP-21 primary MXR antibody at 1:25 v/v in blocking buffer overnight at 4°C. Each well was washed twice with 1 mL 1X PBS and then incubated with the fluorescence-conjugated secondary antibody Alexa 488 goat anti-mouse at 1:100 v/v in blocking buffer for 1 hr at room temperature in the dark. Wells were gently washed twice with 1 mL 1X PBS, the chamber slides and gasket removed and the well allowed to dry. Cells were covered with ProLong Gold Antifade plus DAPI mounting reagent, fitted with a cover slide and dried for 4 hr at room temperature and 24 hr at 4°C. Slides were stored at -20°C until imaged using a Retiga CCD-cooled camera and associated QCapture Pro software (QImaging Surrey, BC Canada) filtered for green (MXR) and blue (DAPI) fluorescence with 10 to 25 sec exposures at both 10X and 40X magnification.

2.3.11. qRT-PCR

ABCG2 mRNA levels were quantified in HEK293 Flp-in stable cell lines using reverse-transcription polymerase chain reaction (RT-PCR). RNA (3 µg) extracted from

stably transfected HEK293 Flp-in colonies were reverse transcribed by the SuperScript® III First-Strand Synthesis System in a 10 μL reaction containing 0.1 U SuperScript III (SSIII) reverse transcriptase, 1X SSIII reaction buffer, 500 μM dNTPs, 1X random hexamers, 20 U RNase OUT and 5 mM $MgCl_2$, with the residual volume filled with RNase-free water. Samples were incubated at the following conditions: 5 min at 65°C, 5 min at 25ºC, 50 min at 50ºC and 10 min at 85ºC. Gene expression was then quantified in a reaction containing 1X TaqMan Universal Master Mix, 1X gene expression assay, and 1 μL cDNA in a 10 μL volume. The reaction was then analyzed in the 7900HT Fast Real-Time PCR System under the following conditions: 95°C for 2 min, then 35 cycles between 95°C for 15 sec and 60°C for 1 min. Gene expression of ABCG2 and an internal control, either GAPDH or GusB, were analyzed in each sample. Expression of ABCG2 was normalized to either the expression of GAPDH or GusB and expressed as ΔΔCt for each sample. The expression of each ABCG2 variant was compared to the expression of reference ABCG2.

2.3.12. Vesicle Isolation

Membrane fractions of HEK293 Flp-in stably transfected cells were isolated and formed as previously described[42] with modifications. First, cells were grown to confluency in a HYPERflask (yields ~2 x 10^8 cells), trypsinized with 0.05% trypsin until cells detached, centrifuged at 500*g* for 5 min and the pellet washed twice with 1X PBS. All further steps were done with ice cold buffers, on ice or at 4°C. Cells were then lysed with 10 mL hypotonic lysis buffer (consisting of 0.5 mM Tris-HEPES and 0.1 mM EGTA at pH 7.5) using 10 strokes of a Potter-Elvenjem homogenizer. The lysate was

centrifuged at 2000*g* for 10 min and the supernatant saved while the pellet was homogenized again in another aliquot of 10 mL hypotonic lysis buffer. After centrifuging the re-homogenized cells at 2000*g*, the supernatants were combined, homogenized by 10 strokes of a Potter-Elvenjem homogenizer and then centrifuged at 100,000*g* for 30 min. The resulting pellets were suspended in 7.2 mL of 250 mM sucrose/10 mM Tris-HEPES and homogenized by 10 strokes of a Potter-Elvenjem homogenizer. Homogenate was layered in 1.2 mL aliquots over 1.2 mL of 40% w/v sucrose and centrifuged at 100,000*g* for 30 min. The middle cloudy layer was extracted (~2.25 mL), brought to a final volume of 9 mL with 250 mM sucrose/10 mM Tris-HEPES and centrifuged at 100,000*g* for 30 min. The resulting pellet was resuspended in 100 µL 250 mM sucrose/10 mM Tris-HEPES, protein was quantified using a BSA assay and samples were frozen at -80°C in 10-20 µL aliquots. Before use, vesicles were slowly thawed, incubated with 0.05% Brij58, a detergent previously identified to support the formation of sealed inside-out vesicles[90,91], and formed by passing through a 23 gauge needle at least 10 times.

2.3.13. Vanadate Sensitive ATPase Assay

Membrane vesicles isolated from HEK293 Flp-in stable cell lines were assayed for their ATPase activity. Uptake buffer for the ATPase assay was 250 mM sucrose/10 mM Tris-HCl with 2.5 mM $MgCl_2$, 0.5 mM ATP, 2 mM ouabain and 3 mM sodium azide. Vanadate sensitive ATPase activity was determined by calculating the difference between the activities of the vesicles obtained in the presence and absence of 2 mM sodium orthovanadate. Vesicles were stimulated with 5 µM of sulfasalazine, mitoxantrone, SN-38, pheophorbide A or estrone-3-sulfate. A 90 µL aliquot of uptake

buffer with drugs was warmed to 37°C, and then formed vesicles were added to the uptake buffer. The reaction was incubated for 30 min at 37°C, and the release of inorganic phosphate was immediately determined using the colorimetric PiColorLock ATPase Assay kit following the manufacturer's protocol. Absorbance of the samples were determined at 635 nm and compared to a standard curve to quantify liberated inorganic phosphate. The sulfasalazine experiment was repeated twice with triplicate wells per condition; whereas the other three drugs were only tested in one experiment with at least triplicates per condition. Results were analyzed as described below with BD CT empty vesicles used as the negative control.

2.3.14. H^+/ATPase Assay

Vesicles were tested for their ability to simultaneously generate a proton gradient and for ATPase activity to determine the extent of inside-out and intact vesicles. The dual H^+-ATPase assay was based on a previously published protocol[92] , with slight alterations, which allows for the monitoring of acridine orange and NADH absorbance simultaneously. The quenching of acridine orange occurs inside the vesicle once protons are pumped into the vesicles, thus creating an acidic environment and altering the absorbance of acridine orange at 495 nm[93]. The ATPase activity is monitored by coupling inorganic phosphate cleavage with the oxidation of NADH, which can be monitored by a decrease in absorbance at 340 nm[92]. Vesicles were obtained either from HEK293 Flp-in cells as described above or purchased from commercially available sources which were made from mock transfected (BD CT) and overexpressing MXR (BD BCRP) cells. The reaction buffer consisted of 10 mM MOP-BTP at pH 6.5 plus 140 mM KCl, 2 mM ATP,

1 mM EDTA, 1 mM DTT, 50 μM acridine orange, 1 mg/mL BSA, 0.05% Brij58, 250 μM NADH, 1 mM PEP, 25 μg/mL LD and 50 μg/mL PK. First, 10 μg of membranes were diluted to 100 μL by 10 mM MOP-BTP with 0.05% Brij58, and then vesicles were formed by passing through a 23 gauge needle 10 times. Vesicles were incubated with equal volume 2X reaction buffer for 10 min. The reaction was initiated by the addition of 4 mM $MgCl_2$, and the absorbance at wavelengths 495 and 340 nm was read every 30 sec for 60 min. The proton gradient was abolished by permeablizing the membrane with 0.015 % w/v Triton X-100.

2.3.15. Vesicle Uptake Assay

The ability of inside-out vesicles to uptake MXR substrates was determined by adapting and optimizing previously published vesicle uptake protocols[42,45,56,62,81,94,95]. Vesicle uptake buffer consisted of 250 mM sucrose, 10 mM Tris-HCl, 1 mM ATP, 5 mM $MgCl_2$ and an ATP-regenerating system (5 mM creatine phosphate, 0.5 μg creatine kinase). Reaction stop buffer consisted of ice cold 250 mM sucrose, 10 mM Tris-HCl and 10 mM EDTA. Uptake reactions were performed using cold 0-100 μM SN-38 and 10 μM mitoxantrone with 1 μg vesicles in uptake buffer at 37°C for 0-5 min. Reactions were quenched with ice cold stop buffer, vacuum filtered through an MCE filter plate and washed with 1 mL cold stop buffer. Vesicles were dissolved in 10% DMSO plus 1% acetic acid for mitoxantrone and 0.1N NaOH plus 0.1% SDS for SN-38. Mitoxantrone absorbance was read at 670 nm, and SN-38 fluorescence emission was measured at 545 nm after excitation at 414 nm. Uptake reactions for sulfasalazine and pheophorbide A were performed using 50 μM sulfasalazine and 10 μM pheophorbide A with 1 μg vesicles

in uptake buffer at 37°C for 0 - 5 min. Sephadex G-25 columns were prepared with stop buffer per the manufacturer's instructions. Reactions were quenched with 150 µL ice cold stop buffer and vesicles isolated by spinning through a G-25 sephadex column at 700*g* for 2 min. The elute was made basic by the addition of 50 µL of 10 N NaOH and the absorbance at 460 nm (sulfasalazine) or 410 nm (pheophorbide A) was measured. The uptake of substrates was normalized for µg of protein and time for each reaction.

2.3.16. Statistics

The expression of MXR protein or ABCG2 mRNA in MXR transiently or stably transfected cell lines and vesicles was considered different between reference and pcDNA5/FRT if $P < 0.05$ when tested with a Student's *t*-test. The expression of MXR protein or ABCG2 mRNA in MXR transiently or stably transfected cell lines and vesicles was considered different between reference and variant MXR constructs, if $P < 0.05$ when tested with an ANOVA followed with a post-hoc Bonferroni *t*-test. Differences in populations separated by flow cytometry were detected by testing the cumulative distribution function (CDF) plots, which exhibit the distribution of fluorescence through the two populations. CDFs were tested for differences between the distribution of MXR variants and MXR reference proteins using a generalized Chi-squared test to provide a value for T(x). Degrees of freedom were determined by the general formula "k-c", where k is bins and c is parameters plus 1. For all flow data there were 100 bins used for the distribution of the data and parameters were the 14 gates used on both samples (7 each: FSC, SSC, FL1-FL4H and Count). Therefore degrees of freedom (DFs) were calculated by 100 bins – 14 parameters +1 = 85 DFs and critical T(x) values >108 for 85 DFs were

considered significant at the $P < 0.05$ level, the actual P values noted on the cell histograms. For efflux assays, the "Inhibitable Efflux" (IE) is defined as the difference in median fluorescence with pantoprazole ($FL_{inhibitor}$) minus mean fluorescence without pantoprazole (FL_o), divided by mean fluorescence without pantoprazole[67] (Equation 2.1). Significance between MXR WT and variants was determined by an ANOVA followed by a post-hoc Bonferroni *t*-test with $P < 0.05$ considered significant.

$$IE = \frac{FL_{inhibitor} - FL_o}{FL_o} \qquad \textbf{Equation 2.1}$$

For ATPase assays, the vanadate-sensitive ATPase activity was determined by taking the difference in ATPase activity without and with sodium orthovanadate treatment. The velocity of ATP hydrolysis was then calculated by dividing the μmole of liberated inorganic phosphate by mg of vesicles and reaction time. Vanadate-sensitive ATPase velocity was tested for differences between MXR reference and EV using a Student's *t*-test and MXR reference was tested for differences from MXR variants using an ANOVA followed by a post-hoc Bonferroni's multiple comparison *t*-test with $P < 0.05$ considered significant. Statistics were determined using the Graphpad Prism 5 (La Jolla, CA) software.

2.4. Results

2.4.1. Nonsynonymous Variants of MXR in the SOPHIE Cohort

Sequencing of the SOPHIE cohort identified six nonsynonymous variants in *ABCG2*; none of the variant amino acids fall within the key ABC domains, but five of six

are evolutionarily conserved (Table 2.3). These variants include the widely described V12M and Q141K variants, both with >25% MAF in one population and MAF >5% in almost all populations. The valine at position 12 is the only non-conserved amino acid; most species have a methionine at this position (data not shown). All three methods used to estimate the extent of disruption by the amino acid change predicted that these two SNPs would have low to medium disruption of the protein function. The V12M and Q141K polymorphisms were in low linkage disequilibrium (r^2=0.16), thus the haplotype V12M/Q141K occurred at a frequency of 0.6% in the Caucasian and African American populations of the SOPHIE cohort.

All other nonsynonymous variants in *ABCG2* had MAF <2% in the SOPHIE cohorts and were generally only present in one or two populations. The I206L and D620N variants have MAF of ~2% in African American and Caucasian populations, respectively. The D620N SNP was predicted to have little effect on protein function by both Grantham and SIFT score, but PolyPhen predicted it was potentially damaging (Table 2.3). The sequencing of the SOPHIE cohort also resulted in the first report of the T542A variant, which has since been confirmed[95]. The P269S SNP had <1% MAF in the Asian population, and was predicted to be the most detrimental to protein function by all three prediction methods (Table 2.3). Variants from the MXR sequencing have been deposited in dbSNP and are available on the Pharmacogenomics of Membrane Transporter (PMT)[76] and PharmGKB[96] websites. Expression plasmids for all six nonsynonymous variants present in the SOPHIE cohort, and the V12M/Q141K haplotype, were generated and the resulting proteins tested for alterations in expression and activity.

Table 2.3. MXR Nonsynonymous Variants from the SOPHIE Cohort

SNP ID	ΔAmino Acid	MAF[1] (%)						Amino Acid Conservation[3]	Grantham Value[4]	SIFT Prediction[4]	PolyPhen Prediction[4]
		AA	CA	AS	ME	PA	Other[2]				
rs2231137	Val12Met	7.7	6.6	27.2	14.9	0.0	0 - 27	ch	21	Tolerated	Benign
rs2231142	Gln141Lys	1.3	8.1	40.8	26.0	16.7	1 - 41	ch, d, co, m, r	53	Tolerated	Benign
rs12721643	Ile206Leu	0.0	1.5	0.0	0.0	0.0	0.6-20	ch, d, co, m, r	5	Tolerated	Benign
rs34678167	Pro269Ser	0.0	0.0	0.8	0.0	0.0	0.8	ch, d, co, m, r, z	74	Deleterious	PD
rs35965584	Thr542Ala	0.0	0.0	0.8	0.0	0.0	1.9	ch, d, co, m, r, z	58	Tolerated	Benign
rs34783571	Asp620Asn	1.9	0.0	0.0	0.0	0.0	0.6-1.1	ch, co, r	23	Tolerated	PD
-	Val12Met/ Gln141Lys	0.6	0.6	0.0	0.0	0.0	1.5	-	-	-	-

Abbreviations: SNP, Single Nucleotide Polymorphism; AA, Amino Acid; MAF, Minor Allele Frequency; PD, Possibly Damaging

[1]MAF for African American (AA), Caucasian (CA), Asian (AS), Mexican (ME) and Pacific Islander (PA) populations obtained from the Pharmacogenomics Membrane Transporters (PMT) database

[2]MAF from the 1000 Genomes database and/or reported in other populations[79–82]

[3]Determined from sequence alignment with chimp (ch), dog (d), cow (co), mouse (m), rat (r) and zebrafish (z)

[4]Calculated as described in *Materials and Methods*

2.4.2. Expression and Function of MXR Variants in Transiently Transfected MCF-7s

To test if MXR variant transporters have altered function, expression plasmids were transiently transfected into MCF-7 cells, the cells were loaded with substrate and then allowed to efflux. The remaining internal drug concentration was measured using flow cytometry and intracellular drug concentration was inversely correlated with MXR function. The V12M/Q141K haplotype was not tested in the transient transfection studies. MXR reference (WT) and most of the MXR variant transporters were transiently expressed in MCF-7 cells, although the expression was only moderately greater than the background expression in the cells (Figure 2.1). Despite this low level of overexpression, cells transfected with MXR reference had a significant decrease in internal drug fluorescence for mitoxantrone and pheophorbide A compared to cells transfected with the pcDNA5/FRT vector (Figure 2.2). As expected, reference MXR did not transport doxorubicin (Figure 2.2). Although the PE-conjugated external epitope MXR antibody 5D3 is available, attempts to utilize it for isolation of MXR positive cells were unsuccessful because of crosstalk of the PE fluorophore with the drug fluorescence and more importantly, because the 5D3 antibody is an inhibitor of MXR transport[97,98].

Due to the potential differences in internal drug concentrations of the transfected cells after being loaded with substrate, we utilized the MXR inhibitor pantoprazole, as described in *Materials and Methods*, to determine IE for each variant. Mitoxantrone transport in MCF-7 cells transiently expressing MXR reference or variants was inhibitable by pantoprazole (Figure 2.3). In contrast, pheophorbide A transport was less sensitive to pantoprazole and the Q141K and T542A variants were almost completely resistant to inhibition with pantoprazole (Figure 2.4). Using IE as a specific measure of

MXR transport, there was no difference between mitoxantrone transport by the reference and variant MXR transporters (Figure 2.5A). For pheophorbide A IE, the I206L variant had higher transport activity than the reference protein (Figure 2.5B), but there were no differences in transport of pheophorbide A for any other variant.

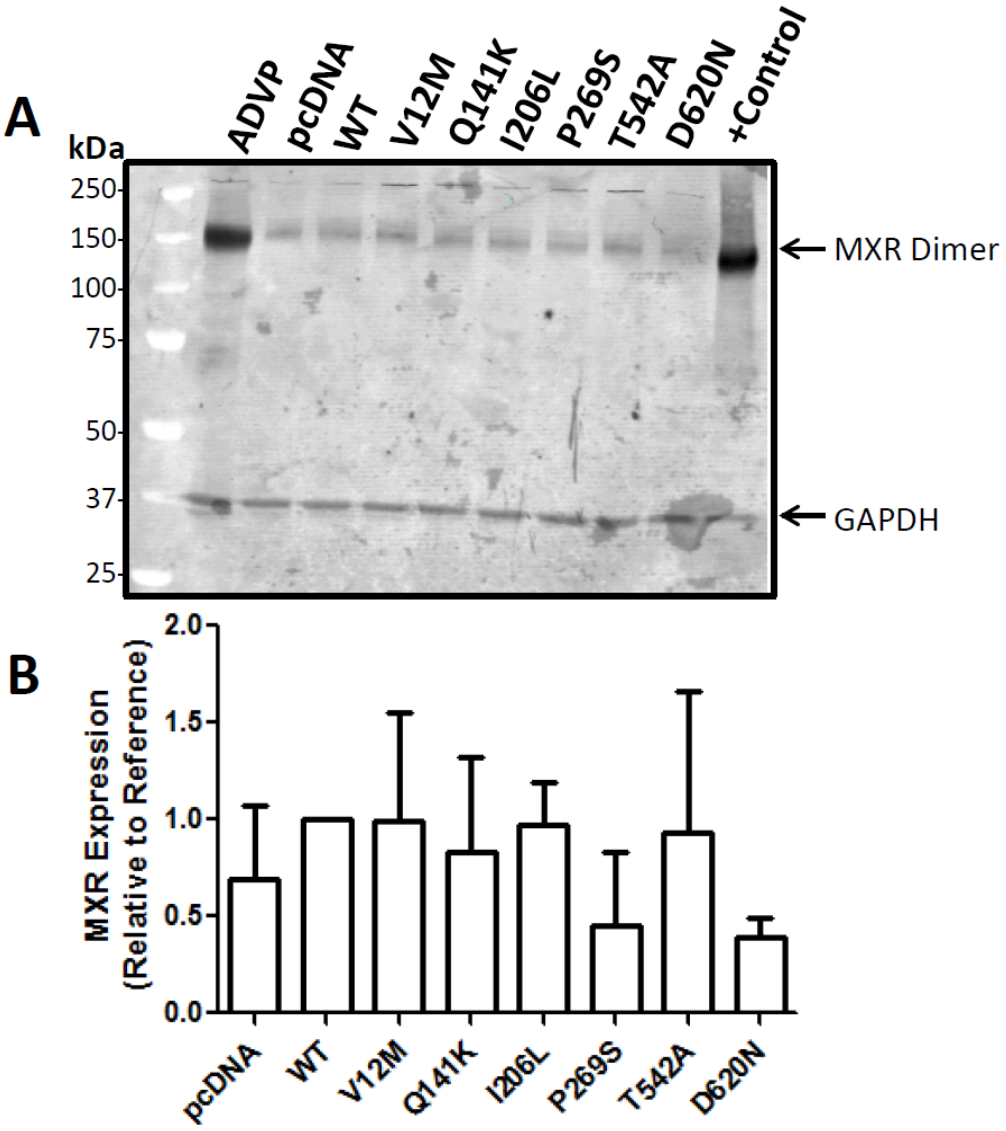

Figure 2.1. Expression levels of MXR in transiently transfected MCF-7 cells. Expression of MXR determined by (A) immunoblot and then represented in (B) as GAPDH normalized expression with MXR reference (WT) set to 1. Whole cell lysates were prepared from cells transiently transfected with reference or variant MXR, 10 µg

was loaded per lane. MCF-7 AdVp cells (10 µg) and MXR vesicles (+Control) were also used as a positive control (4 µg). The homodimer of MXR is indicated at 144-150 kD and GAPDH is indicated at ~35 kD. Relative expression levels of MXR and GAPDH in each sample were determined by densitometric analysis as described in *Materials and Methods*. A representative immunoblot was selected from two separate experiments, whose densitometric analyses are both represented in the graph.

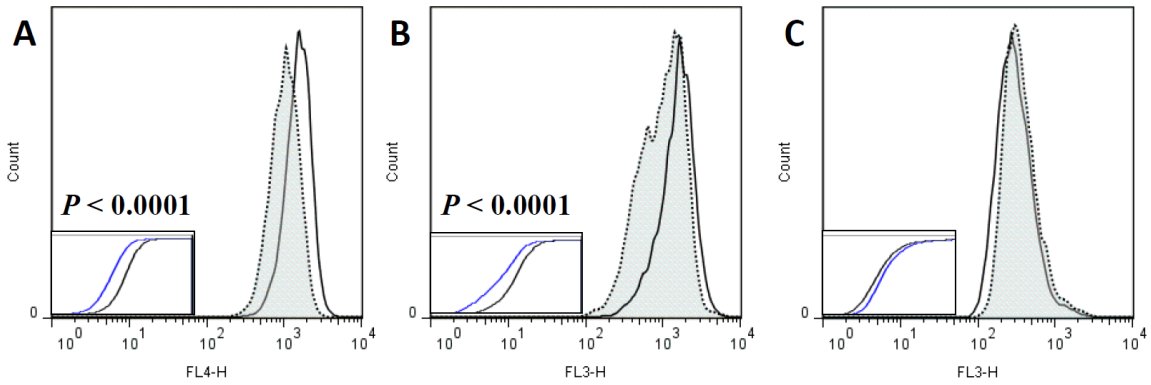

Figure 2.2. Efflux of mitoxantrone, pheophorbide A and doxorubicin in MXR and pcDNA5/FRT transfected MCF-7 cells. MCF-7 cells were transiently transfected with reference MXR (dotted shaded line) or pcDNA5/FRT (black line) vectors. Efflux assays were then performed with (A) 10 µM mitoxantrone, (B) 1 µM pheophorbide A or (C) 10 µM doxorubicin as described under *Materials and Methods*. Histograms show the distribution of fluorescence (FL) from transfected cells in channels 3 or 4 (FL3-H, FL4-H) and in the lower left corner are the CDF plots which show the distribution of fluorescence throughout the two populations. CDFs were tested for differences between the distribution of pcDNA and MXR reference transfected cells using a generalized Chi-squared T(x) test. T(x) values over the critical value of 108 significant at $P < 0.05$, were observed for mitoxantrone and pheophorbide A.

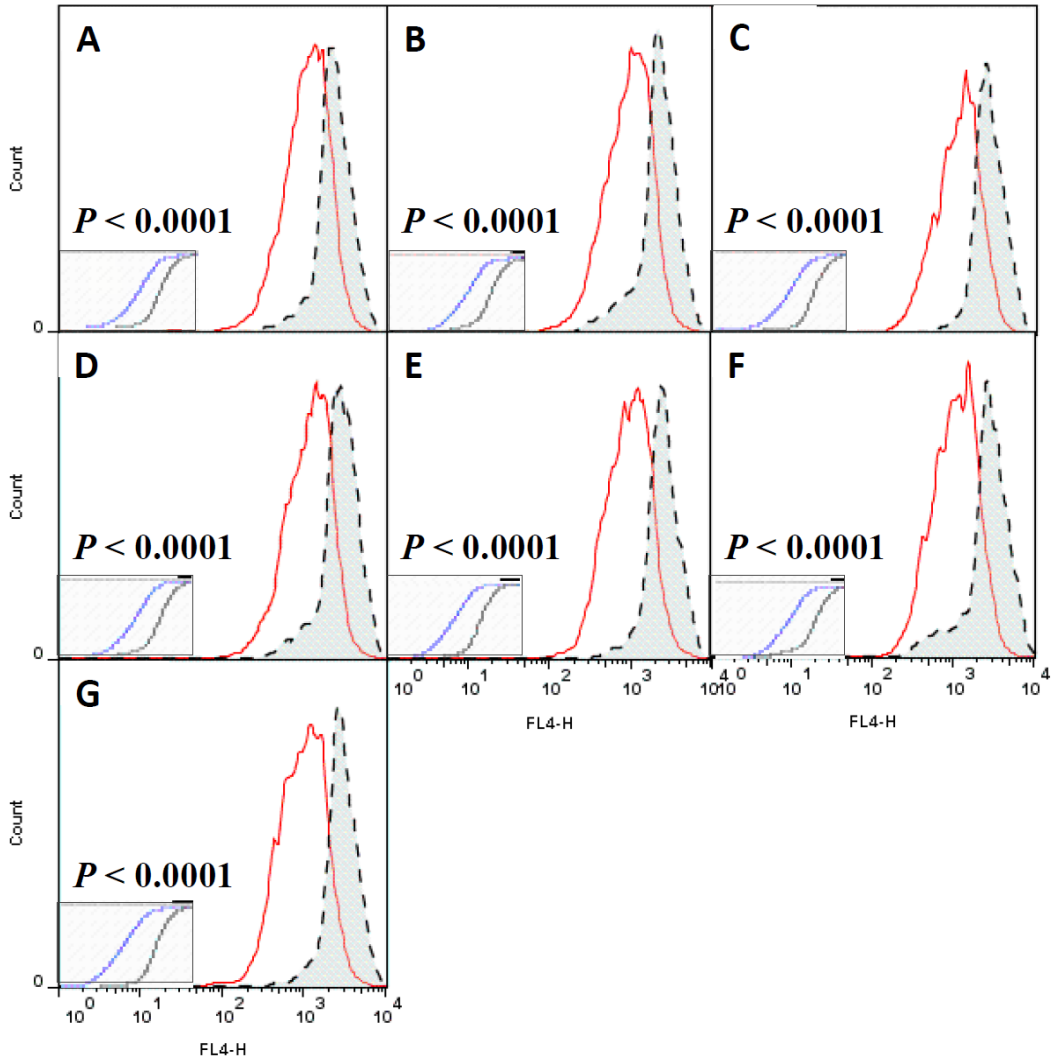

Figure 2.3. Inhibition of MXR mediated mitoxantrone efflux in transiently transfected MCF-7 cells. MCF-7 cells were transiently transfected with (A) reference, (B) V12M, (C) Q141K, (D) I206L, (E) P269S, (F) T542A and (G) D620N MXR plasmids. Efflux assays were then performed with 10 μM mitoxantrone in the presence (black dotted line) or absence (red line) of pantoprazole as described under *Materials and Methods*. Histograms show the distribution of channel 4 fluorescence (FL4-H) from MXR transfected cells. CDFs were tested for differences between each variant with and without pantoprazole using a Chi-squared T(x) test, resulting *P* values are indicated. Results are shown from a representative experiment from up to seven replicates.

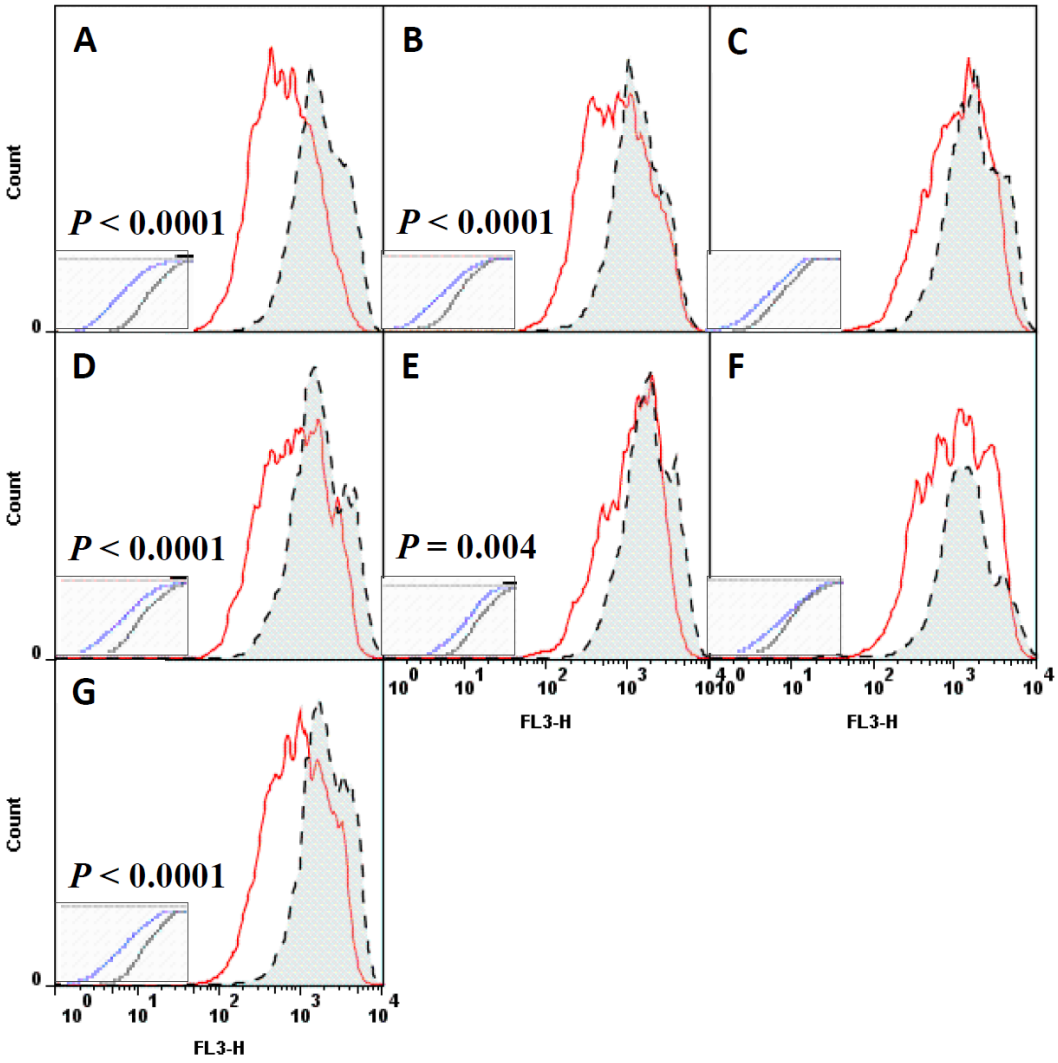

Figure 2.4. Inhibition of MXR mediated pheophorbide A efflux in transiently transfected MCF-7 cells. MCF-7 cells were transiently transfected with (A) reference, (B) V12M, (C) Q141K, (D) I206L, (E) P269S, (F) T542A and (G) D620N MXR plasmids. Efflux assays were then performed with 1 μM pheophorbide A in the presence (black dotted line) or absence (red line) of pantoprazole as described in *Materials and Methods*. Histograms show the distribution of channel 3 fluorescence (FL3-H) from MXR transfected cells. CDFs were tested for differences between each variant with and without pantoprazole using a Chi-squared T(x) test, resulting *P* values are indicated. Results are shown from a representative experiment from up to seven replicates.

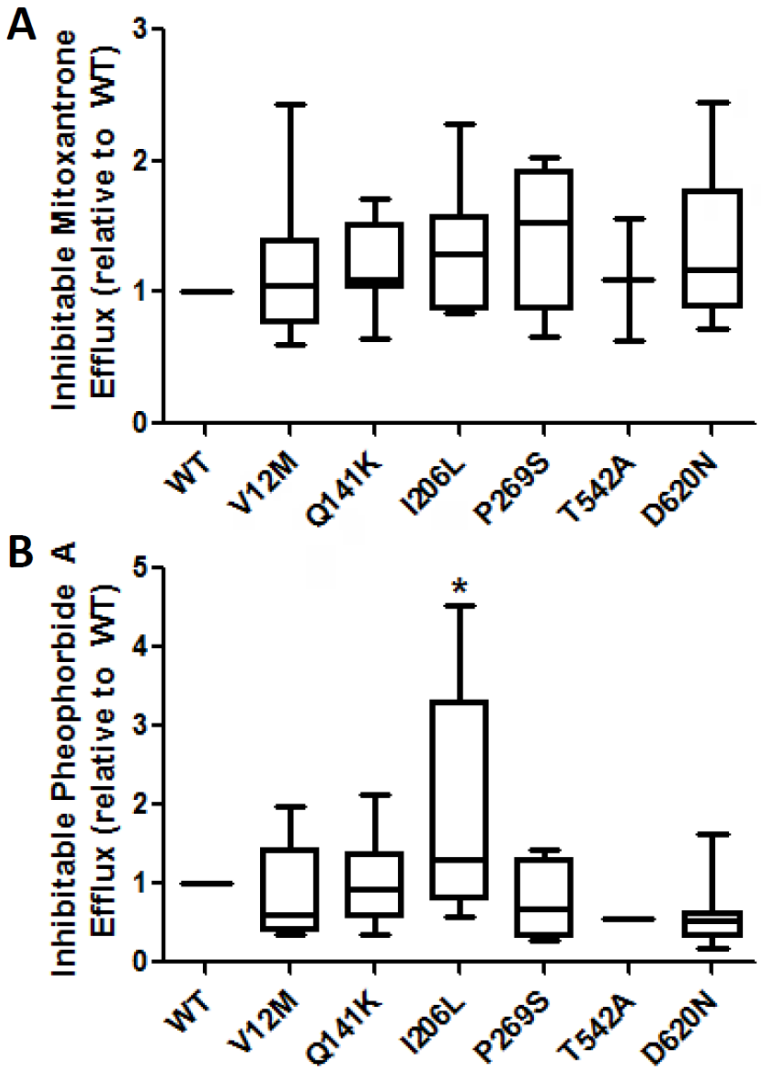

Figure 2.5. Box and whisker plot of MXR inhibitable efflux. Inhibitable efflux of (A) mitoxantrone and (B) pheophorbide A in MCF-7 cells transiently transfected with MXR reference (WT) and variant plasmids. After transfection, cells were loaded with drug and allowed to efflux in the presence or absence of pantoprazole. Inhibitable efflux (IE), as defined in *Materials and Methods*, is normalized to WT for MXR variants within each experiment. Whisker plots show the data from seven replicate experiments (except for T542A which was only tested twice and P269S which was tested four times). WT and variant MXR proteins were tested with an ANOVA followed with a post-hoc Bonferroni *t*-test, * $P < 0.05$.

2.4.3. Generation of Stably Transfected MXR Variant Cell Lines

The HEK293 Flp-in system was utilized to generate stably transfected cell lines for all MXR variants listed in Table 2.3. The MXR WT sequence was previously cloned in the Kroetz lab into the pcDNA5/FRT (pcDNA) vector, and from that, all MXR variants were generated by SDM. These plasmids were all successfully transfected into HEK293 Flp-in cells, and at least 12 colonies expressing each variant MXR protein were isolated. Colonies for each of the variant MXR proteins, and empty vector transfected HEK293 Flp-in cells, were screened for their expression of MXR mRNA, MXR whole cell protein and MXR membrane protein. The pcDNA transfected cells with the lowest expression of MXR were selected, while MXR variant protein colonies with MXR expression levels most similar to MXR WT were selected.

2.4.4. *Expression and Localization of MXR Variants*

ABCG2 mRNA levels in pcDNA transfected cells were <5% of MXR WT cells. The expression of ABCG2 mRNA in MXR variant colonies was similar to WT (Figure 2.6). Consistent with the high ABCG2 mRNA levels in the stable cell lines, whole cell MXR expression was 5-fold higher in the reference MXR cells compared to the empty vector transfected cells; MXR protein in the variant cell lines were similar to WT except for Q141K which had a 50% decrease (Figure 2.7). As expected, the MXR cell-surface expression in empty vector transfected cells was significantly lower than that of the MXR WT cell lines (Figure 2.8). The MXR variants had reduced membrane expression compared to MXR WT as determined via flow cytometry (Figure 2.8). This was consistent with a 40% reduction in MXR expression in the Q141K and D620N membrane

vesicles isolated from the HEK293 Flp-in cells (Figure 2.9). Immunocytochemistry showed that MXR WT protein stained to the plasma membrane of the HEK293 Flp-in cells (Figure 2.10 and Figure 2.11) and was virtually nonexistent in the pcDNA transfected cells (Figure 2.12). None of the MXR variant proteins exhibited any altered localization within the cell (Figure 2.10 and Figure 2.11).

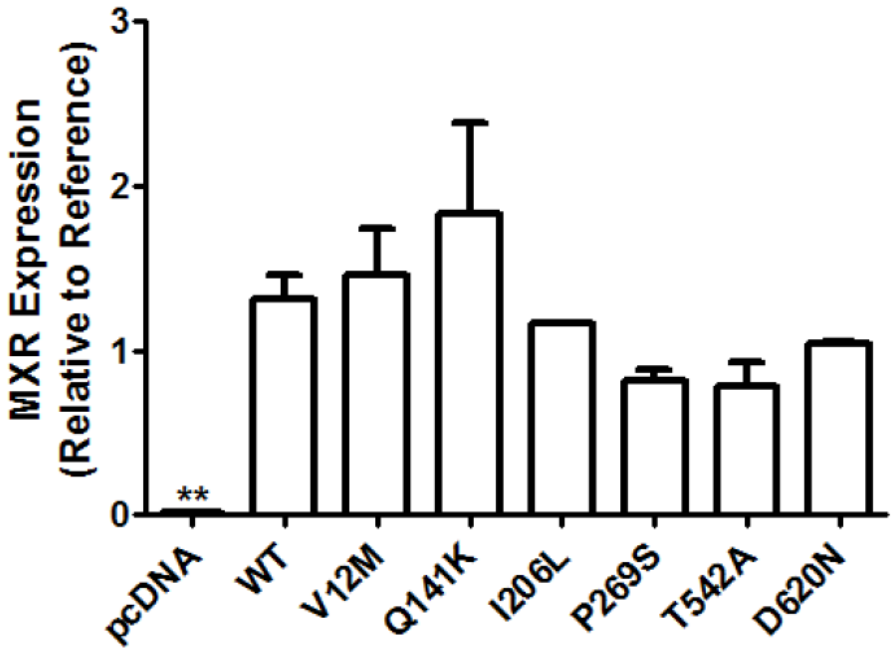

Figure 2.6. Expression of ABCG2 mRNA in stably transfected cell lines. Quantitative RT-PCR analysis of ABCG2 mRNA in stably transfected MXR variant and reference HEK293 Flp-in cells was performed and ABCG2 mRNA expression levels were expressed as ΔΔCt compared to GAPDH and normalized to reference. Shown are the mRNA expression values of 2-6 clones for each plasmid stably transfected into HEK293 Flp-in cells. The difference in ABCG2 expression between pcDNA and MXR reference colonies was tested with a Student's *t*-test, ** $P < 0.001$. Expression of ABCG2 in MXR variant cells were considered different from reference if $P < 0.05$ when tested with an ANOVA followed with a post-hoc Bonferroni *t*-test.

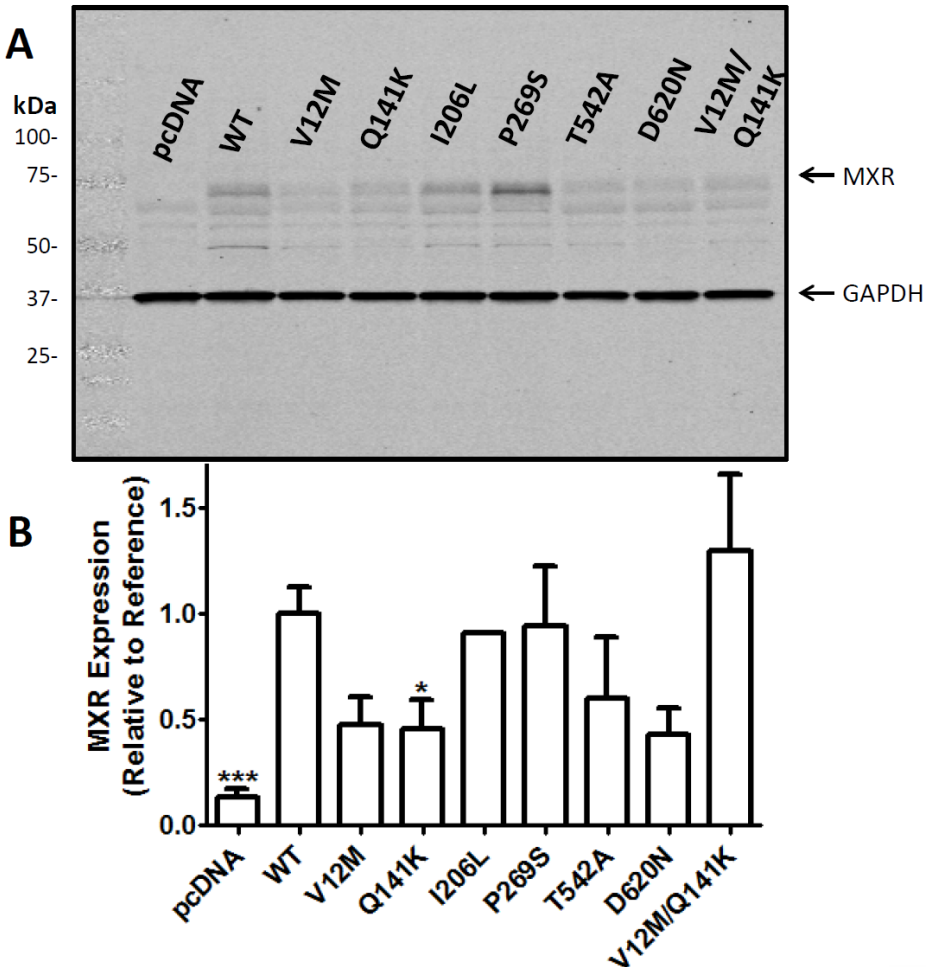

Figure 2.7. Expression levels of MXR in stably transfected HEK293 Flp-in cells. Expression of MXR was determined by (A) immunoblot and (B) quantified by densitometry, normalized by GAPDH and expressed relative to WT as described in *Materials and Methods*. An aliquot (10 µg) of whole cell lysate from the indicated cell lines was loaded into each lane. The monomer of MXR (75 kD) and GAPDH (~35kD) are noted. A representative immunoblot is shown from upto four replicate experiments. The difference in ABCG2 expression between pcDNA and MXR reference cells was tested with a Student's *t*-test, *** $P < 0.0001$. The difference in ABCG2 expression between variant and reference MXR cells was tested with an ANOVA followed with a post-hoc Bonferroni *t*-test, * $P < 0.05$.

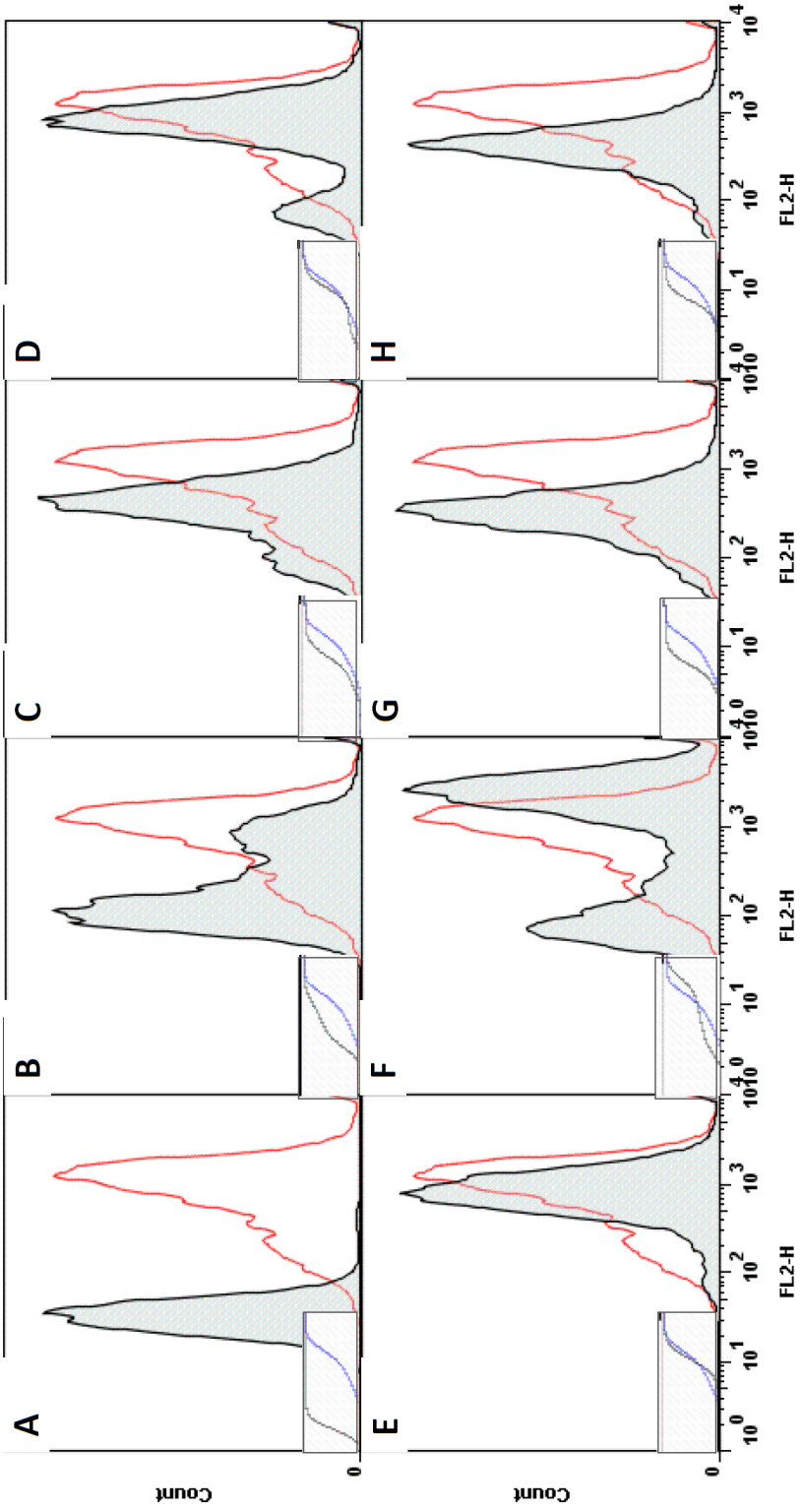

Figure 2.8. Cell surface expression of MXR in stable cell lines. HEK293 Flp-in cells stably transfected with reference (WT) MXR (red line in all the graphs), or with (A)

pcDNA empty vector, (B) V12M, (C) Q141K, (D) I206L, (E) P269S, (F) T542A, (G) D620N and H) V12M/Q141K MXR plasmids shown as the black shaded lines. MXR staining was performed using 5D3-PE conjugated antibody as described in *Materials and Methods* and histograms show the distribution of fluorescence (FL) in channel 2 (FL2-H). Cumulative distribution function plots (CDFs) were tested for differences between each variant and WT MXR using a generalized Chi-squared T(x) test. Critical T(x) values > 108 were considered significant. All X^2 values are >108 and $P < 0.0001$ compared to WT. Results are shown for a representative experiment from three replicates.

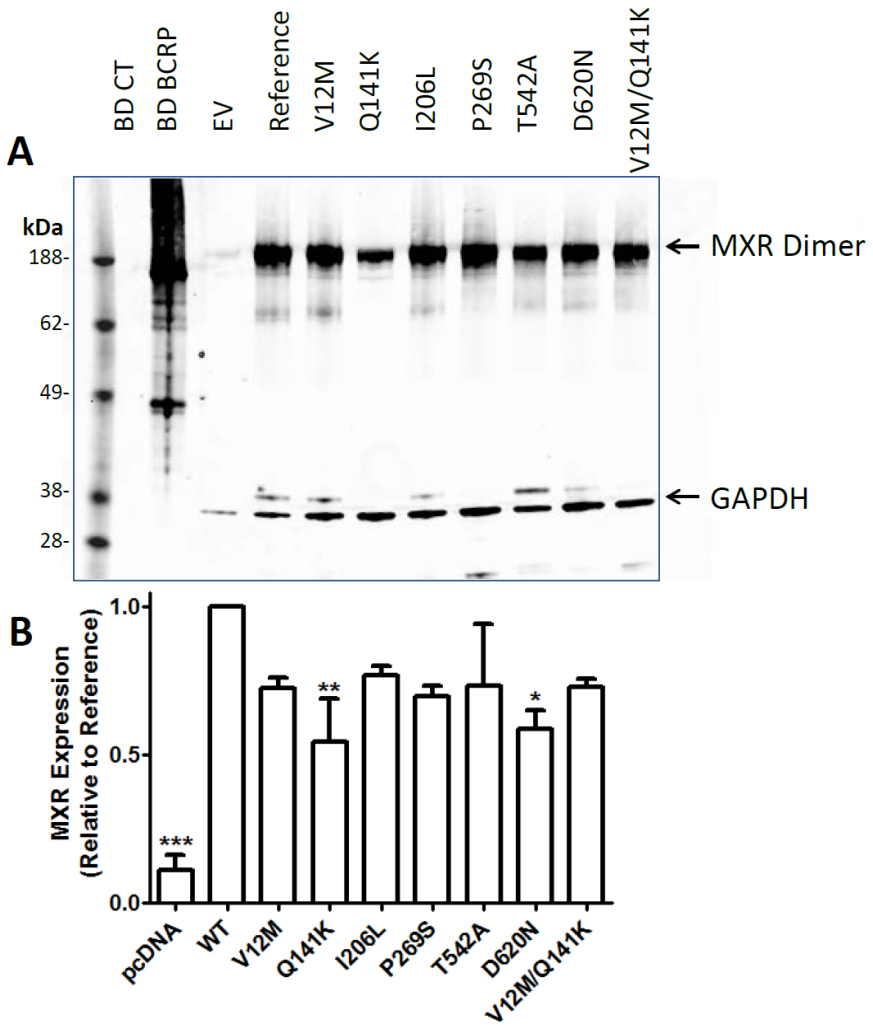

Figure 2.9. Expression levels of MXR in vesicles. Expression of MXR was determined by (A) immunoblot and (B) quantified using densitometric analysis, normalized by GAPDH and expressed relative to WT, as described in *Materials and Methods*. An aliquot of membrane vesicles (5 µg) either purchased (BD CT and BD BCRP) or prepared from the HEK293 Flp-in stable cell lines was loaded onto the gel. MXR dimer (144-150 kD) and GAPDH (~35 kD) are indicated. The immunoblot is representative of two separate experiments, whose values are combined in the graph. The difference in ABCG2 expression between pcDNA and MXR reference vesicles was tested with a Student's *t*-test, *** $P < 0.0001$, and between variant and reference MXR cells with an ANOVA followed with a post-hoc Bonferroni *t*-test, * $P < 0.05$ and ** $P < 0.001$.

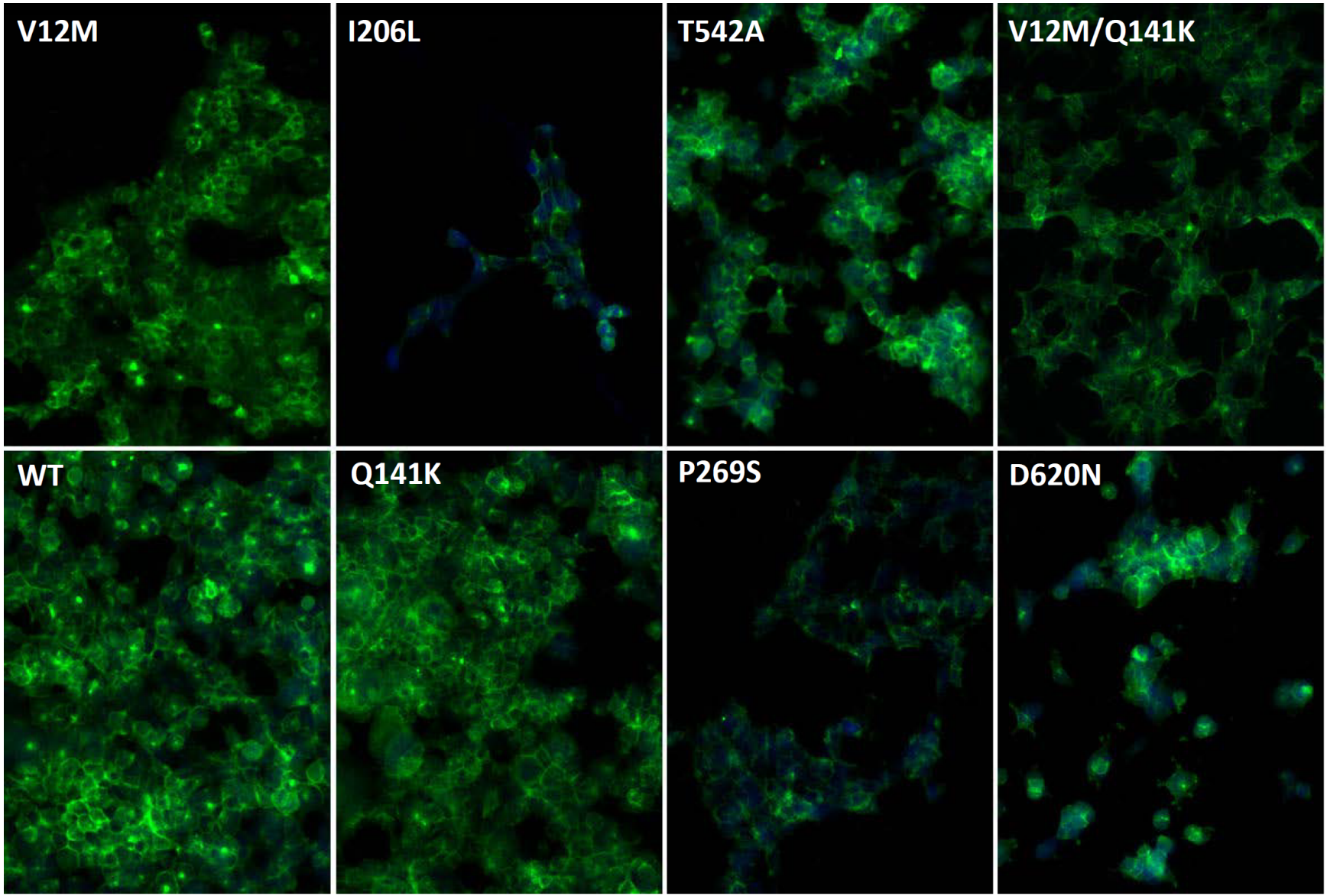
V12M
I206L
T542A
V12M/Q141K
WT
Q141K
P269S
D620N

Figure 2.10. Localization of MXR variants in stably transfected HEK293 Flp-in cells at 10X magnification. Stably transfected HEK293 Flp-in cells were stained for MXR (green) expression using the BXP-21 MXR antibody followed by 488-Alexa conjugated anti-mouse secondary antibody and DAPI as described in *Materials and Methods*. Shown are representative images at 10X magnification selected from three replicate experiments.

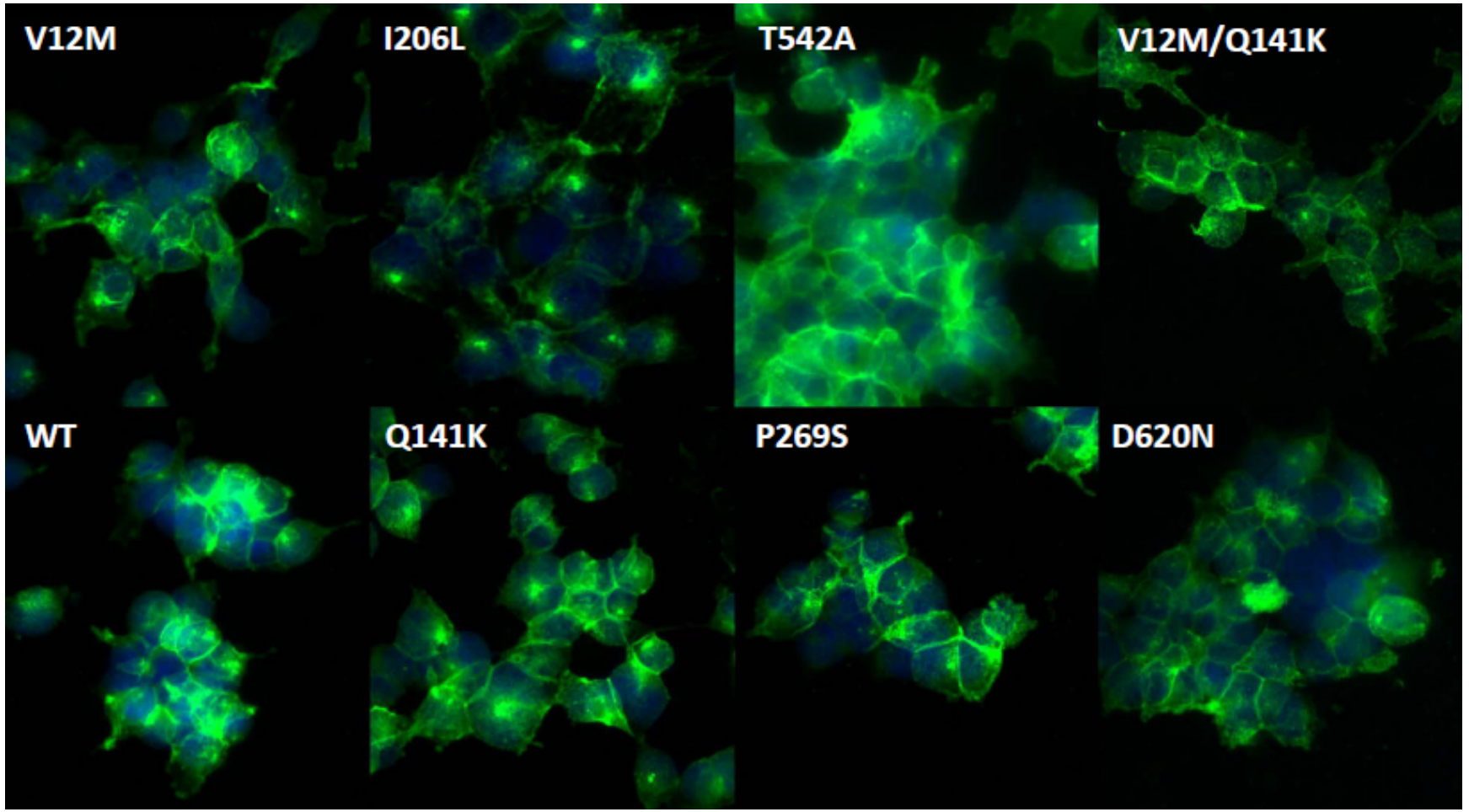
V12M
I206L
T542A
V12M/Q141K
WT
Q141K
P269S
D620N

Figure 2.11. Localization of MXR variants in stably transfected HEK293 Flp-in cells at 40X magnification. Stably transfected HEK293 Flp-in cells were stained for MXR (green) expression using the BXP-21 MXR antibody followed by 488-Alexa conjugated anti-mouse secondary antibody and DAPI as described in *Materials and Methods*. Shown are representative images at 40X magnification selected from three replicate experiments.

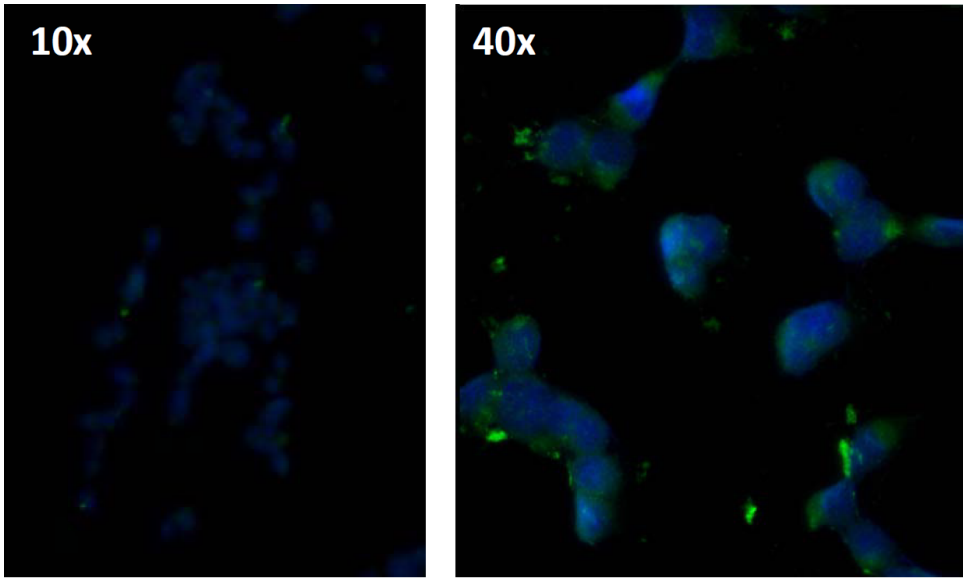

Figure 2.12. Localization of MXR in HEK293 Flp-in cells stably transfected with empty pcDNA5/FRT vector. Stably transfected HEK293 Flp-in cells were stained for MXR (green) using the BXP-21 MXR antibody followed by FITC-conjugated anti-mouse secondary antibody and DAPI as described in *Materials and Methods*. Shown are representative images at 10X (left) and 40X (right) magnification selected from three replicate experiments.

2.4.5. Transport Activity of MXR Vesicles

To ensure that vesicles were forming inside-out and with intact (not leaky) membranes, we utilized a previously published protocol[91] to simultaneously measure the development of a proton (H^+) pump gradient and ATPase activity. We initiated the reaction by addition of $MgCl_2$ and tested that the H^+ gradient could be abolished with the addition of Triton X-100 (Figure 2.13), which permeablizes the membrane[90]. All MXR variants, EV and commercially purchased vesicles exhibited dual H^+- ATPase activity (Figure 2.14). We saw no differences in activity between commercially purchased vesicles and the HEK293 Flp-in vesicle preps (data not shown). Also, all MXR and EV vesicles were above the signal of reactions without vesicles and MXR vesicles generally had higher ATPase activities, but similar H^+ gradients to EV vesicles (data not shown and Figure 2.14). We also observed that the reaction was only initiated upon the addition of $MgCl_2$ (Figure 2.13 and zero point in Figure 2.14) and that addition of Brij58 increased both H^+ and ATPase activity of the vesicles (data not shown).

A colorimetric ATPase assay[99] was used to measure changes in ATPase activity in the presence and absence of MXR substrates. Sodium orthovanadate did not inhibit all ATPase activity in the vesicle reactions (data not shown), indicating slight contamination by non-plasma membrane ATPases. Therefore, we also included sodium azide to inhibit mitochondrial membrane ATPase activity[100] and ouabain to inhibit sodium-potassium ATPase channels. MXR WT vesicle ATPase activity was ~3-fold higher than EV vesicles upon exposure to sulfasalazine, mitoxantrone, SN-38 and pheophorbide A (Figure 2.15). There was no difference in ATPase activity between MXR WT and EV with estrone-3-sulfate treatment (data not shown). The V12M variant vesicles had

significantly higher ATPase activity than MXR WT vesicles upon exposure to sulfasalazine, mitoxantrone, SN-38 and pheophorbide A (Figure 2.15). The D620N variant vesicles had significantly higher ATPase activity than MXR WT vesicles upon exposure to sulfasalazine, SN-38 and pheophorbide A (Figure 2.15). The ATPase assays were only completed once and replicate experiments are needed to confirm the results.

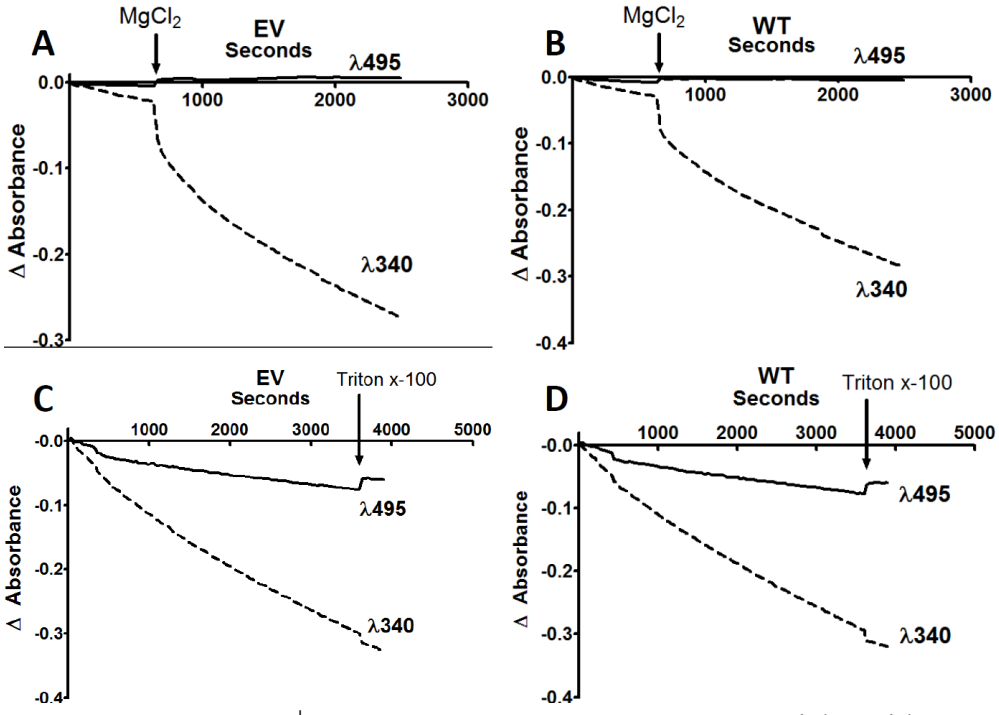

Figure 2.13. Vesicle dual H^+-ATPase activity assay controls. Vesicles with no MXR expression [EV (A, C)] or overexpressing MXR protein [WT (B, D)] were tested for their ability to quench acridine orange and NADH absorbance. The hydrolysis of ATP was coupled to the oxidation of NADH and was monitored through the quenching of NADH absorbance at 395 nm (dashed line). The reaction was initiated through the addition of $MgCl_2$ (indicated by an arrow in A and B). At the same time, formation of a pH gradient over time was monitored by absorbance quenching of acridine orange at 495 nm (solid black line). The detergent Triton X-100 was added near the end of the reaction (indicated by an arrow in C and D) to disrupt the vesicle membrane and abolish the proton gradient.

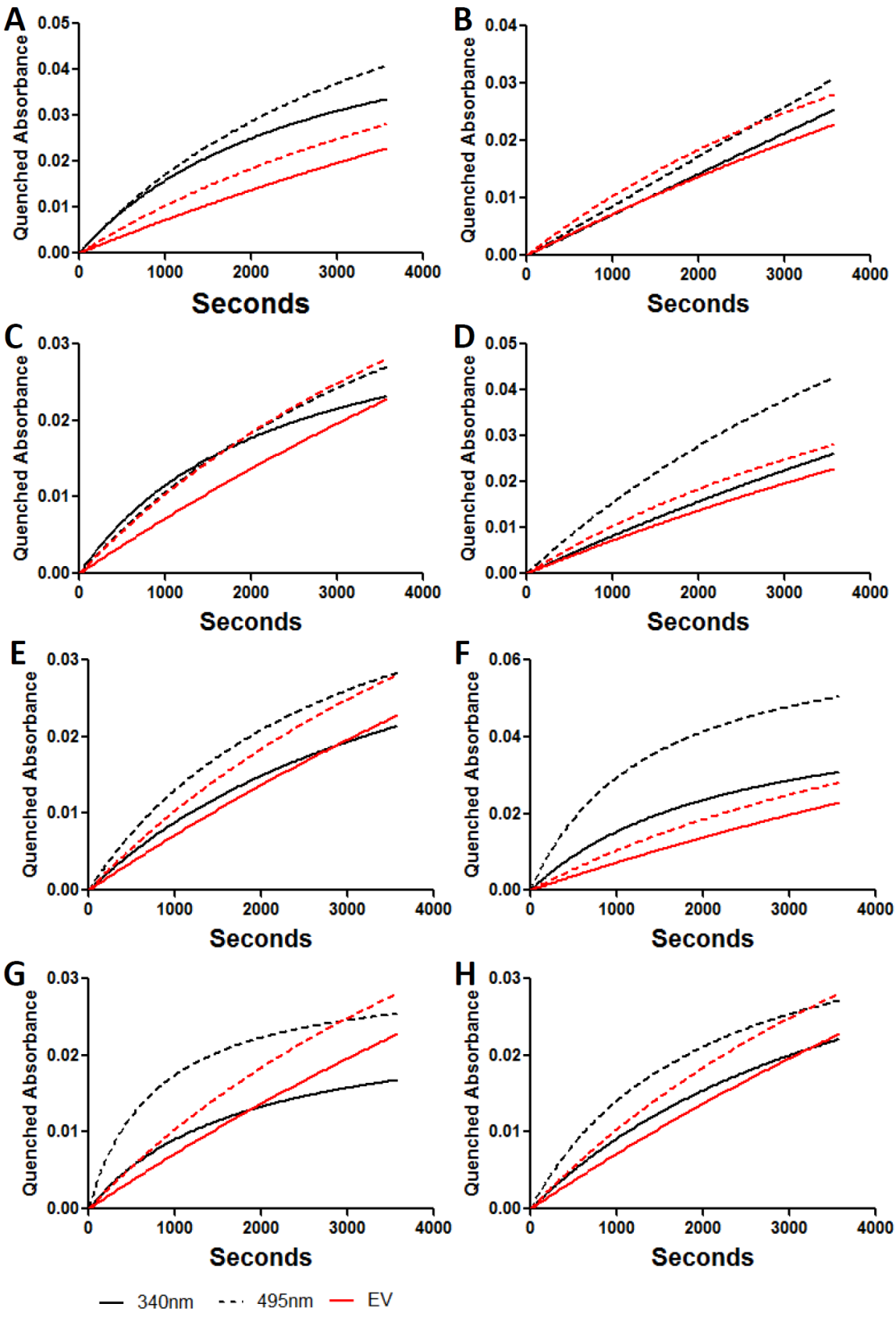
A
B
C
D
E
F
G
H
Quenched Absorbance
Seconds
0
1000
2000
3000
4000
340nm
495nm
EV

Figure 2.14. Dual H^+-ATPase activity of MXR expressing vesicles. Vesicles with no MXR expression (EV, red lines all graphs) or overexpressing MXR protein variants (black lines), A) WT, B) V12M, C) Q141K, D) I206L, E) P269S, F) T542A, G) D620N and H) V12M/Q141K, were tested for their H^+-ATPase activity as described in *Materials and Methods*. Formation of a pH gradient over time was monitored by absorbance quenching of acridine orange at 495 nm (dashed lines). At the same time, the hydrolysis of ATP was coupled to the oxidation of NADH and was monitored through the quenching of NADH absorbance at 395 nm (solid lines).

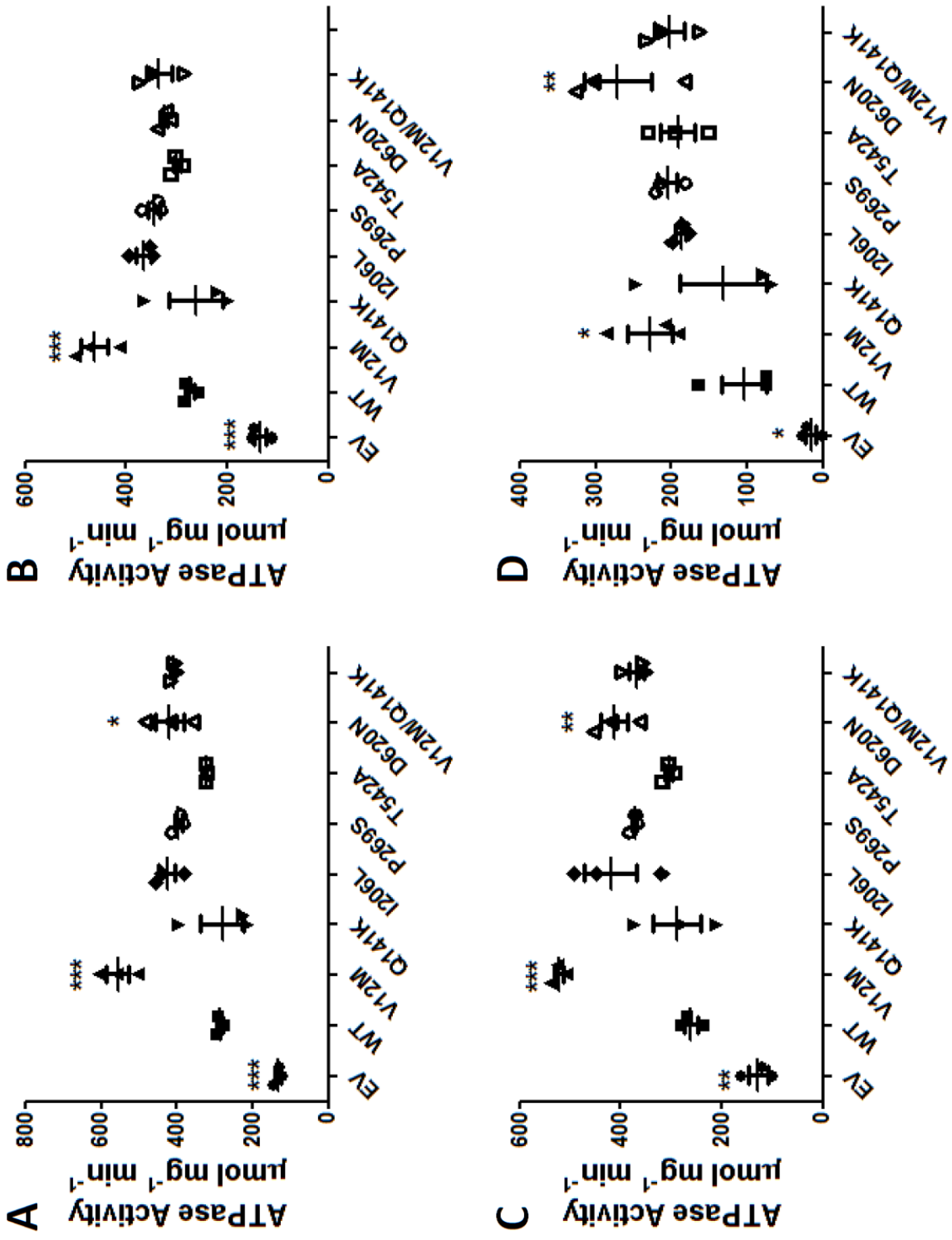

Figure 2.15. Vanadate sensitive ATPase activity of MXR vesicles. Vanadate-sensitive ATPase activity of vesicles after stimulation with (A) 5 μM sulfasalazine, (B) 5 μM mitoxantrone, (C) 5 μM SN-38 and (D) 5 μM pheophorbide A. Vesicles were made from

HEK293 Flp-in cell membranes stably expressing EV, MXR reference (WT) or MXR variant proteins. The ATPase activities of the vesicles were determined using a colorimetric assay to detect vanadate-sensitive liberation of inorganic phosphate as described in *Materials and Methods*. Vanadate-sensitive ATPase activity is expressed as μmole of liberated inorganic phosphate (Pi) divided by mg of vesicle protein and reaction time. Results are from one experiment with triplicate wells per condition with EV data from BD CT vesicles. Vanadate-sensitive ATPase activity for EV was tested for differences from reference MXR using a Student's *t*-test and variant MXR proteins were tested for differences from reference MXR using an ANOVA followed by a post-hoc Bonferroni *t*-test, * $P < 0.05$, ** $P < 0.01$, *** $P < 0.001$.

2.4.6. Substrate Uptake by MXR Vesicles

Inside-out vesicles were used for direct uptake assays. Since the majority of MXR tested substrates were fluorescent, MXR transport was measured through fluorescence detection of the drug inside vesicles. Uptake of mitoxantrone, SN-38 and sulfasalazine was linear before 1 min (Figure 2.16). There were no differences in the linear range of uptake between MXR WT and the MXR variant vesicles (data not shown). We were unable to isolate the linear range of uptake for pheophorbide A (data not shown). The difference between WT and EV vesicles in uptake of mitoxantrone, SN-38 and sulfasalazine was 2- to 4- fold after 30 sec (Figure 2.16). Although the initial tests and optimization of MXR vesicles had promising results, further kinetic assays were inconsistent. Our attempts to calculate kinetics for MXR WT and variant vesicles with fluorescent substrates were unsuccessful due to a loss of specific transport in the MXR

expressing cells (data not shown) and studies are ongoing to optimize reaction conditions and detection methods.

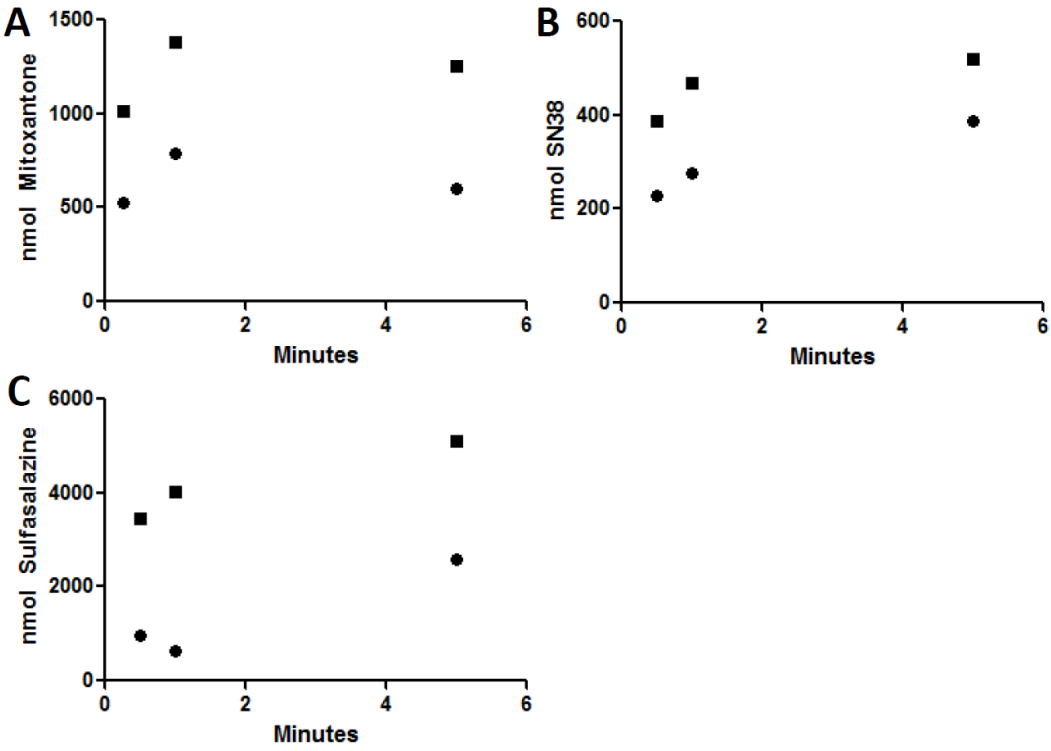

Figure 2.16. Time dependent uptake of fluorescent drugs into inside-out vesicles. Uptake of (A) mitoxantrone, (B) SN-38 and (C) sulfasalazine into EV (●) and MXR WT (■) inside-out vesicles was measured as described in *Materials and Methods*. Vesicles (1 µg) were treated with 10 µM mitoxantrone, 10 µM SN-38 or 50 µM sulfasalazine for 30 sec, 1 min or 5 min, and the reaction was quenched and vesicles separated from uptake buffer using MCE filter plates (mitoxantrone and SN-38) or sephadex columns (sulfasalazine). The amount of substrate from lysed vesicles was quantified via fluorescence at 414 nm following excitation at 545 nm for SN-38, absorbance at 460 nm for sulfasalazine and absorbance at 670 nm for mitoxantrone.

2.5. Discussion

The sequencing of the SOPHIE cohort identified six non-synonymous variants and one haplotype of the MXR transporter. In this study, these protein variants were functionally characterized by expressing the MXR variant transporters using the HEK293 Flp-in system. The HEK293 Flp-in system has been well validated as a system to identify MXR variants that might have altered protein expression, degradation and function[41,45,54,101–104]. The overexpression of MXR variants in HEK293 Flp-in cells indicated that none of the SNPs cause a complete loss in MXR expression or alter the localization of the protein. Although there were slight fluctuations in the MXR expression levels in the vesicles isolated from the HEK293 Flp-in stable cells, MXR expression for all vesicle preps, except pcDNA, was very high.

Inside-out and intact membrane vesicles from these overexpressing cell lines were used to functionally characterize the MXR variants. The MXR vanadate-sensitive ATPase activity of the vesicles was stimulated 2-fold with mitoxantrone, sulfasalazine, SN-38 and pheophorbide A. Although there is generally over a 4-fold stimulation in ATPase activity that occurs with P-glycoprotein (P-gp), 2-fold simulation of MXR activity is consistent with what has been seen with other MXR substrates[82,105–109]. Further conclusions regarding the function of the MXR variant transporters relative to the reference require additional experiments.

The MAF of MXR variants have been well summarized in reviews and are population-specific[7,45,79,103,104,110,111]. The two most common SNPs were the V12M and the Q141K variants and the MAF found in the Caucasian, Asian and African American SOPHIE samples was similar to reported values[15,22,68,80,110,112–116]. Both the V12M and

Q141K variants are most common in Asians (15-45%[15,22,80,110,112] and 15-36%[15,22,68,80,110,112,113], respectively), followed by Caucasians (2-12%[22,114–116] and 6-14%[22,68,114–116], respectively), and African Americans (0% and 0-5%[22,68], respectively). The I206L, P269S and D620N variants are much less common in most populations[22,80,114,117]. The PMT project was the first to report the T542A SNP, which has since been noted in another population[95]. The V12M and Q141K SNPs occur together at a low frequency (<1% in Caucasians and African Americans), consistent with other reports that show these SNPs to be in linkage disequilibrium[80] and therefore not part of a common haplotype[113].

Due to its high MAF in different ethnic populations, the V12M variant is well studied. The V12M variant is located in the NH_2-terminal intracellular region of the MXR protein. The observed decreased expression of MXR V12M compared to WT is consistent with another report of low V12M protein levels in cell lines[45]. However, there have been many reports noting that V12M mRNA and/or protein expression levels were the same as MXR WT in either human tissues or cell lines[41,54,81,103,111,112]. A single report in Hispanic livers noted an association of the V12M variant with lower mRNA levels of ABCG2[20]. Altered localization of the V12M protein was not observed in the current study using non-polarized cells but has been reported in a polarized cell system[116].

There is evidence for substrate-dependent effects of the V12M variant as it has been reported to cause lower porphyrin[45] and higher methotrexate[42] transport. In vesicle assays, the V12M MXR exhibited significantly higher ATPase activity compared to WT MXR when stimulated with sulfasalazine, mitoxantrone, SN-38 and pheophorbide A. These results are consistent with reports that V12M has protective effects against

pheophorbide A[103] and SN-38 cytotoxicity[54]. Alterations of V12M transport are of note because V12M has been clinically associated with a poor response to imatinib mesylate treatment[118]. Further studies are needed to determine if V12M can impact the pharmacokinetics or dynamics of porphyrins, irinotecan and its active metabolite SN-38.

The Q141K variant is the most common MXR variant and has been associated with chemotherapy-induced diarrhea[119], acute lymphoblastic leukemia complications[120] and neutropenia in cancer patients treated with irinotecan[121]. It lies between the Walker A motif and the ABC signature region. Not all of the data regarding MXR Q141K function has been in agreement. In the current study using HEK293 Flp-in stable cells, MXR Q141K had similar levels of mRNA to WT but reduced whole cell and membrane protein expression. This reduction in Q141K expression is in agreement with other reports of normal mRNA but low protein expression levels of Q141K[41,45,81,103,111,112,122,123] and has been linked to an increase in the proteosomal degradation of the Q141K variant [101,102]. Although the Q141K variant has not been linked to alterations in human intestine mRNA levels[22], it could still have an impact on protein expression. Analysis of intestinal biopsy samples showed equal protein and mRNA expression between Q141K and WT[21], but the variant did have lower protein expression in human erythrocytes[123] and placental samples[15].

Without normalizing for Q141K expression, the ATPase assays showed no difference in mitoxantrone stimulated ATPase activity, consistent with that of Morisaki et al[67]. Additionally, the Q141K variant exhibits low porphyrin transport[45] and low IC_{50}s in topotecan, SN-38 and mitoxantrone cytotoxicity assays[54,111,112]. However, there is no change in pheophorbide A IC_{50} for the MXR Q141K variant[103] and it has similar MTX

ATP-dependent transport compared to WT[42]. Additionally, the Q141K variant alters the pharmacokinetic parameters of SN-38 and its glucuronide[68], sulfasalazine[21], diflomotecan[124], fluvastatin, pravastatin and simvastatin[125], and rosuvastatin[126]. The Q141K variant has no effect on the pharmacokinetic properties of nitrofurantoin[127], pitavastatin[128], pravastatin[129] or lamivudine[130]. Clearly, further research is needed to clarify the substrate-dependent effects of MXR Q141K and their clinical implications.

The other MXR nonsynonymous SNPs are much less frequent and have been considerably less studied. The I206L variant is located right before the Walker B motif and has been reported to have either no change in expression[20] or reduced expression[131] compared to MXR WT. In the current study, stable HEK293 Flp-in cells showed no differences in I206L mRNA or protein expression. The I206L transiently transfected cells also had a 1.4-fold higher pheophorbide A IE, consistent with previous reports that this variant has a 2.4-fold higher IE[131] and a lower porphyrin transport[45]. Although the I206L variant is functional, in the presence of inhibitors it might play a role in increased exposure to porphyrins. MXR has previously been implicated in pheophorbide A elimination[43]; phototoxicity is present in humans after injection of foods rich in pheophorbide A[52] and patients taking MXR inhibitors or substrates have evidence for photosensitivity[47–50]. Thus, it would be of interest to elucidate the link between MXR variants and phototoxicity and whether they play a clinical role in the presentation of phototoxicity.

P269S is another low frequency MXR SNP that has been relatively unstudied. It is located right before the first transmembrane domain. There was no difference in P269S mRNA or protein expression compared to the reference transporter, consistent with

Kondo et al[81]. ATPase activity of P269S vesicles was not altered relative to the reference transporter in the presence of sulfasalazine, SN-38, mitoxantrone or pheophorbide A. Others have reported that the P269S variant exhibits a 35-40% decrease in vesicular uptake of estrone-3-sulfate and methotrexate compared to WT[80]. The PMT project was the first to identify the T542A MXR variant, and its function has thus not been previously evaluated. The T542A variant is very near or in the 5th transmembrane domain. The T542A variant had higher membrane expression, evident both via flow cytometry and immunohistochemistry. However, there were no significant changes in T542A MXR function compared to the MXR WT protein. The effect of the V12M/Q141K haplotype on MXR function has also not been previously studied. Although we noted some decrease in protein expression, it did not translate into any alteration in protein function.

Stable cell lines expressing the D620N variant, which is in extracellular loop 3 of the transporter, had similar mRNA levels, but decreased membrane and whole cell MXR expression. Decreased[79], increased[131] and no change[45] in protein expression have all been reported for the D620N variant. Both the current study and previous reports showed no effect of the D620N amino acid change on mitoxantrone stimulated ATPase activity[67]. In contrast, ATPase activity was increased for this variant in the presence of sulfasalazine, SN-38 and pheophorbide A. More research is necessary to elucidate whether this variant alters function.

Although vesicles have been successfully used in previous research to characterize MXR substrates, the system was difficult to optimize. Rapid counter-flux of the drugs was observed after 1 minute, a phenomenon attributed to the expression of uptake transporters[132]. This is consistent with mitoxantrone transport by many

transporters[71]. The use of Sf9 cells to generate vesicles expressing human MXR proteins could be used to circumvent this problem. However, the cholesterol composition of both Sf9 and HEK293 membranes affects the activity of MXR[106]. Cholesterol was not added to our system, but it could be a useful tool in the future to increase the difference between the EV and WT ATPase activity or substrate transport. The current vesicle assay could also benefit by further optimization focusing on pH, temperature and sucrose molarity, since all have been shown to affect the transport of MXR substrates into vesicles[56]. Although the sucrose concentration was at the published optimal concentration, the pH was higher[56], and therefore modulating the pH could be another avenue to improve the vesicle assays. MXR is a high capacity transporter, and it would be of interest to determine if reducing the temperature of the reaction could prolong the linear range of MXR transport. Finally, there were difficulties obtaining no transport in conditions in which only AMP was present (data not shown). However, there is evidence that ATP hydrolysis is not necessary for the conformational changes that occur in the MXR protein upon drug binding[108], and instead ATP hydrolysis is relevant for resetting the MXR conformation after transport of substrates[133]. It is possible that in the AMP reactions, drug that binds to the MXR transporter and not drug that was effectively transported into the vesicle was being measured. Thus, further optimization of the vesicle reaction's cholesterol content, pH and temperature, and identification of a different negative control than AMP could be beneficial.

2.6. Conclusion

Preliminary evidence was presented for altered substrate-dependent function of V12M, I206L and D620N variants of MXR. The Q141K variant exhibited lower protein expression, however, the Q141K MXR protein itself is functional. Additionally, the HEK293 Flp-in stable cell lines and inside-out vesicle assay have potential for being a useful tool to determine the expression and function of different MXR variants and substrates. However, further optimization of the substrate uptake assays are needed before final conclusions can be made on kinetic parameters.

2.7. References

(1) Dean, M.; Hamon, Y.; Chimini, G. The human ATP-binding cassette (ABC) transporter superfamily. *Journal of lipid research* **2001**, *42*, 1007–17.

(2) Choudhuri, S.; Klaassen, C. D. Structure, function, expression, genomic organization, and single nucleotide polymorphisms of human ABCB1 (MDR1), ABCC (MRP), and ABCG2 (BCRP) efflux transporters. *International journal of toxicology* **2006**, *25*, 231–59.

(3) Kusuhara, H.; Sugiyama, Y. ATP-binding cassette, subfamily G (ABCG family). *Pflügers Archiv : European journal of physiology* **2007**, *453*, 735–44.

(4) Xu, J.; Liu, Y.; Yang, Y.; Bates, S.; Zhang, J. Characterization of oligomeric human half-ABC transporter ATP-binding cassette G2. *The Journal of biological chemistry* **2004**, *279*, 19781–9.

(5) Bhatia, A.; Schäfer, H.-J.; Hrycyna, C. a Oligomerization of the human ABC transporter ABCG2: evaluation of the native protein and chimeric dimers. *Biochemistry* **2005**, *44*, 10893–904.

(6) Velamakanni, S.; Wei, S. L.; Janvilisri, T.; Van Veen, H. W. ABCG transporters: structure, substrate specificities and physiological roles : a brief overview. *Journal of bioenergetics and biomembranes* **2007**, *39*, 465–71.

(7) Ishikawa, T.; Tamura, A.; Saito, H.; Wakabayashi, K.; Nakagawa, H. Pharmacogenomics of the human ABC transporter ABCG2: from functional evaluation to drug molecular design. *Die Naturwissenschaften* **2005**, *92*, 451–63.

(8) Robey, R. W.; To, K. K. K.; Polgar, O.; Dohse, M.; Fetsch, P.; Dean, M.; Bates, S. E. ABCG2: a perspective. *Advanced drug delivery reviews* **2009**, *61*, 3–13.

(9) Doyle, L. a; Yang, W.; Abruzzo, L. V; Krogmann, T.; Gao, Y.; Rishi, a K.; Ross, D. D. A multidrug resistance transporter from human MCF-7 breast cancer cells. *Proceedings of the National Academy of Sciences of the United States of America* **1998**, *95*, 15665–70.

(10) Maliepaard, M.; Scheffer, G. L.; Faneyte, I. F.; Gastelen, A. Van; Pijnenborg, A. C. L. M. Subcellular Localization and Distribution of the Breast Cancer Resistance Protein Transporter in Normal Human Tissues Subcellular Localization and Distribution of the Breast Cancer Resistance Protein Transporter in Normal Human Tissues 1. **2001**, 3458–3464.

(11) Fetsch, P. a; Abati, A.; Litman, T.; Morisaki, K.; Honjo, Y.; Mittal, K.; Bates, S. E. Localization of the ABCG2 mitoxantrone resistance-associated protein in normal tissues. *Cancer letters* **2006**, *235*, 84–92.

(12) Doyle, L. A.; Ross, D. D. Multidrug resistance mediated by the breast cancer resistance protein BCRP (ABCG2). *Oncogene* **2003**, *22*, 7340–58.

(13) Allikmets, R.; Schriml, L. M.; Hutchinson, A.; Romano-Spica, V.; Dean, M. A human placenta-specific ATP-binding cassette gene (ABCP) on chromosome 4q22 that is involved in multidrug resistance. *Cancer research* **1998**, *58*, 5337–9.

(14) Mao, Q. BCRP/ABCG2 in the placenta: expression, function and regulation. *Pharmaceutical research* **2008**, *25*, 1244–55.

(15) Kobayashi, D.; Ieiri, I.; Hirota, T.; Takane, H. Functional assessment of ABCG2 (BCRP) gene polymorphisms to protein expression in human placenta. *Drug metabolism and* **2005**, *33*, 94–101.

(16) Yeboah, D.; Sun, M.; Kingdom, J.; Baczyk, D.; Lye, S. J.; Matthews, S. G.; Gibb, W. Expression of breast cancer resistance protein (BCRP / ABCG2) in human placenta throughout gestation and at term before and after labor. **2006**, *1258*, 1251–1258.

(17) Cooray, H. C.; Blackmore, C. G.; Maskell, L.; Barrand, M. a Localisation of breast cancer resistance protein in microvessel endothelium of human brain. *Neuroreport* **2002**, *13*, 2059–63.

(18) Jonker, J. W.; Merino, G.; Musters, S.; Van Herwaarden, A. E.; Bolscher, E.; Wagenaar, E.; Mesman, E.; Dale, T. C.; Schinkel, A. H. The breast cancer resistance protein BCRP (ABCG2) concentrates drugs and carcinogenic xenotoxins into milk. *Nature medicine* **2005**, *11*, 127–9.

(19) Noguchi, K.; Katayama, K.; Mitsuhashi, J.; Sugimoto, Y. Functions of the breast cancer resistance protein (BCRP/ABCG2) in chemotherapy. *Advanced drug delivery reviews* **2009**, *61*, 26–33.

(20) Poonkuzhali, B.; Lamba, J.; Strom, S. Association of breast cancer resistance protein/ABCG2 phenotypes and novel promoter and intron 1 single nucleotide polymorphisms. *Drug Metabolism and ...* **2008**, *36*, 780–795.

(21) Urquhart, B. L.; Ware, J. a; Tirona, R. G.; Ho, R. H.; Leake, B. F.; Schwarz, U. I.; Zaher, H.; Palandra, J.; Gregor, J. C.; Dresser, G. K.; Kim, R. B. Breast cancer resistance protein (ABCG2) and drug disposition: intestinal expression, polymorphisms and sulfasalazine as an in vivo probe. *Pharmacogenetics and genomics* **2008**, *18*, 439–48.

(22) Zamber, C. P.; Lamba, J. K.; Yasuda, K.; Farnum, J.; Thummel, K.; Schuetz, J. D.; Schuetz, E. G. Natural allelic variants of breast cancer resistance protein (BCRP) and their relationship to BCRP expression in human intestine. *Pharmacogenetics* **2003**, *13*, 19–28.

(23) Ross, D. D.; Karp, J. E.; Chen, T. T.; Doyle, L. A. Expression of breast cancer resistance protein in blast cells from patients with acute leukemia. *Blood* **2000**, *96*, 365–8.

(24) Suvannasankha, a; Minderman, H.; O'Loughlin, K. L.; Nakanishi, T.; Greco, W. R.; Ross, D. D.; Baer, M. R. Breast cancer resistance protein (BCRP/MXR/ABCG2) in acute myeloid leukemia: discordance between expression and function. *Leukemia : official journal of the Leukemia Society of America, Leukemia Research Fund, U.K* **2004**, *18*, 1252–7.

(25) Suvannasankha, A.; Minderman, H.; O'Loughlin, K. L.; Nakanishi, T.; Ford, L. a; Greco, W. R.; Wetzler, M.; Ross, D. D.; Baer, M. R. Breast cancer resistance protein (BCRP/MXR/ABCG2) in adult acute lymphoblastic leukaemia: frequent expression and possible correlation with shorter disease-free survival. *British journal of haematology* **2004**, *127*, 392–8.

(26) Benderra, Z.; Faussat, A.-M.; Sayada, L.; Perrot, J.-Y.; Chaoui, D.; Marie, J.-P.; Legrand, O. Breast cancer resistance protein and P-glycoprotein in 149 adult acute myeloid leukemias. *Clinical cancer research : an official journal of the American Association for Cancer Research* **2004**, *10*, 7896–902.

(27) Tsunoda, S.; Okumura, T.; Ito, T.; Kondo, K.; Ortiz, C.; Tanaka, E.; Watanabe, G.; Itami, A.; Sakai, Y.; Shimada, Y. ABCG2 expression is an independent unfavorable prognostic factor in esophageal squamous cell carcinoma. *Oncology* **2006**, *71*, 251–8.

(28) Usuda, J.; Tsunoda, Y.; Ichinose, S.; Ishizumi, T.; Ohtani, K.; Maehara, S.; Ono, S.; Tsutsui, H.; Ohira, T.; Okunaka, T.; Furukawa, K.; Sugimoto, Y.; Kato, H.; Ikeda, N. Breast cancer resistant protein (BCRP) is a molecular determinant of the outcome of photodynamic therapy (PDT) for centrally located early lung cancer. *Lung cancer (Amsterdam, Netherlands)* **2010**, *67*, 198–204.

(29) Uggla, B.; Ståhl, E.; Wågsäter, D.; Paul, C.; Karlsson, M. G.; Sirsjö, A.; Tidefelt, U. BCRP mRNA expression v. clinical outcome in 40 adult AML patients. *Leukemia research* **2005**, *29*, 141–6.

(30) Yoh, K. Breast Cancer Resistance Protein Impacts Clinical Outcome in Platinum-Based Chemotherapy for Advanced Non-Small Cell Lung Cancer. *Clinical Cancer Research* **2004**, *10*, 1691–1697.

(31) Bates, S. E.; Robey, R.; Miyake, K.; Rao, K.; Ross, D. D.; Litman, T. The role of half-transporters in multidrug resistance. *Journal of bioenergetics and biomembranes* **2001**, *33*, 503–11.

(32) Mao, Q.; Unadkat, J. D. Role of the breast cancer resistance protein (ABCG2) in drug transport. *The AAPS journal* **2005**, *7*, E118–33.

(33) Mo, W.; Zhang, J.-T. Human ABCG2: structure, function, and its role in multidrug resistance. *International journal of biochemistry and molecular biology* **2012**, *3*, 1–27.

(34) Miyake, K.; Mickley, L.; Litman, T.; Zhan, Z.; Robey, R.; Cristensen, B.; Brangi, M.; Greenberger, L.; Dean, M.; Fojo, T.; Bates, S. E. Molecular cloning of cDNAs which are highly overexpressed in mitoxantrone-resistant cells: demonstration of homology to ABC transport genes. *Cancer research* **1999**, *59*, 8–13.

(35) Litman, T.; Brangi, M.; Hudson, E.; Fetsch, P.; Abati, A.; Ross, D. D.; Miyake, K.; Resau, J. H.; Bates, S. E. The multidrug-resistant phenotype associated with overexpression of the new ABC half-transporter, MXR (ABCG2). *Journal of cell science* **2000**, *113 (Pt 1*, 2011–21.

(36) Posner, L. E.; Dukart, G.; Goldberg, J.; Bernstein, T.; Cartwright, K. Mitoxantrone: an overview of safety and toxicity. *Investigational new drugs* **1985**, *3*, 123–32.

(37) Scott, L. J.; Figgitt, D. P. Mitoxantrone: a review of its use in multiple sclerosis. *CNS drugs* **2004**, *18*, 379–96.

(38) Carles, J.; Castellano, D.; Climent, M. Á.; Maroto, P.; Medina, R.; Alcaraz, A. Castration-resistant metastatic prostate cancer: current status and treatment possibilities. *Clinical & translational oncology : official publication of the Federation of Spanish Oncology Societies and of the National Cancer Institute of Mexico* **2012**, *14*, 169–76.

(39) Atiba, J. O.; Green, S. J.; Hynes, H. E.; Osborne, C. K.; Miller, T. P.; Davidner, M. Phase II evaluation of mitoxantrone plus cis-platinum in patients with advanced breast cancer. A Southwest Oncology Group study. *Investigational new drugs* **1994**, *12*, 129–32.

(40) An, G.; Morris, M. E. Effects of single and multiple flavonoids on BCRP-mediated accumulation, cytotoxicity and transport of mitoxantrone in vitro. *Pharmaceutical research* **2010**, *27*, 1296–308.

(41) Tamura, A.; Wakabayashi, K.; Onishi, Y.; Nakagawa, H.; Tsuji, M.; Matsuda, Y.; Ishikawa, T. Genetic polymorphisms of human ABC transporter ABCG2: development of the standard method for functional validation of SNPs by using the

Flp recombinase system. *Journal of experimental therapeutics & oncology* **2006**, *6*, 1–11.

(42) Ishikawa, T.; Sakurai, A.; Kanamori, Y.; Nagakura, M.; Hirano, H.; Takarada, Y.; Yamada, K.; Fukushima, K.; Kitajima, M. High-speed screening of human ATP-binding cassette transporter function and genetic polymorphisms: new strategies in pharmacogenomics. *Methods in enzymology* **2005**, *400*, 485–510.

(43) Jonker, J. W.; Buitelaar, M.; Wagenaar, E.; Van Der Valk, M. a; Scheffer, G. L.; Scheper, R. J.; Plosch, T.; Kuipers, F.; Elferink, R. P. J. O.; Rosing, H.; Beijnen, J. H.; Schinkel, A. H. The breast cancer resistance protein protects against a major chlorophyll-derived dietary phototoxin and protoporphyria. *Proceedings of the National Academy of Sciences of the United States of America* **2002**, *99*, 15649–54.

(44) Desuzinges-Mandon, E.; Arnaud, O.; Martinez, L.; Huché, F.; Di Pietro, A.; Falson, P. ABCG2 transports and transfers heme to albumin through its large extracellular loop. *The Journal of biological chemistry* **2010**, *285*, 33123–33.

(45) Tamura, A.; Watanabe, M.; Saito, H.; Nakagawa, H.; Kamachi, T.; Okura, I.; Ishikawa, T. Functional validation of the genetic polymorphisms of human ATP-binding cassette (ABC) transporter ABCG2: identification of alleles that are defective in porphyrin transport. *Molecular pharmacology* **2006**, *70*, 287–96.

(46) Krishnamurthy, P.; Schuetz, J. D. The ABC transporter Abcg2/Bcrp: role in hypoxia mediated survival. *Biometals : an international journal on the role of metal ions in biology, biochemistry, and medicine* **2005**, *18*, 349–58.

(47) Wan, P.; Moat, S.; Anstey, A. Pellagra: a review with emphasis on photosensitivity. *The British journal of dermatology* **2011**, *164*, 1188–200.

(48) Ho, A. Y. L.; Deacon, A.; Osborne, G.; Mufti, G. J. Precipitation of porphyria cutanea tarda by imatinib mesylate? *British journal of haematology* **2003**, *121*, 375.

(49) Brazzelli, V.; Prestinari, F.; Barbagallo, T.; Rona, C.; Orlandi, E.; Passamonti, F.; Locatelli, F.; Zecca, M.; Villani, S.; Borroni, G. A long-term time course of colorimetric assessment of the effects of imatinib mesylate on skin pigmentation: a study of five patients. *Journal of the European Academy of Dermatology and Venereology : JEADV* **2007**, *21*, 384–7.

(50) Brazzelli, V.; Muzio, F.; Manna, G.; Moggio, E.; Vassallo, C.; Orlandi, E.; Fiandrino, G.; Lucioni, M.; Borroni, G. Photoinduced dermatitis and oral lichenoid reaction in a chronic myeloid leukemia patient treated with imatinib mesylate. *Photodermatology, photoimmunology & photomedicine* **2012**, *28*, 2–5.

(51) Boumendjel, a; Macalou, S.; Valdameri, G.; Pozza, a; Gauthier, C.; Arnaud, O.; Nicolle, E.; Magnard, S.; Falson, P.; Terreux, R.; Carrupt, P.; Payen, L.; Di Pietro, a Targeting the multidrug ABCG2 transporter with flavonoidic inhibitors: in vitro optimization and in vivo validation. *Current medicinal chemistry* **2011**, *18*, 3387–401.

(52) Jitsukawa, K.; Suizu, R.; Hidano, A. Chlorella photosensitization. New phytophotodermatosis. *International journal of dermatology* **1984**, *23*, 263–8.

(53) Robey, R. W.; Steadman, K.; Polgar, O.; Morisaki, K.; Blayney, M.; Mistry, P.; Bates, S. E. Pheophorbide a is a specific probe for ABCG2 function and inhibition. *Cancer research* **2004**, *64*, 1242–6.

(54) Tamura, A.; Wakabayashi, K.; Onishi, Y.; Takeda, M.; Ikegami, Y.; Sawada, S.; Tsuji, M.; Matsuda, Y.; Ishikawa, T. Re-evaluation and functional classification of non-synonymous single nucleotide polymorphisms of the human ATP-binding cassette transporter ABCG2. *Cancer Science* **2007**, *98*, 231–239.

(55) Robey, R. W.; Steadman, K.; Polgar, O.; Bates, S. E. ABCG2-mediated transport of photosensitizers: potential impact on photodynamic therapy. *Cancer biology & therapy* **2005**, *4*, 187–94.

(56) Jani, M.; Szabó, P.; Kis, E.; Molnár, E.; Glavinas, H.; Krajcsi, P.; Ani, M. J.; Zabó, P. S.; Is, E. K.; Olnár, É. M.; Lavinas, H. G.; Rajcsi, P. K. Kinetic characterization of sulfasalazine transport by human ATP-binding cassette G2. *Biological & pharmaceutical bulletin* **2009**, *32*, 497–9.

(57) Cantini, F.; Niccoli, L.; Nannini, C.; Kaloudi, O.; Bertoni, M.; Cassarà, E. Psoriatic arthritis: a systematic review. *International journal of rheumatic diseases* **2010**, *13*, 300–17.

(58) Ford, A. C.; Achkar, J.-P.; Khan, K. J.; Kane, S. V; Talley, N. J.; Marshall, J. K.; Moayyedi, P. Efficacy of 5-aminosalicylates in ulcerative colitis: systematic review and meta-analysis. *The American journal of gastroenterology* **2011**, *106*, 601–16.

(59) Adkison, K. K.; Vaidya, S. S.; Lee, D. Y.; Koo, S. H.; Li, L.; Mehta, A. A.; Gross, A. S.; Polli, J. W.; Humphreys, J. E.; Lou, Y.; Lee, E. J. D. Oral sulfasalazine as a clinical BCRP probe substrate: pharmacokinetic effects of genetic variation (C421A) and pantoprazole coadministration. *Journal of pharmaceutical sciences* **2010**, *99*, 1046–62.

(60) Kusuhara, H.; Furuie, H.; Inano, A.; Sunagawa, A.; Yamada, S.; Wu, C.; Fukizawa, S.; Morimoto, N.; Ieiri, I.; Morishita, M.; Sumita, K.; Mayahara, H.; Fujita, T.; Maeda, K.; Sugiyama, Y. Pharmacokinetic interaction study of

sulphasalazine in healthy subjects and the impact of curcumin as an in vivo inhibitor of BCRP. *British journal of pharmacology* **2012**, *166*, 1793–1803.

(61) De Jong, F. a; De Jonge, M. J. a; Verweij, J.; Mathijssen, R. H. J. Role of pharmacogenetics in irinotecan therapy. *Cancer letters* **2006**, *234*, 90–106.

(62) Nakatomi, K.; Yoshikawa, M.; Oka, M.; Ikegami, Y.; Hayasaka, S.; Sano, K.; Shiozawa, K.; Kawabata, S.; Soda, H.; Ishikawa, T.; Tanabe, S.; Kohno, S. Transport of 7-ethyl-10-hydroxycamptothecin (SN-38) by breast cancer resistance protein ABCG2 in human lung cancer cells. *Biochemical and biophysical research communications* **2001**, *288*, 827–32.

(63) Bates, S. E.; Medina-Pérez, W. Y.; Kohlhagen, G.; Antony, S.; Nadjem, T.; Robey, R. W.; Pommier, Y. ABCG2 mediates differential resistance to SN-38 (7-ethyl-10-hydroxycamptothecin) and homocamptothecins. *The Journal of pharmacology and experimental therapeutics* **2004**, *310*, 836–42.

(64) Bessho, Y.; Oguri, T.; Achiwa, H.; Muramatsu, H.; Maeda, H.; Niimi, T.; Sato, S.; Ueda, R. Role of ABCG2 as a biomarker for predicting resistance to CPT-11/SN-38 in lung cancer. *Cancer science* **2006**, *97*, 192–8.

(65) Takahata, T.; Ookawa, K.; Suto, K.; Tanaka, M.; Yano, H.; Nakashima, O.; Kojiro, M.; Tamura, Y.; Tateishi, T.; Sakata, Y.; Fukuda, S. Chemosensitivity determinants of irinotecan hydrochloride in hepatocellular carcinoma cell lines. *Basic & clinical pharmacology & toxicology* **2008**, *102*, 399–407.

(66) Jada, S. R.; Lim, R.; Wong, C. I.; Shu, X.; Lee, S. C.; Zhou, Q.; Goh, B. C.; Chowbay, B. Role of UGT1A1*6, UGT1A1*28 and ABCG2 c.421C>A polymorphisms in irinotecan-induced neutropenia in Asian cancer patients. *Cancer science* **2007**, *98*, 1461–7.

(67) Morisaki, K.; Robey, R. W.; Ozvegy-Laczka, C.; Honjo, Y.; Polgar, O.; Steadman, K.; Sarkadi, B.; Bates, S. E. Single nucleotide polymorphisms modify the transporter activity of ABCG2. *Cancer chemotherapy and pharmacology* **2005**, *56*, 161–72.

(68) De Jong, F. a; Marsh, S.; Mathijssen, R. H. J.; King, C.; Verweij, J.; Sparreboom, A.; McLeod, H. L. ABCG2 pharmacogenetics: ethnic differences in allele frequency and assessment of influence on irinotecan disposition. *Clinical cancer research : an official journal of the American Association for Cancer Research* **2004**, *10*, 5889–94.

(69) IEIRI, I. Functional Significance of Genetic Polymorphisms in P-glycoprotein (MDR1, ABCB1) and Breast Cancer Resistance Protein (BCRP, ABCG2). *Drug metabolism and pharmacokinetics* **2011**.

(70) Cascorbi, I. Role of pharmacogenetics of ATP-binding cassette transporters in the pharmacokinetics of drugs. *Pharmacology & therapeutics* **2006**, *112*, 457–73.

(71) Sarkadi, B.; Homolya, L.; Szakács, G.; Váradi, A. Human multidrug resistance ABCB and ABCG transporters: participation in a chemoimmunity defense system. *Physiological reviews* **2006**, *86*, 1179–236.

(72) Urban, T. J.; Sebro, R.; Hurowitz, E. H.; Leabman, M. K.; Badagnani, I.; Lagpacan, L. L.; Risch, N.; Giacomini, K. M. Functional genomics of membrane transporters in human populations. *Genome research* **2006**, *16*, 223–30.

(73) Giri, N.; Agarwal, S.; Shaik, N.; Pan, G.; Chen, Y.; Elmquist, W. F. Substrate-Dependent Breast Cancer Resistance Protein (Bcrp1 / Abcg2) -Mediated Interactions : Consideration of Multiple Binding Sites in in Vitro Assay Design. *Pharmacology* **2009**, *37*, 560–570.

(74) Robey, R. W.; Honjo, Y.; Morisaki, K.; Nadjem, T. a; Runge, S.; Risbood, M.; Poruchynsky, M. S.; Bates, S. E. Mutations at amino-acid 482 in the ABCG2 gene affect substrate and antagonist specificity. *British journal of cancer* **2003**, *89*, 1971–8.

(75) Meyer, H. E.; Kroemer, H. K. *Drug Transporters: In Vitro and In Vivo Evidence for the Importance of Breast Cancer Resistance Protein Transporters (BCRP/MXR/ABCP/ABCG2)*; Fromm, M. F.; Kim, R. B., Eds.; Springer Berlin Heidelberg: Berlin, Heidelberg, 2011; Vol. 201.

(76) Kroetz, D. L.; Yee, S. W.; Giacomini, K. M. The pharmacogenomics of membrane transporters project: research at the interface of genomics and transporter pharmacology. *Clinical pharmacology and therapeutics* **2010**, *87*, 109–16.

(77) Africa, W. A map of human genome variation from population-scale sequencing. *Nature* **2010**, *467*, 1061–73.

(78) Frazer, K. a; *et. al*. A second generation human haplotype map of over 3.1 million SNPs. *Nature* **2007**, *449*, 851–61.

(79) Yoshioka, S.; Katayama, K.; Okawa, C.; Takahashi, S.; Tsukahara, S.; Mitsuhashi, J.; Sugimoto, Y. The identification of two germ-line mutations in the human breast cancer resistance protein gene that result in the expression of a low/non-functional protein. *Pharmaceutical research* **2007**, *24*, 1108–17.

(80) Lee, S. S.; Jeong, H.; Yi, J.; Jung, H.; Jang, J.; Kim, E.; Lee, S.; Shin, J.; Al, L. E. E. E. T. Identification and Functional Assessment of BCRP Polymorphisms in a Korean Population. *Pharmacology* **2007**, *35*, 623–632.

(81) Kondo, C.; Suzuki, H.; Itoda, M.; Ozawa, S.; Sawada, J.; Kobayashi, D.; Ieiri, I.; Mine, K.; Ohtsubo, K.; Sugiyama, Y. Functional analysis of SNPs variants of BCRP/ABCG2. *Pharmaceutical research* **2004**, *21*, 1895–903.

(82) Ozvegy, C.; Váradi, A.; Sarkadi, B. Characterization of drug transport, ATP hydrolysis, and nucleotide trapping by the human ABCG2 multidrug transporter. Modulation of substrate specificity by a point mutation. *The Journal of biological chemistry* **2002**, *277*, 47980–90.

(83) Hesselson, S. E.; Matsson, P.; Shima, J. E.; Fukushima, H.; Yee, S. W.; Kobayashi, Y.; Gow, J. M.; Ha, C.; Ma, B.; Poon, A.; Johns, S. J.; Stryke, D.; Castro, R. a; Tahara, H.; Choi, J. H.; Chen, L.; Picard, N.; Sjödin, E.; Roelofs, M. J. E.; Ferrin, T. E.; Myers, R.; Kroetz, D. L.; Kwok, P.-Y.; Giacomini, K. M. Genetic variation in the proximal promoter of ABC and SLC superfamilies: liver and kidney specific expression and promoter activity predict variation. *PloS one* **2009**, *4*, e6942.

(84) Barrett, J. C.; Fry, B.; Maller, J.; Daly, M. J. Haploview: analysis and visualization of LD and haplotype maps. *Bioinformatics (Oxford, England)* **2005**, *21*, 263–5.

(85) Grantham, R. Amino acid difference formula to help explain protein evolution. *Science (New York, NY)* **1974**, *185*, 862–864.

(86) Kumar, P.; Henikoff, S.; Ng, P. C. Predicting the effects of coding non-synonymous variants on protein function using the SIFT algorithm. *Nature protocols* **2009**, *4*, 1073–81.

(87) Adzhubei, I. a; Schmidt, S.; Peshkin, L.; Ramensky, V. E.; Gerasimova, A.; Bork, P.; Kondrashov, A. S.; Sunyaev, S. R. A method and server for predicting damaging missense mutations. *Nature methods* **2010**, *7*, 248–9.

(88) Schneider, C. A.; Rasband, W. S.; Eliceiri, K. W. NIH Image to ImageJ: 25 years of image analysis. *Nature methods* **2012**, *9*, 671–5.

(89) Palmgren, M. G.; Askerlund, P.; Fredrikson, K.; Widell, S.; Sommarin, M.; Larsson, C. Sealed inside-out and right-side-out plasma membrane vesicles : optimal conditions for formation and separation. *Plant physiology* **1990**, *92*, 871–80.

(90) Palmgren, M. G.; Sommarin, M.; Ulvskov, P.; Larsson, C. Effect of detergents on the H(+)-ATPase activity of inside-out and right-side-out plant plasma membrane vesicles. *Biochimica et Biophysica Acta* **1990**, *1021*, 133–140.

(91) Palmgren, M. G. An H-ATPase Assay: Proton Pumping and ATPase Activity Determined Simultaneously in the Same Sample. *Plant physiology* **1990**, *94*, 882–6.

(92) Palmgren, M. G. Acridine orange as a probe for measuring pH gradients across membranes: mechanism and limitations. *Analytical biochemistry* **1991**, *192*, 316–21.

(93) Imai, Y.; Asada, S.; Tsukahara, S.; Ishikawa, E.; Tsuruo, T.; Sugimoto, Y. Breast cancer resistance protein exports sulfated estrogens but not free estrogens. *Molecular pharmacology* **2003**, *64*, 610–8.

(94) Chen, Z.; Robey, R. W.; Belinsky, M. G.; Shchaveleva, I.; Ren, X.; Sugimoto, Y.; Ross, D. D.; Bates, S. E.; Kruh, G. D. Transport of methotrexate, methotrexate polyglutamates, and 17beta-estradiol 17-(beta-D-glucuronide) by ABCG2: effects of acquired mutations at R482 on methotrexate transport. *Cancer research* **2003**, *63*, 4048–54.

(95) Ishikawa, T.; Nakagawa, H.; Hagiya, Y.; Nonoguchi, N.; Miyatake, S.-I.; Kuroiwa, T. Key Role of Human ABC Transporter ABCG2 in Photodynamic Therapy and Photodynamic Diagnosis. *Advances in pharmacological sciences* **2010**, *2010*, 587306.

(96) Nguyen, T. D.; Gow, J. M.; Chinn, L. W.; Kelly, L.; Jeong, H.; Huang, C. C.; Stryke, D.; Kawamoto, M.; Johns, S. J.; Carlson, E.; Taylor, T.; Ferrin, T. E.; Sali, A.; Giacomini, K. M.; Kroetz, D. L. PharmGKB submission update: IV. PMT submissions of genetic variations in ATP-Binding cassette transporters to the PharmGKB network. *Pharmacological reviews* **2006**, *58*, 1–2.

(97) Zhou, S.; Schuetz, J. D.; Bunting, K. D.; Colapietro, a M.; Sampath, J.; Morris, J. J.; Lagutina, I.; Grosveld, G. C.; Osawa, M.; Nakauchi, H.; Sorrentino, B. P. The ABC transporter Bcrp1/ABCG2 is expressed in a wide variety of stem cells and is a molecular determinant of the side-population phenotype. *Nature medicine* **2001**, *7*, 1028–34.

(98) Ozvegy-Laczka, C.; Katalin, N.; Sarkadi, B.; Német, K.; Váradi, A. ABCG2 -- a transporter for all seasons. *FEBS letters* **2004**, *567*, 116–20.

(99) Kova, R.; Va, E.; Richter, O. Von; Koomen, G. ABCG2 (Breast Cancer Resistance Protein / Mitoxantrone Resistance-Associated Protein) ATPase Assay : A Useful Tool to Detect Drug-Transporter Interactions ABSTRACT : **2007**, *35*, 1533–1542.

(100) Noumi, T.; Maeda, M.; Futai, M. Mode of inhibition of sodium azide on H+-ATPase of Escherichia coli. *FEBS letters* **1987**, *213*, 381–384.

(101) Furukawa, T.; Wakabayashi, K.; Tamura, A.; Nakagawa, H.; Morishima, Y.; Osawa, Y.; Ishikawa, T. Major SNP (Q141K) variant of human ABC transporter ABCG2 undergoes lysosomal and proteasomal degradations. *Pharmaceutical research* **2009**, *26*, 469–79.

(102) Wakabayashi-Nakao, K.; Tamura, A.; Furukawa, T.; Nakagawa, H.; Ishikawa, T. Quality control of human ABCG2 protein in the endoplasmic reticulum: ubiquitination and proteasomal degradation. *Advanced drug delivery reviews* **2009**, *61*, 66–72.

(103) Tamura, A.; Onishi, Y.; An, R.; Koshiba, S.; Wakabayashi, K.; Hoshijima, K.; Priebe, W.; Yoshida, T.; Kometani, S.; Matsubara, T.; Mikuriya, K.; Ishikawa, T. In vitro evaluation of photosensitivity risk related to genetic polymorphisms of human ABC transporter ABCG2 and inhibition by drugs. *Drug metabolism and pharmacokinetics* **2007**, *22*, 428–40.

(104) Wakabayashi, K.; Tamura, A.; Saito, H.; Onishi, Y.; Ishikawa, T. Human ABC transporter ABCG2 in xenobiotic protection and redox biology. *Drug metabolism reviews* **2006**, *38*, 371–91.

(105) Ni, Z.; Bikadi, Z.; Rosenberg, M. F.; Mao, Q. Structure and function of the human breast cancer resistance protein (BCRP/ABCG2). *Current drug metabolism* **2010**, *11*, 603.

(106) Pál, A.; Méhn, D.; Molnár, E.; Gedey, S.; Mészáros, P.; Nagy, T.; Glavinas, H.; Janáky, T.; Von Richter, O.; Báthori, G.; Szente, L.; Krajcsi, P. Cholesterol potentiates ABCG2 activity in a heterologous expression system: improved in vitro model to study function of human ABCG2. *The Journal of pharmacology and experimental therapeutics* **2007**, *321*, 1085–94.

(107) Ozvegy, C.; Litman, T.; Szakács, G.; Nagy, Z.; Bates, S.; Váradi, a; Sarkadi, B. Functional characterization of the human multidrug transporter, ABCG2, expressed in insect cells. *Biochemical and biophysical research communications* **2001**, *285*, 111–7.

(108) Rosenberg, M. F.; Bikadi, Z.; Chan, J.; Liu, X.; Ni, Z.; Cai, X.; Ford, R. C.; Mao, Q. The human breast cancer resistance protein (BCRP/ABCG2) shows conformational changes with mitoxantrone. *Structure (London, England : 1993)* **2010**, *18*, 482–93.

(109) Glavinas, H.; Kis, E.; Pál, A.; Kovács, R.; Jani, M.; Vági, E.; Molnár, E.; Bánsághi, S.; Kele, Z.; Janáky, T.; Báthori, G.; Von Richter, O.; Koomen, G.-J.; Krajcsi, P. ABCG2 (breast cancer resistance protein/mitoxantrone resistance-associated protein) ATPase assay: a useful tool to detect drug-transporter interactions. *Drug metabolism and disposition: the biological fate of chemicals* **2007**, *35*, 1533–42.

(110) Kim, K.; Joo, H.-J.; Park, J.-Y. ABCG2 polymorphisms, 34G>A and 421C>A in a Korean population: analysis and a comprehensive comparison with other populations. *Journal of clinical pharmacy and therapeutics* **2010**, *35*, 705–12.

(111) Yanase, K.; Tsukahara, S.; Mitsuhashi, J.; Sugimoto, Y. Functional SNPs of the breast cancer resistance protein-therapeutic effects and inhibitor development. *Cancer letters* **2006**, *234*, 73–80.

(112) Ingelheim, B.; Imai, Y.; Nakane, M.; Kage, K.; Tsukahara, S.; Ishikawa, E.; Tsuruo, T.; Miki, Y.; Sugimoto, Y. C421A polymorphism in the human breast cancer resistance protein gene is associated with low expression of Q141K protein and low-level drug resistance. *Molecular cancer therapeutics* **2002**, *1*, 611–6.

(113) ITODA, M.; SAITO, Y.; SHIRAO, K. Eight novel single nucleotide polymorphisms in ABCG2/BCRP in Japanese cancer patients administered irinotacan. *Drug metabolism and ...* **2003**, *18*, 212–217.

(114) Honjo, Y.; Morisaki, K.; Huff, L.; Robey, R. W.; Hung, J.; Dean, M.; Bates, S. E. Single-nucleotide polymorphism (SNP) analysis in the ABC half-transporter ABCG2 (MXR/BCRP/ABCP1). *Cancer biology & ...* **2002**, *2*, 696–702.

(115) Bäckström, G.; Taipalensuu, J.; Melhus, H.; Brändström, H.; Svensson, A.-C.; Artursson, P.; Kindmark, A. Genetic variation in the ATP-binding cassette transporter gene ABCG2 (BCRP) in a Swedish population. *European journal of pharmaceutical sciences : official journal of the European Federation for Pharmaceutical Sciences* **2003**, *18*, 359–64.

(116) Mizuarai, S.; Aozasa, N.; Kotani, H. Single nucleotide polymorphisms result in impaired membrane localization and reduced atpase activity in multidrug transporter ABCG2. *International journal of cancer. Journal international du cancer* **2004**, *109*, 238–46.

(117) Bosch, T. M.; Kjellberg, L. M.; Bouwers, A.; Koeleman, B. P. C.; Schellens, J. H. M.; Beijnen, J. H.; Smits, P. H. M.; Meijerman, I. Detection of single nucleotide polymorphisms in the ABCG2 gene in a Dutch population. *American journal of pharmacogenomics : genomics-related research in drug development and clinical practice* **2005**, *5*, 123–31.

(118) Kim, D. H. D.; Sriharsha, L.; Xu, W.; Kamel-Reid, S.; Liu, X.; Siminovitch, K.; Messner, H. a.; Lipton, J. H. Clinical relevance of a pharmacogenetic approach using multiple candidate genes to predict response and resistance to imatinib therapy in chronic myeloid leukemia. *Clinical cancer research : an official journal of the American Association for Cancer Research* **2009**, *15*, 4750–8.

(119) Kim, I.-S.; Kim, H.-G.; Kim, D. C.; Eom, H.-S.; Kong, S.-Y.; Shin, H.-J.; Hwang, S.-H.; Lee, E.-Y.; Lee, G.-W. ABCG2 Q141K polymorphism is associated with chemotherapy-induced diarrhea in patients with diffuse large B-cell lymphoma who received frontline rituximab plus cyclophosphamide/doxorubicin/vincristine/prednisone chemotherapy. *Cancer science* **2008**, *99*, 2496–501.

(120) Erdilyi, D. J.; Kámory, E.; Csókay, B.; Andrikovics, H.; Tordai, a; Kiss, C.; Filni-Semsei, a; Janszky, I.; Zalka, a; Fekete, G.; Falus, a; Kovács, G. T.; Szalai, C. Synergistic interaction of ABCB1 and ABCG2 polymorphisms predicts the prevalence of toxic encephalopathy during anticancer chemotherapy. *The pharmacogenomics journal* **2008**, *8*, 321–7.

(121) Sai, K.; Saito, Y.; Maekawa, K.; Kim, S.-R.; Kaniwa, N.; Nishimaki-Mogami, T.; Sawada, J.; Shirao, K.; Hamaguchi, T.; Yamamoto, N.; Kunitoh, H.; Ohe, Y.; Yamada, Y.; Tamura, T.; Yoshida, T.; Matsumura, Y.; Ohtsu, A.; Saijo, N.; Minami, H. Additive effects of drug transporter genetic polymorphisms on irinotecan pharmacokinetics/pharmacodynamics in Japanese cancer patients. *Cancer chemotherapy and pharmacology* **2010**, *66*, 95–105.

(122) Sugimoto, Y.; Tsukahara, S.; Ishikawa, E.; Mitsuhashi, J. Breast cancer resistance protein: molecular target for anticancer drug resistance and pharmacokinetics/pharmacodynamics. *Cancer science* **2005**, *96*, 457–65.

(123) Kasza, I.; Várady, G.; Andrikovics, H.; Koszarska, M.; Tordai, A.; Scheffer, G. L.; Németh, A.; Szakács, G.; Sarkadi, B. Expression Levels of the ABCG2 Multidrug Transporter in Human Erythrocytes Correspond to Pharmacologically Relevant Genetic Variations. *PloS one* **2012**, *7*, e48423.

(124) Sparreboom, A.; Gelderblom, H.; Marsh, S.; Ahluwalia, R.; Obach, R.; Principe, P.; Twelves, C.; Verweij, J.; McLeod, H. L. Diflomotecan pharmacokinetics in relation to ABCG2 421C>A genotype. *Clinical pharmacology and therapeutics* **2004**, *76*, 38–44.

(125) Keskitalo, J. E. J.; Pasanen, M. K. M.; Neuvonen, P. J.; Niemi, M. Different effects of the ABCG2 c. 421C> A SNP on the pharmacokinetics of fluvastatin, pravastatin and simvastatin. *Pharmacogenomics* **2009**, *10*, 1617–1624.

(126) Zhang, W.; Yu, B.-N.; He, Y.-J.; Fan, L.; Li, Q.; Liu, Z.-Q.; Wang, A.; Liu, Y.-L.; Tan, Z.-R.; Fen-Jiang; Huang, Y.-F.; Zhou, H.-H. Role of BCRP 421C>A polymorphism on rosuvastatin pharmacokinetics in healthy Chinese males. *Clinica chimica acta; international journal of clinical chemistry* **2006**, *373*, 99–103.

(127) Adkison, K. K.; Vaidya, S. S.; Lee, D. Y.; Koo, S. H.; Li, L.; Mehta, A. a; Gross, A. S.; Polli, J. W.; Lou, Y.; Lee, E. J. D. The ABCG2 C421A polymorphism does not affect oral nitrofurantoin pharmacokinetics in healthy Chinese male subjects. *British journal of clinical pharmacology* **2008**, *66*, 233–9.

(128) Ieiri, I.; Suwannakul, S.; Maeda, K.; Uchimaru, H.; Hashimoto, K.; Kimura, M.; Fujino, H.; Hirano, M.; Kusuhara, H.; Irie, S.; Higuchi, S.; Sugiyama, Y. SLCO1B1 (OATP1B1, an Uptake Transporter) and ABCG2 (BCRP, an Efflux Transporter) Variant Alleles and Pharmacokinetics of Pitavastatin in Healthy Volunteers. *Clinical Pharmacology & Therapeutics* **2007**, *82*, 541–547.

(129) Ho, R. H.; Choi, L.; Lee, W.; Mayo, G.; Schwarz, U. I.; Tirona, R. G.; Bailey, D. G.; Michael Stein, C.; Kim, R. B. Effect of drug transporter genotypes on pravastatin disposition in European- and African-American participants. *Pharmacogenetics and genomics* **2007**, *17*, 647–56.

(130) Kim, H.-S.; Sunwoo, Y. E.; Ryu, J. Y.; Kang, H.-J.; Jung, H.-E.; Song, I.-S.; Kim, E.-Y.; Shim, J.-C.; Shon, J.-H.; Shin, J.-G. The effect of ABCG2 V12M, Q141K and Q126X, known functional variants in vitro, on the disposition of lamivudine. *British journal of clinical pharmacology* **2007**, *64*, 645–54.

(131) Vethanayagam, R. R.; Wang, H.; Gupta, A.; Zhang, Y.; Lewis, F.; Unadkat, J. D.; Mao, Q. Functional analysis of the human variants of breast cancer resistance protein: I206L, N590Y, and D620N. *Drug metabolism and disposition: the biological fate of chemicals* **2005**, *33*, 697–705.

(132) Xie, H. Activity assay of membrane transport proteins. *Acta Biochimica et Biophysica Sinica* **2008**, *40*, 269–277.

(133) McDevitt, C. a; Crowley, E.; Hobbs, G.; Starr, K. J.; Kerr, I. D.; Callaghan, R. Is ATP binding responsible for initiating drug translocation by the multidrug transporter ABCG2? *The FEBS journal* **2008**, *275*, 4354–62.

Chapter 3: Functional Characterization of the *ABCG2* Promoter and its Genetic Variants

3.1. Abstract

ABCG2 encodes the mitoxantrone resistance protein (MXR, BCRP), a membrane transporter responsible for the efflux of its substrates out of the cell and important in detoxification of the body. In the present study, we examine the basal activity of the *ABCG2* promoter in HepG2 (liver), HEK293T (kidney), HCT116 (intestine) and MCF-7 (breast) cell lines. We then proceed to test the effect of variants on the *ABCG2* promoter activity *in vitro* and on *in silico* predictions for transcription factor binding. Reference and variant *ABCG2* promoter sequences, cloned into a promoter assay vector, were tested for their ability to increase luciferase activity when transiently transfected into these four cell lines. We found that the *ABCG2* promoter was strongest in the HepG2 and HCT116 cell lines. We also identified four SNPs in the basal *ABCG2* promoter (rs76656413, rs66664036, rs139256004 and rs59370292) that decreased the activity of the *ABCG2* promoter by 50% in at least three of the four cell lines. Three of these SNPs (rs76656413 and rs59370292) significantly decreased *in vivo* liver promoter activity, from 50-80%. The *in silico* transcription factor binding analysis found alterations in binding probabilities of several transcription factors for each of these SNPs that could explain their ability to alter *ABCG2* promoter activity *in vitro*. In conclusion, genetic variants in the *ABCG2* promoter could be a contributing factor to the variability of ABCG2 expression in the liver and intestine.

3.2. Introduction

The mitoxantrone resistance protein (MXR, BCRP) is an efflux membrane transporter and part of the ATP-binding cassette (ABC) transporter family. It transports a variety of dietary toxins, endogenous nutrients and pharmaceutical compounds[1]. MXR is expressed in the side population of hematological stem cells[2–4], endothelium of veins and capillaries (including in the brain)[5–7], intestinal and colon epithelium[5,7–9], placental syncytiotrophoblasts[5,7–13], ducts and lobules of the breast[5], the bile canalicular membrane of hepatocytes[5,7–9] and to a lesser extent the renal cortex tubules[7–9]. *ABCG2* is essential for detoxification processes, transport of nutrients into milk and protection of vital organs and tissues like the brain, fetus, prostate and eye[14].

Inter-individual expression of ABCG2 mRNA has been shown to be highly variable. One analysis of human livers has shown as much as a 500-fold difference in mRNA expression across samples, without detectable copy number variations[15]. ABCG2 mRNA levels varied 1000-fold in the blast cells of leukemic patients[16] and 1.8- to 78-fold in human intestine[17,18]. Our own liver and kidney expression data show large variation in human liver and kidney ABCG2 mRNA (*Chapter 1* Figure 1.2). High ABCG2 expression has been linked to decreased disease-free survival in several different cancers[18–25]. Variability in ABCG2 expression might also influence drug response and toxicity. Understanding the mechanisms that regulate the expression of ABCG2 can help to predict cancer outcomes, drug response and toxicity.

MXR is transcribed by *ABCG2* located on the anti-strand of chromosome 4q22 between *PKD2* and *PPM1K*. *ABCG2* spans over 66 kb with the translational start site in exon 2, the Walker A domain in exon 3 and the Walker B and ABC signature domains in

exon 6[10]. There are several tissue-specific isoforms of *ABCG2* that occur due to the creation of splice variants of the 5'-UTR of *ABCG2* from use of alternate promoters[26–28]. Examples of exon 1 splice variants are E1a[15,29] (the most common, generated by three adjacent promoters and detected in drug-resistance cell lines[27]), E1b (associated with lower ABCG2 mRNA in livers[15] and with a murine equivalent expressed in the intestine[28]) and E1c (contains an intron 1 that is approximately 90 kb longer than the others and detected in human leukemia[26] and murine erythroid differentiation[30]). Due to this evidence of tissue specific use of promoters, the relevance of the basal *ABCG2* promoter in different tissues and how the variants of its promoter effect the expression of ABCG2 needs to be investigated.

Promoters regulate the basal expression of genes and are generally located within 2.5 kb of the transcriptional start site (TSS), with the core promoter usually ~50 bp in length and adjacent to the TSS of the gene[31,32]. The core promoter is responsible for binding of transcriptional machinery, such as RNA polymerase II, and is the minimal amount of promoter required to drive transcription of the gene[33]. The region adjacent to the core promoter, generally within 250 bp, is called the proximal promoter. The proximal promoter is typically comprised of binding sites for other transcription factors (TFs) which are important for the tethering of regulatory elements (such as enhancers) which interact with the general transcriptional machinery[34]. Promoters work in concert with other regulatory regions, including insulators, suppressors and enhancers, to modulate the level of gene expression. Promoters are often associated with a high frequency of cytosine followed by guanine (CpG) sites[32]. Clusters of CpG sites, at a frequency higher than what would randomly be expected through the genome, are called CpG islands[35].

Methylation occurs at the 5'-position on the cytosine of CpG sites, and methylation of multiple CpG sites over a gene promoter is associated with gene suppression[35].

The basal *ABCG2* promoter is a TATA-less promoter and was previously identified as the 312 bp upstream of the TSS[29]. The basal promoter includes a CCAAT box and numerous SP1, AP1 and AP2 sites (black boxes in Figure 3.1)[29]. The proximal promoter of *ABCG2* has a functional aryl hydrocarbon receptor response element between -194 to -190[36,37] (purple box Figure 3.1) that overlaps with its functional progesterone[38] (turquoise box Figure 3.1) and estrogen[39] response elements (pink box Figure 3.1). There is also an NF-κB response element at -23, which works in concert with estrogen to increase ABCG2 expression[40] (orange bar in Figure 3.1). Additionally, there is a hypoxia inducible factor (HIF)-1α response element (HRE) between -116 and -112[41] (red bar in Figure 3.1) and an antioxidant response element (ARE) at -431 to -420[42] (blue bar in Figure 3.1). The basal promoter is on the edge of a large CpG island that covers most of the *ABCG2* proximal promoter (green bar in Figure 3.1). Hypomethylation of the *ABCG2* CpG island is a factor in the increased expression levels of ABCG2 during development of drug resistance in both cell lines and human tumor cells[43–46].

Genetic polymorphisms in the proximal promoter of transporter genes have been linked to variation in gene expression[47–50]. Additionally, genetic variations in promoters for other pharmacogenes have been linked to adverse drug reactions[51–55]. The general function of the basal *ABCG2* promoter has been previously identified[29]; however no further research has been done looking at genetic variation in the *ABCG2* promoter and its effect on the basal activity of the promoter.

In the present study, the basal activity of the major *ABCG2* promoter (-499 to +21 bp relative to the TSS) was investigated in transiently transfected kidney (HEK293T), liver (HepG2), intestine (HCT116) and breast (MCF-7) cell lines. The activity of twelve variant *ABCG2* promoter constructs was characterized in these same cell lines to identify SNPs that alter *ABCG2* promoter activity. Furthermore, SNPs that caused significant *in vitro* decreases in *ABCG2* promoter activity were tested in the mouse hydrodynamic tail vein assay for their effect on *in vivo* promoter activity. The functional significance of these SNPs was investigated by predicting changes in TFBS using *in silico* TFBS modeling. In some cases, preliminary support for the binding of these TFBS to the *ABCG2* promoter was obtained from the public chromatin immunoprecipitation with parallel sequencing (ChIP-seq) database ENCODE.

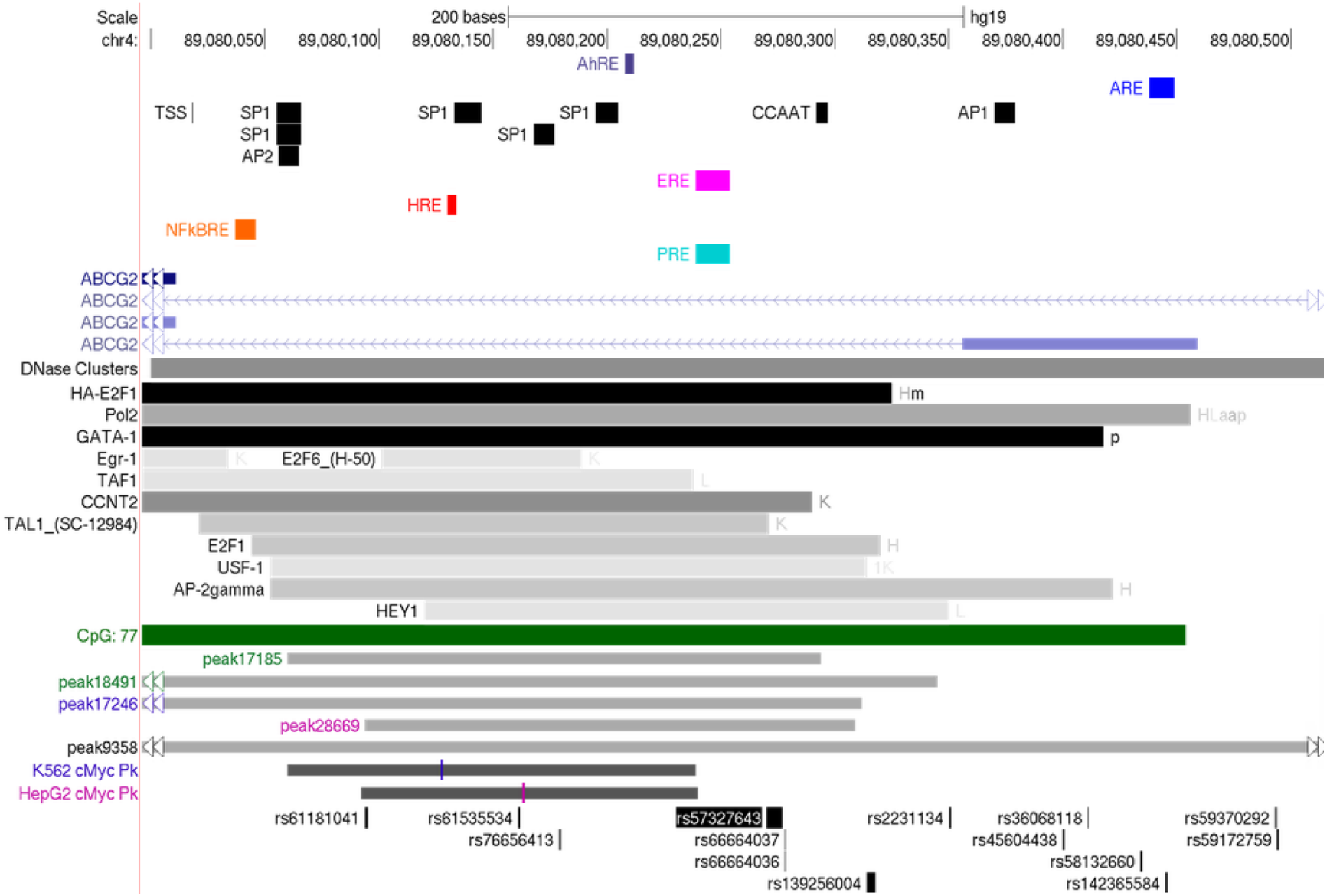
Scale
chr4:
200 bases
hg19
89,080,050
89,080,100
89,080,150
89,080,200
89,080,250
89,080,300
89,080,350
89,080,400
89,080,450
89,080,500
AhRE
ARE
TSS
SP1
SP1
AP2
SP1
SP1
SP1
CCAAT
AP1
ERE
HRE
NFkBRE
PRE
ABCG2
ABCG2
ABCG2
ABCG2
DNase Clusters
HA-E2F1
Pol2
GATA-1
Egr-1
E2F6_(H-50)
TAF1
CCNT2
TAL1_(SC-12984)
E2F1
USF-1
AP-2gamma
HEY1
CpG: 77
peak17185
peak18491
peak17246
peak28669
peak9358
K562 cMyc Pk
HepG2 cMyc Pk
rs61181041
rs61535534
rs76656413
rs57327643
rs66664037
rs66664036
rs139256004
rs2231134
rs36068118
rs45604438
rs59370292
rs59172759
rs58132660
rs142365584

Figure 3.1. Schematic of the *ABCG2* promoter region. From top to bottom: the genomic coordinates (chr4:89079997-89080517; hg19) followed by black boxes indicating where basal transcription factors have been reported to bind[29]. The transcriptional start site is indicated by a black box labeled TSS. The colored boxes indicate where nuclear response elements for aryl hydrocarbon[36] (purple), antioxidant[42] (blue), estrogen[39] (pink), hypoxia[41] (red), NF-κB[40] (orange) and progesterone[38] (turquoise) receptors have been reported to bind. Below this is ChIP-seq data from ENCODE with each TF on its own line followed by a bar, with the length indicating the breadth of the peak and the shading indicating its strength. Each bar is followed by letters to indicate the cell line the signal was found in: K, K562; H, HeLa-S3; L, HepG2; a, A549; p, PAC-1; m, MCF-7. This is followed by a green bar depicting a CpG island covering almost the entire basal promoter. Below the CpG island are seven additional peaks from ENCODE ChIP-seq data. The first five grey bars are for USF-1, with peaks 17185 and 18491 in H1-hESC cells, peak 17246 in K562 cells, peak 28669 in HepG2 cells and peak 9358 in ECC1 cells. The last two peaks are for cMyc in K562 and HepG2 cells. Finally, the location and rs number for single nucleotide polymorphisms (SNP) reported in dbSNP 135 are indicated.

3.3. Materials and Methods

3.3.1. *Chemicals and Materials*

The vectors pGL4.11b [*luc2*P], pGL4.74 [*hRluc*/TK], pGL4.13 [*luc2*/SV40], the Dual-Luciferase® Reporter Assay System and HB101 competent cells were all purchased from Promega (Madison, WI). The human embryonic kidney (HEK293T/17), human

colorectal carcinoma (HCT116), human hepatocellular carcinoma (HepG2) and human breast adenocarcinoma (MCF-7) cell lines were all purchased from the American Type Culture Collection (ATCC, Manassas, VA). The One Shot INV110 *dcm*$^-$/*dam*$^-$ competent cells, high-glucose Dulbecco's modified Eagle's medium (DMEM), Opti-Minimal Essential Medium (Opti-MEM) and Lipofectamine 2000 were all purchased from Invitrogen (Carlsbad, CA). The 100 mm LB Amp-100 agar plates and LB Broth supplemented with 100 μg/mL ampicilin were purchased from Teknova (Hollister, CA). DMSO, phosphate buffered saline (PBS), 0.05% trypsin and 100X penicillin and streptomycin were all purchased from the UCSF Cell Culture Facility (San Francisco, CA). The GeneJet PCR Purification Kits, GeneJET Gel Purification Kits and GeneJet Plasmid Miniprep Kits were all purchased from Fermentas (Glen Burnie, MD). High-Fidelity Phusion Buffer, Phusion High-Fidelity DNA Polymerase, bovine serum albumin (BSA), Buffer 2, *Nhe*I, *Hind*III, T4 Ligase, Ligase buffer, *Dpn*I, *Dpn*I digestion buffer, antarctic phosphatase and 10 mM ATP were all purchased from New England Biolabs (Ipswich, MA). Endotoxin-Free Maxiprep Kits and placental genomic DNA were purchased from Sigma Aldrich (St. Louis, MO). All other materials including10% fetal bovine serum (FBS) (Axenia BioLogix, Dixon, CA), GenElute HP Improved Minimum Essential Medium (IMEM) without phenol red (Mediatech Inc, Manassas, VA), PolyJet™ DNA *In Vitro* Transfection Reagent (SignaGen Laboratories, Rockville, MD), PfuTurbo DNA Polymerase (Agilent Technologies, Santa Clara, CA) and dNTPs (Denville, Metuchen, NJ) were all purchased from the indicated manufacturers.

3.3.2. *ABCG2 Promoter Plasmid Construction*

A 524 bp region of the *ABCG2* promoter (chr4:89079995-89080518, hg19) was targeted for PCR amplification using the forward primer 5'-TCAGGCTAGCAAGCATCCACTTTCTCAGA-3' and reverse primer 5'-TTATAAGCTTCAGGCAGCGCTGACACGAA-3'. This region was selected as it includes the proximal promoter (-312 bp upstream of the TSS)[29], adjacent TF response elements including the antioxidant response element (ARE) at -431 to -420[42] and the CpG island that extends to ~500 bp upstream of the TSS[29]. The core of the primers were designed using the Primer3 program[56] and the sequences for restriction sites *Nhe*I and *Hind*III were added to the forward and reverse primers, respectively (underlined in above sequences). Primers were synthesized by Integrated DNA Technologies (San Diego, CA). The UCSC genome browser's *in silico* PCR program was used to confirm predicted specific amplification of the target region with the selected primer set. The region was amplified from human placenta genomic DNA using 1 unit PfuTurbo DNA polymerase, 1X PfuTurbo buffer, 200 μM dNTPs, 150 ng genomic DNA, 400 nM of each primer, and 1 μL DMSO in a final reaction volume of 50 μL. PCR conditions were 95°C for 2 min, followed by 35 cycles of 30 sec at 95°C, 30 sec at 60°C and 1 min at 68°C, then a final extension of 10 min at 72°C. The PCR reaction was imaged on a 1% agarose gel and the specific band at 542 bp was gel purified using the GeneJet Gel Purification Kit following the manufacturer's protocol. For cloning, the pGL4.11b [*luc2*P] vector was grown in One Shot INV110 dcm^-/dam^- competent cells so methylation would not interfere with enzyme digestion. The pGL4.11b vector is a promoterless firefly luciferase vector designed to accept a putative promoter sequence before the luciferase gene. The purified promoter

region and the pGL4.11b vector were enzyme digested in a reaction of 1X Buffer 2, 1 unit *Nhe*I, 1 unit *Hind*III and 0.5 µL BSA at 37°C for 1 hr. Vectors were dephosphorylated using 4 units of antarctic phosphatase at 37°C for 2 hr. The reaction was purified using the GeneJet PCR Purification Kit following the manufacturer's protocol and the concentration of the cleaned DNA was checked using spectrophotometry (NanoDrop Spectrophotometer, Thermo Scientific).

The amplified *ABCG2* promoter region was ligated into the pGL4.11b vector through a 96:32 fmol insert to vector reaction comprised of the insert and vector plus 1 unit Ligase T4, 1X Ligase Buffer, and 65 nM ATP in a final reaction volume of 20 µL. The ligation was allowed to sit overnight at room temperature before purification using the GeneJet PCR Purification kit. A portion of the purified ligation reaction (5 µL) was transformed into 35 µL HB101 competent cells following the manufacturer's protocol. The transformed bacteria was plated onto 100 mm LB Amp-100 plates and grown at 37°C for 24 hr. Selected colonies were grown in 2-5 mL LB Broth with 100 µg/mL ampicillin at 37°C with shaking for up to 24 hr. DNA was isolated from the bacteria using a GeneJet Plasmid Miniprep Kit and sequenced with the RVPrimer3 to verify the presence and orientation of the *ABCG2* promoter in the pGL4.11b vector. Colonies having the promoter in both the forward (positive strand sequence) and reverse (reverse strand sequence) orientation were isolated. Other vectors used in the transfection assays include the pGL4.74 [*hRluc*/TK] vector, which has a Renilla luciferase reporter gene, a highly active HSV-TK promoter, and is co-transfected into each cell so that the transfection efficiency can be controlled by the expression of Renilla, and the pGL4.13 [*luc2*/SV40] vector, which has a luciferase reporter gene and a highly active SV40

promoter and is used as a positive control. DNA for the selected promoter plasmids, empty pGL4.11b [*luc2*P], pGL4.74 [*hRluc*/TK] and pGL4.13 [*luc2*/SV40] vectors were isolated from transformed bacteria grown in 150 mL LB Broth with 100 μg/mL ampicillin overnight at 37°C with shaking, using the GenElute HP Endotoxin-Free Maxiprep Kit following the manufacturer's protocol. The forward promoter (+) plasmid was only used for basal promoter activity assays in HEK293T and HepG2 cell lines and is labeled as the (+) promoter. In all other assays and for site-directed mutagenesis, the reverse (-) promoter plasmid was used and is termed the 'reference' promoter vector.

3.3.3. *Genetic Analysis of ABCG2 Promoter Region*

SNPs in the *ABCG2* promoter region were retrieved for all available ethnic populations from publicly available databases, including 1000 Genomes (phase 1 release 02/14/2012)[57], dbSNP build 135, and HapMap release 28[58] and were combined with those from the SOPHIE cohort reported in the Pharmacogenetics of Membrane Transporter Database (UCSF, San Francisco, CA). The SOPHIE cohort is a group of 247 ethnically diverse individuals who have donated DNA and are willing to be a part of future clinical pharmacogenomic studies[59]. The *ABCG2* promoter region from -674 to +85 bp was sequenced for variants in the SOPHIE cohort. Details regarding the sequencing of SOPHIE samples for *ABCG2* promoter SNPs has already been published[48]. Genotypes from 1000 Genomes (phase 1 release 05/21/2011) were used for calculating haplotypes. Haplotypes were determined by downloading each region's genotype and information files from the 1000 Genomes browser for all available ethnic groups

combined. Genotype and information files were then loaded into Haploview version 4.2[60] and haplotypes were determined using all available SNPs.

3.3.4. *Site-Directed Mutagenesis*

Site-directed mutagenesis (SDM) primers for each of the *ABCG2* promoter SNPs (Table 3.1) were designed using the PrimerX© program and then synthesized by Integrated DNA Technologies (San Diego, CA). PCR reaction components for all primers are as follows: 1X High-Fidelity Phusion Buffer, 1 unit Phusion High-Fidelity DNA Polymerase, 200 nM dNTPs, 1 μM each primer and 100 ng *ABCG2* reference promoter plasmid, all in a final volume of 50 μL. PCR reaction conditions for all primers except rs139256004 are as follows: An initial cycle for 30 sec at 98°C, followed by 20 cycles of 10 sec at 98°C, melting temperature (varies per primer pair) for 30 sec and 3 min at 72°C, then a final extension for 10 min at 72°C. The SDM PCR reactions were then digested for at least 20 min at 37°C with 1 unit *Dpn*I enzyme in 1X *Dpn*I digestion buffer. The reactions were then purified using the GeneJet PCR purification kit per the manufacturer's protocol, and 5 μL of the purified SDM reaction was transformed into 35 μL HB101 competent cells. After growing for 24 hr on 100 mm LB Amp-100 agar plates, colonies were selected for expansion overnight at 37°C with shaking in LB broth supplemented with 100 μg/mL ampicillin . DNA was then isolated from the bacteria using the GeneJet Miniprep Kit and the vector was sequenced with the RVPrimer3 primer to confirm the presence of the SNP. Large bacterial preps of the correctly mutagenized vectors were grown in 150 mL LB broth supplemented with 100 μg/mL ampicillin overnight at 37°C with shaking and DNA isolated with the GenElute HP

Endotoxin-Free Maxiprep Kit per the manufacturer's protocol. All DNA used for the *in vitro* and *in vivo* luciferase assays were endotoxin-free to avoid the cytotoxic effects of toxins released from the bacteria during lysis, which also allowed for more reproducible results.

Table 3.1 *ABCG2* Site-Directed Mutagenesis Primers

SNP ID	Δnt[1]	Primer Sequence[2]	Tm[3]
rs61181041	G>A	GAACCCCGAC[T]TGGGGAAAC	58.4
		GTTTCCCCA[A]GTCGGGGTTC	
rs61535534	C>G	CTTTCAGCCG[C]GTCGCAGGG	64
		CCCTGCGAC[G]CGGCTGAAAG	
rs76656413	C>T	GCGGCAGGACA[T]GTGTGCGCTTTC	65.2
		GAAAGCGCACAC[A]TGTCCTGCCGC	
rs66664036	->G	GGAGGCGGG[G]AGTGTTTGG	61.2
		CCAAACACT[C]CCCGCCTCC	
rs139256004	GTTA>-	TCGTA[-]ATCACTCTGGTTCATTCCGTTC	58.4
		GTGAT[-]TACGAGAATCACCAGGCGC	59.9
rs2231134	C>G	GACGAGGTACT[C]ATCAGCCCAATG	59.2
		CATTGGGCTGAT[G]AGTACCTCGTC	
rs45604438	G>A	GTGCTTCGG[T]GCTCCGGCC	64.4
		GGCCGGAGC[A]CCGAAGCAC	
rs36068118	->C	CAGCGTCCCC[C]GGTGCTTCG	65.9
		CGAAGCACC[G]GGGGACGCTG	
rs58132660	C>T	CTTGTGACTG[A]GCAACCTGTG	56.1
		CACAGGTTGC[T]CAGTCACAAG	
rs142365584	G>C	GTGCGAGCAG[G]GCTTGTGAC	61.6
		GTCACAAGC[C]CTGCTCGCAC	
rs59370292	G>A	CTTTCTCAGAAT[T]CCATTCACCAG	53.8
		CTGGTGAATGG[A]ATTCTGAGAAAG	
rs59172759	A>T	CTTTCTCAGAA[A]CCCATTCACCAG	55.9
		CTGGTGAATGGG[T]TTCTGAGAAAG	

[1]Change in reference to variant nucleotide of the anti-strand

[2]Forward and reverse primers per SNP with mutagenized nucleotide in brackets

[3]Melting temperature used for annealing step of SDM PCR

3.3.5. *Deletion Mutagenesis PCR Amplification*

The deletion SNP rs139256004 was introduced into the *ABCG2* promoter using a special protocol illustrated in Figure 3.2 and previously reported to work for both deletion and insertion mutatgenesis[61]. Primers were designed to overlap on their 5'- end so that the deletion is missing from both primers (see Figure 3.2B) and to ensure that the melting temperature of the non-overlapping section of the primers was greater than that of the overlapping section of the primers by 5-10°C. PCR reaction components were the same as described above with PCR conditions as follows: an initial cycle of 5 min at 95°C, then 12 cycles of 95°C for 1 min, 45°C for 1 min and 72°C for 9 min, with a final cycle of 1 min at 36°C and 30 min at 72°C. Promoter SNP rs57327643 was also attempted via this protocol, but no colonies were successfully isolated.

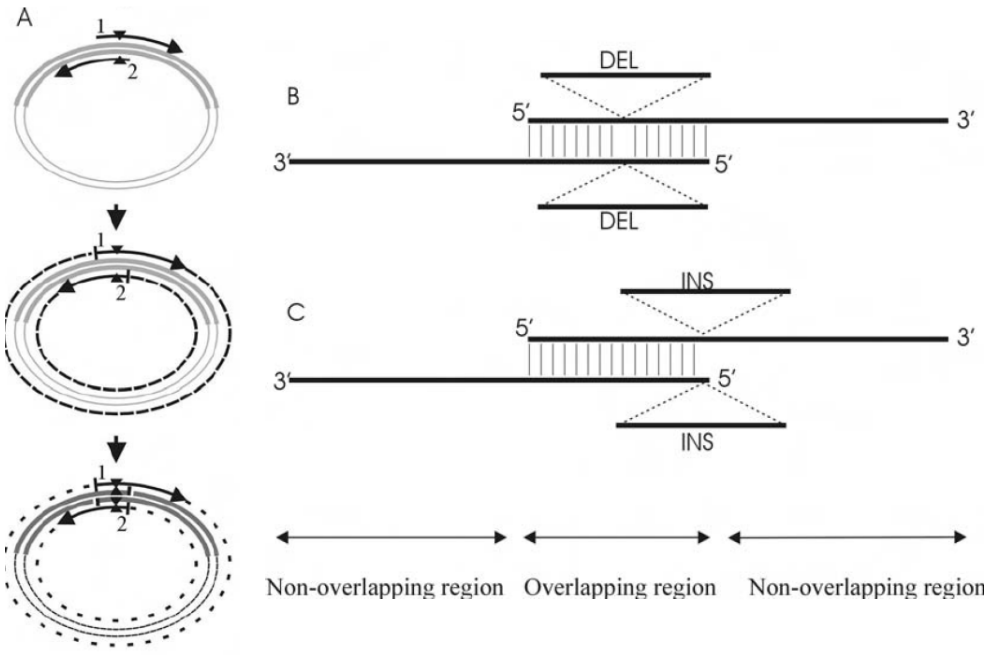

Figure 3.2. Schematic of mutagenesis protocol for large deletion or insertion polymorphisms. The PCR amplification protocol (A) and primer design to create the large deletion (B) or insertion (C) polymorphisms is illustrated. Solid circles represent the

parent plasmid and dashed circles represent the amplified plasmid. Arrows indicate primers and triangles represent the polymorphism. Figure is reproduced from Liu et. al.[61].

3.3.6. *Cell Culture*

HEK293T/17, HCT116 and HepG2 were grown in high-glucose DMEM supplemented with 10% FBS, 100 units/mL of penicillin and 0.1 mg/mL of streptomycin. The MCF-7 cell line was grown in IMEM without phenol red, supplemented with 10% FBS, 100 units/mL of penicillin and 0.1 mg/mL of streptomycin. All cell lines were grown in a 5% CO_2 incubator at 37°C. To maintain cells, they were split upon reaching confluency by treatment with 0.05% Trypsin-EDTA, washing with 1X PBS and suspension in fresh media at a 1:5 to 1:20 dilution.

3.3.7. *Transient Transfection*

The HEK293T/17 (kidney), HepG2 (liver), HCT116 (intestine) and MCF-7 (breast) cell lines were chosen to represent their primary tissue source. For transient transfections of the HEK293T/17, HepG2 and HCT116 cell lines, cells were seeded at approximately 1.8 x 10^4 cells per well of a 96-well plate in fresh DMEM with 10% FBS, but without antibiotics, and grown for at least 24 hr to 80% confluency. Cells were then transfected with Lipofectamine 2000 following guidelines suggested in the manufacturer's protocol. In short, 0.5 µL of Lipofectamine 2000 was incubated in 25 µL Opti-MEM for 5 min and then gently mixed with a 25 µL solution of 0.08 µg of the pGL4.11b [*luc2*P] plasmids (plus 0.02 µg pGL4.74 [*hRluc*/TK]) diluted with Opti-MEM. The DNA-Lipofectamine mixture was allowed to incubate at room temperature for 30

min before being placed onto cells with 50 µL of antibiotic-free media. MCF-7 cells were split with 0.05% Trypsin-EDTA and seeded at ~2.5 x 10^4 cells per well and transfected only once they reached 95% confluency with the PolyJet™ DNA *In Vitro* Transfection Reagent; transfection efficiency was optimized by following the manufacturer's guidelines. Briefly, media on the cells were replaced with 100 µL fresh IMEM (supplemented with FBS and antibiotics as above) 30 min before transfection. A mix of 75 ng *ABCG2* plasmid and 25 ng of pGL4.74 [*hRluc*/TK], to control for transfection efficiency, was diluted to 5 µL with IMEM supplemented with 10% FBS (no antibiotics). A 0.4 µL aliquot of PolyJet was diluted to 5 µL with IMEM supplemented with 10% FBS (no antibiotics) and then immediately added to the DNA mix with gentle mixing. The PolyJet/DNA mix was allowed to incubate at room temperature for 15 min before being added to the cells. All cell lines were incubated with their transfection agents for 18-24 hr before assaying.

3.3.8. *Luciferase Reporter Assay*

The day after transfection, each well was washed with 100 µL 1X PBS before being lysed with 50 µL of 1X passive lysis buffer for 1 hr with shaking. Then 20 µL of HEK293T/17 or 30 µL of HepG2, HCT116 and MCF-7 lysates were measured for firefly and Renilla luciferase activity using 70 µL each of the Luciferase Assay Reagent II and Stop & Glo® reagents from the Dual-Luciferase® Reporter Assay System in a GloMax 96 microplate Dual Injector Luminometer. The firefly activity was normalized to the Renilla activity per well to control for transfection efficiency. Each experiment also included the empty pGL4.11b vector as the negative control and the pGL4.13 [*luc2*/SV40] vector as

the positive control. The promoter activity for each plasmid was calculated as the ratio of the normalized firefly activity to that of the empty vector.

3.3.9. *Hydrodynamic Tail Vein Assay*

Positive *in vitro* variant enhancer elements were screened for their effect on *in vivo* liver enhancer activity through the hydrodynamic tail vein injection[62] adapted for enhancer element screening[63] (see *Chapter 4*, Figure 4.10). Each variant enhancer, along with their reference enhancer plasmid, was injected into the tail vein of 4-5 mice using the TransIT EE *In Vivo* Gene Delivery System following the manufacturer's protocol. Briefly, 10 μg of pGL4.23 [*luc2*/minP] vector with or without enhancer element, or the *ApoE*[64] positive control liver enhancer, along with 2 μg of pGL4.74 [*hRluc*/TK] were injected into the tail vein of CD1 mice (Charles River Laboratory). After 24 hr, mice were euthanized and livers from the mice were harvested. Each liver was homogenized in 3 mL of 1X Promega Passive Lysis Buffer and then centrifuged at 4°C for 30 min at 14,000 rpm. The supernatant was then diluted 1:20 with additional lysis buffer and measured for firefly and *Renilla* luciferase activity using the Dual-luciferase® reporter assay system according to the manufacturer's protocol in a Synergy 2 (BioTek Instruments, Winooski, VT) microplate reader. Each mouse liver lysate was read in replicate 3-6 times, with each sample's firefly activity normalized to the *Renilla* activity and then averaged across the replicates. Average normalized luciferase activity is expressed as the mean of 4-5 mice. Enhancer or ApoE normalized luciferase activity was then compared to the empty pGL4.23 vector activity and expressed as fold activation

relative to pGL4.23. All mouse work was done following a protocol approved by the UCSF Institutional Animal Care and Use Committee.

3.3.10. *Predictions of Transcription Factor Binding Site Changes*

Two separate computation tools were used to predict differences in the binding probability of TFs between reference and variant promoter sequences. First, the Consite[65] program, which directly compares the transcription factor binding sites (TFBS) shared between two aligned genomic sequences. For this analysis, promoter reference and variant sequences were extracted from UCSC genome browser (hg19) and imputed as orthologous pairs of genomic sequences. The regions were scanned for vertebrate TFs provided by the program, with a minimum specificity of 10 bits. With no conservation cut off, the TF score threshold was set to 70% and TFs with greater than 20% change in binding probability were extracted. The second computation tool was the TRANSFAC Match program[66]. Individually, the genomic sequence of the reference and variant promoters were scanned for the probability of TF binding using the TRANSFAC release 2012.2 matrix table of all non-redundant vertebrate TFs. Parameters were set to select only high quality matrices and to minimize false positives. The probabilities for TF binding of enhancer and reference promoters were compiled and those that altered TF binding were extracted. Consite and TRANSFAC also provided alignments of the consensus TF matrix sequence with that of the reference and variant promoter sequences. We compared any alterations in TFBS with that of ChIP-seq validated TF binding sites through the RegulomeDB[67] database.

3.3.11. *Statistical Analysis*

Promoter activity was expressed relative to the empty vector (as described above). Results for each transfection, with 3-16 wells per plasmid in each transfection, were combined for each cell line and analyzed by an ANOVA followed by a Bonferroni's multiple comparison *t*-test. A representative experiment (n=6-16 wells per plasmid) is shown for each cell line. Basal forward and reverse promoter activity in the HEK293T and HepG2 cell lines was considered to be statistically significant from the empty pGL4.11b vector if the ANOVA analysis followed by a Bonferroni's multiple comparison *t*-test had a $P < 0.05$. Basal promoter activity in the HCT116 and MCF-7 cell lines was considered to be statistically significant from the empty pGL4.11b vector when $P < 0.05$ using a Student's *t*-test. Variant promoter plasmids tested *in vitro* or *in vivo* were compared to the reference *ABCG2* promoter by an ANOVA analysis followed by a Bonferroni's multiple comparison *t*-test. Variant *ABCG2* promoter sequences identified for *in vivo* testing were significantly different ($P < 0.05$) from the reference promoter in three of four cell lines. In the *in vivo* experiments, the reference sequence and ApoE controls were tested for difference from the empty vector sequence using an unpaired Students's *t*-test. All statistics were run using the GraphPad Prism 5 program.

3.4. Results

3.4.1. *Genetic Polymorphisms of the ABCG2 Promoter*

A total of 13 SNPs were obtained for the *ABCG2* promoter region from publicly available databases and from the SOPHIE cohort, and are displayed in Table 3.2. Of the 13 SNPs, rs57327643, rs66664036, rs2231134, rs45604438 and rs59172759 had MAF

above 4% in at least one of the ethnic populations (Table 3.2). The *ABCG2* promoter SNPs included two single nucleotide insertions, rs66664036 and rs36068118. There were also two multiple base pair deletions, rs57327643 and rs139256004. Attempts to construct the rs57327643 variant promoter plasmid were unsuccessful and this SNP was not evaluated in the functional assays. Variant promoter plasmids for all other SNPs in Table 3.2 were successfully made and tested for their luciferase activity relative to reference in four cell lines. There was no notable linkage disequilibrium between SNPs in the *ABCG2* promoter (data not shown).

Table 3.2 *ABCG2* Promoter SNPs

SNP ID	Position[1]	Δnt	MAF (%)[2]			
			AA	CA	AS	ME
rs61181041	-84	G>A	0.00	0.00	0.80	0.00
rs61535534	-151	C>G	0.00	0.00	0.00	0.80
rs76656413	-169	C>T	0.00	0.00	1.00	0.00
rs57327643	-266	AGTGTTT>-	3.80	4.20	0.00	4.70
rs66664036	-267	->G	nr	6.00	nr	nr
rs139256004	-267	GTTA>-	nr	nr	nr	nr
rs2231134	-307	C>G	2.50	6.50	0.00	6.00
rs45604438	-340	G>A	7.50	0.00	0.00	1.70
rs36068118	-390	->C	nr	nr	nr	nr
rs58132660	-400	C>T	0.00	0.00	0.00	0.90
rs142365584	-424	G>C	0.00	0.00	0.00	0.30
rs59370292	-435	G>A	0.00	0.00	0.80	0.00
rs59172759	-483	A>T	4.20	0.00	0.00	0.00

[1]SNP position is noted relative to the transcriptional start site

[2]Minor allele frequency (MAF) for African American (AA), Caucasian (CA), Asian (AS) and Mexican (ME) populations

Abbreviations: nr, not reported

3.4.2. *Basal Activity of the ABCG2 Promoter In Vitro*

The baseline activity of the reverse and forward strand *ABCG2* promoter sequence (chr4:89079947-89080567, hg19), cloned into the firefly luciferase reporter vector pGL4.11b, was investigated in transiently transfected HEK293T and HepG2 cell lines, while the reverse strand promoter plasmids were screened in the HCT116 and MCF-7 cell lines (Figure 3.3). This region includes the basal promoter of *ABCG2* (previously reported) and the structural elements displayed in Figure 3.1. The promoter drives expression of the firefly luciferase gene, and firefly luciferase activity is used as a marker of promoter activity. In both HEK293T and HepG2 cell lines, the forward and reverse orientation promoter plasmids exhibited an increased promoter activity ($P < 0.05$) when compared to pGL4.11b empty vector (Figure 3.3). The reverse *ABCG2* promoter activity was strongest in the HEK293T and HCT116 cell lines, with average activation of 15- and 14-fold, respectively; in the HepG2 and MCF-7 cell lines promoter activity was weaker, with average activation of 4- and 1.5- fold, respectively (Figure 3.3). The forward *ABCG2* promoter sequence exhibited the same promoter activity as the reverse *ABCG2* promoter sequence in the HepG2 and HEK293T cell lines (Figure 3.3).

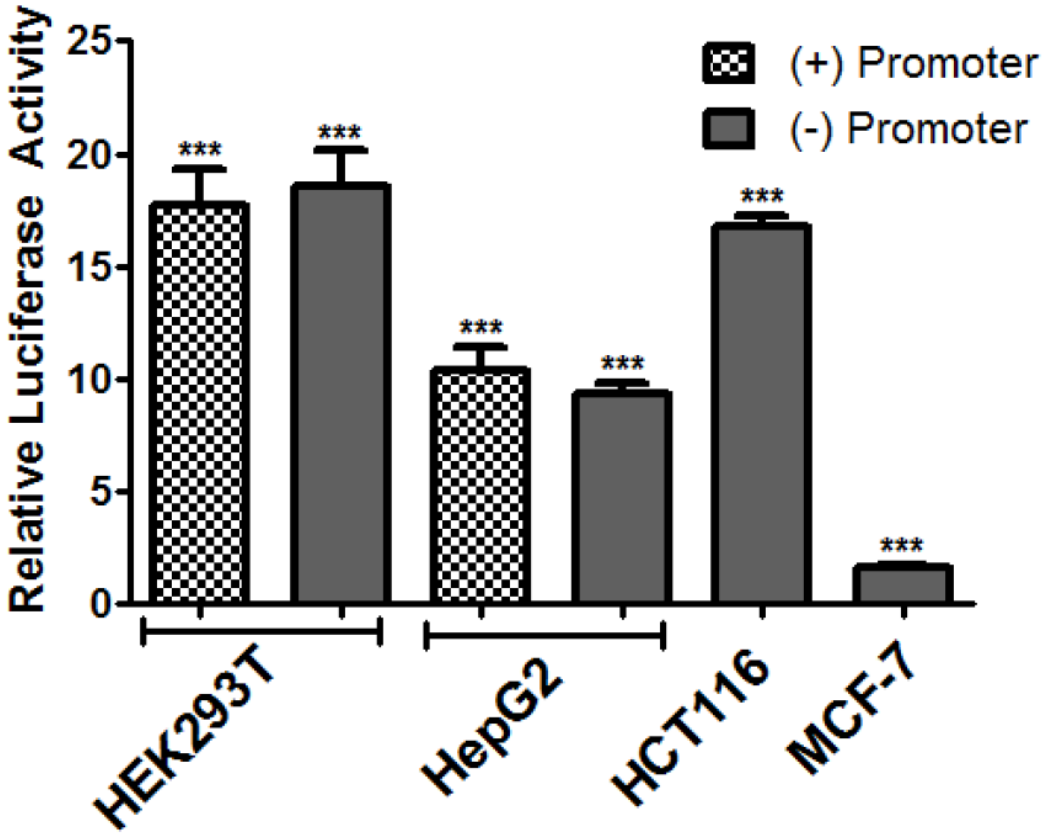

Figure 3.3. Basal *ABCG2* promoter activity *in vitro*. Luciferase activity of the forward (checkered) and reverse (solid grey) reference promoter was measured in transiently transfected liver (HepG2) and kidney (HEK293T) cell lines, while the reverse reference promoter was also measured in the intestine (HCT116) and breast (MCF-7) cell lines. Promoter activity is expressed as the ratio of the normalized firefly to *Renilla* luciferase activity relative to the empty vector (pGL4.11b) activity. Data is expressed as the mean ± SEM from a representative experiment (n=16 wells per construct). Differences between reference and empty vector, and forward and reverse promoter constructs, were tested by an ANOVA followed by a post-hoc Bonferroni's multiple comparison test (HEK293T and HepG2 cells) or a Student's *t*-test (HCT116 and MCF-7 cells) for difference between reference and empty vector; *** $P < 0.0001$.

3.4.3. *Effect of SNPs on Basal ABCG2 Promoter Activity In Vitro*

The effect of twelve SNPs on the basal *ABCG2* promoter activity was investigated by transient transfections of HEK293T, HepG2, HCT116 and MCF-7 cell lines with the reference and variant *ABCG2* promoter plasmids. Two SNPs had significantly decreased promoter activity in HepG2 cells (Figure 3.4A); rs76656413 and rs66664036 had a 50% decrease in promoter activity relative to the reference promoter. Five SNPs had significantly decreased promoter activity in HEK293T cells (Figure 3.4B). Three of them (rs61181041, rs139258004 and rs2231134) had a 25% decrease in activity relative to reference, while the other two (rs59370292 and rs76656413) had over a 50% decrease in promoter activity relative to the reference promoter. In HCT116 cells, six SNPs had decreased activity relative to the reference promoter including a 25% decrease with SNPs rs61181041, rs66664036 and rs142365584, a 50% decrease with rs76656413 and rs139256004, and over a 75% decrease with rs59370292 (Figure 3.4C). Finally in the MCF-7 cells, four SNPs (rs76656413, rs66664036, rs139256004 and rs59370292) have a 50% decrease relative to reference promoter (Figure 3.4D). Both the rs66664036 and rs139256004 SNPs had 25-50% decreased promoter activity relative to reference in three of the four cell lines (Figure 3.4). The rs76656413 SNP had over a 50% decreased promoter activity in all four of the cell lines (Figure 3.4). The rs59370292 SNP was the most detrimental SNP in both HepG2 (Figure 3.4A) and HCT116 (Figure 3.4C) cell lines with an almost 75% decreased promoter activity; it also had a 50% decrease in promoter activity in MCF-7 (Figure 3.4D) cells. Due to their decreased promoter activity in at least three of four cell lines, rs66664036, rs139256004, rs76656413 and rs59370292 were chosen for follow up in the *in vivo* hydrodynamic tail vein injection assay.

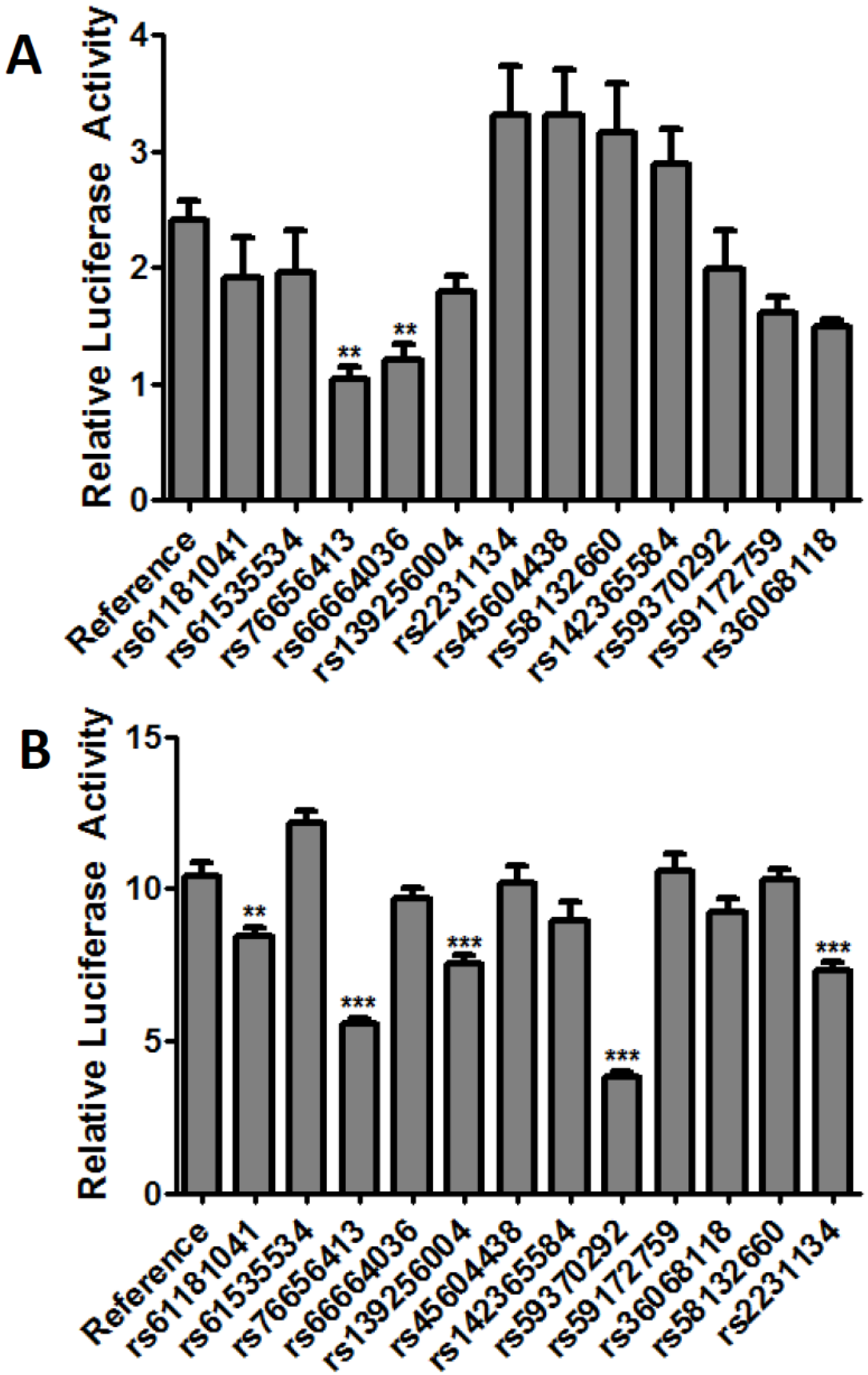
A
Relative Luciferase Activity
0
1
2
3
4
**
**
Reference
rs61181041
rs61535534
rs76656413
rs66664036
rs139256004
rs2231134
rs45604438
rs58132660
rs142365584
rs59370292
rs59172759
rs36068118
B
Relative Luciferase Activity
0
5
10
15
**
***
***
***
***
Reference
rs61181041
rs61535534
rs76656413
rs66664036
rs139256004
rs45604438
rs142365584
rs59370292
rs59172759
rs36068118
rs58132660
rs2231134

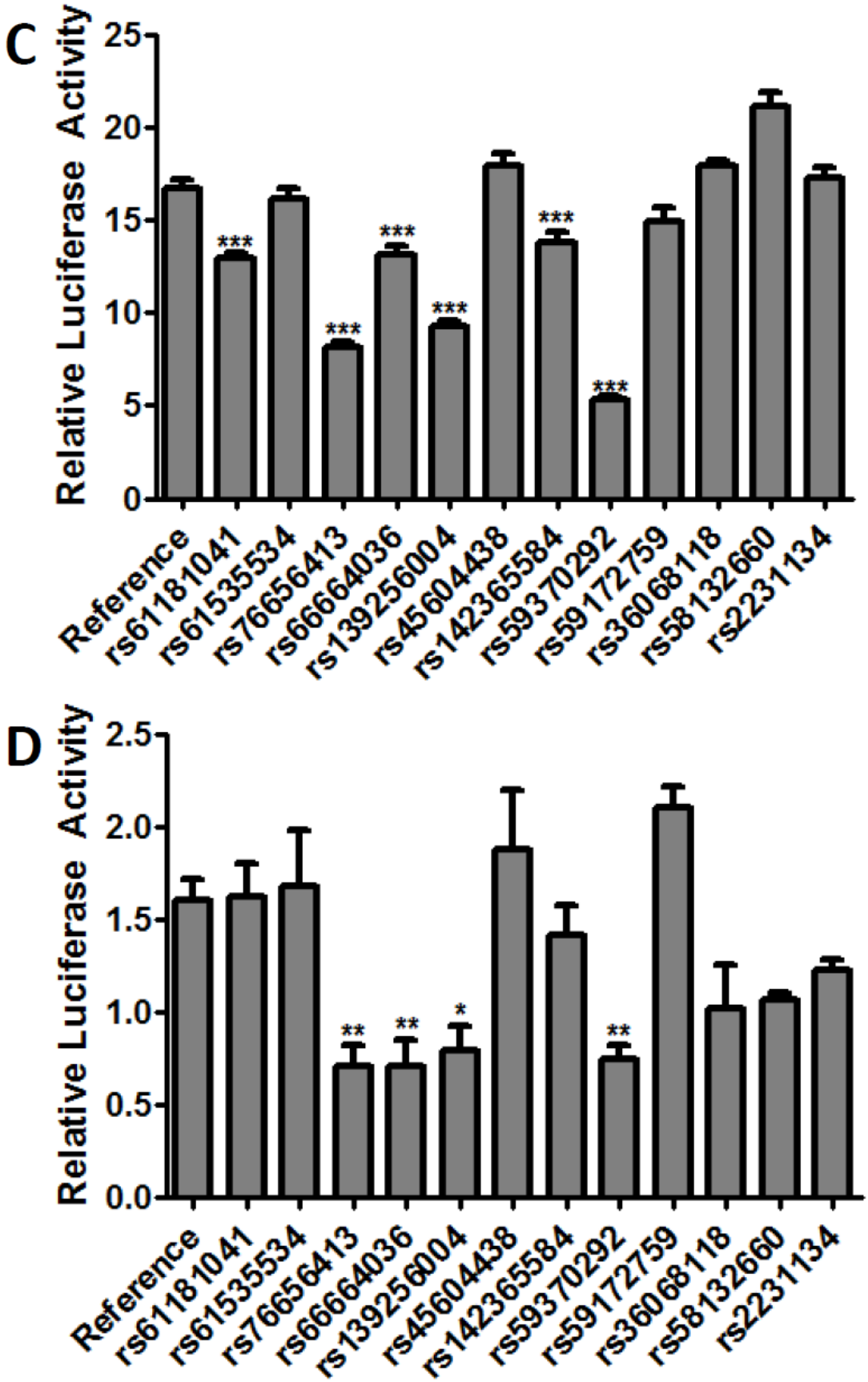
C
Relative Luciferase Activity
25
20
15
10
5
0
***
***
***
***
***
Reference
rs61181041
rs61535534
rs76656413
rs66664036
rs139256004
rs45604438
rs142365584
rs59370292
rs59172759
rs36068118
rs58132660
rs2231134
D
Relative Luciferase Activity
2.5
2.0
1.5
1.0
0.5
0.0
**
**
*
**
Reference
rs61181041
rs61535534
rs76656413
rs66664036
rs139256004
rs45604438
rs142365584
rs59370292
rs59172759
rs36068118
rs58132660
rs2231134

Figure 3.4. Effect of promoter variants *in vitro.* Luciferase assay of *ABCG2* reference and variant promoter sequences was measured in transiently transfected A) liver (HepG2), B) kidney (HEK293T), C) intestine (HCT116) and D) breast (MCF-7) cell lines. Promoter activity is expressed as the ratio of the normalized firefly to *Renilla* luciferase activity relative to the empty vector (pGL4.11b) activity. Data is expressed as the mean ± SEM from a representative experiment (N = 6-12 wells per construct). Differences between reference and variant promoter constructs were tested by an ANOVA followed by a post-hoc Bonferroni's Multiple Comparison *t*-test; *** $P < 0.0001$, ** $P < 0.001$, * $P < 0.05$.

3.4.4. *Effect of SNPs on Basal ABCG2 Promoter Activity In Vivo*

Four SNPs were screened for their effect on *in vivo* liver enhancers using the hydrodynamic tail vein injection assay. In this assay, we used the ApoE liver enhancer positive control, which had more than 200-fold activation over empty vector (pGL4.11b). The *ABCG2* promoter construct exhibited a strong 35-fold activation over empty pGL4.11b. Two of the four promoter SNPs screened showed a significant decrease in promoter activity *in vivo* (Figure 3.5). The rs59370292 SNP had the largest decrease in activity, with over 80% decrease in promoter activity, while the rs76656413 resulted in a 70% decrease in promoter activity *in vivo*. After multiple comparison adjustment, rs66664036 showed a trend toward significance (p=0.078) and reduced promoter activity by 50%. The *in vivo* and *in vitro* fold activities, relative to empty vector, for the five *ABCG2* promoter variants tested *in vivo* are shown in Table 3.3.

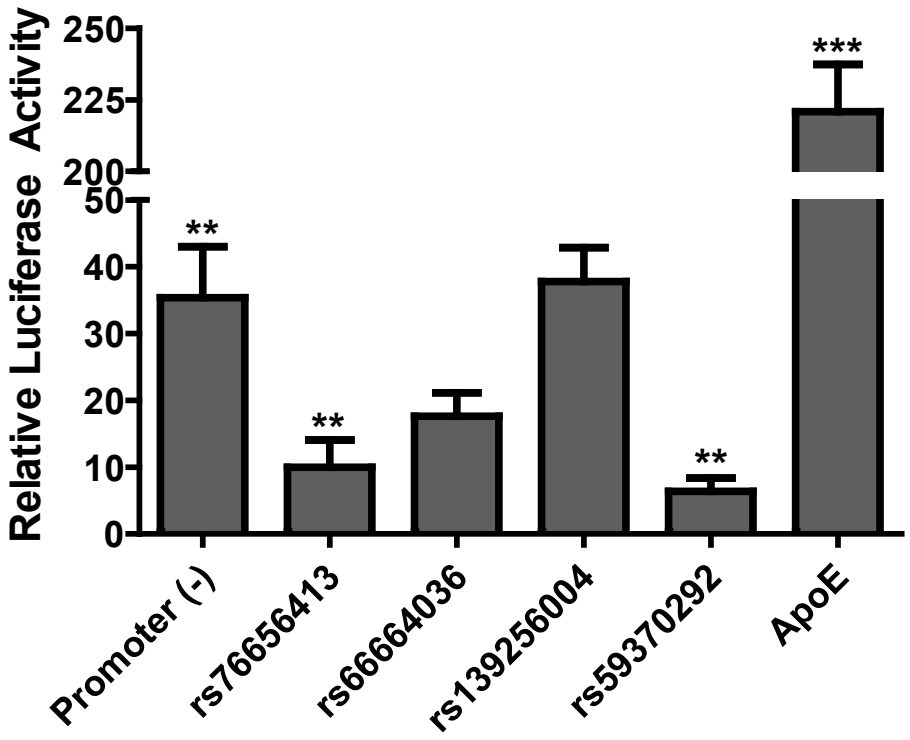

Figure 3.5. Effect of promoter variants *in vivo*. The luciferase activity in mouse liver homogenates was measured 24 hr after plasmid injection. Promoter activity is expressed as the ratio of firefly to *Renilla* luciferase activity normalized to the empty vector (pGL4.11b) activity. SNPs are displayed respective to their genomic orientation. Data is expressed as the mean ± SEM for 4-5 mice. Differences between reference promoter or ApoE and empty vector were tested by an unpaired Student's *t*-test, and reference and variant promoter sequences were compared using a one-way ANOVA followed by a Bonferroni's multiple comparison *t*-test; ** $P < 0.001$.

Table 3.3. *ABCG2* Promoter Variants *In Vitro* and *In Vivo* Activity

Genotype	Relative Fold Activation									
	HEK293T		HepG2		HCT116		MCF-7		*In Vivo*	
Reference	10.40		2.42		16.74		1.60		35.36	
rs76656413	5.59	***	1.04	**	13.14	***	0.71	**	9.99	**
rs66664036	9.70	ns	1.21	**	9.31	***	0.71	**	17.60	ns
rs139256004	7.52	***	1.80	ns	17.88	***	0.80	*	37.79	ns
rs59370292	3.81	***	1.99	ns	5.28	***	0.75	**	6.37	**

* P <0.05; ** P < 0.001; *** P < 0.0001; ns, not significant

3.4.5. *Effect of SNPs on Predicted Binding of TFs in the ABCG2 Promoter*

To investigate the mechanism for decreased *ABCG2* promoter activity associated with some of the SNPs, TFBS predictions were made on both reference and promoter sequences using ConSite and TRANSFAC Match programs. Predicted probability score changes from ConSite are shown in Figure 3.6 and Figure 3.7 sections A and B, while any TRANSFAC predicted losses and gains in TF binding sites are shown in sections C and D of the figures. rs76656413 caused a 41% gain in the binding probability score for p53 and binding probability score losses for Myc-Max (33%), USF (37%), n-Myc (37%) and Max (98%) (Figure 3.6A and B). The predicted loss of Myc-Max binding was corroborated by TRANSFAC (Figure 3.6C), which predicted no probable binding of Myc-Max (>0.7) to the variant sequence. rs59370292 had predicted gains in TF binding probability scores for p65 (20%), Pax-4 (24%), Chop-cEBP (47%) and c-REL (50%), as well as decreases in the binding probability scores for RREB-1 (34%) and RXR-VDR (38%) (Figure 3.7 A and B). The RegulomeDB[67] database also predicted that rs59370292 is likely to affect TF binding and provides evidence for the binding of GATA1, STAT1 and STAT5A to this region (data not shown).

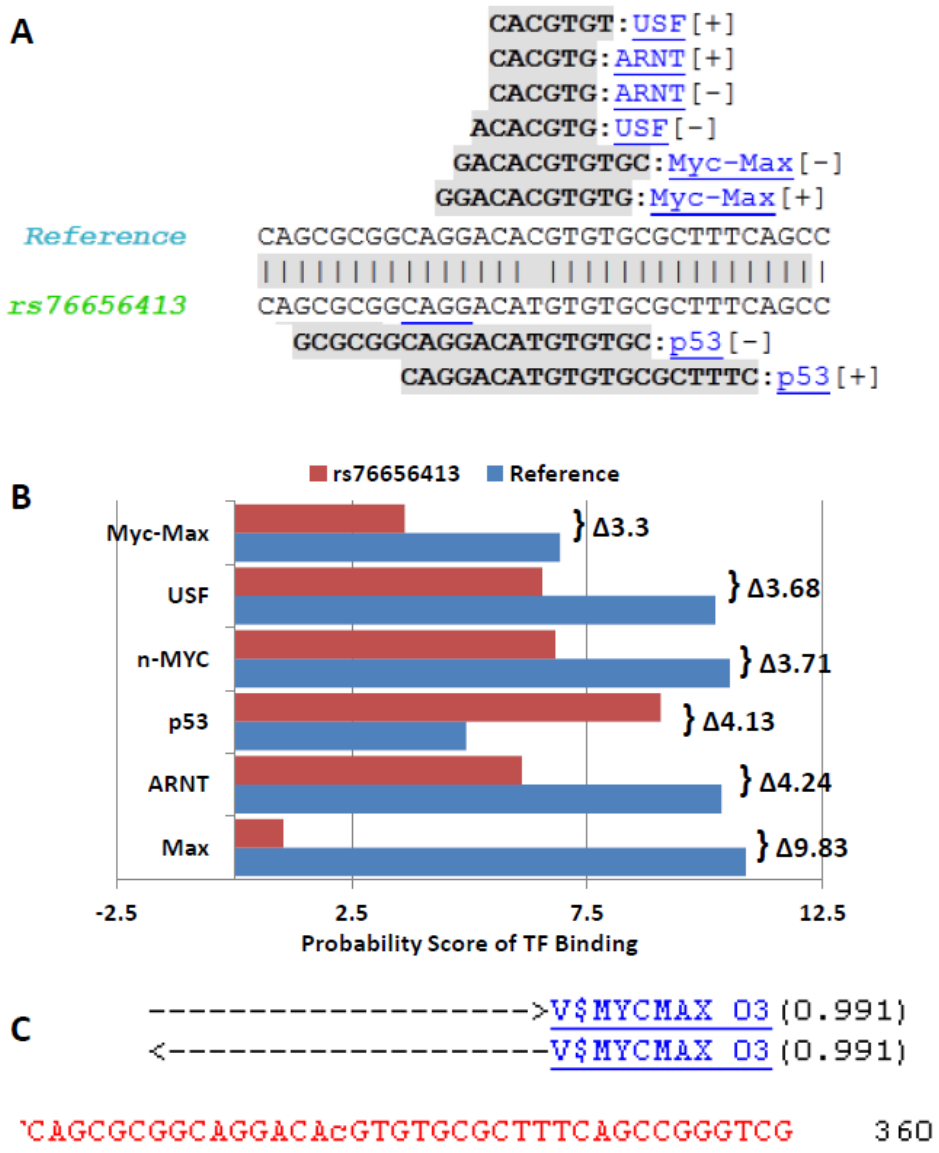

Figure 3.6. Predicted TFBS for rs76656413. The TFBS predicted by (A, B) Consite aligned with reference and SNP sequences that are lost (above alignment) or gained (below alignment) and the corresponding binding probability scores (B) for the reference (blue) and SNP (red) sequences. The absolute change in binding probability scores for each TF, between reference and variant sequences, are indicated as a Δ value. TFBS changes as determined by (C) TRANSFAC, showing sequence alignments of TFBS that are lost.

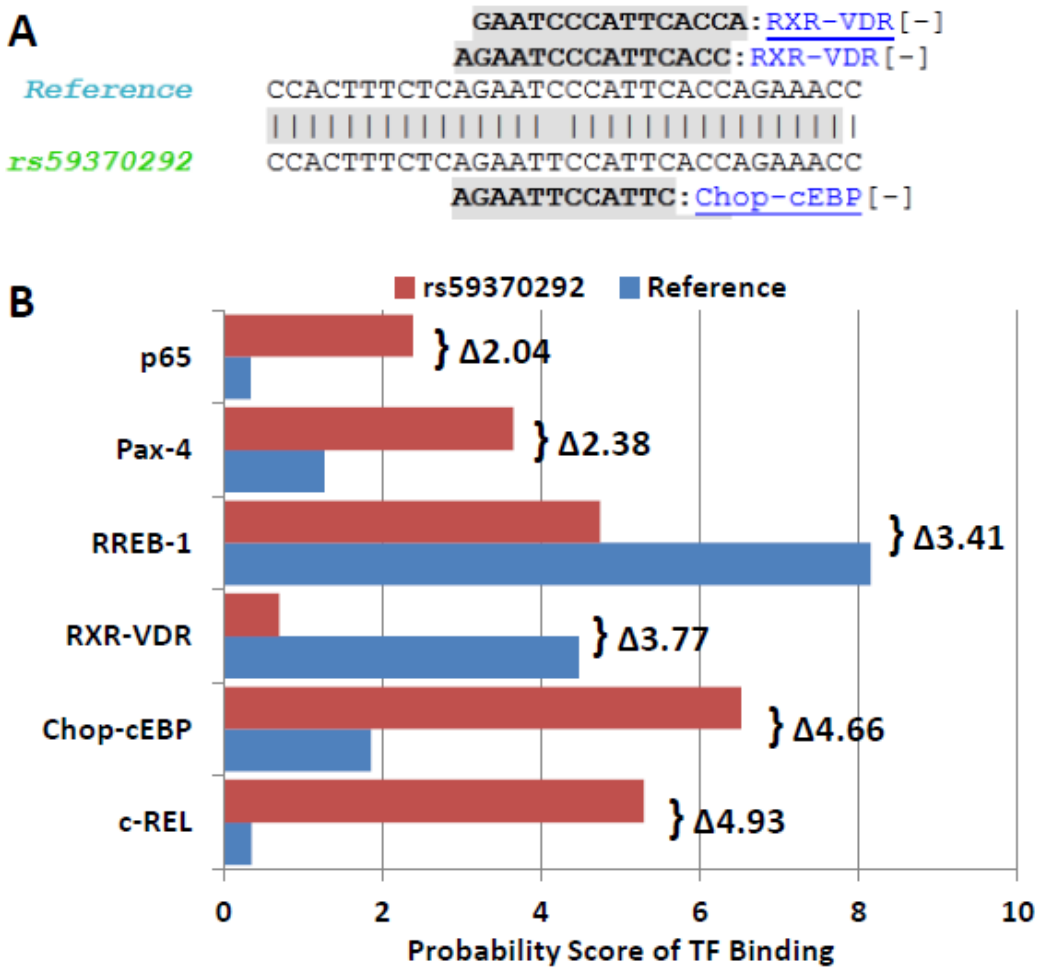

Figure 3.7. Predicted TFBS for rs59370292. The TFBS predicted by (A, B) Consite aligned with reference and SNP sequences that are lost (above alignment) or gained (below alignment) and the corresponding binding probability scores (B) for the reference (blue) and SNP (red) sequences. The absolute change in binding probability scores for each TF, between reference and variant sequences, are indicated as a Δ value.

3.5. Discussion

The results of this study indicate that the *ABCG2* promoter is highly active in the intestinal HCT116 and liver HepG2 cell lines, has medium activity in the kidney HEK293T cell line and low but detectable activity in the breast MCF-7 cell line. It also had a strong *in vivo* liver activity. These results correlate with the high expression of ABCG2 in intestine and liver and more moderate expression of ABCG2 in kidney[5]. In contrast, the low promoter activity in the MCF-7 cells is not consistent with the high expression of ABCG2 in breast tissue[5]. Previously, luciferase assays on the -628/+362 *ABCG2* promoter segment indicated suppressed activity in MCF-7 cells, whereas the -312/+362 promoter segment was highly active. It is possible that a suppressor element within the -499 to -312 segment reduces the activity of our *ABCG2* promoter construct in MCF-7 cells[29]. Recently, an interferon-gamma activated sequence (GAS) at -448/-422 was shown to increase the *ABCG2* promoter activity upon stimulation of the JAK2/STAT5 pathway by prolactin[68]. This overlaps with the antioxidant response element stimulated by Nrf2 in stem cells[42]. STAT5 is well documented for its importance in regulating expression of genes essential for mammary development and lactogenesis[69]. Naturally occurring dominant-negative isoforms of STAT5 have also been shown to suppress the transcriptional activity of the estrogen receptor (ER) in MCF-7 cells[70]. Although the MCF-7 cell line does express the ER, previous research has shown discordant results in the ability of the *ABCG2* promoter to be upregulated in cell lines with ER expression when treated with 17β-estradiol[71,72]. Therefore, it is possible that without stimulation of the STAT5 pathways, there is a suppressive factor bound between -499 and -312 of the *ABCG2* promoter in MCF-7 cells that inhibits promoter activity.

This indicates a fragile and complex network of TFs that bind to the *ABCG2* promoter and regulate its expression specific to each cell line and tissue.

Similar to promoter SNPs in other pharmacogenes[47–50], several of the *ABCG2* promoter SNPs affect the activity of the *ABCG2* promoter *in vitro* and *in vivo* through the predicted alteration of TF binding. Although four SNPs in the *ABCG2* promoter altered promoter activity *in vitro*, all except rs66664036 have reported low minor allele frequencies. This is in concordance with a large analysis of ABC and SLC gene promoter variation that found the proximal promoters of these gene families had low nucleotide diversity[48]. Therefore, when present, these SNPs could have effects on the expression levels of ABCG2, but due to their low frequency may not contribute significantly to the wide variability in ABCG2 expression. Also, due to the low frequency of these SNPs, we were unable to correlate them with the expression of ABCG2 in tissue samples (data not shown). Further research is needed to successfully associate these SNPs with the expression of ABCG2 and the function of the MXR transporter.

Of the four SNPs identified in the *in vitro* screen, two were confirmed to have a significantly decreased *in vivo* activity, while one more SNP's drop in activity showed a trend toward significance. There was no cell line whose pattern of SNPs' activity was comparable to, or could be used to predict, *in vivo* activity. Therefore, a combination of cell lines is necessary for future screens in order to identify SNPs that would also be positive *in vivo*. This is consistent with the use of multiple cell lines in other transporter promoter SNP assays[49]. Overall, the *in vitro* activity of *ABCG2* promoter SNPs in four cell lines was an adequate predictor of the SNPs' activity *in vivo*.

The *ABCG2* promoter SNP rs76656413 has strong evidence for altering the transcriptional activity of the *ABCG2* promoter. It was able to attenuate the relative luciferase activity of the *ABCG2* promoter by 50% in all four cells lines and decreased *ABCG2* liver promoter activity by 70% *in vivo*. It was also predicted to have large losses in USF-1, n-Myc, Max and Myc-Max binding, as predicted by multiple TFBS analysis programs. The USF and Myc-Max TFs are all reported to bind to the same canonical E-box sequence[73]. The rs76656413 lies in the middle of several reported ChIP-seq peaks for USF-1 and c-Myc. Additionally, c-Myc has been reported to direct the transcriptional regulation of *ABC* genes, particularly the unmethylated *ABCG2* promoter, in human leukemic hematopoietic progenitor cells[74]. Furthermore, the expression of ABCG2 was altered by the overexpression of c-Myc in human breast epithelial cells[75]. Since the USF-1 and c-Myc transcription factors bind to the *ABCG2* promoter in several cell types, it is possible that the rs76656413 SNP is able to disrupt this binding and alter the transcriptional activity of the *ABCG2* promoter.

The *ABCG2* promoter SNP rs66664036 significantly decreased the relative luciferase activity of the *ABCG2* promoter in three of the four cell lines tested by 35 to 50% and trended towards significant with altering the liver *in vivo* activity by 50%. It was predicted to reduce binding of the AP-1 TF to the *ABCG2* promoter (data not shown). There are both AP-1 and AP-2 predicted sites in the *ABCG2* promoter, and ChIP-seq evidence from ENCODE for the binding of the AP-2γ TF over the rs66664036 SNP. AP-1 is a TF shown to regulate both basal and inducible transcription of target genes[76,77]. Previously it was shown that ER works in concert with AP-1 and Sp1 to activate its target genes[78], and promoters with Sp1 and AP-1 sites had substantially more modulation of

activity with estrogen treatment[79]. Additionally, AP-1 physically interacts with ERβ to modulate the transcription of genes upon treatment with estrogen[80]. We have done further experiments on the reference and variant promoter plasmids to show that rs66664036 increased response to 17β-estradiol treatment compared to the reference promoter (see Chapter 6, Figure 6.4). It is possible that the rs6666403 SNP alters the basal transcriptional activity of the *ABCG2* promoter through reduced binding of the AP-1 TF, but does not alter the inducible activity of the *ABCG2* promoter by 17β-estradiol. Further experiments are necessary to test this hypothesis.

The *ABCG2* promoter SNP rs59370292 has the lowest reported minor allele frequencies of the four SNPs that alter *in vitro ABCG2* promoter activity. The rs59370292 SNP is just upstream of the antioxidant response element in the *ABCG2* promoter. It altered the relative luciferase activity of the *ABCG2* promoter in three of four cell lines and had the largest effect of any *ABCG2* promoter SNP *in vivo*, decreasing the promoter activity by 80%. The top TF predicted to have reduced binding due to rs139256004 is the vitamin D receptor (VDR). We could not find evidence for binding of this TFs to the *ABCG2* promoter in ChIP-seq databases or for the regulation of *ABCG2* by VDR. However, the genomic binding locations of VDR are not yet in the publicly available ChIP-seq databases. Although VDR has not been directly linked to *ABCG2*, VDR is important in regulating bile acid transporters, and its ligands include bile acid derivatives and steroids[81,82]. Since *ABCG2* encodes a bile acid transporter[83] and has been shown to be important for the pharmacokinetics and pharmacodynamics of statins[84], VDR could be the link for statin regulation of ABCG2 expression. However, further

studies are needed to determine if VDR binding to the proximal promoter of *ABCG2* is involved in *ABCG2* transcription.

3.6. Conclusions

The basal promoter of *ABCG2* from -499 to +21 has strong activity in HepG2, HCT116 and HEK293T cell lines; it has low activity in the MCF-7 cell line. The rs76656413 and rs59370292 SNPs within the basal promoter of *ABCG2* affect its function both *in vitro* and *in vivo*. Additionally, these SNPs are predicted to alter TFBS relevant to the transcriptional regulation of *ABCG2*. Taken together, these SNPs could account for some of the reported variability of *ABCG2* expression in liver and intestine.

3.7. References

(1) Ni, Z.; Bikadi, Z.; Rosenberg, M. F.; Mao, Q. Structure and function of the human breast cancer resistance protein (BCRP/ABCG2). *Current drug metabolism* **2010**, *11*, 603.

(2) Abbott, B. L. ABCG2 (BCRP): a cytoprotectant in normal and malignant stem cells. *Clinical advances in hematology & oncology : H&O* **2006**, *4*, 63–72.

(3) Hirschmann-Jax, C.; Foster, a E.; Wulf, G. G.; Nuchtern, J. G.; Jax, T. W.; Gobel, U.; Goodell, M. a; Brenner, M. K. A distinct "side population" of cells with high drug efflux capacity in human tumor cells. *Proceedings of the National Academy of Sciences of the United States of America* **2004**, *101*, 14228–33.

(4) Zhou, S.; Schuetz, J. D.; Bunting, K. D.; Colapietro, a M.; Sampath, J.; Morris, J. J.; Lagutina, I.; Grosveld, G. C.; Osawa, M.; Nakauchi, H.; Sorrentino, B. P. The ABC transporter Bcrp1/ABCG2 is expressed in a wide variety of stem cells and is a molecular determinant of the side-population phenotype. *Nature medicine* **2001**, *7*, 1028–34.

(5) Maliepaard, M.; Scheffer, G. L.; Faneyte, I. F.; Gastelen, A. Van; Pijnenborg, A. C. L. M. Subcellular Localization and Distribution of the Breast Cancer Resistance Protein Transporter in Normal Human Tissues Subcellular Localization and Distribution of the Breast Cancer Resistance Protein Transporter in Normal Human Tissues 1. **2001**, 3458–3464.

(6) Cooray, H. C.; Blackmore, C. G.; Maskell, L.; Barrand, M. a Localisation of breast cancer resistance protein in microvessel endothelium of human brain. *Neuroreport* **2002**, *13*, 2059–63.

(7) Doyle, L. A.; Ross, D. D. Multidrug resistance mediated by the breast cancer resistance protein BCRP (ABCG2). *Oncogene* **2003**, *22*, 7340–58.

(8) Doyle, L. a; Yang, W.; Abruzzo, L. V; Krogmann, T.; Gao, Y.; Rishi, a K.; Ross, D. D. A multidrug resistance transporter from human MCF-7 breast cancer cells. *Proceedings of the National Academy of Sciences of the United States of America* **1998**, *95*, 15665–70.

(9) Fetsch, P. a; Abati, A.; Litman, T.; Morisaki, K.; Honjo, Y.; Mittal, K.; Bates, S. E. Localization of the ABCG2 mitoxantrone resistance-associated protein in normal tissues. *Cancer letters* **2006**, *235*, 84–92.

(10) Allikmets, R.; Schriml, L. M.; Hutchinson, A.; Romano-Spica, V.; Dean, M. A human placenta-specific ATP-binding cassette gene (ABCP) on chromosome 4q22 that is involved in multidrug resistance. *Cancer research* **1998**, *58*, 5337–9.

(11) Mao, Q. BCRP/ABCG2 in the placenta: expression, function and regulation. *Pharmaceutical research* **2008**, *25*, 1244–55.

(12) Kobayashi, D.; Ieiri, I.; Hirota, T.; Takane, H. Functional assessment of ABCG2 (BCRP) gene polymorphisms to protein expression in human placenta. *Drug metabolism and* **2005**, *33*, 94–101.

(13) Yeboah, D.; Sun, M.; Kingdom, J.; Baczyk, D.; Lye, S. J.; Matthews, S. G.; Gibb, W. Expression of breast cancer resistance protein (BCRP / ABCG2) in human placenta throughout gestation and at term before and after labor. **2006**, *1258*, 1251–1258.

(14) Leslie, E. M.; Deeley, R. G.; Cole, S. P. C. Multidrug resistance proteins: role of P-glycoprotein, MRP1, MRP2, and BCRP (ABCG2) in tissue defense. *Toxicology and applied pharmacology* **2005**, *204*, 216–37.

(15) Poonkuzhali, B.; Lamba, J.; Strom, S. Association of breast cancer resistance protein/ABCG2 phenotypes and novel promoter and intron 1 single nucleotide polymorphisms. *Drug Metabolism and ...* **2008**, *36*, 780–795.

(16) Ross, D. D.; Karp, J. E.; Chen, T. T.; Doyle, L. A. Expression of breast cancer resistance protein in blast cells from patients with acute leukemia. *Blood* **2000**, *96*, 365–8.

(17) Urquhart, B. L.; Ware, J. a; Tirona, R. G.; Ho, R. H.; Leake, B. F.; Schwarz, U. I.; Zaher, H.; Palandra, J.; Gregor, J. C.; Dresser, G. K.; Kim, R. B. Breast cancer resistance protein (ABCG2) and drug disposition: intestinal expression, polymorphisms and sulfasalazine as an in vivo probe. *Pharmacogenetics and genomics* **2008**, *18*, 439–48.

(18) Zamber, C. P.; Lamba, J. K.; Yasuda, K.; Farnum, J.; Thummel, K.; Schuetz, J. D.; Schuetz, E. G. Natural allelic variants of breast cancer resistance protein (BCRP) and their relationship to BCRP expression in human intestine. *Pharmacogenetics* **2003**, *13*, 19–28.

(19) Suvannasankha, a; Minderman, H.; O'Loughlin, K. L.; Nakanishi, T.; Greco, W. R.; Ross, D. D.; Baer, M. R. Breast cancer resistance protein (BCRP/MXR/ABCG2) in acute myeloid leukemia: discordance between expression and function. *Leukemia : official journal of the Leukemia Society of America, Leukemia Research Fund, U.K* **2004**, *18*, 1252–7.

(20) Suvannasankha, A.; Minderman, H.; O'Loughlin, K. L.; Nakanishi, T.; Ford, L. a; Greco, W. R.; Wetzler, M.; Ross, D. D.; Baer, M. R. Breast cancer resistance protein (BCRP/MXR/ABCG2) in adult acute lymphoblastic leukaemia: frequent expression and possible correlation with shorter disease-free survival. *British journal of haematology* **2004**, *127*, 392–8.

(21) Benderra, Z.; Faussat, A.-M.; Sayada, L.; Perrot, J.-Y.; Chaoui, D.; Marie, J.-P.; Legrand, O. Breast cancer resistance protein and P-glycoprotein in 149 adult acute myeloid leukemias. *Clinical cancer research : an official journal of the American Association for Cancer Research* **2004**, *10*, 7896–902.

(22) Tsunoda, S.; Okumura, T.; Ito, T.; Kondo, K.; Ortiz, C.; Tanaka, E.; Watanabe, G.; Itami, A.; Sakai, Y.; Shimada, Y. ABCG2 expression is an independent unfavorable prognostic factor in esophageal squamous cell carcinoma. *Oncology* **2006**, *71*, 251–8.

(23) Usuda, J.; Tsunoda, Y.; Ichinose, S.; Ishizumi, T.; Ohtani, K.; Maehara, S.; Ono, S.; Tsutsui, H.; Ohira, T.; Okunaka, T.; Furukawa, K.; Sugimoto, Y.; Kato, H.; Ikeda, N. Breast cancer resistant protein (BCRP) is a molecular determinant of the outcome of photodynamic therapy (PDT) for centrally located early lung cancer. *Lung cancer (Amsterdam, Netherlands)* **2010**, *67*, 198–204.

(24) Uggla, B.; Ståhl, E.; Wågsäter, D.; Paul, C.; Karlsson, M. G.; Sirsjö, A.; Tidefelt, U. BCRP mRNA expression v. clinical outcome in 40 adult AML patients. *Leukemia research* **2005**, *29*, 141–6.

(25) Yoh, K. Breast Cancer Resistance Protein Impacts Clinical Outcome in Platinum-Based Chemotherapy for Advanced Non-Small Cell Lung Cancer. *Clinical Cancer Research* **2004**, *10*, 1691–1697.

(26) Campbell, P. K.; Zong, Y.; Yang, S.; Zhou, S.; Rubnitz, J. E.; Sorrentino, B. P. Identification of a novel, tissue-specific ABCG2 promoter expressed in pediatric acute megakaryoblastic leukemia. *Leukemia research* **2011**, *35*, 1321–9.

(27) Nakanishi, T.; Bailey-Dell, K. J.; Hassel, B. a; Shiozawa, K.; Sullivan, D. M.; Turner, J.; Ross, D. D. Novel 5' untranslated region variants of BCRP mRNA are differentially expressed in drug-selected cancer cells and in normal human tissues: implications for drug resistance, tissue-specific expression, and alternative promoter usage. *Cancer research* **2006**, *66*, 5007–11.

(28) Natarajan, K.; Xie, Y.; Nakanishi, T.; Beck, W. T.; Bauer, K. S.; Ross, D. D. Identification and characterization of the major alternative promoter regulating Bcrp1/Abcg2 expression in the mouse intestine. *Biochimica et biophysica acta* **2011**, *1809*, 295–305.

(29) Bailey-Dell, K. J.; Hassel, B.; Doyle, L. a; Ross, D. D. Promoter characterization and genomic organization of the human breast cancer resistance protein (ATP-binding cassette transporter G2) gene. *Biochimica et biophysica acta* **2001**, *1520*, 234–41.

(30) Zong, Y.; Zhou, S.; Fatima, S.; Sorrentino, B. P. Expression of mouse Abcg2 mRNA during hematopoiesis is regulated by alternative use of multiple leader exons and promoters. *The Journal of biological chemistry* **2006**, *281*, 29625–32.

(31) Kim, T. H.; Barrera, L. O.; Zheng, M.; Qu, C.; Singer, M. a; Richmond, T. a; Wu, Y.; Green, R. D.; Ren, B. A high-resolution map of active promoters in the human genome. *Nature* **2005**, *436*, 876–80.

(32) Cooper, S. J.; Trinklein, N. D.; Anton, E. D.; Nguyen, L.; Myers, R. M. Comprehensive analysis of transcriptional promoter structure and function in 1% of the human genome. *Genome research* **2006**, *16*, 1–10.

(33) Smale, S. T.; Kadonaga, J. T. The RNA polymerase II core promoter. *Annual review of biochemistry* **2003**, *72*, 449–79.

(34) Calhoun, V. C.; Stathopoulos, A.; Levine, M. Promoter-proximal tethering elements regulate enhancer-promoter specificity in the Drosophila Antennapedia complex. *Proceedings of the National Academy of Sciences of the United States of America* **2002**, *99*, 9243–7.

(35) Takai, D.; Jones, P. a Comprehensive analysis of CpG islands in human chromosomes 21 and 22. *Proceedings of the National Academy of Sciences of the United States of America* **2002**, *99*, 3740–5.

(36) To, K. K. W.; Robey, R.; Zhan, Z.; Bangiolo, L.; Bates, S. E. Upregulation of ABCG2 by romidepsin via the aryl hydrocarbon receptor pathway. *Molecular cancer research : MCR* **2011**, *9*, 516–27.

(37) Tan, K. P.; Wang, B.; Yang, M.; Boutros, P. C.; Macaulay, J.; Xu, H.; Chuang, A. I.; Kosuge, K.; Yamamoto, M.; Takahashi, S.; Wu, A. M. L.; Ross, D. D.; Harper, P. A.; Ito, S. Aryl Hydrocarbon Receptor Is a Transcriptional Activator of the Human Breast Cancer Resistance Protein (BCRP / ABCG2) □. **2010**.

(38) Wang, H.; Lee, E.; Zhou, L.; Leung, P. C. K.; Ross, D. D.; Unadkat, J. D.; Mao, Q. Progesterone receptor (PR) isoforms PRA and PRB differentially regulate expression of the breast cancer resistance protein in human placental choriocarcinoma BeWo cells. *Molecular pharmacology* **2008**, *73*, 845–54.

(39) Ee, P. L. R. Identification of a Novel Estrogen Response Element in the Breast Cancer Resistance Protein (ABCG2) Gene. *Cancer Research* **2004**, *64*, 1247–1251.

(40) Pradhan, M.; Bembinster, L. a; Baumgarten, S. C.; Frasor, J. Proinflammatory cytokines enhance estrogen-dependent expression of the multidrug transporter gene ABCG2 through estrogen receptor and NF{kappa}B cooperativity at adjacent response elements. *The Journal of biological chemistry* **2010**, *285*, 31100–6.

(41) Krishnamurthy, P.; Ross, D. D.; Nakanishi, T.; Bailey-Dell, K.; Zhou, S.; Mercer, K. E.; Sarkadi, B.; Sorrentino, B. P.; Schuetz, J. D. The stem cell marker Bcrp/ABCG2 enhances hypoxic cell survival through interactions with heme. *The Journal of biological chemistry* **2004**, *279*, 24218–25.

(42) Singh, A.; Wu, H.; Zhang, P.; Happel, C. Expression of ABCG2 (BCRP) is regulated by Nrf2 in cancer cells that confers side population and chemoresistance phenotype. *Molecular cancer ...* **2010**, *9*, 2365–2376.

(43) Turner, J. G.; Gump, J. L.; Zhang, C.; Cook, J. M.; Marchion, D.; Hazlehurst, L.; Munster, P.; Schell, M. J.; Dalton, W. S.; Sullivan, D. M. ABCG2 expression, function, and promoter methylation in human multiple myeloma. *Blood* **2006**, *108*, 3881–9.

(44) To, K. K. W.; Zhan, Z.; Bates, S. E. Aberrant promoter methylation of the ABCG2 gene in renal carcinoma. *Molecular and cellular biology* **2006**, *26*, 8572–85.

(45) Bram, E.; Stark, M.; Raz, S. Chemotherapeutic drug-induced ABCG2 promoter demethylation as a novel mechanism of acquired multidrug resistance. *Neoplasia (New York, NY)* **2009**, *11*, 1359–1370.

(46) Nakano, H.; Nakamura, Y.; Soda, H.; Kamikatahira, M.; Uchida, K.; Takasu, M.; Kitazaki, T.; Yamaguchi, H.; Nakatomi, K.; Yanagihara, K.; Kohno, S.; Tsukamoto, K. Methylation status of breast cancer resistance protein detected by methylation-specific polymerase chain reaction analysis is correlated inversely with its expression in drug-resistant lung cancer cells. *Cancer* **2008**, *112*, 1122–30.

(47) Ha Choi, J.; Wah Yee, S.; Kim, M. J.; Nguyen, L.; Ho Lee, J.; Kang, J.-O.; Hesselson, S.; Castro, R. a; Stryke, D.; Johns, S. J.; Kwok, P.-Y.; Ferrin, T. E.; Goo Lee, M.; Black, B. L.; Ahituv, N.; Giacomini, K. M. Identification and characterization of novel polymorphisms in the basal promoter of the human transporter, MATE1. *Pharmacogenetics and genomics* **2009**, *19*, 770–80.

(48) Hesselson, S. E.; Matsson, P.; Shima, J. E.; Fukushima, H.; Yee, S. W.; Kobayashi, Y.; Gow, J. M.; Ha, C.; Ma, B.; Poon, A.; Johns, S. J.; Stryke, D.; Castro, R. a; Tahara, H.; Choi, J. H.; Chen, L.; Picard, N.; Sjödin, E.; Roelofs, M. J. E.; Ferrin, T. E.; Myers, R.; Kroetz, D. L.; Kwok, P.-Y.; Giacomini, K. M. Genetic variation in the proximal promoter of ABC and SLC superfamilies: liver and kidney specific expression and promoter activity predict variation. *PloS one* **2009**, *4*, e6942.

(49) Yee, S. W.; Shima, J. E.; Hesselson, S.; Nguyen, L.; De Val, S.; Lafond, R. J.; Kawamoto, M.; Johns, S. J.; Stryke, D.; Kwok, P.; Ferrin, T. E.; Black, B. L.; Gurwitz, D.; Ahituv, N.; Giacomini, K. M. Identification and characterization of proximal promoter polymorphisms in the human concentrative nucleoside

transporter 2 (SLC28A2). *The Journal of pharmacology and experimental therapeutics* **2009**, *328*, 699–707.

(50) Li, L.; Koo, S. H.; Hong, I. H. K.; Lee, E. J. D. Identification of functional promoter haplotypes of human concentrative nucleoside transporter 2, hCNT2 (SLC28A2). *Drug metabolism and pharmacokinetics* **2009**, *24*, 161–6.

(51) Wang, D.; Chen, H.; Momary, K. M.; Cavallari, L. H.; Johnson, J. a; Sadée, W. Regulatory polymorphism in vitamin K epoxide reductase complex subunit 1 (VKORC1) affects gene expression and warfarin dose requirement. *Blood* **2008**, *112*, 1013–21.

(52) Kenna, G. a; Zywiak, W. H.; McGeary, J. E.; Leggio, L.; McGeary, C.; Wang, S.; Grenga, A.; Swift, R. M. A within-group design of nontreatment seeking 5-HTTLPR genotyped alcohol-dependent subjects receiving ondansetron and sertraline. *Alcoholism, clinical and experimental research* **2009**, *33*, 315–23.

(53) McLeod, H. L.; Sargent, D. J.; Marsh, S.; Green, E. M.; King, C. R.; Fuchs, C. S.; Ramanathan, R. K.; Williamson, S. K.; Findlay, B. P.; Thibodeau, S. N.; Grothey, A.; Morton, R. F.; Goldberg, R. M. Pharmacogenetic predictors of adverse events and response to chemotherapy in metastatic colorectal cancer: results from North American Gastrointestinal Intergroup Trial N9741. *Journal of clinical oncology : official journal of the American Society of Clinical Oncology* **2010**, *28*, 3227–33.

(54) Toffoli, G.; Cecchin, E.; Gasparini, G.; D'Andrea, M.; Azzarello, G.; Basso, U.; Mini, E.; Pessa, S.; De Mattia, E.; Lo Re, G.; Buonadonna, A.; Nobili, S.; De Paoli, P.; Innocenti, F. Genotype-driven phase I study of irinotecan administered in combination with fluorouracil/leucovorin in patients with metastatic colorectal cancer. *Journal of clinical oncology : official journal of the American Society of Clinical Oncology* **2010**, *28*, 866–71.

(55) Innocenti, F.; Undevia, S. D.; Iyer, L.; Chen, P. X.; Das, S.; Kocherginsky, M.; Karrison, T.; Janisch, L.; Ramírez, J.; Rudin, C. M.; Vokes, E. E.; Ratain, M. J. Genetic variants in the UDP-glucuronosyltransferase 1A1 gene predict the risk of severe neutropenia of irinotecan. *Journal of clinical oncology : official journal of the American Society of Clinical Oncology* **2004**, *22*, 1382–8.

(56) Rozen, S.; Skaletsky, H. Primer3 on the WWW for general users and for biologist programmers. *Methods in molecular biology (Clifton, N.J.)* **2000**, *132*, 365–86.

(57) Africa, W. A map of human genome variation from population-scale sequencing. *Nature* **2010**, *467*, 1061–73.

(58) Frazer, K. a; *et. al.* A second generation human haplotype map of over 3.1 million SNPs. *Nature* **2007**, *449*, 851–61.

(59) Kroetz, D. L.; Yee, S. W.; Giacomini, K. M. The pharmacogenomics of membrane transporters project: research at the interface of genomics and transporter pharmacology. *Clinical pharmacology and therapeutics* **2010**, *87*, 109–16.

(60) Barrett, J. C.; Fry, B.; Maller, J.; Daly, M. J. Haploview: analysis and visualization of LD and haplotype maps. *Bioinformatics (Oxford, England)* **2005**, *21*, 263–5.

(61) Liu, H.; Naismith, J. H. An efficient one-step site-directed deletion, insertion, single and multiple-site plasmid mutagenesis protocol. *BMC biotechnology* **2008**, *8*, 91.

(62) Liu, F.; Song, Y.; Liu, D. Hydrodynamics-based transfection in animals by systemic administration of plasmid DNA. *Gene therapy* **1999**, *6*, 1258–66.

(63) Kim, M. J.; Ahituv, N. The Hydrodynamic Tail Vein Assay as a Tool for the Study of Liver Promoters and Enhancers. In *Pharmacogenomics: Methods and Protocols*; Innocenti, F.; van Schaik, R. H. N., Eds.; 2012.

(64) Simonet, W. S.; Bucay, N.; Lauer, S. J.; Taylor, J. M. A far-downstream hepatocyte-specific control region directs expression of the linked human apolipoprotein E and C-I genes in transgenic mice. *The Journal of biological chemistry* **1993**, *268*, 8221–9.

(65) Sandelin, A.; Wasserman, W. W.; Lenhard, B. ConSite: web-based prediction of regulatory elements using cross-species comparison. *Nucleic acids research* **2004**, *32*, W249–52.

(66) Wingender, E.; Chen, X.; Hehl, R.; Karas, H.; Liebich, I.; Matys, V.; Meinhardt, T.; Prüss, M.; Reuter, I.; Schacherer, F. TRANSFAC: an integrated system for gene expression regulation. *Nucleic acids research* **2000**, *28*, 316–9.

(67) Boyle, A. P.; Hong, E. L.; Hariharan, M.; Cheng, Y.; Schaub, M. a; Kasowski, M.; Karczewski, K. J.; Park, J.; Hitz, B. C.; Weng, S.; Cherry, J. M.; Snyder, M. Annotation of functional variation in personal genomes using RegulomeDB. *Genome research* **2012**, *22*, 1790–7.

(68) Wu, A. M. L.; Dalvi, P.; Lu, X.; Yang, M.; Riddick, D. S.; Matthews, J.; Clevenger, C. V; Ross, D. D.; Harper, P. a; Ito, S. *Induction of Multidrug Resistance Transporter ABCG2 by Prolactin in Human Breast Cancer Cells.*; 2012.

(69) Watson, C. J. Stat transcription factors in mammary gland development and tumorigenesis. *Journal of mammary gland biology and neoplasia* **2001**, *6*, 115–27.

(70) Yamashita, H.; Iwase, H.; Toyama, T.; Fujii, Y. Naturally occurring dominant-negative Stat5 suppresses transcriptional activity of estrogen receptors and induces apoptosis in T47D breast cancer cells. *Oncogene* **2003**, *22*, 1638–52.

(71) Imai, Y.; Ishikawa, E.; Asada, S.; Sugimoto, Y. Estrogen-mediated post transcriptional down-regulation of breast cancer resistance protein/ABCG2. *Cancer research* **2005**, *65*, 596–604.

(72) Yasuda, S.; Kobayashi, M.; Itagaki, S.; Hirano, T.; Iseki, K. Response of the ABCG2 promoter in T47D cells and BeWo cells to sex hormone treatment. *Molecular biology reports* **2009**, *36*, 1889–96.

(73) Boyd, K. E.; Farnham, P. J. Coexamination of Site-Specific Transcription Factor Binding and Promoter Activity in Living Cells Coexamination of Site-Specific Transcription Factor Binding and Promoter Activity in Living Cells. *Society* **1999**, *19*.

(74) Porro, A.; Iraci, N.; Soverini, S.; Diolaiti, D.; Gherardi, S.; Terragna, C.; Durante, S.; Valli, E.; Kalebic, T.; Bernardoni, R.; Perrod, C.; Haber, M.; Norris, M. D.; Baccarani, M.; Martinelli, G.; Perini, G. c-MYC Oncoprotein Dictates Transcriptional Profiles of ATP-Binding Cassette Transporter Genes in Chronic Myelogenous Leukemia CD34+ Hematopoietic Progenitor Cells. *Molecular cancer research : MCR* **2011**, *9*, 1054–66.

(75) Kang, K. W.; Im, Y. Bin; Go, W.-J.; Han, H.-K. C-myc amplification altered the gene expression of ABC- and SLC-transporters in human breast epithelial cells. *Molecular pharmaceutics 6*, 627–33.

(76) Hess, J.; Angel, P.; Schorpp-Kistner, M. AP-1 subunits: quarrel and harmony among siblings. *Journal of cell science* **2004**, *117*, 5965–73.

(77) Angel, P.; Karin, M. The role of Jun, Fos and the AP-1 complex in cell-proliferation and transformation. *Biochimica et biophysica acta* **1991**, *1072*, 129–57.

(78) Safe, S. Transcriptional activation of genes by 17 beta-estradiol through estrogen receptor-Sp1 interactions. *Vitamins and hormones* **2001**, *62*, 231–52.

(79) Schultz, J. R.; Petz, L. N.; Nardulli, A. M. Cell- and ligand-specific regulation of promoters containing activator protein-1 and Sp1 sites by estrogen receptors alpha and beta. *The Journal of biological chemistry* **2005**, *280*, 347–54.

(80) Zhao, C.; Gao, H.; Liu, Y.; Papoutsi, Z.; Jaffrey, S.; Gustafsson, J.-A.; Dahlman-Wright, K. Genome-wide mapping of estrogen receptor-beta-binding regions reveals extensive cross-talk with transcription factor activator protein-1. *Cancer research* **2010**, *70*, 5174–83.

(81) Halilbasic, E.; Claudel, T.; Trauner, M. Bile acid transporters and regulatory nuclear receptors in the liver and beyond. *Journal of hepatology* **2012**, *58*, 155–168.

(82) Germain, P.; Staels, B.; Dacquet, C.; Spedding, M.; Laudet, V. Overview of Nomenclature of Nuclear Receptors. **2006**, *58*, 685–704.

(83) Blazquez, A. G.; Briz, O.; Romero, M. R.; Rosales, R.; Monte, M. J.; Vaquero, J.; Macias, R. I. R.; Cassio, D.; Marin, J. J. G. Characterization of the role of ABCG2 as a bile acid transporter in liver and placenta. *Molecular pharmacology* **2012**, *81*, 273–83.

(84) Generaux, G. T.; Bonomo, F. M.; Johnson, M.; Doan, K. M. M. Impact of SLCO1B1 (OATP1B1) and ABCG2 (BCRP) genetic polymorphisms and inhibition on LDL-C lowering and myopathy of statins. *Xenobiotica; the fate of foreign compounds in biological systems* **2011**, *41*, 639–51.

Chapter 4 : Identification and Characterization of *ABCG2* Regulatory Regions

4.1. Abstract

ABCG2 encodes the mitoxantrone resistance protein (MXR, BCRP), a membrane transporter responsible for the efflux of substrates out of the cell and body. In this study we computationally analyzed a ~300 kb stretch of DNA surrounding *ABCG2* (chr4:88911376-89220011, hg19) and identified 30 regions with potential *cis*-regulatory capabilities based on high evolutionary conservation, determined by comparative genomics (ECR and Vista browsers), and the presence of specialized transcription factor binding sites (TFBS), identified with computational methods (rVista, TRANSFAC, and Cister). These regions were cloned from human DNA and inserted into the enhancer assay vector pGL4.23 and suppressor assay vector pGL3-promoter. Plasmids were transiently transfected into HepG2, HEK293T, HCT116 and MCF-7 cell lines, and luciferase activity was measured as a surrogate for the transcriptional activity of the genomic region. Nine positive *in vitro* enhancers were selected for *in vivo* validation in the mouse tail vein injection luciferase assay. The *in vivo* tail vein assay confirmed six of the nine regions to have liver enhancer activity. The *in vitro* suppressor assays identified seven regions capable of decreasing gene expression in at least one cell line. Our study provides evidence that there are genomic regions surrounding *ABCG2* capable of altering gene expression. The results from this research will drive future clinical investigations examining how interindividual variation in MXR expression and function contributes to differences in drug response. The effect of genetic variants within these regulatory regions on enhancer activity and ABCG2 expression were also studied and will be discussed in Chapter 5.

4.2. Introduction

The mitoxantrone resistance protein (MXR; BCRP; ABCG2) is an efflux membrane transporter expressed apically in several tissues[1–12] with a broad range of both exogenous and endogenous substrates. The transport activity, tissue distribution and cellular localization of MXR suggest that it plays a pivotal role in endogenous substrate disposition as well as protection from and detoxification of xenobiotics[13,14]. Overexpression of MXR is associated with drug resistance to a variety of anticancer drugs and has been linked with decreased disease-free survival in several cancers[15–22]. An individual's susceptibility to certain drug-induced side effects has also been linked to MXR expression, and both coding and non-coding single nucleotide polymorphisms (SNPs) in the *ABCG2* gene encoding MXR[23–25].

Interindividual variation in drug absorption, distribution, metabolism and excretion (ADME) has been correlated with genetic variation in genes encoding drug-metabolizing enzymes and transporters[26]. New research has highlighted that single nucleotide polymorphisms (SNPs) in non-coding genomic regions can also effect ADME gene transcription and expression levels, and thus drug disposition[27,28]. Additional variation in ADME gene expression can be brought on by ligand-activated transcription factors (TFs) from the nuclear receptor (NR) family; these TFs temporally alter gene expression in response to changes in the cell environment[29]. In addition, complex tissue-specific pathways of TFs have been shown to regulate expression for selected tissues[30,31].

The expression of ABCG2 has wide tissue-specific variability among individuals. There are reports of significant ABCG2 variation in intestine[15,32], liver[33],and blast cells[34],

and we have shown wide variation in ABCG2 mRNA in a local bank of human livers and kidneys (*Chapter 1* Figure 1.2). In addition, the expression of ABCG2 is altered by many types of stimuli, including hypoxia[35], inflammation[36], xenobiotics[37], hormones[38,39] and nutrients[40,41]. ABCG2 expression is tissue-specific[4] and modulated by NR ligands[37]. Several nuclear response elements (NRE) have been mapped to the proximal promoter of *ABCG2*[36,38,42–44]. However, it is speculated that in order to regulate the expression of a gene, multiple response elements for a NR must interact together, causing looping of the DNA between them, to stabilize the transcriptional machinery and increase gene expression[45]. For tissue-specific genes like *ABCG2* that have a CpG island in their promoter, methylation of the CpG island can block the access of NRs to their recognition sequence, thus *cis*-elements are necessary to respond to NR signals[46]. In addition, there have been no reported SNPs in these NREs mapped in the proximal promoter, indicating that even if they regulate expression of ABCG2, these NREs do not contribute to basal *ABCG2* variation. Therefore, we hypothesized that there are *cis*-regulatory elements in the *ABCG2* gene locus that are responsible for the expression of ABCG2. The aim of this study was to identify and characterize those regulatory regions both *in vitro* and *in vivo*.

NRs are a large family of TFs, including the glucocorticoid receptor (GR), estrogen receptor (ER), progesterone receptor (PR), aryl hydrocarbon receptor (AhR), androgen receptor (AR), pregnane X receptor (PXR), retinoid X receptor (RXR), farnesoid X receptor (FXR), hepatocyte nuclear factor 4α (HNF4α) and vitamin D receptor (VDR). NRs are ligand-induced in response to environmental stimuli and their ligands include a variety of fatty acids, vitamins and steroids[47]. NRs prefer to binding to *cis*-elements as opposed to the proximal promoter of their genes[48–51]. In addition NR

response elements have been shown to be composite elements, consisting of binding sites for other TFs[48,50–53]. Therefore, the identification of TF clustering through a gene locus would be a good approach for the identification of regulatory elements.

There are several factors that influence whether predicted regulatory elements are likely functional. Among them is the evolutionary conservation of the region, excluding the coding regions and promoter regions of genes. This is due to well established evidence for the conservation of regulatory elements through different species[54,55], especially for developmental enhancers[56,57] and tissue-specific enhancers[31,58]. Recently it has been shown that the ~1000 bp surrounding a GRE is evolutionarily conserved and the level of conservation for a predicted GRE is correlated to the extent of GR occupancy at that element[59]. Therefore, consideration of conservation of non-coding regions can aid in identifying putative functional elements. However, it is important to note that due to recent selection in primates, conservation is not necessary for some enhancer regions[60].

The existence of large public databases including genome sequencing, comparative genomics, TF profiling, and gene expression studies has made the identification of *cis*-regulatory elements and the characterization of the effect of genetic variation within them possible[30,31,60]. A previous screen looking for tissue-specific enhancers of genes successfully used gene expression, TFBS and conservation to identify tissue-specific enhancers, showing the power of combining complementary genomic data sets[31]. To identify *cis*-regulatory elements in the *ABCG2* gene locus, a layered *in silico* analysis was developed that incorporated predicted TFBS and evolutionary conservation, in combination with the clustering of multiple TFs.

In this study, a computational analysis of the *ABCG2* gene locus for TFBS clustering and evolutionary conservation was performed to identify putative regulatory regions of *ABCG2* (Figure 4.1). Putative regulatory regions were ranked based on the prevalence of TFs linked to ABCG2 expression or tissue-specific expression in liver or kidney, degree of evolutionary conservation and presence of preliminary ChIP-seq data supporting binding of TFs to the genomic region. High priority regulatory regions were cloned into the pGL4.23 [*luc2*/minP] enhancer assay vector and assayed for their activity in transiently transfected kidney (HEK293T), liver (HepG2), intestine (HCT116) and breast (MCF-7) cell lines. The pGL4.23 vector is a firefly luciferase vector with a multiple cloning site designed to accept a putative enhancer element upstream of a minimal promoter and the luciferase gene, once cloned and transfected into cells, the luciferase activity can be measured as a surrogate for enhancer function. The cell lines were each chosen to represent their primary tissue source. Positive *in vitro* enhancer elements were tested for their *in vivo* liver enhancer activity through the hydrodynamic tail vein assay in mice. Elements with suppressor activity were cloned into the pGL3-promoter [*luc*+/SV40] luciferase expression vector and assayed for their ability to suppress luciferase activity in transiently transfected kidney (HEK293T), liver (HepG2), intestine (HCT116) and breast (MCF-7) cell lines. The pGL3-promoter vector is a firefly luciferase vector with a multiple cloning site designed to accept a putative suppressor element upstream of the strong SV40 promoter and the luciferase gene. ChIP-seq databases were mined for evidence to support the activity of the positive *in vivo* enhancer activity. The identified *in vivo* enhancers and *in vitro* suppressors provide elements of the *ABCG2* gene locus that could be responsible for the tissue-specific expression of *ABCG2*.

Further research assessing the effect of SNPs in these regions on enhancer activity is addressed in Chapter 5.

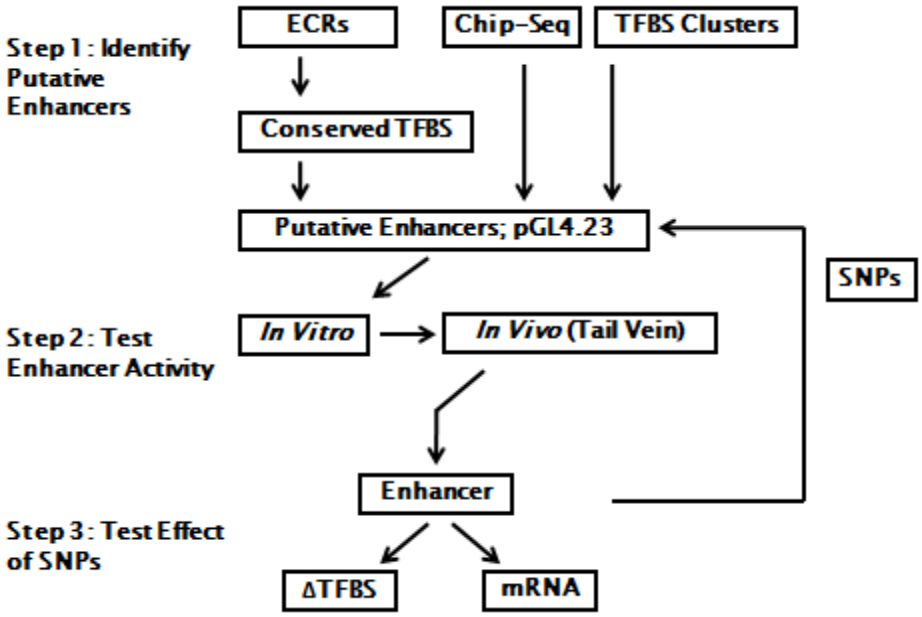

Figure 4.1. Pipeline to identify and characterize *ABCG2* regulatory elements. Experimental design begins with bioinformatic analyses to identify putative enhancer elements (Step 1). Putative enhancers are first tested *in vitro* using luciferase assays for enhancer activity followed by confirmation of enhancer activity *in vivo* (Step 2). Further functional characterization of SNP effects on enhancer activity are performed in Step 3 and will be addressed in Chapter 5.

4.3. Materials and Methods

4.3.1. *Chemicals and Materials*

The vectors pGL4.23 [*luc2*/minP], pGL4.74 [*hRluc*/TK], pGL4.13 [*luc2*/SV40], pGL3-promoter [*luc*+/SV40], the Dual-Luciferase® Reporter Assay System and HB101

competent cells were all purchased from Promega (Madison, WI). The human embryonic kidney (HEK293T/17), human colorectal carcinoma (HCT116), human hepatocellular carcinoma (HepG2) and human breast adenocarcinoma (MCF-7) cell lines were all purchased from the American Type Culture Collection (ATCC, Manassas, VA). One Shot INV110 *dcm*$^{-}$/*dam*$^{-}$ competent cells, high-glucose Dulbecco's modified Eagle's medium (DMEM), Opti-Minimal Essential Medium (Opti-MEM) and Lipofectamine 2000 were all purchased from Invitrogen (Carlsbad, CA). TE buffer, 100 mm LB Amp-100 agar plates and LB Broth 100 μg/mL ampicilin were purchased from Teknova (Hollister, CA). DMSO, phosphate buffered saline (PBS), 0.05% trypsin, and 100X penicillin and streptomycin were all purchased from the UCSF cell culture facility (San Francisco, CA). The GeneJet PCR Purification Kits, GeneJET Gel Purification Kits and GeneJet Plasmid Miniprep Kits were all purchased from Fermentas (Glen Burnie, MD). Bovine serum albumin (BSA), Buffer 2, Buffer 3, *Xho*I, *Acc65*I, *Nhe*I, *Hind*III, T4 Ligase, Ligase buffer, *Dpn*I, *Dpn*I digestion buffer, antarctic phosphatase and 10 mM ATP were all purchased from New England Biolabs (Ipswich, MA). Other materials including 10% fetal bovine serum (FBS) (Axenia BioLogix, Dixon, CA), GenElute HP Endotoxin-Free Maxiprep Kits (Sigma Aldrich), Improved Minimum Essential Medium (IMEM) without phenol red (Mediatech Inc, Manassas, VA), PolyJet™ DNA *In Vitro* Transfection Reagent (SignaGen Laboratories, Rockville, MD), TransIT EE *In Vivo* Gene Delivery System (Mirus Bio, Madison, WI), CD1 mice (Charles Rivers Laboratories, Wilminton, MA), placental genomic DNA (Sigma Aldrich, St. Louis, MO), PfuTurbo DNA Polymerase (Agilent Technologies, Santa Clara, CA) and dNTPs (Denville, Metuchen, NJ) were all purchased from the indicated manufacturers.

4.3.2. *In Silico Analysis of the ABCG2 Locus to Identify Putative Regulatory Elements*

A list of putative regulatory regions in the *ABCG2* gene locus was generated by combining data from several computational programs which looked for high evolutionary conservation to mouse and increased clustering of *cis*-elements. The analyzed *ABCG2* gene locus was defined as a ~300,000 bp region, stretched from one gene upstream (*PPM1K*) and downstream (*PKD2*) of *ABCG2* (chr4:89130400-89439035, hg18; chr4:88911376-89220011, hg19). Using both the Evolutionary Conserved Regions (ECR) browser[61] and Vista browser[62], the *ABCG2* gene locus was scanned for regions larger than 100 bp and with greater than 70% conservation to mouse. Regions from this analysis were numbered ECR1-85 for ECR browser, ECR86-98 for Vista browser, and those with >400 bp of conservation were named ECR400s. Conservation alignments from the ECR browser were submitted to rVista[63], which analyzes them for conserved TFBS using all vertebrate TF matrices from TRANSFAC professional. Next, the genomic region was examined for regions with increased clustering of predicted transcription factor binding sites (TFBS), regardless of conservation, using the Cister program[64]. Matrices used for *cis*-elements included those preprogrammed into the Cister program (TATA, Sp1, CRE, ERE, Nf-1, E2F, Mef-2, Myf, CCAAT, AP-1, Ets, Myc, GATA, LSF, SRF, Tef) and several additional matrices obtained from TRANSFAC[65] and listed in Table 4.1. The *ABCG2* gene locus was split into fourths and analyzed in the Cister program with the default settings: width of window was set to 100 bp, average distance between motifs within a cluster was set to 35 bp, average number of motifs in cluster (b) was set to 6, average distance between clusters (g) was set to 30,000, half-width of sliding window (w) was set to 1000 bp, motif probability threshold was set to 0.1, and pseudocount was set to

1. Regions obtained from this analysis were named cister regions (CR) 1-23. Overlapping regions from the conservation and Cister plot analyses were combined into one putative enhancer region keeping the name of the longer region. Regions consisting of repeat or coding elements were eliminated from further analysis.

Table 4.1. TRANSFAC TFBS Matrices Used in Cister Plot Analysis

Accession Number[1]	Transcription Factor	Accession Number[1]	Transcription Factor
M00054	NF-κB	M00206	HNF-1
M00109	C/EBPβ	M00208	NF-κB
M00117	C/EBPβ	M00235	AhR:Arnt
M00131	HNF-3β	M00236	Arnt
M00132	HNF-1	M00237	AhR:Arnt
M00134	HNF-4	M00242	PPARα:RXRα
M00139	AhR	M00269	XFD-3
M00155	ARP-1	M00289	HFH-3
M00156	RORα1	M00411	HNF-4α
M00157	RORα2	M00512	PPARγ
M00158	COUP-TF, HNF-4	M00515	PPARγ
M00191	ER	M00526	GCNF
M00192	GR	M00528	PPAR
M00194	NF-κB		

[1]Accession number in the TRANSFAC database

4.3.3. *Ranking of Putative Regulatory Elements*

To select high priority putative regulatory elements for *in vitro* testing, putative enhancer regions were ranked based on several criteria. First, regions were scored based on their percent identity to mouse and the number of predicted TFBS per length of region. Then regions were scored for total number of TFBS with extra weight given to TFBS associated with *ABCG2*, liver and kidney gene expression (see Table 4.2). Finally, putative enhancer regions were overlaid with ChIP-seq data peaks from the

TRANSFAC[65] and ENCODE[66] databases. The mining of the ENCODE database is explained in further detail below. Regions with ChIP-seq data supporting association of the region with TFs were given additional weight.

Table 4.2. High Priority Transcription Factors

ABCG2					**Kidney**	**Liver**
NF-κB		VDR		PPARγ	HFH-3	HNF-1
C/EBPβ		LXR		GCNF (RTR)	Kid-1	HNF-3β
ARP-1		FXR		PPARα	FREAC-4	HNF-4α
RORα1		RXRα		ER	Ets-1	HNF-4γ
RORα2		PXR		GR		HNF-3α
AhR		AR		HIF		p300

4.3.4. *Primer Design*

The reverse strand DNA sequences for the putative enhancer regions were pulled from the UCSC genome browser with an additional 30 bp on either side to aid in primer design. Regions were scanned with the NEBcutter V2.0[67] for the presence of any *Nhe*I, *Hind*III, *Xho*I or *Acc65*I restriction sites. Primers for the regions were designed with the aid of Primer3[68]. Extensions were added for the restriction sites *Acc65*I (forward primers) and *Xho*I (reverse primers) for all regions except ECR400, for which *Nhe*I (forward primer) and *Hind*III (reverse primer) were used, to ensure that the anti-strand sequence of the enhancer element would be oriented in the same manner as the element is to the *ABCG2* promoter. The UCSC genome browser *in silico* PCR program was used to confirm predicted specific amplification of the target region with the selected primer set. Sequences and primer locations for ECR cloning primers are shown in Table 4.3. Sequencing primers were developed for ECRs too long to be sequenced by both

RVprimer3 and a reverse primer p150R specific for reverse sequencing of pGL4.23 restriction sites (Table 4.4). Primers were synthesized by Integrated DNA Technologies (San Diego, CA) and diluted to 100 μM stocks in TE Buffer.

Table 4.3. Cloning Primers for Putative Enhancer Regions

Primer	Sequence	Genomic Location[1]	Tm[2]
ECR400F	TCAGGCTAGCAGTGTGCTAGATCTTCCTGG	89143422-89143443	55
ECR400R	GCCGAAGCTTCCAGAGAAGGAAATTGAGAT	89142802-89142823	
ECR402F	TCAGGGTACCTGGCATAAAAACTCTGCTCT	89159089-89159110	55
ECR402R	TCAGCTCGAGTATAGGCCAAGCAATACCAC	89157927-89157947	
ECR17F	TCAGGGTACCTTTGAAACCTTTCCTTCCAA	89190684-89190705	60
ECR17R	TTATCTCGAGCCTGGCCCGACTAATTCAT	89190442-89190463	
ECR410F	TCAGGGTACCGAAAGACCATGGAAGAGATC	89198522-89198542	60
ECR410R	TCAGCTCGAGACAACACTTGGCCACTTTGA	89197061-89197082	
ECR412F	CCCGGGTACCATTGGTAGAAATATGTGAAA	89208738-89208759	60
ECR412R	TCAGCTCGAGTTGGCTATTCCTTGCTGTTA	89207879-89207901	
CR6F	TCAGGGTACCAAAAGAAACAAAACAGCCAC	89230482-89230503	60
CR6R	CCCGCTCGAGTACATTTCTACTTTATAAGA	89229977-89229999	
ECR25F	TCAGGGTACCACATGCAGAGGAGAAGAGTT	89235940-89235960	60
ECR25R	TCAGCTCGAGTAAGAAACATTGCTGCATGT	89234523-89234544	
ECR38F	TCAGGGTACCTGTACTTGATCAGCCAATGG	89272336-89272357	60
ECR38R	TCAGCTCGAGTCAGAGTGCCCATCACAACA	89271364-89271385	
CR7F	TCAGGGTACCGCATACACATACATGCATAA	89276397-89276418	55
CR7R	TCAGCTCGAGTGTACATACAAGATATTCTT	89275033-89275054	
ECR43F	TTATGGTACCGTTGTGCTTAGGAGGACTGT	89281325-89281346	60
ECR43R	CCCGCTCGAGGTGAACTATTTCATTAAACA	89281134-89281154	
CR8F	CCCGGGTACCTTTCACTTAATAGGAATAAT	89287794-89287815	55
CR8R	TCAGCTCGAGGCAATAGACAGGTTAATATG	89286463-89286484	
ECR44F	TCAGGGTACCTTGGATTCAGTCTCTTATGG	89292425-89292446	60
ECR44R	TCAGCTCGAGGGTCTCAAATCCTTTTCTCA	89292195-89292217	
CR9F	TTATGGTACCCTGACCTTGCCAGGGAAAAT	89303202-89303223	60
CR9R	TCAGCTCGAGCAGGAAAGTGTTCATTTGTT	89302387-89302400	
CR10F	TCAGGGTACCTCCAGCATCTGGGCTCTTAC	89308251-89308272	60
CR10R	TCAGCTCGAGGTCCCACGGTTTGAACACGA	89307110-89307132	
CR11F	TCAGGGTACCAGAAGACAGGGAACAAAGCC	89313050-89313070	60
CR11R	TCAGCTCGAGTCTTTGTGTTTCTGGTTGTA	89311815-89311837	
CR15F	TCAGGGTACCTCAAAATTTTCACCTCTTGT	89332525-89332546	60
CR15R	TCAGCTCGAGCACGTGCCCTTTTCTAAACG	89331014-89331035	
CR16F	TCAGGGTACCCTACAGCTCTGTCTGAACCA	89334895-89334917	67

Primer	Sequence	Genomic Location[1]	Tm[2]
CR16R	TCAGCTCGAGGAAGGCTGCCATGAATGTAG	89333859-89333880	
ECR48F	TCAGGGTACCAGGAGGTAAAACGTGGGCCC	89336908-89336930	55
ECR48R	TCAGCTCGAGCTGTCAAGTGCATCTCCTGT	89336705-89336727	
ECR420F	TCAGGGTACCTAGCAGATTTTCAACAGGCA	89346301-89346322	60
ECR420R	TCAGCTCGAGCTGTCAAAAGATTTGCCATT	89345102-89345123	
ECR52F	TCAGGGTACCACTTCATGGAGAAGGTGGGC	89346901-89346880	60
ECR52R	TCAGCTCGAGCAATGCCTTAACTGTGTGCT	89346636-89346657	
ECR55F	TCAGGGTACCTTTCTGGTAGTTCTGACCTC	89364013-89364035	60
ECR55R	TCAGCTCGAGCAGCGAACACACACCACTAC	89363840-89363862	
CR19F	TCAGGGTACCATAAAATAACGTGTTACATC	89383418-89383439	60
CR19R	TCAGCTCGAGCTATAGAGGTGGTAAGACTT	89382285-89382307	
ECR423F	TCAGGGTACCTCCATGGGCTCAAGTAGACC	89409470-89409482	55
ECR423R	TCAGCTCGAGACAATGGTGTGATATGTAGA	89408527-89408548	
ECR425F	TCAGGGTACCAGTGAATGTGTATATGCGTG	89411732-89411754	55
ECR425R	TCAGCTCGAGAAGGTTGTAATACAAAGAGG	89409846-89409868	
ECR426F	TCAGGGTACCTGTTGGGAACTCCAATTAAT	89417136-89417157	55
ECR426R	TCAGCTCGAGGATGAACCAAATACAGATCA	89416468-89416490	
ECR428F	TCAGGGTACCTTGGCCATTCTTTGGAAACA	89419430-89419409	60
ECR428R	TCAGCTCGAGATTTTGGTTAATGCTTTCCC	89418093-89418115	
ECR429F	TCAGGGTACCTTCTTCCCAGATTCCAGCTT	89431770-89431792	55
ECR429R	TCAGCTCGAGCTGTGGGAAATGGTGCATAA	89430870-89430892	
ECR33F	TCAGGGTACCAGCCCATTTCTTGTTTTT	89248403-89248422	56.5
ECR33R	TCAGCTCGAGGGGAAGAGTTTCAATTAGAG	89247469-89247490	
ECR31F	TTATGGTACCAGTCACAGTGGACCCTTAAA	89245696-89245716	60
ECR31R	TTATCTCGAGACTGCACTACTGCACACCAG	89244915-89244935	
ECR54F	TTATGGTACCAAGGTAGTCAGAGGCCAGA	89352633-89352652	60
ECR54R	TTATCTCGAGCCAGAGGGGAAAGTCTTTC	89352026-89352045	

[1]Genomic location of the primers on chromosome 4 build hg18

[2]Melting temperature used in cloning polymerase chain reaction for the primer pair

Abbreviations: F, Forward; R, Reverse

Table 4.4. Sequencing Primers for Putative Regulatory Elements

Primer	Sequence	Genomic Location[1]
ECR402 Seq1	CACCAGCACTGAGAGTGGAGCAT	chr4:89158678-89158701
ECR423 Seq1	TTGAACTGGTTGTAGCCAGTGTTGG	chr4:89408981-89409006
CR10 Seq1	AAGGCAGAAGGGACAGTTGGGTT	chr4:89307834-89307857
CR8 Seq1	TTGACAGGGTTACGCTGTTGCTTAG	chr4:89287234-89287259
ECR25 Seq1	CAAACAAGAACGAAAGATTGTCACTG	chr4:89235274-89235299
ECR428 Seq1	GAACCAGGTGAGAAGGAGAGTGCTG	chr4:89418805-89418830
ECR429 Seq1	GCTTGACAACCAGTGACAAACAGGC	chr4:89431362-89431387
CR7 Seq1	GCCTAGTGGGGGATTCAGAACACA	chr4:89274236-89274260
ECR38 Seq1	AGGCAGGGAGAATCTGGAATATGGC	chr4:89271905-89271930
ECR425 Seq1	GGTTCCCACATCTCTTTGTCCCA	chr4:89411209-89411231
CR15 Seq1	CCACATCATCTCGCCAACACCTG	chr4:89331631-89331653
pGL4.23 SEQ p150R	GGCATCTTCCATGGTGGCTTTACC	na

[1]Genomic location in build hg19

Abbreviations: na, not applicable

4.3.5. *Cloning of Putative Regulatory Elements*

The region of interest was amplified from human placenta genomic DNA using 1 unit PfuTurbo DNA polymerase, 1X PfuTurbo buffer, 200 μM dNTPs, 150 ng genomic DNA, 400 nM each primer (Table 4.3) and when needed,1 μL DMSO in a final reaction volume of 50 μL. PCR conditions were 95°C for 2 min, followed by 35 cycles of 30 sec at 95°C, 30 sec at melting temperature (see Table 4.3) and 2.5 min at 72°C, and then a final extension of 10 min at 72°C. The PCR reaction was imaged on a 1% agarose gel, and the specific band at the correct size was gel purified using the GeneJet Gel Purification Kit following the manufacturer's protocol. For cloning, the pGL4.23 [*luc2*/minP] and pGL3-promoter [*luc*+/SV40] were grown in One Shot INV110 *dcm*$^-$ /*dam*$^-$ competent cells so methylation would not interfere with enzyme digestion. The purified putative enhancer regions, 500 ng of pGL4.23 [*luc2*/minP] and 500 ng of pGL3-promoter [*luc*+/SV40] vector were digested in separate reactions of 1X Buffer 3, 1 unit

*Acc65*I, 1 unit *Xho*I and 0.5 µL BSA at 37°C for 1 hr. For ECR400, the purified enhancer region, 500 ng of pGL4.23, and 500 ng of pGL3-promoter vector were digested in separate reactions of 1X Buffer 2, 1 unit *Nhe*I, 1 unit *Hind*III, and 0.5 µL BSA, at 37°C for 1 hr. Vectors were dephosphorylated after enzyme digestion using 4 units of antarctic phosphatase at 37°C for 2 hr. The reaction was purified using the GeneJet PCR Purification Kit following the manufacturer's protocol, and the concentration of the cleaned DNA measured using a NanoDrop spectrophotometer (Thermo Scientific).

The amplified *ABCG2* putative enhancer region was ligated into the pGL4.23 vector through a 96:32 fmol insert to vector reaction comprised of the insert and vector plus 1 unit Ligase T4, 1X Ligase Buffer, 65 nM ATP and a final reaction volume of 20 µL. The ligation was allowed to sit overnight at room temperature before purification using the GeneJet PCR Purification Kit. A portion of the purified ligation reaction (5 µL) was transformed into 35 µL HB101 competent cells following the manufacturer's protocol. The transformed bacteria was plated onto 100mm LB Amp plates and grown at 37°C for 24 hr. Selected colonies were grown in 2-5 mL LB Broth with 100 µg/mL ampicillin at 37°C with shaking for up to 24 hr. DNA was isolated from the bacteria using a GeneJet Plasmid Miniprep Kit and sequenced with the RVPrimer3 and p150R primers (Table 4.4) to confirm the presence and orientation of the putative enhancer element in the pGL4.23 vector. If needed, additional sequencing primers (see Table 4.4) were used to verify the correct sequence of the putative enhancer. Other vectors used in the transfection assays include the pGL4.74 [*hRluc*/TK] vector, which has a Renilla luciferase reporter gene, a highly active HSV-TK promoter and is co-transfected into each cell so that the transfection efficiency can be controlled by the expression of Renilla,

and the pGL4.13 [*luc2*/SV40] vector, which has a luciferase reporter gene and a highly active SV40 promoter. DNA for the selected enhancer plasmids, empty pGL4.23, *APOE*[69] (liver specific enhancer in pGL4.23 kindly provided by Dr. Nadav Ahituv, University of California San Francisco), pGL4.13, and pGL4.74 vectors were isolated from transformed bacteria grown overnight at 37°C with shaking in 150 mL LB Broth with 100 μg/mL ampicillin, using the GenElute HP Endotoxin-Free Maxiprep Kit following the manufacturer's protocol. For follow-up studies on negative regulatory regions, putative suppressor regions were re-amplified from the pGL4.23 vectors and cloned, using the same restriction sites, into the pGL3-promoter vector. Constructs were sequenced to verify their identity and orientation in the pGL3-promoter vector.

4.3.6. *Cell Culture*

HEK293T/17, HCT116 and HepG2 cell lines were grown in high-glucose DMEM supplemented with 10% FBS, 100 units/mL of penicillin and 0.1 mg/mL of streptomycin. The MCF-7 cell line was grown in IMEM without phenol red, supplemented with 10% FBS, 100 units/mL of penicillin and 0.1 mg/mL of streptomycin. All cell lines were grown in a 5% CO_2 incubator at 37°C. To maintain cells, they were split upon reaching confluency by treatment with 0.05% Trypsin-EDTA, washing with 1X PBS and suspending in fresh media at a 1:5 to 1:20 dilution.

4.3.7. *Transient Transfections*

For transient transfections of the HEK293T/17, HepG2 and HCT116 cell lines, cells were seeded at approximately 1.8 x 10^4 cells per well of a 96-well plate in fresh

DMEM with 10% FBS, but without antibiotics, and grown for at least 24 hr to 80% confluency. Cells were then transfected with Lipofectamine 2000 following guidelines suggested in the manufacturer's protocol. In short, 0.5 μL of Lipofectamine 2000 was incubated in 25 μL Opti-Minimal Essential Medium (Opti-MEM) for 5 min and then gently mixed with a 25 μL solution of 0.08 μg construct (pGL4.23 [*luc2*/minP], Enhancer-pGL4.23 [*luc2*/minP], pGL3 promoter [*luc*+/SV40], Supressor-pGL3 promoter [*luc*+/SV40], APOE-pGL4.23 or pGL4.13 [*luc2*/SV40]) plus 0.02 μg pGL4.74 [*hRluc*/TK] diluted with Opti-MEM. The DNA-Lipofectamine mixture was allowed to incubate at room temperature for 30 min before being placed onto cells with fresh 50 μL of antibiotic-free media. MCF-7 cells were split with 0.05% Trypsin-EDTA and seeded at ~2.5 x 10^4 cells per well and transfected once they reached 95% confluency with the PolyJet™ DNA *In Vitro* Transfection Reagent; transfection efficiency was optimized by following the manufacturer's guidelines. Briefly, media on the cells were replaced with 100 μL fresh IMEM (supplemented with FBS and antibiotics as above) 30 min before transfection. A mix of 75 ng ABCG2 plasmid and 25 ng of pGL4.74 [*hRluc*/TK], to control for transfection efficiency, was diluted to 5 μL with IMEM supplemented with 10% FBS (no antibiotics). A 0.4 μL aliquot of PolyJet was diluted to 5 μL with IMEM supplemented with 10% FBS (no antibiotics) and then immediately added to the DNA mix with gentle mixing. The PolyJet/DNA mix was allowed to incubate at room temperature for 15 min before being added to the cells. All cell lines were incubated with their transfection reagents for 18-24 hr before assaying.

4.3.8. *Luciferase Assay*

The day after transfection, each well was washed with 100 µL 1X PBS before being lysed with 50 µL of 1X passive lysis buffer for 1 hr with shaking. Then 20 µL of HEK293T/17 or 30 µL of HepG2, HCT116 and MCF-7 lysates were measured for firefly and *Renilla* luciferase activity using 70 µL each of the Luciferase Assay Reagent II and Stop & Glo® reagents from the Dual-Luciferase® Reporter Assay System in a GloMax 96 microplate Dual Injector Luminometer. The firefly activity was normalized to the *Renilla* activity per well to control for transfection efficiency. Each experiment also included the empty pGL4.23 or pGL3-promoter vector as the negative control and the *APOE*-pGL4.23 or pGL4.13 vector as the positive control. The enhancer activity for each plasmid was calculated as the ratio of its normalized firefly activity to that of the empty vector.

4.3.9. *Hydrodynamic Tail Vein Injection*

Positive *in vitro* enhancer elements were screened for *in vivo* liver enhancer activity through the hydrodynamic tail vein injection[70] adapted for enhancer element screening[71] (see Figure 4.10). Each construct was injected into the tail vein of 4-5 mice using the TransIT EE *In Vivo* Gene Delivery System following the manufacturer's protocol. Briefly, 10 µg of pGL4.23 vector with or without enhancer element, or the *ApoE*[69] positive control liver enhancer, along with 2 µg of pGL4.74 were injected into the tail vein of CD1 mice. After 24 hr, mice were euthanized and their livers were harvested. Each liver was homogenized in 3 mL of 1X passive lysis buffer and then centrifuged at 4°C for 30 min at 14,000 rpm. The supernatant was diluted 1:20 with lysis buffer and measured for firefly and *Renilla* luciferase activity using the Dual-luciferase® reporter

assay system according to the manufacturer's protocol in a Synergy 2 (BioTek Instruments, Winooski, VT) microplate reader. Each sample lysate was read in replicate 3-6 times, with firefly activity normalized to the *Renilla* activity and then averaged across the replicates. The enhancer or ApoE normalized firefly activity was expressed as fold activation relative to pGL4.23. All mouse work was done following a protocol approved by the UCSF Institutional Animal Care and Use Committee.

4.3.10. *Data Mining and Retrieval from ENCODE*

The Encyclopedia of DNA Elements (ENCODE) consortium is constantly adding to the available data from a variety of assays and methods to identify functional regulatory elements in the genome[66]. Through the UCSC genome browser portal to the ENCODE data, information on the occupancy density of histone modifications for an enhancer region of the genome was extracted. Histone modifications associated with active regulatory elements (H3K27ac)[72] and general regulatory elements (H3K4me1)[72,73] were the focus of his analysis. Sensitivity of the DNA region to the DNaseI nuclease was also analyzed. DNaseI hypersensitivity sites are an indication of open chromatin around active genes[74], and they are also present when TFs bind and displace histones[46,75,76]. The last, and by far most extensive, ENCODE dataset that was mined was mapping of TFs bound to the genome through the ChIP-seq approach[77]. In addition to utilizing the TF ChIP-seq clustering from ENCODE to identify priority putative enhancer elements, additional ChIP-seq peaks for each of the positive *in vivo* enhancers were analyzed in order to get an idea of which TFs are binding to the enhancer element. There are five separate experiments of ENCODE ChIP-seq data available through the UCSC genome

browser, each named for the centers that did them: HAIB, SYDH, UChicago, UTA and UW. The strongest genome-wide peaks that are replicated are combined in the Txn Factor track[77]; the density of TFBS from this track was used in our initial weighting of putative enhancer elements. For further analysis of the positive *in vivo* enhancers, the density of TF signals in each of the ChIP-seq experiments for all available cell lines and TFs was analyzed. TFs that had strong signal density, in both replicates, for multiple cell lines and reported interesting findings in Figure 4.12-Figure 4.17 were of most interest. ENCODE data was accessed through the full or preview UCSC genome browser portal (http://genome.ucsc.edu/ENCODE). Data from this analysis is displayed as shaded density bars indicating both strength of signal for TF and histone association with the DNA region and degree of sensitivity of the DNA to DNaseI.

4.3.11. *Statistical Analysis*

Putative enhancer elements were considered to have statistically significant enhancer activity over the empty pGL4.23 vector activity if the ANOVA analysis, followed by a Bonferroni's multiple comparison *t*-test, had a $P < 0.05$ in each experiment (with 3-6 wells per plasmid) replication. Positive *in vitro* enhancer elements were chosen for follow-up *in vivo* testing when they had significant enhancer activity over the reference enhancer in two of the four cell lines. For analysis of *in vivo* results, normalized enhancer activity from 4 to 5 mice per plasmid was compared to the empty pGL4.23 vector using an ANOVA analysis followed by a Student's *t*-test. Constructs were considered positive *in vivo* if they had a $P < 0.05$. Constructs were chosen for *in vitro* suppressor follow-up in the pGL3-promoter vector if they exhibited luciferase activity

75% reduced from empty vector in one cell line and at least 50% reduced in an additional cell line. Results for suppressor luciferase assays were expressed as normalized reporter activity compared to the empty pGL3-promoter vector. Results from each transfection, with 5 to 10 wells per plasmid, were analyzed with an ANOVA followed by a Bonferroni's multiple comparison *t*-test to compare suppressor constructs to the empty pGL3-promoter vector with significance determined if $P < 0.05$. All statistics were run using the GraphPad Prism 5 software program.

4.4. Results

4.4.1. *Identification of High Priority Putative Enhancer Elements*

A multistep pipeline was developed to identify and then characterize putative regulatory elements of *ABCG2* (Figure 4.1). A list of over 100 putative enhancer elements was generated by the *in silico* analysis of the *ABCG2* gene locus (Step 1 of Figure 4.1). Different characteristics for these elements were compiled through the *in silico* analysis; Figure 4.2 is a snapshot of such features, including evolutionary conservation, predicted TF binding and ChIP-seq data with selected regions highlighted by red boxes. Regions were ranked and a list of high priority elements were selected based on evolutionary conservation (Figure 4.2A, Figure 4.2C and Figure 4.2D), the clustering of predicted *cis*-elements from Cister plot[64] (Figure 4.2E) and ChIP-seq data available from ENCODE[66] (Figure 4.2B) and TRANSFAC[65] databases. A list of 30 high priority elements was generated (Table 4.5 and Figure 4.3), and these regions were cloned into pGL4.23 [*luc2*/minP] for *in vitro* screening. None of the high priority elements fulfilled the criteria of being 'core' ECRs, core ECRs have been previously

defined as > 350 bp and > 77% conservation and are associated with developmental enhancers[78]. There were five regions that appeared in both the evolutionary conservation and Cister plot analyses, all of which were ranked in the top thirty. Three regions, ECR31, ECR33 and ECR52 had preliminary ChIP-seq data from ENCODE and were also ranked in the top thirty. The high priority putative enhancer elements were evenly distributed across the *ABCG2* gene locus and their relative sizes and locations are depicted in Figure 4.3.

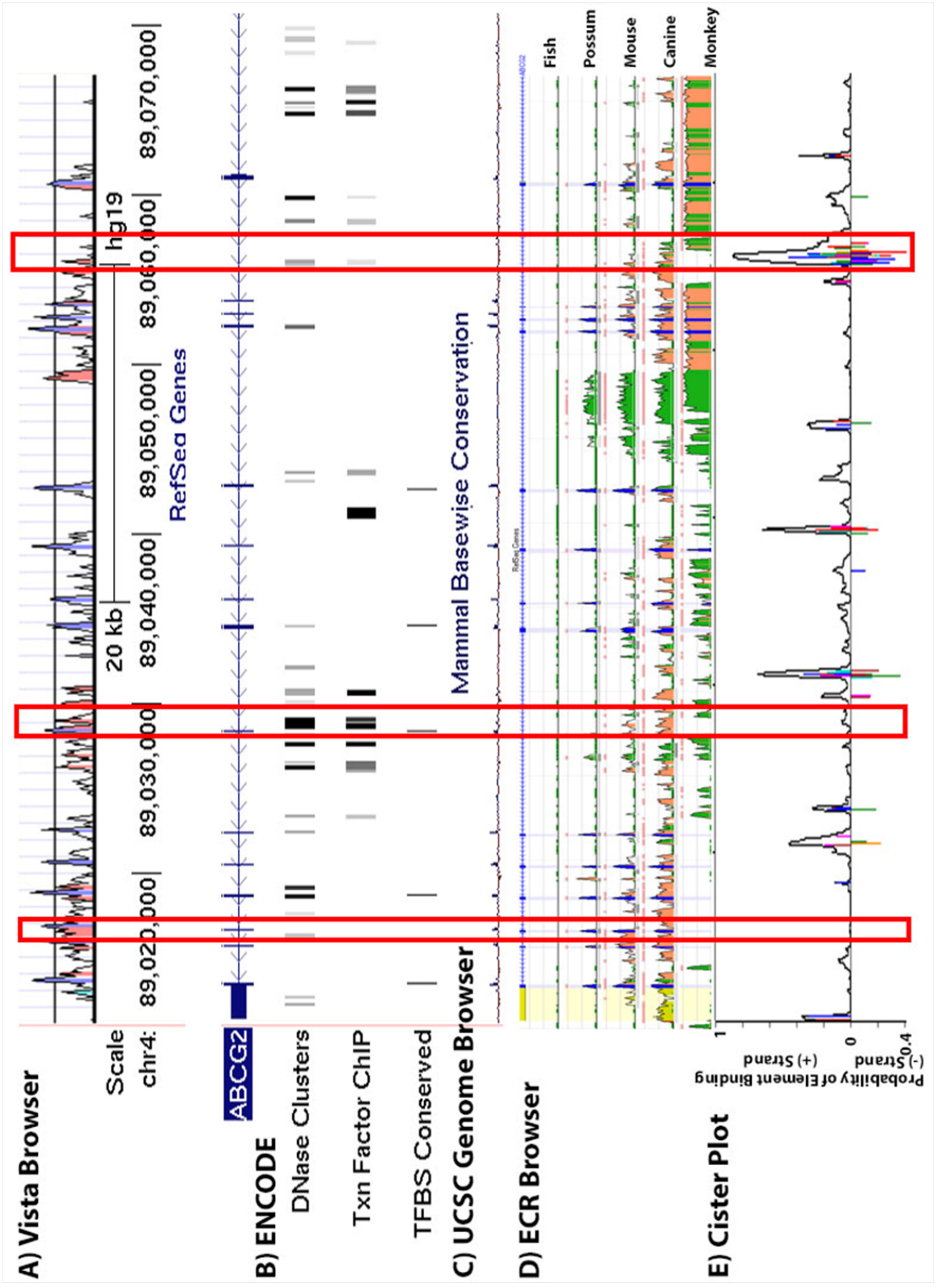
A) Vista Browser
Scale
chr4:
89,020,000
89,030,000
20 kb
89,040,000
89,050,000
89,060,000
89,070,000
hg19
RefSeq Genes
B) ENCODE
ABCG2
DNase Clusters
Txn Factor ChIP
TFBS Conserved
C) UCSC Genome Browser
Mammal Basewise Conservation
D) ECR Browser
Fish
Possum
Mouse
Canine
Monkey
E) Cister Plot
Probability of Element Binding
(-) Strand
(+) Strand
1
0.4
0

Figure 4.2. Snapshot from *ABCG2* locus illustrating representative results from bioinformatic analyses. Red boxes indicate high priority putative ECR regions that were chosen for further study based on conservation as determined by the Vista Browser (A), UCSC genome browser mammal base wise conservation (C) or ECR browser conservation to fish, possum, mouse, canine and monkey (D). Regions were also chosen based on clusters of TF elements with a probability of binding >0.7 as determined by Cister plot (E) and overlap of these regions with ENCODE DNaseI, ChIP-seq and conserved TFBS data (B).

Table 4.5. High Priority Putative Enhancer Regions

Rank	Region	Genomic position[1] hg18	Genomic position[1] hg19	Length
1	ECR425	89409846-89411754	89190822-89192730	1909
2	CR8	89286463-89287815	89067439-89068791	1353
3	ECR423	89408527-89409482	89189503-89190458	956
4	CR9	89302387-89303223	89083363-89084199	837
5	ECR402	89157927-89159110	88938903-88940086	1184
6	CR19	89382285-89383439	89163261-89164415	1155
7	ECR410	89197061-89198542	88978037-88979518	1482
8	ECR400	89142824-89143421	88923800-88924397	598
9	CR10	89307110-89308272	89088086-89089248	1163
10	ECR420	89345102-89346322	89126078-89127298	1221
11	CR7	89275033-89276418	89056009-89057394	1386
12	ECR412	89207879-89208759	88988855-88989735	881
13	ECR25	89234523-89235960	89015499-89016936	1438
14	ECR48	89336705-89336930	89117681-89117906	226
15	ECR429	89430870-89431792	89211846-89212768	923
16	CR15	89331014-89332546	89111990-89113522	1533
17	ECR426	89416468-89417157	89197444-89198133	690
18	ECR17	89190442-89190705	88971418-88971681	264
19	CR16	89333859-89334917	89114835-89115893	1059
20	ECR428	89418093-89419430	89199069-89200406	1338
21	ECR401	89147687-89148807	88928663-88929783	1121
22	ECR38	89271364-89272357	89052340-89053333	994
23	ECR44	89292195-89292446	89073171-89073422	251
24	ECR52	89346636-89346901	89127612-89127877	266
25	CR6	89229977-89230503	89010953-89011479	527
26	ECR55	89363840-89364013	89144816-89144989	174
27	ECR43	89281134-89281346	89062110-89062322	213
28	ECR31	89244906-89245725	89025882-89026701	819
29	ECR54	89352017-89352661	89132993-89133637	644
30	ECR33	89247461-89248430	89028437-89029406	969

[1]Genomic location on Chromosome 4

Abbreviations: ECR, Evolutionarily Conserved Region; CR, Cister Region

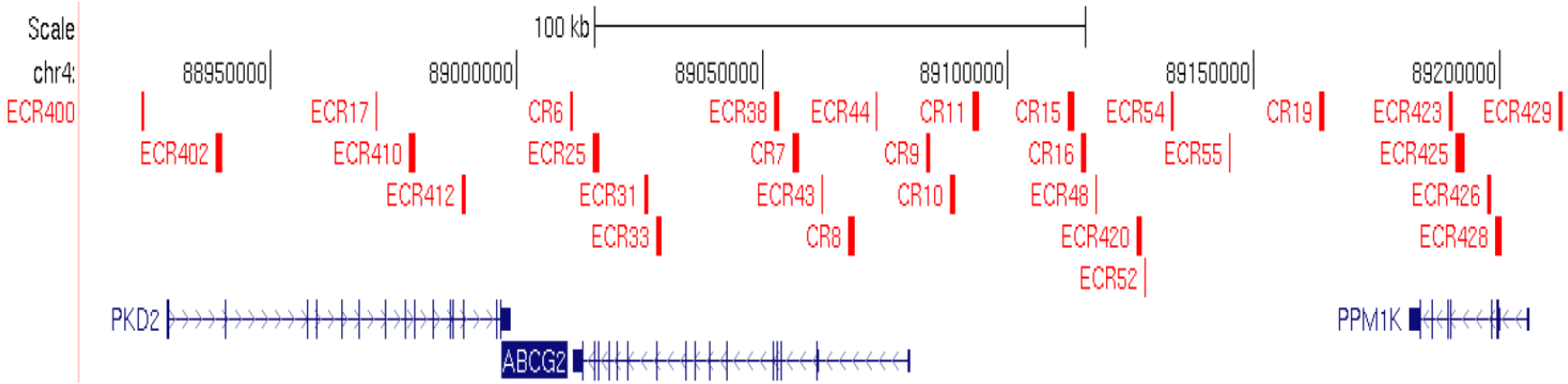

Figure 4.3. Genomic representation of 30 high priority putative *ABCG2* enhancer regions. The genome sequence runs 3' to 5' from left to right. *ABCG2* is on the anti-strand flanked by *PKD2* and *PPMIK* (also on the anti-strand). Putative enhancer regions are denoted by a red box indicating their size and location.

4.4.2. *System Controls*

For the second step of the enhancer discovery pipeline (Figure 4.1 Step 2), high priority putative enhancer regions were cloned into pGL4.23 [*luc2*/minP]. The pGL4.23 vector is a luciferase expression vector with only a minimal promoter before the luciferase gene. Thus the luciferase gene is only transcribed when an enhancer element is placed upstream, and the activity of the luciferase gene can be used as a marker of enhancer activity. The putative enhancer constructs were transiently transfected into four cell lines to test for their *in vitro* enhancer activity; top *in vitro* enhancers were then injected into the tail vein of mice for quantification of their *in vivo* enhancer activity. Putative enhancer elements displaying suppressor characteristics in pGL4.23 were cloned into the pGL3-promoter vector to be tested for suppressor activity. For all *in vitro* and *in vivo* luciferase experiments an empty vector (either pGL4.23 or pGL3-promoter) was also transfected as a baseline marker for luciferase activity. The normalized luciferase activity for the empty vector was set at 1.0 in all experiments (see white bars in Figure 4.4). The experimental set up for screening the *in vitro* enhancers was validated using two different controls. The first is the pGL4.13 [*luc2*/SV40] vector which has the SV40 early enhancer driving the expression of the luciferase gene. This construct was an excessively strong enhancer in all four cell lines ranging from ~100- to ~4000-fold activation relative to pGL4.23 (checkered bars in Figure 4.4). The second positive control for the *in vitro* assay, which was also the positive control for the *in vivo* tail vein luciferase assay, was a pGL4.23 construct with the *ApoE* liver specific enhancer[69]. This construct exhibited selected enhancer activity depending upon the cell line. The *ApoE* enhancer had strong activity in HepG2 and MCF-7 cells, no enhancer activity in HEK293T and HCT116 cells

and strong enhancer activity *in vivo* (grey bars Figure 4.4). These results indicate that the *in vitro* and *in vivo* luciferase assay systems are capable of finding global enhancers as well as identifying possible liver-specific tissue enhancers.

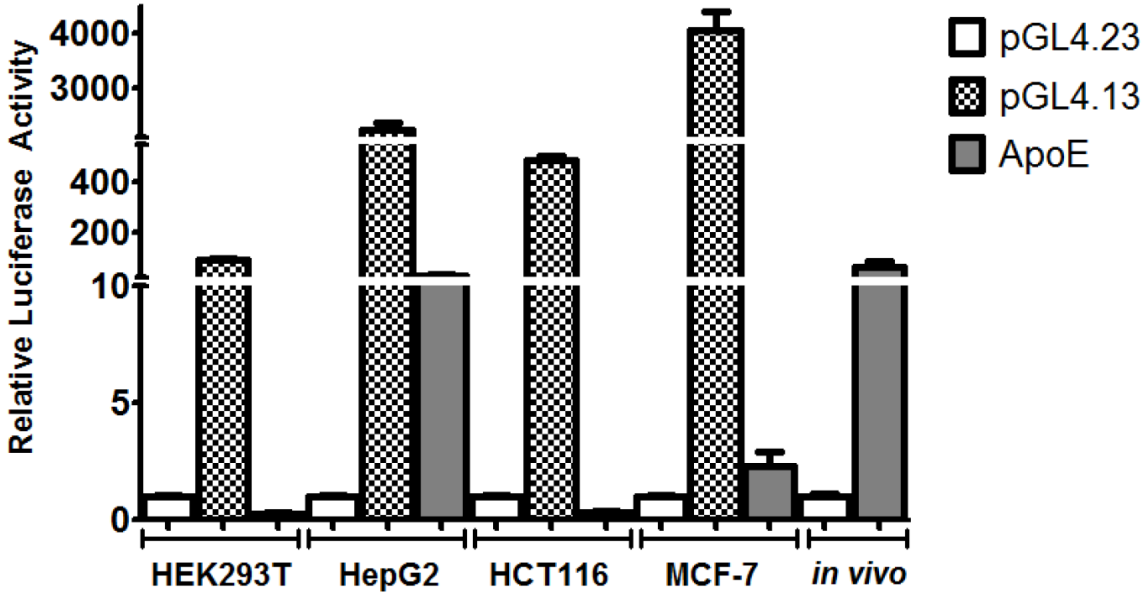

Figure 4.4. System controls for the *in vitro* and *in vivo* luciferase enhancer assay. Luciferase activity of the empty vector pGL4.23 (white), global positive control vector pGL4.13 (checkered) and liver-specific positive control *ApoE* (grey) was measured in transiently transfected kidney (HEK293T), liver (HepG2), intestine (HCT116) and breast (MCF-7) cell lines. The activity of the empty pGL4.23 (white) and ApoE (grey) controls were also determined *in vivo* and their luciferase activity is represented by the last two bars on the right. Enhancer activity is expressed as the ratio of the firefly to *Renilla* luciferase activity normalized to the empty vector activity. Data is expressed as the mean ± SEM of one representative experiment (N=3-6 wells per plasmid).

4.4.3. *In Vitro Enhancers*

The thirty high priority putative enhancer elements (listed in Table 4.2) were transiently transfected into HEK293T (Figure 4.5), HepG2 (Figure 4.6), HCT116 (Figure 4.7) and MCF-7 (Figure 4.8) cell lines and their luciferase activity quantified relative to empty vector. The HEK293T cells had both the highest number of positive enhancer elements and the highest activity of putative enhancer elements, with regions such as CR6, ECR31 and ECR44 showing 32-, 16- and 6-fold activation relative to empty vector (Figure 4.5). There were five more regions with significant enhancer activity in HEK293T cells: ECR400, ECR38, ECR52, ECR423 and ECR429. HepG2 cells had six enhancer regions, of which CR6 had the highest activity with >12-fold activation over empty vector. The other five enhancers, ECR402, ECR33, ECR44, ECR52 and ECR423, ranged from 2-4 fold activation (Figure 4.6). In HCT116 cells, only five enhancer elements were active, the least of any of the tested cells lines (Figure 4.7). The enhancer activity of CR6 in HCT116 cells was >14-fold, and ECR400, ECR31, ECR33 and ECR44, ranged from 1.8- to 3- fold activation. Six putative enhancer regions showed positive activity in MCF-7 cells, although relative enhancer activity was lower than in the other cell lines (Figure 4.8). ECR400, CR6, ECR31, ECR44, ECR52 and CR19 had enhancer activities ranging from 1.8- to 3.5-fold activation in MCF-7 cells (Figure 4.8).

Collective data across all of the cell lines was taken into consideration for selection of enhancer regions for *in vivo* follow-up. For simplification, enhancers were binned according to their ‘strong’ (4-fold and above activation), moderate (2- to 4-fold activation) and weak (1.5- to 2-fold activation) enhancer activities. The strong and most reproducible enhancer element was CR6. It was a strong enhancer element in all four cell

lines, with up to 32-fold increase relative to empty vector. The next most reproducible enhancer element was ECR44; it had strong enhancer activity in HEK293T cells and moderate enhancer activity in the other three cell lines. ECR31 had over a 16-fold activation in HEK293T cells, was a moderate enhancer in HCT116 cells and a weak enhancer in MCF-7s. Two more regions had enhancer activity in three of the four cells lines: ECR52 was a moderate enhancer in both HEK293T and HepG2 cells and a weak enhancer in MCF-7 cells, while ECR400 had moderate activity in MCF-7 cells and weak activity in both HEK293T and HCT116 cell lines. Two regions had enhancer activity in two of the four cell lines: ECR33 was a moderate enhancer in HepG2 cells and a weak enhancer in HCT116 cells, whereas ECR423 had moderate enhancer activity in both HEK293T and HCT116 cell lines. Finally, three regions had enhancer activity in only one of the four cells lines: CR19 was a moderate enhancer in MCF-7 cells, ECR429 was a weak enhancer in HEK293T cells and ECR402 was a weak enhancer in HepG2 cells. All elements that had significant enhancer activity in at least one cell line, except for ECR402, were followed up *in vivo*. The ECR402 was not included in the *in vivo* follow-up because its enhancer activity in the HepG2 cells was barely significant ($P = 0.05$) and not over 1.5-fold. The other two regions that were significant in only one cell line both had activities over 1.8-fold above empty vector.

The pGL4.23 vector has very little basal luciferase activity. However, it can still be useful to obtain a sense of which regions might have suppressive qualities. Regions that had at least 50% reduction in activity for all cell lines (relative to empty pGL4.23), along with one region with suppressive activity in two cell lines, were cloned into the pGL3-promoter [*luc*+/SV40] vector. The pGL3-promoter vector has a much higher basal

transcription of luciferase and is thus a better system to screen regions for suppressor activity. Of the thirty regions analyzed in the enhancer screen, seven (ECR410, ECR17, CR7, CR11, CR15, ECR43 and ECR425) had a 50% decrease in luciferase activity in all four cell lines. All of these, except ECR43, CR11 and CR15, were followed up for suppressor activity in the pGL3-promoter. Three enhancer regions (ECR25, CR16 and ECR428) showed a 75% decrease in three cell lines and 50% in the fourth. All three of these regions were chosen for suppressor follow-up. The final construct chosen for suppressor follow-up was ECR429, which was only suppressive in HepG2 and HCT116 cells. It was chosen for follow-up over other suppressor regions because it had significant enhancer activity in HEK293T and slight activity in MCF-7 cells (although it did not reach significance), suggesting the possibility of finding elements with tissue specific enhancer or suppressor activity.

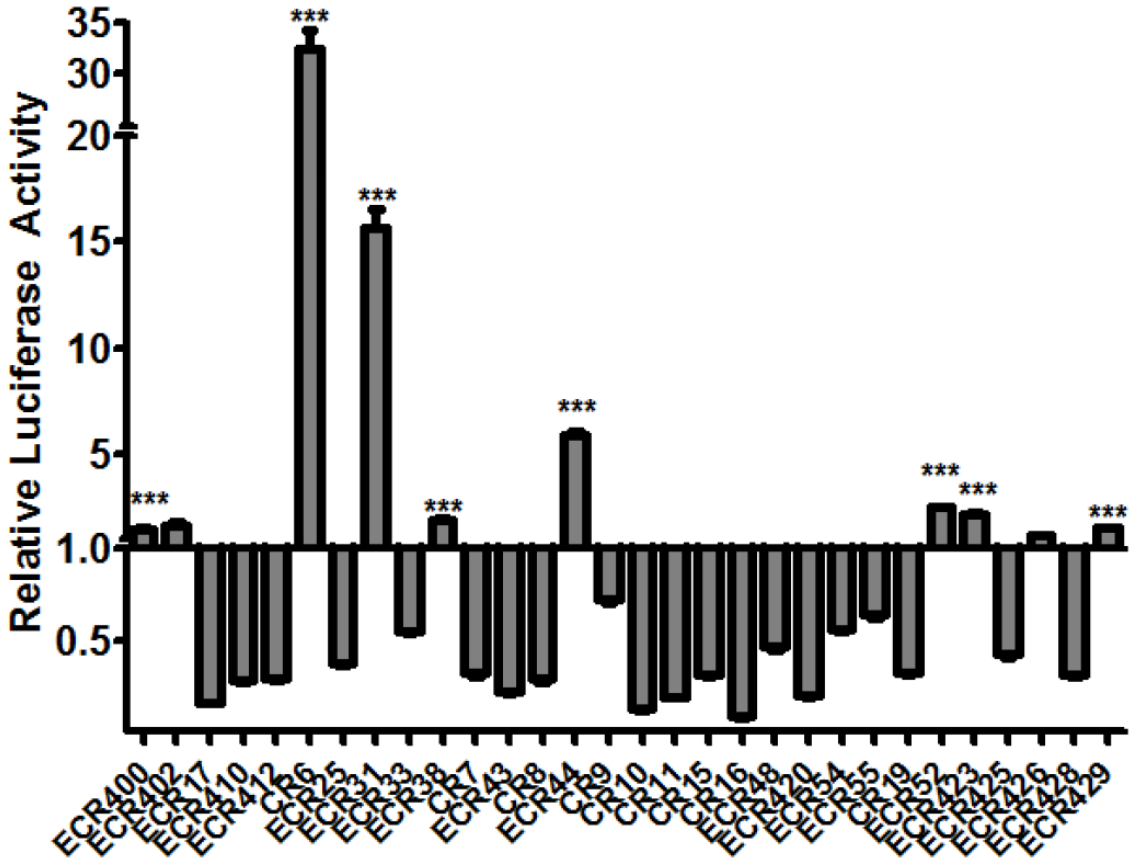

Figure 4.5. Activity of putative enhancer elements in HEK293T cells. Luciferase activity was measured in the transiently transfected kidney (HEK293T) cell line. Enhancer activity is expressed as the ratio of firefly to *Renilla* luciferase activity normalized to the empty vector (pGL4.23) activity. ECRs are displayed respective to their genomic orientation. Data is expressed as the mean ± SEM from a representative experiment (n = 6 wells per construct). Differences between enhancer elements and empty vector were tested by an ANOVA followed by a post-hoc Bonferonni's multiple comparison *t*-test; *** $P < 0.0001$.

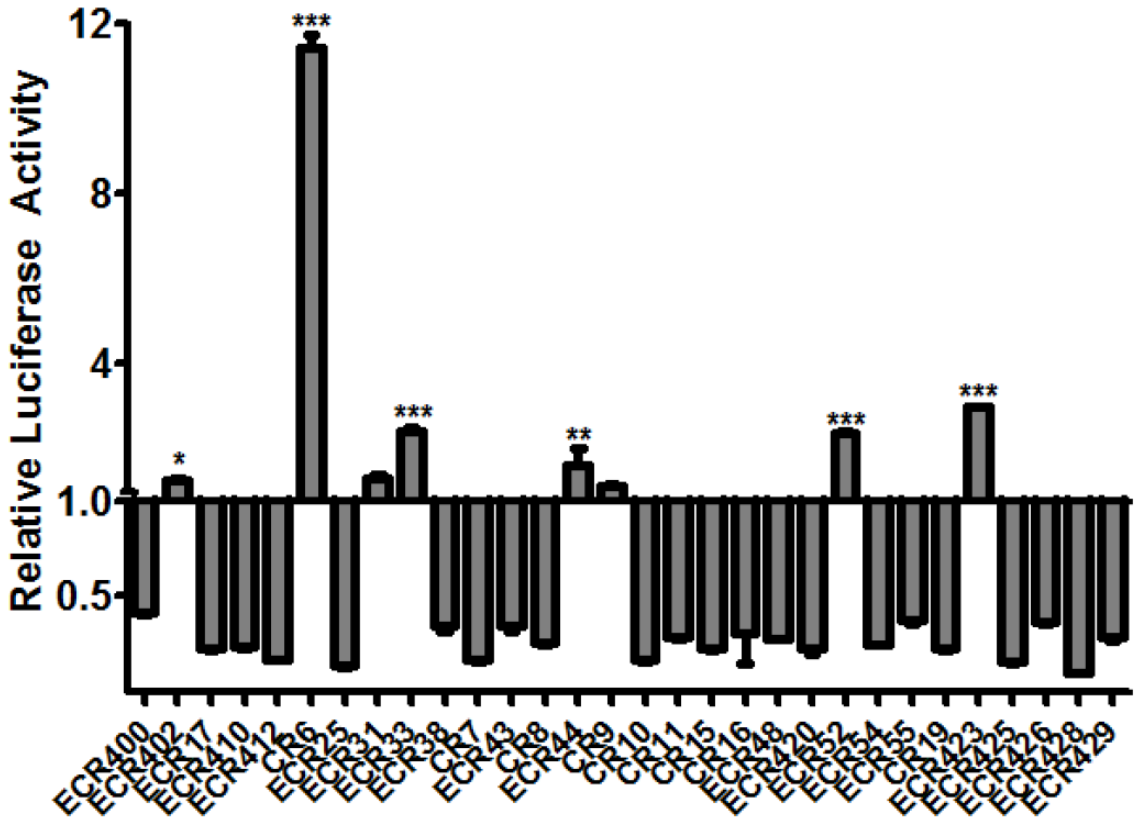

Figure 4.6. Activity of putative enhancer elements in HepG2 cells. Luciferase activity was measured in the transiently transfected liver (HepG2) cell line. Enhancer activity is expressed as the ratio of firefly to *Renilla* luciferase activity normalized to the empty vector activity (pGL4.23). ECRs are displayed respective to their genomic orientation. Data is expressed as the mean ± SEM from a representative experiment (n = 3 wells per construct). Differences between enhancer elements and empty vector were tested by an ANOVA followed by a post-hoc Bonferonni's multiple comparison *t*-test; *** $P < 0.0001$, ** $P < 0.001$, * $P < 0.05$.

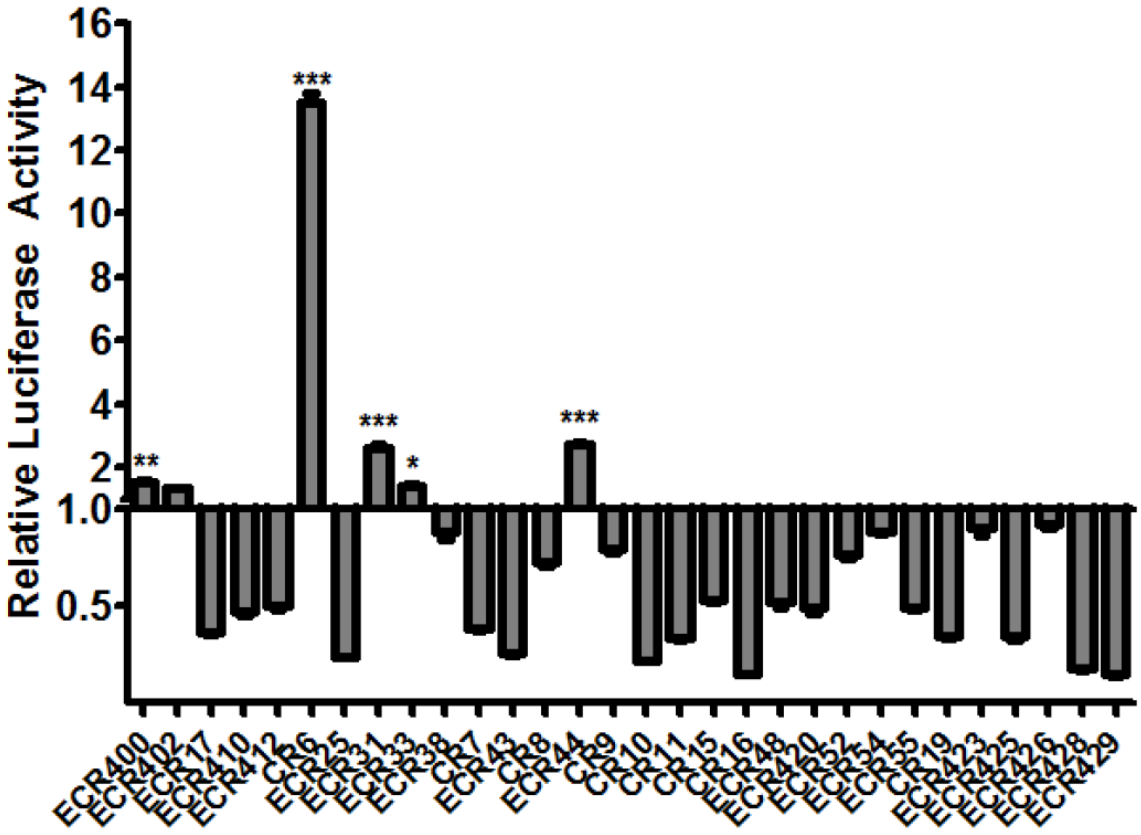

Figure 4.7. Activity of putative enhancer elements in HCT116 cells. Luciferase activity was measured in the transiently transfected intestine (HCT116) cell line. Enhancer activity is expressed as the ratio of firefly to *Renilla* luciferase activity normalized to the empty vector activity (pGL4.23). ECRs are displayed respective to their genomic orientation. Data is expressed as the mean ± SEM from a representative experiment (n = 6 wells per construct). Differences between enhancer elements and empty vector were tested by an ANOVA followed by a post-hoc Bonferonni's multiple comparison *t*-test; *** $P < 0.0001$, ** $P < 0.001$, * $P < 0.05$.

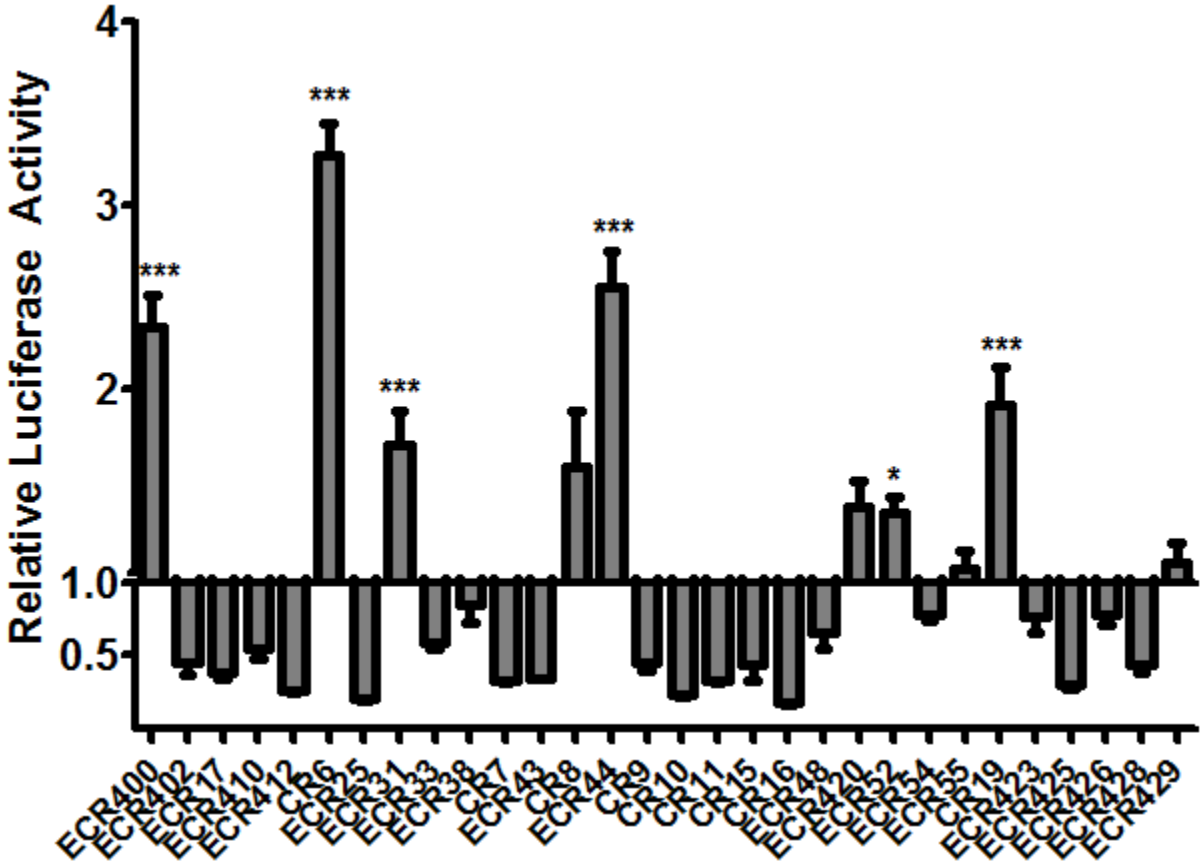

Figure 4.8. Activity of putative enhancer elements in MCF-7 cells. Luciferase activity was measured in the transiently transfected breast (MCF-7) cell line. Enhancer activity is expressed as the ratio of firefly to *Renilla* luciferase activity normalized to the empty vector activity (pGL4.23). ECRs are displayed respective to their genomic orientation. Data is expressed as the mean ± SEM from a representative experiment (n = 6 wells per construct). Differences between enhancer elements and empty vector were tested by an ANOVA followed by a post-hoc Bonferonni's multiple comparison *t*-test; *** $P < 0.0001$, * $P < 0.05$.

4.4.4. *In Vitro Suppressors*

Suppressor activity of ten regions was determined by cloning them into the pGL3-promoter vector, transiently transfecting them into four cell lines and measuring the resulting luciferase activity relative to empty vector. The strongest and most consistent suppressor was ECR25 (Figure 4.9). It had >75% decrease in luciferase activity in both HepG2 (Figure 4.9A) and HCT116 (Figure 4.9C), and a 50% decrease in HEK293T (Figure 4.9B) and MCF-7 (Figure 4.9D) cells. ECR25 was the only significant suppressor in the HEK293T cell line (Figure 4.9B). Three elements: ECR428, CR7 and ECR429 had significantly decreased luciferase activity in the HepG2 (Figure 4.9A) and HCT116 (Figure 4.9C) cell lines. ECR412 luciferase activity was significantly decreased in both the HCT116 (Figure 4.9C) and MCF-7 (Figure 4.9D) cell lines. ECR412 and ECR25 were the only two suppressors in the MCF-7 (Figure 4.9D) cell line. The last two elements with suppressor activity, CR10 and ECR425, were only significant in the HCT116 (Figure 4.9C) cell line. ECR429 had 2-fold increase in activity in both HEK293 and MCF-7 cells, the same cells it was an enhancer in with the pGL4.23 screen, and 50% decreased activity in the HEK293T and HCT116 cell lines.

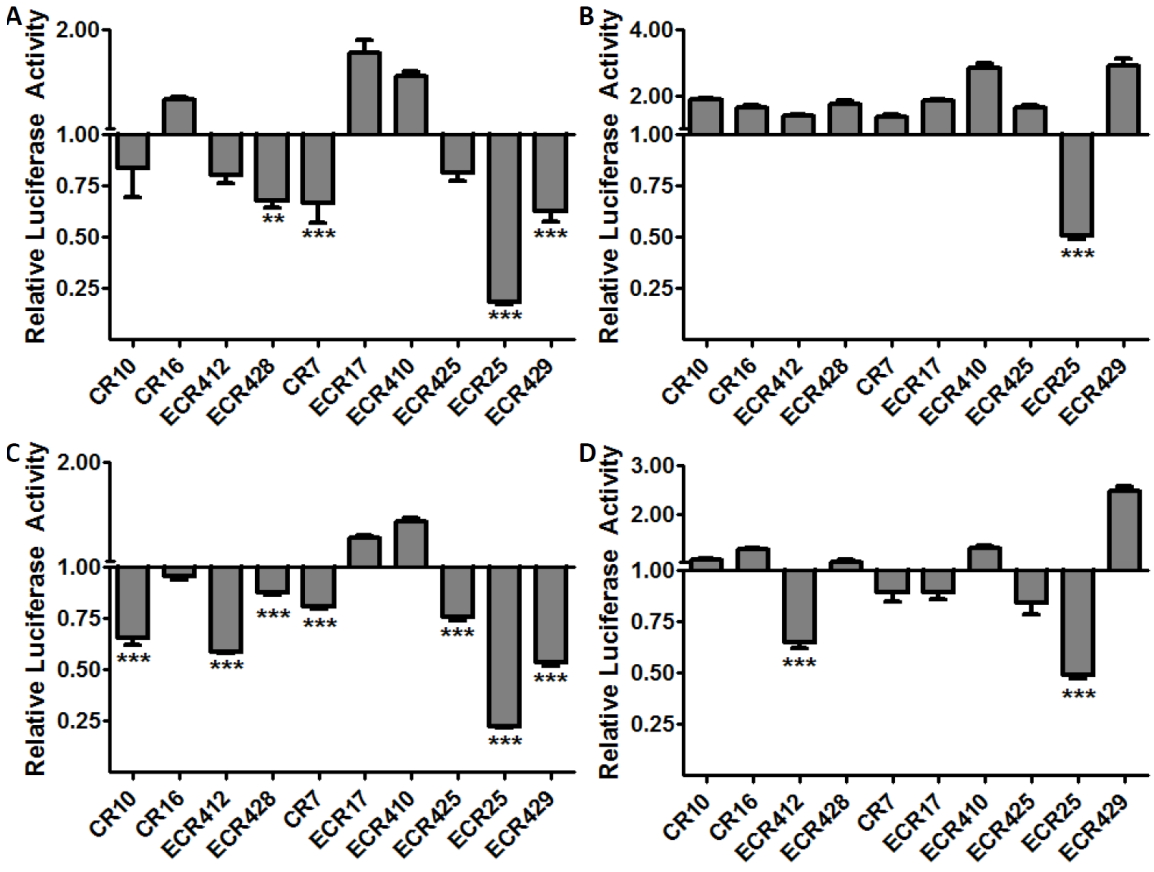

Figure 4.9. Activity of putative suppressor elements *in vitro.* Luciferase activity of selected regions cloned into the pGL3-promoter vector and transiently transfected into A) liver (HepG2), B) kidney (HEK293T), C) intestinal (HCT116) and D) breast (MCF-7) cell lines. Suppressor activity is expressed as the ratio of firefly to *Renilla* luciferase activity normalized to the empty vector activity (pGL3-promoter). Data is expressed as the mean ± SEM from a representative experiment (n = 5-10 wells per construct). Differences between suppressor elements and empty vector were tested by an ANOVA followed by a post-hoc Bonferonni's multiple comparison *t*-test; *** $P < 0.0001$, * $P < 0.05$.

4.4.5. *In Vivo Enhancers*

Nine of the *in vitro* enhancers were selected for *in vivo* validation using the hydrodynamic tail vein injection technique (Figure 4.10). In this technique, naked DNA is injected quickly into the tail vein of the mouse, which due to overload of the heart, causes hepatocytes to take up the DNA[70,79]. At some point after injection, the liver of the mice is extracted and the hepatic lysate luciferase activity is measured. The positive control for this assay was the *ApoE* liver-specific enhancer in the pGL4.23 vector, previously shown to be a strong enhancer *in vivo*[69] and an effective control for the hydrodynamic tail vein injection[80]. This enhancer gave consistently strong enhancer activity, with over 40-fold activation, confirming that the tail vein injection assay was working (Figure 4.11). Of the nine enhancer elements tested *in vivo*, six of them had significant enhancer activity (Figure 4.11), giving a 67% rate of successful *in vivo* activity when picking enhancers based on *in vitro* enhancer activity in four separate cell lines. The CR6 construct had the lowest significant enhancer activity *in vivo*, barely reaching 1.8-fold activation. The next four strongest enhancers, ECR31, ECR33, ECR44 and ECR423, all had enhancer activity ranging from 5- to 12- fold relative activation. The strongest enhancer was the ECR400 region; it had consistent activation over 120-fold relative to empty vector, which is almost three times that of the positive *ApoE* control. The strong *in vivo* enhancer capabilities of these regions lead to the question of whether SNPs within these regions alter their enhancer capabilities.

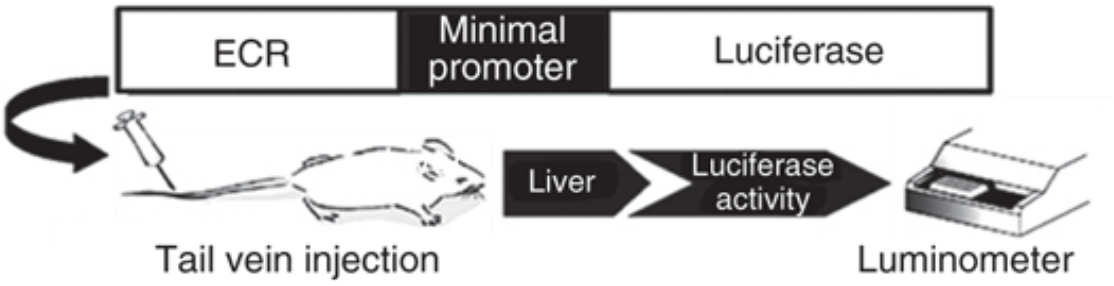

Figure 4.10. Schematic of the *in vivo* hydrodynamic tail vein injection assay. DNA sequences with *in vitro* enhancer activity are injected into the tail vein of a mouse with a large volume of water (10% of mouse weight) over a short time (5-8 seconds). Relative luciferase activity is measured in liver homogenates 24 hr post injection, image is reproduced from Kim, *et al.* 2011[80].

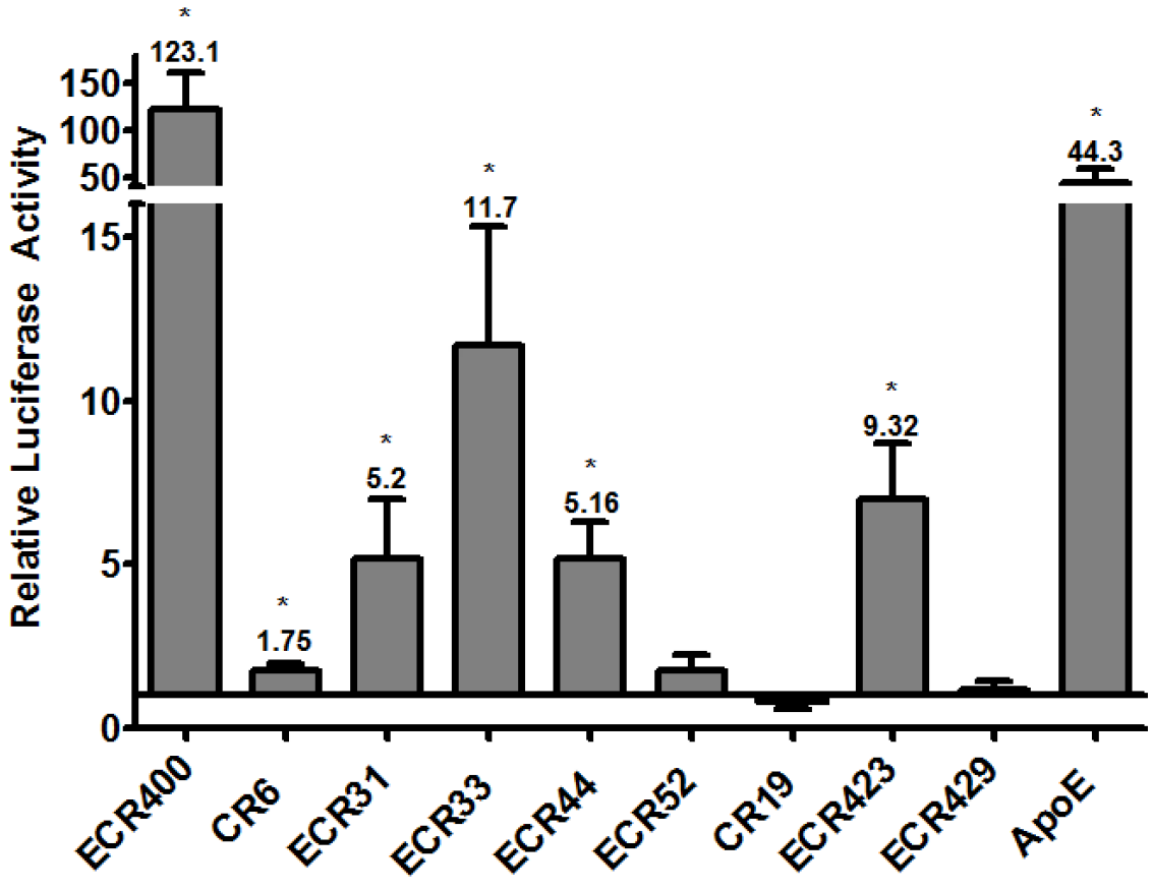

Figure 4.11. *In vivo* liver enhancer activity in mice. Luciferase activity in liver homogenates was measured 24 hr after plasmid injection. Enhancer activity is expressed as the ratio of the firefly to *Renilla* luciferase activity normalized to the empty vector activity (pGL4.23). Data is expressed as the mean ± SEM for 4-5 mice. Differences between enhancer elements and empty vector were tested by an unpaired Student's *t*-test; * $P < 0.05$. The *ApoE* construct was injected as a positive control liver specific enhancer[69].

4.4.6. *Predicted Functional Elements of the In Vivo Enhancers*

The association of the positive *in vivo* enhancers with markers of regulatory elements was examined using the UCSC genome browser (http://genome.ucsc.edu/) and

ENCODE[66] database. The ECR400 enhancer was highly sensitive to DNaseI in multiple cell lines and in CD34- maturating myeloid cells, but not in CD34+ hematopoietic stem cells (Figure 4.12). There are three conserved TFBS in ECR400: Oct1, MIF1 and RFX (Figure 4.12). The only TF that had consistent signal peaks in the ENCODE ChIP-seq data for ECR400 was CTCF; it was present in several cell lines including the MCF-7 and HepG2 cell lines (Figure 4.12). In contrast, the CR6 enhancer had no hypersensitivity to DNaseI, but it did have several dense ChIP-seq peaks, particularly in the center of the region (Figure 4.13). The ChIP-seq signal peaks in the CR6 enhancer region include CEBPB, CREB1, E2F6, Max, USF1, TEAD4, PML, SRF, FOSL2, NFIC, p300, CTCF and Egr-1 (Figure 4.13).

The two enhancers with the most functional markers were ECR31 (Figure 4.14) and ECR33 (Figure 4.15). The ECR31 enhancer region was associated with both H3K27ac and H3K4me1 histone markers; it was also very sensitive to DNaseI in over 100 cell lines (Figure 4.14). Additionally, there were many dense ChIP-seq peaks in the ECR31 region (Figure 4.14). TFs that mapped to ECR31 include GATA-2 and -3, AP-2γ, AP-2α, p300, c-Fos, JunD, c-Jun, CEBPB, PRDM1 and FOXA1 (Figure 4.14). Several of these TFs, including AP-2γ, AP-2α, JunD, c-Jun and CEBPB were in the HepG2 cell line. The ECR33 enhancer also had extensive transcriptional marker associations including strong H3K4me1 markers, heavy DNaseI sensitivity clusters and many TF ChIP-seq peaks (Figure 4.15). TFs bound to the ECR33 region are p300, Pol2, FOXA1, TBP, ELF1, FOSL2, HEY1, TCF4, FOXA2, HNF4α, GR, HDAC2, CEBPB, RXRα, c-Jun, JunD, MafF and MafK. Interestingly, GR was bound to the ECR33 region in A549 cells when they were treated with increasing concentrations of dexamethasone. Also, CEBPB

was bound to ECR33 in both untreated HepG2 and after forskolin treatment. Additional ChIP-seq signal peaks occurred for GATA3 and Max in MCF-7 and HCT116 cell lines (Figure 4.15).

The last two enhancer regions ECR44 and ECR423 had considerably fewer markers of functional transcription as compared to ECR31 and ECR33. The ECR44 enhancer region, located in intron 1 of *ABCG2*, had both histone and TFs markers associated with it (Figure 4.16). Moderate peaks for H3K27ac and weak peaks for H3K4me1 markers were located over the ECR44 enhancer (Figure 4.16). TFs with dense signal peaks in the ECR44 region included CREB1, CEBPB, GATA3, Max, NRF2, p300, TAF1, ATF3 and JunD. Several of these TFs, such as Max and CEBPB were in the MCF-7 and HCT116 cell lines (Figure 4.16). The ECR423 enhancer region, located over an exon of PPM1K, was also associated with H3K27ac and H3K4me1 markers, but it was not sensitive to DNaseI (Figure 4.17). Additionally it had ChIP-seq signal peaks for TFs including CREB1, CEBPB, Max, NRF2, p300, FOSL2 and SRF (Figure 4.17).

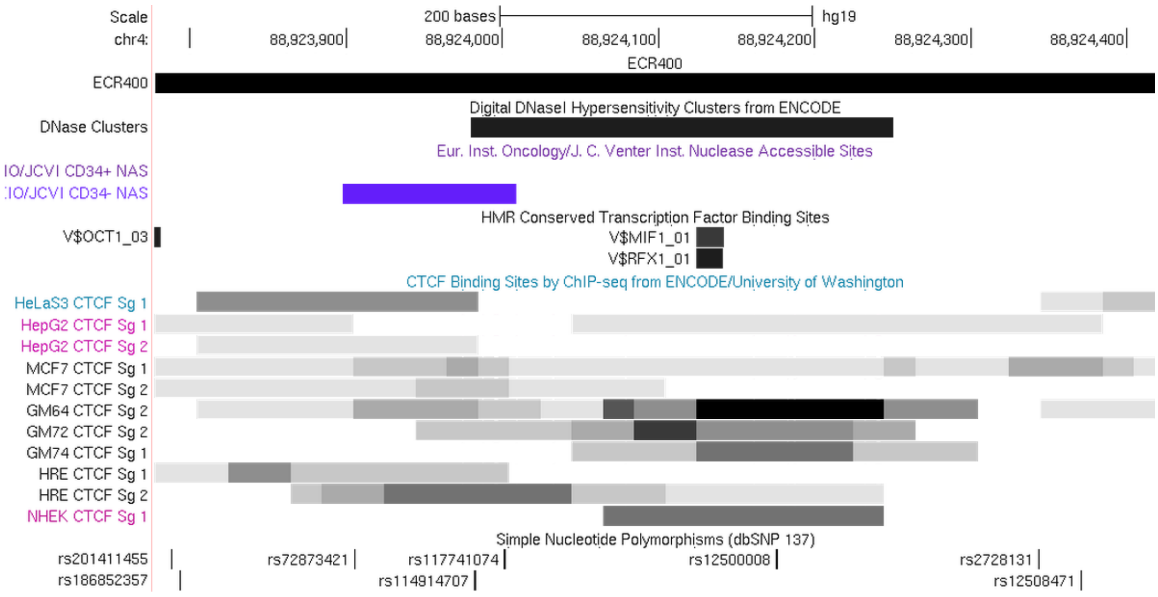

Figure 4.12. ENCODE data in ECR400. From top to bottom: the genomic coordinates (chr4:88923800-88924397; hg19) followed by a black bar indicating the area covered by the ECR400 enhancer. This is followed by a density bar indicating the accessibility of the DNA to DNaseI from all cell types (black shaded bar) and then in CD34+/- cells (blue bar). Next are the locations of three conserved TFBs as determined by rVista. Following this is the DNA occupancy of the CTCF TF as determined by ChIP-seq. Each cell line is on its own line followed by a bar, with the length indicating the breadth of the peak and the shading density indicating its strength. Finally, black lines indicate locations with associated rs numbers for the SNPs reported in dbSNP 137. Schematic was made using the UCSC genome preview browser.

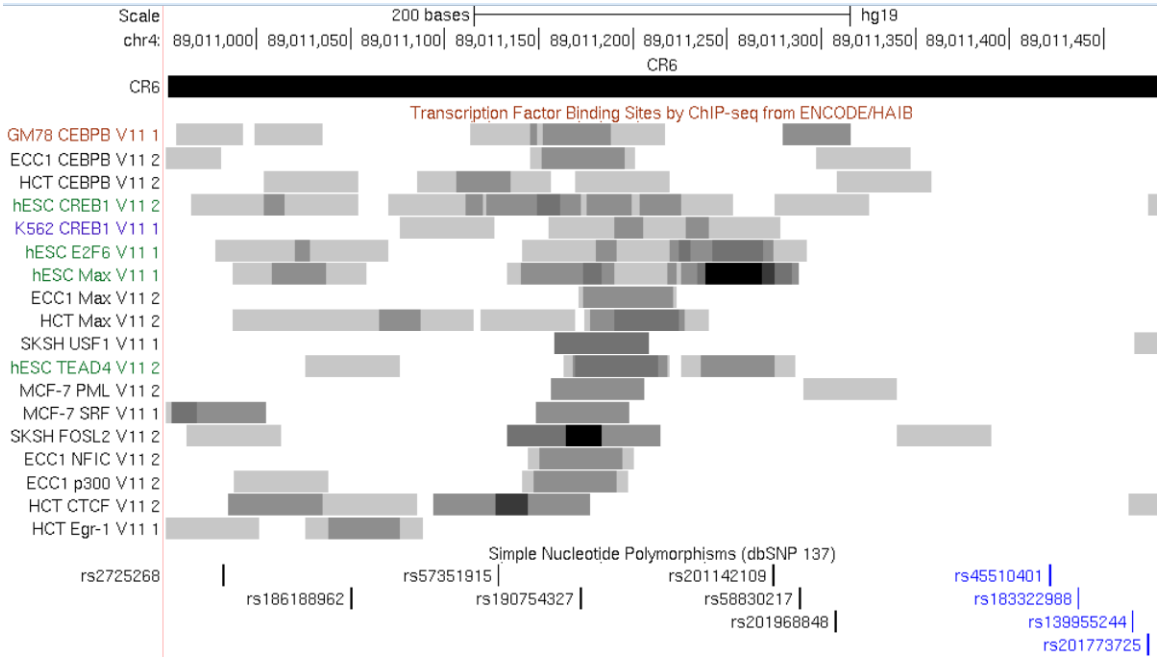

Figure 4.13. ENCODE data in CR6. From top to bottom: the genomic coordinates (chr4:89010953-89011479; hg19) followed by a black bar to indicating the area covered by the CR6 enhancer. Following this is the DNA occupancy of several transcription TFs as determined by ChIP-seq. Representative cell lines for each TF are grouped together, with the length indicating the breadth of the peak and the shading density indicating its strength. Cell lines include GM12878 (GM78), ECC1, HCT116 (HCT), H1-hESC (hESC), SK-N-SH (SKSH), and MCF-7. Finally, black lines indicate locations with associated rs numbers for the SNPs reported in dbSNP 137, blue SNPs indicate those in the 3'UTR of *ABCG2*. Schematic was made using the UCSC genome preview browser.

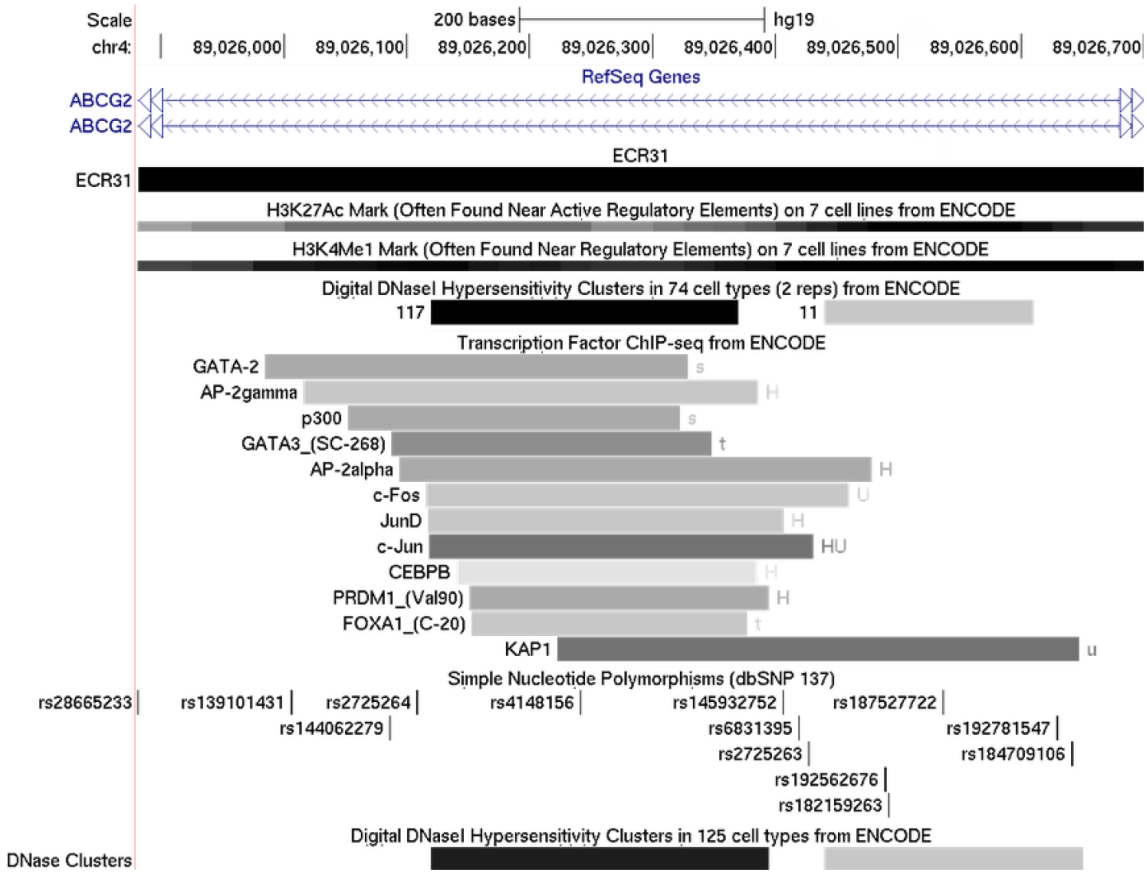

Figure 4.14. ENCODE data in ECR31. From top to bottom: the genomic coordinates (chr4:89025882-89026701; hg19), blue hatched lines indicating intron 10 of *ABCG2* and then black boxes indicating the area covered by the ECR31 enhancer. These are followed by density bars indicating the DNA occupancy of H3K27ac and H3K4me1, and the accessibility of the DNA to DNaseI in all cell types. Next is ChIP-seq data from the combined TxN ChIP-seq ENCODE data, with each TF on its own line followed by a bar, with the length indicating the breadth of the peak and the shading indicating its strength. Each bar is followed by letters to indicate the cell line the signal was found in: H, HeLa-S3; U, HUVEC; s, SH-SY5Y; t, T-47D; u, U2OS. Finally, black lines indicate locations with associated rs numbers for the SNPs reported in dbSNP 137. Schematic was made using the UCSC genome preview browser.

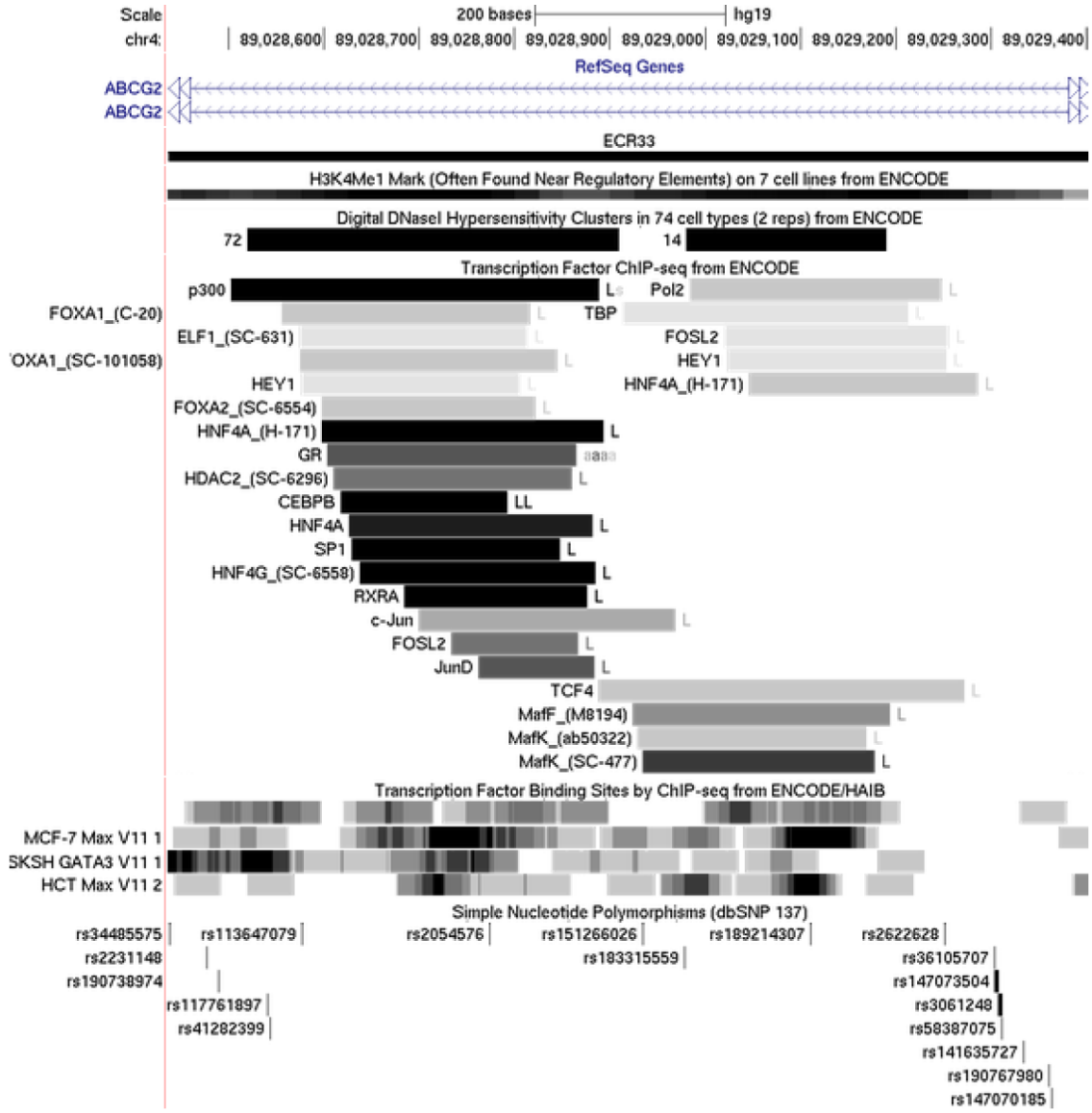

Figure 4.15. ENCODE data in ECR33. From top to bottom: genomic coordinates (chr4:89028437-89029406; hg19), blue hatched lines indicating intron 9 and then black boxes indicating the area covered by the ECR33 enhancer. Next are density bars indicating the DNA occupancy of H3K4me1 and the accessibility of the DNA to DNaseI in all cell types. Following this is ChIP-seq data from the combined TxN ChIP-seq ENCODE data, with each TF on its own line followed by a bar, with the length indicating the breadth of the peak and the shading indicating its strength. Each bar is followed by

letters to indicate the cell line the signal was found in: L, HepG2, s, SH-SY5Y; a, A549; u, U2OS. Multiple repeats of a letter behind a TF bar indicate the peak came up in the cell line when treated with a drug. For GR it is from the A549 cell line when treated with (in order) 5 nM, 50 nM, 500 pM and 100 nM dexamethasone. For CEBPB it is from the HepG2 cell line untreated and after forskolin treatment. Next are ENCODE ChIP-seq peaks. Representative cell lines for each TF are grouped together, with each cell line on its own line followed by a bar, with the length indicating the breadth of the peak and the shading density indicating its strength. TFs are GATA3 and Max in the cell lines MCF-7, HCT116 (HCT) and SK-N-SH (SKSH). Finally, black lines indicate locations with associated rs numbers for the SNPs reported in dbSNP 137. Schematic was made using the UCSC genome preview browser.

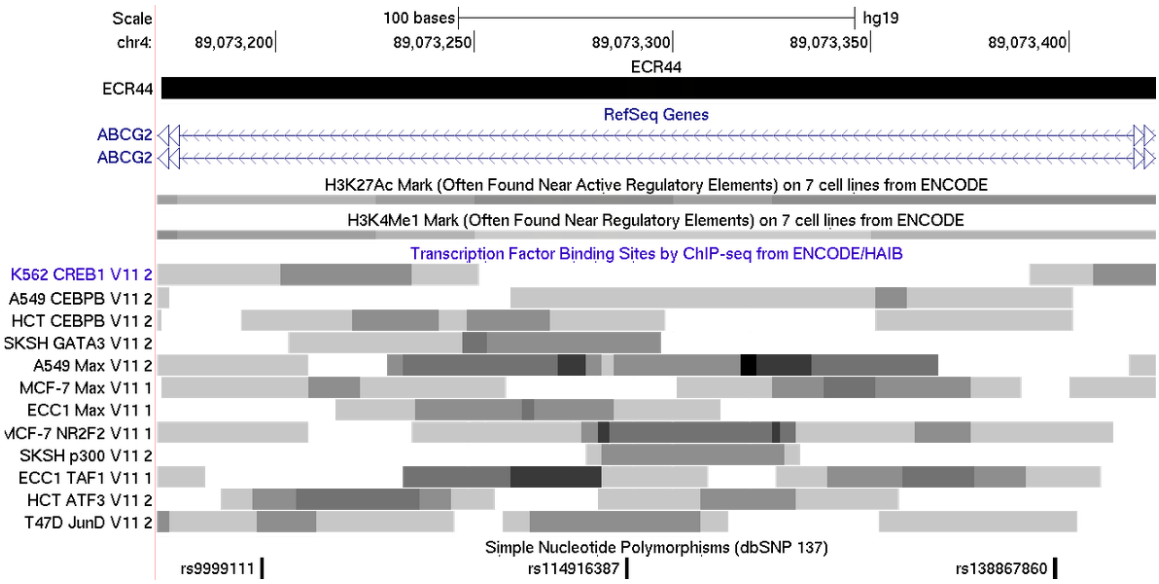

Figure 4.16. ENCODE data in ECR44. From top to bottom: the genomic coordinates (chr4: 89073171-89073422; hg19) followed by black boxes indicating the area covered by the ECR44 enhancer. Following this are blue hatched lines indicating intron 1 of *ABCG2*. Two density bars indicate the DNA occupancy of H3K27ac and H3K4me1. Following this is the DNA occupancy of several TFs as determined by ChIP-seq. Representative cell lines for each TF are grouped together, with each cell line on its own line followed by a bar, with the length indicating the breadth of the peak and the shading density indicating its strength. Cell lines include K562, A549, T47D, ECC1, HCT116 (HCT), SK-N-SH (SKSH), and MCF-7. Finally, black lines indicate locations with associated rs numbers for the SNPs reported in dbSNP 137. Schematic was made using the UCSC genome preview browser.

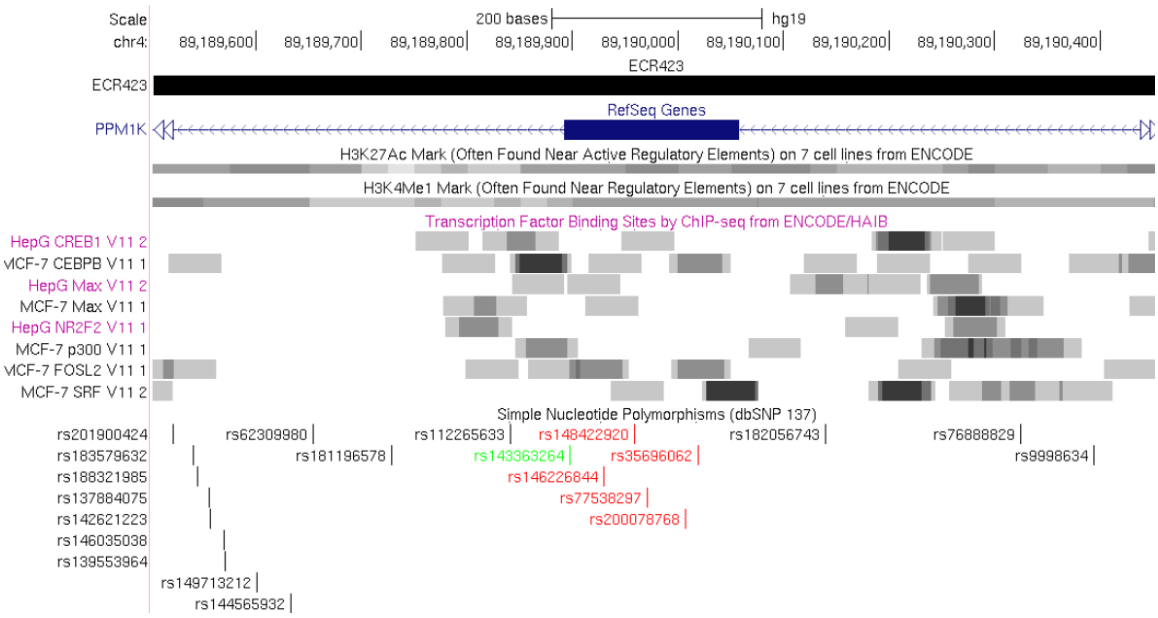

Figure 4.17. ENCODE data in ECR423. From top to bottom: the genomic coordinates (chr4:89189503-89190458; hg19), followed by black boxes indicating the area covered by the ECR423 enhancer. Following this are blue hatched lines indicating intron 1 and exons of PPM1K. Two density bars indicate the DNA occupancy of H3K27ac and H3K4me1. Following this is the DNA occupancy of several TFs as determined by ChIP-seq. Representative cell lines for each TF are grouped together, with each cell line on its own line followed by a bar, with the length indicating the breadth of the peak and the shading density indicating its strength. Cell lines include HepG2 (HepG) and MCF-7. Finally, black lines indicate locations with associated rs numbers for the SNPs reported in dbSNP 137: non-coding SNPs are in black, non-synonymous SNPs are in red and synonymous SNPs are in green. Schematic was made using the UCSC genome preview browser.

4.5. Discussion

Alteration of ABCG2 gene expression has been shown after many types of stimulus including hypoxia[35], inflammation[36], xenobiotics[37], hormones[38,39] and nutrients[40,41]. Additionally ABCG2 is only expressed in select tissues, such as liver, intestine and breast[4]. Variability of ABCG2 expression has not been accounted for by non-synonymous variants of *ABCG2*[33], and thus additional mechanisms are indicated as a cause of variation in expression[28]. There is much evidence for *cis*-elements in the regulation of tissue-specific genes[81], and it is becoming rapidly apparent that many TFs prefer to bind at *cis*-elements rather than proximal promoters to confer gene induction[48,50]. Thus, the several response elements for NRs and other TFs that have been mapped to the *ABCG2* proximal promoter might contribute less to the variability of ABCG2 expression and indeed no SNPs have been reported within these response elements[33]. Aside from elements in the proximal promoter, very little has been done to identify either nuclear response elements or tissue-specific suppressors and enhancers of *ABCG2* within its gene locus. The possibility of finding a tissue-specific *cis*-regulatory element of *ABCG2* could have implications on ABCG2 variation within those tissues. In the present study regulatory elements in the *ABCG2* gene locus were identified and characterized through *in silico*, *in vitro* and *in vivo* methods.

Our *in silico* scheme, considering DNA conservation, TFBS conservation, TF clustering and ChIP-seq, was able to identify over 110 putative enhancer elements and thirty high priority regions were selected for *in vitro* screening. Of the thirty high priority putative regulatory elements screened *in vitro*, eleven had *in vitro* enhancer activity in at least one cell line. Additionally, ten of the high priority regulatory elements were

screened for suppressor activity and seven of the ten elements had suppressor activity in at least one cell line, with the ECR429 region having cell-dependent suppressor and enhancer activity. Therefore, based on *in silico* predictions we were able to identify seventeen regions with *in vitro* regulatory activity, a 57% success rate. The *in vitro* assays allowed us to have stringent criteria for selecting enhancer elements for *in vivo* follow up. We screened nine regions in the *in vivo* hydrodynamic tail vein assay and identified six regions with positive *in vivo* enhancer activity, a 67% success rate. Of the thirty regions that entered the *in vitro* characterization steps, six of them were positive *in vivo* liver enhancers, an overall 20% success rate. Our *in vivo* success rate was two-fold higher than in a previous liver membrane transporter enhancer screen which utilized conservation and liver-specific TFBS as criteria to screen regions for *in vivo* liver enhancer activity[80], indicating that an additional layer of *in vitro* cell-based screening or the addition of ChIP-seq data could improve the selection process for *in vivo* enhancers. We also observed that none of the positive *in vivo* enhancer elements were greater than 1000 bp, which is less than that seen for developmental enhancers[57] but consistent with other *in vivo* liver enhancer regions[80]. Only two of the suppressor regions, ECR25 (1438 bp) and ECR425 (1909 bp) were over 1000 bp long. The current understanding is that regulatory elements can range from 100 to several kb, but are on average 500 bp[55].

The strength of our enhancers both *in vitro* and *in vivo* was quite high. Our *in vivo* liver enhancer activity ranged from ECR400 at >120-fold activation, three times that of the positive ApoE control, to 1.7- fold in the CR6 enhancer; the remaining enhancers showed 5- to 12- fold relative activation. This degree of activation is in the range of the strong enhancer elements previously discovered in screens for regulatory elements of

membrane transporters[80,82]. Additionally, these elements have strong enough enhancer activity that alterations in activity due to SNPs could be detected. Characterization of SNP effects on these *in vivo* liver enhancer elements is reported in Chapter 5.

At the beginning of our screen, only a few of the ENCODE ChIP-seq experiments had been completed and the data publicly available. However, there are now many experiments on the ChIP-seq database, including cells before and after treatment with NR ligands that would be an excellent source for future regulatory element searches[66]. It is worth noting that not all of the regions with ChIP-seq data were enhancers. ECR54 for example has many ChIP-seq peaks, especially strong and reproducible signals for CTCF (data not shown), but ECR54 showed neither enhancer nor suppressor activity in most of the cell lines. This could be because CTCF can act as a general TF, but it is most well known for its ability to act as an insulator and modulator of chromatin structure[76,83]. Additionally, our highest *in vivo* enhancer ECR400 was fairly devoid of ChIP-seq data. Clearly we cannot just rely on ChIP-seq data to find regulatory elements, as there are many TFs that have either not been characterized or do not have reliable antibodies for use in ChIP-seq experiments.

In order to investigate possible mechanisms driving the activity of our positive *in vivo* enhancers, we mined the ENCODE database for ChIP-seq signals of TF binding and DNaseI hypersensitivity; additional data from our original *in silico* screen, such as conserved TFBS was also considered for these regions. Our strongest *in vivo* enhancer was ECR400, but it was a relatively weak *in vitro* enhancer and had no activity in HepG2 cells. ECR400 has a conserved binding site for Octamer 1 (Oct1, POU2F1), a TF which has been shown to interact with NRs RXRα[84], GR, AR and PR[85,86] and general TFs like

Sp1[87,88]. ECR400 has only weak ChIP-seq peaks for CTCF in several cell lines but strong DNaseI sensitivity. CTCF has also been reported to act on its own as both a suppressive and activating TF[83], however CTCF is most strongly linked to decreased gene expression[89], therefore it is likely that additional TFs not picked up in the ENCODE ChIP-seq experiments are driving the activity of ECR400. For example, our TRANSFAC analysis of ECR400 predicted binding sites for CAR, LXR, PXR, VDR and AhR (data shown in Chapter 6: Table 6.1). Additional studies to characterize the TFs responsible for this strong activity of the *in vivo* liver enhancer ECR400 are discussed in Chapter 6. It is also important to note with ECR400 that it is ~4000 bp upstream of the *PKD2* promoter and could alternatively be regulating the expression of *PKD2* or be working as a loci enhancer element to regulate both the expression of *PKD2* and *ABCG2*.

In contrast to ECR400, CR6 was the strongest *in vitro* enhancer in all the cell lines, but it had relatively weak enhancer activity *in vivo*, hardly reaching significance with a 1.7-fold activation. CR6 is located just downstream of the 3' end of *ABCG2*, an ideal location for looping around and regulating the transcription of *ABCG2*. Some of the strongest ChIP-seq signals in CR6 were for Max, FOSL2, CTCF and CREB1. FOSL2 is a member of the c-Fos TF family and a TF that can dimerize with other AP-1 proteins at AP-1 sites[90]. AP-1 and CREB1 have both been shown to interact with hormone receptors, like ER, during their response to ligands[91–93]. Additionally, we explore and discuss a PXR-dependent activation of CR6 activity in Chapter 6. If CR6 is relevant to the hormonal alteration of ABCG2 expression, the absence of hormone receptor ligand could account for the lack of *in vivo* activity of CR6. As our cells were cultured in phenol red containing media, it is important to note that this media on cells *in vitro* has been reported

to work as a NR ligand[94]. This could also be the case for CR19, which had no *in vivo* activity, but has ChIP-seq peaks for multiple ER binding sites and is induced by estrogen (see Chapter 6).

Another possible TF relevant for CR6 activity could be Max. Max is a dimer partner to the Myc proteins, and Myc-Max dimers usually activate genes through enhancer elements[95]. Additionally, cMyc-Max have been shown to bind to the proximal promoter of *ABCG2,* only when it is unmethylated, to activate *ABCG2* transcription[95,96]. Since Myc is a well known oncogene and increases in ABCG2 expression cause drug resistance in tumor cells, finding regulatory elements that link Myc with ABCG2 expression could provide additional mechanisms for the acquisition of drug resistance by tumor cells and possible targets to reverse this resistance.

Due to the dynamics of tissue-specific expression of TFs, *cis*-regulatory elements could have either suppressor or enhancer activity depending on the balance of TFs present in the cell. ECR429 is located just upstream of the *PPM1K* promoter, a location that could work to regulate either *PPM1K* or *ABCG2*. ECR429 was chosen for suppressor follow-up due to its 50% reduction in activity in both HepG2 and HCT116; suppressive activity of ECR429 was confirmed in the HEK293T and HCT116 cell lines. ECR429 was also chosen for *in vivo* enhancer follow up but did not show any *in vivo* enhancer activity. We searched for mechanisms that could explain both suppressor and enhancer properties of ECR429 *in vitro*. The ECR429 region has DNaseI sensitivity and a ChIP-seq peak for the Egr-1 TF (data not shown). The Egr-1 is both a suppressive and activating TF[97]; it has been shown to cooperate with p300[98], AP-2 and GR[99] in activating genes, and could be responsible for the cell-specific activity of the region. Interestingly, ECR429 activity was

decreased upon estrogen treatment and increased with 48 hr dexamethasone treatment (see Chapter 6). This indicates the possibility that the binding of Egr-1 in ECR429 could be facilitating the binding of NRs, such as GR, while competing with others, such as ER, to elicit the activity of ECR429. ECR429 is located upstream of *ABCG2* by ~ 120,000 kb and upstream of PPM1K by ~2,000 bp. Both ER and GR response elements have been shown to prefer binding to elements far away from the proximal promoter[48,49]. The only known ERE for *ABCG2* is in the proximal promoter, therefore the location of ECR429 could facilitate the ability of ECR429 to regulate *ABCG2* through both ER and GR. *PPM1K* has been shown to be a ERα response gene[100] and ECR429 could be a possible ERE for *PPM1K* too. Further discussion on the hormone regulation of the ECR429 region will be made in Chapter 6.

Three of the *in vivo* liver enhancers (3 out of 9, 33%) were within intronic regions of *ABCG2*, which is consistent with the finding that 40% of enhancers are in intronic regions[81]. The *ABCG2* intron 10 enhancer ECR31 exhibited activity of 16- fold in HEK293T and over 2- fold in HCT116 and MCF-7 cells, which were confirmed by *in vivo* liver enhancer activity of 5-fold. There were many strong ChIP-seq peaks in the ECR31 enhancer including sites for GATA-2, AP-2γ, AP-2α, p300, GATA3, c-Fos, JunD, c-Jun, CEBPB, FoxAl and KAP1. JunD, c-Jun and c-Fos are all members of the AP-1 TF complex[90]. JunD is a central player in lymphoid cells[90], c-Jun, which can dimerize with c-Fos, is essential for hepatic development[90,101] and c-Fos is a well known oncogene implemented in osteogenesis[102,103]. Additionally, c-Fos and c-Jun were found bound to ECR31 in human umbilical vein endothelial cells (HUVEC, represented by H in Figure 4.14). ABCG2 is highly expressed in the side population of hematopoietic stem

cells, placental syncytiotrophoblasts and hepatocytes[4]; it would be interesting to see if ECR31 assists in this tissue-specific expression of ABCG2. AP-2γ and FoxA1 have been shown to work as long-range tethering sites for the ERα-mediated transcription[53]. The evidence for these TFs binding to ECR31, along with that of p300, could mean that ECR31 is also relevant to NR regulation of ABCG2 expression. Additional studies are needed to confirm that these TFs are driving ECR31 activity *in vivo*.

The second *ABCG2* intronic enhancer was ECR33. The *ABCG2* intron 9 enhancer ECR33 was active in HepG2 and HCT116 cells, as well as *in vivo*. There are many strong ChIP-seq signals for TFs bound to the ECR33 region. Among them is the HNF4γ nuclear receptor, which often confers tissue specific expression and is expressed in kidney and intestine, but not liver[104]. Since ECR33 was active in the human colon carcinoma cell line (HCT116), ECR33 could be playing a role in the tissue-specific expression of ABCG2 in the intestines. Other TFs bound to ECR33 are RXRα and HNF4α. In addition to RXRα's importance in the placenta, both TFs are important liver specific nuclear factors[105,106]. RXRα and HNF4α have also been shown to interact with each other and with ERα[107]. While CAR and PXR crosstalk with FoxA2 to regulate hepatic genes[108], the presence of GR, FoxA1, Sp1, RXRα and a strong p300 ChIP-seq signal indicate a likely role of ECR33 in hormone response and possibly the expression of ABCG2 in the intestines, liver and placenta. Interestingly, the GR ChIP-seq peak was seen in A549 cells treated with increasing concentrations of dexamethasone. Our own assays show ECR33 responds to both rifampin and estrogen treatment (see Chapter 6). The presence of all these NRs supports the theory that these TFs work as parts of a functional composite NR response complex[46,48]. ECR33 is in intron 9, only 2,000 bp downstream of ECR31; the enhancer's

adjacent locations could allow for them to work together in recruiting additional TFs necessary to moderate ABCG2 expression in a tissue-specific manner.

The last indentified *ABCG2* intronic enhancer, ECR44, is in intron 1. Another study that utilized conservation and TFBS clustering in order to identify high priority regions of *ABCG2* intron 1 for sequencing, also identified a section of intron 1 that includes the ECR44 genomic region[33]. Although this study didn't test the *cis*-element activity of the region, it is promising that our *in silico* screen was able to identify this region as having potential *cis*-regulatory activity. ECR44 had enhancer activity in all four cell lines and in the liver *in vivo*. ChIP-seq data shows a signal for binding of TFs including Max, p300, TAF1 and NR2F2 to ECR44. The NR2F2 TF, also known as COUP-TFII, is a member of the steroid receptor family and is important in glucose, cholesterol and xenobiotic metabolism pathways[109]. The ABCG family has been heavily associated with the transport of cholesterol steroids[110], and ABCG2 itself has been linked with reducing the efficacy of statin drugs[111]. COUP-TFII binds to the same direct repeat segments as VDR, thyroid hormone receptor (TR), retinoic acid receptor (RAR), RXR, PPAR and HNF-4; therefore its exerts negative regulatory function on these NR by competing for their common response element[109]. GR binding stimulates COUP-TFII induced transactivation by attracting cofactors, while COUP-TFII represses the GR-governed transcriptional activity by tethering repressors[112]. With the presence of p300 at ECR44, this element could be working through NR2F2 to regulate ABCG2 expression in response to steroids such as cholesterol.

In addition to intronic enhancers, we identified the ECR423 enhancer which encompasses exon 4 of PPM1K. This is not the first example of a coding exon working

as an enhancer to regulate the tissue-specific expression of a neighboring gene[113]. However, these examples have been infrequent, probably since *in silico* pipelines to identify conserved enhancer elements eliminate coding regions under the assumption that they are conserved due to being necessary for the protein, not due to *cis*-regulatory activity. Since exon 4 of PPM1K is relatively short, we decided not to exclude this region for our analysis because it also held numerous conserved and non-conserved predicted TFBS (data not shown) and it is a region with overlapping *cis*-element clusters and evolutionary conservation. Unfortunately, there has been very little TF binding information available from ChIP-seq databases for the ECR423 region. As one of the strongest *in vivo* liver enhancers in our screen, additional follow-up assays are warranted to identify which TFs are driving the activity of ECR423.

The entire pipeline to indentify *cis*-regulatory elements in the *ABCG2* gene locus yielded many *in vivo* liver enhancers with strong support of their activity by ChIP-seq data. It is important to note that although we screened 30 regions in the *ABCG2* gene locus, there is a possibility that we missed other important regulatory regions. Since the enhancer assay is set up as a putative *cis*-element cloned into a reporter vector, it is not able to assess possible long-range dynamics, like enhancer-enhancer interactions. Additionally, many nuclear response elements work in coordination with other TFs, like p300, in order to remodel chromatin, and the chromatin context is extremely important in the TF activity[46,114]. Without the complex chromatin context that a vector is unable to provide, in addition to the possibility of not having necessary TFs present in the cells, some of these regions could still be *in vivo cis*-regulatory elements. Furthermore, there are limitations of the hydrodynamic tail vein assay that include possible incompatibilities

of mouse TFs with that of human TFBS. Also, we only used livers that were harvested from mice injected with the enhancer plasmids, so we were not able to address other tissue-specific enhancers. Some of the *in vitro* enhancers could possibly be enhancers for other tissues where ABCG2 is expressed such as in the breast, placenta and intestine. A developmental screen would be needed to confirm other tissue enhancer activity for these regions. Although there is the possibility of examining kidney-enhancers through a renal vein injection[115], such an experiment was unsuccessful in our hands due to the difficulty of injecting mouse renal veins.

4.6. Conclusions

Through detailed *in silico*, *in vitro* and *in vivo cis*-regulatory assays, we identified multiple regions in the *ABCG2* gene locus that function as enhancers and suppressors. These regions have evidence for TF binding that could link them with tissue-specific or nuclear receptor responsive expression of ABCG2. Through computational genetics, *in vitro* and *in vivo* assays, regulatory regions can be successfully identified and characterized. With increasing evidence for the effects of *cis*-regulatory regions on drug disposition and efficacy[28], identification of these elements can help elucidate how genetic variants in non-coding regions of the genome cause clinical variation in ADME gene expression, pharmacokinetics and pharmacodynamics of drug response or disease progression.

4.7. References

(1) Abbott, B. L. ABCG2 (BCRP): a cytoprotectant in normal and malignant stem cells. *Clinical advances in hematology & oncology : H&O* **2006**, *4*, 63–72.

(2) Hirschmann-Jax, C.; Foster, a E.; Wulf, G. G.; Nuchtern, J. G.; Jax, T. W.; Gobel, U.; Goodell, M. a; Brenner, M. K. A distinct "side population" of cells with high drug efflux capacity in human tumor cells. *Proceedings of the National Academy of Sciences of the United States of America* **2004**, *101*, 14228–33.

(3) Zhou, S.; Schuetz, J. D.; Bunting, K. D.; Colapietro, a M.; Sampath, J.; Morris, J. J.; Lagutina, I.; Grosveld, G. C.; Osawa, M.; Nakauchi, H.; Sorrentino, B. P. The ABC transporter Bcrp1/ABCG2 is expressed in a wide variety of stem cells and is a molecular determinant of the side-population phenotype. *Nature medicine* **2001**, *7*, 1028–34.

(4) Maliepaard, M.; Scheffer, G. L.; Faneyte, I. F.; Gastelen, A. Van; Pijnenborg, A. C. L. M. Subcellular Localization and Distribution of the Breast Cancer Resistance Protein Transporter in Normal Human Tissues Subcellular Localization and Distribution of the Breast Cancer Resistance Protein Transporter in Normal Human Tissues 1. **2001**, 3458–3464.

(5) Cooray, H. C.; Blackmore, C. G.; Maskell, L.; Barrand, M. a Localisation of breast cancer resistance protein in microvessel endothelium of human brain. *Neuroreport* **2002**, *13*, 2059–63.

(6) Doyle, L. A.; Ross, D. D. Multidrug resistance mediated by the breast cancer resistance protein BCRP (ABCG2). *Oncogene* **2003**, *22*, 7340–58.

(7) Doyle, L. a; Yang, W.; Abruzzo, L. V; Krogmann, T.; Gao, Y.; Rishi, a K.; Ross, D. D. A multidrug resistance transporter from human MCF-7 breast cancer cells. *Proceedings of the National Academy of Sciences of the United States of America* **1998**, *95*, 15665–70.

(8) Allikmets, R.; Schriml, L. M.; Hutchinson, A.; Romano-Spica, V.; Dean, M. A human placenta-specific ATP-binding cassette gene (ABCP) on chromosome 4q22 that is involved in multidrug resistance. *Cancer research* **1998**, *58*, 5337–9.

(9) Mao, Q. BCRP/ABCG2 in the placenta: expression, function and regulation. *Pharmaceutical research* **2008**, *25*, 1244–55.

(10) Kobayashi, D.; Ieiri, I.; Hirota, T.; Takane, H. Functional assessment of ABCG2 (BCRP) gene polymorphisms to protein expression in human placenta. *Drug metabolism and* **2005**, *33*, 94–101.

(11) Yeboah, D.; Sun, M.; Kingdom, J.; Baczyk, D.; Lye, S. J.; Matthews, S. G.; Gibb, W. Expression of breast cancer resistance protein (BCRP / ABCG2) in human placenta throughout gestation and at term before and after labor. **2006**, *1258*, 1251–1258.

(12) Fetsch, P. a; Abati, A.; Litman, T.; Morisaki, K.; Honjo, Y.; Mittal, K.; Bates, S. E. Localization of the ABCG2 mitoxantrone resistance-associated protein in normal tissues. *Cancer letters* **2006**, *235*, 84–92.

(13) Jonker, J. W.; Merino, G.; Musters, S.; Van Herwaarden, A. E.; Bolscher, E.; Wagenaar, E.; Mesman, E.; Dale, T. C.; Schinkel, A. H. The breast cancer resistance protein BCRP (ABCG2) concentrates drugs and carcinogenic xenotoxins into milk. *Nature medicine* **2005**, *11*, 127–9.

(14) Noguchi, K.; Katayama, K.; Mitsuhashi, J.; Sugimoto, Y. Functions of the breast cancer resistance protein (BCRP/ABCG2) in chemotherapy. *Advanced drug delivery reviews* **2009**, *61*, 26–33.

(15) Zamber, C. P.; Lamba, J. K.; Yasuda, K.; Farnum, J.; Thummel, K.; Schuetz, J. D.; Schuetz, E. G. Natural allelic variants of breast cancer resistance protein (BCRP) and their relationship to BCRP expression in human intestine. *Pharmacogenetics* **2003**, *13*, 19–28.

(16) Suvannasankha, a; Minderman, H.; O'Loughlin, K. L.; Nakanishi, T.; Greco, W. R.; Ross, D. D.; Baer, M. R. Breast cancer resistance protein (BCRP/MXR/ABCG2) in acute myeloid leukemia: discordance between expression and function. *Leukemia : official journal of the Leukemia Society of America, Leukemia Research Fund, U.K* **2004**, *18*, 1252–7.

(17) Suvannasankha, A.; Minderman, H.; O'Loughlin, K. L.; Nakanishi, T.; Ford, L. a; Greco, W. R.; Wetzler, M.; Ross, D. D.; Baer, M. R. Breast cancer resistance protein (BCRP/MXR/ABCG2) in adult acute lymphoblastic leukaemia: frequent expression and possible correlation with shorter disease-free survival. *British journal of haematology* **2004**, *127*, 392–8.

(18) Benderra, Z.; Faussat, A.-M.; Sayada, L.; Perrot, J.-Y.; Chaoui, D.; Marie, J.-P.; Legrand, O. Breast cancer resistance protein and P-glycoprotein in 149 adult acute myeloid leukemias. *Clinical cancer research : an official journal of the American Association for Cancer Research* **2004**, *10*, 7896–902.

(19) Tsunoda, S.; Okumura, T.; Ito, T.; Kondo, K.; Ortiz, C.; Tanaka, E.; Watanabe, G.; Itami, A.; Sakai, Y.; Shimada, Y. ABCG2 expression is an independent unfavorable prognostic factor in esophageal squamous cell carcinoma. *Oncology* **2006**, *71*, 251–8.

(20) Usuda, J.; Tsunoda, Y.; Ichinose, S.; Ishizumi, T.; Ohtani, K.; Maehara, S.; Ono, S.; Tsutsui, H.; Ohira, T.; Okunaka, T.; Furukawa, K.; Sugimoto, Y.; Kato, H.; Ikeda, N. Breast cancer resistant protein (BCRP) is a molecular determinant of the outcome of photodynamic therapy (PDT) for centrally located early lung cancer. *Lung cancer (Amsterdam, Netherlands)* **2010**, *67*, 198–204.

(21) Uggla, B.; Ståhl, E.; Wågsäter, D.; Paul, C.; Karlsson, M. G.; Sirsjö, A.; Tidefelt, U. BCRP mRNA expression v. clinical outcome in 40 adult AML patients. *Leukemia research* **2005**, *29*, 141–6.

(22) Yoh, K. Breast Cancer Resistance Protein Impacts Clinical Outcome in Platinum-Based Chemotherapy for Advanced Non-Small Cell Lung Cancer. *Clinical Cancer Research* **2004**, *10*, 1691–1697.

(23) Mo, W.; Zhang, J.-T. Human ABCG2: structure, function, and its role in multidrug resistance. *International journal of biochemistry and molecular biology* **2012**, *3*, 1–27.

(24) Cusatis, G.; Gregorc, V.; Li, J.; Spreafico, A.; Ingersoll, R. G.; Verweij, J.; Ludovini, V.; Villa, E.; Hidalgo, M.; Sparreboom, A.; Baker, S. D. Pharmacogenetics of ABCG2 and adverse reactions to gefitinib. *Journal of the National Cancer Institute* **2006**, *98*, 1739–42.

(25) Sai, K.; Saito, Y.; Maekawa, K.; Kim, S.-R.; Kaniwa, N.; Nishimaki-Mogami, T.; Sawada, J.; Shirao, K.; Hamaguchi, T.; Yamamoto, N.; Kunitoh, H.; Ohe, Y.; Yamada, Y.; Tamura, T.; Yoshida, T.; Matsumura, Y.; Ohtsu, A.; Saijo, N.; Minami, H. Additive effects of drug transporter genetic polymorphisms on irinotecan pharmacokinetics/pharmacodynamics in Japanese cancer patients. *Cancer chemotherapy and pharmacology* **2010**, *66*, 95–105.

(26) Daly, A. K. Pharmacogenetics and human genetic polymorphisms. *The Biochemical journal* **2010**, *429*, 435–49.

(27) Georgitsi, M.; Zukic, B.; Pavlovic, S.; Patrinos, G. P. Transcriptional regulation and pharmacogenomics. *Pharmacogenomics* **2011**, *12*, 655–73.

(28) Smith, R. P.; Lam, E. T.; Markova, S.; Yee, S. W.; Ahituv, N. Pharmacogene regulatory elements: from discovery to applications. *Genome medicine* **2012**, *4*, 45.

(29) Urquhart, B.; Tirona, R.; Kim, R. Nuclear receptors and the regulation of drug-metabolizing enzymes and drug transporters: implications for interindividual variability in response to drugs. *The Journal of Clinical …* **2007**.

(30) Ong, C.-T.; Corces, V. G. Enhancer function: new insights into the regulation of tissue-specific gene expression. *Nature reviews. Genetics* **2011**, *12*, 283–93.

(31) Pennacchio, L. a; Loots, G. G.; Nobrega, M. a; Ovcharenko, I. Predicting tissue-specific enhancers in the human genome. *Genome research* **2007**, *17*, 201–11.

(32) Urquhart, B. L.; Ware, J. a; Tirona, R. G.; Ho, R. H.; Leake, B. F.; Schwarz, U. I.; Zaher, H.; Palandra, J.; Gregor, J. C.; Dresser, G. K.; Kim, R. B. Breast cancer resistance protein (ABCG2) and drug disposition: intestinal expression, polymorphisms and sulfasalazine as an in vivo probe. *Pharmacogenetics and genomics* **2008**, *18*, 439–48.

(33) Poonkuzhali, B.; Lamba, J.; Strom, S. Association of breast cancer resistance protein/ABCG2 phenotypes and novel promoter and intron 1 single nucleotide polymorphisms. *Drug Metabolism and ...* **2008**, *36*, 780–795.

(34) Ross, D. D.; Karp, J. E.; Chen, T. T.; Doyle, L. A. Expression of breast cancer resistance protein in blast cells from patients with acute leukemia. *Blood* **2000**, *96*, 365–8.

(35) Cheng, G. M. Y.; To, K. K. W. Adverse Cell Culture Conditions Mimicking the Tumor Microenvironment Upregulate ABCG2 to Mediate Multidrug Resistance and a More Malignant Phenotype. *ISRN oncology* **2012**, *2012*, 746025.

(36) Pradhan, M.; Bembinster, L. a; Baumgarten, S. C.; Frasor, J. Proinflammatory cytokines enhance estrogen-dependent expression of the multidrug transporter gene ABCG2 through estrogen receptor and NF{kappa}B cooperativity at adjacent response elements. *The Journal of biological chemistry* **2010**, *285*, 31100–6.

(37) Jigorel, E.; Vee, M. Le; Boursier-neyret, C.; Parmentier, Y.; Fardel, O. Differential Regulation of Sinusoidal and Canalicular Hepatic Drug Transporter Expression by Xenobiotics Activating Drug-Sensing Receptors in Primary Human Hepatocytes ABSTRACT : **2006**, *34*, 1756–1763.

(38) Wang, H.; Lee, E.; Zhou, L.; Leung, P. C. K.; Ross, D. D.; Unadkat, J. D.; Mao, Q. Progesterone receptor (PR) isoforms PRA and PRB differentially regulate expression of the breast cancer resistance protein in human placental choriocarcinoma BeWo cells. *Molecular pharmacology* **2008**, *73*, 845–54.

(39) Zhang, Y.; Zhou, G.; Wang, H.; Zhang, X.; Wei, F.; Cai, Y.; Yin, D. Transcriptional upregulation of breast cancer resistance protein by 17beta-estradiol in ERalpha-positive MCF-7 breast cancer cells. *Oncology* **2006**, *71*, 446–55.

(40) Lemos, C.; Kathmann, I.; Giovannetti, E.; Dekker, H.; Scheffer, G. L.; Calhau, C.; Jansen, G.; Peters, G. J. Folate deprivation induces BCRP (ABCG2) expression and mitoxantrone resistance in Caco-2 cells. *International journal of cancer. Journal international du cancer* **2008**, *123*, 1712–20.

(41) Lemos, C.; Kathmann, I.; Giovannetti, E.; Calhau, C.; Jansen, G.; Peters, G. J. Impact of cellular folate status and epidermal growth factor receptor expression on BCRP/ABCG2-mediated resistance to gefitinib and erlotinib. *British journal of cancer* **2009**, *100*, 1120–7.

(42) Tan, K. P.; Wang, B.; Yang, M.; Boutros, P. C.; Macaulay, J.; Xu, H.; Chuang, A. I.; Kosuge, K.; Yamamoto, M.; Takahashi, S.; Wu, A. M. L.; Ross, D. D.; Harper, P. A.; Ito, S. Aryl Hydrocarbon Receptor Is a Transcriptional Activator of the Human Breast Cancer Resistance Protein (BCRP / ABCG2) □. **2010**.

(43) Singh, A.; Wu, H.; Zhang, P.; Happel, C. Expression of ABCG2 (BCRP) is regulated by Nrf2 in cancer cells that confers side population and chemoresistance phenotype. *Molecular cancer …* **2010**, *9*, 2365–2376.

(44) Ee, P. L. R. Identification of a Novel Estrogen Response Element in the Breast Cancer Resistance Protein (ABCG2) Gene. *Cancer Research* **2004**, *64*, 1247–1251.

(45) Pike, J. W.; Meyer, M. B.; Watanuki, M.; Kim, S.; Zella, L. a; Fretz, J. a; Yamazaki, M.; Shevde, N. K. Perspectives on mechanisms of gene regulation by 1,25-dihydroxyvitamin D3 and its receptor. *The Journal of steroid biochemistry and molecular biology* **2007**, *103*, 389–95.

(46) Wiench, M.; Miranda, T. B.; Hager, G. L. Control of nuclear receptor function by local chromatin structure. *The FEBS journal* **2011**, *278*, 2211–30.

(47) Germain, P.; Staels, B.; Dacquet, C.; Spedding, M.; Laudet, V. Overview of Nomenclature of Nuclear Receptors. **2006**, *58*, 685–704.

(48) So, A. Y.-L.; Chaivorapol, C.; Bolton, E. C.; Li, H.; Yamamoto, K. R. Determinants of cell- and gene-specific transcriptional regulation by the glucocorticoid receptor. *PLoS genetics* **2007**, *3*, e94.

(49) Carroll, J. S.; Meyer, C. a; Song, J.; Li, W.; Geistlinger, T. R.; Eeckhoute, J.; Brodsky, A. S.; Keeton, E. K.; Fertuck, K. C.; Hall, G. F.; Wang, Q.; Bekiranov, S.; Sementchenko, V.; Fox, E. a; Silver, P. a; Gingeras, T. R.; Liu, X. S.; Brown, M. Genome-wide analysis of estrogen receptor binding sites. *Nature genetics* **2006**, *38*, 1289–97.

(50) Bolton, E. C.; So, A. Y.; Chaivorapol, C.; Haqq, C. M.; Li, H.; Yamamoto, K. R. Cell- and gene-specific regulation of primary target genes by the androgen receptor. *Genes & development* **2007**, *21*, 2005–17.

(51) Weltmeier, F.; Borlak, J. A high resolution genome-wide scan of HNF4α recognition sites infers a regulatory gene network in colon cancer. *PloS one* **2011**, *6*, e21667.

(52) Wang, Q.; Li, W.; Liu, X. S.; Carroll, J. S.; Jänne, O. a; Keeton, E. K.; Chinnaiyan, A. M.; Pienta, K. J.; Brown, M. A hierarchical network of transcription factors governs androgen receptor-dependent prostate cancer growth. *Molecular cell* **2007**, *27*, 380–92.

(53) Tan, S. K.; Lin, Z. H.; Chang, C. W.; Varang, V.; Chng, K. R.; Pan, Y. F.; Yong, E. L.; Sung, W. K.; Sung, W. K.; Cheung, E. AP-2γ regulates oestrogen receptor-mediated long-range chromatin interaction and gene transcription. *The EMBO journal* **2011**, *30*, 2569–81.

(54) Ahituv, N.; Rubin, E. M.; Nobrega, M. a Exploiting human--fish genome comparisons for deciphering gene regulation. *Human molecular genetics* **2004**, *13 Spec No*, R261–6.

(55) Loots, G. G. Genomic identification of regulatory elements by evolutionary sequence comparison and functional analysis. *Advances in genetics* **2008**, *61*, 269–93.

(56) Woolfe, A.; Goodson, M.; Goode, D. K.; Snell, P.; McEwen, G. K.; Vavouri, T.; Smith, S. F.; North, P.; Callaway, H.; Kelly, K.; Walter, K.; Abnizova, I.; Gilks, W.; Edwards, Y. J. K.; Cooke, J. E.; Elgar, G. Highly conserved non-coding sequences are associated with vertebrate development. *PLoS biology* **2005**, *3*, e7.

(57) Pennacchio, L. a; Ahituv, N.; Moses, A. M.; Prabhakar, S.; Nobrega, M. a; Shoukry, M.; Minovitsky, S.; Dubchak, I.; Holt, A.; Lewis, K. D.; Plajzer-Frick, I.; Akiyama, J.; De Val, S.; Afzal, V.; Black, B. L.; Couronne, O.; Eisen, M. B.; Visel, A.; Rubin, E. M. In vivo enhancer analysis of human conserved non-coding sequences. *Nature* **2006**, *444*, 499–502.

(58) Savic, D.; Bell, G. I.; Nobrega, M. a An in vivo cis-regulatory screen at the type 2 diabetes associated TCF7L2 locus identifies multiple tissue-specific enhancers. *PloS one* **2012**, *7*, e36501.

(59) So, A. Y.-L.; Cooper, S. B.; Feldman, B. J.; Manuchehri, M.; Yamamoto, K. R. Conservation analysis predicts in vivo occupancy of glucocorticoid receptor-binding sequences at glucocorticoid-induced genes. *Proceedings of the National Academy of Sciences of the United States of America* **2008**, *105*, 5745–9.

(60) King, D. C.; Taylor, J.; Zhang, Y.; Cheng, Y.; Lawson, H. a; Martin, J.; Chiaromonte, F.; Miller, W.; Hardison, R. C. Finding cis-regulatory elements using comparative genomics: some lessons from ENCODE data. *Genome research* **2007**, *17*, 775–86.

(61) Ovcharenko, I.; Nobrega, M. a; Loots, G. G.; Stubbs, L. ECR Browser: a tool for visualizing and accessing data from comparisons of multiple vertebrate genomes. *Nucleic acids research* **2004**, *32*, W280–6.

(62) Frazer, K. a; Pachter, L.; Poliakov, A.; Rubin, E. M.; Dubchak, I. VISTA: computational tools for comparative genomics. *Nucleic acids research* **2004**, *32*, W273–9.

(63) Loots, G. G.; Ovcharenko, I. rVISTA 2.0: evolutionary analysis of transcription factor binding sites. *Nucleic acids research* **2004**, *32*, W217–21.

(64) Frith, M.; Hansen, U.; Weng, Z. Detection of cis-element clusters in higher eukaryotic DNA. *Bioinformatics* **2001**, *17*, 878–889.

(65) Wingender, E.; Chen, X.; Hehl, R.; Karas, H.; Liebich, I.; Matys, V.; Meinhardt, T.; Prüss, M.; Reuter, I.; Schacherer, F. TRANSFAC: an integrated system for gene expression regulation. *Nucleic acids research* **2000**, *28*, 316–9.

(66) Encode, T.; Consortium, P. A user's guide to the encyclopedia of DNA elements (ENCODE). *PLoS biology* **2011**, *9*, e1001046.

(67) Vincze, T. NEBcutter: a program to cleave DNA with restriction enzymes. *Nucleic Acids Research* **2003**, *31*, 3688–3691.

(68) Rozen, S.; Skaletsky, H. Primer3 on the WWW for general users and for biologist programmers. *Methods in molecular biology (Clifton, N.J.)* **2000**, *132*, 365–86.

(69) Simonet, W. S.; Bucay, N.; Lauer, S. J.; Taylor, J. M. A far-downstream hepatocyte-specific control region directs expression of the linked human apolipoprotein E and C-I genes in transgenic mice. *The Journal of biological chemistry* **1993**, *268*, 8221–9.

(70) Liu, F.; Song, Y.; Liu, D. Hydrodynamics-based transfection in animals by systemic administration of plasmid DNA. *Gene therapy* **1999**, *6*, 1258–66.

(71) Kim, M. J.; Ahituv, N. The Hydrodynamic Tail Vein Assay as a Tool for the Study of Liver Promoters and Enhancers. In *Pharmacogenomics: Methods and Protocols*; Innocenti, F.; van Schaik, R. H. N., Eds.; 2012.

(72) Wang, Z.; Zang, C.; Rosenfeld, J. a; Schones, D. E.; Barski, A.; Cuddapah, S.; Cui, K.; Roh, T.-Y.; Peng, W.; Zhang, M. Q.; Zhao, K. Combinatorial patterns of histone acetylations and methylations in the human genome. *Nature genetics* **2008**, *40*, 897–903.

(73) Benevolenskaya, E. V Histone H3K4 demethylases are essential in development and differentiation. *Biochemistry and cell biology = Biochimie et biologie cellulaire* **2007**, *85*, 435–43.

(74) Weintraub, H.; Groudine, M. Chromosomal subunits in active genes have an altered conformation. *Science (New York, N.Y.)* **1976**, *193*, 848–56.

(75) Stalder, J.; Larsen, A.; Engel, J. D.; Dolan, M.; Groudine, M.; Weintraub, H. Tissue-specific DNA cleavages in the globin chromatin domain introduced by DNAase I. *Cell* **1980**, *20*, 451–60.

(76) Cockerill, P. N. Structure and function of active chromatin and DNase I hypersensitive sites. *The FEBS journal* **2011**, *278*, 2182–210.

(77) Landt, S. G.; Snyder, M.; *et. al.* ChIP-seq guidelines and practices of the ENCODE and modENCODE consortia. **2012**, 1813–1831.

(78) Ovcharenko, I.; Stubbs, L.; Loots, G. G. Interpreting mammalian evolution using Fugu genome comparisons. *Genomics* **2004**, *84*, 890–5.

(79) Zhang, G.; Gao, X.; Song, Y. K.; Vollmer, R.; Stolz, D. B.; Gasiorowski, J. Z.; Dean, D. a; Liu, D. Hydroporation as the mechanism of hydrodynamic delivery. *Gene therapy* **2004**, *11*, 675–82.

(80) Kim, M. J.; Skewes-Cox, P.; Fukushima, H.; Hesselson, S.; Yee, S. W.; Ramsey, L. B.; Nguyen, L.; Eshragh, J. L.; Castro, R. A.; Wen, C. C.; Stryke, D.; Johns, S. J.; Ferrin, T. E.; Kwok, P.; Relling, M. V; Giacomini, K. M.; Kroetz, D. L.; Ahituv, N. Functional characterization of liver enhancers that regulate drug-associated transporters. *Clinical pharmacology and therapeutics* **2011**, *89*, 571–8.

(81) Heintzman, N. D.; Hon, G. C.; Hawkins, R. D.; Kheradpour, P.; Stark, A.; Harp, L. F.; Ye, Z.; Lee, L. K.; Stuart, R. K.; Ching, C. W.; Ching, K. a; Antosiewicz-Bourget, J. E.; Liu, H.; Zhang, X.; Green, R. D.; Lobanenkov, V. V; Stewart, R.; Thomson, J. a; Crawford, G. E.; Kellis, M.; Ren, B. Histone modifications at human enhancers reflect global cell-type-specific gene expression. *Nature* **2009**, *459*, 108–12.

(82) Matsson, P.; Yee, S. W.; Markova, S.; Morrissey, K.; Jenkins, G.; Xuan, J.; Jorgenson, E.; Kroetz, D. L.; Giacomini, K. M. Discovery of regulatory elements in human ATP-binding cassette transporters through expression quantitative trait mapping. *The pharmacogenomics journal* **2011**, 1–13.

(83) Phillips, J. E.; Corces, V. G. CTCF: master weaver of the genome. *Cell* **2009**, *137*, 1194–211.

(84) Kakizawa, T.; Miyamoto, T.; Ichikawa, K.; Kaneko, A.; Suzuki, S.; Hara, M.; Nagasawa, T.; Takeda, T.; Mori, J. i; Kumagai, M.; Hashizume, K. Functional interaction between Oct-1 and retinoid X receptor. *The Journal of biological chemistry* **1999**, *274*, 19103–8.

(85) Préfontaine, G. G.; Walther, R.; Giffin, W.; Lemieux, M. E.; Pope, L.; Haché, R. J. Selective binding of steroid hormone receptors to octamer transcription factors

determines transcriptional synergism at the mouse mammary tumor virus promoter. *The Journal of biological chemistry* **1999**, *274*, 26713–9.

(86) Préfontaine, G. G.; Lemieux, M. E.; Giffin, W.; Schild-poulter, C.; Pope, L.; Lacasse, E.; Haché, R. J. G. Recruitment of Octamer Transcription Factors to DNA by Glucocorticoid Receptor Recruitment of Octamer Transcription Factors to DNA by Glucocorticoid Receptor. **1998**.

(87) Ström, A. C.; Forsberg, M.; Lillhager, P.; Westin, G. The transcription factors Sp1 and Oct-1 interact physically to regulate human U2 snRNA gene expression. *Nucleic acids research* **1996**, *24*, 1981–6.

(88) Gunther, M.; Laithier, M.; Brison, O. A set of proteins interacting with transcription factor Sp1 identified in a two-hybrid screening. *Molecular and cellular biochemistry* **2000**, *210*, 131–42.

(89) Ernst, J.; Kheradpour, P.; Mikkelsen, T. S.; Shoresh, N.; Ward, L. D.; Epstein, C. B.; Zhang, X.; Wang, L.; Issner, R.; Coyne, M.; Ku, M.; Durham, T.; Kellis, M.; Bernstein, B. E. Mapping and analysis of chromatin state dynamics in nine human cell types. *Nature* **2011**, *473*, 43–9.

(90) Hess, J.; Angel, P.; Schorpp-Kistner, M. AP-1 subunits: quarrel and harmony among siblings. *Journal of cell science* **2004**, *117*, 5965–73.

(91) Dutertre, M.; Smith, C. L. Ligand-independent interactions of p160/steroid receptor coactivators and CREB-binding protein (CBP) with estrogen receptor-alpha: regulation by phosphorylation sites in the A/B region depends on other receptor domains. *Molecular endocrinology (Baltimore, Md.)* **2003**, *17*, 1296–314.

(92) Acevedo, M. L.; Kraus, W. L. Mediator and p300 / CBP-Steroid Receptor Coactivator Complexes Have Distinct Roles , but Function Synergistically , during Estrogen Receptor α -Dependent Transcription with Chromatin Templates Mediator and p300 / CBP-Steroid Receptor Coactivator Complexes. **2003**.

(93) Zhao, C.; Gao, H.; Liu, Y.; Papoutsi, Z.; Jaffrey, S.; Gustafsson, J.-A.; Dahlman-Wright, K. Genome-wide mapping of estrogen receptor-beta-binding regions reveals extensive cross-talk with transcription factor activator protein-1. *Cancer research* **2010**, *70*, 5174–83.

(94) Berthois, Y.; Katzenellenbogen, J. A.; Katzenellenbogen, B. S. Phenol red in tissue culture media is a weak estrogen: implications concerning the study of estrogen-responsive cells in culture. *Proceedings of the National Academy of Sciences of the United States of America* **1986**, *83*, 2496–500.

(95) Herkert, B.; Eilers, M. Transcriptional repression: the dark side of myc. *Genes & cancer* **2010**, *1*, 580–6.

(96) Porro, A.; Iraci, N.; Soverini, S.; Diolaiti, D.; Gherardi, S.; Terragna, C.; Durante, S.; Valli, E.; Kalebic, T.; Bernardoni, R.; Perrod, C.; Haber, M.; Norris, M. D.; Baccarani, M.; Martinelli, G.; Perini, G. c-MYC Oncoprotein Dictates Transcriptional Profiles of ATP-Binding Cassette Transporter Genes in Chronic Myelogenous Leukemia CD34+ Hematopoietic Progenitor Cells. *Molecular cancer research : MCR* **2011**, *9*, 1054–66.

(97) Khachigian, L. M. Early growth response-1 in cardiovascular pathobiology. *Circulation research* **2006**, *98*, 186–91.

(98) Mouillet, J.-F.; Sonnenberg-Hirche, C.; Yan, X.; Sadovsky, Y. p300 regulates the synergy of steroidogenic factor-1 and early growth response-1 in activating luteinizing hormone-beta subunit gene. *The Journal of biological chemistry* **2004**, *279*, 7832–9.

(99) Wong, D. L.; Siddall, B. J.; Ebert, S. N.; Bell, R. A.; Her, S. Phenylethanolamine N-methyltransferase gene expression: synergistic activation by Egr-1, AP-2 and the glucocorticoid receptor. *Brain research. Molecular brain research* **1998**, *61*, 154–61.

(100) Lin, Z.; Reierstad, S.; Huang, C.-C.; Bulun, S. E. Novel estrogen receptor-alpha binding sites and estradiol target genes identified by chromatin immunoprecipitation cloning in breast cancer. *Cancer research* **2007**, *67*, 5017–24.

(101) Eferl, R.; Sibilia, M.; Hilberg, F.; Fuchsbichler, A.; Kufferath, I.; Guertl, B.; Zenz, R.; Wagner, E. F.; Zatloukal, K. Functions of c-Jun in liver and heart development. *The Journal of cell biology* **1999**, *145*, 1049–61.

(102) Wagner, E. F. Functions of AP1 (Fos/Jun) in bone development. *Annals of the rheumatic diseases* **2002**, *61 Suppl 2*, ii40–2.

(103) Durchdewald, M.; Angel, P.; Hess, J. The transcription factor Fos: a Janus-type regulator in health and disease. *Histology and histopathology* **2009**, *24*, 1451–61.

(104) Drewes, T.; Senkel, S.; Holewa, B.; Ryffel, G. U. Human hepatocyte nuclear factor 4 isoforms are encoded by distinct and differentially expressed genes. *Molecular and cellular biology* **1996**, *16*, 925–31.

(105) Schrem, H.; Klempnauer, J.; Borlak, J. Liver-enriched transcription factors in liver function and development. Part I: the hepatocyte nuclear factor network and liver-specific gene expression. *Pharmacological reviews* **2002**, *54*, 129–58.

(106) Germain, P.; Chambon, P.; Eichele, G.; Evans, R. M.; Lazar, M. A.; Leid, M.; De Lera, A. R.; Lotan, R.; Mangelsdorf, D. J.; Gronemeyer, H. International Union of

Pharmacology. LXIII. Retinoid X receptors. *Pharmacological reviews* **2006**, *58*, 760–72.

(107) Lee, S. K.; Choi, H. S.; Song, M. R.; Lee, M. O.; Lee, J. W. Estrogen receptor, a common interaction partner for a subset of nuclear receptors. *Molecular endocrinology (Baltimore, Md.)* **1998**, *12*, 1184–92.

(108) Konno, Y.; Negishi, M.; Kodama, S. The roles of nuclear receptors CAR and PXR in hepatic energy metabolism. *Drug metabolism and pharmacokinetics* **2008**, *23*, 8–13.

(109) Qiu, Y.; Krishnan, V.; Pereira, F. A.; Tsai, S. Y.; Tsai, M. J. Chicken ovalbumin upstream promoter-transcription factors and their regulation. *The Journal of steroid biochemistry and molecular biology* **1996**, *56*, 81–5.

(110) Kusuhara, H.; Sugiyama, Y. ATP-binding cassette, subfamily G (ABCG family). *Pflügers Archiv : European journal of physiology* **2007**, *453*, 735–44.

(111) Generaux, G. T.; Bonomo, F. M.; Johnson, M.; Doan, K. M. M. Impact of SLCO1B1 (OATP1B1) and ABCG2 (BCRP) genetic polymorphisms and inhibition on LDL-C lowering and myopathy of statins. *Xenobiotica; the fate of foreign compounds in biological systems* **2011**, *41*, 639–51.

(112) De Martino, M. U.; Alesci, S.; Chrousos, G. P.; Kino, T. Interaction of the glucocorticoid receptor and the chicken ovalbumin upstream promoter-transcription factor II (COUP-TFII): implications for the actions of glucocorticoids on glucose, lipoprotein, and xenobiotic metabolism. *Annals of the New York Academy of Sciences* **2004**, *1024*, 72–85.

(113) Birnbaum, R. Y.; Clowney, E. J.; Agamy, O.; Kim, M. J.; Zhao, J.; Yamanaka, T.; Pappalardo, Z.; Clarke, S. L.; Wenger, A. M.; Nguyen, L.; Gurrieri, F.; Everman, D. B.; Schwartz, C. E.; Birk, O. S.; Bejerano, G.; Lomvardas, S.; Ahituv, N. Coding exons function as tissue-specific enhancers of nearby genes. *Genome research* **2012**, *22*, 1059–68.

(114) Biddie, S. C.; John, S.; Hager, G. L. Genome-wide mechanisms of nuclear receptor action. *Trends in endocrinology and metabolism: TEM* **2010**, *21*, 3–9.

(115) Kameda, S.; Maruyama, H.; Higuchi, N.; Iino, N.; Nakamura, G.; Miyazaki, J.; Gejyo, F. Kidney-targeted naked DNA transfer by retrograde injection into the renal vein in mice. *Biochemical and Biophysical Research Communications* **2004**, *314*, 390–395.

Chapter 5 : Effect of SNPs on *ABCG2* Locus Enhancer Regions

5.1. Abstract

ABCG2 encodes the mitoxantrone resistance protein (MXR, BCRP), a membrane transporter responsible for the efflux of its substrates out of the cell and important in detoxification. In the present study, the effect of genetic variation on the *in vitro* enhancer activity of six previously identified liver enhancers in the *ABCG2* locus was examined. The effect of variants on enhancer activity *in vivo* and on *in silico* predictions for transcription factor binding was also characterized. Reference and variant *ABCG2* gene locus liver enhancers, cloned into the pGL4.23 expression vector, were tested for their ability to alter luciferase activity when transiently transfected into HepG2 and HEK293T cell lines. Multiple SNPs were found that both increased and decreased enhancer activity *in vitro*. Three SNPs (rs9999111, rs12508471 and rs149713212) decreased the activity of the enhancers by at least 50% and four SNPs (rs72873421, rs183322988, rs190738974 and rs2725263) increased the activity of the enhancers by over 2-fold in both cell lines. Four of these SNPs (rs9999111, rs12508471, rs72873421 and rs149713212) significantly decreased and rs2725263 significantly increased enhancer activity *in vivo*. The *in silico* transcription factor binding analysis found alterations in binding probabilities of prominent transcription factors for each of these SNPs that could explain their ability to alter enhancer activity *in vivo*. Additionally, associations of these SNPs with *ABCG2*, *PPM1K* or *PDK2* expression in liver, kidney, breast, lymphocytes, T-cells and skin cells were detected. In conclusion, genetic variants in *ABCG2* gene locus liver enhancers could be a contributing factor to the variability of *ABCG2*, *PKD2* and *PPM1K* expression in a tissue-specific manner.

5.2. Introduction

The mitoxantrone resistance protein (MXR, BCRP), encoded by the *ABCG2* gene, is a member of the ABC membrane transporter family and is responsible for transport of its substrates across the intestinal epithelial cells back into the intestinal lumen, from the hepatocyte into the bile, into milk, away from the placenta and brain, and into the lumen of the renal proximal tubule[1]. With MXR playing important roles in the disposition of xenobiotics and endogenous ligands throughout the body, it's not surprising that reduced expression and function of MXR is associated with a variety of drug side effects, lower efficacy of treatments and increased susceptibility to cancer[2–10]. Although reduced function variants of MXR occur[11–17], all the variability in ABCG2 expression and MXR substrate pharmacokinetics cannot be accounted for by these nonsynonymous variants. For example, even in individuals without these variants there is a wide range of ABCG2 expression[18].

There are many phenotypes associated with decreased, absent or drug-inhibited MXR. MXR knockout mice (*Abcg2*-/-) experience phototoxicity due to the accumulation of porphyrins[19], which are established MXR substrates[20]. Normally, MXR protects tissues during hypoxia by effluxing heme and porphyrin compounds out of the cell[21]. Reduced porphyrin transport by MXR could thus be an explanation for human phototoxicity in individuals treated with a number of MXR substrates such as statins[22] and imatinib[23]. MXR also transports uric acid, and polymorphisms of *ABCG2* have been repeatedly associated with gout[24]. Statins are proposed as a treatment for gout since they are able to alter ABCG2 expression[25]. Polymorphisms in *ABCG2* have also been linked to increased risk of diarrhea in patients taking gefitinib, another MXR substrate[26]. Altered

ABCG2 expression has been associated with decreased disease-free survival[3–10] as a result of the natural protective role of MXR against carcinogens[27] and its ability to efflux chemotherapeutics out of the cancer cell[28]. Based on the important function of MXR in protection from toxins and intracellular access to drugs, identifying regulatory regions of *ABCG2* and functional SNPs within those regions may inform about the mechanisms of regulation of ABCG2 expression.

MXR is one of many transporters and enzymes important in drug absorption, distribution, metabolism and excretion (ADME). Recently, the transcriptional regulation of ADME genes has been linked to *cis*-regulatory elements, and alterations in their expression due to variants in those regulatory elements are becoming more evident[29,30]. Additionally, expression quantitative trait loci (eQTL) studies of human genes have implicated proximal regulatory variation as a prevalent cause of population variation in gene expression by associating a genetic variation with the expression of a gene of interest[31,32]. *Cis*-regulatory elements include enhancers, suppressors, promoters, insulators and locus control regions that work to regulate the transcriptional activity of the basal transcription machinery. These genomic regions provide binding sites for transcription factors (TFs), which can be ubiquitous or tissue-specific, that work through complex interactions with histones, other TFs and/or RNA polymerase to alter gene transcription. In our previous research, we characterized the *ABCG2* promoter (see Chapter 3) and utilized comparative genomics along with *in vitro* and *in vivo* assays to identify nine liver enhancers in the *ABCG2* gene locus (see Chapter 4).

The *ABCG2* gene locus is shared with the polycystic kidney disease 2 (*PKD2*) and protein phosphatase 1K (*PPM1K*) genes. *PKD2* encodes the polycystin-2 protein, an

integral membrane protein implemented in cell-cell interactions, renal tubular development and calcium homeostasis in the kidney[33]. Germline mutations in *PKD2*, and the resulting reduction in polycystin-2 protein, cause autosomal dominant polycystic kidney disease (ADPKD)[34]. Additionally, somatic mutations in *PKD2* occur in ADPKD patients with germline *PKD1* mutations causing more severe disease[33]. Although they have not been identified, other genetic modifying effects causing wide variability in *PKD1* and *PKD2* expression have been linked to the ADPKD phenotype and disease progression[35].

The other member of the *ABCG2* gene locus is the *PPM1K* gene. *PPM1K* encodes the protein phosphatase 2Cm (PP2Cm) enzyme important in branched-chain amino acid homeostasis and regulation of the mitochondria permeability transition pore[36]. PP2Cm is highly expressed in the brain, heart, liver and kidney and is also transcriptionally regulated in response to nutrient status[37]. Any *cis*-regulatory elements found in the *ABCG2* gene locus could also be important for the regulation of *PKD2* and *PPM1K*. Therefore, it is important to also test the association of enhancer SNPs with the expression of these two genes.

In this study, we test the hypothesis that SNPs in previously identified (see Chapter 4) regulatory regions of the *ABCG2* locus explain the variation in ABCG2, PKD2 or PPM1K expression. Variants in the liver enhancer regions reported in publicly available databases were studied in the pGL4.23 [*luc2*/minP] vector. The pGL4.23 vector is a firefly luciferase vector with a multiple cloning site designed to accept a putative enhancer element upstream of a minimal promoter and the luciferase gene, once cloned and transfected into cells, the luciferase activity can be measured as a surrogate for

enhancer function. Enhancer activity of the variant plasmids was measured *in vitro* in kidney (HEK293T) and liver (HepG2) cells, each chosen to represent their primary tissue source, and variants with altered function were tested *in vivo* using a hydrodynamic tail vein assay. SNPs that significantly altered *in vivo* liver enhancer activity were then tested for association with ABCG2, PKD2 and PPM1K expression in human liver, kidney, breast, lymphocyte, T-cell and fibroblasts. The ability of functional SNPs to alter TFBS was predicted using *in silico* methods. The findings from these studies provide insight into how non-coding genetic variants may lead to altered exposure, and thus toxicity, to MXR substrates.

5.3. Materials and Methods

5.3.1. *Chemicals and Materials*

The vectors pGL4.23 [*luc2*/minP], pGL4.74 [*hRluc*/TK], pGL4.13 [*luc2*/SV40], the Dual-Luciferase® Reporter Assay System and HB101 competent cells were all purchased from Promega (Madison, WI). The human embryonic kidney (HEK293T/17) and human hepatocellular carcinoma (HepG2) cells were purchased from the American Type Culture Collection (ATCC, Manassas, VA). High-glucose Dulbecco's modified Eagle's medium (DMEM), Opti-Minimal Essential Medium (Opti-MEM), Lipofectamine 2000 and Trizol were all purchased from Invitrogen (Carlsbad, CA). Both 100 mm LB Amp-100 agar plates and LB Broth 100 μg/mL ampicilin were purchased from Teknova (Hollister, CA). $RNase^-$ $DNase^-$ water, 1X phosphate buffered saline (PBS), 0.05% trypsin and 100X penicillin and streptomycin were all purchased from the University of California San Francisco (UCSF) cell culture facility (San Francisco, CA). The GeneJet

PCR Purification Kits and GeneJet Plasmid Miniprep Kits are from Fermentas (Glen Burnie, MD). High-Fidelity Phusion Buffer, Phusion High-Fidelity DNA Polymerase, *Dpn*I and *Dpn*I digestion buffer were all purchased from New England Biolabs (Ipswich, MA). AllPrep DNA/RNA Mini Kits, QIAquick PCR Purification Kits, and Qiagen RNeasy MinElute Cleanup Kits were from Qiagen (Valencia, CA). Other materials including 10% fetal bovine serum (FBS) (Axenia BioLogix, Dixon, CA), GenElute HP Endotoxin-Free Maxiprep Kit (Sigma Aldrich), TransIT EE *In Vivo* Gene Delivery System (Mirus Bio, Madison, WI), CD1 mice (Charles Rivers Laboratories, Wilminton, MA), High Capacity cDNA Reverse Transcription Kits (Applied Biosystems, Foster City, CA), 10 U/mL Exonuclease I enzyme (GE Healthcare, Piscataway, New Jersey) and dNTPs (Denville, Metuchen, NJ) were purchased from the indicated manufacturers. The APOE-pGL4.23[38] construct was a gift from Nadav Ahituv (University of California San Francisco, San Francisco, CA).

5.3.2. *Genetic Analysis of Enhancer Regions*

SNPs in each of the *ABCG2 in vivo* enhancer regions were retrieved for all available ethnic populations from publicly available databases, including 1000 Genomes 20120214 phase 1 release[39], dbSNP build 135 and HapMap release 28[40]. Genotypes from 1000 Genomes 20100804 phase 1 release were used for calculating haplotypes. Haplotypes were determined by downloading each region's genotype and information files from the 1000 Genomes browser for Caucasians (CEU), Nigerians (YRI), combined Chinese and Japanese (CHB+JBT) and all available ethnic groups combined (ALL). Genotype and information files were then loaded into Haploview version 4.2[41] and

linkage analysis was performed on each region. Haplotype frequencies are reported as the frequency of one haplotype compared to all other haplotypes. SNP and haplotype frequencies for each enhancer region are displayed in Table 5.7 - Table 5.12. All SNPs were tested *in vitro* regardless of minor allele frequency. SNPs in linkage disequilibrium (LD) with rs12508471, rs72873421, rs149713212, rs9999111 and rs2725263 (r^2 threshold ≥ 0.8) were extracted from 1000 Genomes pilot 1 genotype data using the Broad Institute SNP annotation and proxy search (SNAP) version 2.2[42] for each population (CEU, YRI and CHB+JBT) separately.

5.3.3. *Primer Design*

DNA sequences ±25 bp for each SNP were pulled from the UCSC genome browser. The site-directed mutagenesis (SDM) primers for each SNP in a positive *in vivo* *ABCG2* locus enhancer were designed using the PrimerX© program and synthesized by Integrated DNA Technologies (San Diego, CA). Each primer was diluted to 100 μM in TE buffer and each primer set (forward and reverse) was combined in a 10 μM solution in RNAse and DNase free water for use in SDM PCR. Primers for the deletion SNP rs36105707 were designed according to the large deletion/insertion protocol described in Chapter 3. In short, the primers were designed to overlap on their 5'-end so that the deletion is missing from both primers (see Figure 3.2B) and to ensure that the melting temperature of the non-overlapping section of the primers is larger than that of the overlapping section of the primers by 5-10°C.

Table 5.1. ECR44 Site-Directed Mutagenesis Primers

SNP ID	Δnt[1]	Primer Sequence[2]	Tm[3]
rs9999111	T<G	CCTTTTCTCACTGTG[C]ATTCAATCAACAGA	58
		TCTGTTGATTGAAT[G]CACAGTGAGAAAAGG	
rs138867860	G<T	CTACCAATTTTACTT[A]TTTCCCATAAGAGACT	58
		AGTCTCTTATGGGAAA[T]AAGTAAAATTGGTAG	
rs114916387	A<G	CTTACCAGAGCCTAA[C]AGATAGAAGCTCAC	60
		GTGAGCTTCTATCT[G]TTAGGCTCTGGTAAG	

[1]Change in reference to variant nucleotide of the anti-strand

[2]Forward and reverse primers per SNP with mutagenized nucleotide in brackets

[3]Melting temperature used for annealing step of SDM PCR

Table 5.2. ECR400 Site-Directed Mutagenesis Primers

SNP ID	Δnt[1]	Primer Sequence[2]	Tm[3]
rs72873421	G<A	CCAAATCTATCATGAA[A]AAGGCCACAAATCCTAGC	60
		GCTAGGATTTGTGGCCTT[T]TTCATGATAGATTTGG	
rs117741074	C<T	GTTCTTCTCATAAA[A]CCCAAAACACCAGA	60
		TCTGGTGTTTTGGG[T]TTTATGAGAAGAAC	
rs2728131	C<T	CCTTTTAAAATGG[T]TCCTTCCAGCGTC	60
		GACGCTGGAAGGA[A]CCATTTTAAAAGG	
rs12508471	A<G	ACGGTGGCACTA[G]GACTGAGGTGAG	60
		CTCACCTCAGT[C]CTAGTGCCACCGT	
88924169[4]	T<C	GAAACTCCTTTTGGA[T]TTCCTCTCGAGGTG	58
		CACCTCGAGAGGAA[A]TCCAAAAGGAGTTTC	
rs12500008	G<T	GTCTCCACCTC[T]AGAGGAAATCC	62
		GGATTTCCTCT[A]GAGGTGGAGAC	
rs78901673	A<G	ACCGTGG[G]CGCTGGAAGGA	62
		TCCTTCCAGCG[C]CCACGGT	

[1]Change in reference to variant nucleotide of the anti-strand

[2]Forward and reverse primers per SNP with mutagenized nucleotide in brackets

[3]Melting temperature used for annealing step of SDM PCR

[4]Primer mutates enhancer region back to reference, this is not a reported SNP

Table 5.3. ECR423 Site-Directed Mutagenesis Primers

SNP ID	Δnt[1]	Primer Sequence[2]	Tm[3]
rs137884075	C<T	GGAGGGCAGATCA[T]GAGGTCAGGAGATC	60
		GATCTCCTGACCTC[A]TGATCTGCCCTCC	
rs142621223	G<A	GAGGGCAGATCAC[A]AGGTCAGGAGATC	60
		GATCTCCTGACCT[T]GTGATCTGCCCTC	
rs139553964	G<A	GGTCAGGAGATC[A]AGACCATCCTGG	58
		CCAGGATGGTCT[T]GATCTCCTGACC	
rs149713212	G<A	CACGGTGAAACCCC[A]TCTCTACTAAAAAAC	58
		GTTTTTTAGTAGAGA[T]GGGGTTTCACCGTG	
rs144565932	G<A	CAAAAAATTAGCCGAGC[A]TGTTGGCAGGC	60
		GCCTGCCAACA[T]GCTCGGCTAATTTTTTG	
rs62309980	C<T	GGCGCCTGTAGT[T]CCAGCTACTCAG	60
		CTGAGTAGCTGG[A]ACTACAGGCGCC	
rs76888829	T<C	GCATCACTATCTACAAA[C]GGCCTCTATTCATATC	60
		GATATGAATAGAGGCC[G]TTTGTAGATAGTGATGC	
rs9998634	C<A	GGATATCTGGTGTCCA[T]ACTGAAAGTATTAAA	60
		TTTAATACTTTCAGT[A]TGGACACCAGATATCC	
rs77538297	C<T	CACAAAATAGCC[T]GGCTGTCCCCAAC	60
		GTTGGGGACAGCC[A]GGCTATTTTGTG	
rs35696062	G<-	CATCTCGCAATA[-]GGCTACTGTTGCAGTAG	60
		CTACTGCAACAGTAGCC[-]TATTGCGAGATG	

[1]Change in reference to variant nucleotide of the anti-strand

[2]Forward and reverse primers per SNP with mutagenized nucleotide in brackets

[3]Melting temperature used for annealing step of SDM PCR

Table 5.4. CR6 Site-Directed Mutagenesis Primers

SNP ID	Δnt[1]	Primer Sequence[2]	Tm[3]
rs45510401	A<G	AAAGAATACATAAAATAGGAT[G]TAATTAAATTCTCATTTAT	60
		ATAAATGAGAATTTAATTA[C]ATCCTATTTTATGTATTCTTT	
rs573519157[4]	-<A	CAAAAAAAAAAAA[A]TTAGCCGGGCGTG	60
		CACGCCCGGCTAA[T]TTTTTTTTTTTG	
rs5883021	A<-	CAAAAAAAAAAAAAAAAAAAA [-]GTCCTTAATTTTAAAATGG	60
		CCATTTTAAAATTAAGGAC[-]TTTTTTTTTTTTTTTTTTTTG	
rs186188962	C<T	CCACCCGCTT[T]GGCCTCCCA	65.4
		TGGGAGGCC[A]AAGCGGGTGG	
rs144180103	T<-	GCTAATTTTTTTTTTTT[-]GTATTTTTAGTAGAGAC	58
		GTCTCTACTAAAAATAC[-]AAAAAAAAAAAAATTAGCC	
rs190754327	G<C	GTAATGGCTGG[C]ACTACAGGCTCC	64.9
		GGAGCCTGTAGT[G]CCAGCCATTAC	
rs2725268	A<G	AAAGAATACATAAAATAGGAT[G]TAATTAAATTCTCATTTAT	56
		ATAAATGAGAATTTAATTA[C]ATCCTATTTTATGTATTCTTT	
rs183322988	A<G	ATTAACTTTTTAAATAA[G]TGAGAATTTAATTATATCCT	58
		AGGATATAATTAAATTCTCA[C]TTATTTAAAAAGTTAAT	

[1]Change in reference to variant nucleotide of the anti-strand

[2]Forward and reverse primers per SNP with mutagenized nucleotide in brackets

[3]Melting temperature used for annealing step of SDM PCR

[4]Primer mutates enhancer region back to reference

Table 5.5. ECR31 Site-Directed Mutagenesis Primers

SNP ID	Δnt[1]	Primer Sequence[2]	Tm[3]
rs139101431	T<C	CTGAAGAAACACCTAAGGTTCTTC[T]TTATTTCTC	59.2
		GAGAAATAA[A]GAAGAACCTTAGGTGTTTCTTCAG	
rs144062279	G<A	CAAAGTTCCAGTTG[A]AGACCAGGTTACTCC	65
		GGAGTAACCTGGTC[T]TCAACTGGAACTTTG	
rs2725264[4]	C<T	GTTACTCCATGTCCT[C]TCCAAATGCTTCCTG	60
		CAGGAAGCATTTGGA[G]AGGACATGGAGTAAC	
rs4148156	G<A	GTCTGGAAATAATCT[A]GATACCTCAGCCC	59.6
		GGGCTGAGGTATC[T]AGATTATTTCCAGAC	
rs145932752	A<G	CTTATTCTTTAAAAAATA[G]TCAGCCTTTCCAGACATC	59.2
		GATGTCTGGAAAGGCTGA[C]TATTTTTTAAAGAATAAG	
rs6831395	G<A	ATAATCAGCCTTTCCA[A]ACATCAAAATAGGCTGC	62.1
		GCAGCCTATTTTGATGT[T]TGGAAAGGCTGATTAT	
rs2725263[4]	A<C	CTTTCCAGACATCAA[A]ATAGGCTGCACATAAG	60
		CTTATGTGCAGCCTAT[T]TTGATGTCTGGAAAG	
rs192562676	C<T	GATACTACCATCTA[T]CCCCTCTAAATCAC	55
		GTGATTTAGAGGGG[A]TAGATGGTAGTATC	
rs182159263	C<G	CTACCATCTACCC[G]CTCTAAATCACTGG	62.1
		CCAGTGATTTAGAG[C]GGGTAGATGGTAG	
rs187527722	A<G	GACAGCAAGC[G]CTACGGAGCAC	65
		GTGCTCCGTAG[C]GCTTGCTGTC	
rs192781547	A<G	GCTTATGTTCAGA[G]CACAATACAGTCG	65
		CGACTGTATTGTG[C]TCTGAACATAAGC	
rs184709106	C<T	CAGAACACAATACAGT[T]GATAAAAAGTCCCCTC	59.6
		GAGGGGACTTTTTATC[A]ACTGTATTGTGTTCTG	

[1]Change in reference to variant nucleotide of the anti-strand

[2]Forward and reverse primers per SNP with mutagenized nucleotide in brackets

[3]Melting temperature used for annealing step of SDM PCR

[4]Primer mutates enhancer region back to reference

Table 5.6. ECR33 Site-Directed Mutagenesis Primers

SNP ID	Δnt[1]	Primer Sequence[2]	Tm[3]
rs2231148	T<A	CAATTAGAGATAAAAACTTA[A] ACACACCATTTATTAGTATA	57
		TATACTAATAAATGGTGTGT[T]TAAGTTTTTATCTCTAATTG	
rs190738974	A<G	AACTTATACACACCATTT[G]TTAGTATAATATATGGT	57
		ACCATATATTATACTAA[C]AAATGGTGTGTATAAGTT	
rs117761897	C<T	CATTAAGATAAACACT[T]AATGGCTTGGCCAACG	62.7
		CGTTGGCCAAGCCATT[A]AGTGTTTATCTTAATG	
rs41282399	A<C	GATAAACACTCA[C]TGGCTTGGCCAAC	61
		GTTGGCCAAGCCA[G]TGAGTGTTTATC	
rs113647079	C<G	CCCTGGGAGAAAATAAAA[G]AGCATACATTATTTAGAC	61
		GTCTAAATAATGTATGCT[C]TTTTATTTTCTCCCAGGG	
rs2054576	A<G	CAATGCAAGTATGT[G]GCAAAGCAAAGTC	61
		GACTTTGCTTTGC[C]ACATACTTGCATTG	
rs151266026	T<C	AAAAATTTTAAAGCACACA[C] TAAAAAAATTCTAACAATGG	61
		CCATTGTTAGAATTTTTTTA[G]TGTGTGCTTTAAAATTTTT	
rs183315559	G<A	GTGAGGAAATAG[A]GGTGAGATGGAGC	61
		GCTCCATCTCACC[T]CTATTTCCTCAC	
rs189214307	C<T	CACTACCCATCTC[T]TGTCACTGCTTC	61
		GAAGCAGTGACA[A]GAGATGGGTAGTG	
rs36105707[4,5]	-< TTAAA	ATAACGTAACCC[TTAAA]TTAACCCTTTGCTTATTGAA	62
		TTTAAGGGTTACGTTATGATAT[AATTT] ATCTGAGAAAATCC	
rs141635727	A<G	ACGTTATGATATAATTT[G]TCTGAGAAAATCCTATTT	57
		AAATAGGATTTTCTCAGA[C]AAATTATATCATAACGT	
rs190767980	C<T	AGAAAATCCTATTTATATTTA[T] TCGTGAGTTAAATATTAAAA	57
		TTTTAATATTTAACTCACGA[A] TAAATATAAATAGGATTTTCT	
rs147070185	G<A	AAATCCTATTTATATTTACTCA[T] GAGTTAAATATTAAAAAAC	57
		GTTTTTTAATATTTAACTC[A] TGAGTAAATATAAATAGGATTT	
rs2622628[4]	C<A	CTGGACAAACAC[C]AATCTTGTTTCTAGG	56
		CCTAGAAACAAGATT[G]GTGTTTGTCCAG	

[1]Change in reference to variant nucleotide of the anti-strand

[2]Forward and reverse primers per SNP with mutagenized nucleotide in brackets

[3]Melting temperature used for annealing step of SDM PCR

[4]Primer mutates enhancer region back to reference

[5]This primer is used with special PCR conditions

5.3.4. *Variant Enhancer Plasmid Construction*

Reference enhancer plasmids, in the pGL4.23 [*luc2*/minP] vector, were constructed as described in Chapter 4. SDM on the reference plasmids were performed to create each of the variant enhancer constructs using the primers listed in Table 5.1 - Table 5.6. PCR reaction components for all SNP primer sets were as follows: 1X High-Fidelity Phusion Buffer, 1 unit Phusion High-Fidelity DNA Polymerase, 200 nM dNTPs, 1 μM each primer and 100 ng *ABCG2* reference enhancer vector, all in a final volume of 50 μL. PCR reaction conditions for all primers except for rs36105707 were as follows: An initial cycle for 30 sec at 98°C, followed by 20 cycles of 10 sec at 98°C, melting temperature (varies per primer pair) for 30 sec and 3 min at 72°C, then a final extension for 10 min at 72°C. The SDM PCR reactions were then digested for at least 20 min at 37°C with 1 unit *Dpn*I in 1X *Dpn*I digestion buffer. The reactions were then purified using the GeneJet PCR purification kit per the manufacturer's protocol, and 5 μL of the purified SDM reaction was transformed into 35 μL HB101 competent cells per the manufacturer's protocol. After growing for 24 hr on 100 mm LB Amp-100 agar plates, colonies were selected for expansion in LB broth supplemented with 100 μg/mL ampicillin overnight at 37°C with shaking. DNA was then isolated from the bacteria using the GeneJet Miniprep Kit and the vector was sequenced with the RVPrimer3, p150R or region-specific primer (see Table 4.4) to confirm the presence of the SNP. Large bacterial preparations of the correctly mutagenized plasmids were grown in 150 mL LB broth supplemented with 100 μg/mL ampicillin overnight at 37°C with shaking and DNA was isolated with the GenElute HP Endotoxin-Free Maxiprep Kit per the manufacturer's protocol. In order to make the ECR400 rs7287321/rs12508471/rs12500008 haplotype, the SNPs for

rs7287321 and rs12508471 were introduced into the rs12500008 construct. The ECR33 rs412823991/rs2622628 haplotype was made by mutating the rs412823991 SNP into the rs2622628 construct. The ECR31 rs2725264/rs2725263 haplotype was the genotype of the originally cloned ECR31 region and was mutated back to reference. All DNA used for the *in vitro* and *in vivo* luciferase assays were endotoxin-free to avoid the cytotoxic effects of toxins released from the bacteria during lysis; this also allowed for more reproducible results.

5.3.5. *Deletion Mutagenesis PCR Amplification*

The protocol for large insertion/deletion amplification is explained in detail in Chapter 3. The deletion SNP rs36105707 was mutated back to reference in the ECR33 plasmid using a special protocol illustrated in Figure 3.2 and previously reported to work for both deletion and insertion mutatgenesis[43]. Primers were designed as described above. PCR reaction components were the same as described above. PCR conditions were as follows: an initial cycle of 5 min at 95°C, then 12 cycles of 95°C for 1 min, 46.5°C for 1 min and 72°C for 9 min, with a final cycle of 1 min at 36°C and 30 min at 72°C.

5.3.6. *Cell Culture*

HEK293T/17 and HepG2 cell lines were grown in high-glucose DMEM supplemented with 10% FBS, 100 units/mL of penicillin and 0.1 mg/mL of streptomycin. Both cell lines were grown in 5% CO_2 at 37°C. To maintain cells, they were split upon

reaching confluency by treatment with 0.05% Trypsin-EDTA, washing with 1X PBS and suspension in fresh media at a 1:5 to 1:20 dilution.

5.3.7. *Transient Transfection*

For transient transfections of the HEK293T/17 and HepG2 cell lines, cells were seeded at approximately 1.8 x 10^4 cells per well of a 96-well plate in fresh DMEM with 10% FBS without antibiotics and grown for at least 24 hrs to 80% confluency. Cells were then transfected with Lipofectamine 2000 following guidelines suggested in the manufacturer's protocol. In short, 0.5 µL of Lipofectamine 2000 was incubated in 25 µL Opti-MEM for 5 min and then gently mixed with a 25 µL solution of 0.08 µg plasmid (pGL4.23 [*luc2*/minP], reference or variant enhancer-pGL4.23 [*luc2*/minP], APOE-pGL4.23 or pGL4.13 [*luc2*/SV40]) plus 0.02 µg pGL4.74 [*hRluc*/TK] diluted with Opti-MEM. The DNA-Lipofectamine mixture was allowed to incubate at room temperature for 30 min before being placed onto cells with 50 µL of antibiotic-free media. Cells were incubated with their transfection reagents for 18-24 hr before analysis.

5.3.8. *Luciferase Reporter Assay*

The day after transfection, each well was washed with 100 µL 1X PBS before being lysed with 50 µL of 1X passive lysis buffer for 1 hr with shaking. Then 20 µL of HEK293T/17 or 30 µL of HepG2 lysates were measured for firefly and *Renilla* luciferase activity using 70 µL each of the Luciferase Assay Reagent II and Stop & Glo® reagents from the Dual-Luciferase® Reporter Assay System in a GloMax 96 microplate Dual Injector Luminometer. The firefly activity was normalized to the *Renilla* activity per well

to control for transfection efficiency. Each experiment also included the empty pGL4.23 vector as the negative control and the *APOE*-pGL4.23 or pGL4.13 [*luc2*/SV40] plasmids as a positive control. Enhancer activity was expressed as the ratio of the plasmid firefly luciferase activity to *Renilla* activity; the activity of each variant plasmid was then normalized relative to that of the reference plasmid, setting the reference activity to one.

5.3.9. *Hydrodynamic Tail Vein Assay*

Positive *in vitro* variant enhancer elements were screened for their effect on *in vivo* liver enhancer activity through the hydrodynamic tail vein injection[44] adapted for enhancer element screening[45] (see Chapter 4, Figure 4.10). Each variant enhancer, along with their reference enhancer construct, was injected into the tail vein of 4-5 mice using the TransIT EE *In Vivo* Gene Delivery System following the manufacturer's protocol. Briefly, 10 μg of pGL4.23 [*luc2*/minP] vector with or without enhancer element, or the *ApoE*[38] positive control liver enhancer, along with 2 μg of pGL4.74 [*hRluc*/TK] were injected into the tail vein of CD1 mice. After 24 hr, mice were euthanized and livers from the mice were harvested. Each liver was homogenized in 3 mL of 1X Passive Lysis Buffer and then centrifuged at 4°C for 30 min at 14,000 rpm. The supernatant was then diluted 1:20 with additional lysis buffer and measured for firefly and *Renilla* luciferase activity using the Dual-luciferase® reporter assay system according to the manufacturer's protocol in a Synergy 2 (BioTek Instruments, Winooski, VT) microplate reader. Each liver's lysate was read in replicate 3-6 times, with each sample's firefly activity normalized to the *Renilla* activity and then averaged across the replicates for a per mouse value. The enhancer or ApoE normalized luciferase activity was compared to that of the

empty pGL4.23 vector. All mouse work was done following a protocol approved by the UCSF institutional Animal Care and Use Committee.

5.3.10. *Predictions of Transcription Factor Binding Site Changes*

Two separate computational tools were used to predict differences in the binding probability of TFs between reference and variant enhancer sequences. First, Consite[46]was used to directly compare the transcription factor binding sites (TFBS) shared between two aligned genomic sequences. For this analysis, enhancer reference and variant sequences were extracted from UCSC genome browser (hg19) and imputed as orthologous pairs of genomic sequences. The regions were scanned for vertebrate TFs provided by the program, with a minimum specificity of 10 bits. With no conservation cut off, the TF score threshold was set to 70%, and TFs with greater than 20% change in binding probability were extracted. The second computational tool was the TRANSFAC's Match program[47]. Individually, the genomic sequence of the reference and variant enhancers were scanned for the probability of TF binding using the TRANSFAC release 2012.2 matrix table of all non-redundant vertebrate TFs with high quality matrices. TRANSFAC determines TF matrices to be high quality if they produce a minimal amount of false positives when used to scan a control sequence of DNA. Additionally, default settings were used to minimize false positives, which are calculated by TRANSFAC by setting a minFP value for each matrix equal to the lowest value which yields no hits when scanning a control region. The probabilities for TF binding to reference and variant enhancer sequences of TF's with a matrix score >0.70 were compiled, and TFs which had a gain or loss of binding were identified. Consite and

TRANSFAC also provided alignments of the consensus TF matrix sequence with that of the reference and variant enhancer sequences.

5.3.11. *Liver and Kidney Tissues*

Kidney (n=60) and liver (n=60) samples were procured by the Pharmacogenomics of Membrane Transporters (PMT) research group at the University of California San Francisco (San Francisco, CA)[48]. These tissues were purchased from Asterand (Detroit, MI), Capital Biosciences (Rockville, MD) and SRI International (Menlo Park, CA). The Asterand samples included both postmortem tissues and surgical resections from donors; the Capital Biosciences specimens included surgical resections from normal tissue surrounding cancer tissues and SRI International included postmortem tissues. All samples were stored frozen at -80°C until processing for DNA and RNA. Information on the age, sex, and ethnicity of the patient was available for all samples.

DNA was extracted from the tissues using a Qiagen AllPrep DNA/RNA Mini Kit following the manufacturer's protocol, with additional DNA clean-up using the QIAquick PCR Purification Kit. RNA was extracted from the tissues following the protocol for Trizol reagent, followed by RNA clean-up with the Qiagen RNeasy MinElute Cleanup Kit following the manufacturer's protocol. Good-quality RNA (260/280 >1.7 and 260/230 >1.8, RNA Integrity number 3-8) was isolated from 58 kidney samples and 60 liver samples, and these were used to correlate SNP genotype with total ABCG2 mRNA expression. RNA (2 μg) was reverse transcribed to cDNA using the High Capacity cDNA Reverse Transcription Kit and the following incubation conditions: 10 min at 22ºC, 2 hr at 37ºC, 5 min at 4ºC, 10 min at 75ºC and 5 min at 4ºC.

Exonuclease I enzyme (10 U/mL) was added to each sample and the following incubation conditions were used to remove excess primers: 1 hr at 37ºC, 5 min at 4ºC and then 10 min at 85ºC to inactivate the exonuclease enzyme. Samples were then stored at -20ºC until assayed for gene expression or genotype.

5.3.12. *ABCG2 mRNA Expression and Genotype in PMT Liver and Kidney Tissues*

Gene expression for ABCG2 (along with other transporters) was evaluated in 60 kidney and 60 liver samples from surgical resection or postmortem collections in Caucasian males and females using the Biotrove Open Array™ qPCR platform (Life Technologies, Carlsbad, CA) according to the manufacturer's protocol. ABCG2 mRNA expression was normalized to a geometric mean of the expression of GAPDH, β-2 microglobin, and β-actin and expressed as $2^{-\Delta\Delta Ct}$ per gene for each sample. All ΔCt values for a given tissue type were quantile normalized across samples using the open source R preprocessCore package[49,50]. Expression data was quality controlled using principal component analysis to identify outliers. Of these samples, 58 kidney samples and 34 liver samples were successfully genotyped on the Affymetrix Axiom (Santa Clara, CA) genotyping platform using the Axiom® Genome-Wide CEU 1 Array Plate (Affymetrix, Santa Clara, CA). The samples were tested for quality control (QC) using sex-check, identity by descent and call rate tests, of which six kidney samples failed and were excluded from further analysis. After initial QC, 52 kidney samples and 34 liver samples were included in subsequent analyses.

5.3.13. *Association of SNPs with Gene Expression*

Associations between variants and ABCG2 expression levels in the PMT liver and kidney tissues were identified by imputing genotypes using 1000 Genomes data and then testing for correlation between gene expression and genotype using a linear regression adjusted for gender. Additional liver genotype and expression data provided by Schadt *et al.*[51] was also analyzed for correlation between genotype and gene expression. Additionally, gene expression and genotyping data from The Cancer Genome Atlas (TCGA) breast tissue[52] was analyzed in a similar manner. All data were analyzed using liner regression between SNPs with *in vivo* effects on enhancer activity and the expression of ABCG2, PPM1K and PKD2 using the Affymetrix Genotyping Console (Affymetrix, Santa Clara, CA).

Recently, a database for integrated analysis and visualization of SNP-gene associations in eQTL studies has become available[53]. This database includes data from several sequence and gene expression profiling studies: the MuTHER study[54,55] with data from female twins in adipose, skin and lymphoblastoid cell lines (LCLs), the Stranger study[56–59] with data from HapMap LCLs, and the GenCord study[60] with data from human umbilical fibroblasts, LCLs and T-cells. The expression of ABCG2, PPM1K and PKD2 was correlated to the *ABCG2* locus SNPs that altered enhancer activity *in vivo*, or when the SNP was not genotyped, with SNPs in LD (r^2>0.08, as determined above) with these SNPs. Using the GeneVar 3.2.0 eQTL analysis program, Spearman rank correlation coefficients (rho) for 10,000 permutations per SNP between reference, heterozygous and variant alleles were calculated.

5.3.14. *Statistical Analysis*

Enhancer activity was expressed relative to the reference sequence as described above. Normalized enhancer activities were determined per transfection, with a minimum of three and maximum of eight wells per plasmid. All polymorphic enhancer constructs were compared to the reference enhancer construct by an ANOVA analysis followed by a Bonferroni's multiple comparison *t*-test; $P < 0.05$ was considered significant. Polymorphic enhancer constructs identified for *in vivo* testing had either a 2-fold increase or 50% decrease in activity and a $P < 0.0001$ in both cell lines. Results from the hydrodynamic tail vein injection were analyzed using an unpaired Student's *t*-test between the reference and variant enhancer. All statistics were run using the GraphPad Prism 5 program.

5.4. Results

5.4.1. *Genetic Variation in the ABCG2 Locus Enhancer Regions*

A total of 54 SNPs and 5 haplotypes were obtained from publicly available databases throughout all six enhancer regions with *in vivo* activity. ECR44 had three SNPs (Table 5.7), none of which are in linkage disequilibrium (LD) with each other, and only the rs9999111 SNP had a minor allele frequency (MAF) ≥ 5%. There are six SNPs in the ECR400 region (Table 5.8), as well as a seventh novel SNP found in the cloned region (rs88924169 in Table 5.2). In addition, ECR400 has one major haplotype (referred to as ECR400*1 throughout results), which is a combination of the SNPs rs72873421, rs12500008 and rs12508471. These three SNPs have MAFs ranging from 8.4-38% and are in almost perfect linkage disequilibrium (r^2=0.96-0.98) with each other (Figure 5.1A).

There are ten SNPs in ECR423 (Table 5.9), but only rs76888829 has a MAF above 2%. There are eight SNPs in CR6 (Table 5.10), the most frequent of which is rs2725268, which has a MAF ranging from 8-47%. There are 13 SNPs in ECR 31 (Table 5.11) along with three haplotypes. The most common ECR31 haplotype (referred to as ECR31*1 throughout results) is a combination of the two most frequent SNPs rs2725263 and rs2725264. These two SNPs have MAFs ranging from 8-87% depending on the ethnic population, and the ECR31*1 haplotype has a frequency of approximately 31% with an r^2 = 0.46 between the two SNPs (Figure 5.1B). There are 14 SNPs and two haplotypes in ECR33 (Table 5.12). The two haplotypes of ECR33 (*1, rs41282399/ rs2622628) and (*2, rs2231148/ rs117761897) are comprised of the four most common SNPs in ECR33. ECR33*1 has a frequency of 3.6% and an r^2 = 0.13 between the two SNPs (Figure 5.1C). ECR33*2 has a frequency of 2.9% and an r^2 = 0.07 (Figure 5.1C) between the two SNPs. The minor allele frequencies for each of the SNPs and haplotypes that were reported are displayed in Tables 5.7-5.12, and the LD plots for selected SNPs are in Figure 5.1.

Table 5.7. SNPs in the ECR44 Enhancer

SNP ID	Δnt[1]	Conserved[1]	MAF[2] %			Location[3]
			AA	EUR	AS	
rs9999111	A>C	Yes	4.7	7.3	0.0	chr4:89073197
rs138867860	C>A	No	0.0	0.0	0.0	chr4:89073397
rs114916387	T>C	Yes	2.0	0.0	0.5	chr4:89073289

[1]Nucleotide change and conservation of the reference allele to the variant allele as obtained from the UCSC genome browser

[2]Minor allele frequency (MAF) for African American (AA), European (EUR), and Asian (AS) populations as obtained from databases described in methods

[3]Genomic location obtained from UCSC genome browser's hg19 build

Table 5.8. SNPs in the ECR400 Enhancer

Variant ID[1]	Δnt[2]	Conserved[2]	MAF[3] %			Location[4]
			AA	EUR	AS	
rs72873421	G/A	Yes	21.1	8.4	38.1	chr4:88923906
rs117741074	G/A	Yes	0.0	0.0	1.7	chr4:88924002
rs12500008	C/A	Yes	21.1	8.4	38.3	chr4:88924176
rs2728131	C/T	Yes	1.2	8.4	2.8	chr4:88924344
rs12508471	A/G	Yes	21.1	8.4	38.3	chr4:88924371
rs78901673	A/G	Yes	nr	nr	nr	chr4:88924356
*1[5]	-	-	16.8	16.8	16.8	-

[1]Variant ID as either the rs number or haplotype ID

[2]Nucleotide change and conservation of the reference allele to the variant allele as obtained from the UCSC genome browser

[3]Frequency of minor allele (MAF) or haplotype (as a percent of all haplotypes) for African American (AA), European (EUR) and Asian (AS) populations

[4]Genomic location obtained from UCSC genome browser's hg19 build

[5]rs72873421/rs12500008/rs12508471 (*1)

Abbreviations: nr, not reported

Table 5.9. SNPs in the ECR423 Enhancer

SNP ID	Δnt[1]	Conserved[1]	MAF[2] %			Location[3]
			AA	EUR	AS	
rs137884075	C/T	No	0.0	0.0	0.2	chr4:89189556
rs142621223	G/A	No	0.0	0.0	0.3	chr4:89189557
rs139553964	G/A	No	0.0	0.0	1.2	chr4:89189571
rs149713212	G/A	No	1.6	0.0	0.2	chr4:89189602
rs144565932	G/A	No	0.0	0.0	1.2	chr4:89189634
rs62309980	C/T	Yes	0.0	0.1	0.0	chr4:89189655
rs76888829	T/C	Yes	4.3	1.3	1.2	chr4:89190325
rs9998634	G/C	Yes	0.4	0.0	0.0	chr4:89190395
rs77538297	C/T	Yes	0.2	0.0	0.0	chr4:89189971
rs35696062	G/-	Yes	nr	nr	nr	chr4:89190022

[1]Nucleotide change and conservation of the reference allele to the variant allele as obtained from the UCSC genome browser

[2]Minor allele frequency (MAF) for African American (AA), European (EUR) and Asian (AS) populations as obtained from databases described in methods

[3]Genomic location obtained from UCSC genome browser's hg19 build

Abbreviations: nr, not reported

Table 5.10. SNPs in the CR6 Enhancer

SNP ID	Δnt[1]	Conserved[1]	MAF[2] %			Location[3]
			AA	EUR	AS	
rs45510401	A>G	No	4.5	0.0	0.0	chr4:89011422
rs2725268	A>G	Yes	7.5	47.4	24.0	chr4:89010983
rs57351915	A>-	Yes	nr	nr	nr	chr4:89011141
rs58830217	->A	No	nr	nr	nr	chr4:89011309
rs186188962	G>A	No	0.0	0.5	0.0	chr4:89011051
rs144180103	A>-	No	nr	nr	nr	chr4:89011129
rs190754327	C>G	Yes	nr	nr	nr	chr4:89011173
rs183322988	T>C	No	0.0	0.3	0.3	chr4:89011437

[1]Nucleotide change and conservation of the reference allele to the variant allele as obtained from the UCSC genome browser

[2]Minor allele frequency (MAF) for African American (AA), European (EUR) and Asian (AS) populations as obtained from databases described in methods

[3]Genomic location obtained from UCSC genome browser's hg19 build

Abbreviations: nr, not reported

Table 5.11. SNPs in the ECR31 Enhancer

Variant ID[1]	Δnt[2]	Conserved[2]	Frequency[3]			Location[4]
			AA	EUR	AS	
rs28665233	G/A	Yes	18.9	0.9	0.2	chr4:89025882
rs139101431	A/G	No	1.6	0.0	0.0	chr4:89026007
rs144062279	G/A	No	0.4	0.0	0.0	chr4:89026087
rs2725264	C/T	Yes	83.7	8.2	21.5	chr4:89026109
rs4148156	C/T	Yes	nr	nr	nr	chr4:89026242
rs145932752	A/G	No	1.6	0.0	0.0	chr4:89026407
rs6831395	G/A	Yes	2.2	0.0	0.0	chr4:89026420
rs2725263	A/C	Yes	87.0	48.4	40.0	chr4:89026428
rs192562676	C/T	No	0.0	0.0	1.0	chr4:89026490
rs182159263	C/G	No	0.0	0.7	0.0	chr4:89026493
rs187527722	A/G	No	0.0	0.0	0.2	chr4:89026537
rs192781547	A/G	No	0.0	0.0	0.3	chr4:89026630
rs184709106	C/T	No	0.0	0.0	0.3	chr4:89026642
*1[5]	-	-	30.6	30.6	30.6	-
*2[5]	-	-	6.1	6.1	6.1	-
*3[5]	-	-	3.6	3.6	3.6	-

[1]Variant ID as either the rs number or haplotype ID

[2]Nucleotide change and conservation of the reference allele to the variant allele as obtained from the UCSC genome browser

[3]Frequency of minor allele (MAF) or haplotype (as a percent of all haplotypes) for African American (AA), European (EUR) and Asian (AS) populations

[4]Genomic location obtained from UCSC genome browser's hg19 build

[5]rs2725264/rs2725263(*1); rs58665233/rs2725263 (*2); rs58665233/rs2725263/rs2725264 (*3)

Abbreviations: nr, not reported

Table 5.12. SNPs in the ECR33 Enhancer

Variant ID[1]	Δnt[2]	Conserved[2]	Frequency[3]			Location[4]
			AA	EUR	AS	
rs34485575	A>-	Yes	nr	nr	nr	chr4:89028439
rs2231148	T>A	Yes	4.3	40.2	18.5	chr4:89028478
rs190738974	A>G	No	0.0	0.0	0.2	chr4:89028490
rs117761897	C>T	Yes	0.0	0.0	0.2	chr4:89028542
rs41282399	A>C	Yes	4.1	1.7	3.3	chr4:89028544
rs113647079	C>G	Yes	nr	nr	nr	chr4:89028578
rs2054576	A>G	Yes	1.2	7.9	25.0	chr4:89028775
rs151266026	T>C	No	0.0	0.0	0.7	chr4:89028935
rs183315559	G>A	No	0.0	0.0	0.3	chr4:89028979
rs189214307	C>T	No	0.0	0.0	0.3	chr4:89029111
rs2622628	A>C	Yes	45.5	4.4	20.8	chr4:89029252
rs36105707	->TTAAT	Yes	nr	nr	nr	chr4:89029304
rs141635727	A>G	No	0.4	0.0	0.0	chr4:89029335
rs190767980	C>T	No	0.0	0.0	0.0	chr4:89029361
rs147070185	G>A	No	0.0	0.0	0.2	chr4:89029364
*1[5]	-	-	3.6	3.6	3.6	-
*2[5]	-	-	2.9	2.9	2.9	-

[1]Variant ID as either the rs number or haplotype ID

[2]Nucleotide change and conservation of the reference allele to the variant allele as obtained from the UCSC genome browser

[3]Frequency of minor allele (MAF) or haplotype (as a percent of all haplotypes) for African American (AA), European (EUR) and Asian (AS) populations

[4]Genomic location obtained from UCSC genome browser's hg19 build

[5]rs412823991/rs2622628 (*1); rs2231148/rs117761897 (*2)

Abbreviations: nr, not reported

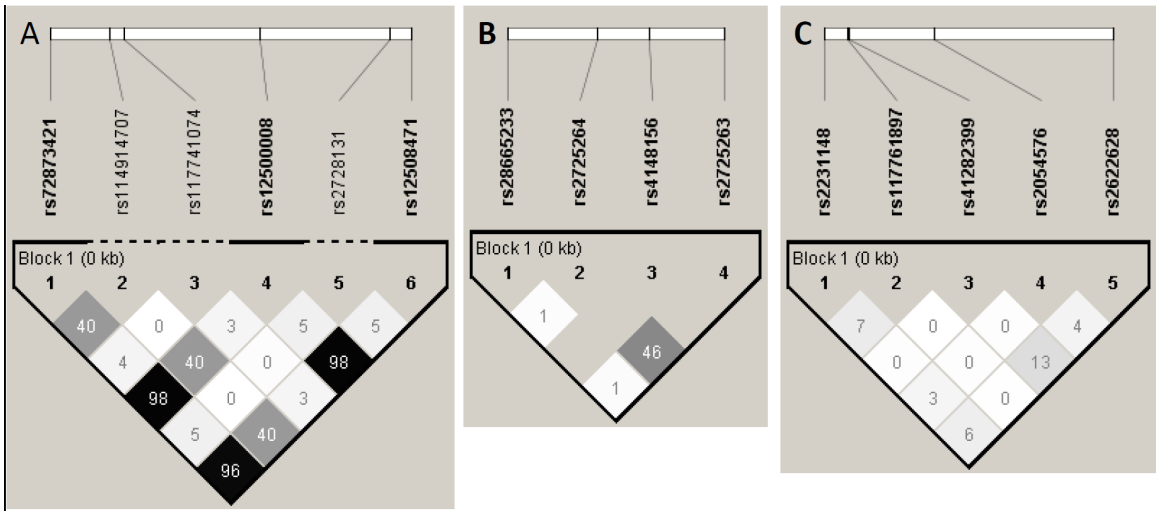

Figure 5.1. Linkage disequilibrium plots of SNPs in *ABCG2* locus enhancers. Plots show the degree of linkage disequilibrium (LD) of SNPs within ECR400 (A), ECR31 (B) and ECR33 (C). The top lane shows the rs numbers for the different SNPs within the region that were reported in any of the 1000 Genomes populations. The r^2 values between each SNP are in the box connecting the two SNPs, i.e., 98 implies $r^2 = 0.98$. Linkage disequilibrium is depicted by the shade of grey, with black being highly linked and white no linkage. LD plots were generated using Haploview v4.2 and incorporated genotype data from all available ethnic groups in the 1000 Genome database.

5.4.2. *Effect of SNPs on ECR44 In Vitro Activity*

All three SNPs in the ECR44 region (Table 5.7) were successfully mutated into the ECR44 enhancer plasmid and tested for their luciferase activity relative to reference ECR44 in HepG2 (Figure 5.2A) and HEK293T (Figure 5.2B) cell lines. rs138867860 caused a 1.3- to 1.5-fold increase in luciferase activity in both cell lines. The rs114916387 SNP had no effect in HepG2 cells, but it was increased by almost 1.5-fold above reference in HEK293T cells. The rs9999111 SNP was chosen for *in vivo* follow up because it displayed over an 80% reduction in activity compared to reference in HepG2 and HEK293T cells, respectively (Figure 5.2).

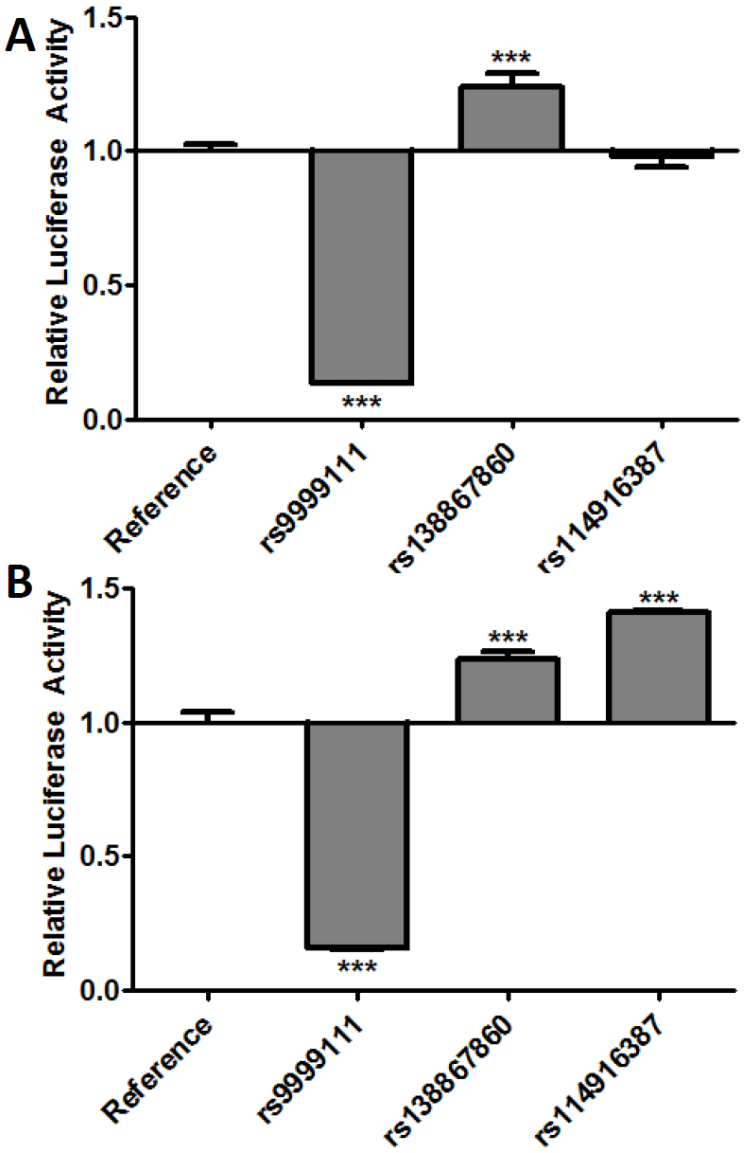

Figure 5.2. Effect of ECR44 genetic variants *in vitro*. The luciferase activity of ECR44 reference and variant enhancer regions was measured in transiently transfected a) liver (HepG2) and b) kidney (HEK293T/17) cell lines. Enhancer activity is expressed as the ratio of firefly to *Renilla* luciferase activity normalized to the reference enhancer activity (reference is set to 1). SNPs are displayed respective to their genomic orientation. Data is expressed as the mean ± SEM from a representative experiment with 4-5 wells per construct. Differences between reference and variant enhancers were tested by an ANOVA followed by a post-hoc Bonferroni's multiple comparison *t*-test; *** $P < 0.0001$.

5.4.3. *Effect of SNPs on ECR400 In Vitro Activity*

Seven SNPs in the ECR400 enhancer and the ECR400*1 haplotype (Table 5.8) were successfully mutated into the ECR400 enhancer plasmid and tested for their luciferase activity relative to reference in HepG2 (Figure 5.3A) and HEK293T (Figure 5.3B) cell lines. Three SNPs caused an increased activity in both cell lines: rs72873421, rs117741074 and rs78901673. rs72873421 caused the highest increase (>2-fold) in enhancer activity relative to the reference sequence. The fifth SNP, significant in both cell lines, was rs12508471, which had almost a complete loss of activity in HepG2 (Figure 5.3A) and HEK293T (Figure 5.3B) cells. The rs72873421/rs12500008/rs12508471 (ECR400*1) haplotype did not have a significant effect in HepG2 cells, but resulted in a 75% reduction of enhancer activity in the HEK293T cell line. Of the four SNPs that significantly altered the ECR400 enhancer activity in both cell lines, two of them, rs72873421 and rs12508471, were chosen for *in vivo* validation.

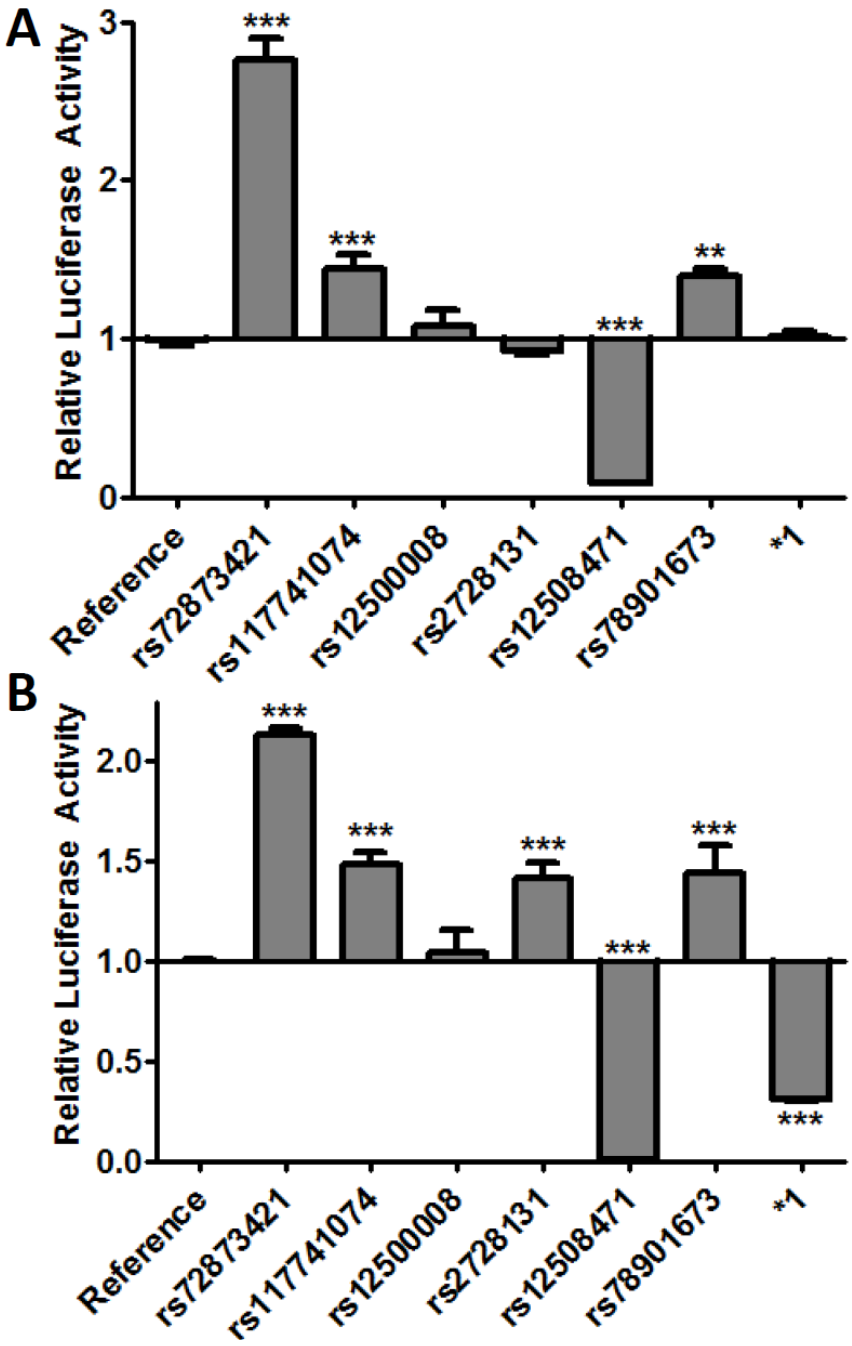

Figure 5.3. Effect of ECR400 genetic variants *in vitro*. The luciferase activity of ECR400 reference and variant enhancer regions was measured in transiently transfected A) liver (HepG2) and B) kidney (HEK293T/17) cells. Enhancer activity is expressed as the ratio of the firefly to *Renilla* luciferase activity normalized to the reference plasmid (reference is set to 1). SNPs are displayed respective to their genomic orientation. The

rs72873421/rs12500008/rs12508471 haplotype is labeled *1. Data is expressed as the mean ± SEM from a representative experiment with 4-6 wells per construct. Differences between reference and variant enhancers were tested by an ANOVA followed by a post-hoc Bonferroni's multiple comparison *t*-test; ** $P < 0.001$, *** $P < 0.0001$.

5.4.4. *Effect of SNPs on ECR423 In Vitro Activity*

All nine SNPs in the ECR423 enhancer (Table 5.9) were successfully introduced into the ECR423 enhancer plasmid and screened for their luciferase activity in HepG2 (Figure 5.4A) and HEK293T (Figure 5.4B) cell lines. Seven of the nine SNPs caused relatively small but significant increases in enhancer activity relative to the reference sequence in both cell lines. Three of these SNPs rs62309980, rs777538297 and rs35696062 had 1.5- to 2-fold increases in activity in both cell lines. The only SNP that led to a decrease in enhancer activity was rs149713212. It was associated with an ~90% reduction in enhancer activity in HepG2 (Figure 5.4A) and HEK293T (Figure 5.4B) cell lines. The ability of the rs149713212 SNP to decrease the enhancer activity of the ECR423 enhancer led to its selection for *in vivo* validation.

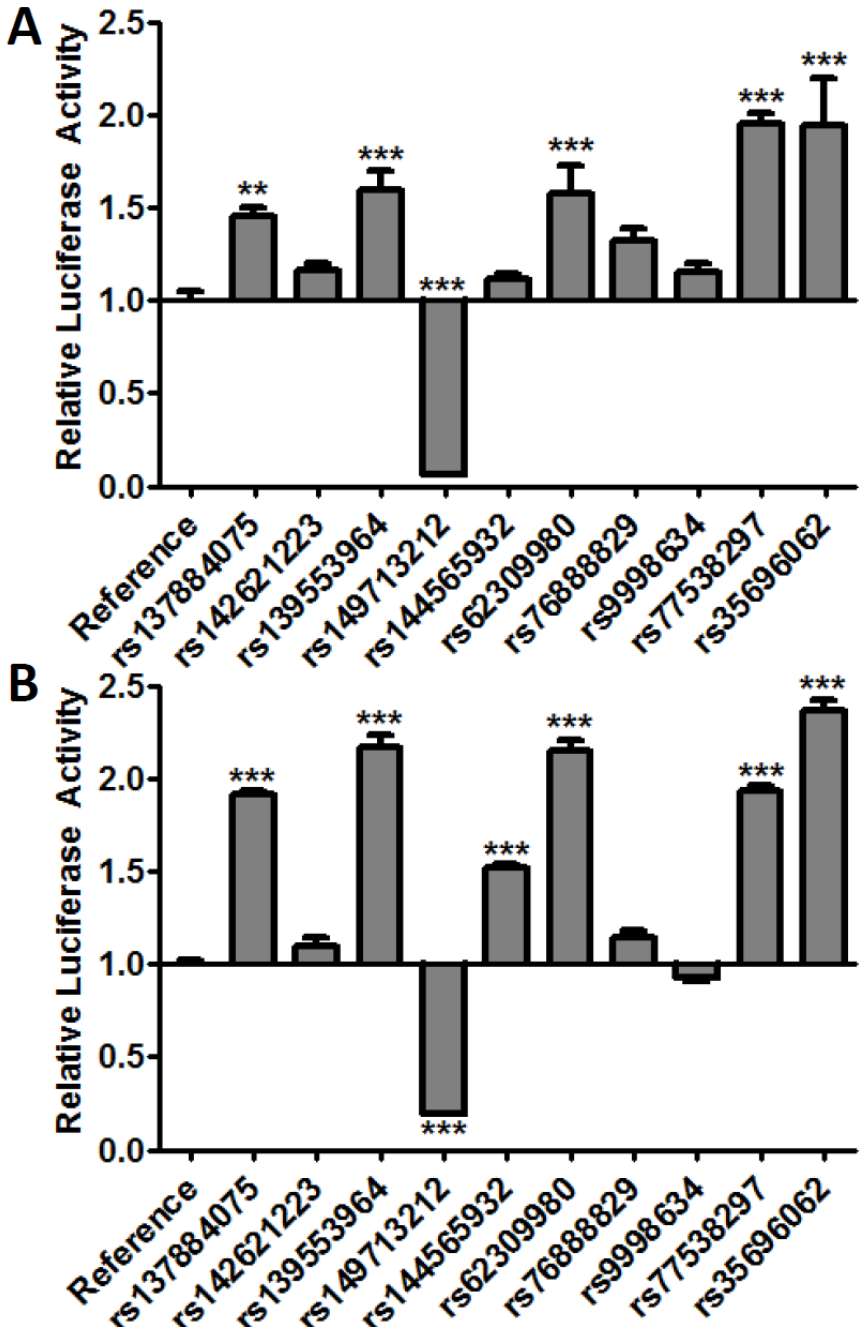

Figure 5.4. Effect of ECR423 genetic variants *in vitro*. The luciferase activity of ECR423 reference and variant enhancer regions was measured in transiently transfected A) liver (HepG2) and B) kidney (HEK293T/17) cell lines. Enhancer activity is expressed as the ratio of firefly to *Renilla* luciferase activity normalized to the reference vector activity (reference is set to 1). SNPs are displayed respective to their genomic orientation.

Data is expressed as the mean ± SEM from a representative experiment with 3-5 wells per construct. Differences between reference and variant enhancers were tested by an ANOVA followed by a post-hoc Bonferroni's multiple comparison *t*-test; ** $P < 0.001$, *** $P < 0.0001$.

5.4.5. *Effect of SNPs on CR6 In Vitro Activity*

All eight SNPs in the CR6 enhancer (Table 5.10) were successfully introduced into the CR6 enhancer plasmid and screened for enhancer activity in HepG2 (Figure 5.5A) and HEK293T (Figure 5.5B) cell lines. Four of the SNPs, rs573519157, rs5883021, rs45510401 and rs190754327, caused small but significant decreases in relative enhancer activity in both cell lines. The most detrimental was rs573519157, which led to a 25-50% reduction in relative luciferase activity in both cell lines. The only SNP to cause a significant increase in enhancer activity was rs183322988, which increased relative enhancer activity by 1.5-fold in both cell lines. Since CR6 was only a weak *in vivo* enhancer (Figure 4.11) only rs183322988 SNP, which enhanced activity, was chosen for *in vivo* validation.

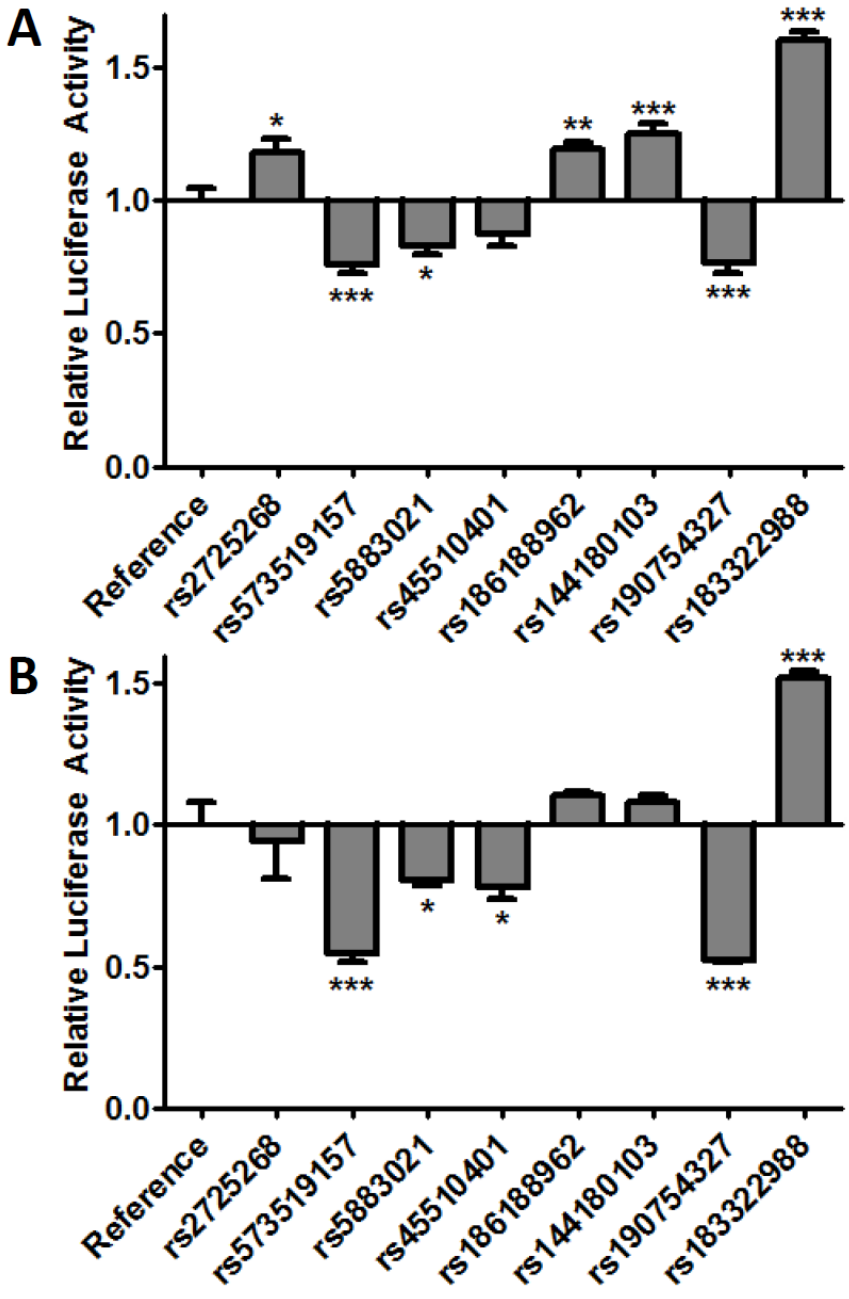

Figure 5.5. Effect of CR6 genetic variants *in vitro*. The luciferase activity of CR6 reference and variant enhancer regions was measured in transiently transfected A) liver (HepG2) and B) kidney (HEK293T/17) cell lines. Enhancer activity is expressed as the ratio of firefly to *Renilla* luciferase activity normalized to the reference vector activity (reference is set to 1). SNPs are displayed respective to their genomic orientation. Data is

expressed as the mean ± SEM of a representative experiment with 4-6 wells per construct. Differences between reference and variant enhancers were tested by an ANOVA followed by a post-hoc Bonferroni's multiple comparison *t*-test; * $P < 0.05$, ** $P < 0.001$, *** $P < 0.0001$.

5.4.6. *Effect of SNPs on ECR31 In Vitro Activity*

All thirteen SNPs in the ECR31 enhancer and the ECR31*1 haplotype (Table 5.11) were successfully introduced into the ECR31 enhancer construct and screened for enhancer activity in HepG2 (Figure 5.6A) and HEK293T (Figure 5.6B) cell lines. Only rs2725263 and rs2725264 had a significant effect on enhancer activity in HepG2 cells (Figure 5.6A); they both caused over a 1.3-fold increase in relative luciferase activity. These SNPs had similar increases in enhancer function in HEK293T cells. Interestingly, the ECR31*1 haplotype, a combination of both rs2725263 and rs2725264, did not affect enhancer activity. Three other SNPs, rs139101431, rs144062279 and rs184709106, also had modest increases in enhancer activity in the HEK293T cell line (Figure 5.6B). Only rs2725263 was chosen for *in vivo* follow-up because it had a more consistent increase in enhancer function than the rs2725264 SNP.

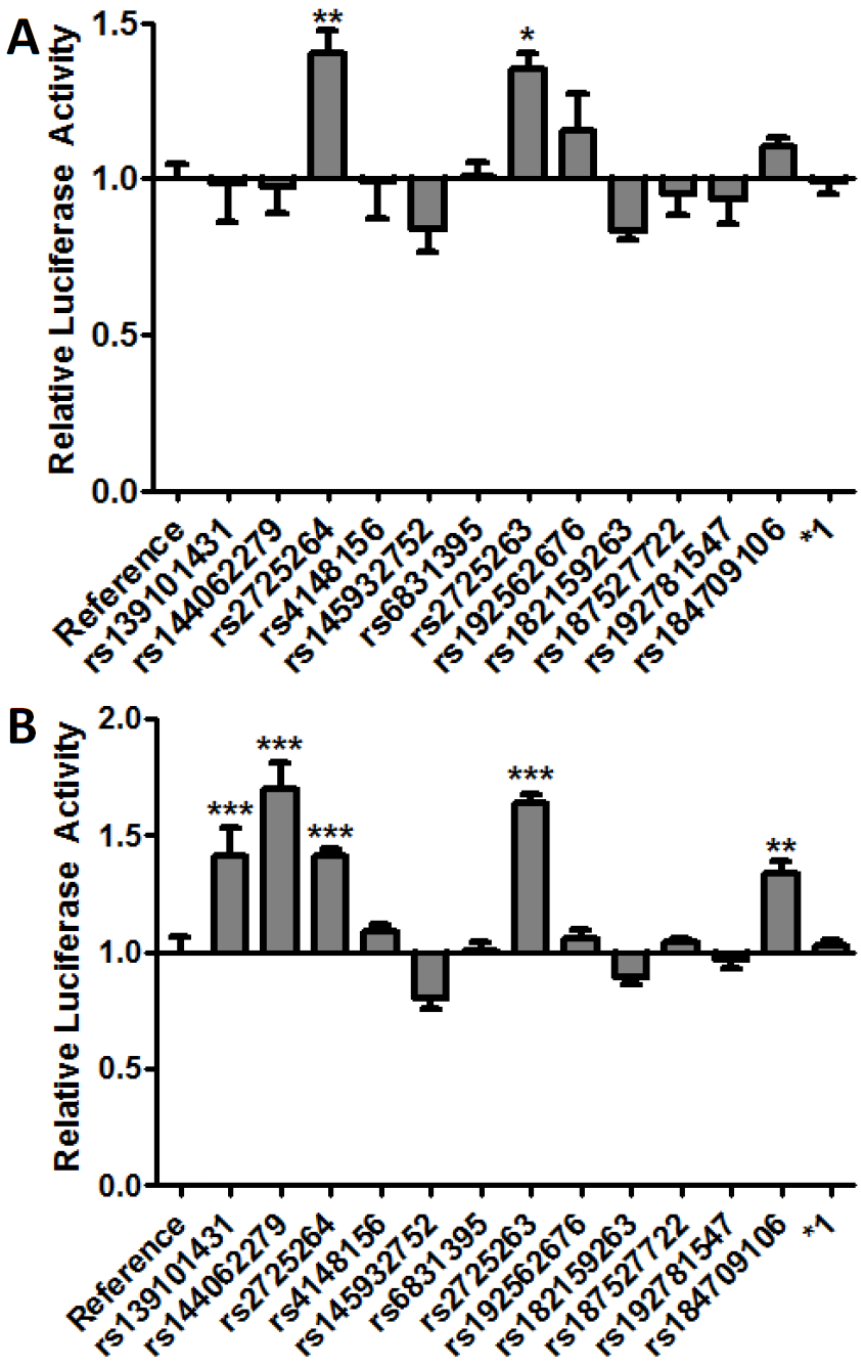

Figure 5.6. Effect of ECR31 genetic variants *in vitro*. The luciferase activity of ECR31 reference and variant enhancer regions was measured in transiently transfected A) liver (HepG2) and B) kidney (HEK293T/17) cell lines. Enhancer activity is expressed as the ratio of firefly to *Renilla* luciferase activity normalized to the reference vector activity (reference is set to 1). SNPs are displayed respective to their genomic orientation. The

rs2725263/rs2725264 haplotype is labeled *1. Data is expressed as the mean ± SEM of a representative experiment with 4-6 wells per construct. Differences between reference and variant enhancers were tested by an ANOVA followed by a post-hoc Bonferroni's multiple comparison *t*-test; * $P < 0.05$, ** $P < 0.001$, *** $P < 0.0001$.

5.4.7. *Effect of SNPs on ECR33 In Vitro Activity*

All fourteen SNPs in the ECR33 enhancer and the ECR33*1 haplotype (Table 5.12) were successfully introduced into the ECR31 enhancer construct and screened for enhancer activity in HepG2 (Figure 5.7A) and HEK293T (Figure 5.7B) cell lines. Three SNPs caused significantly increased enhancer activity in both cell lines. rs41282399 had only a slight 1.3- to 1.5-fold increase in function. The other two SNPs, rs190738974 and rs36105707, both had 1.5- to 2-fold increase in enhancer activity which was replicated in the HEK293T cell line. Four additional SNPs, rs2231148, rs117761897, rs151266026 and rs2622628, had decreased enhancer activity in the HEK293T cells, ranging from 25% to 50% reduction. The increased activity of SNP rs41282399 was balanced by the decreased activity of the rs2622628 in the ECR33*1 haplotype in HepG2 cells, but not in the HEK293T cells, where ECR33*1 still had significantly increased activity relative to reference. The only SNP that was chosen for *in vivo* follow-up was the rs190738974; it was chosen over the rs36105707 SNP based on predicted changes in TFBS (Table 5.12).

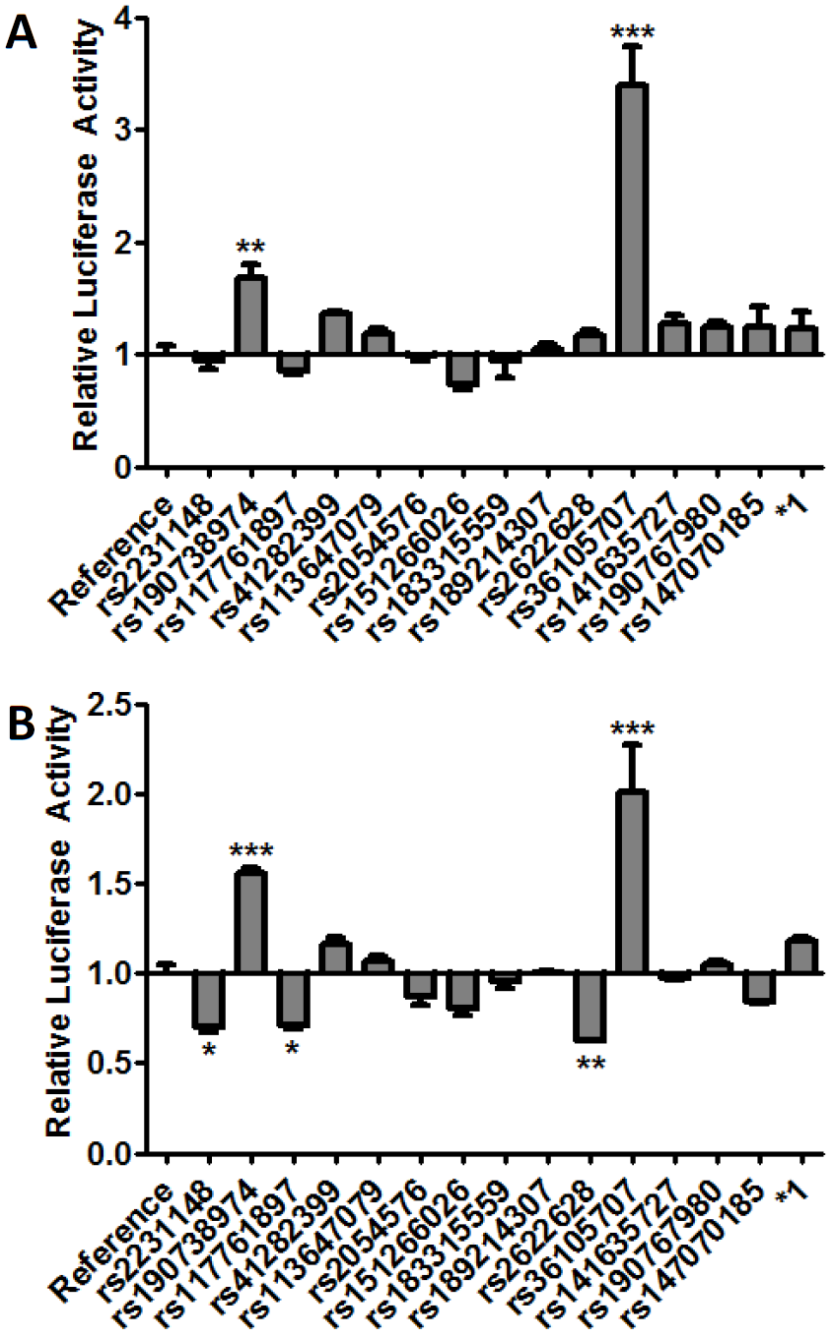

Figure 5.7. Effect of ECR33 genetic variants *in vitro*. The luciferase activity of ECR33 reference and variant enhancer regions was measured in transiently transfected A) liver (HepG2) and B) kidney (HEK293T/17) cell lines. Enhancer activity is expressed as the ratio of firefly to *Renilla* luciferase activity normalized to the reference vector activity (reference is set to 1). SNPs are displayed respective to their genomic orientation. The

rs412823991/rs2622628 haplotype is labeled *1. Data is expressed as the mean ± SEM of a representative experiment with 4-6 wells per construct. Differences between reference and variant enhancers were tested by an ANOVA followed by a post-hoc Bonferroni's multiple comparison *t*-test; * $P < 0.05$, ** $P < 0.001$, *** $P < 0.0001$.

5.4.8. *Effect of SNPs on Enhancer Activity In Vivo*

Seven SNPs were screened for their effect on *in vivo* liver enhancers using the hydrodynamic tail vein injection assay. Four of the seven SNPs resulted in decreased enhancer activity compared to their respective reference enhancer (Figure 5.8). SNP rs9999111 decreased ECR44 enhancer activity by 70% (Figure 5.8, $P < 0.05$), consistent with *in vitro* results (Figure 5.2). SNP rs72873421 decreased the enhancer activity of ECR400 by ~50% *in vivo* but a high level of enhancer activity was still associated with this region (Figure 5.8, $P < 0.05$); *in vitro* this SNP increased the activity of ECR400 in both HepG2 and HEK293T (Figure 5.3) cell lines. The ECR400 SNP rs12508471 resulted in an almost complete loss of enhancer activity (Figure 5.8, $P < 0.0001$), consistent with the complete loss of ECR400 enhancer activity in HepG2 and HEK293T cells transfected with this variant enhancer sequence (Figure 5.3). The ECR423 SNP rs149713212 also led to a complete loss of enhancer activity *in vivo* (Figure 5.8, $P < 0.001$) consistent with its effect *in vitro* (Figure 5.4). The only SNP to increase enhancer activity *in vivo* was the ECR31 SNP rs2725263 (Figure 5.8). This SNP increased the ECR31 *in vivo* enhancer activity by 1.5- fold (Figure 5.8, $P < 0.05$), which was consistent with its effect *in vitro* (Figure 5.6). The CR6 SNP rs183322988 and ECR33 SNP rs190738974 had no effect on enhancer activity *in vivo*.

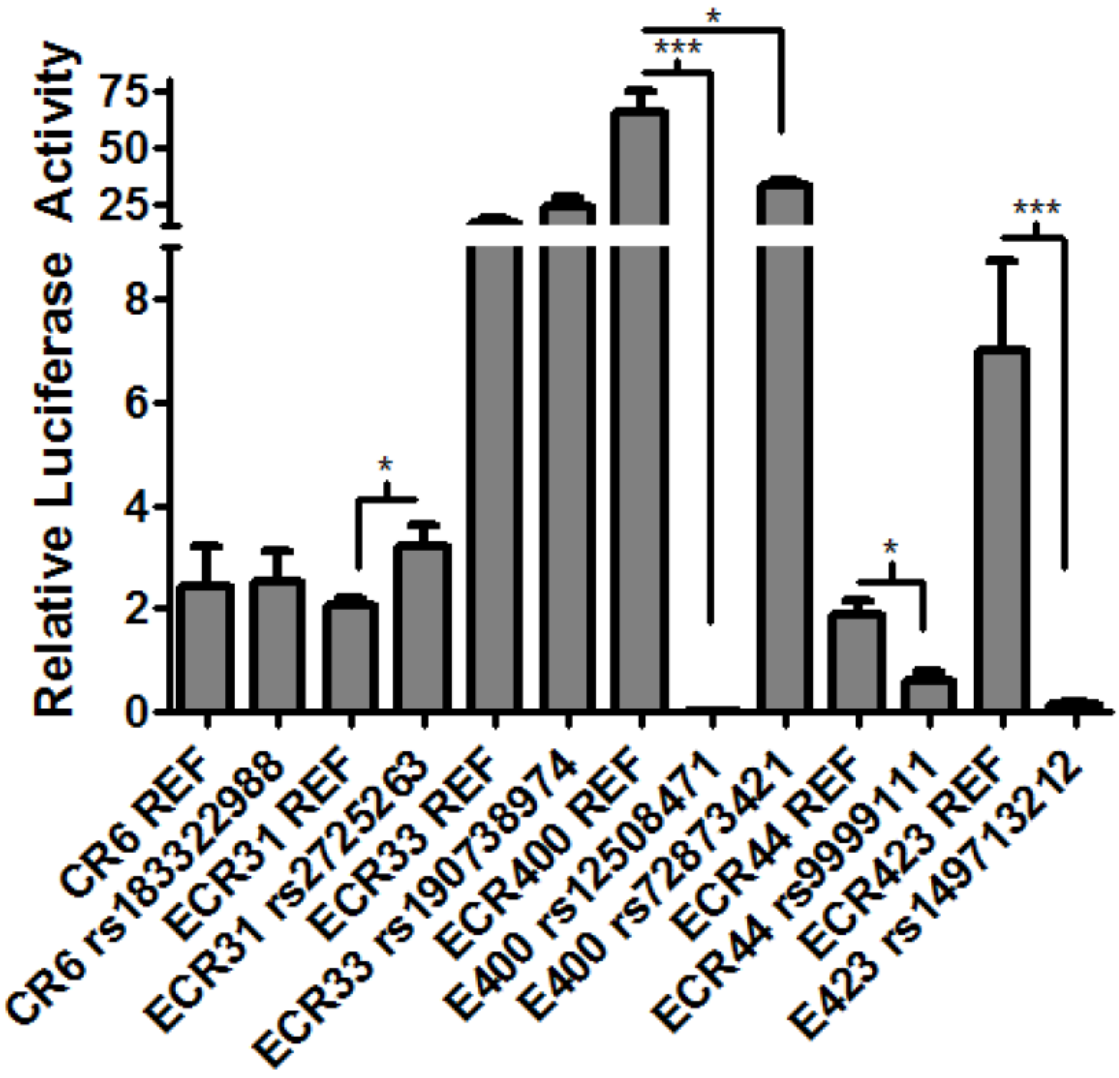

Figure 5.8. *In vivo* liver enhancer activity of *ABCG2* locus variants. The luciferase activity in mouse liver homogenates was measured 24 hr after plasmid injection. Enhancer activity is expressed as the ratio of firefly to *Renilla* luciferase activity normalized to the empty vector activity. SNPs are displayed respective to their genomic orientation. Data is expressed as the mean ± SEM for 4-5 mice. Differences between reference and variant enhancer elements were tested by an unpaired Student's *t*-test; * $P < 0.05$, *** $P < 0.0001$.

5.4.9. *Associations of SNPs with mRNA Expression Levels*

SNPs that showed an effect on *in vivo* liver enhancer activity were tested for their association with expression levels of ABCG2, PKD2 and PPM1K in human liver, kidney, breast, LCLs, T-cell, adipose and skin cells. Genotype and expression data were collected both from tissues analyzed by the PMT group and from previously published literature (Schadt[51], TCGA[52], MuTHER[54], GenCord[60] and Stranger[56]). Since many of the ECRs are in low-coverage areas for sequencing, they are not included in genotyping platforms. Therefore, when possible we utilized linkage disequilibrium from 1000 Genomes to impute genotypes for missing SNPs.

The ECR44 SNP rs9999111 was tested for association with ABCG2 expression in the PMT liver and kidney tissues and, after correction for sex, was associated with decreased expression of ABCG2 in kidney tissues ($P = 0.05$; β=1.814, Figure 5.9B) but had no association with ABCG2 expression in the liver samples. ABCG2 expression was also not correlated with rs9999111 in the Schadt[51] liver tissues (data not shown). However, rs9999111 was significantly associated with lower ABCG2 expression in LCLs and T-cells from the GenCord[60] tissues (Figure 5.9 C and D). Due to the low frequency of rs9999111, very few samples were homozygous for this SNP. Additionally, there were only 52 kidney PMT tissues; therefore follow-up in a cohort with more kidney tissues could help clarify the association of this SNP with ABCG2 expression in kidney.

The three SNPs from ECR400, rs12500008, rs12508471 and rs72873421, are in almost perfect LD (r^2=0.96-0.98, Figure 5.1) and occur together as the ECR400*1 haplotype (Table 5.8). The ECR400*1 haplotype was associated with lower ABCG2 expression in LCLs of Chinese (CHB, rho = 0.251, $P = 0.025$; Figure 5.10A) and trended

toward significance with ABCG2 expression in the Kenyan population (LWK, rho = 0.181, *P* = 0.1; Figure 5.10A). ECR400*1 was also associated with lower PPM1K expression in adipose (rho=0.2, *P*=0.015; Figure 5.10B) and skin (rho=0.32, *P*=0.005; Figure 5.10C). ECR400*1 was also associated with lower PPM1K expression in LCLs using two probes for the PPM1K mRNA (rho=0.22, *P*=0.06 and rho=0.22, *P*=0.47; Figure 5.10D). All ECR400*1 associations with PPM1K and ABCG2 had similar effect sizes (rho ~ 0.25).

There where two SNPs in ECR31 tested for correlation with gene expression in tissues, both the rs2725263 and rs2725264. These two SNPs have a modest linkage disequilibrium of $r^2 = 0.46$ (Figure 5.1), occur together in the ECR31*1 haplotype and both have high minor allele frequencies (Table 5.11). The rs2725263 SNP trended toward significance when associated with PPM1K expression in TCGA[52] breast tissues (*P* = 0.07, β = -0.22; Figure 5.11A) and PKD2 in the Schadt[51] liver tissues (*P* = 0.066, β = -0.07; Figure 5.11B). Additionally, the rs2725264 SNP trended toward significance when associated with PKD2 in the Schadt livers (*P* = 0.057, β = -0.05; Figure 5.12). Neither SNP was associated with ABCG2 expression in any of the tissue sets (data not shown).

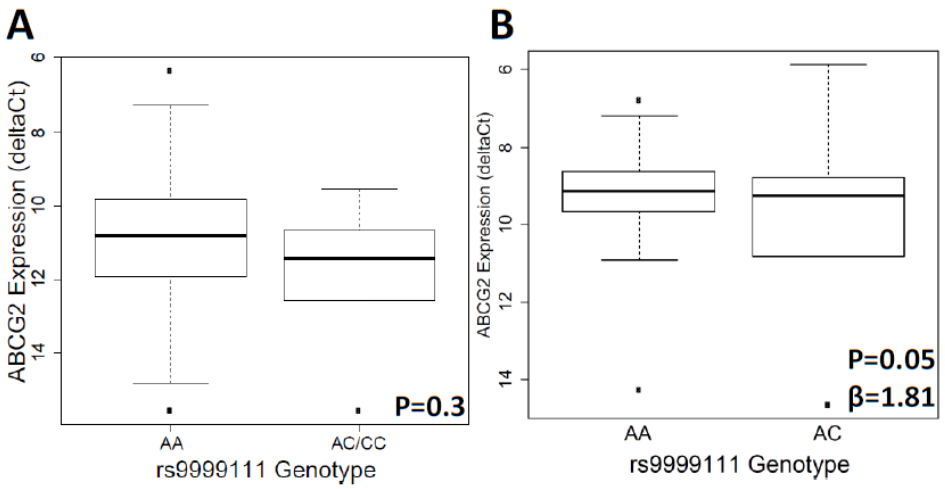
A
ABCG2 Expression (deltaCt)
6
8
10
12
14
P=0.3
AA
AC/CC
rs9999111 Genotype
B
ABCG2 Expression (deltaCt)
6
8
10
12
14
P=0.05
β=1.81
AA
AC
rs9999111 Genotype

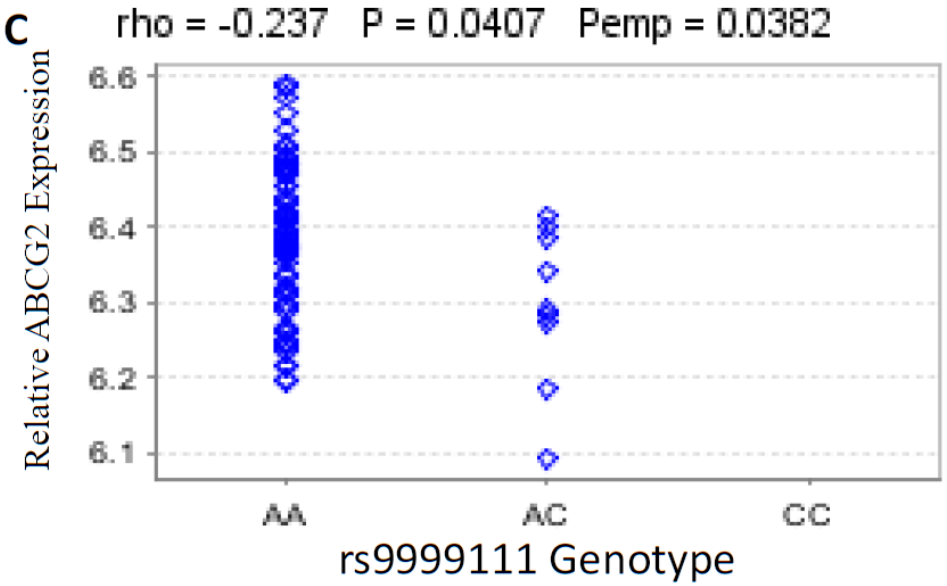
C
rho = -0.237 P = 0.0407 Pemp = 0.0382
Relative ABCG2 Expression
6.6
6.5
6.4
6.3
6.2
6.1
AA
AC
CC
rs9999111 Genotype

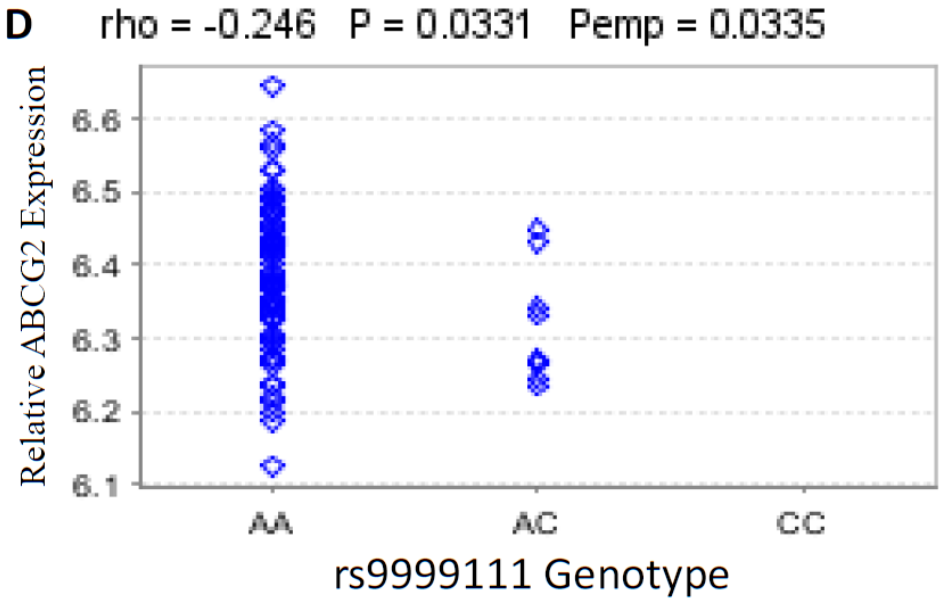
D
rho = -0.246 P = 0.0331 Pemp = 0.0335
Relative ABCG2 Expression
6.6
6.5
6.4
6.3
6.2
6.1
AA
AC
CC
rs9999111 Genotype

Figure 5.9. Association of rs9999111 with ABCG2 expression. Association of the ECR44 SNP rs9999111 with ABCG2 mRNA expression in (A) human livers and (B) kidneys from PMT, and in (C) lymphocytes and (D) T-Cells from GenCord[60]. Analysis on PMT livers and kidneys were done using a linear regression on imputed genotypes versus ABCG2 expression (ΔCT) after correcting for sex. Lymphocyte and T-Cell analysis was done using the GeneVar[53] program as described in the *Materials and Methods* section with a linear regression and are displayed as ABCG2 expression (ΔCT) versus rs9999111 genotype with rho (correlation coefficient), *P* value (P) and empirical *P* value (Pemp) indicated.

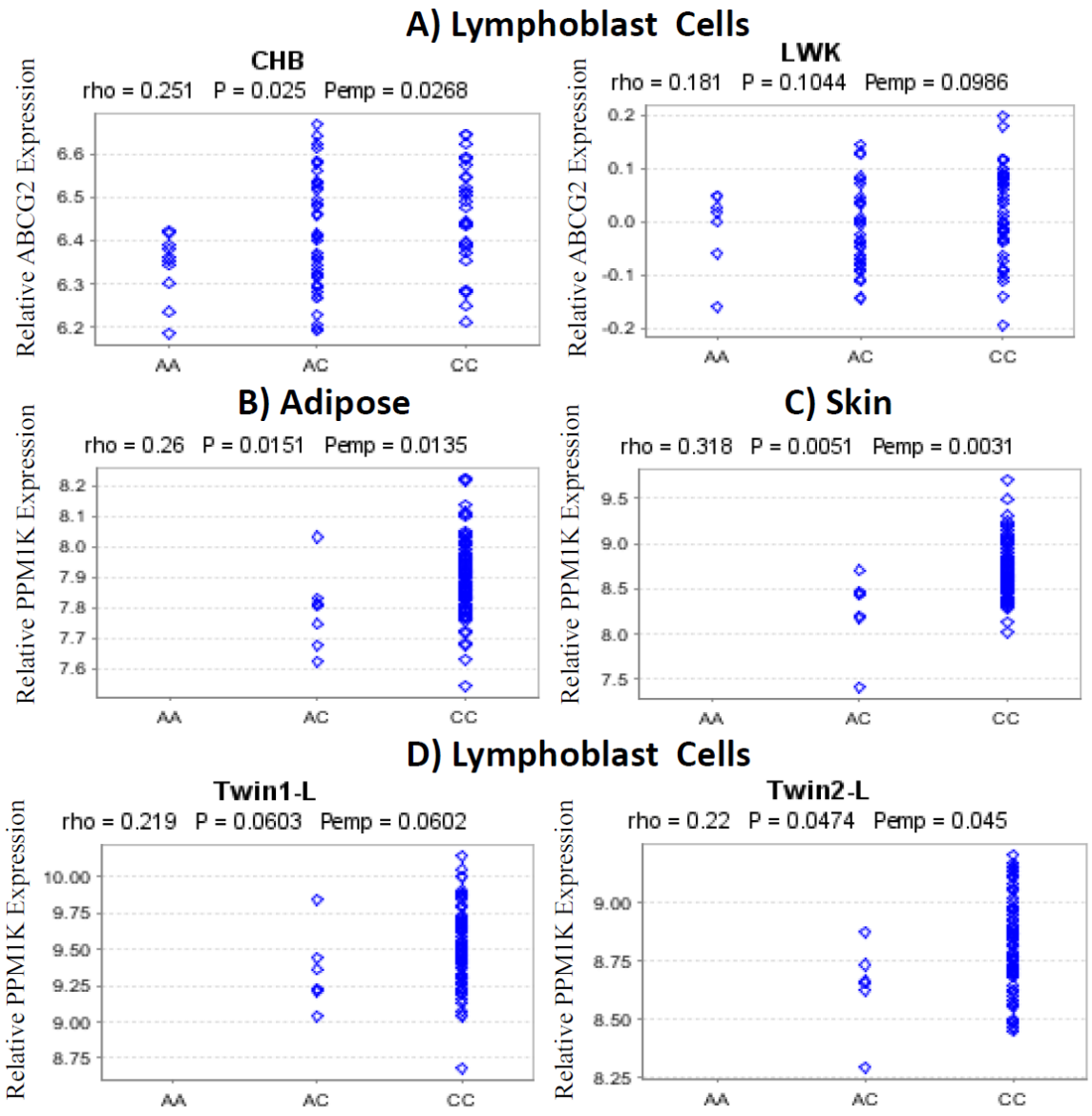

Figure 5.10. Association of rs12500008 with gene expression. Association of the ECR400 SNP rs12500008 with ABCG2 mRNA expression in (A) HapMap LCLs of Han Chinese (CHB) and Kenyan (LWK) from the Stranger study[57]; and with PPM1K in (B) adipose, (C) skin and (D) LCLs (two probes) from the MuTHER study[54]. Analysis was done using the GeneVar[53] program as described in *Materials and Methods* with a linear regression and are displayed as gene expression versus rs12500008 genotype with rho (correlation coefficient), *P* value (P) and empirical *P* value (Pemp) indicated.

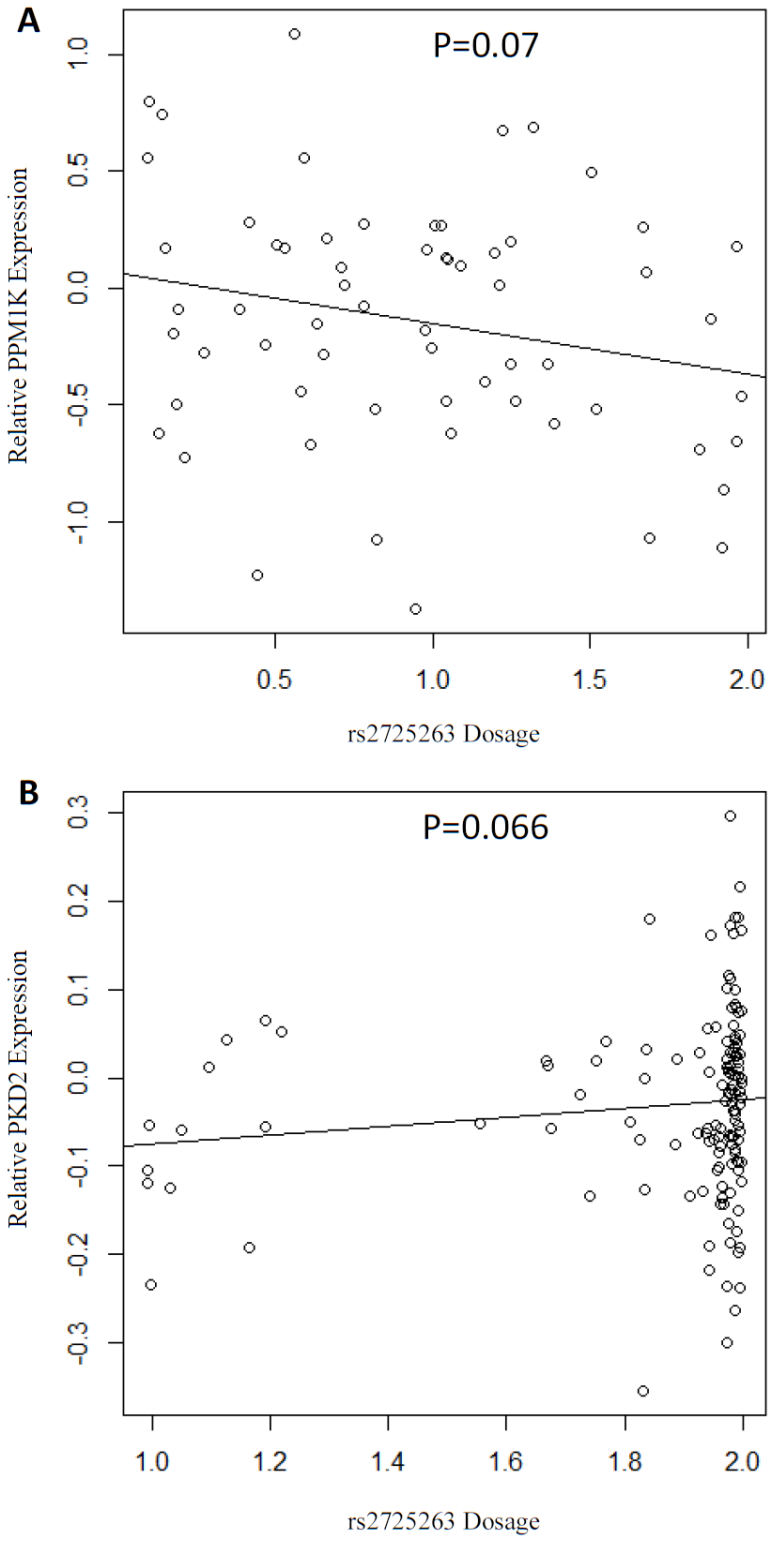

Figure 5.11. Association of rs2725263 with PPM1K and PKD2 expression. Trend for the association of ECR31 rs2725263 with mRNA expression of (A) PPM1K in human

breast tissue from TCGA network[52] and with (B) PKD2 in human liver from Schadt[51]. Analysis was done using a linear regression as described in *Materials and Methods*, and data is displayed as gene expression versus the dosage of rs2725263 with *P* value (P) indicated.

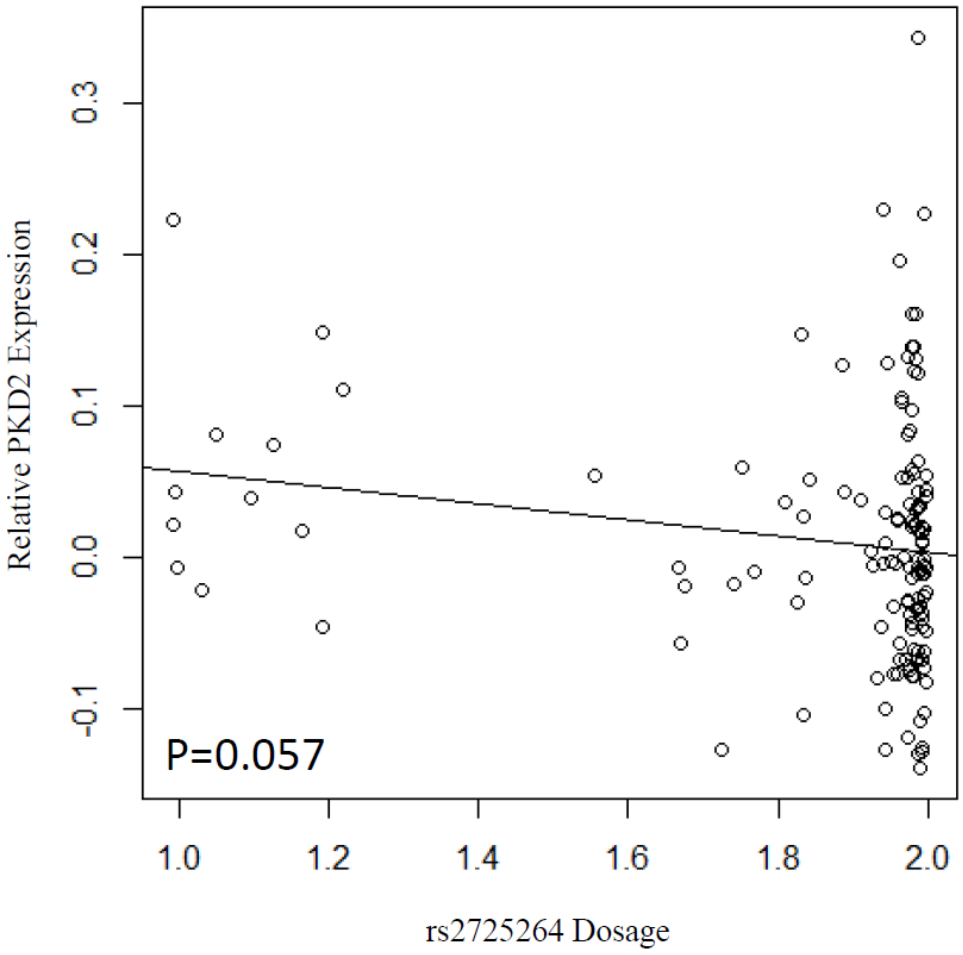

Figure 5.12. Association of rs2725264 with *PKD2* liver expression. Trend for the association of ECR31 rs2725264 with mRNA expression of *PKD2* in human liver from Schadt[51]. Analysis was done using a linear regression as described in *Materials and Methods*, and data is displayed as gene expression versus the dosage of rs2725264 with *P* value (P) indicated.

5.4.10. *Predicted Alterations in TFBS by SNPs*

Functional effects of SNPs on enhancer activity were assessed using TFBS predictions on both the reference and enhancer sequences using ConSite and TRANSFAC Match programs (Figure 5.13Figure 5.17). The ECR44 rs9999111 SNP, which decreased *in vivo* (Figure 5.8) and *in vitro* (Figure 5.2) activity of the ECR44 enhancer, had predicted losses in TFBS for HFH-2, Gfi, HNF-3β and RXR-VDR (Figure 5.13).

The ECR400 SNP rs12508471 was the most detrimental SNP, decreasing ECR400 enhancer activity both *in vitro* (Figure 5.3) and *in vivo* (Figure 5.8). There were no predicted changes in TFBS between the rs12508471 and ECR400 reference sequence using ConSite. However, the TRANSFAC MATCH program predicted gains for the rs12508471 sequence in PPAR (direct repeat 1), GR, SREBP, p300, VDR and PXR, none of which were predicted to bind to the reference ECR400 with a greater than 0.6 core matrix match score (Figure 5.15). The ECR400 rs72873421 SNP, which had a loss of function *in vivo* (Figure 5.8), had predicted gains for PPARγ-RXRα, COUP-TF and HLF binding probabilities (Figure 5.14). It also had predicted losses for SPI-1, SPI-B and CREB binding (Figure 5.14).

The ECR423 SNP rs149713212 was the second most detrimental SNP, decreasing ECR423 activity both *in vitro* (Figure 5.4) and *in vivo* (Figure 5.8). For rs149713212, ConSite predicted gains in TF binding probability for GATA-1, 2&3, RREB-1 and PPARγ-RXRα (Figure 5.16). The ECR31 SNP rs2725263 increased ECR31 activity both *in vitro* (Figure 5.6) and *in vivo* (Figure 5.8). TFBS predictions show gains in binding for hepatic TFs HNF-3β, HFH-1 and HFH-2, as well as for the general TFs AP2α, CREB

and GATA-3 (Figure 5.17). Although many other SNPs in the high priority ECRs were predicted to result in TFBS changes (data not shown), none of those SNPs were screened for their effect on *in vivo* enhancer activity due to their low impact on *in vitro* enhancer activity.

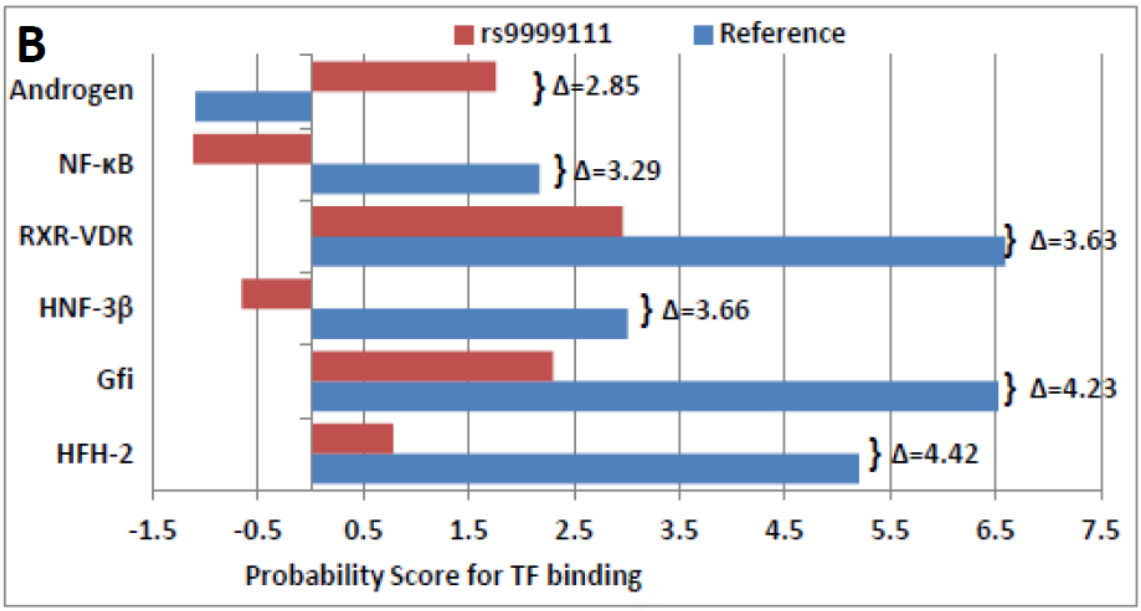

Figure 5.13. Predicted TFBS changes for ECR44 rs9999111. (A) Sequence alignments for reference and variant ECR44 as determined by ConSite indicate TFBS that are lost (above alignment) or gained (below alignment) and (B) the binding probabilities for reference (blue) and SNP (red) sequences. The absolute change in binding probabilities for each TF, between reference and variant sequences, are indicated.

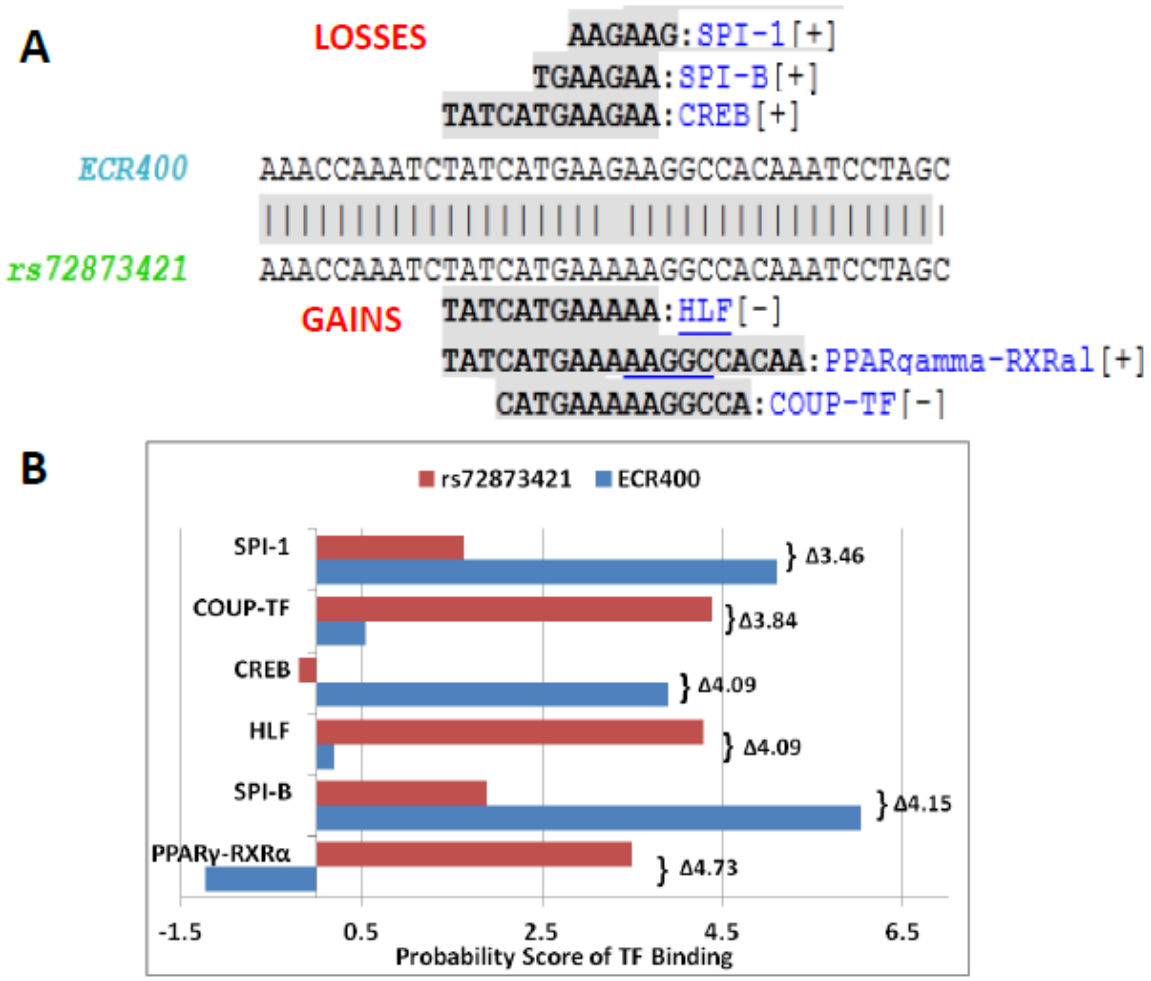

Figure 5.14. Predicted TFBS changes for ECR400 rs72873421. (A) Sequence alignments for reference and variant ECR400 as determined by ConSite indicate TFBS that are lost (above alignment) or gained (below alignment) and (B) the binding probabilities for reference (blue) and SNP (red) sequences. The absolute change in binding probabilities, between reference and variant sequences, for each TF are indicated.

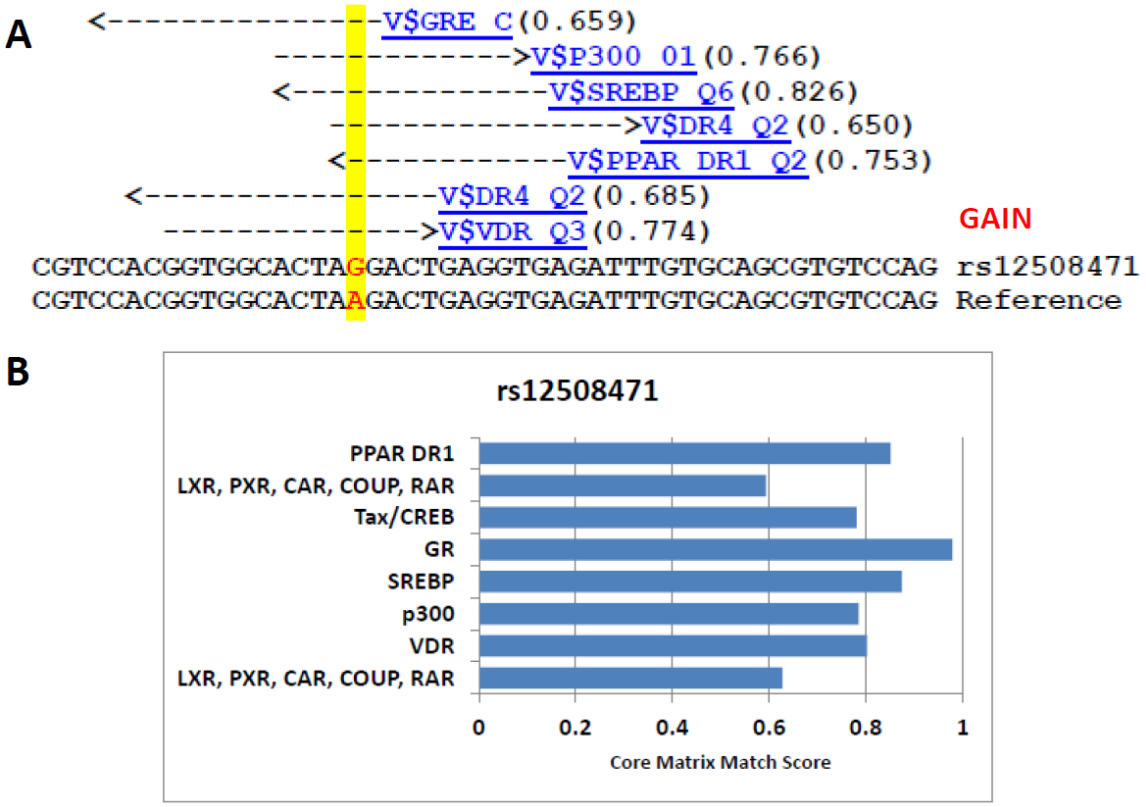

Figure 5.15. Predicted TFBS changes for ECR400 rs12508471. (A) Sequence alignments of reference and variant ECR400 as determined by TRANSFAC indicate TFBS that are gained above alignment and (B) the binding probabilities for variant sequence (blue). None of these TFs had predicted binding for the reference sequence.

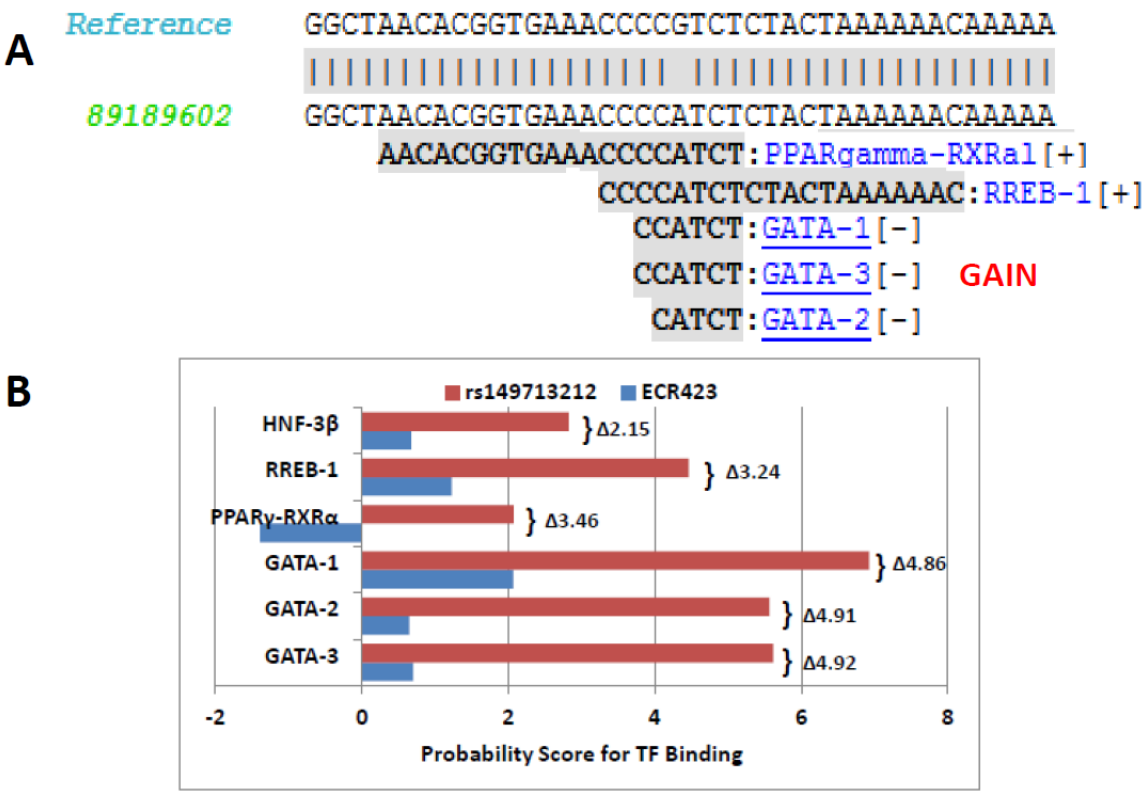

Figure 5.16. Predicted TFBS changes for ECR423 rs149713212. (A) Sequence alignments of reference and variant ECR423 as determined by ConSite indicate TFBS that are gained (below alignment) and (B) the binding probabilities for reference (blue) and SNP (red) sequences. The absolute change in binding probabilities, between reference and variant sequences, for each TF are indicated.

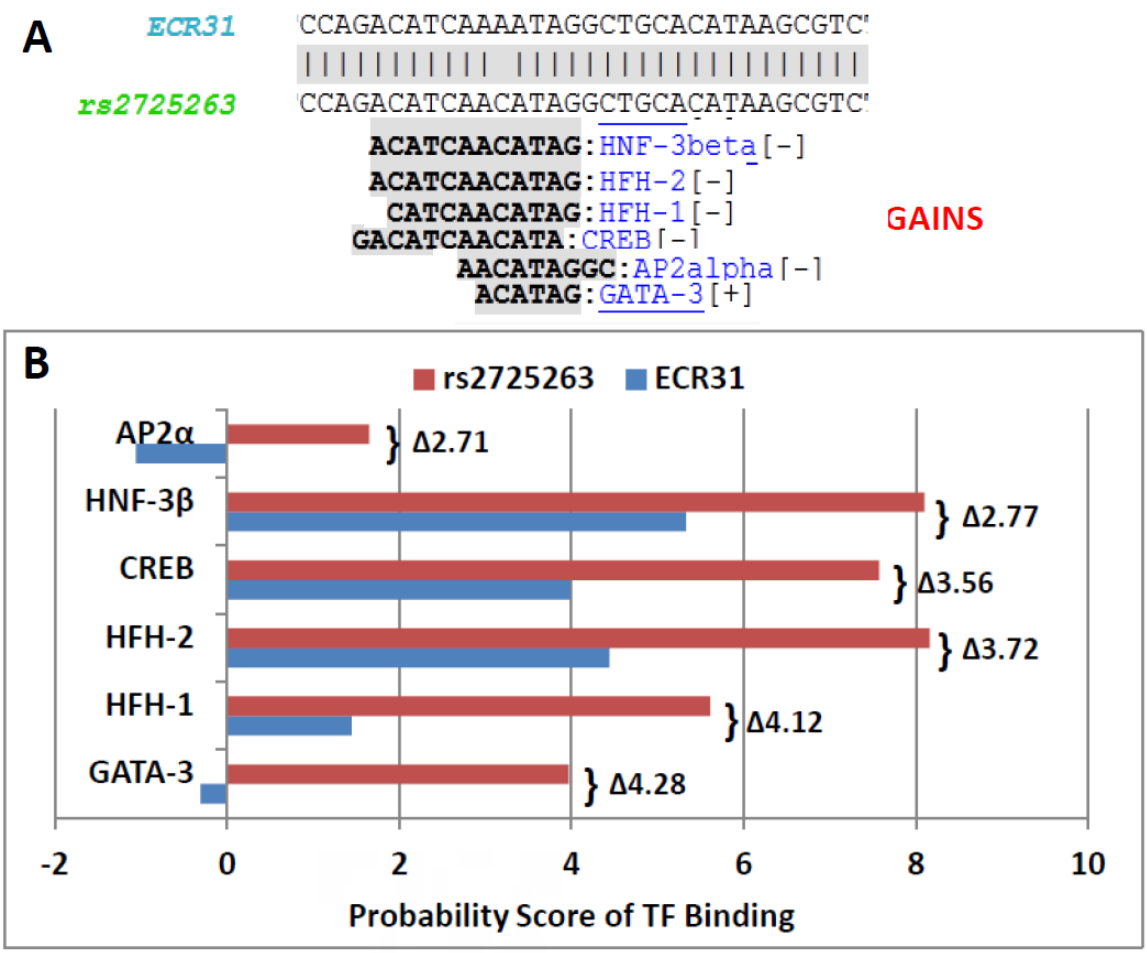

Figure 5.17. Predicted TFBS changes for ECR31 rs2725263. (A) Sequence alignments of reference and variant ECR31 as determined by ConSite indicate TFBS that are gained (below alignment) and (B) the binding probabilities for reference (blue) and SNP (red) sequences. The absolute change in binding probabilities, between reference and variant sequences, for each TF are indicated.

5.5. Discussion

Although non-coding SNPs in the *ABCG2* gene locus have been correlated with drug response[61] and disease progression[62], relatively few have been correlated with gene

expression[18,61] and none have confirmed mechanisms of action. Recent studies on other ADME genes have identified SNPs in *cis*-regulatory regions that are responsible for altering the expression of the gene and contributing to adverse drug effects[29,63,64].

Following a previous *cis*-regulatory screen (see Chapter 4) which identified six *in vivo* liver enhancers in the *ABCG2* gene locus, the *in vitro* and *in vivo* effect of SNPs on enhancer activity was evaluated. There were 54 SNPs throughout the six enhancer regions. After screening these SNPs for their effect on enhancer activity *in vitro*, the SNP in each region with the largest *in vitro* effect was chosen for *in vivo* follow-up; in the case of ECR400, two SNPs were chosen. Of the seven SNPs tested *in vivo*, five significantly altered *in vivo* liver enhancer activity, a 71% success rate, and two of these SNPs (rs9999111 and rs12508471) were correlated with decreased gene expression in human tissues. Our ability to identify functional enhancer SNPs in our pipeline is comparable to other studies that searched first for SNPs associated with transporter expression and then characterized *cis*-element activity[65] and is slightly higher than the identification of SNPs in transporter enhancer regions around drug-associated transporters[63]. Of the SNPs chosen for *in vivo* follow-up, four were expected to increase enhancer activity, of which only one significantly did. However, three of the SNPs decreased enhancer activity both *in vitro* and *in vivo*, suggesting that SNPs decreasing enhancer activity might have a more consistent effect *in vivo*.

With the high success rate of the chosen SNPs to alter enhancer activity *in vivo*, additional SNPs identified in the *in vitro* screen could also benefit from *in vivo* follow-up. Specifically, it would be interesting to follow-up with the CR6 SNPs rs573519157 and rs190754327 to see their effect *in vivo* since they each had a 25% to 50% decrease in

activity in both cell lines. Additionally, the ECR33 SNP rs2622628 elicited an over 50% reduction in enhancer activity in HEK293T cells, and this SNP had a trend for association with decreased PPM1K and ABCG2 expression in human livers (data not shown). It would also be interesting to test the positive *in vivo* SNPs for correlation to gene expression in both kidney and liver samples. Association of SNPs with liver expression was first evaluated in the 195 liver samples from Schadt[51] and then replication was tested in 34 liver samples that were available from the PMT cohort. Unfortunately, only 52 kidney samples were available for the primary analysis with no replication cohort. Many of the enhancer regions are in low sequence coverage areas. Follow-up sequencing on these enhancer regions could allow for gene expression correlation with the few SNPs that we were not able to correlate with gene expression in the selected tissues due to their low MAF and low genotype coverage.

The rs9999111 SNP, which has a MAF of 5%, was chosen for *in vivo* follow-up because it displayed an 80% reduction in activity compared to reference in HepG2 and HEK293T cells, respectively. ECR44 SNP rs9999111, which is located in intron 1 of *ABCG2*, significantly decreased the activity of the ECR44 enhancer sequence *in vivo* by ~70%. The rs9999111 SNP was also associated with decreased ABCG2 expression in human kidney (after adjusting for sex), LCLs and T-cells. The beta coefficient of rs9999111 in the kidney (1.8) and the correlation coefficient for rs9999111 in the other tissues (0.18-0.26) indicate this SNP contributes modestly to the variation in ABCG2 expression. Additionally, the minor allele, rs9999111 is consistently associated with lower ABCG2 expression across these tissues. However, rs9999111 was not associated with liver expression of ABCG2 and previously was not found to influence liver or

intestinal expression of ABCG2[18]. These data suggest that rs9999111 could regulate ABCG2 in a tissue-specific manner and possibly play a role in the response of ABCG2 expression to hormones. rs9999111 is predicted to cause a decrease in binding for HFH-2, Gfi, HNF-3β, RXR-VDR and NF-κB. The zinc-finger transcriptional repressor (Gfi-1) plays an essential role in hematopoietic development, of interest in lymphoid and T-cells[66]. Binding sites for Gfi-1 are enriched around genes specific for liver and whole blood[67]. It has been linked to repressed genes in LCLs and K562, but not HepG2 cells[68]. However, the dynamic for Gfi-1 to repress genes depends heavily on the expression of its co-repression TFs and the state of cell differentiation[69]. Working against the Gfi-1 suppression would be the NF-κB TF, which is an activator for lymphoblastoid enhancers[68]. Current literature suggests Gfi-1 works as a transcriptional repressor to stimulate T-cells, hematopoietic stem cells and liver regeneration, whereas NF-κB works to activate genes in these cell lines. In addition, HNF-3β regulates gene expression in selected tissues including hepatocytes and intestinal epithelium[70]. With the association of rs9999111 with ABCG2 expression in T-cells, predicted changes in Gfi, NF-κB and HNF-3β binding and the relevance of these TFs in hematopoietic cells, the ability of this SNP to alter the binding of these putative TFs needs to be directly tested. Additionally, more knowledge on the dynamic interaction of Gfi-1 and NF-κB or HNF-3β in each tissue could elucidate how the rs9999111 SNP may reduce ABCG2 expression.

ECR400*1 is a common haplotype with a frequency of 20% and is made up of rs12508471, rs72873421 and rs12500008. rs12508471 completely eliminated ECR400 enhancer activity *in vitro* and *in vivo*. In contrast, rs72873421 showed increased activity *in vitro*, which could limit the decrease in activity by rs12508471 when these SNPs occur

together in the ECR400*1 haplotype. However, ECR400*1 showed a 75% decrease in enhancer activity in the HEK293T cells. Both rs12508471 and rs72873421 had decreased activity *in vivo*. The ECR400*1 construct was not tested *in vivo* and requires further testing. ECR400*1 was associated with decreased expression of ABCG2 in LCLs (rho= 0.18-0.26) and with PPM1K in several tissues (rho=0.22-31), indicating that this haplotype may modestly influence the variability in ABCG2 and PPM1K expression in multiple tissues. ECR400 is situated just upstream of the *PKD2* promoter, but it did not correlate with PKD2 expression in any of the tissue sets (data not shown). The *ABCG2* gene is on the anti-strand and *PKD2* downstream of the *ABCG2* promoter running on the positive strand. This puts the *ABCG2* and *PKD2* promoters back-to-back, which would facilitate an enhancer regulating both promoters. Enhancers that regulate the expression of linked genes are locus control regions and play a role in the regulation of multiple genes in a tissue-specific manner[71]. This enhancer region may regulate both ABCG2 and PKD2 expression and the ECR400*1 haplotype could contribute to altered expression of these genes.

TFBS predictions were analyzed to understand the molecular basis for the detrimental effect of rs12508471 on ECR400 enhancer activity. rs12508471 was predicted to cause gains in several TFBS, many of which are NRs, including PPAR, PXR, CREB, GR, p300, SREBP, VDR and multiple COUP-TF sites. NRs need their ligands to be active, but in the absence of ligands, other TFs often bind to their DNA consensus sequence, recruit histone binding proteins and work to repress transcriptional function[72]. For example, COUP-TF suppresses the GR transcriptional activity by tethering co-repressors and tightening the chromatin structure[73]. Additionally, COUP-TF

has been shown to repress the transcriptional activity of several other NRs including RAR, TR, VDR and PPAR by competing for DNA binding, forming inactive heterodimers or tethering the co-repressor silencing mediator for retinoid and thyroid hormone receptor (SMRT)[74,75]. The ECR400 SNP rs72873421 is predicted to gain a COUP-TF site and lose sites for the general TF SP1. This brings up an interesting possibility that the rs12508471 and rs72873421 SNPs create multiple new COUP-TF binding sites which suppress the activity of any NR binding to that region of ECR44. Further experiments are needed to directly test alteration in binding for these variant enhancer sequences to the COUP-TF protein. Additionally, follow-up is warranted on SNPs that correlate with ABCG2 expression (such as rs9999111 and ECR400*1) in cohorts of patients with drug treatment to see the effect of these SNPs on pharmacokinetics and pharmacodynamics of MXR substrates.

The ECR423 SNP rs149713212 also caused an extreme loss in enhancer activity both *in vitro* and *in vivo*. Due to the low MAF of rs149713212(0.2-2%) we were unable to correlated this SNP to gene expression. However, rs149713212 is predicted to cause a gain in binding of GATA proteins 1, 2, and 3. GATA1 and GATA2 work together or independently to promote or suppress transcription in differentiation-dependent settings[76]. For example, GATA1 will replace GATA2 to suppress genes during the development of erythrocytes[76]. Coupled with the changes in GATA1 and GATA2 expression patterns during erythropoieses[77], it will be of interest to investigate whether this SNP is associated with gene suppression in hematopoietic stem cells or differentiated cells where ABCG2 is normally expressed.

The only SNP to exhibit increased *in vivo* liver enhancer activity was rs2725263 in the ECR31 enhancer region. rs2725263 is common, with MAFs ranging from 40% in Asians to 84% in African Americans. The rs2725263 SNP was associated with decreased PPM1K expression in the TCGA breast tissues[52], but with increased PKD2 expression in liver[51]. The rs2725263 genotype accounted for 22% of variation in PKD2 liver expression, while it accounted for only 7% of PPM1K breast expression. This SNP is predicted to increase binding of APα and GATA3, two TFs already shown to bind to ECR31 over the rs2725263 SNP by ChIP-seq. GATA3 is a TF linked to tissue-specific gene expression in kidney and breast and is associated with the development of these tissues[76,78]. Also, GATA3 is integral to the ERα receptor pathway in several tissues including kidney and breast[78]. Although the ECR31 enhancer lies in the middle of *ABCG2* intron 10, SNPs in it are correlated to expression of neighboring genes, indicating this enhancer might play a more relevant role in their expression.

The other common ECR31 SNP, rs2725264, was present with a MAF ranging from 8.2% in Europeans to 84% in African Americans. This SNP was not screened *in vivo*, but caused a 1.25- to 1.5-fold increase in relative luciferase activity *in vitro*. It is possible that this SNP and the rs2725264 ECR31 SNP, which showed a trend for association with decreased PKD2 expression, could also be relevant for the regulation of PKD2 through the GATA and ER pathways. This is important because it has been noted that the severity of polycystic kidney disease is associated with hormonal factors in both male and female disease progression, and specifically with estrogen exposure in females[35]. In Chapter 6, data is presented showing that ECR31 activity changes upon NR ligand treatment, however further research would be necessary to test if the rs2725263

and rs2725264 SNPs respond differently than reference ECR31 to hormone exposure. Additionally, direct experiments are needed to test if GATA-3 and ERα have altered binding to the sequence containing rs2725263.

Although we are able to show some correlation between *ABCG2* locus enhancer SNPs and gene expression, further association studies in larger cohorts and in additional tissues are needed to validate these findings. Electrophoretic mobility shift assays are needed to confirm the predicted alterations by these SNPs in the proposed TF binding to the enhancer.

5.6. Conclusions

Liver enhancers identified in the *ABCG2* gene locus have many genetic polymorphisms that alter their activity *in vitro*. Several of these SNPs, including rs9999111, rs125084721, rs72873421, rs2725263 and rs149713212 alter enhancer activity *in vivo*. The rs9999111 SNP and ECR400*1 haplotype were correlated with ABCG2 and PPM1K expression in a tissue-specific manner. Predicted alterations in TFBS provide testable hypotheses for the mechanism by which these SNPs alter enhancer activity. Taken together, these SNPs could account for some of the reported variability in ABCG2 and PPM1K expression in various tissues and may influence the correlation between these genes and disease risk for cancers, ADPKD or gout. Finally, these novel regulatory SNPs may influence the pharmacokinetics and pharmacodynamics of *ABCG2* substrates.

5.7. References

(1) Robey, R. W.; To, K. K. K.; Polgar, O.; Dohse, M.; Fetsch, P.; Dean, M.; Bates, S. E. ABCG2: a perspective. *Advanced drug delivery reviews* **2009**, *61*, 3–13.

(2) Mo, W.; Zhang, J.-T. Human ABCG2: structure, function, and its role in multidrug resistance. *International journal of biochemistry and molecular biology* **2012**, *3*, 1–27.

(3) Zamber, C. P.; Lamba, J. K.; Yasuda, K.; Farnum, J.; Thummel, K.; Schuetz, J. D.; Schuetz, E. G. Natural allelic variants of breast cancer resistance protein (BCRP) and their relationship to BCRP expression in human intestine. *Pharmacogenetics* **2003**, *13*, 19–28.

(4) Suvannasankha, a; Minderman, H.; O'Loughlin, K. L.; Nakanishi, T.; Greco, W. R.; Ross, D. D.; Baer, M. R. Breast cancer resistance protein (BCRP/MXR/ABCG2) in acute myeloid leukemia: discordance between expression and function. *Leukemia : official journal of the Leukemia Society of America, Leukemia Research Fund, U.K* **2004**, *18*, 1252–7.

(5) Suvannasankha, A.; Minderman, H.; O'Loughlin, K. L.; Nakanishi, T.; Ford, L. a; Greco, W. R.; Wetzler, M.; Ross, D. D.; Baer, M. R. Breast cancer resistance protein (BCRP/MXR/ABCG2) in adult acute lymphoblastic leukaemia: frequent expression and possible correlation with shorter disease-free survival. *British journal of haematology* **2004**, *127*, 392–8.

(6) Benderra, Z.; Faussat, A.-M.; Sayada, L.; Perrot, J.-Y.; Chaoui, D.; Marie, J.-P.; Legrand, O. Breast cancer resistance protein and P-glycoprotein in 149 adult acute myeloid leukemias. *Clinical cancer research : an official journal of the American Association for Cancer Research* **2004**, *10*, 7896–902.

(7) Tsunoda, S.; Okumura, T.; Ito, T.; Kondo, K.; Ortiz, C.; Tanaka, E.; Watanabe, G.; Itami, A.; Sakai, Y.; Shimada, Y. ABCG2 expression is an independent unfavorable prognostic factor in esophageal squamous cell carcinoma. *Oncology* **2006**, *71*, 251–8.

(8) Usuda, J.; Tsunoda, Y.; Ichinose, S.; Ishizumi, T.; Ohtani, K.; Maehara, S.; Ono, S.; Tsutsui, H.; Ohira, T.; Okunaka, T.; Furukawa, K.; Sugimoto, Y.; Kato, H.; Ikeda, N. Breast cancer resistant protein (BCRP) is a molecular determinant of the outcome of photodynamic therapy (PDT) for centrally located early lung cancer. *Lung cancer (Amsterdam, Netherlands)* **2010**, *67*, 198–204.

(9) Uggla, B.; Ståhl, E.; Wågsäter, D.; Paul, C.; Karlsson, M. G.; Sirsjö, A.; Tidefelt, U. BCRP mRNA expression v. clinical outcome in 40 adult AML patients. *Leukemia research* **2005**, *29*, 141–6.

(10) Yoh, K. Breast Cancer Resistance Protein Impacts Clinical Outcome in Platinum-Based Chemotherapy for Advanced Non-Small Cell Lung Cancer. *Clinical Cancer Research* **2004**, *10*, 1691–1697.

(11) Kim, K.; Joo, H.-J.; Park, J.-Y. ABCG2 polymorphisms, 34G>A and 421C>A in a Korean population: analysis and a comprehensive comparison with other populations. *Journal of clinical pharmacy and therapeutics* **2010**, *35*, 705–12.

(12) Tamura, A.; Onishi, Y.; An, R.; Koshiba, S.; Wakabayashi, K.; Hoshijima, K.; Priebe, W.; Yoshida, T.; Kometani, S.; Matsubara, T.; Mikuriya, K.; Ishikawa, T. In vitro evaluation of photosensitivity risk related to genetic polymorphisms of human ABC transporter ABCG2 and inhibition by drugs. *Drug metabolism and pharmacokinetics* **2007**, *22*, 428–40.

(13) Wakabayashi, K.; Tamura, A.; Saito, H.; Onishi, Y.; Ishikawa, T. Human ABC transporter ABCG2 in xenobiotic protection and redox biology. *Drug metabolism reviews* **2006**, *38*, 371–91.

(14) Ishikawa, T.; Tamura, A.; Saito, H.; Wakabayashi, K.; Nakagawa, H. Pharmacogenomics of the human ABC transporter ABCG2: from functional evaluation to drug molecular design. *Die Naturwissenschaften* **2005**, *92*, 451–63.

(15) Yanase, K.; Tsukahara, S.; Mitsuhashi, J.; Sugimoto, Y. Functional SNPs of the breast cancer resistance protein-therapeutic effects and inhibitor development. *Cancer letters* **2006**, *234*, 73–80.

(16) Tamura, A.; Watanabe, M.; Saito, H.; Nakagawa, H.; Kamachi, T.; Okura, I.; Ishikawa, T. Functional validation of the genetic polymorphisms of human ATP-binding cassette (ABC) transporter ABCG2: identification of alleles that are defective in porphyrin transport. *Molecular pharmacology* **2006**, *70*, 287–96.

(17) Yoshioka, S.; Katayama, K.; Okawa, C.; Takahashi, S.; Tsukahara, S.; Mitsuhashi, J.; Sugimoto, Y. The identification of two germ-line mutations in the human breast cancer resistance protein gene that result in the expression of a low/non-functional protein. *Pharmaceutical research* **2007**, *24*, 1108–17.

(18) Poonkuzhali, B.; Lamba, J.; Strom, S. Association of breast cancer resistance protein/ABCG2 phenotypes and novel promoter and intron 1 single nucleotide polymorphisms. *Drug Metabolism and …* **2008**, *36*, 780–795.

(19) Jonker, J. W.; Buitelaar, M.; Wagenaar, E.; Van Der Valk, M. a; Scheffer, G. L.; Scheper, R. J.; Plosch, T.; Kuipers, F.; Elferink, R. P. J. O.; Rosing, H.; Beijnen, J. H.; Schinkel, A. H. The breast cancer resistance protein protects against a major chlorophyll-derived dietary phototoxin and protoporphyria. *Proceedings of the National Academy of Sciences of the United States of America* **2002**, *99*, 15649–54.

(20) Desuzinges-Mandon, E.; Arnaud, O.; Martinez, L.; Huché, F.; Di Pietro, A.; Falson, P. ABCG2 transports and transfers heme to albumin through its large extracellular loop. *The Journal of biological chemistry* **2010**, *285*, 33123–33.

(21) Krishnamurthy, P.; Schuetz, J. D. The ABC transporter Abcg2/Bcrp: role in hypoxia mediated survival. *Biometals : an international journal on the role of metal ions in biology, biochemistry, and medicine* **2005**, *18*, 349–58.

(22) Wan, P.; Moat, S.; Anstey, A. Pellagra: a review with emphasis on photosensitivity. *The British journal of dermatology* **2011**, *164*, 1188–200.

(23) Ho, A. Y. L.; Deacon, A.; Osborne, G.; Mufti, G. J. Precipitation of porphyria cutanea tarda by imatinib mesylate? *British journal of haematology* **2003**, *121*, 375.

(24) Reginato, A. M.; Mount, D. B.; Yang, I.; Choi, H. K. The genetics of hyperuricaemia and gout. *Nature reviews. Rheumatology* **2012**, *8*, 610–21.

(25) Rodrigues, A. C.; Curi, R.; Genvigir, F. D. V.; Hirata, M. H.; Hirata, R. D. C. The expression of efflux and uptake transporters are regulated by statins in Caco-2 and HepG2 cells. *Acta pharmacologica Sinica* **2009**, *30*, 956–64.

(26) Cusatis, G.; Gregorc, V.; Li, J.; Spreafico, A.; Ingersoll, R. G.; Verweij, J.; Ludovini, V.; Villa, E.; Hidalgo, M.; Sparreboom, A.; Baker, S. D. Pharmacogenetics of ABCG2 and adverse reactions to gefitinib. *Journal of the National Cancer Institute* **2006**, *98*, 1739–42.

(27) Jonker, J. W.; Merino, G.; Musters, S.; Van Herwaarden, A. E.; Bolscher, E.; Wagenaar, E.; Mesman, E.; Dale, T. C.; Schinkel, A. H. The breast cancer resistance protein BCRP (ABCG2) concentrates drugs and carcinogenic xenotoxins into milk. *Nature medicine* **2005**, *11*, 127–9.

(28) Noguchi, K.; Katayama, K.; Mitsuhashi, J.; Sugimoto, Y. Functions of the breast cancer resistance protein (BCRP/ABCG2) in chemotherapy. *Advanced drug delivery reviews* **2009**, *61*, 26–33.

(29) Georgitsi, M.; Zukic, B.; Pavlovic, S.; Patrinos, G. P. Transcriptional regulation and pharmacogenomics. *Pharmacogenomics* **2011**, *12*, 655–73.

(30) Smith, R. P.; Lam, E. T.; Markova, S.; Yee, S. W.; Ahituv, N. Pharmacogene regulatory elements: from discovery to applications. *Genome medicine* **2012**, *4*, 45.

(31) Ge, B.; Pokholok, D. K.; Kwan, T.; Grundberg, E.; Morcos, L.; Verlaan, D. J.; Le, J.; Koka, V.; Lam, K. C. L.; Gagné, V.; Dias, J.; Hoberman, R.; Montpetit, A.; Joly, M.-M.; Harvey, E. J.; Sinnett, D.; Beaulieu, P.; Hamon, R.; Graziani, A.; Dewar, K.; Harmsen, E.; Majewski, J.; Göring, H. H. H.; Naumova, A. K.;

Blanchette, M.; Gunderson, K. L.; Pastinen, T. Global patterns of cis variation in human cells revealed by high-density allelic expression analysis. *Nature genetics* **2009**, *41*, 1216–22.

(32) Pastinen, T. Genome-wide allele-specific analysis: insights into regulatory variation. *Nature reviews. Genetics* **2010**, *11*, 533–8.

(33) Tan, Y.-C.; Blumenfeld, J.; Rennert, H. Autosomal dominant polycystic kidney disease: genetics, mutations and microRNAs. *Biochimica et biophysica acta* **2011**, *1812*, 1202–12.

(34) Peters, D. J.; Spruit, L.; Saris, J. J.; Ravine, D.; Sandkuijl, L. A.; Fossdal, R.; Boersma, J.; Van Eijk, R.; Nørby, S.; Constantinou-Deltas, C. D. Chromosome 4 localization of a second gene for autosomal dominant polycystic kidney disease. *Nature genetics* **1993**, *5*, 359–62.

(35) Rossetti, S.; Harris, P. C. Genotype-phenotype correlations in autosomal dominant and autosomal recessive polycystic kidney disease. *Journal of the American Society of Nephrology : JASN* **2007**, *18*, 1374–80.

(36) Lu, G.; Ren, S.; Korge, P.; Choi, J.; Dong, Y.; Weiss, J.; Koehler, C.; Chen, J.; Wang, Y. A novel mitochondrial matrix serine/threonine protein phosphatase regulates the mitochondria permeability transition pore and is essential for cellular survival and development. *Genes & development* **2007**, *21*, 784–96.

(37) Zhou, M.; Lu, G.; Gao, C.; Wang, Y.; Sun, H. Tissue-specific and nutrient regulation of the branched-chain α-keto acid dehydrogenase phosphatase, protein phosphatase 2Cm (PP2Cm). *The Journal of biological chemistry* **2012**, *287*, 23397–406.

(38) Simonet, W. S.; Bucay, N.; Lauer, S. J.; Taylor, J. M. A far-downstream hepatocyte-specific control region directs expression of the linked human apolipoprotein E and C-I genes in transgenic mice. *The Journal of biological chemistry* **1993**, *268*, 8221–9.

(39) Africa, W. A map of human genome variation from population-scale sequencing. *Nature* **2010**, *467*, 1061–73.

(40) Frazer, K. a; *et. al.* A second generation human haplotype map of over 3.1 million SNPs. *Nature* **2007**, *449*, 851–61.

(41) Barrett, J. C.; Fry, B.; Maller, J.; Daly, M. J. Haploview: analysis and visualization of LD and haplotype maps. *Bioinformatics (Oxford, England)* **2005**, *21*, 263–5.

(42) Johnson, A. D.; Handsaker, R. E.; Pulit, S. L.; Nizzari, M. M.; O'Donnell, C. J.; De Bakker, P. I. W. SNAP: a web-based tool for identification and annotation of proxy SNPs using HapMap. *Bioinformatics (Oxford, England)* **2008**, *24*, 2938–9.

(43) Liu, H.; Naismith, J. H. An efficient one-step site-directed deletion, insertion, single and multiple-site plasmid mutagenesis protocol. *BMC biotechnology* **2008**, *8*, 91.

(44) Liu, F.; Song, Y.; Liu, D. Hydrodynamics-based transfection in animals by systemic administration of plasmid DNA. *Gene therapy* **1999**, *6*, 1258–66.

(45) Kim, M. J.; Ahituv, N. The Hydrodynamic Tail Vein Assay as a Tool for the Study of Liver Promoters and Enhancers. In *Pharmacogenomics: Methods and Protocols*; Innocenti, F.; van Schaik, R. H. N., Eds.; 2012.

(46) Sandelin, A.; Wasserman, W. W.; Lenhard, B. ConSite: web-based prediction of regulatory elements using cross-species comparison. *Nucleic acids research* **2004**, *32*, W249–52.

(47) Wingender, E.; Chen, X.; Hehl, R.; Karas, H.; Liebich, I.; Matys, V.; Meinhardt, T.; Prüss, M.; Reuter, I.; Schacherer, F. TRANSFAC: an integrated system for gene expression regulation. *Nucleic acids research* **2000**, *28*, 316–9.

(48) Kroetz, D. L.; Yee, S. W.; Giacomini, K. M. The pharmacogenomics of membrane transporters project: research at the interface of genomics and transporter pharmacology. *Clinical pharmacology and therapeutics* **2010**, *87*, 109–16.

(49) Bolstad, B. M.; Irizarry, R. A.; Astrand, M.; Speed, T. P. A comparison of normalization methods for high density oligonucleotide array data based on variance and bias. *Bioinformatics (Oxford, England)* **2003**, *19*, 185–93.

(50) Boes, T.; Neuhäuser, M. Normalization for Affymetrix GeneChips. *Methods of information in medicine* **2005**, *44*, 414–7.

(51) Schadt, E. E.; Molony, C.; Chudin, E.; Hao, K.; Yang, X.; Lum, P. Y.; Kasarskis, A.; Zhang, B.; Wang, S.; Suver, C.; Zhu, J.; Millstein, J.; Sieberts, S.; Lamb, J.; GuhaThakurta, D.; Derry, J.; Storey, J. D.; Avila-Campillo, I.; Kruger, M. J.; Johnson, J. M.; Rohl, C. a; Van Nas, A.; Mehrabian, M.; Drake, T. a; Lusis, A. J.; Smith, R. C.; Guengerich, F. P.; Strom, S. C.; Schuetz, E.; Rushmore, T. H.; Ulrich, R. Mapping the genetic architecture of gene expression in human liver. *PLoS biology* **2008**, *6*, e107.

(52) The Cancer Genome Atlas Network Comprehensive molecular portraits of human breast tumours. *Nature* **2012**, *490*, 61–70.

(53) Yang, T.-P.; Beazley, C.; Montgomery, S. B.; Dimas, A. S.; Gutierrez-Arcelus, M.; Stranger, B. E.; Deloukas, P.; Dermitzakis, E. T. Genevar: a database and Java application for the analysis and visualization of SNP-gene associations in eQTL studies. *Bioinformatics (Oxford, England)* **2010**, *26*, 2474–6.

(54) Nica, A. C.; Parts, L.; Glass, D.; Nisbet, J.; Barrett, A.; Sekowska, M.; Travers, M.; Potter, S.; Grundberg, E.; Small, K.; Hedman, A. K.; Bataille, V.; Tzenova Bell, J.; Surdulescu, G.; Dimas, A. S.; Ingle, C.; Nestle, F. O.; Di Meglio, P.; Min, J. L.; Wilk, A.; Hammond, C. J.; Hassanali, N.; Yang, T.-P.; Montgomery, S. B.; O'Rahilly, S.; Lindgren, C. M.; Zondervan, K. T.; Soranzo, N.; Barroso, I.; Durbin, R.; Ahmadi, K.; Deloukas, P.; McCarthy, M. I.; Dermitzakis, E. T.; Spector, T. D. The architecture of gene regulatory variation across multiple human tissues: the MuTHER study. *PLoS genetics* **2011**, *7*, e1002003.

(55) Grundberg, E.; Small, K. S.; Hedman, Å. K.; Nica, A. C.; Buil, A.; Keildson, S.; Bell, J. T.; Yang, T.; Meduri, E.; Barrett, A.; Nisbett, J.; Sekowska, M.; Wilk, A.; Shin, S.; Glass, D.; Travers, M.; Min, J. L.; Ring, S.; Ho, K.; Thorleifsson, G.; Kong, A.; Thorsteindottir, U.; Ainali, C.; Dimas, A. S.; Hassanali, N.; Ingle, C.; Knowles, D.; Krestyaninova, M.; Lowe, C. E.; Meglio, P. Di; Montgomery, S. B.; Parts, L.; Potter, S.; Surdulescu, G.; Tsaprouni, L.; Tsoka, S.; Bataille, V.; Durbin, R.; Nestle, F. O.; Rahilly, S. O.; Soranzo, N.; Lindgren, C. M.; Zondervan, K. T.; Ahmadi, K. R.; Schadt, E. E.; Stefansson, K.; Smith, G. D.; Mccarthy, M. I.; Deloukas, P.; Dermitzakis, E. T.; Spector, T. D.; Multiple, T.; Human, T. Articles Mapping cis- and trans-regulatory effects across multiple tissues in twins. **2012**, *44*.

(56) Stranger, B. E.; Nica, A. C.; Forrest, M. S.; Dimas, A.; Bird, C. P.; Beazley, C.; Ingle, C. E.; Dunning, M.; Flicek, P.; Koller, D.; Montgomery, S.; Tavaré, S.; Deloukas, P.; Dermitzakis, E. T. Population genomics of human gene expression. *Nature genetics* **2007**, *39*, 1217–24.

(57) Stranger, B. E.; Forrest, M. S.; Clark, A. G.; Minichiello, M. J.; Deutsch, S.; Lyle, R.; Hunt, S.; Kahl, B.; Antonarakis, S. E.; Tavaré, S.; Deloukas, P.; Dermitzakis, E. T. Genome-wide associations of gene expression variation in humans. *PLoS genetics* **2005**, *1*, e78.

(58) Stranger, B. E.; Forrest, M. S.; Dunning, M.; Ingle, C. E.; Beazley, C.; Thorne, N.; Redon, R.; Bird, C. P.; De Grassi, A.; Lee, C.; Tyler-Smith, C.; Carter, N.; Scherer, S. W.; Tavaré, S.; Deloukas, P.; Hurles, M. E.; Dermitzakis, E. T. Relative impact of nucleotide and copy number variation on gene expression phenotypes. *Science (New York, N.Y.)* **2007**, *315*, 848–53.

(59) Stranger, B. E.; Montgomery, S. B.; Dimas, A. S.; Parts, L.; Stegle, O.; Ingle, C. E.; Sekowska, M.; Smith, G. D.; Evans, D.; Gutierrez-Arcelus, M.; Price, A.; Raj, T.; Nisbett, J.; Nica, A. C.; Beazley, C.; Durbin, R.; Deloukas, P.; Dermitzakis, E.

T. Patterns of cis regulatory variation in diverse human populations. *PLoS genetics* **2012**, *8*, e1002639.

(60) Dimas, A.; Deutsch, S.; Stranger, B. Common regulatory variation impacts gene expression in a cell type–dependent manner. *Science* **2009**, *325*, 1246–1250.

(61) Rudin, C. M.; Liu, W.; Desai, A.; Karrison, T.; Jiang, X.; Janisch, L.; Das, S.; Ramirez, J.; Poonkuzhali, B.; Schuetz, E.; Fackenthal, D. L.; Chen, P.; Armstrong, D. K.; Brahmer, J. R.; Fleming, G. F.; Vokes, E. E.; Carducci, M. A.; Ratain, M. J. Pharmacogenomic and pharmacokinetic determinants of erlotinib toxicity. *Journal of clinical oncology : official journal of the American Society of Clinical Oncology* **2008**, *26*, 1119–27.

(62) Campa, D.; Butterbach, K.; Slager, S. L.; Skibola, C. F.; De Sanjosé, S.; Benavente, Y.; Becker, N.; Foretova, L.; Maynadie, M.; Cocco, P.; Staines, A.; Kaaks, R.; Boffetta, P.; Brennan, P.; Conde, L.; Bracci, P. M.; Caporaso, N. E.; Strom, S. S.; Camp, N. J.; Cerhan, J. R.; Consortium, G.; Canzian, F.; Nieters, A. A comprehensive study of polymorphisms in the ABCB1, ABCC2, ABCG2, NR1I2 genes and lymphoma risk. *International journal of cancer. Journal international du cancer* **2012**, *131*, 803–12.

(63) Kim, M. J.; Skewes-Cox, P.; Fukushima, H.; Hesselson, S.; Yee, S. W.; Ramsey, L. B.; Nguyen, L.; Eshragh, J. L.; Castro, R. A.; Wen, C. C.; Stryke, D.; Johns, S. J.; Ferrin, T. E.; Kwok, P.; Relling, M. V; Giacomini, K. M.; Kroetz, D. L.; Ahituv, N. Functional characterization of liver enhancers that regulate drug-associated transporters. *Clinical pharmacology and therapeutics* **2011**, *89*, 571–8.

(64) McLeod, H. L.; Sargent, D. J.; Marsh, S.; Green, E. M.; King, C. R.; Fuchs, C. S.; Ramanathan, R. K.; Williamson, S. K.; Findlay, B. P.; Thibodeau, S. N.; Grothey, A.; Morton, R. F.; Goldberg, R. M. Pharmacogenetic predictors of adverse events and response to chemotherapy in metastatic colorectal cancer: results from North American Gastrointestinal Intergroup Trial N9741. *Journal of clinical oncology : official journal of the American Society of Clinical Oncology* **2010**, *28*, 3227–33.

(65) Matsson, P.; Yee, S. W.; Markova, S.; Morrissey, K.; Jenkins, G.; Xuan, J.; Jorgenson, E.; Kroetz, D. L.; Giacomini, K. M. Discovery of regulatory elements in human ATP-binding cassette transporters through expression quantitative trait mapping. *The pharmacogenomics journal* **2011**, 1–13.

(66) Hock, H.; Orkin, S. H. Zinc-finger transcription factor Gfi-1: versatile regulator of lymphocytes, neutrophils and hematopoietic stem cells. *Current opinion in hematology* **2006**, *13*, 1–6.

(67) Girgis, H. Z.; Ovcharenko, I. Predicting tissue specific cis-regulatory modules in the human genome using pairs of co-occurring motifs. *BMC bioinformatics* **2012**, *13*, 25.

(68) Ernst, J.; Kheradpour, P.; Mikkelsen, T. S.; Shoresh, N.; Ward, L. D.; Epstein, C. B.; Zhang, X.; Wang, L.; Issner, R.; Coyne, M.; Ku, M.; Durham, T.; Kellis, M.; Bernstein, B. E. Mapping and analysis of chromatin state dynamics in nine human cell types. *Nature* **2011**, *473*, 43–9.

(69) Saleque, S.; Kim, J.; Rooke, H. M.; Orkin, S. H. Epigenetic regulation of hematopoietic differentiation by Gfi-1 and Gfi-1b is mediated by the cofactors CoREST and LSD1. *Molecular cell* **2007**, *27*, 562–72.

(70) Schrem, H.; Klempnauer, J.; Borlak, J. Liver-enriched transcription factors in liver function and development. Part I: the hepatocyte nuclear factor network and liver-specific gene expression. *Pharmacological reviews* **2002**, *54*, 129–58.

(71) Li, Q.; Peterson, K. R.; Fang, X.; Stamatoyannopoulos, G. Locus control regions. *Blood* **2002**, *100*, 3077–86.

(72) Wiench, M.; Miranda, T. B.; Hager, G. L. Control of nuclear receptor function by local chromatin structure. *The FEBS journal* **2011**, *278*, 2211–30.

(73) De Martino, M. U.; Alesci, S.; Chrousos, G. P.; Kino, T. Interaction of the glucocorticoid receptor and the chicken ovalbumin upstream promoter-transcription factor II (COUP-TFII): implications for the actions of glucocorticoids on glucose, lipoprotein, and xenobiotic metabolism. *Annals of the New York Academy of Sciences* **2004**, *1024*, 72–85.

(74) Shibata, H.; Nawaz, Z.; Tsai, S. Y.; O'Malley, B. W.; Tsai, M. J. Gene silencing by chicken ovalbumin upstream promoter-transcription factor I (COUP-TFI) is mediated by transcriptional corepressors, nuclear receptor-corepressor (N-CoR) and silencing mediator for retinoic acid receptor and thyroid hormone receptor (SMRT). *Molecular endocrinology (Baltimore, Md.)* **1997**, *11*, 714–24.

(75) Qiu, Y.; Krishnan, V.; Pereira, F. A.; Tsai, S. Y.; Tsai, M. J. Chicken ovalbumin upstream promoter-transcription factors and their regulation. *The Journal of steroid biochemistry and molecular biology* **1996**, *56*, 81–5.

(76) Bresnick, E. H.; Katsumura, K. R.; Lee, H.-Y.; Johnson, K. D.; Perkins, A. S. Master regulatory GATA transcription factors: mechanistic principles and emerging links to hematologic malignancies. *Nucleic acids research* **2012**, *40*, 5819–31.

(77) Bresnick, E. H.; Lee, H.-Y.; Fujiwara, T.; Johnson, K. D.; Keles, S. GATA switches as developmental drivers. *The Journal of biological chemistry* **2010**, *285*, 31087–93.

(78) Wilson, B. J. Does GATA3 act in tissue-specific pathways ? A meta-analysis-based approach. **2008**, 1–6.

Chapter 6 : Characterization of Inducible Regulatory Elements of the *ABCG2* Locus

6.1. Abstract

The mitoxantrone resistance protein (MXR, BCRP) is one of many drug transporters, and its gene *ABCG2* is regulated by nuclear receptors (NR). NRs are ligand-dependent transcription factors that upon activation by their ligand, bind to specific sequences in DNA and work to activate or repress target genes. In the present study, we examine the effect of NR ligands on the activity of putative regulatory regions from the *ABCG2* locus. Reference and variant *ABCG2* enhancers, suppressors and promoter were cloned into luciferase reporter vectors, transiently transfected into MCF-7 and HepG2 cell lines and then treated with rifampin, 17β-estradiol (E_2), dexamethasone and benzo[a]pyrene (B[a]P). The *ABCG2* promoter responded to E_2, dexamethasone and B[a]P, and the promoter SNP rs66664036 had a significantly altered response to E_2 compared to the reference promoter. Nine rifampin, six E_2 and three dexamethasone responsive regulatory regions were identified. The ECR400 SNP rs12508471 has a significantly altered response to E_2 compared to reference ECR400. Finally, the CR6 SNPs rs573519157 and rs190754327 both responded differently to E_2 than reference CR6. These results describe novel hormone response elements within the *ABCG2* gene locus and SNPs within these regions that could explain clinical variation in *ABCG2* expression.

6.2. Introduction

Drug metabolism and transporter genes are regulated by nuclear receptors (NR) which stimulate drug detoxification pathways in the body[1,2]. NRs are ligand-dependent

transcription factors (TFs) that bind to consensus sequences in the genome and promote the transcription or transrepression of target genes[3]. NRs exist as homo- and heterodimers with each partner recognizing specific DNA sequences, called response elements[4]. These response elements exist as direct, indirect or inverted half-sites separated by variable length nucleotide spacers[5]. NRs have been classified depending upon their binding partner and the type of response element to which they bind[4]. Class I NRs include the steroid hormones and bind to inverted repeats[6], and Class II NRs are heterodimeric partners of RXR and bind to direct repeats[7]. The other two classes of NRs are orphan receptors binding to direct repeats and NRs acting as monomers to bind to a single half-site[4,5]. NRs can also be categorized based upon their mechanism of action, which includes their ligand binding while the NR is located in the cytosol (Type I) or nucleus (Type II)[8]. The large number of heterodimer combinations between different NRs and their diversity of isoform expression depending on cell type and development could generate significant diversity in gene regulation[9]. The study of NRs has been rapidly developing, and there are many good reviews in the literature[3–5,7,8,10–13]. Additionally, ~13% of current drugs target NRs[14]; therefore it is imperative we understand the transcriptional regulation of drug enzymes and transporters by NR ligands.

NRs are a large family of TFs that include the glucocorticoid receptor (GR), estrogen receptor (ER), progesterone receptor (PR), aryl hydrocarbon receptor (AhR), androgen receptor (AR), pregnane X receptor (PXR), retinoid X receptor (RXR), farnesoid X receptor (FXR), hepatocyte nuclear factor 4α (HNF4α) and vitamin D receptor (VDR). NRs are ligand-induced in response to environmental stimuli and their ligands include a variety of fatty acids, vitamins and steroids[15]. Through ChIP-seq

experiments many NRs were shown to prefer binding to *cis*-elements as opposed to the proximal promoter of their genes. Over 63% of glucocorticoid response elements (GRE) are >10 kb from the transcriptional start site (TSS) of glucocorticoid responsive genes, split evenly between up- and downstream of the TSS, with only 9% of GREs in the proximal promoter[16]. Similarly, only 4% of estrogen responsive elements (ERE) are in the proximal promoter of estrogen responsive genes[17] and ~33% of androgen responsive elements (ARE) are within 10 kb of androgen responsive genes[18]. Similarly, more that 90% of HNF4α sites map to distal promoter elements[19]. In addition to preferring distal locations from the proximal promoter, the ERE, ARE, GREs and HNF4α response elements (HRE) are composite elements, consisting of binding sites for other TFs. AP-1, ETS, C/EBP and HNF4 bind to GREs[16], Oct1, GATA2, AP-1, RAR, ZNF4α, HNF4α and EGR[18,20] to AREs, and ERα, AP-1, GATA, HNF1α, AP-2γ and FoxA1 with HNF1α sites[19,21]. Therefore, when searching for NR response elements, it is necessary to take into consideration the binding of other NRs, especially the multiple NR dimer partner RXR.

The efflux transporter *ABCG2* is not excepted from NR regulation and there is evidence supporting its regulation by the ER, PR, PXR, constitutive androstane receptor (CAR), AhR, GR, hypoxia inducible factor (HIF), retinoid-related orphan receptor (ROR), peroxisome proliferator-activated receptor (PPAR) and NF-E2 related factor-2 (Nrf2)[22–31]. In addition, the expression of ABCG2 is altered by many types of stimuli, including hypoxia[32], inflammation[29] and nutrient status[33,34]. Several nuclear response elements (NRE) have been mapped to the proximal promoter of *ABCG2*[22,27–31]. Due to the necessity of dynamic regulation of gene transcription, NRs prefer to bind to *cis*-

regulatory elements as opposed to proximal promoter elements[12]. Therefore, it is likely that there are NREs in the *ABCG2* locus.

One NR prominent in the regulation of drug metabolizing enzyme and transporter genes is PXR. PXR expression correlates with the expression of ABCG2[35,36], and the PXR ligand rifampin[37] induces ABCG2 expression[24,38]. However, no PXR or retinoid X receptor (RXR), a binding partner of PXR, response element has been mapped to the *ABCG2* locus. PXR is activated by other ligands, including statins and the bile acid lithocholic acid[39]. *ABCG2* is integral in statin response[40] and the development of gout[41], so the identification of PXR response elements and a better understanding of the PXR induction pathway for *ABCG2* could identify new therapeutic targets.

Hormones and their receptors are common pathways to regulate drug metabolizing enzymes and transporters. For example, the ER both induces[23,42,43] and downregulates[44–46] ABCG2 expression. Also, ER often shares response elements with the PR, such as the ER/PR element found in the *ABCG2* proximal promoter[22]. ER also interacts with HNF3α (FOXA1) and genomic variants in the ERE where it binds are a major risk factor for breast cancer[47]. Understanding the ER regulation pathway for *ABCG2* is vital because of the role both of these hormones play in the placenta and mammary tissues[48,49]. For example, the ER and PR have a normal role in the upregulation of ABCG2 during pregnancy to augment protection of the fetus[31,49,50]. In contrast, upregulation of ABCG2 in ER and PR positive breast cancer cells is associated with decreased response to chemotherapy[51]. ABCG2 overexpression in breast cancer cells leads to drug resistance as MXR effluxes chemotherapeutics from the cancer cell. Although there is a well characterized ER/PR response element in the *ABCG2*

promoter[22], *in vivo* only 4% of active ERE are within 1 kb of the proximal promoter and almost all ER binding events occur in non-annotated *cis*-regulatory elements[17]. Therefore, identification of ER and PR *cis*-regulatory elements of *ABCG2* could help untangle how drug resistance develops and how *ABCG2* is regulated in placenta and breast.

Glucocorticoids, which are ligands for the GR, have a broad endogenous role in the body, including regulation of growth, metabolic, immune and stress related pathways[52–54]. Due to the powerful anti-inflammatory and immunosuppressive action of glucocorticoids, they are widely utilized for treatment of acute and chronic inflammatory diseases, autoimmune diseases, organ transplant rejection, and malignancies of the lymphoid system[53,55]. The GR ligand dexamethasone decreases ABCG2 expression both *in vivo*[56] and i*n vitro*[57]. Additionally, dexamethasone also increases the expression of both PXR and RXR[58]. Due to dexamethasone's ability to induce PXR expression, it has been proposed that dexamethasone acts via direct GR-dependent mechanisms at either low concentrations or short (up to 24 hr) treatment and via a PXR-dependent mechanism at high or long (48 hr) treatment[59–61]. Most NRs are known for activating gene expression; after being released from its repressors by its ligand, GR works to trans-repress target genes by binding to other TFs in the nucleus such as AP-1 or NF-κB and inhibiting them from activating transcription of the target gene[62]. Identification of GR response elements (GRE) for *ABCG2* could help unravel the GR response pathway and its effect on ABCG2 expression in inflammatory diseases as well as after glucocorticoid treatment.

Many carcinogens are known ligands of AhR and through AhR induce many metabolizing enzymes and drug transporters[63]. This allows the body to protect its vital organs from exposure to these carcinogens. Exposure to carcinogens causes DNA

damage that leads to DNA mutations[64], and exposure to exogenous carcinogens are a factor in the development, severity and aggressiveness of cancer. MXR not only transports carcinogens[65], but ABCG2 expression is increased with carcinogen exposure[65–67]. The expression of ABCG2 to has been linked to severity and disease-free survival in cancer[68–75] and low functioning alleles of *ABCG2* with the occurrence of cancer[76]. Identification of AhR response elements (AhRE) for *ABCG2* would allow for better understanding of the AhR pathway regulation of *ABCG2* and for identification of variants that have altered response to carcinogen exposure, thus leading to increasing carcinogen exposure and cancer severity.

Due to the multitude of NR ligands and environmental stimuli that regulate *ABCG2*, we hypothesized that some of the putative *cis*-regulatory elements of the *ABCG2* locus are NRE. In this study, liver (HepG2) or breast (MCF-7) cells expressing variant and reference *ABCG2* promoter plasmids (see Chapter 3) and previously identified reference and variant high priority regulatory regions in the *ABCG2* gene locus (see Chapter 4) were treated with ligands for PXR, ER, GR and AhR. The identification of putative NREs in the *ABCG2* gene locus adds to the previously identified *cis*-regulatory elements of *ABCG2* (see Chapter 4 and references[22,27–31]) and provides novel links between genetic variants and ABCG2 expression.

6.3. Materials and Methods

6.3.1. *Chemicals and Materials*

The vectors pGL4.23 [*luc2*/minP], pGL3-promoter [*luc*+/SV40], pGL4.11b [*luc2*P], pGL4.74 [*hRluc*/TK], pGL4.13 [*luc2*/SV40], the Dual-Luciferase® Reporter

Assay System and HB101 competent cells were all purchased from Promega (Madison, WI). The human hepatocellular carcinoma (HepG2) and human breast adenocarcinoma (MCF-7) cell lines were both purchased from the American Type Culture Collection (ATCC, Manassas, VA). High-glucose Dulbecco's modified Eagle's medium (DMEM), Opti-Minimal Essential Medium (Opti-MEM) and Lipofectamine 2000 were all purchased from Invitrogen (Carlsbad, CA). DMSO, 1X phosphate buffered saline (PBS), 0.05% trypsin and 100X penicillin and streptomycin were all purchased from the UCSF Cell Culture Facility (San Francisco, CA). Rifampin, 17β-estradiol, benzo[a]pyrene, dexamethasone and 10% charcoal stripped fetal bovine serum (FBS) were all purchased from Sigma Aldrich (St. Louis, MO). Improved Minimum Essential Medium (IMEM) without phenol red (Mediatech Inc, Manassas, VA), 10% FBS (Axenia BioLogix, Dixon, CA), and PolyJet™ DNA *In Vitro* Transfection Reagent (SignaGen Laboratories, Rockville, MD) were all purchased from the indicated manufacturers. The CYP3A4 Xrem[77] in the pGL4.23 [*luc2*/minP] vector and hPXR-pcDNA3.1 were a gift from Kathy Giacomini (University of California San Francisco, San Francisco, CA).

6.3.2. *Computational Predictions of Nuclear Response Elements*

Three web-based computational tools and two chromatin immunoprecipitation (ChIP) coupled with deep sequencing (ChIP-seq) databases were used to either predict or provide evidence for the binding of NRs to putative enhancer elements. For the prediction analysis, either the entire *ABCG2* locus, which we defined as the ~300,000 bp region, stretching from one gene up- (*PPM1K*) and downstream (*PKD2*) of *ABCG2* (chr4:89130400-89439035 hg18; chr4:88911376-89220011 hg19), or selected putative

enhancer sequences were extracted from UCSC genome browser (hg19). These sequences were then compared with NR consensus sequences using Cister, rVista and TRANSFAC MATCH programs to detect which putative *cis*-regulatory elements have high probability of NR binding. The prediction analyses with Cister and rVista, were originally done during the initial *in silico* screen for putative enhancer elements (see Chapter 4) on the entire *ABCG2* gene locus. First the entire *ABCG2* locus was scanned using the rVista[78] program, which analyzes sequences for conserved TFBS, using all vertebrate TF matrices from TRANSFAC professional. NREs were isolated from the list of all predicted TFBS, and regions with NREs predicted by rVista are indicated in Table 6.1. Next, the *ABCG2* locus was examined for regions with increased clustering of predicted transcription factor binding sites (TFBS), regardless of conservation, using the Cister program[79]. Matrices used for *cis*-elements included those preprogrammed into the Cister program (see Chapter 4 *Material and Methods* for full list) and several additional matrices obtained from TRANSFAC[80] and listed in Table 4.1. The *ABCG2* gene locus was split into fourths and analyzed in the Cister program with the default settings described in *Chapter 4 Materials and Methods*. Enhancer regions with NREs (such as ERE) predicted by Cister are indicated in Table 6.1. The third computational tool was the TRANSFAC Match program[80]. For this tool, the genomic sequence for each putative enhancer element was individually scanned for the probability of TF binding using the TRANSFAC release 2012.2 matrix table of all non-redundant vertebrate TFs. Parameters were set to select only high quality matrices and to minimize false positives. The probabilities for TF binding in putative enhancer elements were compiled and those elements with predicted NREs were extracted. To provide evidence for the actual binding

of NRs to putative enhancer regions, overlap of NR ChIP-seq peaks with putative enhancer elements were pulled from the TRANSFAC[80] ChIP-seq database. Additionally, all putative enhancer elements were visualized using the UCSC genome browser, and NR peaks occurring in the ENCODE[81] TF ChIP-seq (Txn ChIP) track were noted in Table 6.1. Many of the putative enhancer elements with *in silico* evidence-based predictions for NR binding are compiled under the respective NR in Table 6.1; the NR predictions shown were those utilized to select putative enhancer elements for testing in *in vitro* induction assays.

Table 6.1. Nuclear Response Elements in ECRs

ER	HNF3α/β[6]	RXR[7]	PXR	GR	AhR
ECR420[4]	ECR44[2]	CR9[2]	ECR17[2]	ECR31[2]	ECR420[2,4]
CR15[3]	ECR402[1,2]	ECR52[2]	ECR425[2]	ECR52[2]	ECR429[1]
ECR410[4]	ECR423[2]	ECR426[2]	CR6[2]	ECR426[1,2]	CR10[4]
CR10[4]	ECR426[2]	CR6[2]	ECR420[2]	ECR410[2,4]	CR15[2,4]
CR11[4]	CR9[4]	ECR400[2]	CR10[2]	CR10[4]	CR16[2,4]
CR16[4]	ECR43[2]	ECR38[2]	CR11[2]	ECR38[2]	ECR410[2,4]
CR19[2,4]	CR7[2]	CR7[2]	ECR428[2]	CR7[2]	ECR400[2]
CR8[2]	ECR25[2]	ECR429[2]	ECR400[2]	ECR428[2]	
ECR425[2]	CR10[2]	ECR428[2]		CR8[2]	
	CR15[2]	CR19[2]		ECR402[2]	
	CR16[2]	ECR25[2]		ECR412[2,4]	
	ECR31[2]	CR8[2]		ECR25[2]	
		ECR402[2]		ECR33[5]	
		ECR410[2]			
		ECR412[2]			
		ECR423[2]			
		CR10[2]			
		ECR425[2]			
		CR11[2]			
		CR15[2]			
		CR16[2]			
		ECR33[2,5]			
		ECR31[2]			
		ECR55[2]			

[1]rVista predicted
[2]TRANSFAC predicted
[3]TRANSFAC ChIP-seq evidence
[4]Cister predicted
[5]ENCODE evidence
[6]Either HNF3α (FOXA1) or HNF3β;
[7]Due to the flexibility of RXR as a binding partner, these predictions are from matrices that target different combinations of direct repeats

6.3.3. *Cell Culture*

The HepG2 cell line was obtained from the ATCC and grown in high-glucose DMEM supplemented with 10% FBS, 100 units/mL of penicillin and 0.1 mg/mL of streptomycin. The MCF-7 cell line was also obtained from ATCC and cells were grown in IMEM, without phenol red, supplemented with 10% charcoal stripped FBS, 100 units/mL of penicillin and 0.1 mg/mL of streptomycin. All cell lines were grown in a 5% CO_2 incubator at 37°C. To maintain cells, they were split upon reaching confluency by treatment with 0.05% Trypsin-EDTA, washed with 1X PBS and suspended in fresh media at a 1:5 to 1:20 dilution.

6.3.4. *Transient Transfections*

ABCG2 promoter reference and variant plasmids were made as described in the *Materials and Methods* of Chapter 3, enhancer and suppressor constructs as described in Chapter 4, and variant enhancer constructs as described in Chapter 5. The pGL4.23 vector is a firefly luciferase vector with a multiple cloning site designed to accept a putative enhancer element upstream of a minimal promoter and the luciferase gene. The pGL3-promoter vector is a firefly luciferase vector with a multiple cloning site designed to accept a putative suppressor element upstream of the strong SV40 promoter and the luciferase gene. The pGL4.11b vector is a promoterless firefly luciferase vector designed to accept a putative promoter sequence before the luciferase gene. Once the target sequence is cloned into one of these vectors and transfected into cells, the luciferase activity can be measured as a surrogate for the regulatory region function. The cell lines were each chosen to represent their primary tissue source. Plasmids for hPXR and Xrem

were a gift from Kathy Giacomini and are described below. For transient transfections of the HepG2 cell lines, cells were split with 0.05% Trypsin-EDTA and seeded at approximately 1.8 x 10^4 cells per well of a 96-well plate in fresh DMEM with 10% FBS without antibiotics and grown for at least 24 hr to 80% confluency. Cells were then transfected with Lipofectamine 2000 following guidelines suggested in the manufacturer's protocol. In short, 0.5 µL of Lipofectamine 2000 was incubated in 25 µL Opti-MEM for 5 min and then gently mixed with a 25 µL solution of 100 ng *ABCG2* plasmid, 50 ng of hPXR plasmid and 10 ng pGL4.74 [*hRluc*/TK] (Promega, Madison, WI) diluted with Opti-MEM. The DNA-Lipofectamine mixture was allowed to incubate at room temperature for 30 min before being placed onto cells with 50 µL of antibiotic-free media. MCF-7 cells were split with 0.05% Trypsin-EDTA and seeded at ~2.5 x 10^4 cells per well and transfected with the PolyJet™ DNA *In Vitro* Transfection Reagent once they reached 80-90% confluency; transfection efficiency was optimized by following the manufacturer's guidelines. Briefly, media on the cells was replaced with 100 µL fresh IMEM (supplemented with FBS and antibiotics as above) 30 min before transfection. A mix of 75 ng *ABCG2* plasmid and 25 ng of pGL4.74 [*hRluc*/TK], to control for transfection efficiency, was diluted to 5 µL with IMEM supplemented with 10% FBS (no antibiotics). A 0.4 µL aliquot of PolyJet was diluted to 5 µL with IMEM supplemented with 10% FBS (no antibiotics) and then immediately added to the DNA with gentle mixing. The PolyJet/DNA mix was incubated at room temperature for 15 min before being added to the cells. All cell lines were incubated with their transfection reagents for 6-24 hr before drug media was added for induction assays.

6.3.5. *Rifampin Induction*

The protocol for induction of the *ABCG2* constructs with rifampin was adapted from previously published rifampin induction protocols[77,82]. The positive control plasmid for induction was a xenobiotic response element (Xrem) that induces CYP3A4 expression upon rifampin treatment[77]. Additionally, we co-transfected with a human PXR plasmid to ensure the expression of PXR. Plasmids used in the rifampin induction assays included empty pGL4.23 [*luc2*/minP], enhancer-pGL4.23, hPXR-pcDNA3.1 and Xrem-pGL4.23. Since almost all putative *cis*-regulatory elements had either a PXR or RXR predicted binding site, we screened them all in the rifampin induction assay. HepG2 cells were transiently transfected as above and 18 hr after transfection each well in a 96-well plate was given new media. Each plasmid was treated with either 200 µL of DMEM with 25 µM rifampin dissolved in DMSO or with 200 µL of DMEM with 0.1% DMSO. Cells were incubated for 24 hr with drug media before being assayed for luciferase activity.

6.3.6. *17β-estradiol Exposure*

Treatment of the *ABCG2* constructs with E_2 was adapted from previously published ER induction protocols[31,44]. The positive control plasmid for induction was the *ABCG2* promoter construct, which includes an ERE at -180 that responds to E_2 treatment[29,31,43]. MCF-7 cells were used for the E_2 induction assay because they express the ER and estrogen treatment modulates ABCG2 expression[45,83]. Plasmids used in the E_2 induction assays included pGL4.23 [*luc2*/minP], enhancer-pGL4.23, variant enhancer-pGL4.23, pGL3 promoter [*luc*+/SV40], *ABCG2* promoter-pGL4.11b [*luc*+/minP], variant *ABCG2* promoter-pGL4.11b and pGL4.11b [*luc2*+/minP]. Since a significant

faction of putative *cis*-regulatory elements have predicted HNF3α or ER binding sites and ER also binds to nontraditional recognition sequences[84], we hypothesized that there are both novel and traditional ERE in our putative *cis*-regulatory elements. Since ER is such an important regulator of *ABCG2*, all high priority putative *cis*-regulatory elements were screened in the E_2 induction assays, whether or not they were predicted to have ER response elements (Table 6.1). MCF-7 cells were transiently transfected as above, and 6 hr after transfection, media was changed to 200 μL of IMEM (without phenol red) with 100 nM E_2 (dissolved in DMSO) or with 200 μL of IMEM with 0.2% DMSO for each well of the 96-well plate. Cells were incubated for 48 hr with drug media before being assayed for luciferase activity.

6.3.7. *Aryl Hydrocarbon Receptor Induction*

Induction of the *ABCG2* plasmids with B[a]P was adapted from a previously published AhR induction protocol[85]. The positive control plasmid for induction was the *ABCG2* promoter construct, which includes AhR response elements at -55 and -189 that are important in response of the *ABCG2* promoter to aryl hydrocarbon treatment[30,85,86]. MCF-7 cells were used for the AhR induction assay because they express the AhR and their ABCG2 expression responds to aryl hydrocarbon treatment[66]. Plasmids used in the AhR induction assays included pGL4.23 [*luc2*/minP], enhancer-pGL4.23 [*luc2*/minP], *ABCG2* promoter-pGL4.11b [*luc*+/minP] and pGL4.11b [*luc2*+/minP]. Only enhancer elements predicted to have AhR response elements were screened in the B[a]P induction assays (Table 6.1). MCF-7 cells were transiently transfected as above, and 18 hr after transfection, media was changed to 200 μL of IMEM (without phenol red) with 500 nM

or 10 μM B[a]P dissolved in DMSO or with 200 μL of IMEM with 0.2% DMSO. Cells were incubated for 24 hr with drug media before being assayed for luciferase activity.

6.3.8. *Dexamethasone Induction*

Induction of the *ABCG2* plasmids with dexamethasone (DEX) was adapted from previously published GR induction protocols[60,61]. MCF-7 cells were used for the DEX induction assay because they express GR[87] and their expression of ABCG2 responds to glucocorticoid treatment[60]. Plasmids used in the DEX induction assays included pGL4.23 [*luc2*/minP], enhancer-pGL4.23, variant enhancer-pGL4.23, pGL3 promoter [*luc*+/SV40], supressor-pGL3 promoter [*luc*+/SV40], *ABCG2* promoter-pGL4.11b [*luc2*+/minP], variant *ABCG2* promoter-pGL4.11b and pGL4.11b [*luc2*+/minP]. Only putative enhancer elements predicted to have GR response elements were screened in the dexamethasone induction assays. MCF-7 cells were transiently transfected as above, and 18 hr after transfection, media was changed to 200 μL of IMEM (without phenol red) with 500 nM DEX (dissolved in DMSO) or with 200 μL of IMEM with 0.2% DMSO. Cells were incubated for 24 with drug media before being assayed for luciferase activity.

6.3.9. *Luciferase Assay*

After cells were treated with drug or DMSO, each well was washed with 100 μL 1X PBS and lysed with 50 μL of 1X passive lysis buffer for 1 hr with shaking. HepG2 or MCF-7 lysates (30 μL) were measured for firefly and *Renilla* luciferase activity using 70 μL each of the Luciferase Assay Reagent II and Stop & Glo® reagents from the Dual-Luciferase® Reporter Assay System in a GloMax 96 microplate Dual Injector

Luminometer. The firefly activity was normalized to the *Renilla* activity per well to control for transfection efficiency. Each experiment also included the empty pGL4.23, pGL4.11b or pGL3-promoter vector as the negative control and the *Xrem*-pGL4.23 or *ABCG2* promoter plasmid as the positive control. Luciferase activity for each plasmid was expressed as the ratio of the normalized firefly to *Renilla* activity to that of either the DMSO treatment or the empty vector treated with or without drug.

6.3.10. *Statistical Analysis*

Luciferase activity was first normalized to *Renilla* activity and then by the activity of the drug-treated empty vector (EV). For presentation in figures, the difference from EV with NR ligand treatment was divided by the activity with DMSO treatment to yield a relative fold activity (RFA). Putative enhancer elements treated with drug were considered to have statistically significant activity compared to the DMSO treated vector if the unpaired Student's *t*-test had a $P < 0.05$ in each experimental replication. For statistical analysis of variant versus reference regulatory regions, the RFA for the variant regulatory region was tested against the RFA of the reference regulatory region using either an unpaired Student's *t*-test (when analyzing only one variant) or an ANOVA followed by a post-hoc Bonferroni's multiple comparison *t*-test (when comparing multiple variants) with statistical significance set at $P < 0.05$. All statistics were run using the GraphPad Prism 5 program.

6.4. Results

6.4.1. *Predicted Nuclear Response Elements*

Utilizing several web-based TF prediction programs and publically available ChIP-seq databases, putative enhancer elements were analyzed for the occurrence of various NREs (Table 6.1). The NRE for RXR, from matrices that include different direct repeat configurations, was present in 24 of the 30 putative enhancer elements, making it the most abundant putative NRE. All but one RXR response elements were predicted using the TRANSFAC MATCH program[80]; only ECR33 had additional evidence from the ENCODE ChIP-seq database[81] for the binding of RXR (Table 6.1). The glucocorticoid response element (GRE) was predicted in 13 of 30 putative enhancer elements with the GREs in ECR426, ECR410 and ECR412 being predicted by more than one program. Additionally, the ECR426 predicted GRE was conserved through mouse. The next most abundant NRE, in 12 of the 30 putative enhancer elements, was for HNF-3α (FOXA1, a binding partner of ER) or HNF-3β. ERE were predicted in 9 of the 30 putative *cis*-regulatory regions and AhR response elements in only 7 of 30 putative *cis*-regulatory regions. Besides RXR binding in ECR33, the only other ChIP-seq evidence for NR binding was for p300, a co-activator for many NRs, in both ECR31 and ECR33 and ER in CR15 (Table 6.1).

6.4.2. *System Controls*

To test the validity of our induction assays, MCF-7 cells transiently transfected with the *ABCG2* promoter plasmid were treated for 18 to 48 hr with ligands for different nuclear receptors (Figure 6.1A). Initial conditions for the induction assays were based on

previous literature for E_2[31,44], DEX[60,61] and B[a]P[85]. Treatment with 100 nM E_2 caused increased *ABCG2* promoter activity within 18 hours and increased activity was maintained for 48 hours (Figure 6.1A). Treatment with 500 nM DEX caused increased *ABCG2* promoter activity at 24 hours and decreased promoter activity after 48 hours (Figure 6.1A). Any cell toxicity from the DEX, or other NR ligands, is accounted for by the *Renilla* activity. However, we did not notice excessive cell toxicity at any of the NR ligand doses used. Due to the ability of DEX to act via a GR mediated mechanism at 24 hr and a PXR mechanism at 48 hr[60,61], regulatory regions were tested at 24 hr post DEX treatment. Treatment with 500 nM or 10 μM B[a]P caused 2-fold induction of the *ABCG2* promoter at 18 hr and this increased to 4-fold induction only with the lower dose (Figure 6.1A). There was no induction by B[a]P at 48 hr (Figure 6.1A). Based on these results and a previous study[85] cells were treated for 24 hr with 10 μM B[a]P. To test the validity of the rifampin induction assay, HepG2 cells were treated with 10 μM and 25 μM of rifampin for 24 hr after transient transfection with the XREM element. These conditions were based on the literature[77,82], and the positive control, Xrem, was a known rifampin-inducible element upstream of CYP3A4[77]. Treatment with 10 μM rifampin caused an 8-fold induction of the XREM enhancer activity after 24 hr, while treatment with 25 μM rifampin caused an 18-fold induction of the XREM enhancer activity (Figure 6.1B). Therefore, cells expressing putative regulatory regions were treated with 25 μM rifampin for 24 hr.

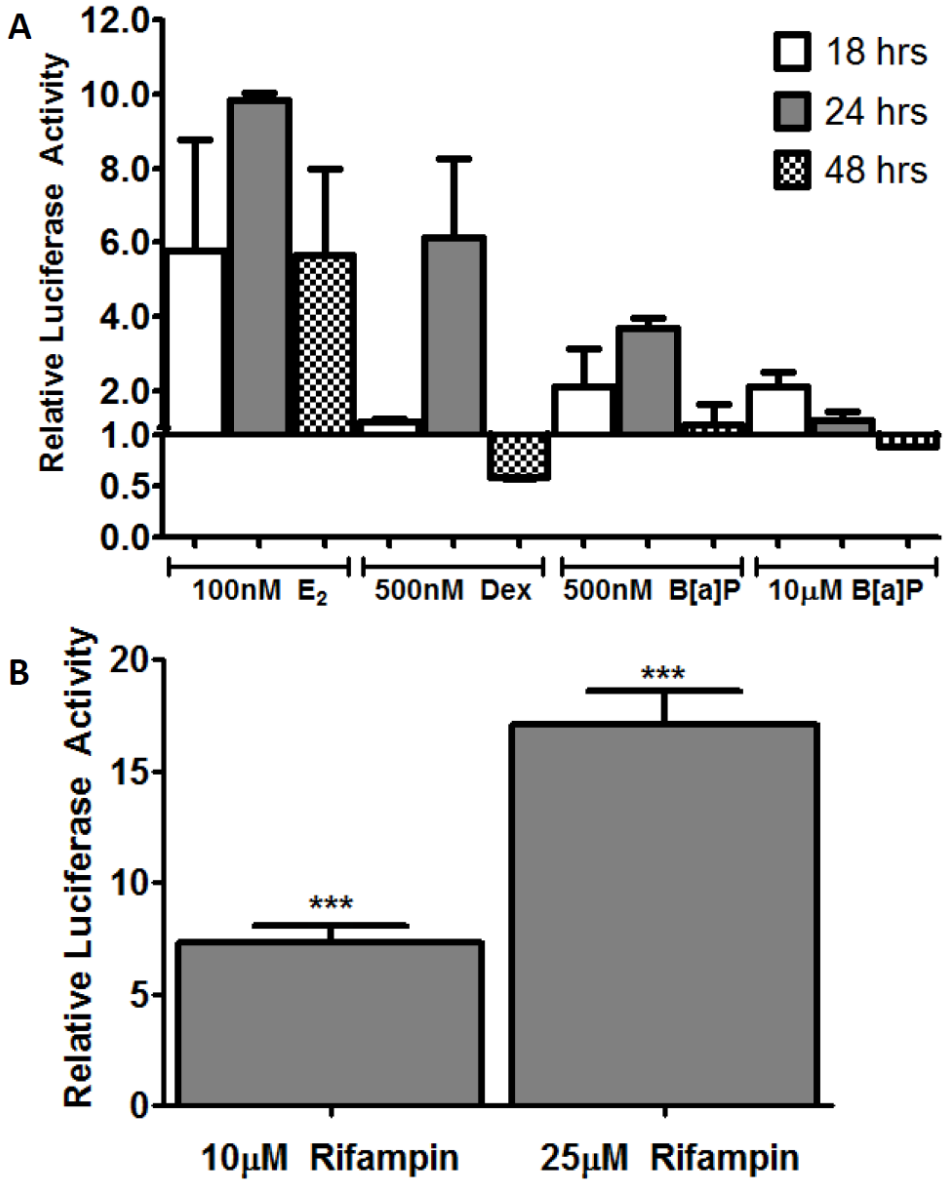

Figure 6.1. System controls for *in vitro* nuclear response element assays. Breast (MCF-7) cells (A) were transiently transfected with the *ABCG2* promoter plasmid (in pGL4.11b) and then treated with 17β-estradiol (E_2, 100 nM), dexamethasone (Dex, 500 nM), benzo[a]pyrene (B[a]P, 500 nM or 10 μM) or 0.2% DMSO. Liver (HepG2) cells (B) were transiently transfected with the Xrem plasmid (in pGL4.23) and then treated with rifampin (10 μM or 25 μM) or 0.1% DMSO. Cells were treated with drug for 18 (white bars), 24 (grey bars) or 48 (checkered bars) hr before luciferase activity was

measured. Normalized firefly to *Renilla* luciferase activity post ligand treatment is shown for each plasmid relative to its activity when treated with DMSO (DMSO treatment is set to '1'). Normalized luciferase values less than one are due to attenuation of luciferase activity with ligand treatment. Data is expressed as the mean ± SEM from a representative experiment (n = 4-9). Differences between XREM activity in the absence and presence of rifampin were tested by an unpaired Student's *t*-test. *** $P < 0.0001$.

6.4.3. *Rifampin Induction*

The ability of putative enhancer elements to respond to a PXR ligand was tested in transiently transfected HepG2 cells after 24 hr of rifampin treatment. After DMSO and rifampin treatment, cell lysates were tested for differences in normalized enhancer activity. Relative luciferase activity for each plasmid is expressed as the enhancer activity with ligand treatment to that measured after DMSO treatment (Figure 6.2). Of the 30 screened enhancer elements, nine of them had significant rifampin-inducible activity (Figure 6.2). Most of the regions (CR8, CR9, CR10, ECR38, ECR400, ECR410 and ECR412) responded weakly to rifampin treatment (Figure 6.2). ECR25 and ECR33 responded moderately (~3-fold induction) to rifampin treatment, and the ECR33 enhancer had the highest induction (Figure 6.2). This screen identified several regulatory elements that respond to the PXR ligand rifampin and could be potential nuclear response elements for the *ABCG2* gene.

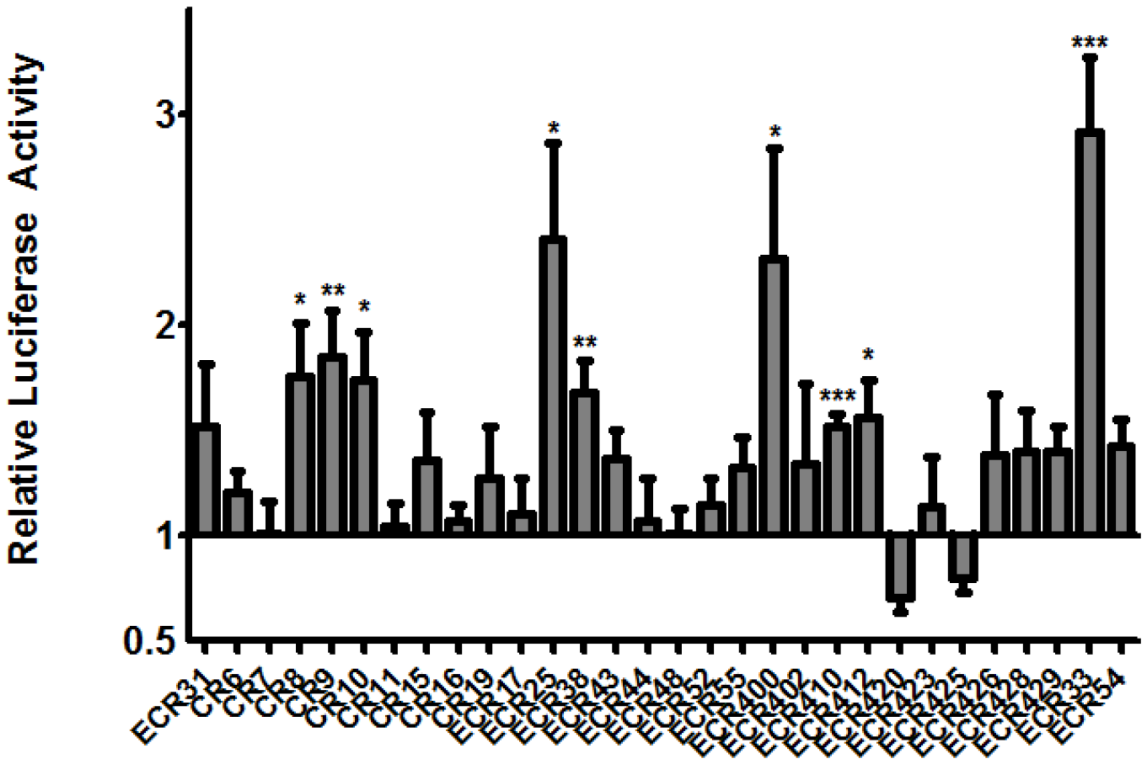

Figure 6.2. Effect of rifampin treatment on enhancer activity. Luciferase activity of putative enhancer regions was measured in transiently transfected liver (HepG2) cells 24 hr after treatment with 0.1% DMSO or 25μM rifampin. Enhancer activity is expressed as the ratio of firefly to *Renilla* luciferase activity in the presence of rifampin to the same ratio after DMSO treatment. Data is expressed as the mean ± SEM from a representative experiment (n = 6 wells per construct and treatment). Differences between the enhancer activity in the absence and presence of rifampin were tested by an unpaired Student's *t*-test. *** $P < 0.0001$, ** $P < 0.001$, * $P < 0.05$.

6.4.4. *Estrogen Receptor Mediated Induction*

Many different regulatory sequences were tested for their response to E_2 treatment after 48 hours. First, the response of 30 putative enhancer constructs and the *ABCG2*

promoter construct to E_2 were tested (Figure 6.3). There were six enhancer elements, ECR400, CR6, ECR33, CR7, CR8 and CR9, with significantly decreased activity (25 to 50%) upon E_2 treatment (Figure 6.3). Most of these regions were moderate to strong enhancers with DMSO treatment and their activity was reduced or abolished with E_2 treatment. The only putative enhancer region with induced activity after E_2 treatment was CR19, which exhibited a moderate induction upon E_2 treatment (Figure 6.3). The *ABCG2* promoter construct activity was also weakly induced by E_2 treatment (Figure 6.3 and Figure 6.4).

After confirmation that the *ABCG2* promoter was inducible with E_2 treatment (Figure 6.3 and Figure 6.4), the nine variant *ABCG2* promoter plasmids (described in Chapter 3) were tested for changes in E_2 induction. Four of nine *ABCG2* promoter variants responded to E_2 treatment, and rs66664036 increased induction compared to the reference sequence (Figure 6.4).

Since CR6 enhancer activity was significantly decreased upon treatment with E_2 (Figure 6.3), the effect of E_2 on the seven variant CR6 enhancer regions described in Chapter 5 was evaluated. Three SNPs were associated with reduced enhancer activity in response to E_2, and the suppression with rs573519157 was greater than that for the reference sequence (Figure 6.5). rs190754327 was associated with loss of E_2 induction (Figure 6.5).

Since the ECR400 enhancer activity was significantly decreased upon treatment with E_2 (Figure 6.3) the effect of genetic variation in ECR400 on the response to E_2 was evaluated. With one exception, the ECR400 SNPs did not affect the ability of the

ECR400 enhancer to respond to E_2 (Figure 6.6). rs12508471 caused a loss of E_2-induced suppression of ECR400 enhancer activity (Figure 6.6).

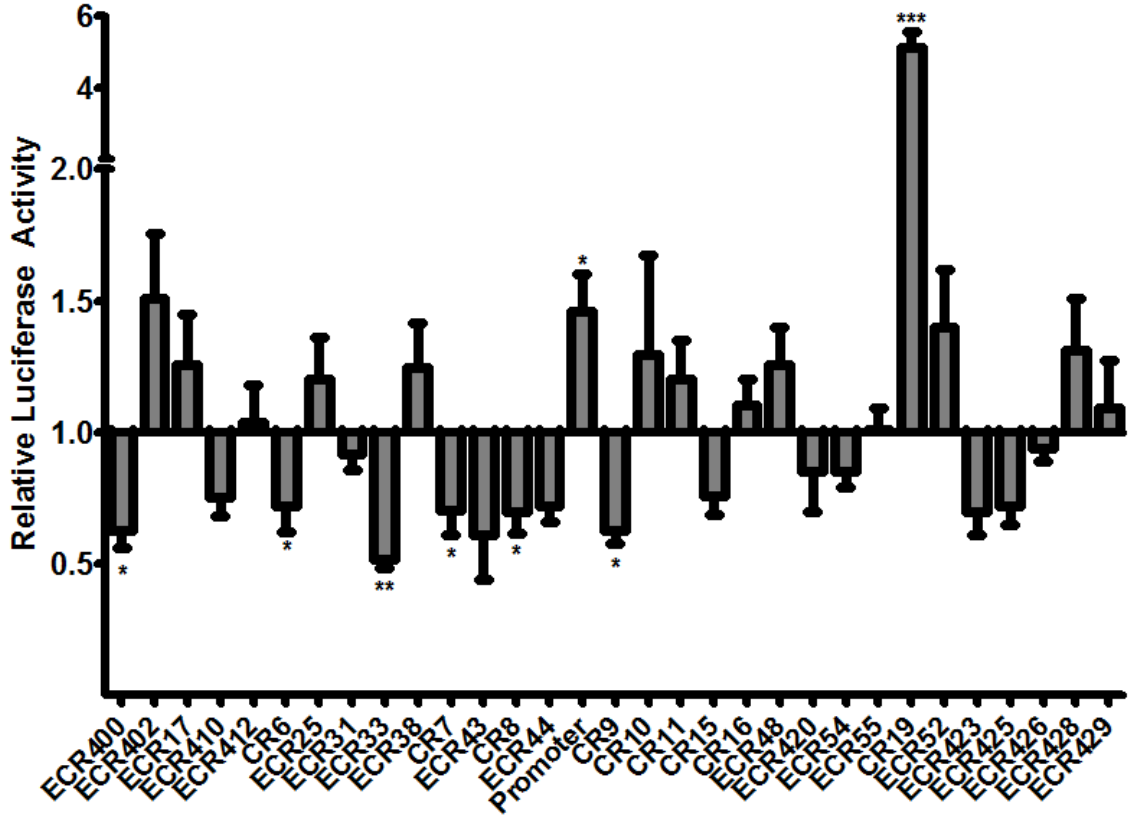

Figure 6.3. Effect of 17β-estradiol treatment on promoter and enhancer activity. The luciferase activity of *ABCG2* promoter (in pGL4.11b) and putative enhancer regions (in pGL4.23) was measured in transiently transfected breast (MCF-7) cells 48 hr after treatment with 0.2% DMSO or 100 nM 17β-estradiol (E_2). Enhancer activity is expressed as the ratio of firefly to *Renilla* luciferase activity in the presence of E_2 to the same ratio after DMSO treatment. Relative luciferase activity less than one is due to reduction of the enhancer activity with E_2 treatment. Data is expressed as the mean ± SEM from a representative experiment (n = 6-8 wells per construct and treatment). Differences between enhancer activity in the absence and presence of E_2 were tested by an unpaired Student's *t*-test. *** $P < 0.0001$, ** $P < 0.001$, * $P < 0.05$.

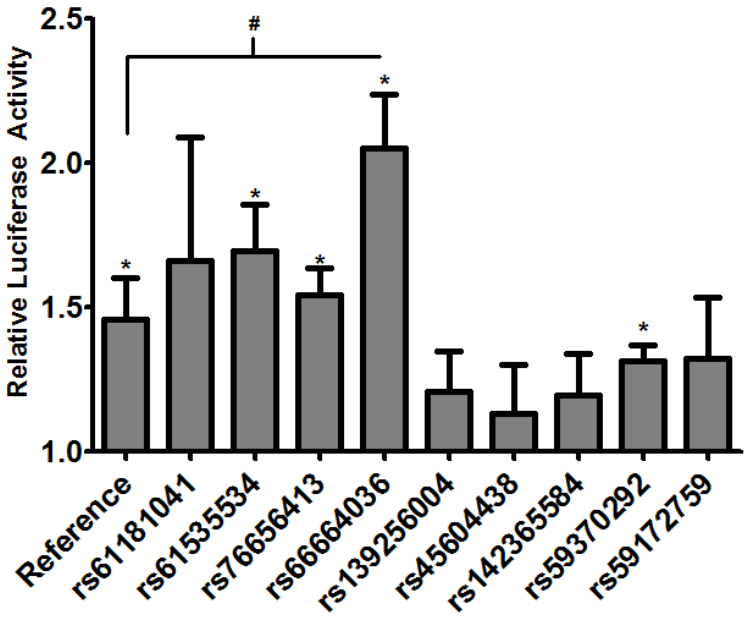

Figure 6.4. Effect of 17β-estradiol treatment on reference and variant promoter activity. The luciferase activity of reference and variant promoter plasmids (in pGL4.11b) was measured in transiently transfected breast (MCF-7) cells 48 hr after treatment with 0.2% DMSO or 100 nM 17β-estradiol (E_2). Enhancer activity is expressed as the ratio of firefly to *Renilla* luciferase activity in the presence of E_2 to the same ratio after DMSO treatment. Data is expressed as the mean ± SEM from a representative experiment (n = 6-8 wells per plasmid and treatment). Differences between promoter activity in the absence and presence of E_2 were tested by an unpaired Student's *t*-test; * $P < 0.05$. Differences in promoter activity between variants and the reference were compared by an ANOVA followed by a Bonferroni multiple comparison *t*-test; $^{\#}$ $P < 0.05$.

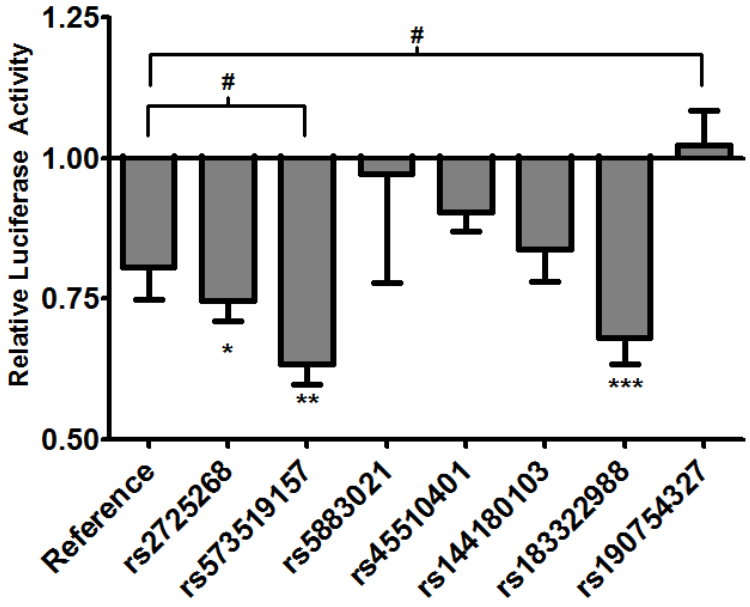

Figure 6.5. Effect of 17β-estradiol treatment on reference and variant CR6 enhancer activity. The luciferase activity of reference and variant CR6 enhancer plasmids (in pGL4.23) was measured in transiently transfected breast (MCF-7) cells 48 hr after treatment with 0.2% DMSO or 100 nM 17β-estradiol (E_2). Enhancer activity is expressed as the ratio of firefly to *Renilla* luciferase activity in the presence of E_2 to the same ratio after DMSO treatment. Relative luciferase activity less than one indicates reduction of enhancer activity with E_2 treatment. Data is expressed as the mean ± SEM from a representative experiment (n = 6-8 wells per construct and treatment). Differences between the enhancer activity in the absence and presence of E_2 were tested by an unpaired Student's *t*-test; * $P < 0.05$, ** $P < 0.001$. Differences between variant and reference CR6 enhancer RFA were compared by an ANOVA followed by a Bonferroni multiple comparison *t*-test; $^{\#}$ $P < 0.05$.

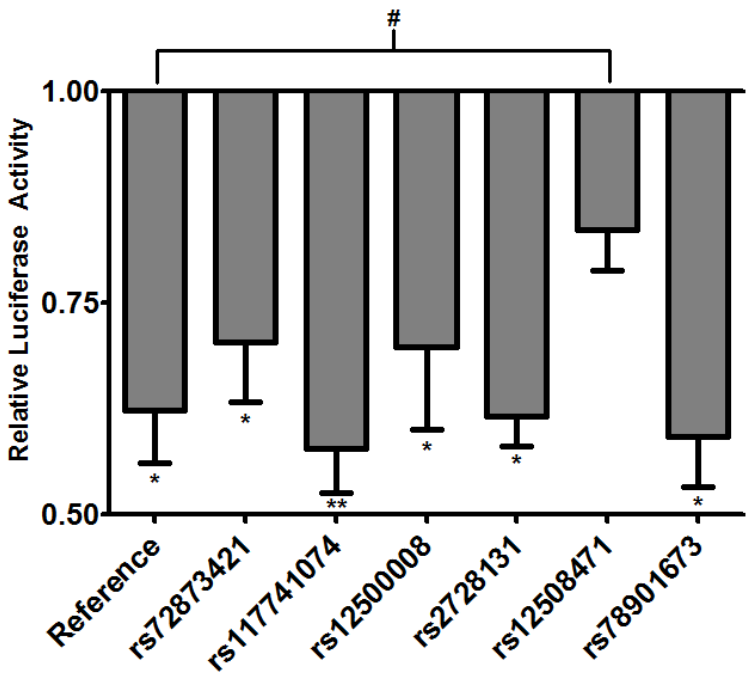

Figure 6.6. Effect of 17β-estradiol treatment on reference and variant ECR400 enhancer activity. The luciferase activity of reference and variant ECR400 enhancer constructs (in pGL4.23) was measured in transiently transfected breast (MCF-7) cells 48 hr after treatment with 0.2% DMSO or 100 nM 17β-estradiol (E_2). Enhancer activity is expressed as the ratio of firefly to *Renilla* luciferase activity in the presence of E_2 to the same ratio after DMSO treatment. Relative luciferase activities less than one indicate reduction of enhancer activity with E_2 treatment. Data is expressed as the mean ± SEM from a representative experiment (n = 6-8 wells per construct and treatment). Differences between enhancer activity in the absence and presence of E_2 were tested by an unpaired Student's *t*-test; * $P < 0.05$, ** $P < 0.001$. Differences between the response of reference and variant ECR400 enhancers to E_2 were compared by an ANOVA followed by a Bonferroni multiple comparison *t*-test; $^{\#}$ $P < 0.05$.

6.4.5. *Glucocorticoid Receptor Mediated Induction*

Selected putative enhancer constructs were tested for their response to dexamethasone (DEX) treatment. First, putative enhancer constructs, and when available their suppressor constructs, with predicted GREs (Table 6.1) were transiently transfected into MCF-7 cells and then treated with DEX or DMSO for 24 hours and their relative luciferase activity measured. Three regions had significantly decreased luciferase activity relative to DMSO treatment respectively. ECR25 (in pGL4.23) had a 60% decrease in RFA with DEX treatment (Figure 6.8). However, the ECR25 (pGL3-promoter) suppressor construct did not have altered RFA with DEX treatment (Figure 6.8). ECR410, which had GREs predicted by both Cister and TRANSFAC (Table 6.1), had a 50% to 75% decrease in RFA after DEX treatment when this region was tested in either the in pGL4.23 or pGL3-promoter vectors (Figure 6.8). The last construct with a significant decrease in relative luciferase activity was ECR400 rs12508471 plasmid. Although ECR400 is not predicted to have a GRE (Table 6.1), the rs12508471 SNP was predicted to gain a GR site (see *Chapter 5*, Figure 5.15), which was why this SNP was screened. The ECR400 enhancer was not significantly decreased with DEX treatment, dropping a little over 25% (Figure 6.8). In contrast, the rs12508471 SNP had over an 80% decreased RFA with DEX treatment (Figure 6.8).

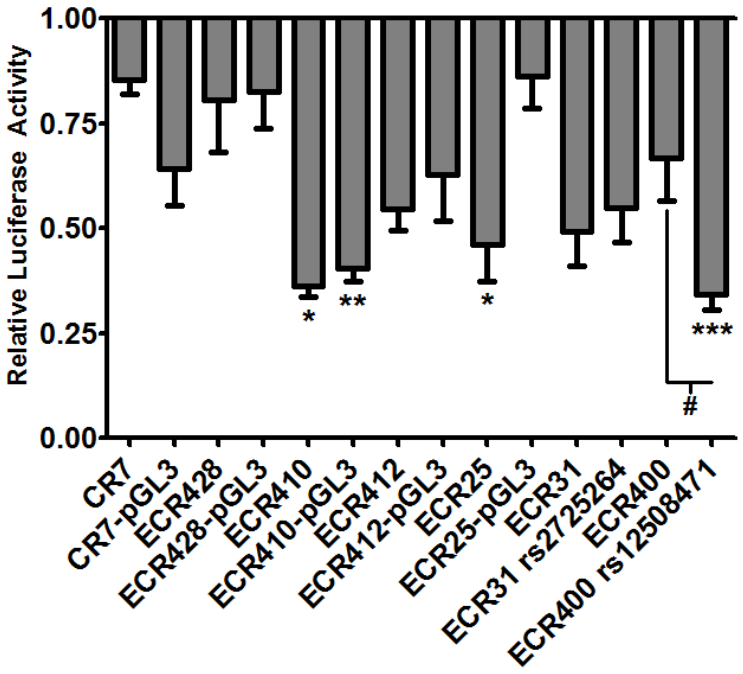

Figure 6.7. Effect of 24 hour dexamethasone treatment on selected reference and variant enhancers' and suppressors' activities. The luciferase activity of reference and variant enhancer constructs (in pGL4.23) and suppressor constructs (in pGL3-promoter) was measured in transiently transfected breast (MCF-7) cells 24 hours after treatment with 0.2% DMSO or 500nM dexamethasone (DEX). Enhancer activity is expressed as the ratio of firefly to *Renilla* luciferase activity in the presence of DEX to the same ratio after DMSO treatment. Relative fold activation values less than one are due to reduction of the enhancer's activity with DEX treatment. Data is expressed as the mean ± SEM from a representative experiment (n=6-8 wells per construct and treatment). Differences between reference enhancer activity in the absence and presence of DEX were tested by an unpaired Student's *t*-test * $P < 0.05$, ** $P < 0.001$, *** $P < 0.0001$. Differences between the RFA of reference and variant enhancers were compared by a Student's *t*-test, $^{\#}$ $P <$ 0.05.

6.4.6. *Aryl Hydrocarbon Receptor Mediated Induction*

Putative enhancer constructs that were predicted by more than one program to have aryl hydrocarbon (AhR) response elements (Table 6.1) and the *ABCG2* promoter construct, were transiently transfected into MCF-7 cells and then treated with B[a]P for 24 hr and their relative luciferase activity measured (Figure 6.8). Only the *ABCG2* promoter showed increased activity when treated with B[a]P and the induction was modest (Figure 6.8).

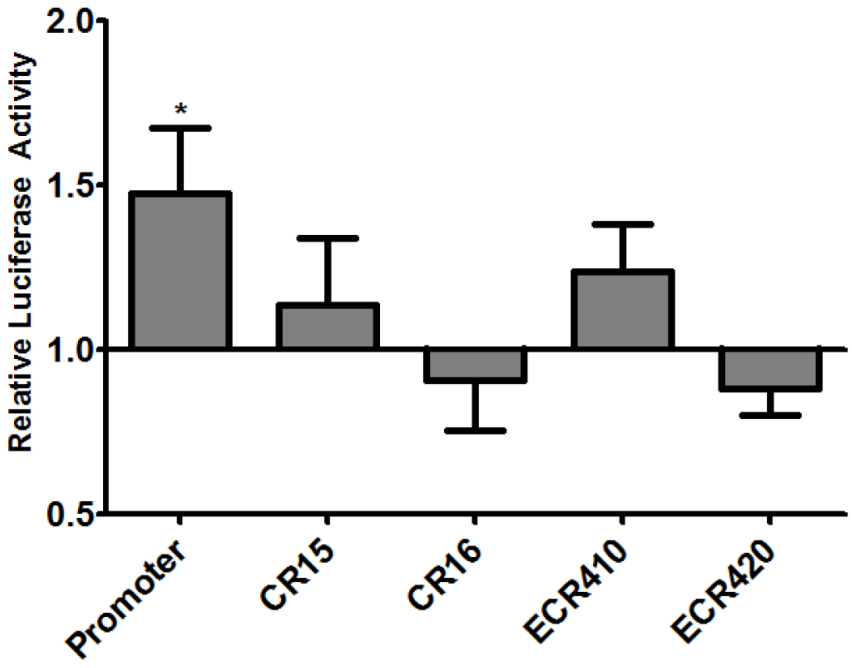

Figure 6.8. Effect of 24 hour benzo[a]pyrene treatment on selected enhancer and promoter activities. The luciferase activity of enhancer regions (in pGL4.23) and the *ABCG2* promoter (in pGL4.11b) was measured in transiently transfected breast (MCF-7) cells 24 hr after treatment with 0.2% DMSO or 10 μM benzo[a]pyrene (B[a]P). Enhancer activity is expressed as the ratio of firefly to *Renilla* luciferase activity in the presence of B[a]P to the same ratio after DMSO treatment. Relative luciferase activities less than one

indicate reduction in enhancer activity with B[a]P treatment. Data is expressed as the mean ± SEM from a representative experiment (n = 8 wells per construct and treatment). Differences between reference enhancer activity in the absence and presence of B[a]P were tested by a Student's *t*-test; * $P < 0.05$.

6.4.7. *Accuracy of NRE and HRE Predictions*

There were 12 of the 30 high priority enhancer regions that responded to at least one nuclear receptor (NR) ligand (listed in Table 6.2), six regions responded to at least two different NR ligands and ECR400 (or its variant) responded to all the NR ligands tested (Table 6.2).

All regions were challenged with rifampin and 17β-estradiol (E_2), in an attempt to see if prediction of NRRE were sufficient to determine *in vitro* activity. Of the nine elements that responded to rifampin, only two had predicted PXR response elements (22%) and of the eight regions with predicted PXR response elements only two responded to rifampin (25%). Of the 22 regions not predicted to harbor a PXR response element, six responded to rifampin treatment (27%). For E_2 response, of the nine regions with predicted ERE, only three responded to E_2 treatment (33%), and CR15, which had ChIP-seq support for ER binding (Table 6.1), did not respond to E_2 treatment (Figure 6.3). Of the 21 regions without predicted ER response elements, six (29%) responded to E_2 treatment. These results suggest that *in silico* prediction or preliminary ChIP-seq data of NR binding was not indicative of response to ligand treatment (summarized in Table 6.2). Additionally, excluding regions without predicted NR binding could allow for false negatives.

Only selected regions with predicted GR and AhR (Table 6.1) were challenged with dexamethasone and B[a]P. Of the three regions that responded to dexamethasone treatment, one (33%) had predicted GR binding. Of the three elements with predicted GR binding only one (33%) responded to dexamethasone. None of the regions with predicted AhR binding responded to B[a]P treatment.

Table 6.2. Response of *ABCG2* Locus Regulatory Regions to Xenobiotic Treatment

Region	Treatment				Predicted NRE
	Rifampin	Estrogen	Dex	B[a]P	
ECR33	↑	↓	•	•	RXR, GR
CR16	↔	↔	•	↔	ER, RXR, AhR
CR6	↔	↓	•	•	RXR, PXR
ECR400	↑	↓	↓	•	RXR, PXR, AhR
CR8	↑	↓	•	•	ER, RXR, GR
CR9	↑	↓	•	•	RXR
CR10	↑	↔	•	•	ER, RXR, PXR, AhR
ECR25	↑	↔	↓	•	RXR, ER
ECR38	↑	↔	•	•	RXR, GR
ECR410	↑	↔	↓[1]	↔	ER, RXR, GR, AhR
ECR412	↑	↔	↔	•	RXR, GR
CR7	↔	↓	↔	•	RXR, GR
CR19	↔	↑	•	•	ER, RXR
ECR429	↔	•	•	•	RXR, AhR
ECR425	↔	↔	•	•	ER, RXR, PXR
CR11	↔	↔	•	•	ER, RXR, PXR
ECR17	↔	↔	•	•	PXR
ECR31	↔	↔	↔	•	RXR, GR
ECR52	↔	↔	•	•	RXR
ECR402	↔	↔	•	•	RXR, GR
ECR426	↔	↔	•	•	GR
ECR420	↔	↔	•	↔	ER, PXR, AhR
Promoter	•	↑	↑	↑	ER

↑Increase, ↓Decrease, ↔No Response, • Not Tested

[1] Significant in both pGL4.23 and pGL3-suppressor vectors

Abbreviations: Dex, Dexamethasone; hr, hour; B[a]P, Benzo[a]pyrene; NRE, Nuclear Response Elements; ER, Estrogen Receptor; RXR, Retinoic Acid Receptor; PXR, Pregnane X Receptor; GR, Glucocorticoid Receptor; AhR, Aryl Hydrocarbon Receptor

6.5. Discussion

The evidence that *ABCG2* is regulated by NR pathways[22–25,27,29–31,33,34] and that multiple NREs work together to modulate expression of a gene[88] suggest that there are multiple hormone and xenobiotic response elements in the *ABCG2* gene locus. Therefore, the previous screen for regulatory elements of *ABCG2* (see Chapter 4) was extended with *in vitro* induction assays for PXR, ER, GR and AhR to identify if any of these putative regulatory elements are *cis*- hormone or xenobiotic response elements.

Rifampin induction of XREM (8- to 16- fold) was lower than the 45- fold induction reported in the literature[77], and reflects to some degree differences in the experimental conditions. The *ABCG2* promoter was inducible ~6-fold with E_2 treatment, similar to previous reports[31]. The 2- to 4- fold induction of the *ABCG2* promoter with an AhR ligand was also consistent with earlier studies[85,86].

The use of *in silico* TFBS prediction programs was moderately successful in identifying regions that would respond to ER, AhR, PXR and GR ligand challenge. Regions screened in both the GR and AhR induction assays were selected based on predicted binding of GR or AhR. However, the regions that were selected to be tested had response rates of 33% for GR and 0% with AhR. Predictive programs for TF binding are fairly inconsistent, but can only be as good as the TF matrices currently available. For example, only 60% of AhR bound DNA from ChIP-seq studies contained a core AhRE (5'-GCGTG-3')[89]. This is due to the variability in published cistrome data; for example, replication attempts to identify ER binding sites using ChIP-seq and ChIP-ChIP have success rates between 10-76%[90]. Continued development of TF binding consensus

sequence libraries and ChIP-seq databases, such as that from ENCODE, are likely to increase our ability to predict NRE.

In addition to variability in TF consensus sequences, binding of NRs to DNA found in ChIP-seq screens do not guarantee the region is a regulatory element. For example, 66%[91] - 91%[18] of androgen receptor response elements based on ChIP-seq data responded to androgens. Since both PXR and ER are important NRs in the regulation of *ABCG2*, all high priority regulatory elements in the *ABCG2* locus were challenged with representative ligands. Of the regions with a predicted NRE, 25-30% responded to the respective ligand; 29-77% of regions without a predicted NRE were modulated by the NR ligands. Inconsistent prediction of ERE by ER ChIP-seq has been previously reported[90]. The CR15 enhancer region had ChIP-seq data from ENCODE[81] supporting the binding of ER, however, CR15 did not respond to E_2. The CR19 region was significantly induced by E_2 treatment, consistent with ChIP-seq data that identified two peaks for binding of ER, and the ERα tethering protein FOXA1[21], to CR19. ChIP-seq data suggests that NRE are often composite elements, consisting of binding sites for NR co-activators as well as other NRs and TFs[12]. There is a wide variation in NR dimer partners for ER, including HNF-4, TR, RAR, RXR, and VDR[9]. The use of additional TFBS to identify composition sites, as well as the continual addition to ChIP-seq databases, would improve our current prediction methods for the identification of NRE.

The ER is perhaps the most well defined NR system, as it is integral in many biological responses and has many clinical applications[5]. Additionally, E_2 is a key regulator of growth and development and it functions in a wide array of target tissues[92]. In the current study, the activity of the *ABCG2* promoter was induced with E_2 treatment,

consistent with previous studies[31]. Additionally, the promoter SNP rs66664036 had significantly greater response to E_2 than the reference promoter. The rs6664036 SNP does not lie in the promoter's documented ERE and therefore does not effect ER binding. Interestingly, this same SNP reduced *in vivo* promoter activity 50% (see Chapter 3), a response that might be negated in the presence of E_2.

Although this ERE in the *ABCG2* promoter responds to E_2 treatment, the ER, like many other hormone receptors, prefers to bind to *cis*-regulatory regions versus proximal promoters[17], especially for genes with tissue-specific expression. Due to significant evidence supporting the ability of ER ligands to either increase or decrease ABCG2 expression depending on the tissue and presence of other NR[23,42–46], regulatory regions within the *ABCG2* gene locus were tested for response to E_2 treatment. CR6, a region just downstream of *ABCG2* with strong *in vitro* enhancer activity and weak *in vivo* activity, had decreased activity upon E_2 treatment. Additionally, regulation of ABCG2 expression by CR6 could be confounded by the CR6 SNP rs190754327 which eliminated the response to E_2 or the E_2-sensitive CR6 SNP rs573519157. Both of these SNPs resulted in reduced enhancer activity in HepG2 and HEK293T cells but further studies would be needed to test their activity *in vivo*. Thus the decreased *in vivo* activity of CR6 could be dependent on the availability of E_2 in a given tissue.

The expression of ABCG2 and activity of its promoter are both altered by exposure to AhR ligands[30,85,86]. In addition to crosstalk between ER and AhR[93], AhR dimerizes with several other NRs[94] and has recently been shown to recognize nontraditional AhRE motifs[89,95]. Although only elements with predicted AhR binding sites were screened, future studies should test the induction of other putative regulatory

regions regardless of predicted AhR binding, especially those we have shown to respond to E_2. The *ABCG2* promoter was the only region that responded to AhR; it was also induced by E_2 treatment. Interestingly, ECR420 and ECR410 also had predicted response elements for both ER and AhR but these regions did not respond to either E_2 or B[a]P. AhR and ER reportedly can dimerize[93]; whether this is important for the function of the *ABCG2* promoter requires further study. The response of the *ABCG2* promoter to both ER and AhR supports the hypothesis that there is an overlap in the genomic regions that bind both ER and AhR[93].

A goal of these experiments was to identify PXR response elements in the *ABCG2* locus since none have been reported despite strong evidence of *ABCG2* regulation by PXR[24,35,36,38]. PXR is a well known regulator of multiple hepatic drug transporters and metabolizing enzymes, and it is activated by many structurally diverse xenobiotic and endogenous ligands[96]. The most promising PXR response element in the *ABCG2* locus is the ECR33 enhancer region. ChIP-seq data from ENCODE supports the binding of two PXR interaction partners[7], p300 and RXR, to ECR33. ECR33 activity was also suppressed by treatment with E_2. ChIP-seq data also suggests that many other NRs bind to ECR33, including HNF4α, HNF4γ and GR, and the ER co-activator FOXA1 (HNF3α)[21]. RXRα and HNF4α have also been shown to interact with each other and with ERα[9]. Therefore, ER could be tethered to the ECR33 element through interactions with FOXA1, RXRα and HNF4α. The binding of so many NRs to the ECR33 region and the ability of multiple NR ligands to regulate ECR33 enhancer activity suggests that ECR33 is a composite response element. Knowledge of *ABCG2* PXR response elements, such as ECR33, could also aid in the identification of underlying protective or causative genetic

variants for altered statin response or gout, such as the rs2622628 ECR33 variant that reduces function or the rs190738974 ECR 33 variant that increases function.

As in the enhancer and suppressor screens, the most interesting inducible region was ECR400. ECR400 responded to multiple ligands, increasing with rifampin treatment and decreasing with E_2. The ECR400 has a conserved binding site for the Oct-1 TF, an important coactivator of many NRs including GR, PR, AR, RXR and ER[17,97–99]. Although there is no ChIP-seq data available from ENCODE or TRANSFAC indicating binding of any NRs to ECR400, the response of ECR400 to multiple NR ligands suggests that it is an important hormone and xenobiotic response element. Further studies are needed to confirm the binding of these NRs and Oct-1 to ECR400.

The ECR400 element has SNPs within it that completely abolish its activity both *in vitro* and *in vivo* (see Chapter 5). The ECR400 SNP rs12508471 had reduced activity *in vivo* and was modestly associated with reduced expression of ABCG2 and PPM1K in different tissues (see Chapter 5). rs12508471 had predicted gains for several NRs including PPAR, PXR, LXR, GR, p300 and VDR. Therefore, the rs12508471 enhancer plasmid was challenged in the induction assays to see if it had a different response to NR ligands than the reference ECR400 sequence. rs12508471 was associated with a reduced response to E_2 and increased response to dexamethasone treatment. ER and PXR both dimerize with RXR, and RXR dimers with PPAR, CAR or LXR have been shown to bind to GR or ER response elements and inhibit ER or GR response[100–103]. The gain in predicted binding for RXR could explain the alteration in rs12508471 response to E_2 and dexamethasone. Additionally, rs12508471 was predicted to induce binding of chicken ovalbumin upstream promoter-transcription factor (COUP-TF), which has been shown to

repress the transcriptional activity of several NRs by forming inactive heterodimers that compete for DNA binding, tether co-repressors and tighten the chromatin structure[104–106]. The restrictive expression patterns for RXRα/β[7] and COUP-TF[107] could explain how this SNP affects expression of genes in selected tissues. Future studies are needed to confirm this change in binding of rs12508471 to RXR or COUP-TF.

The reporter gene assays used in the current studies do not provide local chromatin structure that is integral in the regulation of expression by nuclear receptors[12,88,108]. It will be interesting to see if chromosome confirmation capture assays are able to detect the interaction of the *ABCG2* promoter with these *cis*-regulatory elements. Additionally, only a few NR ligands and environmental stimuli were investigated. Many of the putative regulatory elements had predicted binding for PPAR, LXR, ROR and several HNF isoforms. Other cell-based assays for induction by RXR[109], PPAR[110], HIFα[111], LXR[112], HNF4[113] and ROR[114] could identify additional nuclear response elements important for the regulation of *ABCG2*.

6.6. Conclusions

Through the use of NR ligand induction assays, multiple regions in the *ABCG2* gene locus, including the *ABCG2* promoter, were identified as NREs. Additionally, some SNPs within these regions were shown to have altered response to NR ligands compared to the reference regulatory regions. In addition to the previously identified enhancer and suppressor regions surrounding *ABCG2* and their SNPs, (see Chapter 4 and 5), these regions could explain the reported NR regulation of *ABCG2*. The SNPs within these regions could also explain clinical variability in ABCG2 gene expression, drug

pharmacokinetics and pharmacodynamics and disease risk for cancer, ADPKD or gout. Additionally, the discovery of NRE in the *ABCG2* locus extends our understanding of the architecture and regulation of *ABCG2*.

6.7. References

(1) Tirona, R. Molecular mechanisms of drug transporter regulation. *Drug Transporters* **2011**, *201*.

(2) Urquhart, B.; Tirona, R.; Kim, R. Nuclear receptors and the regulation of drug-metabolizing enzymes and drug transporters: implications for interindividual variability in response to drugs. *The Journal of Clinical …* **2007**.

(3) Schupp, M.; Lazar, M. a Endogenous ligands for nuclear receptors: digging deeper. *The Journal of biological chemistry* **2010**, *285*, 40409–15.

(4) Mangelsdorf, D. J.; Thummel, C.; Beato, M.; Herrlich, P.; Schütz, G.; Umesono, K.; Blumberg, B.; Kastner, P.; Mark, M.; Chambon, P.; Evans, R. M. The nuclear receptor superfamily: the second decade. *Cell* **1995**, *83*, 835–9.

(5) Olefsky, J. M. Nuclear receptor minireview series. *The Journal of biological chemistry* **2001**, *276*, 36863–4.

(6) Klinge, C. M.; Bodenner, D. L.; Desai, D.; Niles, R. M.; Traish, a M. Binding of type II nuclear receptors and estrogen receptor to full and half-site estrogen response elements in vitro. *Nucleic acids research* **1997**, *25*, 1903–12.

(7) Germain, P.; Chambon, P.; Eichele, G.; Evans, R. M.; Lazar, M. A.; Leid, M.; De Lera, A. R.; Lotan, R.; Mangelsdorf, D. J.; Gronemeyer, H. International Union of Pharmacology. LXIII. Retinoid X receptors. *Pharmacological reviews* **2006**, *58*, 760–72.

(8) Novac, N.; Heinzel, T. Nuclear receptors: overview and classification. *Current drug targets. Inflammation and allergy* **2004**, *3*, 335–46.

(9) Lee, S. K.; Choi, H. S.; Song, M. R.; Lee, M. O.; Lee, J. W. Estrogen receptor, a common interaction partner for a subset of nuclear receptors. *Molecular endocrinology (Baltimore, Md.)* **1998**, *12*, 1184–92.

(10) Whitfield, G. K.; Jurutka, P. W.; Haussler, C. a; Haussler, M. R. Steroid hormone receptors: evolution, ligands, and molecular basis of biologic function. *Journal of cellular biochemistry* **1999**, *Suppl 32-3*, 110–22.

(11) Prologue, M. Thematic Minireview Series on Nuclear Receptors in Biology and. **2010**, *285*, 38741–38742.

(12) Biddie, S. C.; John, S.; Hager, G. L. Genome-wide mechanisms of nuclear receptor action. *Trends in endocrinology and metabolism: TEM* **2010**, *21*, 3–9.

(13) Michalik, L.; Auwerx, J.; Berger, J. P.; Chatterjee, V. K.; Glass, C. K.; Gonzalez, F. J.; Grimaldi, P. A.; Kadowaki, T.; Lazar, M. A.; Rahilly, S. O.; Palmer, C. N. A.; Plutzky, J.; Reddy, J. K.; Spiegelman, B. M.; Staels, B. International Union of Pharmacology . LXI . Peroxisome Proliferator-Activated Receptors. **2006**, *58*, 726–741.

(14) Overington, J. P.; Al-Lazikani, B.; Hopkins, A. L. How many drug targets are there? *Nature reviews. Drug discovery* **2006**, *5*, 993–6.

(15) Germain, P.; Staels, B.; Dacquet, C.; Spedding, M.; Laudet, V. Overview of Nomenclature of Nuclear Receptors. **2006**, *58*, 685–704.

(16) So, A. Y.-L.; Chaivorapol, C.; Bolton, E. C.; Li, H.; Yamamoto, K. R. Determinants of cell- and gene-specific transcriptional regulation by the glucocorticoid receptor. *PLoS genetics* **2007**, *3*, e94.

(17) Carroll, J. S.; Meyer, C. a; Song, J.; Li, W.; Geistlinger, T. R.; Eeckhoute, J.; Brodsky, A. S.; Keeton, E. K.; Fertuck, K. C.; Hall, G. F.; Wang, Q.; Bekiranov, S.; Sementchenko, V.; Fox, E. a; Silver, P. a; Gingeras, T. R.; Liu, X. S.; Brown, M. Genome-wide analysis of estrogen receptor binding sites. *Nature genetics* **2006**, *38*, 1289–97.

(18) Bolton, E. C.; So, A. Y.; Chaivorapol, C.; Haqq, C. M.; Li, H.; Yamamoto, K. R. Cell- and gene-specific regulation of primary target genes by the androgen receptor. *Genes & development* **2007**, *21*, 2005–17.

(19) Weltmeier, F.; Borlak, J. A high resolution genome-wide scan of HNF4α recognition sites infers a regulatory gene network in colon cancer. *PloS one* **2011**, *6*, e21667.

(20) Wang, Q.; Li, W.; Liu, X. S.; Carroll, J. S.; Jänne, O. a; Keeton, E. K.; Chinnaiyan, A. M.; Pienta, K. J.; Brown, M. A hierarchical network of transcription factors governs androgen receptor-dependent prostate cancer growth. *Molecular cell* **2007**, *27*, 380–92.

(21) Tan, S. K.; Lin, Z. H.; Chang, C. W.; Varang, V.; Chng, K. R.; Pan, Y. F.; Yong, E. L.; Sung, W. K.; Sung, W. K.; Cheung, E. AP-2γ regulates oestrogen receptor-mediated long-range chromatin interaction and gene transcription. *The EMBO journal* **2011**, *30*, 2569–81.

(22) Wang, H.; Lee, E.; Zhou, L.; Leung, P. C. K.; Ross, D. D.; Unadkat, J. D.; Mao, Q. Progesterone receptor (PR) isoforms PRA and PRB differentially regulate expression of the breast cancer resistance protein in human placental choriocarcinoma BeWo cells. *Molecular pharmacology* **2008**, *73*, 845–54.

(23) Zhang, Y.; Zhou, G.; Wang, H.; Zhang, X.; Wei, F.; Cai, Y.; Yin, D. Transcriptional upregulation of breast cancer resistance protein by 17beta-estradiol in ERalpha-positive MCF-7 breast cancer cells. *Oncology* **2006**, *71*, 446–55.

(24) Jigorel, E.; Vee, M. Le; Boursier-neyret, C.; Parmentier, Y.; Fardel, O. Differential Regulation of Sinusoidal and Canalicular Hepatic Drug Transporter Expression by Xenobiotics Activating Drug-Sensing Receptors in Primary Human Hepatocytes ABSTRACT : **2006**, *34*, 1756–1763.

(25) Cheng, G. M. Y.; To, K. K. W. Adverse Cell Culture Conditions Mimicking the Tumor Microenvironment Upregulate ABCG2 to Mediate Multidrug Resistance and a More Malignant Phenotype. *ISRN oncology* **2012**, *2012*, 746025.

(26) Szatmari, I.; Vámosi, G.; Brazda, P.; Balint, B. L.; Benko, S.; Széles, L.; Jeney, V.; Ozvegy-Laczka, C.; Szántó, A.; Barta, E.; Balla, J.; Sarkadi, B.; Nagy, L. Peroxisome proliferator-activated receptor gamma-regulated ABCG2 expression confers cytoprotection to human dendritic cells. *The Journal of biological chemistry* **2006**, *281*, 23812–23.

(27) Singh, A.; Wu, H.; Zhang, P.; Happel, C. Expression of ABCG2 (BCRP) is regulated by Nrf2 in cancer cells that confers side population and chemoresistance phenotype. *Molecular cancer ...* **2010**, *9*, 2365–2376.

(28) Krishnamurthy, P.; Ross, D. D.; Nakanishi, T.; Bailey-Dell, K.; Zhou, S.; Mercer, K. E.; Sarkadi, B.; Sorrentino, B. P.; Schuetz, J. D. The stem cell marker Bcrp/ABCG2 enhances hypoxic cell survival through interactions with heme. *The Journal of biological chemistry* **2004**, *279*, 24218–25.

(29) Pradhan, M.; Bembinster, L. a; Baumgarten, S. C.; Frasor, J. Proinflammatory cytokines enhance estrogen-dependent expression of the multidrug transporter gene ABCG2 through estrogen receptor and NF{kappa}B cooperativity at adjacent response elements. *The Journal of biological chemistry* **2010**, *285*, 31100–6.

(30) Tan, K. P.; Wang, B.; Yang, M.; Boutros, P. C.; Macaulay, J.; Xu, H.; Chuang, A. I.; Kosuge, K.; Yamamoto, M.; Takahashi, S.; Wu, A. M. L.; Ross, D. D.; Harper, P. A.; Ito, S. Aryl Hydrocarbon Receptor Is a Transcriptional Activator of the Human Breast Cancer Resistance Protein (BCRP / ABCG2) □. **2010**.

(31) Ee, P. L. R. Identification of a Novel Estrogen Response Element in the Breast Cancer Resistance Protein (ABCG2) Gene. *Cancer Research* **2004**, *64*, 1247–1251.

(32) Krishnamurthy, P.; Schuetz, J. D. The ABC transporter Abcg2/Bcrp: role in hypoxia mediated survival. *Biometals : an international journal on the role of metal ions in biology, biochemistry, and medicine* **2005**, *18*, 349–58.

(33) Lemos, C.; Kathmann, I.; Giovannetti, E.; Dekker, H.; Scheffer, G. L.; Calhau, C.; Jansen, G.; Peters, G. J. Folate deprivation induces BCRP (ABCG2) expression and mitoxantrone resistance in Caco-2 cells. *International journal of cancer. Journal international du cancer* **2008**, *123*, 1712–20.

(34) Lemos, C.; Kathmann, I.; Giovannetti, E.; Calhau, C.; Jansen, G.; Peters, G. J. Impact of cellular folate status and epidermal growth factor receptor expression on BCRP/ABCG2-mediated resistance to gefitinib and erlotinib. *British journal of cancer* **2009**, *100*, 1120–7.

(35) Albermann, N.; Schmitz-Winnenthal, F. H.; Z'graggen, K.; Volk, C.; Hoffmann, M. M.; Haefeli, W. E.; Weiss, J. Expression of the drug transporters MDR1/ABCB1, MRP1/ABCC1, MRP2/ABCC2, BCRP/ABCG2, and PXR in peripheral blood mononuclear cells and their relationship with the expression in intestine and liver. *Biochemical pharmacology* **2005**, *70*, 949–58.

(36) Gahir, S. S.; Piquette-miller, M. Gestational and Pregnane X Receptor-Mediated Regulation of Placental ATP-Binding Cassette Drug Transporters in Mice □. **2011**, 465–471.

(37) Lehmann, J. M.; McKee, D. D.; Watson, M. a; Willson, T. M.; Moore, J. T.; Kliewer, S. a The human orphan nuclear receptor PXR is activated by compounds that regulate CYP3A4 gene expression and cause drug interactions. *The Journal of clinical investigation* **1998**, *102*, 1016–23.

(38) Lemmen, J.; Tozakidis, I. E. P.; Galla, H.-J. Pregnane X receptor upregulates ABC-transporter Abcg2 and Abcb1 at the blood-brain barrier. *Brain research* **2012**, 1–13.

(39) Kliewer, S. a.; Goodwin, B.; Willson, T. M. The nuclear pregnane X receptor: a key regulator of xenobiotic metabolism. *Endocrine reviews* **2002**, *23*, 687–702.

(40) Generaux, G. T.; Bonomo, F. M.; Johnson, M.; Doan, K. M. M. Impact of SLCO1B1 (OATP1B1) and ABCG2 (BCRP) genetic polymorphisms and inhibition on LDL-C lowering and myopathy of statins. *Xenobiotica; the fate of foreign compounds in biological systems* **2011**, *41*, 639–51.

(41) Reginato, A. M.; Mount, D. B.; Yang, I.; Choi, H. K. The genetics of hyperuricaemia and gout. *Nature reviews. Rheumatology* **2012**, *8*, 610–21.

(42) Ee, P. L. R.; He, X.; Ross, D. D.; Beck, W. T. Modulation of breast cancer resistance protein (BCRP / ABCG2) gene expression using RNA interference Modulation of breast cancer resistance protein (BCRP / ABCG2) gene expression using RNA interference. **2005**, 1577–1584.

(43) Yasuda, S.; Kobayashi, M.; Itagaki, S.; Hirano, T.; Iseki, K. Response of the ABCG2 promoter in T47D cells and BeWo cells to sex hormone treatment. *Molecular biology reports* **2009**, *36*, 1889–96.

(44) Wang, H.; Zhou, L.; Gupta, A.; Vethanayagam, R. R.; Zhang, Y.; Unadkat, J. D.; Mao, Q. Regulation of BCRP/ABCG2 expression by progesterone and 17beta-estradiol in human placental BeWo cells. *American journal of physiology. Endocrinology and metabolism* **2006**, *290*, E798–807.

(45) Imai, Y.; Ishikawa, E.; Asada, S.; Sugimoto, Y. Estrogen-mediated post transcriptional down-regulation of breast cancer resistance protein/ABCG2. *Cancer research* **2005**, *65*, 596–604.

(46) Imai, Y.; Tsukahara, S.; Ishikawa, E.; Tsuruo, T.; Sugimoto, Y. Estrone and 17beta-estradiol reverse breast cancer resistance protein-mediated multidrug resistance. *Japanese journal of cancer research : Gann* **2002**, *93*, 231–5.

(47) Meyer, K. B.; Carroll, J. S. FOXA1 and breast cancer risk. *Nature genetics* **2012**, *44*, 1176–7.

(48) Yeboah, D.; Sun, M.; Kingdom, J.; Baczyk, D.; Lye, S. J.; Matthews, S. G.; Gibb, W. Expression of breast cancer resistance protein (BCRP / ABCG2) in human placenta throughout gestation and at term before and after labor. **2006**, *1258*, 1251–1258.

(49) Mao, Q. BCRP/ABCG2 in the placenta: expression, function and regulation. *Pharmaceutical research* **2008**, *25*, 1244–55.

(50) Jonker, J. W.; Smit, J. W.; Brinkhuis, R. F.; Maliepaard, M.; Beijnen, J. H.; Schellens, J. H.; Schinkel, A. H. Role of breast cancer resistance protein in the bioavailability and fetal penetration of topotecan. *Journal of the National Cancer Institute* **2000**, *92*, 1651–6.

(51) Wang, H.; Zhou, L.; Gupta, A.; Vethanayagam, R. R.; Zhang, Y.; Unadkat, J. D.; Mao, Q.; Robert, R. Regulation of BCRP/ABCG2 expression by progesterone and 17beta-estradiol in human placental BeWo cells. *American journal of physiology. Endocrinology and metabolism* **2006**, *290*, E798–807.

(52) Charmandari, E.; Kino, T.; Chrousos, G. P. Glucocorticoids and their actions: an introduction. *Annals of the New York Academy of Sciences* **2004**, *1024*, 1–8.

(53) Oakley, R. H.; Cidlowski, J. a Cellular processing of the glucocorticoid receptor gene and protein: new mechanisms for generating tissue-specific actions of glucocorticoids. *The Journal of biological chemistry* **2011**, *286*, 3177–84.

(54) Glass, C. K.; Saijo, K. Nuclear receptor transrepression pathways that regulate inflammation in macrophages and T cells. *Nature reviews. Immunology* **2010**, *10*, 365–76.

(55) Rhen, T.; Cidlowski, J. a Antiinflammatory action of glucocorticoids--new mechanisms for old drugs. *The New England journal of medicine* **2005**, *353*, 1711–23.

(56) Petropoulos, S.; Gibb, W.; Matthews, S. G. Glucocorticoid regulation of placental breast cancer resistance protein (Bcrp1) in the mouse. *Reproductive sciences (Thousand Oaks, Calif.)* **2011**, *18*, 631–9.

(57) Elahian, F.; Kalalinia, F.; Behravan, J. Dexamethasone downregulates BCRP mRNA and protein expression in breast cancer cell lines. *Oncology research* **2009**, *18*, 9–15.

(58) Pascussi, J. M.; Drocourt, L.; Fabre, J. M.; Maurel, P.; Vilarem, M. J. Dexamethasone induces pregnane X receptor and retinoid X receptor-alpha expression in human hepatocytes: synergistic increase of CYP3A4 induction by pregnane X receptor activators. *Molecular pharmacology* **2000**, *58*, 361–72.

(59) Bhadhprasit, W.; Sakuma, T.; Hatakeyama, N.; Fuwa, M.; Kitajima, K.; Nemoto, N. Involvement of Glucocorticoid Receptor and Pregnane X Receptor in the Regulation of Mouse CYP3A44 Female-Predominant Expression by Glucocorticoid Hormone ABSTRACT : **2007**, *35*, 1880–1885.

(60) Honorat, M.; Mesnier, A.; Di Pietro, A.; Lin, V.; Cohen, P.; Dumontet, C.; Payen, L. Dexamethasone down-regulates ABCG2 expression levels in breast cancer cells. *Biochemical and biophysical research communications* **2008**, *375*, 308–14.

(61) Pascussi, J. M.; Drocourt, L.; Gerbal-Chaloin, S.; Fabre, J. M.; Maurel, P.; Vilarem, M. J. Dual effect of dexamethasone on CYP3A4 gene expression in human hepatocytes. Sequential role of glucocorticoid receptor and pregnane X receptor. *European journal of biochemistry / FEBS* **2001**, *268*, 6346–58.

(62) Ray, a; Prefontaine, K. E. Physical association and functional antagonism between the p65 subunit of transcription factor NF-kappa B and the glucocorticoid receptor. *Proceedings of the National Academy of Sciences of the United States of America* **1994**, *91*, 752–6.

(63) Nguyen, L. P.; Bradfield, C. a The search for endogenous activators of the aryl hydrocarbon receptor. *Chemical research in toxicology* **2008**, *21*, 102–16.

(64) Pfeifer, G. P.; Denissenko, M. F.; Olivier, M.; Tretyakova, N.; Hecht, S. S.; Hainaut, P. Tobacco smoke carcinogens, DNA damage and p53 mutations in smoking-associated cancers. *Oncogene* **2002**, *21*, 7435–51.

(65) Ebert, B.; Seidel, A.; Lampen, A. Identification of BCRP as transporter of benzo[a]pyrene conjugates metabolically formed in Caco-2 cells and its induction by Ah-receptor agonists. *Carcinogenesis* **2005**, *26*, 1754–63.

(66) Ebert, B.; Seidel, A.; Lampen, A. Phytochemicals induce breast cancer resistance protein in Caco-2 cells and enhance the transport of benzo[a]pyrene-3-sulfate. *Toxicological sciences : an official journal of the Society of Toxicology* **2007**, *96*, 227–36.

(67) Advance, T. The fungicide prochloraz and environmental pollutant dioxin induce the ABCG2 transporter in bovine mammary epithelial cells by the arylhydrocarbon receptor signalling pathway. **2012**.

(68) Zamber, C. P.; Lamba, J. K.; Yasuda, K.; Farnum, J.; Thummel, K.; Schuetz, J. D.; Schuetz, E. G. Natural allelic variants of breast cancer resistance protein (BCRP) and their relationship to BCRP expression in human intestine. *Pharmacogenetics* **2003**, *13*, 19–28.

(69) Suvannasankha, a; Minderman, H.; O'Loughlin, K. L.; Nakanishi, T.; Greco, W. R.; Ross, D. D.; Baer, M. R. Breast cancer resistance protein (BCRP/MXR/ABCG2) in acute myeloid leukemia: discordance between expression and function. *Leukemia : official journal of the Leukemia Society of America, Leukemia Research Fund, U.K* **2004**, *18*, 1252–7.

(70) Suvannasankha, A.; Minderman, H.; O'Loughlin, K. L.; Nakanishi, T.; Ford, L. a; Greco, W. R.; Wetzler, M.; Ross, D. D.; Baer, M. R. Breast cancer resistance protein (BCRP/MXR/ABCG2) in adult acute lymphoblastic leukaemia: frequent expression and possible correlation with shorter disease-free survival. *British journal of haematology* **2004**, *127*, 392–8.

(71) Benderra, Z.; Faussat, A.-M.; Sayada, L.; Perrot, J.-Y.; Chaoui, D.; Marie, J.-P.; Legrand, O. Breast cancer resistance protein and P-glycoprotein in 149 adult acute myeloid leukemias. *Clinical cancer research : an official journal of the American Association for Cancer Research* **2004**, *10*, 7896–902.

(72) Tsunoda, S.; Okumura, T.; Ito, T.; Kondo, K.; Ortiz, C.; Tanaka, E.; Watanabe, G.; Itami, A.; Sakai, Y.; Shimada, Y. ABCG2 expression is an independent unfavorable prognostic factor in esophageal squamous cell carcinoma. *Oncology* **2006**, *71*, 251–8.

(73) Usuda, J.; Tsunoda, Y.; Ichinose, S.; Ishizumi, T.; Ohtani, K.; Maehara, S.; Ono, S.; Tsutsui, H.; Ohira, T.; Okunaka, T.; Furukawa, K.; Sugimoto, Y.; Kato, H.; Ikeda, N. Breast cancer resistant protein (BCRP) is a molecular determinant of the outcome of photodynamic therapy (PDT) for centrally located early lung cancer. *Lung cancer (Amsterdam, Netherlands)* **2010**, *67*, 198–204.

(74) Uggla, B.; Ståhl, E.; Wågsäter, D.; Paul, C.; Karlsson, M. G.; Sirsjö, A.; Tidefelt, U. BCRP mRNA expression v. clinical outcome in 40 adult AML patients. *Leukemia research* **2005**, *29*, 141–6.

(75) Yoh, K. Breast Cancer Resistance Protein Impacts Clinical Outcome in Platinum-Based Chemotherapy for Advanced Non-Small Cell Lung Cancer. *Clinical Cancer Research* **2004**, *10*, 1691–1697.

(76) Korenaga, Y.; Naito, K.; Okayama, N.; Hirata, H.; Suehiro, Y.; Hamanaka, Y.; Matsuyama, H.; Hinoda, Y. Association of the BCRP C421A polymorphism with nonpapillary renal cell carcinoma. *International journal of cancer. Journal international du cancer* **2005**, *117*, 431–4.

(77) Goodwin, B.; Hodgson, E.; Liddle, C. The orphan human pregnane X receptor mediates the transcriptional activation of CYP3A4 by rifampicin through a distal enhancer module. *Molecular pharmacology* **1999**, *56*, 1329–39.

(78) Loots, G. G.; Ovcharenko, I. rVISTA 2.0: evolutionary analysis of transcription factor binding sites. *Nucleic acids research* **2004**, *32*, W217–21.

(79) Frith, M.; Hansen, U.; Weng, Z. Detection of cis-element clusters in higher eukaryotic DNA. *Bioinformatics* **2001**, *17*, 878–889.

(80) Wingender, E.; Chen, X.; Hehl, R.; Karas, H.; Liebich, I.; Matys, V.; Meinhardt, T.; Prüss, M.; Reuter, I.; Schacherer, F. TRANSFAC: an integrated system for gene expression regulation. *Nucleic acids research* **2000**, *28*, 316–9.

(81) Encode, T.; Consortium, P. A user's guide to the encyclopedia of DNA elements (ENCODE). *PLoS biology* **2011**, *9*, e1001046.

(82) Chen, Y.; Ferguson, S. S.; Negishi, M.; Goldstein, J. A.; Carolina, N. Induction of Human CYP2C9 by Rifampicin , Hyperforin , and Phenobarbital Is Mediated by the Pregnane X Receptor. **2004**, *308*, 495–501.

(83) Kamalakaran, S.; Radhakrishnan, S. K.; Beck, W. T. Identification of estrogen-responsive genes using a genome-wide analysis of promoter elements for transcription factor binding sites. *The Journal of biological chemistry* **2005**, *280*, 21491–7.

(84) Lin, Z.; Reierstad, S.; Huang, C.-C.; Bulun, S. E. Novel estrogen receptor-alpha binding sites and estradiol target genes identified by chromatin immunoprecipitation cloning in breast cancer. *Cancer research* **2007**, *67*, 5017–24.

(85) To, K. K. W.; Robey, R.; Zhan, Z.; Bangiolo, L.; Bates, S. E. Upregulation of ABCG2 by romidepsin via the aryl hydrocarbon receptor pathway. *Molecular cancer research : MCR* **2011**, *9*, 516–27.

(86) Tompkins, L. M.; Li, H.; Li, L.; Lynch, C.; Xie, Y.; Nakanishi, T.; Ross, D. D.; Wang, H. A novel xenobiotic responsive element regulated by aryl hydrocarbon receptor is involved in the induction of BCRP/ABCG2 in LS174T cells. *Biochemical pharmacology* **2010**, *80*, 1754–61.

(87) Rossini, G. P.; Malaguti, C. Nanomolar concentrations of untransformed glucocorticoid receptor in nuclei of intact cells. *The Journal of steroid biochemistry and molecular biology* **1994**, *51*, 291–8.

(88) Pike, J. W.; Meyer, M. B.; Watanuki, M.; Kim, S.; Zella, L. a; Fretz, J. a; Yamazaki, M.; Shevde, N. K. Perspectives on mechanisms of gene regulation by 1,25-dihydroxyvitamin D3 and its receptor. *The Journal of steroid biochemistry and molecular biology* **2007**, *103*, 389–95.

(89) Advance, T. High-resolution genome-wide mapping of AHR and ARNT binding sites by ChIP-Seq High-resolution genome-wide mapping of AHR and ARNT binding sites by ChIP-Seq Raymond Lo * and Jason Matthews * * Department of Pharmacology and Toxicology , University of Toron. **2012**.

(90) Zhao, C.; Gao, H.; Liu, Y.; Papoutsi, Z.; Jaffrey, S.; Gustafsson, J.-A.; Dahlman-Wright, K. Genome-wide mapping of estrogen receptor-beta-binding regions reveals extensive cross-talk with transcription factor activator protein-1. *Cancer research* **2010**, *70*, 5174–83.

(91) Jia, L.; Berman, B. P.; Jariwala, U.; Yan, X.; Cogan, J. P.; Walters, A.; Chen, T.; Buchanan, G.; Frenkel, B.; Coetzee, G. a Genomic androgen receptor-occupied regions with different functions, defined by histone acetylation, coregulators and transcriptional capacity. *PloS one* **2008**, *3*, e3645.

(92) Hall, J. M.; Couse, J. F.; Korach, K. S. The multifaceted mechanisms of estradiol and estrogen receptor signaling. *The Journal of biological chemistry* **2001**, *276*, 36869–72.

(93) Ahmed, S.; Valen, E.; Sandelin, A.; Matthews, J. Dioxin increases the interaction between aryl hydrocarbon receptor and estrogen receptor alpha at human promoters. *Toxicological sciences : an official journal of the Society of Toxicology* **2009**, *111*, 254–66.

(94) Hankinson, O. Role of coactivators in transcriptional activation by the aryl hydrocarbon receptor. *Archives of biochemistry and biophysics* **2005**, *433*, 379–86.

(95) Patel, R. D.; Murray, I. a; Flaveny, C. a; Kusnadi, A.; Perdew, G. H. Ah receptor represses acute-phase response gene expression without binding to its cognate response element. *Laboratory investigation; a journal of technical methods and pathology* **2009**, *89*, 695–707.

(96) Chen, Y.; Nie, D. Pregnane X receptor and its potential role in drug resistance in cancer treatment. *Recent patents on anti-cancer drug discovery* **2009**, *4*, 19–27.

(97) Préfontaine, G. G.; Walther, R.; Giffin, W.; Lemieux, M. E.; Pope, L.; Haché, R. J. Selective binding of steroid hormone receptors to octamer transcription factors determines transcriptional synergism at the mouse mammary tumor virus promoter. *The Journal of biological chemistry* **1999**, *274*, 26713–9.

(98) Kakizawa, T.; Miyamoto, T.; Ichikawa, K.; Kaneko, A.; Suzuki, S.; Hara, M.; Nagasawa, T.; Takeda, T.; Mori, J. i; Kumagai, M.; Hashizume, K. Functional interaction between Oct-1 and retinoid X receptor. *The Journal of biological chemistry* **1999**, *274*, 19103–8.

(99) Gonzalez, M. I.; Robins, D. M. Oct-1 preferentially interacts with androgen receptor in a DNA-dependent manner that facilitates recruitment of SRC-1. *The Journal of biological chemistry* **2001**, *276*, 6420–8.

(100) Nuñez, S. B.; Medin, J. a; Braissant, O.; Kemp, L.; Wahli, W.; Ozato, K.; Segars, J. H. Retinoid X receptor and peroxisome proliferator-activated receptor activate an estrogen responsive gene independent of the estrogen receptor. *Molecular and cellular endocrinology* **1997**, *127*, 27–40.

(101) Keller, H.; Givel, F.; Perroud, M.; Wahli, W. Signaling cross-talk between peroxisome proliferator-activated receptor/retinoid X receptor and estrogen receptor through estrogen response elements. *Molecular endocrinology (Baltimore, Md.)* **1995**, *9*, 794–804.

(102) Min, G.; Kim, H.; Bae, Y.; Petz, L.; Kemper, J. K. Inhibitory cross-talk between estrogen receptor (ER) and constitutively activated androstane receptor (CAR). CAR inhibits ER-mediated signaling pathway by squelching p160 coactivators. *The Journal of biological chemistry* **2002**, *277*, 34626–33.

(103) Nader, N.; Ng, S. S. M.; Wang, Y.; Abel, B. S.; Chrousos, G. P.; Kino, T. Liver x receptors regulate the transcriptional activity of the glucocorticoid receptor: implications for the carbohydrate metabolism. *PloS one* **2012**, *7*, e26751.

(104) De Martino, M. U.; Alesci, S.; Chrousos, G. P.; Kino, T. Interaction of the glucocorticoid receptor and the chicken ovalbumin upstream promoter-transcription factor II (COUP-TFII): implications for the actions of glucocorticoids on glucose, lipoprotein, and xenobiotic metabolism. *Annals of the New York Academy of Sciences* **2004**, *1024*, 72–85.

(105) Shibata, H.; Nawaz, Z.; Tsai, S. Y.; O'Malley, B. W.; Tsai, M. J. Gene silencing by chicken ovalbumin upstream promoter-transcription factor I (COUP-TFI) is mediated by transcriptional corepressors, nuclear receptor-corepressor (N-CoR) and silencing mediator for retinoic acid receptor and thyroid hormone receptor (SMRT). *Molecular endocrinology (Baltimore, Md.)* **1997**, *11*, 714–24.

(106) Qiu, Y.; Krishnan, V.; Pereira, F. A.; Tsai, S. Y.; Tsai, M. J. Chicken ovalbumin upstream promoter-transcription factors and their regulation. *The Journal of steroid biochemistry and molecular biology* **1996**, *56*, 81–5.

(107) Park, J.-I.; Tsai, S. Y.; Tsai, M.-J. Molecular mechanism of chicken ovalbumin upstream promoter-transcription factor (COUP-TF) actions. *The Keio journal of medicine* **2003**, *52*, 174–81.

(108) Wiench, M.; Miranda, T. B.; Hager, G. L. Control of nuclear receptor function by local chromatin structure. *The FEBS journal* **2011**, *278*, 2211–30.

(109) Zou, a; Elgort, M. G.; Allegretto, E. a Retinoid X receptor (RXR) ligands activate the human 25-hydroxyvitamin D3-24-hydroxylase promoter via RXR heterodimer binding to two vitamin D-responsive elements and elicit additive effects with 1,25-dihydroxyvitamin D3. *The Journal of biological chemistry* **1997**, *272*, 19027–34.

(110) Mochizuki, K.; Suruga, K.; Fukami, H.; Kiso, Y.; Takase, S.; Goda, T. Selectivity of fatty acid ligands for PPARalpha which correlates both with binding to cis-element and DNA binding-independent transactivity in Caco-2 cells. *Life sciences* **2006**, *80*, 140–5.

(111) Xia, M.; Huang, R.; Sun, Y.; Semenza, G. L.; Aldred, S. F.; Witt, K. L.; Inglese, J.; Tice, R. R.; Austin, C. P. Identification of chemical compounds that induce HIF-1alpha activity. *Toxicological sciences : an official journal of the Society of Toxicology* **2009**, *112*, 153–63.

(112) Berrodin, T. J.; Shen, Q.; Quinet, E. M.; Yudt, M. R.; Freedman, L. P. Identification of 5 ␣ , 6 ␣ -Epoxycholesterol as a Novel Modulator of Liver X Receptor Activity. **2010**, *78*, 1046–1058.

(113) Lucas, B.; Grigo, K.; Erdmann, S.; Lausen, J.; Klein-Hitpass, L.; Ryffel, G. U. HNF4alpha reduces proliferation of kidney cells and affects genes deregulated in renal cell carcinoma. *Oncogene* **2005**, *24*, 6418–31.

(114) Wilkinson, J.; Hallis, T.; Hermanson, S.; Bi, K. Development and validation of a cell-based assay for the nuclear receptor retinoid-related orphan receptor gamma. *Assay and drug development technologies* **2011**, *9*, 125–35.

Chapter 7 : DNA Methylation in the *ABCG2* Gene Locus

7.1. Abstract

ABCG2 encodes for a multidrug efflux transporter called the mitoxantrone resistance protein (MXR, BCRP). MXR is an important player in the natural detoxification and protection pathways of the body and is responsible for the efflux of substrates from the cell. The methylation of cytosine paired with guanine (CpG) sites in the *ABCG2* promoter has been correlated with ABCG2 expression. In this study, eleven clusters of CpG sites, called CpG islands (CGIs), were predicted in the *ABCG2* gene locus. Sodium bisulfite treatment and pyrosequencing was used to quantify percent methylation of CpG sites in two CGIs, CpG4 and CpG6. Finally, methylation of these sites was correlated with the expression of ABCG2 in human liver and kidney tissues. CpG4, the CGI over the *ABCG2* promoter, has little methylation through its center, but variable methylation on its sides; methylation of a specific CpG site within CpG4 (#77) is correlated with ABCG2 expression in the kidney. Methylation of the edges of CpG4 is significantly lower in liver than in kidney and methylation of the entire CpG6 is significantly higher in kidney than in liver. There was no correlation of methylation of the entire CpG4 or CpG6 with ABCG2 expression. These findings add to knowledge of *ABCG2* CGI methylation in liver and kidney, and identify regions of interest for future studies on the development of drug resistance.

7.2. Introduction

The mitoxantrone resistance protein (MXR, BCRP) is an efflux membrane transporter, a member of the ATP-binding cassette (ABC) transporter family and is

encoded by *ABCG2*. MXR is expressed in many tissues including the liver[1–4] and kidney[2–4] and plays a role in protecting these vital organs from natural dietary toxins and in elimination of xenobiotics from the body. Not only has wide variability of ABCG2 expression been reported in normal tissues[5–7], but overexpression of ABCG2 is seen in cancers[7–15] and is associated with disease-free survival of patients with these cancers[7,9–15]. The majority of studies investigating mechanisms regulating the expression of ABCG2 have focused on identifying binding sites for transcription factors (TFs) in the *ABCG2* promoter region[16–23]. However, methylation of CpG sites affects the binding of TFs, especially over gene promoters[24,25]. Therefore, further research looking at the effect of *ABCG2* promoter methylation on ABCG2 expression is warranted.

Methylation refers to the addition of a methyl group to the 5' position of cytosine (C) when it is directly linked with a guanine (G). DNA methylation occurs in the human genome at these "CpG" sites (the 'p' refers to the phosphate group linking the two nucleotides). Methylated cytosine accounts for ~1% of total DNA bases and affects 70-80% of all CpG dinucleotides in the genome[26]. CpG sites were first noted because they occur in the genome at a much lower rate than is expected by the random combination of four bases[27]. It was also noted that these CpG sites cluster into specific regions of the genome and were termed 'CpG islands' (CGIs)[27]. Gardiner-Gardner and Frommer originally described CGIs as having a length greater than 200 bp, a G and C content greater than 50% and a CpG observed to expected ratio (O/E) greater than 0.6[28]. Promoters are often associated with a high frequency of CpG sites[29,30], and when multiple CpG sites over a gene promoter are methylated gene suppression occurs[31]. CGIs are

particularly associated with the promoters for tissue-specific and housekeeping genes[28], and their methylation is important for maintaining gene silence[31].

The natural role of CpG methylation is important for the process of imprinting and the regulation of tissue-specific genes (see Bird 2002[32] for review). Global alterations in the epigenetic landscape, such as hypomethylation or hypermethylation of CGIs, are a hallmark of cancer[33–35]. Hypomethylation at CGIs for drug efflux transporters causes aberrant expression of the transporter gene and allows for cancer to acquire drug resistance[36]. Thus, epigenetic mechanisms have become a new target for pharmaceutical agents[37–40].

The *ABCG2* promoter has a CGI, the core of which is just upstream of the transcriptional start site (TSS) (Figure 7.1)[16]. Minimal to absent methylation of the *ABCG2* promoter CGI has been reported in human liver tissues[41] and in renal cell lines[42]. The degree of *ABCG2* promoter methylation correlates to ABCG2 mRNA levels in cancer cell lines[42–45] and hypomethylation of the *ABCG2* promoter contributes to drug-resistance in cell lines and patients[42–47]. Demethylation of the *ABCG2* promoter has also been correlated with metastasis and stage of cancer, but not with the development of cancer itself[48]. Treatment with the demethylating agent 5-aza-2'-deoxycytidine in cell lines induces ABCG2 expression while the hypermethylated *ABCG2* promoter is associated with gene silencing[42–44]. The degree of *ABCG2* promoter methylation in sheep was inversely correlated with xenobiotic resistance, and specific methylated CpG sites in the *ABCG2* promoter correlated to ABCG2 expression [49]. Methylation of the *ABCG2* promoter is implicated in allele-specific expression in certain tissues (shown for ABCG2

in placenta[50]). Characterization of epigenetic expression profiles in liver, intestine and kidney would be of interest.

The methylation of CpG sites over a promoter works to repress gene expression through two mechanisms. The first is limiting binding for activating TFs[24,25], and the second is the recruitment of methyl binding domain (MBDs) proteins that in turn recruit histones and condense chromatin[51]. Recent genome wide studies correlating gene expression with DNA methylation patterns in cancer and normal tissues have identified methylated CpG sites of atypical distances from the gene TSS[52], *trans*- and *cis*-association of CGI methylation with expression[53] and methylation quantitative trait loci (mQTL) for SNP-CpG methylation-expression associations[54–56]. These studies support the hypothesis that 'orphan CGIs', CGIs that are not over the TSS of genes, have functional significance[57]. The most likely explanation for how orphan CGIs affect gene expression is through disruption of *cis*-regulatory regions[58].

The methylation status of cytosines cannot be determined by traditional sequencing methods. CpG methylation is evaluated by treatment of single stranded DNA with sodium bisulfite and subsequent sequencing[59]. Sodium bisulfite converts unmethylated cytosines to uracil (Figure 7.2), whereby 5-methylcytosine (5-MeC) is nonreactive. Treated DNA is then amplified in a methylation specific PCR (MSP), in which converted cytosines amplify as thymine and 5-MeC residues amplify as cytosine. DNA is then sequenced before and after bisulfite treatment, with primers designed to target the expected sequence after bisulfite treatment, to determine which CpG sites are methylated. This technique, called bisulfite sequencing, was the original method for determining the sequence of CGIs and required the sequencing of multiple DNA samples

to obtain quantitative methylation data for the CpG site. Bisulfite treatment has now been coupled with new sequencing methods, such as pyrosequencing, to overcome many of the challenges of MSP[60]. Pyrosequencing is a robust, high-throughput technique that quantifies percent methylation of CpG sites by coupling nucleotide incorporation to a luciferase reaction[61].

In this study, the hypothesis that methylation of CGIs in the *ABCG2* gene locus associates with the expression of ABCG2 was tested. CGIs in the *ABCG2* gene locus were predicted using *in silico* modeling programs based on the accepted definition of a CGI[28]. Pyrosequencing was used to determine the methylation percentage of CpG sites within two of the computed CGIs in the *ABCG2* gene locus for human liver and kidney tissues. Finally, the degree of methylation for individual CpG sites and entire CGIs was correlated to the expression of ABCG2 in these tissues. Results from this study can direct further research to identify key CpG sites important for ABCG2 regulation and the development of drug-resistance.

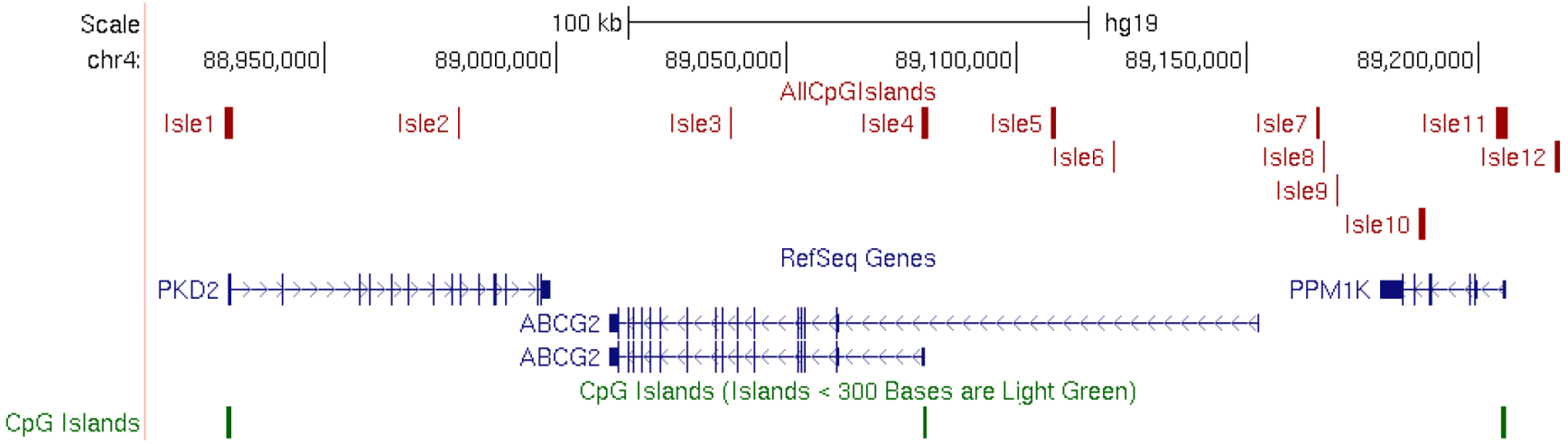

Figure 7.1. Schematic of CpG islands in the *ABCG2* gene locus. From top to bottom: scale for the region followed by the genomic coordinates (chr4:89079997-89080517; hg19). Depicted by red boxes and numbering are the location and relative size of CpG islands predicted by the CpGProD, CpGPlot and CpG Island Searcher analysis as described in *Materials and Methods*. Reference genes from the UCSC Genome Browser are in blue with arrows indicating direction of transcription. CpG islands over 300 bp as predicted by ENCODE are shown in green.

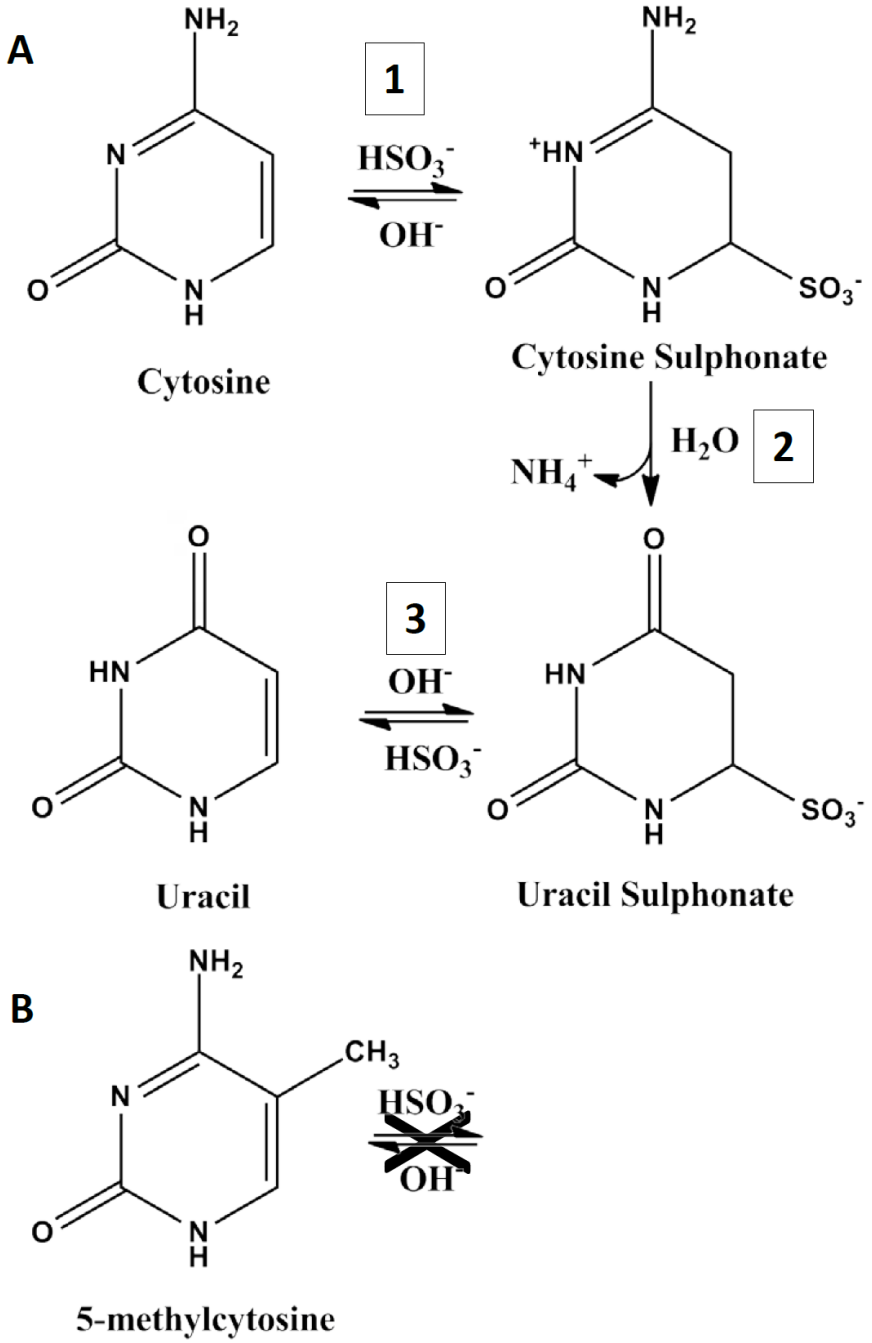

Figure 7.2. Bisulfite conversion of cytosine to uracil. (A) Chemical reaction that occurs when DNA is treated with bisulfite. The bisulfite attacks the aromatic ring leading to sulfonation at the 6' position (Step 1). The ring then goes through a hydrolytic deamination process (Step 2) and finally alkali desulphonation (Step 3) to yield uracil. When there is a methyl group in the 5' position of cytosine (B) this reaction cannot occur.

7.3. Materials and Methods

7.3.1. *Chemicals and Materials*

Qiagen AllPrep DNA/RNA Mini Kit, QIAquick PCR Purification Kit, Qiagen RNeasy MinElute Cleanup Kit, Epitect Bisulfite Kits, Qiagen Pyromark PCR Kits, Strepavidin beads, PyroMark Vacuum System and Qiagen Pyro Gold reagents were all purchased from Qiagen (Valencia, CA). Trizol (Invitrogen, Carlsbad, CA), High Capacity cDNA Reverse Transcription Kit (Applied Biosystems, Foster City, CA) and Exonuclease I (GE Healthcare, Piscataway, NJ) were all purchased from their respective manufacturers.

7.3.2. *In Silico CpG Island Prediction*

CpG island predictions were done using three *in silico* prediction programs (CpGProD[62], CpGPlot by Emboss[63] and CpG Island Searcher[64]) which all utilize baseline criteria for CpG islands described by Gardiner-Gardner and Frommer[28] and the traditional algorithms for predicted CpG islands[65]. The analyzed *ABCG2* gene locus was defined as a ~300,000 bp region from one gene upstream (*PPM1K*) and downstream (*PKD2*) of *ABCG2* (chr4:89130400-89439035, hg18; chr4:88911376-89220011, hg19). Both forward and reverse DNA sequences for the gene locus were obtained from the UCSC Genome browser and utilized in the above prediction programs. For the CpGProD program[62], criteria of GC content $\geq$ 50%, CpG O/E $\geq$ 0.6 and a length greater than 300 bp were used for predictions. This program suggests using a length > 500 bp and it also weights for CpG islands over the transcriptional start site (TSS) of genes[62]. Similar parameters were used for predictions with the CpGPlot program by EMBOSS[63], with the

exception of a required length of 200 bp. The CpG Searcher program uses the algorithm previously described by Takai and Jones[31] and criteria of GC ≥ 55%, O/E ≥ 0.6 and length ≥ 300 bp were used for predictions with this algorithm. No programs that are based on the recently developed algorithms focused on clustering of CpG sites without taking into account baseline DNA content[66] were utilized for these predictions. To help eliminate false positive CpG islands that occur over Alu repeats, a required minimum number of seven CpG sites in 200 bp, described in Table 7.3 as CpG/bp > 0.035, was implemented.

7.3.3. *Liver and Kidney Tissues*

Kidney (n=29) and liver (n=29) samples were procured by the Pharmacogenomics of Membrane Transporters (PMT) research group at the University of California San Francisco (San Francisco, CA)[67]. These tissues were purchased from Asterand (Detroit, MI), Capital Biosciences (Rockville, MD) and SRI International (Menlo Park, CA). The Asterand samples included both postmortem tissues and surgical resections from donors, the Capital Biosciences samples included surgical resections from normal tissue surrounding cancer tissues and SRI International samples were postmortem tissues. All samples were stored frozen at -80°C until processing for DNA and RNA. Information on the age, sex, and ethnicity of the patient was available for all samples.

DNA was extracted from the tissues using the Qiagen AllPrep DNA/RNA Mini Kit following the manufacturer's protocol, with additional DNA clean-up using the QIAquick PCR Purification Kit. RNA was extracted from the tissues following the protocol for Trizol reagent, followed by RNA clean-up with the Qiagen RNeasy

MinElute Cleanup Kit following the manufacturer's protocol. Good-quality RNA (260/280 >1.7 and 260/230 >1.8, RNA Integrity number 3-8) was isolated from 29 kidney samples and 29 liver samples, and all were used to correlate CpG island methylation with total ABCG2 mRNA expression. Two micrograms of RNA were reverse transcribed to cDNA using the High Capacity cDNA Reverse Transcription Kit and the following incubation conditions: 10 min at 22ºC, 2 hr at 37ºC, 5 min at 4ºC, 10 min at 75 ºC and 5 min at 4ºC. Exonuclease I (10U/mL) was added to each sample and the following incubation conditions were used to remove excess primers: 1 hr at 37ºC, 5 min at 4ºC and then 10 min at 85ºC to inactivate the exonuclease enzyme. Samples were then stored at -20ºC until assayed for gene expression or pyrosequenced.

7.3.4. *ABCG2 mRNA Expression in PMT Liver and Kidney Tissues*

ABCG2 expression was evaluated in 29 kidney and 29 liver samples from surgical resection or postmortem collections in Caucasian males and females using the Biotrove Open Array™ qPCR platform (Life Technologies, Carlsbad, CA) according to the manufacturer's protocol. ABCG2 mRNA expression was normalized to a geometric mean of the expression of GAPDH, β-2 microglobin, and β-actin and expressed as $2^{-\Delta\Delta Ct}$ per gene for each sample. All ΔCt values for a given tissue type were quantile normalized across samples using the open source R preprocessCore package[68,69] Expression data was quality controlled using principal component analysis to identify outliers. All samples (N=29 for each tissue) passed initial QC and were pyrosequenced.

7.3.5. *Pyrosequencing Primer Design*

Primers for PCR and pyrosequencing reactions were designed using the PyroMark Assay Design 2.0 software (Qiagen, Valencia, CA). First, CpG4 and CpG6 were split into four and two regions of up to 300 bp, respectively, for PCR reactions. Sequences for each region where extracted from the UCSC Genome Browser and input into the design software. Primers were selected based on melting temperature, percent GC and uniqueness. Multiple sequencing primers were designed per region to cover all CpG sites. All reverse PCR primers were biotin labeled; all primers were synthesized by Integrated DNA Technologies (San Diego, CA).

Table 7.1. Pyrosequencing Primers for CpG Island 4

Primer[1]	Sequence	Location[2]
CpG4 PCR1 F1	TTTTAGAGAAATTGGTTTTATA	89079507-89079528
CpG4 PCR1 R1*	AACTACCTACTATACCCACTCA	89079824-89079845
CpG4 SEQ1 S1	AATTAAAGGTTTAGGATT	89079562-89079570
CpG4 SEQ1 S2	AATAAGATTATTAAGTATGTGTA	89079686-89079708
CpG4 SEQ1 S3	TTTTAATTTTAGTGGGAG	89079764-89079781
CpG4 PCR2 F1	GAATTTTTTGAGTGGGTATAGT	89079816-89079837
CpG4 PCR2 R1*	AACCACTACCTTCAACTCTAAC	89080048-89080069
CpG4 SEQ2 S1	TTTTGAGTGGGTATAGTA	89079821-89079838
CpG4 SEQ2 S2	AATTTTTTTTTTTAATTATAT	89079858-89079878
CpG4 SEQ2 S3	GGTGGTAGTTTGGGGAGA	89079958-89079975
CpG4 PCR3 F1	GTTGTGGATAGTTAGAGTTGAA	89080038-89080059
CpG4 PCR3 R1*	CAATAAACCCCTAATAATTCTC	89080323-89080344
CpG4 SEQ3 S1	GAGTTGAAAGTAGTGGTT	89080052-89080069
CpG4 SEQ3 S2	GTTTAGGGTTTTTTTAGG	89080080-89080097
CpG4 SEQ3 S3	GTTAGTAGGATTGGTATTAT	89080201-89080220
CpG4 PCR4 F1	GTTGAGTAGTTAGTAGGATTGGTAT	89080193-89080217
CpG4 PCR4 R1*	AACCACCCATTTAACTTACTCT	89080461-89080482
CpG4 SEQ4 S1	GTAGGGATAAGTTAAATATT	89080259-89080278
CpG4 SEQ4 S2	TGATTTAGTTGGGTTTGG	89080364-89080381

[1] Primer names indicate CpG island, PCR reaction order per island or overall sequencing reaction number, and a numbered F, R, or S for direction or order of primer in region

[2] Genomic location on chromosome 4 from UCSC genome browser build 19

Asterisks indicate biotin labeled primers

Abbreviations: SEQ, overall sequence reaction; F, forward; R, reverse; S, sequence primer order per region

Table 7.2. Pyrosequencing Primers for CpG Island 6

Primer[1]	Sequence	Location[2]
CpG6 PCR1 F1	AGAGGAATTTGTTGTTAGTATATT	89120804-89120827
CpG6 PCR1 R1*	CCCCACTAATCTTTTTTATATT	89120992-89121013
CpG6 SEQ1 S1	AAAAGTTATTTTATTTTATTTA	89120849-89120870
CpG6 SEQ1 S2	GTTTTAGTATTTTGGGAG	89120898-89120915
CpG6 PCR2 F1	GATTATTTTGGAGAATATAGTGAAA	89120951-89120975
CpG6 PCR2 R1*	AAATTCCTAAACTCAAATAATCTAC	89121251-89121275
CpG6 PCR2 S1	AAAAATATAAAAAAGATTAGT	89120989-89121009
CpG6 SEQ2 S2	GTAGAGTTTGTAGTGAGTAAG	89121085-89121105

[1] Primer names indicate CpG island, PCR reaction order per island or overall sequencing reaction number, and a numbered F, R, or S for direction or order of primer in region

[2] Genomic location on chromosome 4 from UCSC genome browser build 19

Asterisks indicate biotin labeled primers

Abbreviations: SEQ, overall sequence reaction; F, forward; R, reverse; S, sequence primer order per region

7.3.6. *Pyrosequencing*

All bisulfite reactions of DNA and pyrosequencing were done at the Stanford University Protein and Nucleic Acid (PAN) Facility (Stanford, CA). DNA from each tissue was treated with sodium bisulfite using the Qiagen Epitech Bisulfite Kit following the manufacturer's protocol. Regions were amplified using the Qiagen Pyromark PCR kit following the manufacturer's protocol, with the following adjustments per each PCR reaction: 10-20 ng of sodium bisulfite treated DNA, 0.2 μM final primer concentration, 25 mM $MgCl_2$ and an annealing temperature of 54°C. PCR reactions were purified on Strepavidin beads using the Qiagen PyroMark vacuum system following the manufacturer's protocol. Pyrosequencing reactions were run on the Qiagen PyroMark Q24 instrument (Qiagen, Valencia, CA) using Qiagen Pyro Gold reagents following the manufacturer's protocol. Pyrosequencing results were analyzed versus the standard

reference sequence, which was obtained from the UCSC Genome browser, and visualized using the PyroMark Q24 software (Qiagen, Valencia, CA).

7.3.7. *Statistical Analysis*

Results for pyrosequencing reactions were obtained as percent methylation per CpG site. CpG methylation percentages were averaged both per site for all tissues and per CpG island in each tissue. In the case of CpG4, percent methylations for sections of the island were averaged per tissue. Average percent methylation for sections of the CpG4 island or the entire CpG6 island were compared between liver and kidney tissues using an ANOVA followed by a post-hoc Bonferroni's multiple comparison test or a Student's *t*-test, respectively. Regions were considered to have statistically significant differences in methylation with a $P < 0.05$. If the range of percent methylation at a given site was 10% or greater, linear regression was used to evaluate the relationship between ABCG2 expression and methylation. Methylation of whole CpG islands was analyzed in a similar manner. Results were reported for individual CpG sites only if the linear regression had an $R^2 > 0.8$, a $P < 0.05$ and a non-zero slope. Expression of ABCG2 mRNA was analyzed as $2^{-\Delta\Delta Ct}$ values (as described above), and differences in ABCG2 mean expression were examined using a Student's *t*-test on the 29 samples of each tissue. All statistics were run using the GraphPad Prism 5 program.

7.4. Results

7.4.1. *ABCG2 Expression in PMT Liver and Kidney Tissues*

The expression of ABCG2 mRNA in 29 liver and kidney tissues were examined using qRT-PCR. A range of ABCG2 expression was observed in kidney (Figure 7.3). Although there were a few liver samples with high expression of ABCG2, the average expression of ABCG2 in kidney was three times that of liver (0.003 versus 0.001, p = 0.38, data not shown). The lack of statistical difference between the mean of these two tissue sets is likely limited by sample size; analysis of 60 samples for each tissue yields similar mean values of ABCG2 expression but the difference between liver and kidney is significantly different (P = 0.004, data not shown).

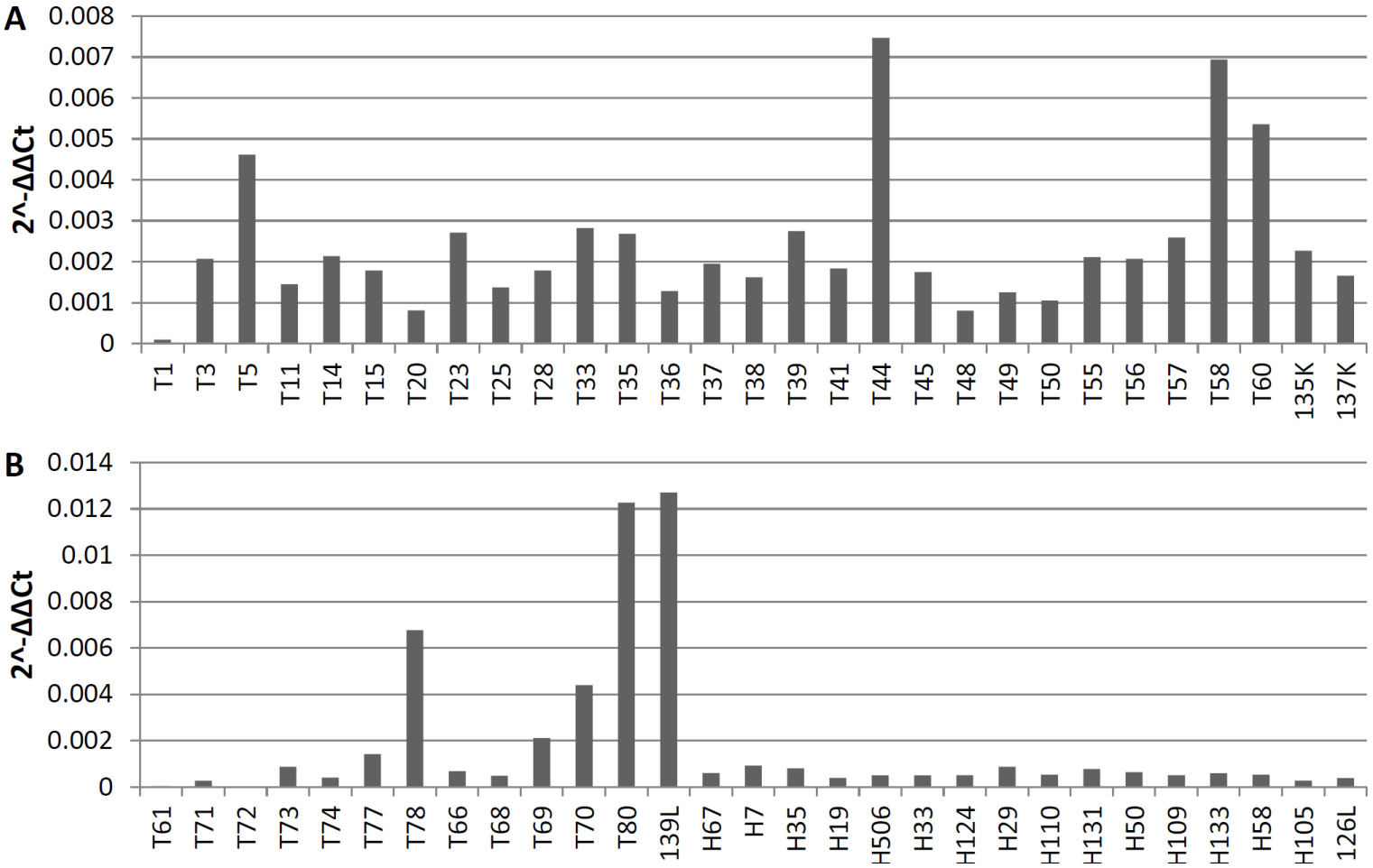

Figure 7.3. Expression profile of ABCG2 mRNA in human tissues. ABCG2 mRNA expression in 29 human (A) kidney and (B) liver tissues, determined by qRT-PCR and displayed as $2^{-\Delta\Delta Ct}$. The mRNA expression of ABCG2 was normalized to the geometric mean of three housekeeping genes and then quantile normalized as described in *Materials and Methods*.

7.4.2. *CpG Island Prediction*

Using the three predictive programs CpGProD, CpGPlot and CpG Island Searcher with criteria described in *Materials and Methods*, 12 predicted CpG islands in the *ABCG2* gene locus were identified (Figure 7.1 and Table 7.3). These CpG Islands ranged in length from 250 bp to 2000 bp, in GC content from 55-70%, in O/E ratio from 0.71-0.95 and in the number of CpG sites from 14-170. As expected, the three largest CpG islands were over the TSS of genes, CpG1 over the *PKD2* TSS, CpG4 over the *ABCG2* TSS and CpG11 over the *PPM1K* TSS. The reverse sequence of the *ABCG2* gene locus yielded slightly more predicted CpG islands than the forward sequence. Since *PKD2* runs on the forward strand and *PPM1K* and *ABCG2* run on the anti-strand, we did not exclude any CpG islands based on their strand orientation.

The three programs predicted similar regions of comparable length. Seven regions were predicted by all three programs: CpG isles 1, 3-6, 9 and 11 (data not shown). The remaining five regions were predicted by both CpGProD and CpGPlot. The Takai/Jones algorithm[31] used in CpGProD was designed to eliminate *Alu* repeats by increasing the minimum length of CpG islands to 500 bp since *Alu* repeats are usually ~300 bp in length[70]. Using a high minimum length requirement suppresses short regions which have been suggested to be active[66]. Therefore, a minimum CpG site of 7 per 200 bp versus the high minimum length to eliminate *Alu* repeats was implemented.

Two CpG islands in the *ABCG2* gene locus were analayzed in both liver and kidney tissues (n = 29 per tissue). The CpG1 and CpG11 islands were eliminated from pyrosequencing analysis due to their orientation over the TSS of neighboring genes, which suggests they are relevant for regulating the expression of those genes (Figure 7.1).

For similar reasons, we choose CpG4 for analysis because it is situated over the TSS of *ABCG2* and there is evidence supporting alteration in methylation correlates with ABCG2 expression[42–45]. CpG islands 3-9 are either intra-*ABCG2* or upstream relative to its TSS (Figure 7.1). Since all of these regions have reliable CpG island criteria (Table 7.3), we selected CpG6 for analysis with pyrosequencing since it was the only region that had preliminary data by ENCODE showing alteration in methylation (data not shown).

Table 7.3. Characteristics of the CpG Islands in the *ABCG2* Locus

Isle ID	%GC[1]	Obs/Exp[2]	Length	#CpG[3]	CpG/bp[4]	Genomic Location[5]
CpG Isle 1	69.6	0.945	1490	170	0.114	88928338-88929827
CpG Isle 2	55.6	0.735	253	14	0.055	88978629-88978881
CpG Isle 3	55.2	0.973	330	22	0.067	89037746-89038075
CpG Isle 4	63	0.834	1040	85	0.082	89079580-89080619
CpG Isle 5	55	0.714	525	28	0.053	89107719-89108243
CpG Isle 6	55	0.841	318	18	0.057	89120882-89121199
CpG Isle 9	55	0.755	318	18	0.057	89169456-89169773
CpG Isle 11	59.3	0.823	1955	139	0.071	89204336-89206290

[1] Percentage G and C content of region

[2] Number of CpG sites divided by number of C and G base pairs

[3] Total number of CpG sites in region

[4] Number of CpG sites per basepair (bp)

[5] Genomic location on chromosome 4 from the UCSC genome browser's hg19 build

7.4.3. *Methylation of CpG4*

Methylation percentages for each CpG site in CpG4 were obtained in seven kidney and liver tissues. Quality of bisulfite conversion and pyrosequencing were checked through analysis of the pyrograms (Figure 7.4) provided by the PyroMark Q24 software. All bisulfite conversions were >90%, and any failed sequencing runs were rerun. Percent methylation for individual CpG sites in both kidney and liver tissues were under 30% (Figure 7.5), and methylation for the entire CpG4 island was under 40% in both tissues (Figure 7.6). The most variability in methylation between samples, for both tissues, occurred on the edges of the CpG4 island, specifically CpG sites 1-13 and 68-87 (Figure 7.5). For both CpG sites 1-13 and 68-87, kidney tissues had a higher percent methylation than liver tissues (Figure 7.7). There was no difference between kidney and liver for the average percent methylation of CpG sites 14-67 in CpG4. Additionally, the individual CpG site percent methylation for CpG sites 1-13 and 68-87 was correlated with the expression of ABCG2 mRNA in kidney and liver. The percent methylation of CpG site 77 of CpG4 was correlated to ABCG2 mRNA in the kidney (Figure 7.8).

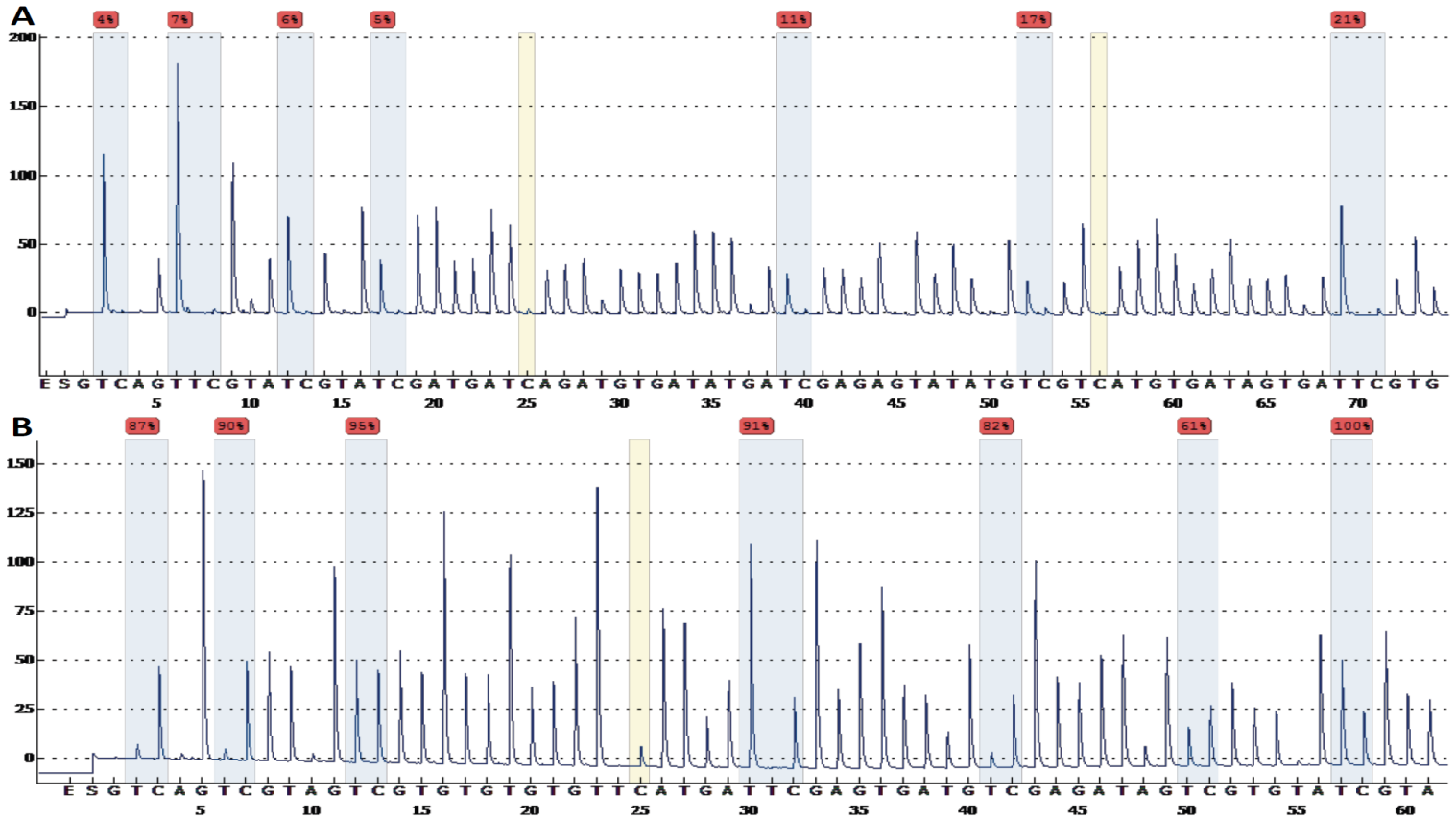

Figure 7.4. Representative program traces obtained by pyrosequencing. Pyrograms from the sequencing of a section of CpG islands (A) CpG4 and (B) CpG6. Red columns indicate methylated CpG sites with the density of the methylation presented at the top of the trace as an average percent for the CpG site analyzed. Highlighted yellow nucleotides indicate quality control flags for failed conversion of cytosine to uracil by the bisulfite treatment. Height of each peak is arbitrary and used by PyroMark within each sample run to calculate percent of methylation. Nucleotide sequence is listed along the bottom below peak traces.

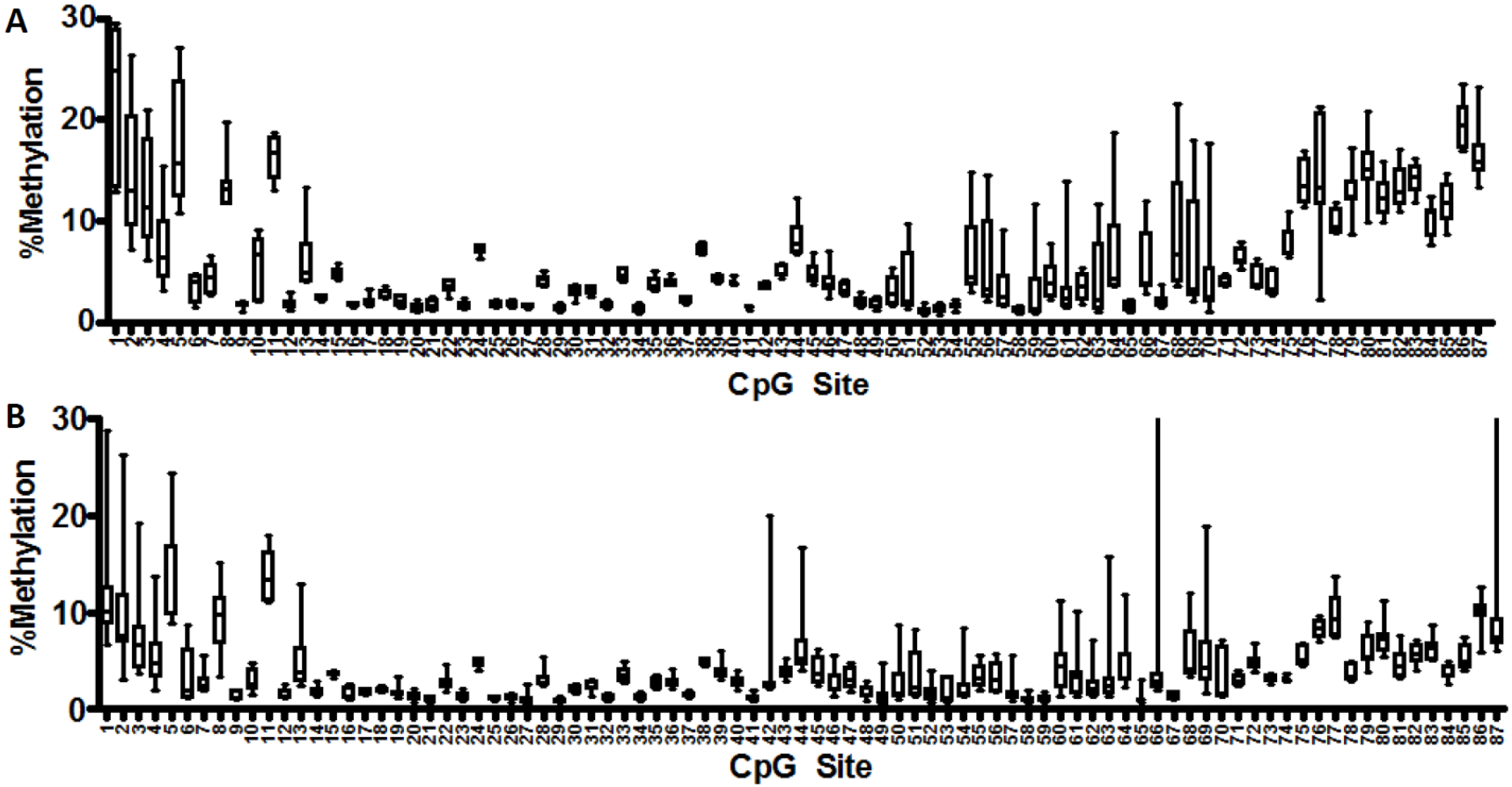

Figure 7.5. Box and whisker plots for range of CpG4 methylation per CpG site. The methylation percent of 87 CpG sites in the CpG4 island for seven (A) kidney and (B) liver tissues. Per each CpG site the box indicates the 25th and 75th percentile, the line in the box the median and the whiskers range from minimum to maximum percent methylation.

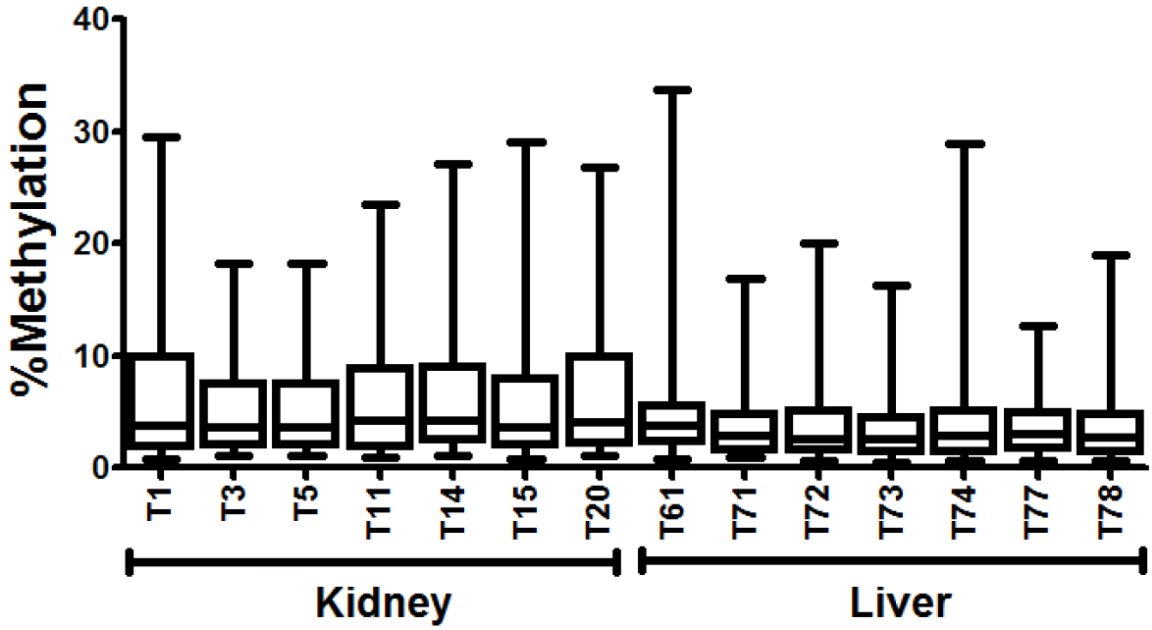

Figure 7.6. Box and whisker plots for range of CpG4 methylation per tissue. The mean methylation percent of all CpG sites in the CpG4 island are combined for each of the seven kidney and liver tissues. Per each tissue, the box indicates the 25th and 75th percentile, the line in the box the median and the whiskers range from minimum to maximum percent methylation.

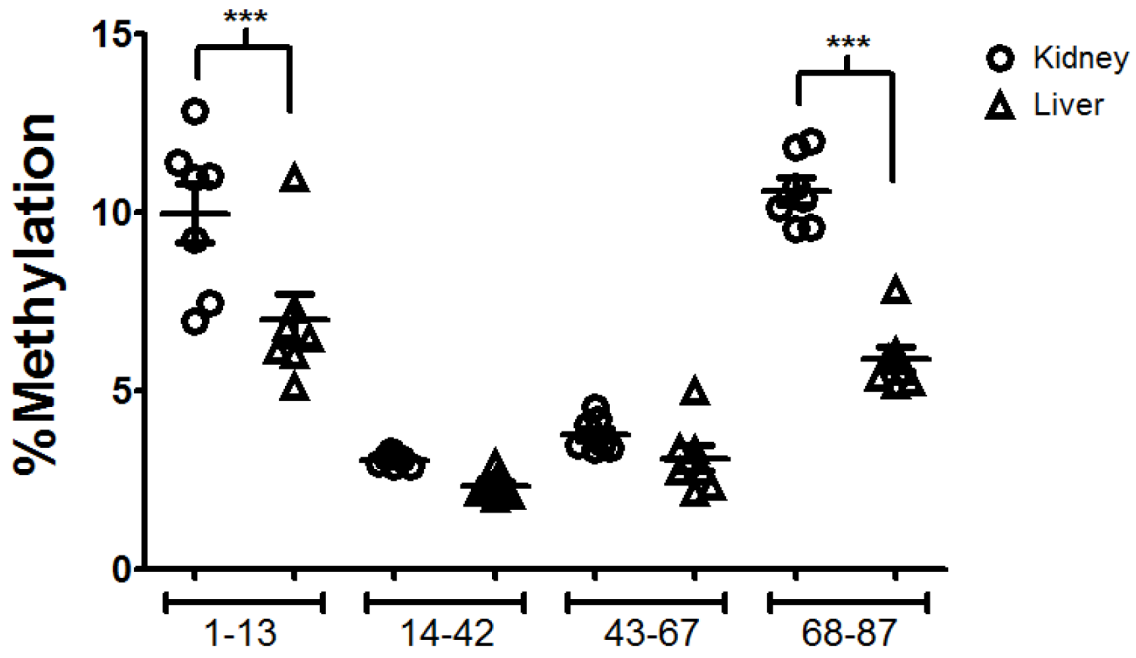

Figure 7.7. Scatter plot of methylation analyses for sections of CpG4. The scatter plot shows the methylation percent of CpG sites in sections of the CpG4 island for (○) Kidney and (△) Liver tissues. The CpG sites contained in each section of the CpG4 island are listed along the x-axis. Per each section of CpG4, the line represents the mean percent methylation of each sample's CpG sites. Analysis between the two tissues were done per each section of CpG4 using an ANOVA followed by a post-hoc Bonferroni's multiple comparison test; *** $P < 0.0001$.

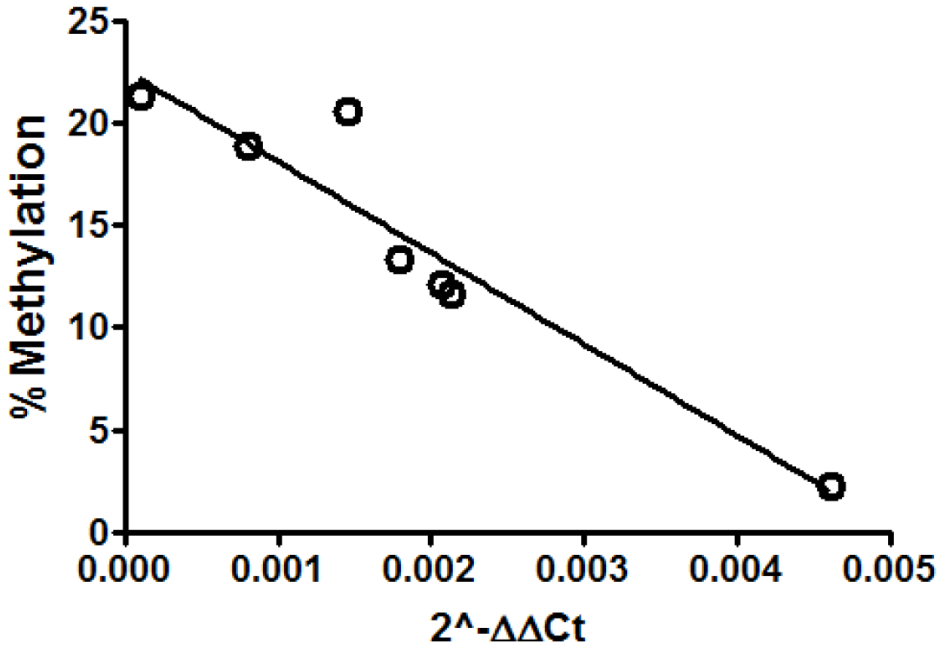

Figure 7.8. Correlation of CpG4 island CpG site 77 methylation with ABCG2 expression in kidney. Percent methylation at CpG site 77 in CpG4 for each of the seven kidney tissues were plotted versus their ABCG2 mRNA expression. ABCG2 mRNA expression is displayed as $2^{-\Delta\Delta Ct}$ as described in *Materials and Methods*. Linear regression was used to determine correlation of methylation with ABCG2 expression; $R^2 = 0.9$, $P = 0.001$.

7.4.4. *Methylation of CpG6*

Methylation percentages for each CpG site in the CpG6 island were obtained in 29 kidney and liver tissues. Quality of bisulfite conversion and pyrosequencing were checked through analysis of the pyrograms (Figure 7.4) provided by the PyroMark Q24 software. All bisulfite conversions were >90%, and any failed sequencing runs were rerun. Percent methylation for individual CpG sites in both kidney and liver tissues had a wide range, but averaged between 50-80% for kidney tissues (Figure 7.9A) and 65-100% for liver tissues (Figure 7.9B). Overall methylation for the entire CpG6 island per tissue sample ranged from 50-90% for kidney tissues (Figure 7.10A) and 85-95% for liver tissues (Figure 7.10B). Since the entire CpG6 island exhibited variability in percent methylation, the average percent methylation for the whole CpG6 island was tested for differences between kidney and liver. Liver had an average percent methylation of 90%, which was significantly higher than the 75% average percent methylation of kidney (Figure 7.11). The average percent methylation for the entire CpG6 island did not correlate with ABCG2 mRNA in either kidney or liver tissues (Figure 7.12). Association between the percent methylation of individual CpG sites in the CpG6 island and ABCG2 mRNA levels was not evident (data not shown).

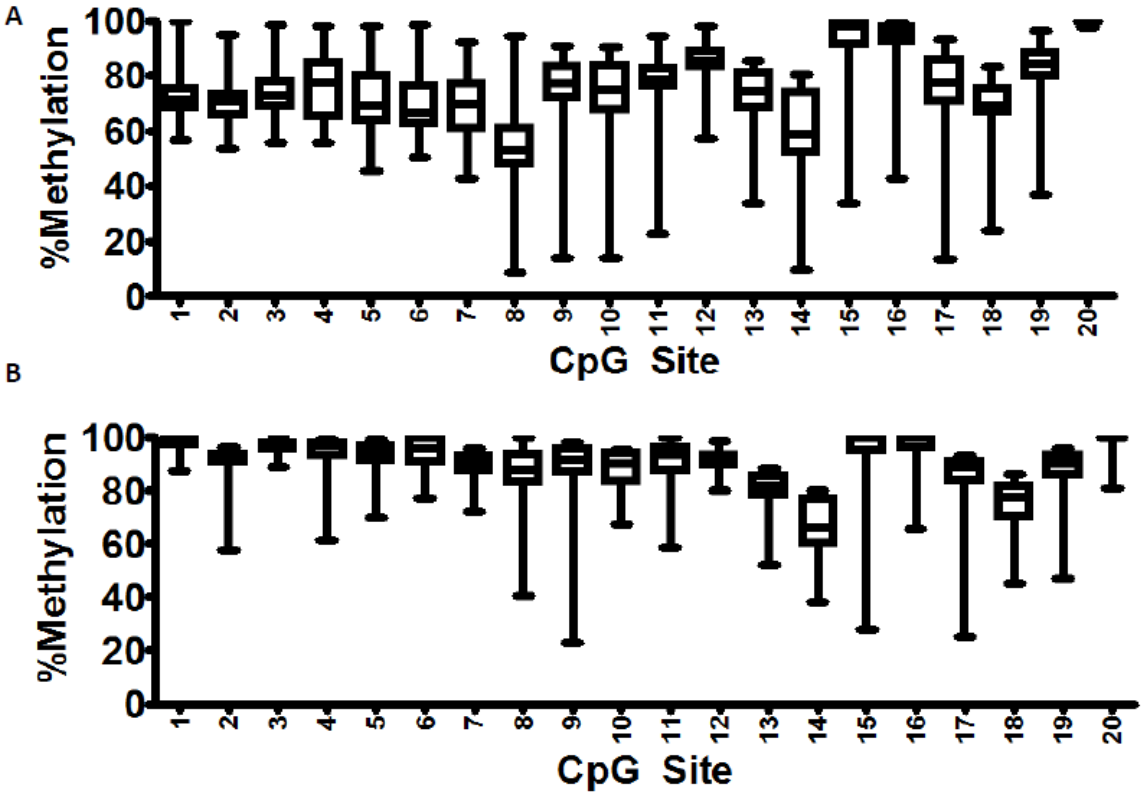

Figure 7.9. Box and whisker plots for range of CpG6 methylation per CpG site. The percent methylation of 20 CpG sites in the CpG6 island for 29 (A) kidney and (B) liver tissues. For each CpG site, the box indicates the 25th and 75th percentile, the line in the box is the median, and the whiskers range from minimum to maximum percent methylation.

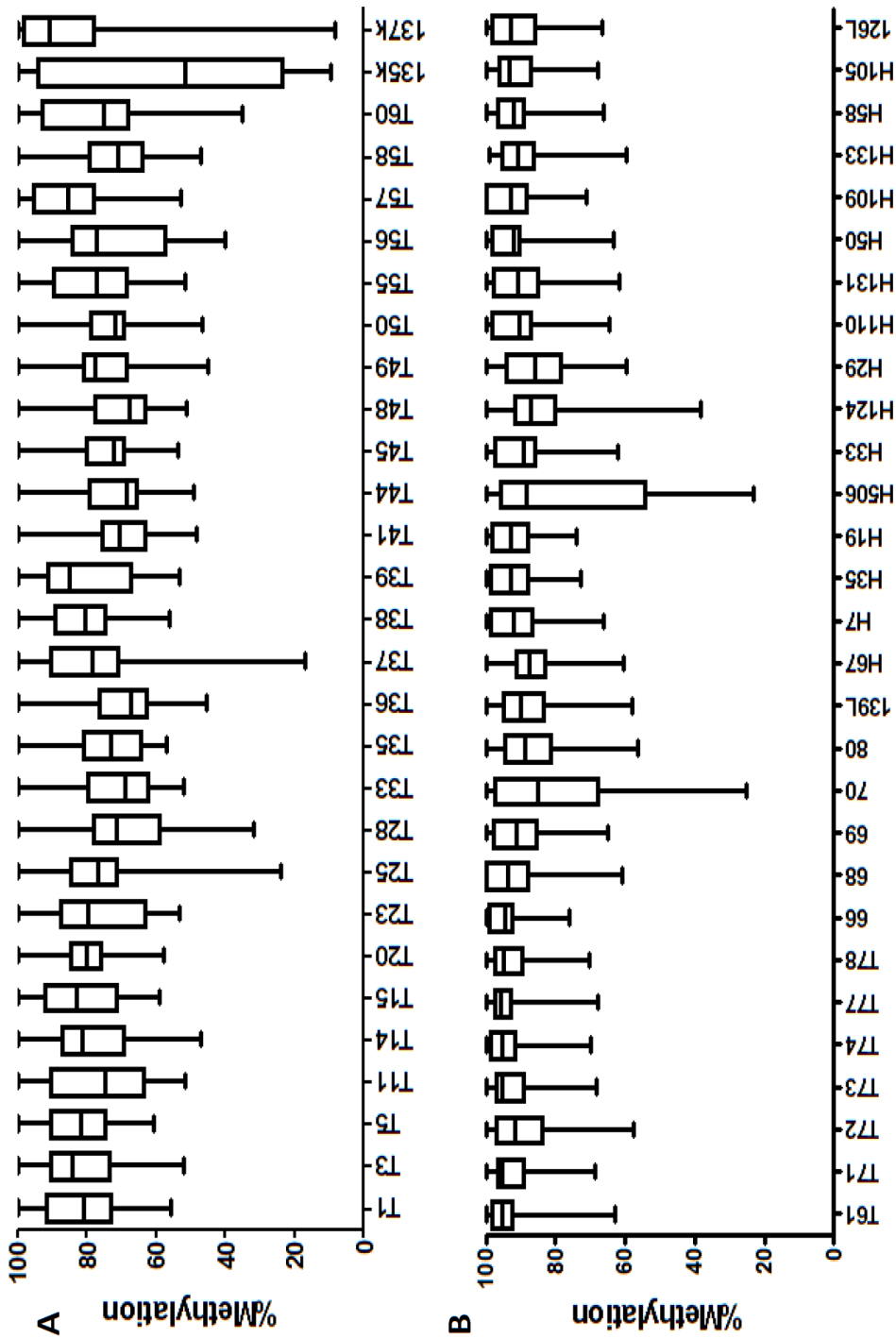

Figure 7.10. Box and whisker plots for range of CpG6 methylation per tissue. The mean percent methylation of all CpG sites in the CpG6 island for 29 (A) kidney and (B) liver tissues. For each tissue, the box indicates the 25th and 75th percentile, the line in the box the median and the whiskers range from minimum to maximum percent

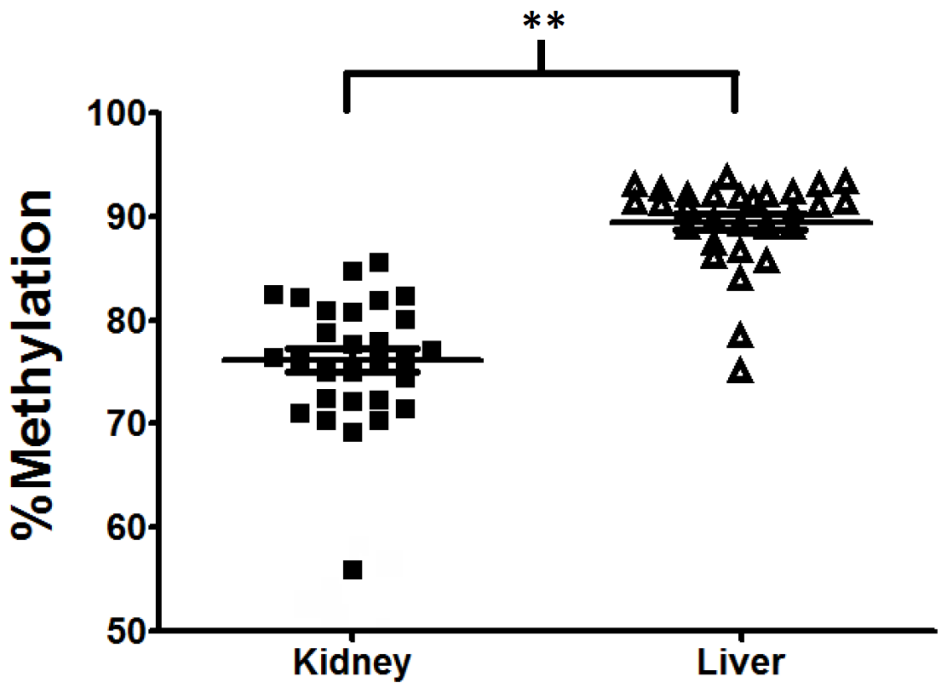

Figure 7.11. Scatter plot of methylation analyses for CpG6. The scatter plot shows the percent methylation of CpG sites in the CpG6 island for (■) kidney and (△) liver tissues. Percent methylation of all 20 CpG sites in CpG6 was averaged per tissue to obtain a single value. For each tissue set, the line represents the mean percent methylation of CpG6. Analysis between the two tissues was done using a Student's *t*-test; ** $P < 0.001$.

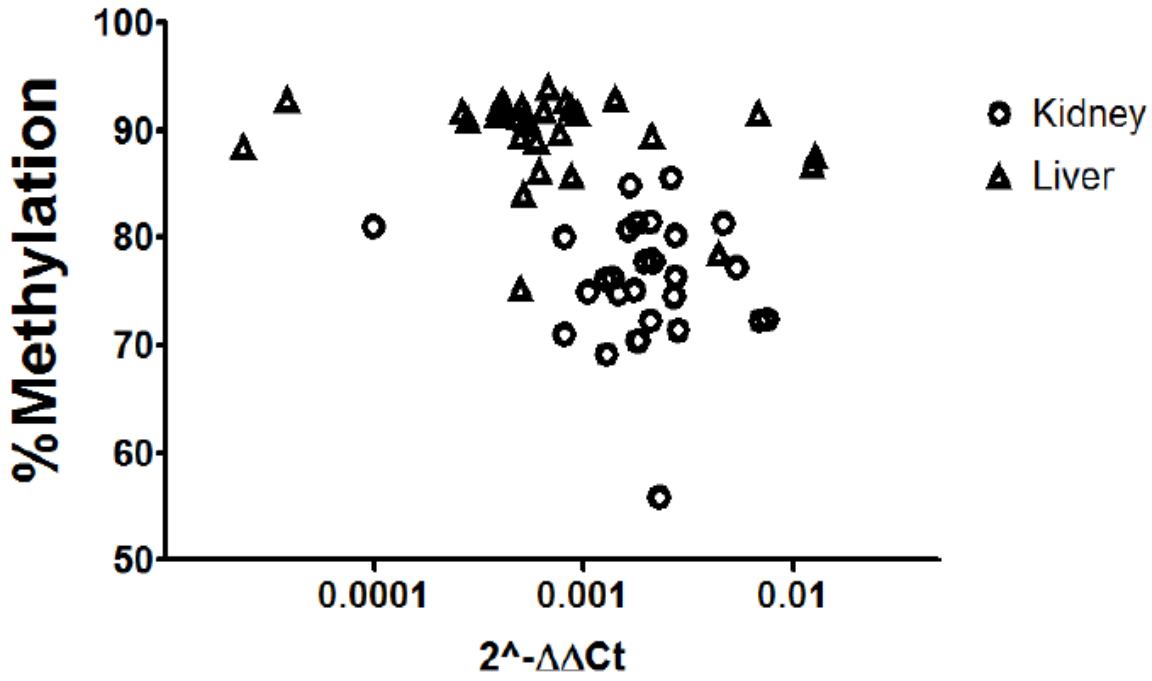

Figure 7.12. Correlation of CpG6 island methylation with ABCG2 expression in kidney and liver. Percent methylation of CpG6 for each of the 29 (○) kidney and (△) liver tissues were plotted versus their ABCG2 mRNA expression. Percent methylation of all 20 CpG sites in CpG6 was averaged per tissue to obtain a single value. ABCG2 mRNA expression is displayed as $2^{-\Delta\Delta Ct}$, as described in *Materials and Methods*. Linear regression was used to determine correlation of CpG6 methylation with ABCG2 expression in either tissue.

7.5. Discussion

The data presented above suggests that the *ABCG2* promoter CpG island, CpG4, has low methylation in liver and kidney. These data are consistent with the absence of methylation for the *ABCG2* promoter CpG island in liver[41] and renal cell lines[42]. Limited methylation and the rank order of methylation between liver and kidney is also consistent with the high expression of ABCG2 in liver and more moderate expression of ABCG2 in kidney[1]. However, the average percent methylation of CpG4 was not correlated with expression of ABCG2. Larger studies are needed to confirm these results.

Previous research correlating the expression of ABCG2 to promoter methylation has been qualitative rather than quantitative in nature. The only report that has shown correlation between ABCG2 mRNA levels and percent methylation of the *ABCG2* promoter used data from before and after mass depletion of promoter methylation by treating cells with the demethylation agent 5-aza-2'deoxycitidine[44]. Other qualitative reports of alteration in ABCG2 expression due to *ABCG2* promoter methylation have also been before and after treatment with 5-aza-2'deoxycitidine or with other xenobiotics[42–46]. The current results demonstrate that in normal kidney and liver tissues the *ABCG2* promoter CpG4 island is not highly methylated and extent of methylation is not a marker for ABCG2 expression.

The use of the pyrosequencing technique allowed the estimation of percent methylation at multiple CpG sites within two CpG islands of the *ABCG2* gene locus. Methylation of one CpG site, CpG site 77 in the CpG4 island, was correlated with ABCG2 expression in the kidney. Alteration in methylation status of CpG sites on the edges, or shores, of CpG islands often relate the strongest to gene expression[71] and it has

been proposed that alterations in methylation status of CpG shores are more relevant to the modulation of gene expression[71]. Consistent with this proposal, CpG4 island CpG site 77 is located in a shore. This insight could continue to direct other studies looking at *ABCG2* promoter methylation in drug resistance.

The smaller CpG6 island, located upstream of the *ABCG2* promoter, showed different extents of methylation in kidney and liver tissues. Traditionally, CpG islands are categorized as being over 200 bp in length[28], with CpG islands over the transcriptional start sites of genes being greater than 500 bp[62]. However, shorter CpG islands (>200 bp) are also functional and can exhibit tissue-specific alterations in methylation and evolutionary conservation[66]. Although there is no correlation between the average percent methylation of CpG6 and ABCG2 expression, there is a significant difference in the average methylation of CpG6 between kidney and liver tissues. This is consistent with reports that functional short CpG islands exhibit tissue-specific alterations in methylation[66], and suggesting that this island may have some other yet unknown function. CpG6 is also upstream of the alternate promoter for *ABCG2*[72], and further studies would be needed to see if the methylation of CpG correlates to expression of individual ABCG2 isoforms or the expression of ABCG2 in other tissues. Additional studies would also be needed to investigate correlation between CpG6 methylation and PPM1K expression, the other gene near CpG6.

7.6. Conclusion

The CpG4 and CpG6 islands in the *ABCG2* gene locus both exhibit tissue-specific patterns in CpG site methylation in kidney and liver tissues. However, the average percent methylation of either island was not correlated to ABCG2 expression. Interestingly, CpG4 had little variability in the methylation of CpG sites located in the center of the island, but its shores exhibited high variability in methylation. The percent methylation of one CpG site in CpG4, site 77, correlated to ABCG2 expression in the kidney. The identification of CpG islands with tissue-specific methylation patterns within the *ABCG2* gene locus, as well as the CpG site 77 that correlates to ABCG2 expression, can help guide further studies investigating the development of drug-resistance in cancer.

7.7. References

(1) Maliepaard, M.; Scheffer, G. L.; Faneyte, I. F.; Gastelen, A. Van; Pijnenborg, A. C. L. M. Subcellular Localization and Distribution of the Breast Cancer Resistance Protein Transporter in Normal Human Tissues Subcellular Localization and Distribution of the Breast Cancer Resistance Protein Transporter in Normal Human Tissues 1. **2001**, 3458–3464.

(2) Doyle, L. a; Yang, W.; Abruzzo, L. V; Krogmann, T.; Gao, Y.; Rishi, a K.; Ross, D. D. A multidrug resistance transporter from human MCF-7 breast cancer cells. *Proceedings of the National Academy of Sciences of the United States of America* **1998**, *95*, 15665–70.

(3) Fetsch, P. a; Abati, A.; Litman, T.; Morisaki, K.; Honjo, Y.; Mittal, K.; Bates, S. E. Localization of the ABCG2 mitoxantrone resistance-associated protein in normal tissues. *Cancer letters* **2006**, *235*, 84–92.

(4) Doyle, L. A.; Ross, D. D. Multidrug resistance mediated by the breast cancer resistance protein BCRP (ABCG2). *Oncogene* **2003**, *22*, 7340–58.

(5) Poonkuzhali, B.; Lamba, J.; Strom, S. Association of breast cancer resistance protein/ABCG2 phenotypes and novel promoter and intron 1 single nucleotide polymorphisms. *Drug Metabolism and …* **2008**, *36*, 780–795.

(6) Urquhart, B. L.; Ware, J. a; Tirona, R. G.; Ho, R. H.; Leake, B. F.; Schwarz, U. I.; Zaher, H.; Palandra, J.; Gregor, J. C.; Dresser, G. K.; Kim, R. B. Breast cancer resistance protein (ABCG2) and drug disposition: intestinal expression, polymorphisms and sulfasalazine as an in vivo probe. *Pharmacogenetics and genomics* **2008**, *18*, 439–48.

(7) Zamber, C. P.; Lamba, J. K.; Yasuda, K.; Farnum, J.; Thummel, K.; Schuetz, J. D.; Schuetz, E. G. Natural allelic variants of breast cancer resistance protein (BCRP) and their relationship to BCRP expression in human intestine. *Pharmacogenetics* **2003**, *13*, 19–28.

(8) Ross, D. D.; Karp, J. E.; Chen, T. T.; Doyle, L. A. Expression of breast cancer resistance protein in blast cells from patients with acute leukemia. *Blood* **2000**, *96*, 365–8.

(9) Suvannasankha, a; Minderman, H.; O'Loughlin, K. L.; Nakanishi, T.; Greco, W. R.; Ross, D. D.; Baer, M. R. Breast cancer resistance protein (BCRP/MXR/ABCG2) in acute myeloid leukemia: discordance between expression and function. *Leukemia : official journal of the Leukemia Society of America, Leukemia Research Fund, U.K* **2004**, *18*, 1252–7.

(10) Suvannasankha, A.; Minderman, H.; O'Loughlin, K. L.; Nakanishi, T.; Ford, L. a; Greco, W. R.; Wetzler, M.; Ross, D. D.; Baer, M. R. Breast cancer resistance protein (BCRP/MXR/ABCG2) in adult acute lymphoblastic leukaemia: frequent expression and possible correlation with shorter disease-free survival. *British journal of haematology* **2004**, *127*, 392–8.

(11) Benderra, Z.; Faussat, A.-M.; Sayada, L.; Perrot, J.-Y.; Chaoui, D.; Marie, J.-P.; Legrand, O. Breast cancer resistance protein and P-glycoprotein in 149 adult acute myeloid leukemias. *Clinical cancer research : an official journal of the American Association for Cancer Research* **2004**, *10*, 7896–902.

(12) Tsunoda, S.; Okumura, T.; Ito, T.; Kondo, K.; Ortiz, C.; Tanaka, E.; Watanabe, G.; Itami, A.; Sakai, Y.; Shimada, Y. ABCG2 expression is an independent unfavorable prognostic factor in esophageal squamous cell carcinoma. *Oncology* **2006**, *71*, 251–8.

(13) Usuda, J.; Tsunoda, Y.; Ichinose, S.; Ishizumi, T.; Ohtani, K.; Maehara, S.; Ono, S.; Tsutsui, H.; Ohira, T.; Okunaka, T.; Furukawa, K.; Sugimoto, Y.; Kato, H.; Ikeda, N. Breast cancer resistant protein (BCRP) is a molecular determinant of the outcome of photodynamic therapy (PDT) for centrally located early lung cancer. *Lung cancer (Amsterdam, Netherlands)* **2010**, *67*, 198–204.

(14) Uggla, B.; Ståhl, E.; Wågsäter, D.; Paul, C.; Karlsson, M. G.; Sirsjö, A.; Tidefelt, U. BCRP mRNA expression v. clinical outcome in 40 adult AML patients. *Leukemia research* **2005**, *29*, 141–6.

(15) Yoh, K. Breast Cancer Resistance Protein Impacts Clinical Outcome in Platinum-Based Chemotherapy for Advanced Non-Small Cell Lung Cancer. *Clinical Cancer Research* **2004**, *10*, 1691–1697.

(16) Bailey-Dell, K. J.; Hassel, B.; Doyle, L. a; Ross, D. D. Promoter characterization and genomic organization of the human breast cancer resistance protein (ATP-binding cassette transporter G2) gene. *Biochimica et biophysica acta* **2001**, *1520*, 234–41.

(17) To, K. K. W.; Robey, R.; Zhan, Z.; Bangiolo, L.; Bates, S. E. Upregulation of ABCG2 by romidepsin via the aryl hydrocarbon receptor pathway. *Molecular cancer research : MCR* **2011**, *9*, 516–27.

(18) Tan, K. P.; Wang, B.; Yang, M.; Boutros, P. C.; Macaulay, J.; Xu, H.; Chuang, A. I.; Kosuge, K.; Yamamoto, M.; Takahashi, S.; Wu, A. M. L.; Ross, D. D.; Harper, P. A.; Ito, S. Aryl Hydrocarbon Receptor Is a Transcriptional Activator of the Human Breast Cancer Resistance Protein (BCRP / ABCG2) □. **2010**.

(19) Wang, H.; Lee, E.; Zhou, L.; Leung, P. C. K.; Ross, D. D.; Unadkat, J. D.; Mao, Q. Progesterone receptor (PR) isoforms PRA and PRB differentially regulate

expression of the breast cancer resistance protein in human placental choriocarcinoma BeWo cells. *Molecular pharmacology* **2008**, *73*, 845–54.

(20) Ee, P. L. R. Identification of a Novel Estrogen Response Element in the Breast Cancer Resistance Protein (ABCG2) Gene. *Cancer Research* **2004**, *64*, 1247–1251.

(21) Pradhan, M.; Bembinster, L. a; Baumgarten, S. C.; Frasor, J. Proinflammatory cytokines enhance estrogen-dependent expression of the multidrug transporter gene ABCG2 through estrogen receptor and NF{kappa}B cooperativity at adjacent response elements. *The Journal of biological chemistry* **2010**, *285*, 31100–6.

(22) Krishnamurthy, P.; Ross, D. D.; Nakanishi, T.; Bailey-Dell, K.; Zhou, S.; Mercer, K. E.; Sarkadi, B.; Sorrentino, B. P.; Schuetz, J. D. The stem cell marker Bcrp/ABCG2 enhances hypoxic cell survival through interactions with heme. *The Journal of biological chemistry* **2004**, *279*, 24218–25.

(23) Singh, A.; Wu, H.; Zhang, P.; Happel, C. Expression of ABCG2 (BCRP) is regulated by Nrf2 in cancer cells that confers side population and chemoresistance phenotype. *Molecular cancer ...* **2010**, *9*, 2365–2376.

(24) Reik, W.; Murrell, A. Silence across the border. **2000**, *405*, 408–409.

(25) Wolffe, a P. Transcriptional control: imprinting insulation. *Current biology : CB* **2000**, *10*, R463–5.

(26) Ehrlich, M.; Gama-Sosa, M. Amount and distribution of 5-methylcytosine in human DNA from different types of tissues or cells. *Nucleic acids ...* **1982**, *10*, 11–14.

(27) Bird, A. CpG-rich islands and the function of DNA methylation. *Nature* **1986**.

(28) Gardiner-Garden, M.; Frommer, M. CpG islands in vertebrate genomes. *Journal of molecular biology* **1987**, *196*, 261–82.

(29) Cooper, S. J.; Trinklein, N. D.; Anton, E. D.; Nguyen, L.; Myers, R. M. Comprehensive analysis of transcriptional promoter structure and function in 1% of the human genome. *Genome research* **2006**, *16*, 1–10.

(30) Larsen, F.; Gundersen, G.; Lopez, R.; Prydz, H. CpG islands as gene markers in the human genome. *Genomics* **1992**, *13*, 1095–107.

(31) Takai, D.; Jones, P. a Comprehensive analysis of CpG islands in human chromosomes 21 and 22. *Proceedings of the National Academy of Sciences of the United States of America* **2002**, *99*, 3740–5.

(32) Bird, A. DNA methylation patterns and epigenetic memory. *Genes & development* **2002**, *16*, 6–21.

(33) Sharma, S.; Kelly, T. K.; Jones, P. a Epigenetics in cancer. *Carcinogenesis* **2010**, *31*, 27–36.

(34) GRØNBÆK, K.; HOTHER, C.; JONES, P. Epigenetic changes in cancer. *Apmis* **2007**, *3*, 9.

(35) Barros, S. P.; Offenbacher, S. Epigenetics: connecting environment and genotype to phenotype and disease. *Journal of dental research* **2009**, *88*, 400–8.

(36) Baker, E. K.; El-Osta, A. The rise of DNA methylation and the importance of chromatin on multidrug resistance in cancer. *Experimental Cell Research* **2003**, *290*, 177–194.

(37) Peedicayil, J. Epigenetic therapy--a new development in pharmacology. *The Indian journal of medical research* **2006**, *123*, 17–24.

(38) Baer-Dubowska, W.; Majchrzak-Celińska, A.; Cichocki, M. Pharmocoepigenetics: a new approach to predicting individual drug responses and targeting new drugs. *Pharmacological reports : PR* **2011**, *63*, 293–304.

(39) Szyf, M. Epigenetics, DNA methylation, and chromatin modifying drugs. *Annual review of pharmacology and toxicology* **2009**, *49*, 243–63.

(40) Piekarz, R. L.; Bates, S. E. Epigenetic modifiers: basic understanding and clinical development. *Clinical cancer research : an official journal of the American Association for Cancer Research* **2009**, *15*, 3918–26.

(41) Ding, S.; Gong, B.-D.; Yu, J.; Gu, J.; Zhang, H.-Y.; Shang, Z.-B.; Fei, Q.; Wang, P.; Zhu, J.-D. Methylation profile of the promoter CpG islands of 14 "drug-resistance" genes in hepatocellular carcinoma. *World journal of gastroenterology : WJG* **2004**, *10*, 3433–40.

(42) To, K. K. W.; Zhan, Z.; Bates, S. E. Aberrant promoter methylation of the ABCG2 gene in renal carcinoma. *Molecular and cellular biology* **2006**, *26*, 8572–85.

(43) Nakano, H.; Nakamura, Y.; Soda, H.; Kamikatahira, M.; Uchida, K.; Takasu, M.; Kitazaki, T.; Yamaguchi, H.; Nakatomi, K.; Yanagihara, K.; Kohno, S.; Tsukamoto, K. Methylation status of breast cancer resistance protein detected by methylation-specific polymerase chain reaction analysis is correlated inversely with its expression in drug-resistant lung cancer cells. *Cancer* **2008**, *112*, 1122–30.

(44) Turner, J. G.; Gump, J. L.; Zhang, C.; Cook, J. M.; Marchion, D.; Hazlehurst, L.; Munster, P.; Schell, M. J.; Dalton, W. S.; Sullivan, D. M. ABCG2 expression,

function, and promoter methylation in human multiple myeloma. *Blood* **2006**, *108*, 3881–9.

(45) Bram, E.; Stark, M.; Raz, S.; Assaraf, Y. Chemotherapeutic drug-induced ABCG2 promoter demethylation as a novel mechanism of acquired multidrug resistance. *Neoplasia (New York, NY)* **2009**, *11*, 1359–1370.

(46) Chen, M.; Xue, X.; Wang, F.; An, Y.; Tang, D.; Xu, Y.; Wang, H.; Yuan, Z.; Gao, W.; Wei, J.; Zhang, J.; Miao, Y. Expression and promoter methylation analysis of ATP-binding cassette genes in pancreatic cancer. *Oncology reports* **2012**, *27*, 265–9.

(47) Bram, E.; Stark, M.; Raz, S. Chemotherapeutic drug-induced ABCG2 promoter demethylation as a novel mechanism of acquired multidrug resistance. *Neoplasia (New York, NY)* **2009**, *11*, 1359–1370.

(48) Hiraki, M.; Kitajima, Y.; Sato, S.; Mitsuno, M.; Koga, Y.; Nakamura, J.; Hashiguchi, K.; Noshiro, H.; Miyazaki, K. Aberrant gene methylation in the lymph nodes provides a possible marker for diagnosing micrometastasis in gastric cancer. *Annals of surgical oncology* **2010**, *17*, 1177–86.

(49) Babu, K.; Zhang, J.; Moloney, S.; Pleasants, T.; McLean, C. a; Phua, S. H.; Sheppard, A. M. Epigenetic regulation of ABCG2 gene is associated with susceptibility to xenobiotic exposure. *Journal of proteomics* **2012**, *75*, 3410–8.

(50) Kobayashi, D.; Ieiri, I.; Hirota, T.; Takane, H. Functional assessment of ABCG2 (BCRP) gene polymorphisms to protein expression in human placenta. *Drug metabolism and* **2005**, *33*, 94–101.

(51) Bird, a P.; Wolffe, a P. Methylation-induced repression--belts, braces, and chromatin. *Cell* **1999**, *99*, 451–4.

(52) Zouridis, H.; Deng, N.; Ivanova, T.; Zhu, Y.; Wong, B.; Huang, D.; Wu, Y. H.; Wu, Y.; Tan, I. B.; Liem, N.; Gopalakrishnan, V.; Luo, Q.; Wu, J.; Lee, M.; Yong, W. P.; Goh, L. K.; Teh, B. T.; Rozen, S.; Tan, P. Methylation subtypes and large-scale epigenetic alterations in gastric cancer. *Science translational medicine* **2012**, *4*, 156ra140.

(53) Van Eijk, K. R.; De Jong, S.; Boks, M. P.; Langeveld, T.; Colas, F.; Veldink, J. H.; De Kovel, C. G.; Janson, E.; Strengman, E.; Langfelder, P.; Kahn, R. S.; Van den Berg, L. H.; Horvath, S.; Ophoff, R. a Genetic analysis of DNA methylation and gene expression levels in whole blood of healthy human subjects. *BMC Genomics* **2012**, *13*, 636.

(54) Gibbs, J. R.; Van der Brug, M. P.; Hernandez, D. G.; Traynor, B. J.; Nalls, M. a; Lai, S.-L.; Arepalli, S.; Dillman, A.; Rafferty, I. P.; Troncoso, J.; Johnson, R.;

Zielke, H. R.; Ferrucci, L.; Longo, D. L.; Cookson, M. R.; Singleton, A. B. Abundant quantitative trait loci exist for DNA methylation and gene expression in human brain. *PLoS genetics* **2010**, *6*, e1000952.

(55) Zhang, D.; Cheng, L.; Badner, J. a; Chen, C.; Chen, Q.; Luo, W.; Craig, D. W.; Redman, M.; Gershon, E. S.; Liu, C. Genetic control of individual differences in gene-specific methylation in human brain. *American journal of human genetics* **2010**, *86*, 411–9.

(56) Bell, J. T.; Pai, A. a; Pickrell, J. K.; Gaffney, D. J.; Pique-Regi, R.; Degner, J. F.; Gilad, Y.; Pritchard, J. K. DNA methylation patterns associate with genetic and gene expression variation in HapMap cell lines. *Genome biology* **2011**, *12*, R10.

(57) Deaton, A. M.; Bird, A. CpG islands and the regulation of transcription. *Genes & development* **2011**, *25*, 1010–22.

(58) Jones, P. a Functions of DNA methylation: islands, start sites, gene bodies and beyond. *Nature reviews. Genetics* **2012**, *13*, 484–92.

(59) Clark, S. J.; Harrison, J.; Paul, C. L.; Frommer, M. High sensitivity mapping of methylated cytosines. *Nucleic acids research* **1994**, *22*, 2990–7.

(60) Umer, M.; Herceg, Z. Deciphering the Epigenetic Code: An Overview of DNA methylation Analysis Methods. *Antioxidants & redox signaling* **2012**, *00*.

(61) Uhlmann, K.; Brinckmann, A.; Toliat, M. R.; Ritter, H.; Nürnberg, P. Evaluation of a potential epigenetic biomarker by quantitative methyl-single nucleotide polymorphism analysis. *Electrophoresis* **2002**, *23*, 4072–9.

(62) Mouchiroud, D. CpGProD : identifying CpG islands associated with transcription start sites in large genomic. **2002**, *18*, 631–633.

(63) Rice, P. The European Molecular Biology Open Software Suite EMBOSS : The European Molecular Biology Open Software Suite. **2000**, *16*, 2–3.

(64) Takai, D.; Jones, P. A. The CpG island searcher: a new WWW resource. *In silico biology* **2003**, *3*, 235–40.

(65) Zhao, Z.; Han, L. CpG islands: algorithms and applications in methylation studies. *Biochemical and biophysical research communications* **2009**, *382*, 643–5.

(66) Hackenberg, M.; Barturen, G.; Carpena, P.; Luque-Escamilla, P. L.; Previti, C.; Oliver, J. L. Prediction of CpG-island function: CpG clustering vs. sliding-window methods. *BMC genomics* **2010**, *11*, 327.

(67) Kroetz, D. L.; Yee, S. W.; Giacomini, K. M. The pharmacogenomics of membrane transporters project: research at the interface of genomics and transporter pharmacology. *Clinical pharmacology and therapeutics* **2010**, *87*, 109–16.

(68) Bolstad, B. M.; Irizarry, R. A.; Astrand, M.; Speed, T. P. A comparison of normalization methods for high density oligonucleotide array data based on variance and bias. *Bioinformatics (Oxford, England)* **2003**, *19*, 185–93.

(69) Boes, T.; Neuhäuser, M. Normalization for Affymetrix GeneChips. *Methods of information in medicine* **2005**, *44*, 414–7.

(70) Häsler, J.; Strub, K. Alu elements as regulators of gene expression. *Nucleic acids research* **2006**, *34*, 5491–7.

(71) Irizarry, R. a; Ladd-Acosta, C.; Wen, B.; Wu, Z.; Montano, C.; Onyango, P.; Cui, H.; Gabo, K.; Rongione, M.; Webster, M.; Ji, H.; Potash, J. B.; Sabunciyan, S.; Feinberg, A. P. The human colon cancer methylome shows similar hypo- and hypermethylation at conserved tissue-specific CpG island shores. *Nature genetics* **2009**, *41*, 178–86.

(72) Campbell, P. K.; Zong, Y.; Yang, S.; Zhou, S.; Rubnitz, J. E.; Sorrentino, B. P. Identification of a novel, tissue-specific ABCG2 promoter expressed in pediatric acute megakaryoblastic leukemia. *Leukemia research* **2011**, *35*, 1321–9.

Chapter 8 : Summary and Conclusions

8.1. Summary

The disposition of xenobiotics is dependent upon expression and function of enzymes and transporters. Uptake and efflux transporters are designed to protect the cell and organism from environmental toxins as well as transport dietary nutrients across barriers, such as into the milk[1,2]. The focus of this thesis was the efflux half-transporter mitoxantrone resistance protein (MXR), which has apical expression in select tissues and a broad spectrum of synthetic and natural substrates[3,4]. MXR has emerged as an essential transporter in xenobiotic pharmacokinetics, anticancer drug resistance and protection against xenobioitics[3,4]. Amino acid variants and variability in expression contribute to altered substrate profiles, chemotherapeutic resistance and cancer risk (Chapter 1)[3,5].

Expression of ABCG2 in various normal[6–8] and tumorigenic[9,10] tissues shows wide variability. Considering the importance of MXR in the transport of endogenous compounds and xenobioitics, a clear understanding of MXR function and *ABCG2* regulation is warranted. Identification of *ABCG2* regulatory elements and the effect of genetic variation in these regulatory regions will inform our understanding of the regulation of ABCG2 expression and MXR function. The work presented in this thesis illustrates that there are many mechanisms involved in the regulation and function of the MXR transporter. In addition to function, expression and localization of MXR variants, this research examines variants within the *ABCG2* promoter, *cis*-regulatory enhancers, suppressors and DNA methylation of the *ABCG2* locus in order to better understand the components of MXR function and *ABCG2* regulation.

The identification of MXR substrates and function of MXR amino acid variants have been extensively reported[11–17] (Chapter 1). The identification of novel nonsynonymous *ABCG2* variants in the SOPHIE cohort, as well as discordant functional studies of MXR variants, prompted the hypothesis that MXR variants can have altered expression and/or function. In Chapter 2 of this thesis, expression and localization studies of MXR variants *in vitro* are described. Specific MXR substrates were used to characterize the activity of amino acid variants both in whole cells and in vesicle based assays.

The optimization and use of vesicle assays for specific MXR substrates could be a useful tool in the identification of both other MXR substrates and altered substrate profiles for different MXR variants. Although the results from the MXR variant assays support many conclusions drawn in the literature, such as the reduced expression of Q141K, further studies are needed to confirm the impact of MXR variants *in vitro* and *in vivo*. This is especially important for understanding the defense of tissues from carcinogens and dietary toxins like pheophorbide A, the patient response and toxicity to chemotherapeutics like SN-38 (active metabolite of irinotecan) and the clinical use of MXR specific probes like sulfasalazine.

The majority of research on *ABCG2* regulation is focused on response elements in the proximal promoter of *ABCG2*[18]. Despite the identification of several response elements in the *ABCG2* proximal promoter, nothing has been done to characterize the effect of SNPs on the promoter's activity. This led to the hypothesis that variants within the *ABCG2* promoter were capable of altering its activity *in vitro* and *in vivo*. In Chapter 3, the results from *in vitro* and *in vivo* luciferase assays characterizing the activity of

ABCG2 promoter variants are presented. *In silico* predictions of transcription factor binding sites were used to predict the mechanism by which SNPs alter promoter activity. The predicted alteration in transcription factor binding by these SNPs must be confirmed. Although several *ABCG2* promoter SNPs were found to alter activity *in vivo*, the frequencies of these SNPs are low, and large population studies are needed to address their contribution to the expression of MXR.

The expression of MXR is altered by cellular exposure to xenobiotics or environmental stimuli[18–25]. Recent discoveries have shown that variation in pharmacogene regulatory elements have clinical impact[26]. This led to the hypothesis that there are regions of the *ABCG2* locus that act as *cis*-regulatory elements, and variations within these elements affect their activity. *In silico* prediction programs and *in vitro* and *in vivo* assays were used to identify the first *cis*-regulatory elements in the *ABCG2* locus (Chapter 4) and to show the effect of genetic variants in these regions on enhancer activity (Chapter 5). Some variants in *cis*-regulatory regions were associated with expression of one or more genes in the *ABCG2* locus, including *ABCG2* itself. Some of the putative *cis*-regulatory regions were identified as nuclear receptor response elements, and genetic variations within these elements altered the response to nuclear receptor ligands (Chapter 6). This screen involving *in silico*, *in vitro* and *in vivo* steps could be applied to the identification of genomic regulatory regions for other transporters or enzymes. As promising as these results are, the predicted transcription factors responsible for the activity of *cis*-regulatory elements and the effect of genetic variations on their binding *in vitro* must be confirmed.

The occurrence of hypo- and hypermethylation along the promoter of genes is a mechanism for the development of chemotherapeutic resistance[27]. Current research has highlighted the role of the *ABCG2* promoter and its hypomethylation in the regulation of MXR expression[18]. Aberrant methylation of the *ABCG2* promoter correlates with ABCG2 expression and drug resistance in clinical tumor samples[28–33]. However, most studies on the methylation of the *ABCG2* promoter focus on complete gain or loss of methylation, versus methylation dynamics, and it has yet to be discovered which sections or sites within CpG islands are most relevant for the DNA methylation regulation of MXR. In this thesis, patterns of DNA methylation of CpG islands within the *ABCG2* locus were examined in healthy kidney and liver tissues. Bisulfite treatment coupled with pyrosequencing techniques were used to obtain quantitative methylation values for each target CpG site. Sections of the CpG islands with different methylation between kidney and liver samples and correlation of *ABCG2* expression with the methylation of a key CpG site were characterized. Further studies are needed to expand these results to more tissues and examine similar DNA methylation in other types of tissues. Additionally, to understand the dynamics of DNA methylation, these sites should be examined after cellular stimuli and exposure to xenobiotics.

This dissertation describes novel data regarding mechanisms involved in the function and expression of MXR. Genetic variants within the *ABCG2* locus attributed to one of these mechanisms may be instrumental in understanding interindividual variation in MXR expression as well as drug response and toxicity. Although new avenues to explain the variation in MXR function have been identified, translation of this knowledge into clinical application requires significant effort. Further research on these mechanisms

is imperative and would allow for the clinical implementation of *ABCG2* pharmacogenetic information for the prediction, prevention or avoidance of altered drug response and adverse drug effects.

8.2. References

(1) Schinkel, A. H.; Jonker, J. W. Mammalian drug efflux transporters of the ATP binding cassette (ABC) family: an overview. *Advanced drug delivery reviews* **2003**, *55*, 3–29.

(2) Daly, A. K. Pharmacogenetics and human genetic polymorphisms. *The Biochemical journal* **2010**, *429*, 435–49.

(3) Mo, W.; Zhang, J.-T. Human ABCG2: structure, function, and its role in multidrug resistance. *International journal of biochemistry and molecular biology* **2012**, *3*, 1–27.

(4) Mao, Q.; Unadkat, J. D. Role of the breast cancer resistance protein (ABCG2) in drug transport. *The AAPS journal* **2005**, *7*, E118–33.

(5) Gradhand, U.; Kim, R. B. Pharmacogenomics of MRP transporters (ABCC1-5) and BCRP (ABCG2). *Drug metabolism reviews* **2008**, *40*, 317–54.

(6) Poonkuzhali, B.; Lamba, J.; Strom, S. Association of breast cancer resistance protein/ABCG2 phenotypes and novel promoter and intron 1 single nucleotide polymorphisms. *Drug Metabolism and ...* **2008**, *36*, 780–795.

(7) Urquhart, B. L.; Ware, J. a; Tirona, R. G.; Ho, R. H.; Leake, B. F.; Schwarz, U. I.; Zaher, H.; Palandra, J.; Gregor, J. C.; Dresser, G. K.; Kim, R. B. Breast cancer resistance protein (ABCG2) and drug disposition: intestinal expression, polymorphisms and sulfasalazine as an in vivo probe. *Pharmacogenetics and genomics* **2008**, *18*, 439–48.

(8) Zamber, C. P.; Lamba, J. K.; Yasuda, K.; Farnum, J.; Thummel, K.; Schuetz, J. D.; Schuetz, E. G. Natural allelic variants of breast cancer resistance protein (BCRP) and their relationship to BCRP expression in human intestine. *Pharmacogenetics* **2003**, *13*, 19–28.

(9) Ross, D. D.; Karp, J. E.; Chen, T. T.; Doyle, L. A. Expression of breast cancer resistance protein in blast cells from patients with acute leukemia. *Blood* **2000**, *96*, 365–8.

(10) Nakanishi, T.; Karp, J. E.; Tan, M.; Doyle, L. A.; Peters, T.; Yang, W.; Wei, D.; Ross, D. D. Quantitative analysis of breast cancer resistance protein and cellular resistance to flavopiridol in acute leukemia patients. *Clinical cancer research : an official journal of the American Association for Cancer Research* **2003**, *9*, 3320–8.

(11) Kim, K.; Joo, H.-J.; Park, J.-Y. ABCG2 polymorphisms, 34G>A and 421C>A in a Korean population: analysis and a comprehensive comparison with other populations. *Journal of clinical pharmacy and therapeutics* **2010**, *35*, 705–12.

(12) Tamura, A.; Onishi, Y.; An, R.; Koshiba, S.; Wakabayashi, K.; Hoshijima, K.; Priebe, W.; Yoshida, T.; Kometani, S.; Matsubara, T.; Mikuriya, K.; Ishikawa, T. In vitro evaluation of photosensitivity risk related to genetic polymorphisms of human ABC transporter ABCG2 and inhibition by drugs. *Drug metabolism and pharmacokinetics* **2007**, *22*, 428–40.

(13) Wakabayashi, K.; Tamura, A.; Saito, H.; Onishi, Y.; Ishikawa, T. Human ABC transporter ABCG2 in xenobiotic protection and redox biology. *Drug metabolism reviews* **2006**, *38*, 371–91.

(14) Ishikawa, T.; Tamura, A.; Saito, H.; Wakabayashi, K.; Nakagawa, H. Pharmacogenomics of the human ABC transporter ABCG2: from functional evaluation to drug molecular design. *Die Naturwissenschaften* **2005**, *92*, 451–63.

(15) Yanase, K.; Tsukahara, S.; Mitsuhashi, J.; Sugimoto, Y. Functional SNPs of the breast cancer resistance protein-therapeutic effects and inhibitor development. *Cancer letters* **2006**, *234*, 73–80.

(16) Tamura, A.; Watanabe, M.; Saito, H.; Nakagawa, H.; Kamachi, T.; Okura, I.; Ishikawa, T. Functional validation of the genetic polymorphisms of human ATP-binding cassette (ABC) transporter ABCG2: identification of alleles that are defective in porphyrin transport. *Molecular pharmacology* **2006**, *70*, 287–96.

(17) Yoshioka, S.; Katayama, K.; Okawa, C.; Takahashi, S.; Tsukahara, S.; Mitsuhashi, J.; Sugimoto, Y. The identification of two germ-line mutations in the human breast cancer resistance protein gene that result in the expression of a low/non-functional protein. *Pharmaceutical research* **2007**, *24*, 1108–17.

(18) Robey, R. W.; To, K. K. K.; Polgar, O.; Dohse, M.; Fetsch, P.; Dean, M.; Bates, S. E. ABCG2: a perspective. *Advanced drug delivery reviews* **2009**, *61*, 3–13.

(19) Cheng, G. M. Y.; To, K. K. W. Adverse Cell Culture Conditions Mimicking the Tumor Microenvironment Upregulate ABCG2 to Mediate Multidrug Resistance and a More Malignant Phenotype. *ISRN oncology* **2012**, *2012*, 746025.

(20) Pradhan, M.; Bembinster, L. a; Baumgarten, S. C.; Frasor, J. Proinflammatory cytokines enhance estrogen-dependent expression of the multidrug transporter gene ABCG2 through estrogen receptor and NF{kappa}B cooperativity at adjacent response elements. *The Journal of biological chemistry* **2010**, *285*, 31100–6.

(21) Jigorel, E.; Vee, M. Le; Boursier-neyret, C.; Parmentier, Y.; Fardel, O. Differential Regulation of Sinusoidal and Canalicular Hepatic Drug Transporter Expression by

Xenobiotics Activating Drug-Sensing Receptors in Primary Human Hepatocytes ABSTRACT : **2006**, *34*, 1756–1763.

(22) Wang, H.; Lee, E.; Zhou, L.; Leung, P. C. K.; Ross, D. D.; Unadkat, J. D.; Mao, Q. Progesterone receptor (PR) isoforms PRA and PRB differentially regulate expression of the breast cancer resistance protein in human placental choriocarcinoma BeWo cells. *Molecular pharmacology* **2008**, *73*, 845–54.

(23) Zhang, Y.; Zhou, G.; Wang, H.; Zhang, X.; Wei, F.; Cai, Y.; Yin, D. Transcriptional upregulation of breast cancer resistance protein by 17beta-estradiol in ERalpha-positive MCF-7 breast cancer cells. *Oncology* **2006**, *71*, 446–55.

(24) Lemos, C.; Kathmann, I.; Giovannetti, E.; Dekker, H.; Scheffer, G. L.; Calhau, C.; Jansen, G.; Peters, G. J. Folate deprivation induces BCRP (ABCG2) expression and mitoxantrone resistance in Caco-2 cells. *International journal of cancer. Journal international du cancer* **2008**, *123*, 1712–20.

(25) Lemos, C.; Kathmann, I.; Giovannetti, E.; Calhau, C.; Jansen, G.; Peters, G. J. Impact of cellular folate status and epidermal growth factor receptor expression on BCRP/ABCG2-mediated resistance to gefitinib and erlotinib. *British journal of cancer* **2009**, *100*, 1120–7.

(26) Smith, R. P.; Lam, E. T.; Markova, S.; Yee, S. W.; Ahituv, N. Pharmacogene regulatory elements: from discovery to applications. *Genome medicine* **2012**, *4*, 45.

(27) Baer-Dubowska, W.; Majchrzak-Celińska, A.; Cichocki, M. Pharmocoepigenetics: a new approach to predicting individual drug responses and targeting new drugs. *Pharmacological reports : PR* **2011**, *63*, 293–304.

(28) Turner, J. G.; Gump, J. L.; Zhang, C.; Cook, J. M.; Marchion, D.; Hazlehurst, L.; Munster, P.; Schell, M. J.; Dalton, W. S.; Sullivan, D. M. ABCG2 expression, function, and promoter methylation in human multiple myeloma. *Blood* **2006**, *108*, 3881–9.

(29) Bram, E.; Stark, M.; Raz, S.; Assaraf, Y. Chemotherapeutic drug-induced ABCG2 promoter demethylation as a novel mechanism of acquired multidrug resistance. *Neoplasia (New York, NY)* **2009**, *11*, 1359–1370.

(30) Chen, M.; Xue, X.; Wang, F.; An, Y.; Tang, D.; Xu, Y.; Wang, H.; Yuan, Z.; Gao, W.; Wei, J.; Zhang, J.; Miao, Y. Expression and promoter methylation analysis of ATP-binding cassette genes in pancreatic cancer. *Oncology reports* **2012**, *27*, 265–9.

(31) To, K. K. W.; Zhan, Z.; Bates, S. E. Aberrant promoter methylation of the ABCG2 gene in renal carcinoma. *Molecular and cellular biology* **2006**, *26*, 8572–85.

(32) Bram, E.; Stark, M.; Raz, S. Chemotherapeutic drug-induced ABCG2 promoter demethylation as a novel mechanism of acquired multidrug resistance. *Neoplasia (New York, NY)* **2009**, *11*, 1359–1370.

(33) Nakano, H.; Nakamura, Y.; Soda, H.; Kamikatahira, M.; Uchida, K.; Takasu, M.; Kitazaki, T.; Yamaguchi, H.; Nakatomi, K.; Yanagihara, K.; Kohno, S.; Tsukamoto, K. Methylation status of breast cancer resistance protein detected by methylation-specific polymerase chain reaction analysis is correlated inversely with its expression in drug-resistant lung cancer cells. *Cancer* **2008**, *112*, 1122–30.

Publishing Agreement

It is the policy of the University to encourage the distribution of all theses, dissertations, and manuscripts. Copies of all UCSF theses, dissertations, and manuscripts will be routed to the library via the Graduate Division. The library will make all theses, dissertations, and manuscripts accessible to the public and will preserve these to the best of their abilities, in perpetuity.

Please sign the following statement:

I hereby grant permission to the Graduate Division of the University of California, San Francisco to release copies of my thesis, dissertation, or manuscript to the Campus Library to provide access and preservation, in whole or in part, in perpetuity.

Rachel Eclov
Author Signature

3/23/13
Date